NCHRP Project 12-36(02)
NCHRP Report 406
Appendixes A - F
Copy No. 1

APPENDIX A

LITERATURE REVIEW

A 1984 "State of the Art Report on Redundant Bridge Systems" [A.1] concluded that although analytical techniques to study the response of damaged and undamaged flexural systems to high loads are available, "little work has been done on quantifying the degree of redundancy that is needed". More than a decade later, this statement seems to be still valid. In fact, contacts by the authors with bridge engineers and researchers in the US, Europe and Japan indicated there are no known current or recent research efforts that address the issue of bridge redundancy in the comprehensive approach proposed in this study. The objective of this study is to develop a framework to include redundancy in bridge design and load capacity evaluation. Since redundancy is related to the performance of damaged and undamaged bridge systems under heavy loads, this Appendix reviews recent research findings on subjects related to the behavior of bridge members and bridge systems, and on studies on the reliability evaluation of structural bridge systems as well as proposed measures of structural redundancy.

A-1 REDUNDANCY IN BRIDGE DESIGN AND EVALUATION

The 1996 AASHTO Standard Specifications for Highway Bridges require the consideration of redundancy when designing steel bridge members [A-2]. For example, section 10.3 of the AASHTO manual requires different allowable fatigue stress ranges for "redundant" and "nonredundant load path" structures. By AASHTO's definition, "a component may be considered a nonredundant load path member when the failure of a single element could cause collapse". Examples of nonredundant load path members are given as flange and web plates in one or two girder bridges, main one-element truss members, hanger plates and caps at single or two-column bents. AASHTO's definition hinges on the term collapse that is not defined in the specifications.

The Ontario Highway Bridge Design Code (OHBDC) [A-3] did not favor using nonredundant designs and avoids giving any guidelines for the design of nonredundant bridges. It is not known if any other bridge code contains specific recommendations that address the issue of redundancy.

Kulicki et al. [A-4] proposed the inclusion of system factors in the LRFD AASHTO Specifications. They outline a format explaining how redundancy and other parameters related

to global response can be included in the design process using "load factor modifiers". As proposed, the load factor modifiers are functions of a subjective evaluation of the "operational importance" of a structure, the "level of ductility" and the "level of redundancy". Operational importance concerns "the consequences of the bridge being out of service" based on "social/survival and/or security/defense requirements". These criteria are similar to those used in the design for earthquakes. The classification of members as ductile or non ductile is left up to the designer. For concrete connections, the LRFD Specification mentions that ductility requirements are satisfied if the resistance of the connection is at least 1.3 times the maximum force effect on the adjacent components. The designation of a member as redundant or nonredundant is based on the "member's contribution to the bridge safety". Main elements whose failure is "expected to cause the collapse of the bridge are designated as fracture-critical and the structural system is nonredundant". Collapse is defined as "a major change in the geometry of the bridge rendering it unfit for use". To include "importance, ductility and redundancy" in the design process, each one of these effects is assigned a factor of 0.95, 1.0 or 1.05. The total load factor modifier is the product of the individual factors. Values of the modifiers below 1.0 are for bridges with high levels of ductility and redundancy and a low level of operational importance. Values above 1.0 indicate that bridge members must be strengthened due to potentially inadequate load redistribution capability.

In a recent NCHRP study [A-5], Fred Moses et al. developed a LRFD formulation for the load capacity evaluation of existing bridges. In the recommendations which were incorporated in AASHTO's Guide Specifications for the Evaluation of Steel and Concrete Bridges, different resistance factors were recommended for redundant and nonredundant spans. The different resistance factors were calibrated using structural reliability theory on the basis of providing higher safety indices for nonredundant components as compared to redundant components "because of the differences in failure consequences". Typically, a resistance factor equal to 0.95 is used for redundant bridges and a factor of 0.75 is used for nonredundant bridges. The same AASHTO definition of redundancy cited above for fatigue categories was used in the evaluation procedures.

In a similar activity on redundancy analysis, Moses, Schilling and Raju in NCHRP project 12-28 developed different factors for fatigue checking of steel members [A-6]. These also utilized different reliability targets for redundant and nonredundant attachments. Their work has been incorporated in two AASHTO Guide Specifications, one for fatigue design and one for fatigue

life evaluation of existing bridges.

Moses et al. [A-5] report that several agencies in different states such as New York and Illinois have been using redundancy definitions in selecting stress levels for bridge rating. For example, higher stresses such as operating stress values are used for redundant members, while lower stresses such as inventory stresses are required in the evaluation of nonredundant members.

Autostress Design [A-7] also known as the "alternate load factor design procedure" is a method adopted by AASHTO for guide specifications for steel beam bridges using braced compact sections. This method uses the formation of a plastic mechanism as the limit state under maximum load conditions. For overload conditions in the autostress method, a slight amount of inelastic rotations is allowed at the supports. Thus, the autostress method accounts for redundancy by allowing a longitudinal redistribution of loads. The method, however, uses the current AASHTO transverse load distribution factors. Thus, the benefit from the presence of additional parallel members which may add to the total system capacity is not considered.

In some examples of current practice for the design and evaluation of truss bridges, computer runs are performed to determine which members are fracture critical. The calculations are executed as follows: A given member is assumed to be fractured, the truss is then analyzed for dead load plus some fraction of live load. If under these circumstances, other members reach their limit capacity, thereby leading to the truss' collapse, the given member was classified as fracture critical. Members designated as fracture critical will require that their material, fabrication and testing conform to requirements of the 1978 AASHTO guide specifications for steel bridge members [A-8]. No guidelines are available to determine the portion of live load that should be used in the analysis.

In some States, it is common to require consultants to undertake a special evaluation of nonredundant, fracture critical members. The evaluation would include rating and checking the fatigue life of fracture critical nonredundant members and the evaluation of critical structural details. The feasibility of converting nonredundant designs to redundant designs is investigated, otherwise, the possibility of improving the load rating of nonredundant members is considered.

Until recently redundancy was never considered when checking the system capacity of bridges under extreme load conditions. The evaluation of bridges under extreme loads was restricted to a

check of the load carrying capacity of individual members. Load distribution was calculated using elastic factors, while (for example when using LFD or Autostress criteria) member strength was calculated using ultimate capacity. Currently, due to the tragic failures of several nonredundant bridges, some states prohibit the use of bridges with three or fewer girders if at all possible. This is based on a subjective and unquantified observation that bridges should have four or more girders that satisfy AASHTO's criteria to provide adequate load redistribution capability after the failure of one girder.

The references mentioned in this section indicate that current bridge engineering practice recognizes the importance of structural redundancy in improving the structural safety of highway bridges. However, present specifications and recommended procedures do not provide consistent methods or accurate measures to include redundancy in bridge design and evaluation. The next section reviews research efforts to develop recommendations for bridge redundancy measures. Section A-3 reviews recent proposals to include redundancy in other structural applications.

A-2 MEASURES OF BRIDGE REDUNDANCY

Although most engineers agree on the general goals of structural redundancy, the issue of quantifying redundancy and defining objective and universal measures has not been resolved. Different researchers have proposed alternative measures of redundancy. For example, Galambos et al. in a recent NCHRP study [A-9] developed a method for the inelastic rating of steel beam and girder bridges. The method incorporates the inelastic range of behavior in the bridge rating process and the bridge is treated as a system rather than focusing on the behavior of individual members. The proposed method uses shakedown as the limit state for bridges under cyclic loads. Shakedown is defined as the load that causes a set of residual moments such that the bridge responds to subsequent loads in an elastic fashion. The proposed analysis also compares the results of the following three limit states: 1) first hinge formation, 2) shakedown, and 3) collapse. The analysis assumes a grid model for typical single-span and multi-span steel bridges. Also in this study, a Residual Damage Analysis (RDA) method was developed. This method rates a bridge against an inelastic deflection limit state, defined as the ratio of the span length to the mid-span inelastic deflection.

Frangopol and his co-workers [A-10] also looked at different measures of redundancy. These include deterministic as well as probabilistic measures. These measures compare the load capacity of intact bridges to that of damaged bridges. Two types of damages are compared: a)

corrosion damage where a uniform loss of material in the girders is considered, and b) accidental damage where one or two girders are completely removed from the bridge system. The load capacity of intact bridges was defined in terms of either the nominal (specification defined) capacity or the actual load capacity using a finite element model. On the other hand, using probabilistic definitions, redundancy was defined as a function of the probability of bridge collapse compared to the probability of first failure or the probability of failure of the weakest member. Examples for steel single span multi-beam, and truss bridges were also given in reference [A-10].

According to acceptable engineering practice, the existence of multi-load paths is not by itself sufficient to define redundancy. The structure should be capable of resisting a certain level of dead and live loads after the total failure or loss of any one member. For example Daniels et al. [A-11] recommend that "after-fracture redundancy" be primarily concerned with the serviceability of the bridge and the safety of the public.

Three types of redundancy are defined by Purvis, Graber and Albrecht in a study for the Federal Highway Administration (FHWA) [A-12]. These are:

a) Internal redundancy which means that the failure of one element will not result in the failure of the other elements of the member. For example, cracks that develop in one element do not spread to other elements.

b) Structural redundancy which refers to the redundancy which exists as a result of the continuity within the load path. For example, any structurally indeterminate structure such as continuous beams would belong to this type. AASHTO usually does not assume structural redundancy to be sufficient. For example, even though a continuous two-span two-girder bridge is structurally indeterminate, the AASHTO criteria would technically classify it as nonredundant.

c) Load path redundancy as defined by AASHTO refers to the number of supporting elements, usually girders. A structure is nonredundant if it has one or two load paths. For example a bridge composed of only one or two parallel girders is regarded as nonredundant. According to the AASHTO criteria, failure of one girder of a system with one or two load paths is assumed to result in the collapse of the span, hence, the bridge is considered to be nonredundant and the girder fracture critical.

Sandberg and Parmelee [A-13] defined redundancy as the ability of a failed structure to support a design truck load without exceeding the stresses allowed by AASHTO for occasional overload. Failure of one main girder was defined as the complete failure of the tension flange plus the portion of the web that would be in tension but preserving enough web to transmit shear. They did not provide supporting evidence for their recommendations and criteria, but they insisted that redundancy should be required in all major structures. They recommended that research to define "reasonable criteria" and "allowable stresses for redundancy design" should be undertaken; further, that load and resistance factors that reflect the available system reserve of "a proven redundant design" be developed.

A-3 REDUNDANCY IN OTHER STRUCTURAL APPLICATIONS

Other structural codes have also considered the possibility of including redundancy in the safety evaluation of structures. For example, Gromala [A-14] discussed the introduction of system factors in a proposed LRFD Specifications for wood buildings. The objective is to take advantage of the system's capability due to the "repetitive member use that occur in an assembly of multiple parallel wood framing members". The draft wood specifications propose to calculate a system factor that is equal to the ratio of the tested or computed 5th percentile of the strength of the system divided by the 5th percentile of the strength of the individual members. On the other hand, the system factor can be computed using reliability based code calibration by taking the ratio of the resistance factor for the complete system divided by the resistance factor for the members. Both member and system resistance factors are computed using a common target reliability index. Damage is not examined in this wood specification but rather an examination is made of the ratio of system failure to first element failure. The draft specifications recommend the use of strength-oriented limit states rather than stiffness or deformation-oriented limit states. Gromala lists possible limit states as first member failure, the failure of any second member or the failure of any two adjacent members. He does not recommend the use of collapse as a system limit state because it would require using a different target reliability index for the system. The use of the same target reliability index for member and system resistance factors is based on their assumption that "the consequences of failure when the system limit states are reached are comparable to the consequences of the member reaching its limit state".

In Europe, the Swiss building and Scandinavian codes address redundancy with a fault tree approach [A-15]. That is, the engineer in cooperation with the owner should evaluate a sequence of "what-if" scenarios. For example, a gas explosion in a kitchen or a truck colliding with a lower

level building column. In such cases, the structure must provide sufficient reserve capacity so that collapse does not follow a given damage scenario.

In the United States, the steel offshore platform code has recently been revised based on reliability methods [A-16]. For example, to achieve system reserve in seismic design provisions, specific framing arrangements are recommended along with member and connection details. Specifically, the code requires that: a) Individual members be provided with toughness rules to assure member ductility. These include requirements to preclude local buckling or unloading following gross column buckling. b) Connections are sized to carry full member loads to eliminate any undesirable "weak links" in the system. c) Member geometries with parallel load paths be used. Engineers selecting designs that do not satisfy the recommended member design practices are required to perform a 3-D nonlinear dynamic analysis to assure platform survival under an extreme seismic event. System reserve capacity beyond first element failure has also been investigated for platforms subject to extreme hurricane wave loadings.

In studies on the reliability of offshore platforms, Cornell et. al. [A-17] proposed a definition of "redundancy" in terms of the ratio of the probability of system failure to the probability of member failure. He also defined "robustness" in terms of the probability of the failure of a damaged system compared to the probability of failure of the intact system.

In a study for AISI, Galambos [A-18] proposed to tie the system factors to the level of damage which would occur if a limit state were exceeded. A set of factors varying between 1.1 and 0.7 were proposed for different damage levels ranging from slight to complete including possibility of loss of life. For example, the failure of a compact member in a redundant frame or the yielding of a tension member that would not produce excessive deformations were defined as slight damage. The failure of a column in a statically determinate structure was defined as moderate damage. Serious damage was associated with frame instability under gravity loads and complete damage was associated with the case where any component failure would bring down the whole system.

Sections A-2 and A-3 show that different researchers have proposed several alternative measures of structural redundancy. It is noted that the consensus emerging from current research studies favors the use of structural reliability methods to develop proposed redundancy measures. Such an approach would be compatible with recent trends to use reliability techniques for the development of structural codes and specifications.

A-4 RELIABILITY OF BRIDGE STRUCTURAL SYSTEMS

To account for the uncertainties associated with determining member resistances and applied loads, all recent developments of bridge codes use reliability-based calibrations of the design equations [A-3,4,19,20,21]. The code calibrations include the determination of the nominal design loads and member capacities as well as the resistance and load factors. Most of these efforts, however, were concerned with the reliability of individual structural members. The theory of reliability has also been extended by researchers such as Ang, Moses and Cornell [A-22,23,24,25] to account for the interaction of members into a structural system with several possible failure modes and to account for the true nonlinear behavior of the system.

The system reliability methods that were first developed for the analysis of offshore platforms were later applied to bridge structures. For example, Tabsh and Nowak [A-26] developed a practical method to calculate the system reliability of girder bridges. A reliability analysis was performed for typical steel (composite and non-composite), reinforced concrete and prestressed concrete bridges. Safety indices which give a statistical measure of structural reliability are calculated. Nowak and Tabsh calculated the safety indices of typical bridge systems and compared these to the safety indices of individual members. In their work they defined the ultimate capacity of the system as the load which will cause the failure of the initially intact bridge. System failure is defined as the formation of a plastic hinge mechanism or the load at which "large permanent deformations" are obtained. All members are assumed to have very high levels of ductility with no possibility of member unloading. All the bridges analyzed were designed to satisfy AASHTO's LFD criteria. Bridges with five longitudinal members at 8 ft spacings were analyzed for spans varying between 40 and 100 ft.

The calculation of system reliability was based on a grid model using moment versus curvature plots obtained from simulation studies. The system safety indices obtained were higher than those of individual members due to the redistribution of loads when individual members reached their limit capacities. The system safety indices varied from about 2.5 to about 3.5 for steel bridges and from 3.5 to 4.0 for reinforced concrete and for prestressed concrete bridges. A plot of member safety index versus system safety index showed that if the strength of the members in a

bridge are assumed to be fully correlated, then for typical five-member bridge systems, the relationship between the safety indices can be roughly approximated from an equation of the form:

$$\beta_{ult} = \beta_{member} + 1.0 \qquad \text{(A-1)}$$

where β_{ult} is the safety index for the ultimate capacity of the system, and β_{member} is the safety index of one member. In their calculations, Nowak and Tabsh ignored the possibility of damage to one or more members due to fatigue failure or collision of vehicles, trucks or debris. They also assumed that the bridges have five identical longitudinal members with sufficiently high ductility levels to insure the formation of a collapse mechanism or the development of large permanent deformations. They did not set any displacement limits and did not check the transverse capacity of the slab and secondary elements.

In a doctoral thesis on the system reliability of steel girder bridges, Arwashan [A-27] uses the definitions proposed by Cornell et al [A-17] to study the redundancy and robustness of girder bridges. In this context, redundancy compares the performance of the system to the performance of one member while robustness compares the performance of the damaged system to that of the intact system. Based on a sensitivity analysis, he concluded that the optimum system for a two lane steel girder bridge would have 4 or 5 girders spaced at 9 or 7 ft and that increasing the number of girders while reducing the girder spacing or increasing the spacing while reducing the number of girders would reduce the level of bridge safety. He also observed that the contribution of the diaphragms to the system's reliability was small.

Studying the reliability of complete structural systems in the nonlinear range is very complicated due to the need of enumerating all the pertinent failure modes and studying the statistical correlation between the members' resistances. To reduce the complexity of the problem, many approximate methods have been developed. These include efficient simulation techniques as well as approximate numerical methods [A-28,29]. Cornell [A-30], however, made the observation

that for systems under dynamic loading, the probabilistic effects of randomness in element capacity upon system capacity are small compared to load variability. Therefore, it would be sufficient to perform a deterministic analysis of a system using the median element properties in order to estimate the reliability of the whole system although the coefficient of variation (COV) of the system is usually somewhat smaller than those of the elements' capacities.

The review of recent research work on the reliability of structural systems indicate that simplified methods such as those suggested by Cornell [A-30] can be applied in practice to accurately describe the safety of bridge systems. These methods can provide measures of bridge redundancy by comparing the safety of the complete system to the safety of individual members. The approach assumes that the uncertainties in describing the loading is much higher than that of the resistances. To perform the system reliability analyses, accurate deterministic evaluation of the behavior of the bridge system is required. The following sections review recent analytical and experimental studies of the behavior of typical bridge systems.

A-5 EFFECT OF SECONDARY MEMBERS ON CAPACITY OF BRIDGE SYSTEMS

Bridge redundancy as normally defined consists of the capability of a bridge to continue to carry loads after the damage or the failure of one or more of its members. The capability of a bridge to continue to carry loads after a member's failure, is due to its ability to redistribute these applied loads. This normally involves a potential for transverse and longitudinal redistribution.

Transverse redistribution is usually a function of the longitudinal member properties, the deck slab, the effect of secondary members, and the geometric configuration of the bridge. Important geometric properties include the number of girders, girder spacing, number of spans and the span lengths. The longitudinal redistribution is usually affected by the ductility of bridge members especially at the continuous supports. The capacity of bridge structures to redistribute loads after the failure of a main load-carrying member seems to have been largely underestimated even for

simple two-girder bridges damaged by the loss of a main member [A-11]. Several recent studies attempted to analytically determine the redistribution capacity or to provide guidelines for new designs or techniques to retrofit existing bridges to insure adequate load-carrying capacity after the failure of any member [A-9,11].

The following sections present a discussion on the important parameters that affect bridge redundancy. These are: Effect of deck slab action and secondary members (including diaphragms and bracing), member ductility, and bridge geometry or system effect. The purpose of this discussion is to identify the most important parameters that affect the ultimate capacity of bridge systems in order to include these parameters in the structural models used in this study.

In a study for NCHRP, Daniels et al. [A-11] observed that existing bridges usually exhibit after-fracture redundancy when the bracing system is "properly configured". They presented guidelines explaining how to perform redundancy rating using 3-D analytical models of bridge structures.

Heins and Kato [A-31] presented analytical data which showed the significant contributions of secondary members to load redistribution after the fracture of one girder. Although this study ignored the effect of deck slabs, they still observed that secondary members can contribute to the integrity of "nonredundant" structures effectively creating redundancy and thus inhibiting immediate collapse.

In a detailed analysis of a multi-span, two-girder steel bridge, Idriss et al. [A-32] showed that the bridge system remained stable and was still capable of carrying AASHTO loads after the fatigue fracture of one girder. This capability was mostly due to the ability of the deck to provide transverse load redistribution. They found that the bottom lateral bracing contributed very slightly to load redistribution, while some of the transverse beams contributed more. The stringers showed a large increase in load at the vicinity of the crack and a significant increase in load at the interior supports.

A project to study the effect of diaphragms in prestressed concrete bridges was conducted for the Iowa Department of Transportation. In that study, Abendroth, Klaiber and Shafer [A-33] observed that: "The distribution of the vertical load in prestressed concrete girder bridges with various diaphragms in place at either midspan or one-third points or without diaphragms present was essentially the same". Girders were assumed to be undamaged in these analyses.

Stallings et. al. [A.109] using field data on actual bridge under regular traffic conditions and trucks of known weights observed that removing the diaphragms increased the stresses in some bridge members by 6 to 15 percent.

In summary, section A-5 makes the observation that researchers are still not in agreement on the contribution of the diaphragms to the transverse distribution of the load. In any case, it is clear that the deck is the most important contributor to the transverse distribution of the load in multi-girder bridge systems. The contributions of the lateral bracing and the diaphragms to the transverse distribution may be significant only if they have substantial strength and stiffness or when one girder is heavily damaged. In the latter case, the secondary members in the vicinity of the damage help the deck slab redistribute the load to the intact members.

A-6 DUCTILITY AND NONLINEARITY OF CONCRETE MEMBERS

According to current AASHTO LFD practice [A-2], concrete bridge members are designed to satisfy minimum ultimate moment capacity criteria. But, many bridge members including prestressed concrete members have been designed using WSD methods which use elastic limit criteria. In either case, in order to ensure adequate load redistribution, these members should provide enough ductility after they reach their ultimate capacities [A-34].

Based on studies of the subject [A-35], ductility of concrete members is a function of the compression steel reinforcement but an inverse function of the tension steel reinforcement. In a ductile member the tension steel will yield before the concrete fails and adding more steel may produce an overreinforced beam. Ductility was also found to be a function of concrete compressive strength but an inverse function of the steel yield strength. Some concern has been expressed about buckling of thin long P/S members with high concrete strengths.

The nonlinear behavior and the ductility of concrete members can be modeled using moment versus curvature relationships. These relationships are developed based on member geometry and material properties. Moment versus plastic rotation curves can also be used to model the nonlinear behavior of concrete members. These curves can be obtained using a combination of analytical and empirical methods [A-36].

Concrete members will keep loading until they reach their ultimate moment capacity. As the section goes into the inelastic range, plastic hinge rotations will occur. These plastic hinge rotations are related to the strain in the member. Once the ultimate strain capacity is reached, the member will reach its maximum possible plastic hinge rotation at which point member failure will occur. Unloading will occur suddenly once this maximum plastic hinge rotation value is reached. It was observed that the maximum plastic hinge rotation that a section can sustain is a function of the section geometry, the reinforcement ratio and the level of lateral confinement [A-36].

Several methods have been proposed to estimate this maximum plastic hinge rotation. For example, Skogman, Tadros and Grasmick [A-37] assumed that the maximum plastic rotation is a function of the distance to the neutral axis from the extreme compression fiber at ultimate capacity, the ultimate compressive concrete strain and the effective depth of the section which is the distance from the extreme compression fiber to the centroid of the tension reinforcement.

Skogman et. al. [A-37] assumed that their equation is valid for both T-beams and prestressed concrete members or partially prestressed beams. In the latter case, the effective depth can be calculated as recommended by Naaman [A-38], using the weighted average of the distance to the centroid of the prestressing steel alone and the reinforcing steel alone; the weighing factors are obtained based on the areas of steel and the stresses in the reinforcing steels at ultimate.

Naaman [A-39] also proposed an empirical formula that gives the maximum plastic hinge rotation as a function of the distance to the centroid of the reinforcing steel, the plastic hinge length and the reinforcing index. Naaman's equation was obtained by fitting a curve through analytically derived data points. This proposed equation is valid for reinforced, prestressed or partially prestressed concrete members and is given as a function of the length of the plastic hinge, the effective depth of the section and the reinforcing index which gives the ratio of the forces in the reinforcing steel to those in the concrete. The equation gives a lower bound on the

maximum plastic hinge rotation that can be sustained by typical members.

Thee length of the plastic hinge that forms in concrete members can be estimated based on empirical formulas. For example, reference [A-36] reviews many alternate empirical methods to calculate the length of the plastic hinge. The model proposed by Naaman seem to provide reasonably close lower bounds to experimental data on bending of concrete members such as those performed by Máttock [A-40].

In summary, it is observed that a combination of analytical and empirical methods can be used to produce moment versus plastic rotation curves for typical concrete bridge sections. These curves would provide a description of the nonlinear flexural behavior and the ductility of concrete members and can be used for the analysis of the nonlinear behavior of concrete bridge systems.

A-7 SHEAR NONLINEARITY OF CONCRETE MEMBERS

In addition to nonlinearity under bending, concrete members exhibit nonlinear behavior due to shear. Shear behavior, however, is very difficult to model. Experimental results on the behavior of concrete members under shear show extremely wide scatter and the models available for predicting the ultimate shear capacity are extremely unreliable [A-41,42,43]. Although bridge field tests and model tests have shown that shear failures in bridges under high loads are not usual, modeling the shear transfer mechanism seems to be an important factor for the analysis of concrete box-girder bridges [A-44].

Reference [A-44] assumes that the shear behavior of concrete members follows a tri-linear shear deformation curve. In a first phase, the shear behavior is assumed to be in the linear elastic range, in the second phase shear nonlinearity is observed and softening of the shear stiffness is observed. In the third stage a plastic shear behavior is assumed with a zero shear stiffness until an ultimate shear strain value of 0.01 is measured at which brittle shear failure is assumed. Appendix F of this Report gives a more detailed description of the model and behavior used in reference [A-44].

This model and similar models are widely used although they are known to vastly underpredict the true shear capacity. This is because they ignore many of the physical phenomena that help provide additional shear capacity such as arch action, and aggregate interlock [A-41,42,43]. Many researchers are trying to develop better models based on the theory of fracture mechanics.

These models however require further refinement before they can be used in actual practice [A-46].

Both OHBDC and the LRFD Specifications use modified compression field models for shear strength [A-3,4]. This method accounts for the interaction between moment and shear. The method has not yet been implemented in the programs used in this study.

In a review of the experimental work performed on the shear strength of high-strength concrete beams, Hall [A-47] proposes a set of empirically derived equations that seem to better predict the experimental results published on high strength beams tested in reference [A-48] as well as regular reinforced concrete beams tested in reference [A-49].

The issue of shear behavior is even more complicated for thin webbed sections in general [A-50] due to the possibility of web crushing. Box beams in particular might be subjected to torsional loads which may influence the shear-bending behavior of the beams [A-51]. For segmental beams, even the bonding or unbonding of the prestressing tendons seems to influence the behavior under the combined action of bending shear and torsion [A-52].

This Section shows that models to account for the nonlinear behavior of concrete members under shear loads are available. These models, however, are highly conservative and provide safe lower bounds useful for design but may not produce accurate estimates of ultimate shear capacity of concrete bridge members.

A-8 DUCTILITY OF STEEL MEMBERS

The factors affecting the behavior in the plastic range of steel beams are complex and intricately interrelated. Local flange, local web, and lateral-torsional distortion interact and tend to build up gradually rather than suddenly. Strain hardening on the one side and instability on the other side work against each other and they tend to balance out [A-53]. For this reason, considerable research on the inelastic behavior and the ductility of steel and composite bridge members took place since the mid-1960's. Many of the observations made by researchers in this field are summarized by Maheu [A-54].

As reported in reference [A-54], experimental results showed that composite sections provide large shape factors on the order of 1.5, while it is about 1.15 for naked steel sections. Failure of composite sections with relatively deep slabs was marked by crushing of the slab only after

considerable strain hardening had occurred in the bottom flange of the beams. However, for sections where the plastic neutral axis is located in the steel section, the ultimate moment may not be reached since the concrete may crush before the steel section could yield throughout. Therefore, the location of the plastic neutral axis is an important factor in determining both the capacity and the ductility of a composite section. This is the same approach adopted in the ductility provisions of the AASHTO Specifications. Based on his literature survey, Maheu [A-54] also observed that a minimum number of connectors is needed to reach the maximum moment but beyond that, additional connectors did not contribute to the moment capacity.

Maheu [A-54] also reports that for negative bending, failure was usually caused by local buckling at the point of maximum negative moment; this was dependent on the slenderness of the flange and the web. Therefore, slenderness limits for compact sections and bracing requirements are important to prevent local buckling during plastic rotations. It was also observed that beams made of high strength steels, low strength concrete and thin slabs tended to lack ductility.

Carskaddan et. al. [A-55] as well as several other researchers made observations similar to those of Maheu [A-54]. Based on this work, AASHTO developed the Autostress Design method [A-56]. Autostress design provides a procedure to include longitudinal load redistribution in the design process.

Autostress design is applicable at two load levels: overload and maximum load. The same definitions of overload and maximum load as those of AASHTO LFD criteria are used. In this context, overload is defined as a serviceability limit state at which permanent deformations must not adversely affect rideability. This is achieved by limiting the maximum positive moment to 0.95 of the nominal yield moment for composite sections and 0.80 for non-composite sections. In contrast to the LFD criteria, Autostress design allows partial yielding to occur at the support under overload but a plastic hinge does not form. The maximum load check allows extensive moment redistribution. In fact, the Autostress design required slenderness ratios would permit sufficient plastic rotations at or above the plastic moment. Realizing that, under maximum load, sections which do not satisfy the slenderness limits can still rotate plastically albeit at reduced moments due to local buckling Autostress design allows plastic design of these sections if their flexural capacity is reduced accordingly.

Schilling [A-57] summarizes the results of experimental studies on steel ductilities. These studies resulted in a number of moment-rotation curves that give the relationship between the applied moment and the plastic rotation of simple and continuous steel beams. Schilling's curves give the

total plastic rotation over the finite length in which yielding occurs. Thus, the total plastic rotation is assumed to be concentrated in a small region representing an angular discontinuity, and the rest of the girder is otherwise assumed tn the elastic.

The curves that Schilling proposed were derived from experimental data which account for: "Steel yielding including the effect of residual stresses; the spread of the yielding along the length of the whole beam as the loading progresses; cracking or local crushing of the slab; permanent distortion of the cross sectional shape; and any other factors that cause permanent rotations". Different curves are proposed to cover composite and non-composite, compact and non-compact sections in positive and negative bending. It should be noted that Schilling's curves are valid for the whole length of the beam where each beam can have a maximum of one plastic hinge. To be used in a finite element analysis with multiple beam elements, moment versus curvature relationship will be extracted from Schilling's moment rotation curves. These moment curvature relationship will be used in this study in connection with the nonlinear analysis programs as will be explained in Appendix C.

The results of available experimental moment rotation curves are currently being corroborated by analytical studies such as the one performed by White et. al. [A-58]. In addition to the global behavior under bending, these studies account for local web and flange buckling in negative bending region.

This review shows that the nonlinear behavior of steel members involves the interaction of several complicated structural phenomena that are difficult to describe. On the other hand, available experimentally derived moment versus plastic rotation curves provide a description of the nonlinear behavior and ductility of steel bridge members that can be used in the analysis of the nonlinear behavior of steel bridge systems.

A-9 SYSTEM EFFECTS.

System capacity is defined as the capability of a bridge to carry heavy loads due to the interlocking of members into a complete system. This requires investigation of member performance and transverse as well as longitudinal load redistribution. To calculate this system capacity the nonlinear analysis of a bridge system is required. Many computer programs are available to perform the analysis of bridge systems. For example, reference [A-59] gives a list of some of these programs such as GENDER [A-60], CURVBRG [A-61] and MUPDI [A-62]. These programs, however, are specialized for the analysis of specific bridge types and are

capable of only performing linear elastic analysis.

Several researchers have also developed specialized programs to perform the nonlinear analysis of particular types of bridges [A-63 through 68]. In addition, commercial finite element packages can also be used for the nonlinear analysis of any structure and in particular for bridge structures [A-68 through 73].

The problem with such commercial packages especially for use in the nonlinear range is the complexity of the required input data and the specialized training required before an engineer becomes familiar with their use, capabilities and limitations. Nevertheless, several research studies have used such general purpose packages or specialized packages to study different aspects of the behavior of typical bridge configurations. These studies are classified under two types, the slab on beam types bridges and box bridges. The next sections present a summary of some of the findings on the behavior of such bridge types.

This section shows that many available commercial packages and programs developed by researchers can be used to study the behavior of typical bridge structures. These programs may not be practical for use in this study because: 1) they are either specialized and can be used only for the analysis of one particular type of structure; or 2) are difficult to use requiring complicated input data and advanced specialized learning curves.

A-10 BEHAVIOR OF SLAB ON BEAM BRIDGES

This section reviews the observations made by other researchers who performed analytical studies on the ultimate capacity of typical slab on beam type bridges. The purpose of this review is to help identify the important structural and geometric properties that affect the ultimate capacity of bridge systems. These properties will be used to determine the geometric configurations and the structural parameters that will be analyzed in this study.

No simplified method is currently available to consider nonlinear system effects in the design or evaluation of girder bridges. Even the autostress design method [A-56] considers bridges as combinations of individual continuous longitudinal members and the interaction of these members in two dimensions is not considered. Bridge systems provide considerable postelastic capacity as demonstrated by several analytical and experimental studies. The post elastic behavior of bridges utilizes both transverse and longitudinal redistribution of loads. Analytical

calculations [A-74] concluded that the elastic distribution factors of AASHTO or OHBDC are conservative and methods to calculate the distribution at ultimate were proposed as functions of the number of girders and the number of design lanes by Heins and Kuo [A-75]. In similar studies on the behavior of bridges at ultimate loads, it was found that the effective widths of slabs increased for the outside girders but decreased for the loaded interior girders immediately after yielding. Initial observations indicate that there normally is enough slab moment capacity to achieve complete transverse distribution of loads up to ultimate for both simple and continuous slab-girder bridges [A-54].

A parametric analysis of the transverse load distribution at ultimate limit states showed that it is affected by many factors including the position of the truck across the bridge, the number of lanes loaded, the level of loading and the dimensions of the bridge. Edge distance, bridge width, number of girders, girder spacing and the number of loaded girders have the most effect [A-54]. This analysis assumed that bridge failure is due to the formation of a collapse mechanism which assumes an infinite level of member ductility and also assumes that the slab remains in the linear elastic range.

Maheu [A-54] also reports that bridges with no composite action seem to provide lower capacity for transverse load distribution than composite bridges. While the contributions of the slabs are very important to the transverse distribution of the load, increased slab thickness has negligible beneficial effect on the transverse load distribution [A-54].

Experimental and analytical analysis of the behavior of reinforced concrete bridges at ultimate showed that support fixities, transverse load distribution and compressive membrane action contributed to the strength reserve of reinforced concrete bridges. Transverse distribution at ultimate was found to be limited by flexural yield capacity of the slab and diaphragms [A-76]. This seems to contradict the observation made by Maheu for the steel bridges he studied.

Kennedy et al. [A-77] developed a method for calculating collapse loads of continuous concrete bridges including prestressed bridges based on the orthotropic plate theory. Transverse distribution was found to be more effective as the bridge width to span ratio increases. The introduction of skews reduced the mid-span and support moments and improved the ultimate capacity.

In a parametric analysis of continuous skewed slab on steel girder bridges, Helba and Kennedy [A-78] observed that the effect of the skew on the ultimate capacity of continuous bridges is

negligible although it might be substantial for simple span bridges with low aspect ratio (length to width ratios).

Based on the observations reported in this section, it is concluded that the most important geometric parameters affecting the ultimate capacity of bridge systems are the number of girders, the girder spacings and the span lengths. Therefore, these factors should be included in this study on bridge redundancy. Other geometric factors such as support fixities, as well as the presence of skews improve the ultimate capacity of bridge systems.

The effect of slabs is extremely important to the ultimate capacity of bridge systems. However, their contributions are not sensitive to variations in the slab thickness. One study showed that flexural yielding in the slab might limit the transverse distribution at ultimate of concrete bridges. Therefore, the nonlinear behavior of the slab should be included although there was no mention that failure of slabs should be of concern. Maheu [A-54] observed that experimental results have shown that deck slabs possess much greater strengths than their flexural resistance would suggest and that failure of the slabs in the transverse direction is unlikely.

A-11 BEHAVIOR OF BOX GIRDER BRIDGES

The behavior of box girder bridges differs from that of I girder bridges because of the influence of the large torsional stiffness of hollow box members. The presence of this torsional stiffness creates an interaction between bending, shear and torsional stresses in the nonlinear range which is difficult to model using simple analysis methods. The best method to account for such behavior is through a three-dimensional finite element analysis. The finite element approach, however, requires refined structural models especially if a study of the nonlinear behavior is desired. This might explain the scarcity of studies on the nonlinear behavior of box girder type bridges. Hambly in reference [A-79] proposes an approximate method to model the global behavior of box type bridges as a combination of beam elements (grillage analysis). Although, he proposed his scheme for the linear elastic range, a sensitivity analysis performed for this project, as described in Appendix F, shows that this approach gives reasonable approximations in the nonlinear range as well.

Very few parametric studies on the behavior of box bridges are available. A notable exception is the work of Hand and Kostem [A-68] on the behavior of prestressed concrete spread box beam

bridges. Their study showed that the effect of warping in this type of bridges is negligible and that the torsional moments observed were low enough not to alter the dominant bending mode of failure. The authors also observed that spread box beam bridges exhibit significantly higher ultimate capacity than comparable I-beam bridges because of higher transverse distribution of the loads. However, if one looks at the ratio of the ultimate capacity to the member capacity using linear elastic methods, then one would observe that the box girder bridges would have lower reserve strength than comparable I-beam bridges. The ultimate capacity was not influenced by the lateral position of the load. In these studies a mechanism would not necessarily form since the analysis was stopped when crushing in the concrete was detected.

Choudhury [A-66] and Seible [A-44] in their nonlinear analyses of prestressed and reinforced concrete box girder bridges observed that "depending on the structure and the loading", distortional effects in the cross section can influence the structural behavior of box bridges significantly. They do not, however, provide guidelines as to which actual bridge loading and geometric conditions are most critical. Siddiqui [A-80] has, however, shown that the installation of rigid diaphragms along the span can effectively control the distortional stresses.

More complete parametric analyses are available in the linear elastic range. For example, according to Wallace [A-81], span length and skew angle were found to be the most significant parameters influencing girder shear distribution. While the aspect ratio and skew angle affected longitudinal bending moments. The number of cells and the depth of the box were not found to be important factors.

Chapman [A-82] noted that distortional stresses occur under symmetrical loading if the bridge is skewed or curved or in multi-cell sections. He emphasized the importance of providing adequate restraints against distortion of the cross section especially in steel boxes. In general, it has been found that steel box girder bridges did not provide much redundancy because these bridges always have noncompact sections [A-83].

In summary, the review of studies on box girder bridges shows the importance of their high torsional capacity on their behavior. For practical applications, the effect of warping can be ignored because of the presence of end diaphragms. Therefore, modelling the torsional stiffness is sufficient to describe the behavior of typical box girder bridges in the nonlinear range.

A-12 EXPERIMENTAL INVESTIGATIONS OF BRIDGE SYSTEMS

In recent years, testing of bridges under service loads have been routinely used to verify design assumptions or for the load capacity evaluation of existing bridges. Very little information is however available on full-scale testing of bridges under overloads or for determining their ultimate load-carrying capacity.

The best known full-scale load studies beyond the elastic limits are those performed at the University of Illinois more than four decades ago [A-84] and those performed by Burdette and Goodpasture [A-85] more than two decades ago. In addition, Buckle [A-76] et. al. summarize the results of three reinforced concrete T-beam bridges loaded until failure. The set of steel bridges tested at the University of Illinois were loaded beyond the elastic limits but were not loaded to failure. The other series of tests consisted of steel and concrete (including one prestressed concrete I-beam bridge) that were loaded to reach their ultimate capacities. Recently, Bakht and Jaeger [A-86] reported on the testing of one noncomposite simply supported 6-girder steel bridge. Some additional field tests on slab bridges were performed but these are not of direct interest to this research project. West and McClure [A-87] report on the full scale testing of a prestressed concrete segmental bridge. This seems to be the only known field test on full scale box-girder type bridges.

These full scale field tests were used by many researchers to verify their bridge analysis models and to verify the accuracy of their programs. Burdette, and Goodpasture [A-88] as well as Bakht and Jaeger [A-86], however, caution against the blind use of bridge test results because the field conditions may not be known exactly. For example, although the boundary conditions may be designed as simple supports, it was often observed that they acted semi-rigidly producing some fixities which substantially increase the ultimate load carrying capacities of the tested bridges. Other uncertainties are due to material properties, residual stresses, unintended composite action, unknown dead loads, contributions of secondary members etc. In fact, Bakht [A-86] reports that the measured ultimate capacity of the bridge he tested was more than 30% higher than his estimates.

Because of the above-mentioned uncertainties and the costs involved in executing full scale field tests on actual bridges, many researchers prefer to perform laboratory tests on model scale bridges. For example, Soliman and Kennedy [A-89] report on model tests on two composite simply-supported and two continuous two-span composite bridges. Other model tests are also

reported by Kennedy et al. [A-90]. Scordelis and his co-workers [A-91] performed ultimate load tests on three multicell reinforced concrete bridge models. Mirza et. al. [A-92] report on 1/7 scale models of one-cell and two-cell prestressed concrete box girder bridges that were tested at McGill University in Canada. Also in Canada, Thimshardy [A-93] reports on failure tests on large cantilever steel box girder models. The use of these tests results to verify computer programs and modeling techniques may be easier than the use of full scale field tests because laboratory tests are normally better controlled and provide fewer uncertainties. However, the scale effect should not be ignored because factors that may be important in model tests may not be as important in full scale bridges and vice versa.

A-13 SINGLE BEAM TESTS

To supplement the limited data available from full scale as well as model scale bridge tests, it is often desirable to verify the accuracy of computer programs by comparing their results to those of laboratory tests of individual beams. Many such laboratory test results are available in the literature. For example, Rabbat et. al. [A-94] performed an extensive experimental investigation to determine the behavior and strength of prestressed concrete girders with draped and blanketed strands after subjecting them to repetitive loading.

The same girders were then tested to destruction under static load. Rabbat et. al. observed that the ultimate strength capacity was not affected by the cyclic loading if the repetitive loading did not cause fatigue cracking in the tendons. This was true for both the blanketed and the draped specimens. Plots showing the applied load versus maximum deflection for the static tests were given in reference [A-94].

Hawkins, Sozen and Siess [A-95] give the results of 22 tests of two-span continuous pre-tensioned prestressed concrete beams. They plotted load deflection curves for two tested specimens. The two specimens were quite similar except for the amount of longitudinal steel reinforcement. The behavior of the specimens under static load tests was monitored until failure.

The classical theory for the analysis and design of beams under shear were based on many tests such the ones performed by Leonhardt and Walther [A-96] on prestressed box girders. Edwards [A-97] tested a large scale single cell prestressed box beam under combined transverse and longitudinal bending and shear. Yen and Chen [A-98] also tested large specimens of composite

steel box girders to failure. These as well as other similar tests could be used to verify some of the modelling assumptions used in the preparation of nonlinear analysis programs and to provide bench-mark tests to verify the validity of these programs for combined bending and shear actions in the nonlinear range [A-99,100,101] and for the combined effect of bending and torsion in the linear range [A-102] or the nonlinear range [A-51].

A-14 LIMIT STATES

One important issue in the description of structure capacity, especially in the context of redundancy criteria, is the definition of the limit states. Current design methods [A-2] utilize a linear elastic analysis to determine component forces. Failure occurs when these linearly derived member forces exceed member capacity. This approach to component checking is utilized even when member capacity is attained after extensive nonlinear plastification.

In addition to verifying strength capacity, member serviceability conditions are also checked. These include deflections, cracking where appropriate, and fatigue stresses.

Failure of a structural system in the present context of redundancy occurs when the structure is no longer capable of carrying any additional load. This is defined as its ultimate capacity. Associated with this load will be a very large or infinite displacement and is usually followed by unloading. However, it often observed that a structure may cease to function effectively even at load levels below the ultimate load. These other limiting states are often called large deflection serviceability limit states [A-108].

Although primarily concerned with serviceability of building structures, many of the observations in reference [A-108] are valid for bridges. For example, reference [A-108] defines a serviceability limit state as ".. the condition in which the function of the structure is disrupted because of excessive deflection, human discomfort, impaired function of the structure or damage..." Reference [A-108] notes that in contrast to a collapse limit state the large deflection unserviceability limit may be difficult to define. In fact, unserviceability may be a continuum starting from a limit with unsightly displacements ranging all the way to a situation where occupants refuse to stay in the structure and may in the case of a traffic situation lead to accidents. For example Kulicki et al [A-4] define collapse as " a major change in the geometry

of the bridge structure rendering unfit for use". Such a definition seems to indirectly associate the subjective concept of serviceability to the seemingly better defined concept of collapse.

For buildings, reference [A-108] notes that the lateral deflections at a ratio of 1/300 of the height is clearly visible and causes minor damages while deflections of 1/100 to 1/200 may cause impaired operations of moveable components. Galambos, et. al [A-9] used similar observations to recommend a serviceability limit state for bridge structures of span/300 for bridges designed or rated using nonlinear analysis. This deflection criteria is in addition to any existing serviceability criteria as mentioned above which is to reduce cracking, fatigue effects or possible visual related deflections under working loads.

Daniels, et al. [A-11] also recommends a serviceability deflection limit. Although he suggested that it be left to the evaluator, in his examples he uses limits of the order of 1/300 to 1/200. Similar limits were used by researchers involved in bridge testing. For example, Bakht, et al. [A-86] stopped a load test in Ontario when the maximum deflection reached 1/125 of the span length "because this deflection limit was believed to be compatible with the ultimate capacity of the bridge". It is interesting to note that even at this displacement the external girder away from the loading had almost zero deflections indicating that a true plastic hinge mechanism for the system had not yet really formed,

Similarly, because of the perception of imminent failure, the load tests performed at the University of Illinois were stopped at deflection levels on the order of 1/150 of the span length [A-84]. For concrete bridges, the ultimate capacity occurs at the load level at which concrete crushing occurs [A-85].

In summary, it is herein concluded that to verify the safety and the utility of a bridge structure, it is important to check its ultimate capacity and a large deflection system serviceability limit state. Ultimate capacity is attained when a mechanism forms or when unloading commences. Based on the above discussion, the most suitable large deflection system serviceability criteria should be based on span length. In Phase I, the criterion selected was span/200 other possible criteria used in this study include a span/100 limit. As mentioned earlier, these values seem to be similar to the values at which full-scale bridge test were stopped because of "fear of catastrophic structural failures" although actual collapse was never reported.

In addition to ultimate and system serviceability for the intact bridge system, a loss of member capacity due to accident scenarios is also used herein for the redundancy criteria. Bridge members may be subject to fatigue and fracture as well as corrosion, fire or accidental collisions by trucks, ships or debris which could lead to member loss. To ensure the safety of the public, the redundancy criteria recommended herein consider that bridges should be able to sustain and survive such likely accidental member losses and still operate albeit at reduced strength capacity. Therefore, in Phase I, the redundancy analysis examined the consequences of selected critical member failures and computed the remaining ultimate capacities.

A-15 SUMMARY

The review of the available literature revealed that although recognized as an important component of structural safety, the concept of redundancy has not been fully defined. Efforts for including redundancy in the design and evaluation of structural systems are underway in several structural applications but full implementation in structural codes and specifications are not yet available.

The observations made in this Appendix indicate that most previous studies on bridge systems produced qualitative assessments of system effects. This was not sufficient for the purposes of this study which requires a quantitative assessment of the system effects in order to evaluate the redundancy of common type steel and prestressed concrete bridges. The literature review showed that the deck slab was the most important contributor to the transverse distribution of loads in slabs on I-beam type bridges especially for intact bridges. The behavior of damaged bridges or bridges subjected to partial member failures or cracked members may be more sensitive to the presence of diaphragms.

Several studies verified that modeling the bridge as a grid system was sufficiently accurate to represent the transverse distribution due to the effect of the slab and diaphragms. A grid model does not completely describe the full behavior of the slab because it ignores the effects of membrane action and other factors due to two-dimensional elasticity. The grid model can still be used in this study which is mainly concerned with the global behavior of the superstructure i.e. in studying the distribution of the moment in the main longitudinal members.

The nonlinear bending behavior of the longitudinal bending members as well as the slab and transverse members can be modelled using moment versus rotation curves obtained based on semi-empirical models for concrete members and based on experimentally derived curves for steel members.

Using a grid (grillage) model for the analysis of box girder type bridges is possible if the torsional properties of the bridge are taken into account. The inclusion of shear nonlinearity in the analysis of bridges is possible. However, available models for estimating the shear strength capacity seem to be overly conservative. This provides safe models for design but will not produce accurate estimates of the ultimate capacity of existing structures.

The validity of any model or program for the analysis of bridges should be verified by comparing its results to those of laboratory and full scale field tests of single beams as well as complete bridge systems. However, care should be taken when performing such comparisons because experimental data on ultimate capacity of actual bridges is scarce and in many cases actual field conditions may not be known exactly. This may explain the difficulties often encountered when using field data for checking analytical studies.

REFERENCES

A-1 ASCE-AASHTO Task Committee, "State of the Art Report on Redundant Bridge Systems", ASCE Journal of Structural Engineering, Vol. lll,No. 12,December 1985.

A-2 Standard Specifications for Highway Bridges, 1996, AASHTO,Washington DC.

A-3 Ontario Highway Bridge Design Code, 1983, Ontario Ministry of Transportation and Communications.Toronto, Ontario, CANADA.

A-4 Kulicki, J.M., "Development of Comprehensive Bridge Specification and Commentary", NCHRP 12-33, Draft Report, March 1993 .

AASHTO LRFD Bridge Design Specifications, 1994, AASHTO, Washington DC.

A-5 Moses, F. and Verma, D., December 1987, "Load Capacity Evaluation of Existing Bridges", NCHRP Report 301.TRB. Washinqton D.C.

A-6 Moses, F., Schilling, C.G. and Raju, K.S., November 1987,"Fatigue Evaluation Procedures for Steel Bridges", NCHRP Report 299. TRB.Washington D.C.

A-7 Haaijer, G., Carskaddan, P.S. and Grubb, M.A., "Autostress Design of Steel Bridges", Journal of Structural Engineering, ASCE,Vol. 109, No. 12, Jan. 1983.

A-8 "Guide Specifications for Fracture Critical Non-Redundant Steel Bridqe Members", AASHTO, Washington DC, Sept. 1978.

A-9 Galambos, T.V., Leon T.R. and French C.W., 1992, "Inelastic Rating Procedures for Steel Beam and Girder Bridges", NCHRP project 12-28(12), TRB, Washington D.C.

A-10 Frangopol; D. and Nakib R. "Effects of Damage and Redundancy on the Safety of Existing Bridges", Third Bridge Engineering Conference, TRB 1290. Denver, Colorado, March, 1991

A-11 Daniels, J.H., Kim, W. and Wilson, J.L., "Guidelines for Redundancy Design and Rating of Two-Girder Steel Bridges", NCHRP 12-28 (10), November, 1988.

A-12 Purvis, R.L., Graber, D.R., Albrecht, P. and Flournoy, T.S., "Inspection of Fracture Critical Bridge Members", FHWA IP-86-26,Sept., 1986.

A-13 Sandberg, H.R. and Parmelee, R.A., "Redundancy by Design Its Implications", Third Annual International Bridge Conference,Pittsburgh, Pennsylvania, June 1986.

A-14 Gromala, D.S., "System Factors in LRFD Format: A Multidimensional Judgment Call", Structural Engineering in Natural Hazards, ASCE Structures Congress, Irvine, California, April 1993.

A-15 Matousek, M., "Safety Plans for Buildings, Structures and Technical Facilities", Structural Safety and Reliability, Proceedings of ICOSSAR'89, San Francisco, CA, August 1989.

A-16 Moses, F., "Load and Resistance Factor Format for Design of Fixed Offshore Platforms", API-RP2A, 1989.

A-17 De, R.S., Karamchandani, A. and Cornell, C.A., "Study of Redundancy of near-ideal Parallel Structural Systems, Proceedinqs of ICOSSAR'89, San Francisco, CA, Aug., 1989.

A-18 Galambos, T.V., "Systems Reliability and Structural Design", International Workshop on Structural System Reliability, Boulder, Colorado, Sept. 1988.

A-19 Nowak, A.S., "Calibration of LRFD Bridge Design CodeH NCHRP project 12-33, May 1992.

A-20 Moses, F. and Ghosn, M., "A Comprehensive Study of Bridge Loads and Reliability", Report FHWA/ODOT/ 85-005, 1985.

A-21 Thoft-Christensen, P., and Baker, M.J., Structural Reliability Theory and itR Applications, Springer-Verlag, New York, 1982.

A-22 Cornell, C.A., "Some Thoughts on System and Structural Reliability", Nuclear Engineering and Design, Vol. 71, 1982.

A-23 Bennett, R.M., and Ang, H.S., "Formulations of Structural System Reliability", ASCE Journal of the Engineering Mechanics Division, Nov. 1986.

A-24 Gorman, M.R., and Moses, F., "Reliability of Structural Systems", Report 79.2, Civil Engineering Department, Case Western Reserve University, Ohio, May,1979

A-25 Moses, F., "System Reliability Developments", Journal of Structural Safety, Vol.1, No.1, 1982.

A-26 Tabsh S.W. and Nowak A.S., "Reliability of Highway Girder Bridges", ASCE Journal of Structural Engineering, Vol. 117, No. 8, August 1991.

A-27 Arwashan, N., "Structural Systems Reliability of Girder Bridges", Department of Civil Engineering, The University of Michiqan, Ann Arbor, MI, 1992.

A-28 Ghosn, M., Moses F., and Khedekar, N., "Response Functions and System Reliability of Bridges" IUTAM Symposium on Advances in Structural Reliability, San Antonio, TX, April, 1993.

A-29 Verma, D., and Moses F., "Efficient Structural System Reliability Assessment by Monte Carlo Methods", Proceedings of ICOSSAR'89, San Francisco, CA, August, 1989.

A-30 Cornell, C.A., "Risk-Based Structural Design", Proceedings of a Symposium on Risk Analysis, Department of Civil Engineering, University of Michigan, Ann Arbor, MI,August, 1994.

A-31 Heins C.P. and Kato H., "Load Redistribution of Cracked Girders", ASCE Journal of Structural Engineering, Vol. 108, No. ST8, August 1982.

A-32 Idriss, R.L., White, K.R., and Jauregui, D.V., "AfterFracture Response of a Two-Girder Steel Bridge", Structural Engineering in Natural Hazards, ASCE Structures Congress, Irvine, CA, 1993.

A-33 Abendroth, R.E., Klaiber, F.W. and Shafer, M.W., "Lateral Load Resistance of Diaphragms in Prestressed Concrete Girder Bridqes", Report to Iowa DOT, Project HR-319, December 1991.

A-34 Nilson, A.H., Design of Prestressed Concrete, Wiley and Sons, New York, 1987.

A-35 Park, R. and Ruitong, D. "Ductility of Doubly Reinforced Concrete Beam sections", ACI Structural Journal March -April 1988.

A-36 Park, R. and Pauley, T., Reinforced Concrete Structures, Wiley and Sons, New York, 1975.

A-37 Skogman B.C., Tadros M.K., and Grasmick R., "Ductility of Reinforced and Prestressed Concrete Flexural Members", PCI Journal, December 1988 .

A-38 Naaman, A. "An Approximate Nonlinear Design Procedure for Partially Prestressed Concrete Beams", Computers and Structures, Vol. 17, No. 2, 1983.

A-39 Naaman, A.E., Harajali, M.H., and Wight, J.K., "Analysis of Ductility in Partially Prestressed Concrete Flexural Members", PCI Journal, V. 31, No. 3, May-June 1986.

A-40 Mattock, A.,H., "Rotational Capacity of Hinging Reglon ln Reinforced Concrete Beams", Int. Symp. on Flexural Mechanics of Reinforced Concrete, PCA,Miami,FL, 1964.

A-41 Joint ACI, ASCE Task Committee 426, "The Shear Strength of Reinforced Concrete Members", ASCE Journal of the structural Division, Vol. 99, No. ST6., June, 1973.

A-42. Kim, W., and White, R.N., "Initiation of Shear Cracking in Reinforced Concrete Beams with no Web Reinforcement", ACI Structural Journal, V. 88, No. 3, May-June 1991.

A-43 Leonhardt, F. and Walther R. "The Stuttgart Shear Tests, 1961", Cement and Concrete Association, No. 111, London, 1962.

A-44 Seibel, F., "Nonlinear Analysis and Ultimate Strength of Multi-Cell Reinforced Concrete Box Girder Bridges", UCB/SESM82/02, Department of Civil Engineering, University of California at Berkeley, Berkeley, CA, 1982.

A-45 Zsutty, T.C., "Shear Strength Prediction for Separate Categories of Simple Beam Tests", ACI Journal, V. 68, No. 2, Feb. 1971

A-46 Bazant, Z, P. and Ozbolt, J., and Eligehausen, R.,"Fracture Size Effect: 1. Review of Evidence for Concrete Structures", ASCE Journal of Structural Engineering, 1992.

A-47 Hall, R.T., Discussion on: "Shear Strength of HighStrength Concrete Beams with Web Reinforcement, ACI Structural Journal, V. 87, No. 2, March-April, 1990.

A-48 Roller, J.J. and Russell, H.G., "Shear Strength of HighStrength Concrete Beams with Web Reinforcement, ACI Structural Journal, V. 87, No. 2, March-April, 1990.

A-49 Moody, K.G., Viest,I.M., Elstner,R.C., and Hognestad, E., "Shear Strength of Reinforced Concrete Beams. Part I -Tests of Simple Beams", ACI Journal, V. 51, No. 4,Dec. 1954.

A-50 Roman, G., Rosati, L., and Ferro, G., "Shear Deformability of thin walled-beams with Arbitrary Cross Sections", International Journal for Numerical Methods in Engineering, V. 35, No. 2, Aug. 1992.

A-51 Leonhardt, F., "Effort Tranchant et Torsion en Beton Precontraint",Annales de L'Institut Technique du Batiment et des Travaux Publics,No. 280, Serie Beton Precontraint No. 73, Avril 1971.

A-52 Falkner, H., Teutsch, M. and Huang, Z., "Torsion-BendingShear in Segmental Beams with Unbonded Tendons", Beton und Stahlbetonbau, V.88, No. 7, Jul. 1993.

A-53 Yura, J.A., Galambos, T.V. and Ravindra, M.K., "The Bending Resistance of Steel Beams", ASCE Journal of the Structural Division, Vol. 104,No.ST9,1978.

A-54 Maheu J.M, "Redistribution of Moments in Slab on Girder Bridges", Ontario Ministry of Transportation.

A-55 Carskaddan, P.S., Haaijer, G., and Grubb, M.A.,Computing the Effective Plastic Moment", Engineering Journal, AISC, Vol. 19, No. 1 1982.

A-56 Grubb, M.A., "The AASHTO Guide Specifications for Alternate Load-Factor Design Procedures for Steel Beam Bridges", Engineering Journal, AISC, Vol. 2, No. 1, 1987.

A-57 Schilling, C.G., "A Unified Autostress Method", Report 51,American Iron and Steel Institute, November 1989.

A-58 White, D.W. and Dutta, A., "Numerical Studies of MomentRotation Behavior in Steel Bridge Girders", Conference of the Structural Stability Research Council, St. Louis, MO, April, 1990

A-59 Zokaie, T., Osterkamp, T.A., Imbsen, R.A., "Distribution of Wheel Loads on Highway Bridges", NCHRP project 12-26, TRB, Washington DC,March 1991.

A-60 Pail, G.H., and Buckle I.G., "Computer Programs for Bridge Deck Analysis", Report No. UC SESM 70-6, University of California, Berkeley, April, 1970.

A-61 Mondkar, D.P., and Pail, G.B., "CURVBRG-A Computer Program for Analysis of Curved Open Girder Bridges", Report No. UC SESM 74-17, University of California, Berkeley, December, 1974.

A-62 Lin, C.S., and Scordelis, A.C., "Computer Program for Bridges on Flexible Bents", Report, No. UC SESM 71-24, University of California, Berkeley, December, 1971.

A-63 Peterson, W.S., and Kostem, C.N., "User's Manual for Program BOVA", Fritz Engineering Laboratory Report No. 378B.6A, Lehigh Univ., Bethlehem, PA, 1975.

A-64 Hall, J.C., and Kostem, C.N., "User's Manual for Program BOVAS", Fritz Engineering Laboratory Report No. 435.3A, Lehigh Univ., Bethlehem, PA. 1981.

A-65 Idriss, R.L. and White, K.R., "Secondary Load Paths in Bridge Systems",Transportation Research Records No. 1290., TRB Bridge Engineering Conference March 1991.

A-66 Choudhury, D., "Analysis of Curved Nonprismatic Reinforced and Prestressed Concrete Box Girder Bridges", Report No. UCB/SEMM-86/13, Department of Civil Engineering, University of California, Berkeley, CA, December 1986.

A-67 Scordelis, A.C., "Berkeley Computer Programs for the Analysis of Concrete Box Girder Bridges", Department of Civil Engineering,Division of Structural Engineering, University of California,Berkeley, CA.

A-68 Hand, T. and Rostem, C.N., "Inelastic Analysis of Prestressed Concrete Spread Box-Beam Bridges", Fritz Engineering Laboratory Report No. 432.8,Lehigh University, Bethlehem, PA, Oct. 1984.

A-69 Lopez, L.A., Rehak, D.R., Dodds, R.H., and Schmidt, R.J.,"POLO-FINITE, A Structural Mechanics System for Linear and Nonlinear, Static and Dynamic Analysis, Civil Engineering Systems Laboratory, University of Illinois at UrbanaChampaign.

A-70 Hibbitt, H.D., Karlsson, B.I., and Sorenson, J., "ABAQUS general purpose finite element code", Hibbitt, Karlsson and Sorensen Inc.Providence, R.I.

A-71 Helba, A. and Kennedy, J.B., "Collapse Loads of Continuous Skew Composite Bridges", ASCE Journal of Structural Engineering, Vol. 120, No. 5, May, 1994.

A-72 "NONSAP User Manual", Structural Mechanics Computer Laboratory,University of Southern California, Jan., 1981.

A-73 Hallquist, J.O., "DYNA3D User's Manual (Nonlinear Dynamic Analysis of Structures in Three Dimensions", Lawrence Livermore National Laboratory, April, 1988.

A-74 Razaqpur, A.G., and Nofal, M., "Transverse Load Distribution at Ultimate Limit States in Single Span Slab-OnGirder Bridges with Compact Steel Sections",Ontario Ministry of Transportation, MISC 88-01,September 1988.

A-75 Heins, C.P., and Kuo, T.C., "Ultimate Live Load Distribution Factors for Bridges", ASCE, Journal of Structural Engineering, Vol. 101, 1975.

A-76 Buckle, I.G. and Dickson A.R. and Phillips M.H., Ultimate Strength of Three Reinforced Concrete Highway Bridges", Canadian Journal of Civil of Civil Engineering, Vol. 12, 1985.

A-77 Kennedy, J.B., and El-Sebakhy, I.S., "Collapse Loads of Continuous Orthotropic Bridges", ASCE Journal of Structural Engineering, Vol. 111, No. 8, August, 1985.

A-78 Helba, A. and Kennedy, J.B., "Parametric Study on the Collapse Loads of Skew Composite Bridges", ASCE Journal of Structural Engineering, Vol. 120, No. 5, May, 1995.

A-79 Hambly, E.,C., "Bridge Deck Behavior", Chapman and Hall, London, 1976.

A-80 Siddiqui, A.H., "Effects of Diaphragms on Stress Reduction in Box Girder Bridge Sections", Canadian Journal of Civil Engineering", Vol. 15, No.1, Feb. 1988.

A-81 Wallace, M.R., "Studies of Skewed Concrete Box-Girder Bridges",Transp. Res. Record No. 607, TRB, 1976.

A-82 Chapman, J.C., "The Structural Behavior of Steel and Concrete Box Girder Bridges", Structural Engineer, Vol. 49, No. 3, 1971.

A-83 "Steel Box-Girder Bridges: Ultimate Strength Considerations",ASCE Journal of Structural Engineering, vol. 100, No. ST12, December 1974.

A-84 Siess, C.P. and Viest I.M., "Tests of Continuous Right IBeam Bridges" Engineering Experiment Station Bulletin 416, University of Illinois at Urbana-Champaign, Urbana, Ill., 1953.

A-85 Burdette, E.G., and Goodpasture, D.W., "Tests of Four Highway Bridges to Failure", ASCE Journal of the Structural Division, vol. 99, No. ST3, March 1973.

A-86 Bakht, B., Jaeger, L.G., "Ultimate Load Test of Slab-onGirder Bridge", ASCE Journal of Structural Engineering, Vol. 118, No. 6, June 1992.

A-87 West, H., and McClure, R.M., "Full Scale Testing of a Prestressed Concrete Segmental Bridge", International Conference on Short and Medium Span Bridges, Toronto, 1982.

A-88 Burdette, E.G., and Goodpasture, D.W., "Correlation of Bridge Load Capacity Estimates with Test Data", NCHRP report No. 306, Transp.Res. Board, Washington DC 1988.

A-89 Soliman. M. and Kennedy, J.B., "Load Distribution in Composite Bridges at the Ultimate Limit State", IABSE Conference on Development in Short and Medium Span Bridge Engineering, Toronto, 1990.

A-90 Kennedy, J.B and Grace, N.F. "Prestressed Continuous Composite Bridges under Dynamic Load", ASCE Journal of Structural Engineering, Vol. 116, No. 6,June 1990.

A-91 Scordelis, A.C., Bouwkamp, J.G., and Wasti, S.T., "Structural Behavior of a Two Span Reinforced Concrete Box Girder Bridge Model",Vols. 1,2 and 3, Report Nos. UC SESM, 715, 71-6, 71-7, University of California, Berkeley, CA, 1971.

A-92 Mirza, S.M., et al. "Experimental Study of Static and Dynamic Response of Prestressed Concrete Box Girder Bridges", Canadian Journal of Civil Engineering, V. 17, No. 3, June 1990.

A-93 Thimmhardy, E., "Experimental Investigation of Buckling Strength of Steel Box Girder Bridges", ASCE Conference on Experimental Assessment of Performance of Bridges, Boston, MA, Oct. 1986.

A-94 Rabbat, B.G., Kaar,P.H., Russell H.G. and Bruce Jr., R.N., "Fatigue Tests of Full-Size Prestressed Girders", State of Louisiana Technical Report No. 113, June 1978.

A-95 Hawkins, N.H., Sozen, M.A., and Siess C.P., "Behavior of Continuous Prestressed Concrete Beams"

A-96 Leonhardt, F. and Walther, R., "Torsion and Shear Tests on Prestressed Box Girders", Cement and Concrete Association, (Translation), No. 130,London, 1968.

A-97 Edwards, A.D., "Structural Behavior of a Prestressed Box Beam with Thin Webs under Combined Bending and Shear", Proceedings of Institution of Civil Engineers, Vol. 63, England, 1977.

A-98 Yen, B.T., and Chen, Y.S., "Testing of Large Size Composite Box Girders", Fritz Engineering Laboratory Report, Lehigh University, Report FHWA-PA 82-010, Lehigh, PA, 1982.

A-99 Lopez, A.,R., "Estudio de la Evolucion hasta la Rotura de Tableros Continos de Puentes de Hormigon Pretensado de Planta Curva o Esviada", Universidad Politecnica de Cataluna, Escuela Tecnica Superior de Ingenieros de Caminos, Canales y Puertos,Barcelona, Spain, 1987.

A-100 Serrano, T.B., "Ensayo a Rotura por Esfuerzo Cortante de Vigasen T parcialmente Pretensadas", Hormigon y Acero, Asociacion Tecnica Espanola del Pretensado, No. 143, Spain, 1981

A-101 Serra, I.M. and Mari, A.B. and Lopez, F.A., "Estudio Experimental del Comportamiento de Vigas de Hormigon Armado Descimbradas a Tempranas Edades", Hormigon y Acero, Asociacion Tecnica Espanola del Pretensado, Spain, 1993.

A-102 Calgaro, J.A., and Virlogeux, M. "Projet et Construction des Ponts: Analyse Structurale des Tabliers de Ponts",Presse de L'Ecole Nationale des Ponts et Chaussees, Paris 1 988.

A-103 Soliman, M.I., and Ghali,M.K., "Effect of Diaphragms on the Behavior of R.C. Box Girder Bridges", Fourth International Conference on Short and Medium Span Bridges, CSCE, Halifax, Nova Scotia, CA, Aug.1994.

A-104 Nawy, E.G., Prestressed Concrete: A Fundamental Approach, Prentice Hall, New York.

A-105 US Steel Highway Bridge Manual, US Steel, Pittsburgh, PA.

A-106 Huckelbridge A.A., El-Esnawi, H. and Moses, F., "An Investigation of Load Transfer in Mulit-Beam Prestressed Box Girder Bridges", Report No. FHWA/OH-94/002.

A-107 Wegmuller, A.W., "Overload Behavior of Composite Stee-Concrete Bridges", ASCE Journal of the Structural Division, Vol. 103, No. ST9, Sept. 1977.

A-108 Ad Hoc Commitee on Serviceability Research, "Structural Serviceability: A Critical Appraisal and Research Needs", ASCE Journal of Structural Engineering, Vol. 112, No.2, December, 1986.

A-109 Stallings, J.M., Cousins, T.E., Stafford, T.E. "Effects of Removing Diaphragms from a Steel Girder Bridge", TRB Congress, Washington DC, Jan. 1996.

APPENDIX B

RELIABILITY AND REDUNDANCY OF PRESTRESSED CONCRETE I-BEAM BRIDGES

This appendix gives a detailed discussion on the findings made in this study on the redundancy of prestressed concrete I-beam bridges. The observations made herein are based on the results of the nonlinear analysis of over hundred-fifty bridge configurations designed to satisfy the AASHTO LFD specifications. In addition to analyzing these different basic configurations, a sensitivity analysis is performed to study the effect of various design and analysis assumptions.

This appendix is divided into six sections. Section 1 describes the structural model used in association with NONBAN to analyze the prestressed concrete I-beam bridges. In Section 2, the modeling procedure proposed in Section 1 is verified by comparing the results obtained by NONBAN to the results of field tests on two full-scale prestressed concrete I-beam bridges. Section 3, describes the bridges that are designed for the purposes of this study. This section also gives the assumptions made during the design of these bridges. Section 4, summarizes the results of the nonlinear analysis performed for the bridges described in Section 3. The nonlinear analysis is performed using NONBAN and the bridges are discretized using the procedure described in Section 1. Results of the sensitivity analysis are presented in Section 5. Section 6 presents the results of the reliability analysis and the calibration of the redundancy factors.

B-1. Modeling of Prestressed Concrete I-Beam Bridges.

In this study, the behavior of prestressed concrete I-beam bridges is analyzed using the Nonlinear Bridge Analysis program NONBAN. As mentioned in Appendix F, the program NONBAN uses a modified grillage analysis method to study the nonlinear behavior of typical bridge configurations. The validity of the program was verified by comparing its results to the published results of various beams, bridge models and full scale bridge tests and theoretical analyses. This section describes the structural model adopted in this study to analyze a typical prestressed concrete I-beam bridge using NONBAN.

B-1.1 Mesh Discretization

To use NONBAN, the bridge superstructure is discretized as longitudinal and transverse beam elements laying in the plane of the superstructure. This discretization procedure is typical

for the grillage analysis method as described in several references on structural analysis including the references by West, Jaegar, Bakht, Hambly or Zokaie et. al. which specifically address the modeling of bridge superstructures [B-1,2,3,4].

The discretization procedure used in this study follows the recommendations made by Zokaie, Osterkamp and Imbsen [B-4] for discretizing a bridge superstructure into equivalent longitudinal and transverse members. The recommendations of [B-4] were subsequently adapted in the AASHTO LRFD specifications [B-9]. Specifically, these recommendations stipulate that longitudinal members are placed along girder centerlines. The longitudinal members' properties are taken to be those of the composite deck-member cross section if the beam is designed for composite action. For bridges that are built for non-composite action, longitudinal member properties are those of the girder alone. Thus, for noncomposite sections, the slab will act as a one way slab such that its contribution is only to the transverse distribution of the load without any contributions in the longitudinal direction.

The contributing slab width for composite sections is taken to be half the girder spacing on each side of the girder. For the case of very wide spacings, Zokaie et al [B-4] recommend that the shear lag effect be considered. They do not however, specify how this should be carried out, neither do they specify which spacings should be considered wide. To remain on the conservative side, this study uses the procedure proposed in the AASHTO specifications to determine the effective flange width of composite sections. In this sense, the effective flange width of a composite section is taken to be the minimum of half the girder spacing between adjacent beams, or one third the span length, or twelve times the slab thickness plus the width of the girder. 1/2 the beam spacing governs for most of the cases studied in this appendix. For the few cases where the 1/2 beam spacing did not govern, a sensitivity analysis has shown that the effect of using different effective flange widths did not affect the final conclusions of this study.

For the edge beams, reference [B-4] recommends to"use judgment" to determine how to account for the effect of compositely designed curbs and parapets. For the purposes of this study, the effect of curbs and parapets is generally ignored except for the specific cases where a comparison between field test results and analytical results warrant their consideration. In the cases where the effect of the curbs and parapets is not known, and to partially account for their contributions, the longitudinal edge beams of a bridge are assumed to have the same moment capacities as the interior beams even if the effective flange width is actually smaller.

In a grillage analogy, transverse beams are used to represent the contribution of the slab and diaphragms to the transverse distribution of the load. Zokaie et al. [B-4] recommend to use transverse beam spacings equal to about 1/10 of the effective span length to account for the slab's contribution in the transverse direction. This span/10 division of the girder is generally followed in this study. In addition, to the beams representing the effect of the slab, a transverse beam must be applied wherever a diaphragm exists. Properties of the transverse beams representing the deck slab are taken to be the properties of the tributary section of the deck slab. In the case where the diaphragm acts compositely with the deck, the properties of the composite section

must be used. Otherwise, transverse beams representing the diaphragms are used independently of the beams representing the slab contribution.

This proposed modeling technique which uses beam elements to model the behavior of bridge superstructures including their deck slabs, ignores the effects of membrane action and arching of the slab. Therefore, the proposed scheme may not be accurate enough to analyze possible failures in the deck slab itself. On the other hand, Zokaie et al. [B-4] as well as Hambly [B-3] suggest that a grillage model may be conservatively used for the analysis of a bridge slab for design purposes. This, however, would require that the slab be discretized as an extremely fine grid of longitudinal and transverse beam elements. This project is concerned with the behavior of the main members of the superstructure and the analysis of the behavior of deck slabs is beyond the scope of this study. Therefore, an exact modeling of the deck slab is not carried out in this analysis. Despite the stated limitations in the slab model, section B-2 of this appendix will demonstrate that the proposed modeling scheme is accurate enough to study the distribution of the load to the main bridge members which is the main purpose of this project.

B-1.2 Section properties

Elastic properties

To analyze prestressed concrete I-beam bridges, the program NONBAN requires the same input data that is required by any commercial structural analysis program. For example, to describe the linear elastic properties of the bridge, the program requires that the following properties be defined for each beam element: a) The modulus of elasticity, E, b) the moment of inertia, I, c) the shear modulus, G, and d) the torsional constant J. The contribution of shear deformations to the response of I-beam bridges is generally ignored.

The moments of inertia and the torsional constants of the longitudinal as well as the transverse beams are calculated using the basic principles of structural mechanics. For the transverse beams representing the contribution of the slab, Zokaie et al. [B-4] and Hambly [B-3] recommend to use a torsional constant, J:

$$J = t^3/6 \qquad \text{per unit length of slab.} \qquad \text{(B.1)}$$

Inelastic properties

In addition to the typical elastic properties listed above, the program NONBAN requires information on the nonlinear section properties of each beam element. In particular, the program requires the user to enter a moment versus plastic rotation curve for each beam element.

In this project, the moment versus plastic rotation curve of a (prestressed or reinforced) concrete member is obtained by first calculating the moment versus curvature relationship. The linear elastic part of the curve was already accounted for using the modulus of elasticity and the moment of inertia entered as part of the elastic properties data. Therefore, only the portion of the moment-curvature curve which corresponds to moments higher than the elastic limit is needed at this stage. Realizing that the curvature is the derivative of the rotation with respect to the length, the moment versus plastic rotation curve is obtained by multiplying the curvature by the length of the plastic hinge (see Appendix C of phase I report for further detail). This multiplication implicitly assumes that the moment (and thus the curvature) is constant within the section of the beam element that is inelastic.

For a concrete member (prestressed or reinforced) the moment versus plastic rotation curve is obtained using the basic principles of equilibrium. The steps followed to obtain a moment versus curvature relationship are:

1. A value of curvature is chosen.
2. The location of the neutral axis is assumed.
3. The corresponding strain diagram for every point of the cross section is drawn.
4. Knowing the stress-strain relationships for every material of the cross section, the corresponding stress diagram is also drawn.
5. The location of the section's neutral axis is validated if the forces produced by the stress distribution satisfy equilibrium. If the force equilibrium is not satisfied, assume a new location for the neutral axis and go back to step 3.
6. The moment produced by the stress distribution is calculated.

For prestressed concrete I-beams, many empirical equations are proposed to calculate the length of the plastic hinge [B-13]. This study assumes that the length of the plastic hinge, L_p, is calculated using the equation:

$$L_p = d \qquad \text{(B-2)}$$

where d is the effective depth of the section (distance between the compressive face of the section to the center of steel area). Many other empirically derived formulas are available to calculate L_p. Equation B-2 is chosen herein for prestressed concrete I-beam bridges, because of its simplicity and because it gives a reasonable approximation for this type of bridge members. In addition, a limitation on the plastic hinge length is imposed in this study to insure that the total plastic zone remains smaller than the total length of the element. This limitation requires that the plastic hinge length be always less than half the length of the beam element. 1/2 the element length is used because plasticity could possibly develop on both ends of each element.

In this project it is assumed that a (prestressed or reinforced) concrete section completely unloads when the plastic rotation reaches a limiting value herein called maximum plastic hinge

rotation. This maximum rotation corresponds to the point at which either the concrete crushes, the prestressed tendon or the reinforcing steel rupture which ever occurs first. In most normal cases, concrete crushing occurs before steel rupture. When the maximum plastic hinge rotation is reached, this study assumes that the section will no longer be capable of carrying any load and the section will shed its load to other structural elements of the bridge. This phenomenon is assumed to coincide with the maximum capacity of the whole bridge because it would normally correspond to the actual ultimate bridge capacity or at best is associated with the occurrence of major damage (crushing of the concrete) rendering the bridge unusable.

The value of the maximum plastic hinge rotation for every concrete (prestressed or reinforced) concrete beam element is herein obtained from the moment versus curvature relationship by multiplying the curvature at which concrete crushes, the prestressed tendon or the reinforcing steel rupture by the length of the plastic hinge L_p.

It should be noted that the modeling scheme proposed herein accounts for nonlinearity only in the bending moment about the main (horizontal) axis of bending. The torsional moments are assumed to always remain in the linear elastic range. This assumption is found to be valid for typical bridge configurations based on comparisons with experimental results of model and full scale bridges. Appendix F discusses the issue of torsion in bridge members more fully especially for box girder bridges where the torsional stiffness is more significant than for I-beam bridges. Also, as mentioned earlier, shear deformations are ignored for prestressed concrete I-beam bridges. Although, NONBAN can account for shear deformation, the effect of shear deformations in I-beam bridges is not significant enough to warrant their inclusion as observed from comparisons with field and laboratory tests.

The program NONBAN is also set up to account for axial member deformations and for bending about the secondary (vertical) axis. These two factors, however, do not affect the behavior of the grid and these properties are assumed to remain in the linear elastic range.

The latest version of NONBAN accounts for the bridge construction sequence in the sense that the dead load is divided into two parts. The first part is applied on the noncomposite section of the longitudinal members while the second part is applied on the composite section. To accommodate this new option, two moment versus rotation curves and two sets of elastic properties are entered as part of the input data for the longitudinal beams only. The first moment versus rotation curve and set of elastic properties are those of the noncomposite section of the longitudinal beams. The second moment versus rotation curve and set of elastic properties are those of the composite section of the longitudinal beams. A sensitivity analysis performed for simple span bridges showed that the effect of including the construction sequence in the analysis does not affect the ultimate capacity significantly although some softening in the load deflection curve is observed in the early loading stages. The sensitivity analysis performed below will further discuss the importance of the loading sequence. The program NONBAN is capable of handling cases where the construction sequence warrants the application of the permanent dead loads on the simple spans while the application of the superimposed dead loads act on the

composite sections of the continuous spans. This construction sequence is the most common for prestressed concrete bridges in the US. NONBAN can also account for the construction sequence whereby continuity is acting for both the permanent and the superimposed dead loads.

B-1.3 Support conditions

In this study, it is always assumed that the supports are totally free to rotate. It should be noted however, that the slab discretization scheme adopted in section B-1.1 above will place a transverse beam element at the end of each span. This end transverse beam will often produce some limited rotational constraints at the supports. The rotations will be further constrained if large transverse diaphragms exist at the support.

B-1.4 Loading

The program NONBAN requires that the dead load data and the live load data be entered separately. The dead load is defined as the load that will remain constant throughout the incremental analysis. The dead load can be entered as either distributed load over the longitudinal beam elements or as point loads at the nodes.

The live load data is defined as the load that will be incremented. This load can only be entered as point loads at the nodes. In this study, all the live loads are assumed to be due to vehicular traffic. In the cases studied below, the live load is always assumed to be formed by vehicles having the configuration of the AASHTO HS-20 vehicle except for the cases when comparisons with test data require the use of different configurations. The AASHTO truck is used with a configuration that would create the maximum effect in a simple span bridge. The cases considered herein uses 14 ft spacings between the axles of the AASHTO truck. If the location of a vehicle is chosen such that the wheels do not coincide with any of the mesh nodes, nominal (artificial) beam elements are created to join the wheels of the vehicle to the adjacent nodes. The purpose of these nominal elements is only to distribute the wheel loads to the adjacent nodes and they do not contribute to the strength or stiffness of the structure. Therefore, these nominal beam elements are assumed to remain elastic and they are chosen to have extremely small moments of inertia and modulus of elasticity.

To study the behavior of the bridge superstructure under a critical loading condition, the HS-20 vehicles are placed on the bridge such that the external wheel line of the main vehicle is directly over one of the edge girders. The other vehicles are placed either behind or ahead of the main vehicle in the same line or to the side of the vehicle. This loading condition would give one of the most adverse conditions except for the cases where there are large overhangs. This position is used herein as the base case for comparing the performance of the different bridge configurations considered.

When side-by-side vehicles are considered, AASHTO specifications recommend that the two trucks should be placed at least 4 ft apart. Many of the analyses performed in this section however used a spacing of only two feet. This situation would obviously produce slightly more conservative results and is accepted herein because it would provide a lower bound estimate on the reliability and safety of the bridges studied. A sensitivity analysis has shown that the differences between the results of 2 ft and 4 ft spacings do not affect the final conclusions of this study because the final results are normalized and presented in terms of ratio of the load at ultimate capacity and load at first failure. By taking the ratios of the load at ultimate to the load at first failure, the effect of the truck configuration and truck spacings become less important.

Only bridges with one simple span or bridges with two continuous spans are considered in this study. For simple span bridges, only one vehicle is placed in each lane. For continuous span bridges, three different loading scenarios are used. For load case 1, side-by-side vehicles are placed in one span. This load case studies the behavior of the bridge when the primary failure mechanism is in positive bending. Load case 2 places two vehicles in the edge lane of the bridge such that the vehicles are in separate spans. Only one lane is loaded. This load case studies the behavior of the bridge when the primary failure mechanism is in negative bending. Load case 3 uses a total of four trucks. Two vehicles are placed side-by-side in each of the two spans considered. This load case also studies the effect of primary failure in negative bending. Load cases 2 and 3 are considered separately because load case 2 has a higher probability of occurrence in the lifetime of the structure than load case 3, although load case 3 is obviously the most critical of the two in a deterministic sense. By comparing the results of load case 2 and load case 3, the effect of one-lane versus two-lane loadings is analyzed.

For simple span bridges, the vehicles are placed such that the drive axle of the HS-20 truck coincides with the bridge mid-span. For continuous spans, two different loading positions are considered: When only one span is loaded, the HS-20 vehicles are placed such that the drive axle is at a distance of 0.41 the span length from the end (noncontinuous) support. When two spans are loaded, the vehicles are placed such that the drive axle is at 0.58 the span length from the end support. These two different positions are chosen herein because they correspond to the most critical design positions respectively for positive and negative bending.

It should be noted that the HS-20 design configurations do not correspond to actual vehicular configurations. The HS-20 design vehicles are used herein because most engineers are familiar with them and also because the maximum lifetime load effects used during the LRFD calibration are given in function of the effects of HS-20 vehicles [B-7]. HS-20 design vehicles rather than design lane loads are used during the NONBAN analysis of long spans and for continuous spans in order to have a configuration resembling that of a truck. The load configuration is an important factor while performing nonlinear analyses.

B-2. Model Verification.

The validity of the program NONBAN and the modeling scheme used to study the behavior of prestressed concrete I-beam bridges is verified by comparing the results of NONBAN to those of two full-scale field tests. The first test considered is the one performed by Gosbell and Stevens in Australia [B-5]. The second test is the one performed by Burdette and Goodpasture in Tennessee [B-6].

B-2.1 Australian field test

The Australian field test was performed on a simply-supported bridge with a span length equal to 18.7 m (61.33 ft). The bridge consisted of seven prestressed I-beams at 1.45 m (4.75 ft) spacings supporting a 15 cm (6 in) deck slab. Reference [B-5] gives a detailed description of the tested bridge. Core samples were used to estimate the properties of the concrete in the deck and the beams as well as the strength of the prestressing strands. The beams and the slab were built to act as composite sections. Similarly, the mid-span diaphragm was designed to have composite action with the slab in the transverse direction.

Tests to determine the ultimate load capacity of the bridge were performed by placing two concentrated point loads at the bridge's midspan. The point loads were placed on one side of the deck to simulate unsymmetrical loading conditions. The first load was placed at 69 cm (2.25 ft) from the edge beam and the second load at 183 cm (6 ft) from the first load. The loads were then incremented in "an attempt to estimate the ultimate load capacity". Testing was stopped when the load reached 2090 kN (474 kips). At that point, the measured maximum deflection was about 12.7 cm (5 in) or at about span length/145. The loading was stopped at that level because the field testing team observed that a "large separation had occurred between the diaphragm and the beam ... and because of fear of a catastrophic punching shear failure under the loads ", although "...no shear failures actually occurred ... and no separation between the slab and longitudinal beams was detected". Reference [B-5] observes that the deflection profile across the bridge's cross section remained essentially unchanged as the load was increased from the linear range until the test was discontinued. It was also noted that the curb and railings significantly increased the rigidity of the edge beams "vastly contributing to the ultimate capacity of the bridge". On the other hand, "the diaphragm did not contribute to the strength of the bridge nor to the distribution of the loads". The authors attributed this to the" weak steel reinforcement provided in the diaphragm" [B-5].

The program NONBAN is run assuming that the curbs act compositely with the edge beams but ignoring the effect of the railings because the exact dimensions and material properties of the railings are not provided. The inclusion of the curb's effect to the edge beam produced an increase in the ultimate member capacity of the edge beam by about 20% relative to the interior beams. The moment of inertia of the edge beam was found to be about 70% higher than that of the interior beams. This 70% increase matches the estimate given in reference [B-5].

To prepare the mesh for the NONBAN analysis, each of the seven longitudinal members is divided into six equal segments. Although the actual tendon profile of the beams is not uniform, the NONBAN analysis assumes that the properties of the longitudinal beams are constant having the same properties as those of the cross section of the midspan. The longitudinal beams are connected by seven equally spaced transverse beams representing the transverse capacity of the slab. Because the actual value of the prestressing force is not available, the moment-rotation curves of the longitudinal beams are derived assuming a prestressing force of 2174 kN (493 kips). This value is used herein because it matches the prestressing force that would have been used if the bridge were designed to meet AASHTO's requirements. Several runs were performed in order to match the NONBAN results to the experimental results. Different estimates for the length of the plastic hinge were used. Also, the effect of the construction sequence was investigated. The possibility of having shear failures is not considered in this example.

Best results were obtained using dead loads on the noncomposite section and applying the superimposed load on the composite section and when the plastic hinge length is assumed to be equal to 80% of the effective depth of the section ($L_p = 0.8$ d). Slightly different results were obtained assuming that all loadings were applied on the composite sections while the plastic hinge length is set equal to the effective section depth ($L_p = d$).

Figure B-1 shows a comparison between the field results published in reference [B-5] and the results of NONBAN. Acceptable agreement is observed in the figure although NONBAN predicts that the bridge is capable of withstanding a load much higher than that at which the test was actually stopped. According to NONBAN, the ultimate capacity would be reached at a total load equal to 2847 kN (640 kips) although the test was actually stopped at 2090 kN (474 kips). In this analysis, the ultimate capacity is defined as the load level at which concrete crushing occurs in a main longitudinal member. The differences between the experimental and the NONBAN loading curves may be due to the limited information provided in Ref. [B-5] about the details of the section properties (e.g. prestressing force) and the dimensions of the curbs. The latter affects the estimate of the member capacities and the magnitude of the dead loads. These proved to be important factors in tracing the loading curve although they are less important for estimating the ultimate capacity. The NONBAN analyses assumes that each longitudinal beam carries 9.6 N/mm (55lb/in) and that the superimposed dead load on the end beams is 0.6 N/mm (3.5 lb/in).

Despite all the limitations in the available data and the assumptions that had to be made, it is observed that there are sufficient similarities between the curves obtained by NONBAN and the load deflection curve from the test results up until the 2090 kN (474 kip) level was reached. These similarities illustrate the validity of the program NONBAN to perform the nonlinear analysis of typical bridge configurations and particularly for prestressed concrete I-beam bridges.

B-2.2 Tennessee field test

The Tennessee field test was performed on a simply-supported bridge with a span length equal to 19.8 m (65 ft). The bridge consisted of four prestressed I-beams at 2.74 m (9.0 ft) spacings supporting a 17.8 cm (7 in) deck slab. The bridge had a 75 degree skew and no information was provided concerning the diaphragms. Reference [B-6] gives a detailed description of the tested bridge. Core samples were used to estimate the properties of the concrete in the deck and the beams as well as the strength of the prestressing strands. The beams and the slab were built to act as composite sections.

Tests to determine the ultimate load capacity of the bridge were performed by placing eight concentrated point loads close to the bridge's midspan [B-6]. The first set of four loads was placed on a line parallel to the skew at 6.7 m (22 ft) from the supports. The first load was placed at 69 cm (2.25 ft) from the edge beam and the second load at 192 cm (6.3 ft) from the first load. The third load was placed at 149 cm (4.9 ft) from the second load. The last load was placed at 183 cm (6.0 ft) from the third load. The second set of four loads was placed along a line which was 4.27 m (14 ft) behind the first set. The loads were then incremented to test the bridge to failure.

Reference [B-6] mentions that visible cracking was observed at the center diaphragm at a load of 1926 kN (433 kips). The interior girders cracked at a load of 2317 kN (521 kips). At a load of 4226 kN (950 kips), the authors noticed considerable "dishing" as the interior girders deflected more than the exterior. This caused the separation between the deck and the girders and the loss of composite action of the interior girders. At that point the concrete of the interior girders started crushing. Finally at 5070 kN (1140 kips) the interior girders failed in shear. The authors developed a load versus average deflection curve based on an analytically derived moment curvature relationship. In their analysis, the authors assumed that the whole bridge behaves as one beam and the moment curvature relationship for the whole bridge cross section was obtained.

To prepare the mesh for the NONBAN analysis, each of the four longitudinal members is divided into twelve to thirteen segments (the difference is to accommodate the skew). Although the actual tendon profile of the beams is not uniform, the NONBAN analysis assumes that the properties (including the M-phi curve) of the longitudinal beams are constant having the same properties as those of the cross section of the midspan. The longitudinal beams are connected by eleven equally spaced transverse beams perpendicular to the longitudinal beams to represent the transverse capacity of the slab. In addition, two skewed transverse beams are set along the end supports. In the acute corner, an additional transverse element is added to connect the two edge beams.

The moment-rotation curves of the longitudinal beams used in the analysis of this bridge were obtained from the moment curvature plots provided in reference [B-6]. The dead load estimates were also extracted from the curves of Ref. [B-6] and are assumed to be applied on the composite

section. This is done herein because the moment-rotation curve given in Ref. [B-6] was corrected to account for this effect.

Figure B-2 shows a comparison between the field results published in reference [B-6] and the results of NONBAN. Reference [B-6] gives an average load deflection curve for all the longitudinal beams. Figure B-2 shows the load deflection curve obtained by NONBAN for the edge beam and for the interior beam and the average curve compared to the curve provided in Ref. [B-6]. Good agreement is observed in the figure. According to NONBAN, the ultimate capacity would be reached at a total load equal to 5360 kN (1205 kips). The test was actually stopped at 5070 kN (1140 kips). The difference being on the order of 6%. The deflection measured at the point when the test was stopped is roughly on the order of span length/115.

In the NONBAN analysis, the ultimate capacity is defined as the load level at which concrete crushing occurs in a main longitudinal member. It should be noted that in the first round of analysis, the input data for dead load was overestimated which produced an underestimation of the ultimate bridge capacity. Good agreement was observed when the dead load was extracted from the moment curvature relationships provided in ref. [B-6]. Nonetheless, the similarity between the curve obtained by NONBAN and the load deflection curve from the test results illustrates the validity of the program NONBAN to perform the nonlinear analysis of typical bridge configurations and particularly for prestressed concrete I-beam bridges.

B-2.3 Summary

The comparison between the results of the two full scale field tests and NONBAN illustrates the validity of the program and the modelling scheme used in this study. It is observed that the estimate of the length of the plastic hinge may affect the shape of the loading curve in the early stages. However, this estimate becomes less critical as the loading is increased. In general, it is observed that a plastic hinge length equal to the effective depth of the section (L_p= d) produces good agreement with experimental curves if all the dead load is applied on the composite section. When the dead load is divided into a permanent dead load and a superimposed dead load, a lower estimate of L_p, produces best results. For the latter cases, it is herein suggested to use a value of L_p extracted from the equations proposed by Park and Pauley [B-10] as was explained in the phase I report. The calculations performed in the rest of this appendix assume a value of L_p equal to d for the prestressed concrete I-beam bridges. For the simple span bridges all the dead load is assumed to act on the composite section. For the continuous bridges, the load is divided into a permanent dead load and a superimposed dead load. Using a value of L_p= d will always give conservative estimates of the loading curves in the early stages of loading but will produce little change in the estimate of the ultimate capacity.

B-3. Bridge Configurations.

Design Considerations

To study the behavior of typical prestressed concrete I-beam bridge configurations, a large number of prestressed concrete bridges are designed to cover typical span lengths and cross-sectional configurations. One hundred and two simple span bridges as well as fifty-one continuous two-span bridges with individual span lengths varying between 14 and 46 m (45 and 150 ft) are designed. The designs assume that the deck is supported by 4, 6, 8 or 10 beams with beam spacings varying between 122 and 366 cm (4 and 12 ft). The concrete bridge decks are assumed to vary in depth between 19 and 22 cm (7.5 and 8.5 in) depending on the beam spacing. For each bridge configuration, appropriate AASHTO I-beam sections were chosen based on the span-length and beam spacings. The beams are assumed to have a compressive strength f'c equal to 35 MPa (5 ksi) while the deck's strength is equal to 24 MPa (3.5 ksi).

The bridges are designed for strength to satisfy the AASHTO LFD criteria for HS-20 loading. The LFD criteria are used herein because they are currently the most commonly used strength criteria in the design of prestressed bridges. Also, the AASHTO LRFD code was calibrated to produce on the average the same level of safety as the LFD criteria and thus the recommendations that will be made in this study will be valid on the average for both LFD and LRFD bridges. More importantly, the object of this study is to recommend a redundancy framework that would be valid for all bridges independent of the criteria that they were built to meet. In addition, a sensitivity analysis will study the effect of using sections with higher or lower strengths than those that exactly satisfy the LFD criteria.

During the design process, a resistance factor of 0.95 is used to calculate the required prestressing steel area for positive bending. A resistance factor of 0.90 is used to find the required area of regular steel reinforcement in the negative bending region of the continuous bridges. The LFD criteria are used to proportion the prestressing as well as the regular reinforcing steels. Although the specifications recommend checking the capacity of the section for service load conditions, this check was not performed herein because this study is focusing on the strength capacity of bridges and not on member serviceability. However, as mentioned above, the effect of using sections with higher or lower strengths than those that exactly satisfy the LFD criteria is studied separately in the parametric analysis described in section B-5 below.

Design Example

The design of an example continuous two-span (45-45m) (150-150 ft) prestressed concrete I-beam bridge is presented in this section to illustrate the assumptions made in this study. This bridge example is assumed to be formed by parallel beams at 3.66 m (12 ft) spacings. The beams are chosen to be AASHTO type VI. The beam's section is shown in Figure B-3.

The dead weight of the beam is assumed to be 16.5 kN/m (1.13 kip/ft) given that the cross sectional area of the beam is 700042 mm^2 (1085 in^2). Assuming a slab thickness of 216 mm (8.5 in), the dead weight of the tributary area of the slab becomes 18.6 kN/mm (1.275 kip/ft). The dead weight due to the wearing surface is assumed to be equal to 8.8 kN/mm (0.6 kip/ft). It is herein assumed that the beam's weight and the slab's weight are carried by the non-composite section before span continuity is secured. On the other hand, the wearing surface's weight is carried by the composite continuous beams. These produce a maximum positive bending moment at the mid-span of the beam equal to 4309 kN.m (3178 kip-ft) for the beam's weight. The slab weight produces a maximum positive bending at the mid-span equal to 4861 kN.m (3585 kip-ft). The wearing surface produces a maximum positive bending moment equal to 1257 kN.m (927 kip-ft) and maximum negative bending moment equal to 2289 kN.m (1688 kip-ft).

The live loads are applied on the composite section and are supported by the continuous bridge. The AASHTO HS-20 truck produces a maximum positive bending moment equal to 2677 kN.m (1974 kip-ft). The truck load is placed on the beam such that the drive axle is at 0.43 span length from the free support. The AASHTO lane load produces a maximum negative bending moment equal to 3145 kN.m (2319 kip-ft).

Using the LFD criteria with HS-20 loading, the impact factor for this 46 m (150-ft) span length is 1.182. The girder distribution factor for the 3.66 m (12-ft) girder spacing is 2.182 of a wheel's load. The LFD load factors of 1.3 for the dead loads and 1.3 times 5/3 for the live loads produce a factored maximum positive bending moment equal to 21038 kN.m (15515 kip-ft) and a factored maximum negative bending moment equal to 11762 kN.m (8674 kip-ft). In order to simplify the design process, the maximum positive bending moments from the dead weights and the live load are added together even though, they may not be occurring at the same point.

For this design example, it is assumed that the concrete strength is 24 MPa (3.5 ksi) for the slab and 34.5 MPa (5 ksi) for the girder. The effective flange width is 3.66 m (12 ft) and the effective depth of the section in the region of maximum positive bending is assumed to be 1918 mm (75.5 in) from the top surface of the slab. The prestressing tendons are assumed to be 1862 MPa (270 ksi) steel.

Using a resistance factor equal to 0.95, the area of prestressing steel required is calculated such that:

$$M_n = A_s^* f_{sn} d \left(1 - 0.6 \frac{A_s^* f_{sn}}{b' d f'_c} \right) \qquad \text{(B-3)}$$

where M_n is the nominal moment which is the applied factored moment divided by the resistance factor. A_s^* is the prestressing steel area. f_{sn}^* is the effective prestressing stress. d is the effective section depth. b' is the effective flange width. f'_c is the concrete strength of the compression

zone. For this design example, the neutral axis is in the slab, therefore f'_c is 24 MPa (3.5 ksi). Assuming f^*_{ps} is about 1724 MPa (250 ksi). The required area of prestressing steel A_s^* is found to be equal to 6730 mm^2 (10.43 in^2). Accounting for prestress losses, the effective prestressing force according to the AASHTO requirements is equal to 7014 kN (1577 kips) (0.7x0.8x1860 MPa x A_s^*).

In the negative bending region, the resistance factor is 0.9. The calculation of the required area of reinforcing steel in the negative bending (middle support) region uses equation B-3 with f^*_{ps} substituted by f_y where f_y is the yielding stress of the reinforcing steel. Assuming f_y equal to 414 MPa (60 ksi) and using f_c of 34 MPa (5 ksi), d equal to 2000 mm (79 in) and b' equal to 711 mm (28 in), the required area of reinforcing steel in the support region is obtained as A_s equal to 17788 mm (27.57 in^2).

The slab of the 150 ft continuous bridge with 6 beams at 8 ft spacings was designed to have a capacity of 12833 lb-ft/ft for a 8.5 in thick deck. The calculation of the required slab capacity was based on service load requirements as described in reference [B-12]. The 12833 lb-ft/ft value is found to be higher (by roughly a factor of 2) than the recommended value as obtained from different slab design guidelines and design charts provided by several state DOT's. These design tables and charts were based on the LFD criteria while the designs of the slabs is herein performed using service load requirements. It should be noted, however, that the sensitivity analysis performed below shows that variations in the slab's strength do not affect the conclusions obtained in this study.

Summary of Designs

All the prestressed concrete I-beam bridges designed in this study follow the procedure illustrated in the example detailed above. Table B-1 gives a summary of the designs for the simple span prestressed concrete I-beam bridge members. Table B-2 gives the summary for the two-span continuous bridges.

B-4. Results of Nonlinear Analysis.

The nonlinear analysis of the prestressed I-beam bridge systems designed as described in the previous section is performed using the program NONBAN. This section illustrates how the bridges are modeled and summarizes the results of the analysis.

Preparation of Input Data.

The mesh discretization and modeling procedure used in this study follow the general guidelines given by Zokaie, Osterkamp and Imbsen [B-4] and the procedure outlined in section B-1 of this appendix. The beams in the longitudinal direction account for the composite action between the slab and the I-beams. In addition, it is herein assumed that the bridges have no transverse diaphragms. This means that the lateral distribution of the load is only effected by the transverse properties of the deck slab. This assumption is made herein to provide a lower bound envelope to the results. In fact, current design procedures do not favor the use of diaphragms "except when absolutely necessary for stability requirements" [B-9]. In addition, many of the bridge tests reported in the literature (see for example the tests described in section B-2) show that the diaphragms did not generally contribute to the load distribution. The sensitivity analysis performed further below demonstrates that the presence of the diaphragms does not change the results of intact bridges significantly. The sensitivity analysis, however, shows that the diaphragms would help distribute the load in the cases where the external beams were subjected to heavy damage.

It should be noted that available methods for estimating the torsional rigidities of the slab and transverse members are very approximate. Also, the model used in this study ignores the interaction between torsion and the two directional bending moments in the deck slab. This interaction may be significant under the effect of high torsional loads especially in the inelastic range. Different methods have been suggested to account for the torsional capacity of the longitudinal and transverse beams. For example, Hambly [B-3] suggests to use a torsional constant equal to twice the bending moment of inertia for the slab elements as described by equation B.1 which is used in this study.

In this study, it is assumed that the transverse beam elements representing the contribution of the slab have a torsional constant J calculated as given in equation (B-1). Also, it is assumed that the torsional constant for the longitudinal composite beams is obtained by summing the torsional contributions of the beam's stem and that of the slab. Equation B-1 is used to find the torsional constant of each part (i.e. the stem and the effective portion of slab). This method provides a reasonable estimate of the torsional inertia of the longitudinal members. The sensitivity analysis performed in section B-5 below also shows that the effect of the assumptions made herein produce negligible effect on the final results.

The discretization of the bridge superstructures for the base cases studied herein divides every longitudinal beam into equal segments such that every segment's length is greater than two times the plastic hinge length. The plastic hinge length was calculated using equation B-2. A maximum number of 10 longitudinal beam elements is used.

The moment-rotation curves for the longitudinal and transverse members are calculated based on their section properties using typical concrete, prestressing steel and reinforcing steel stress-strain diagrams. The stress-strain diagrams used in this study are shown in Figure B-4 based on reference [B.12]. It should be observed that the tensile capacity of the concrete is ignored in these stress-strain diagrams. For the transverse elements, however, nonlinear behavior is assumed to begin when first cracking occurs. For the transverse elements representing the contribution of the slab, the cracking moment is calculated as the moment which will produce a stress equal to the modulus of rupture in the outer surface of the tension zone of the beam. All the longitudinal members are assumed to have the same properties. All the interior transverse elements are assumed to have the same properties. The transverse members on the ends are assumed to have properties equal to 1/2 of those of the interior members.

As mentioned earlier, the live loading is assumed to be composed of trucks having the AASHTO HS-20 configurations. "Nominal" members (with negligibly small moments of inertia) are used to transfer the tire loads to the adjacent mesh nodes. These nominal members are assumed to remain in the elastic range.

The dead load is assumed to be uniformly distributed along the length of each longitudinal member. All the longitudinal members are assumed to carry the same dead load. The live load is formed by HS-20 vehicles placed longitudinally in the most critical design points. In general, the outside wheel of the end vehicle is placed over the web of the exterior beam. The spacing between side-by-side trucks is chosen to be 0.6 m (2 ft). The base case assumes two side-by-side HS-20 vehicles. As mentioned in section B-1, the analysis of the continuous spans assumes three different load combinations.

The nonlinear incremental analysis is performed using the program NONBAN. No safety factors, load or impact factors are applied on the resistances or the loads during the analysis. This is done because this part is concerned with studying the resistance capacity of the bridge system. The capacity will be expressed in terms of the number of HS-20 trucks that can be carried before collapse. The effect of the dynamic impact will be included at a later stage on the load side of the safety check equation (during the reliability analysis) when the capacity will be compared to the maximum expected load which will include the dynamic impact.

The AASHTO HS-20 vehicles are incremented until bridge system failure occurs. The load factor at which the system fails is defined as LFu. LFu gives the factor by which the weights of the initial HS-20 vehicles should be multiplied to produce system failure. Failure of the bridge is assumed to occur when one main longitudinal member reaches a plastic hinge rotation equal to the maximum allowable plastic rotation. This maximum allowable plastic rotation is obtained

from the moment-rotation curves and it corresponds to the value at which the concrete crushes or the prestressing steel snaps. It is herein assumed that concrete crushing under transverse bending or in secondary members will only produce local failures. Therefore, the maximum plastic hinge rotations in transverse members or in secondary members are assumed to be infinite and no failures in the transverse direction are considered although the transverse beams will exhibit nonlinear behavior.

In addition to calculating the load factor corresponding to the ultimate capacity of the bridge system (LFu), the load factor corresponding to the level at which the bridge becomes non-functional is recorded. At this point, it is assumed that a bridge becomes non-functional when the maximum live load displacement under a main longitudinal member reaches a value corresponding to the span length/100. The L/100 value is chosen herein because it is similar to the values at which many bridge field tests were stopped when the researchers observed potentially high and dangerous deflections (see for example the tests described in section B-2). The load factor corresponding to a displacement of L/100 is herein designated as LF100. To study the importance of this subjective selection of the functionality criterion, the load factor corresponding to a displacement equal to span length/300 and the load factor corresponding to a displacement equal to the span length/200 are also obtained. These load factors are herein respectively represented as LF300 and LF200.

The choice of L/100 as a functionality criterion is based on a subjective assessment of "unacceptable displacement levels". L/100 is proposed herein rather than L/200 which was used in earlier reports because it was found that the L/100 gives more stable results than the L/200 value. Stability is used herein in the sense that the L/100 value is less sensitive to the modeling assumptions used with NONBAN such as mesh size, length of plastic hinge Lp etc. The L/100 value is also less sensitive to the bridge member design details such as moments of inertia, section depth, etc. It should also be noted that the choice of the serviceability criterion is less important when the calibration of the redundancy factor is based on a reliability analysis. Hence, if an L/200 criterion is used with a low reliability target, it will produce similar results to those obtained when choosing L/100 with a higher reliability targets. The target reliability levels must be chosen based on "acceptable" current designs. The issue of target reliability levels will be further discussed in section B-6.

Following the calculation of the ultimate capacity of the intact structure, a similar analysis is performed assuming damaged conditions. In this study, a bridge's damaged condition assumes that the external girder is so heavily damaged that it can no longer carry any load. This would simulate a situation where the external girder is knocked out of service due to a collision or due to failures of the prestressing tendons. The incremental nonlinear analysis of bridge structures where the external member is assumed to be totally damaged is executed using the same assumptions stated above for the intact structures. The ultimate load capacity for a damaged bridge is designated by the variable LFd. In the NONBAN model, damaged members are represented by very low moments of inertia. The live load positions used for the damaged cases are the same as those used for the intact bridges. This means that the external wheel load of the

HS-20 vehicle lies directly above the damaged external girder. In this analysis as well, failure is assumed to occur when one of the intact girders reaches its maximum plastic hinge rotation. Although the nonlinearity of the transverse members is accounted for, no failures in the transverse direction are considered. This assumption may be unconservative because there is a possibility that the cantilevered portion of the slab would break under the effect of the extruding wheel load. However, it is herein assumed that the parapet and the railing will provide enough support so that the slab will still be able to transfer the load laterally to the adjacent intact girder. This assumption is made because as mentioned earlier, the object of this study is to study the behavior of the main members rather than focus on the behavior of the bridge's slab.

To provide a measure of a bridge's level of redundancy, the load factor at which the intact bridge system fails (LFu) , the load factor at which the bridge becomes non-functional (LF100) as well as the load factor for the damaged bridge scenario (LFd) are compared to the load factor corresponding to the first member failure LF1. LF1 in this case is calculated assuming linear elastic behavior of the bridge members. A linear elastic behavior is assumed in order to be consistent with current member oriented design and analysis procedures. Thus, the LF1 factor represents the estimated bridge member capacity using current traditional member checking methods without consideration of the code-specified safety factors. The calculation of LF1 is illustrated further below.

Because redundancy is essentially a comparison between the system capacity and that of the individual bridge members, the ratios of LFu/LF1, LF100/LF1 and LFd/LF1 are used as objective deterministic measures of bridge redundancy as discussed in Chapter 2 of this report.. Section B-6 of this appendix proposes a probabilistic measure of redundancy as expressed in terms of the reliability indices.

Detailed Example

The analysis of a 100 ft simple span bridge is presented in this section to illustrate the structural model used in the calculations performed on the prestressed concrete I-beam bridges. The bridge is assumed to have 6 beams spaced 8 ft center to center. The slab is assumed to be 8 in thick acting compositely with the girder. The slab has a concrete strength equal to 3.5 ksi while the girder's concrete strength is 5 ksi. The girder is an AASHTO type V beam. The prestressing steel is 5.0 in^2 and the effective depth, d, is 66 in. The prestressing force is 756 kips. The prestressing strands are formed by 270 ksi steel.

The bridge is discretized as shown in Figure B-5. The longitudinal beams represent the contributions of the composite slab-girder section. These beams are placed at the centerline of the girders. The spacings between the longitudinal beams are thus 96 in. The transverse beams represent the contribution of the slab to the transverse distribution of the loads. Transverse beams are placed at 1/10 of the girder's length. Thus, the spacing between the transverse beams is 120 in. It is herein assumed that the slab is reinforced in the transverse direction on the top and the bottom by an equal amount of steel equal to 0.42 in^2/ft.

The dead load on the longitudinal beams is assumed to equal 0.19 kip/in.

Two side-by-side AASHTO HS-20 trucks are used for the live load. The location of the tire loads are indicated by X in Figure B-5. The external wheel line coincides with the external girder. Nominal beams connect the tire loads to the adjacent mesh nodes as shown in the figure.

For the elastic material properties, all the beams are converted into equivalent beams of the weaker concrete. The modulus of elasticity thus becomes 3372 ksi (based on f'_c=3500 psi) and the shear modulus is 1405 ksi assuming that Poisson's ratio is equal to 0.2.

The elastic properties of the composite longitudinal beams are given in Figure B-6 a. All the longitudinal beams are assumed to have the same properties.

The elastic properties of the interior transverse beams are given in Figure B-6 b. The elastic properties of the transverse end beams are given in Figure B-6 c. As can be seen, the end transverse beams are assumed to have properties equal to 1/2 those of the middle transverse beams.

Figure B-5 also shows the moment versus curvature plots obtained for the longitudinal and transverse beams. To obtain the moment versus plastic rotation curves, the slopes of the moment versus curvature plots are divided by L_p which is assumed to be equal to the effective composite beam depth d (i.e. 66 in is used for the longitudinal beams). Since this value is greater than half the length of the element (120 in./2) the actual value of L_p used herein is reduced to 60 in.

The maximum plastic hinge rotation for the longitudinal beams is taken as the maximum curvature obtained from the moment-curvature plot and multiplied by L_p. The transverse beams representing the slab are assumed to have an infinitely high maximum plastic hinge rotation. This means that failure of the bridge system occurs only due to failures in the longitudinal members although the model accounts for the material nonlinearity of the slab.

The supports at the ends of each longitudinal beam are free to rotate in all directions but their displacements in all directions are fixed.

The damage scenario assumes that the external girder immediately below the external wheel line has zero stiffness. The program accounts for this scenario by using a negligibly small moment of inertia for the elements representing the external girder.

The results of the nonlinear analysis for the intact structure and the damaged condition of the example bridge are shown in Figure B-7. The results show that the ultimate capacity is reached when the HS-20 vehicles are incremented by a factor, LFu equal to 5.28. A displacement equal to span length/300 (4 in) is reached when the load factor, LF300 is equal to 1.91. A displacement equal to span length/200 is reached when the loads are incremented by a factor, LF200, equal to 2.42. A displacement equal to span length/100 is reached when the load factor

reaches a value, LF100, equal to 3.65. The analysis of the damaged bridge reveals that the ultimate capacity of the damaged bridge is reached when the HS-20 vehicles are incremented by a factor LFd equal to 2.05.

As mentioned earlier, LF1 gives the load factor corresponding the failure of the first longituindal member of the bridge assuming linear elastic behavior. The calculation of the load factor LF1 is effected using the equation:

$$LF_1 = \frac{R - D}{DF_1 \quad LL_{HS\text{-}20}} \tag{B-4}$$

where R is the member's moment capacity, D is the member's dead load, DF_1 is the linear elastic distribution factor for the member, $LL_{HS\text{-}20}$ is the total live load effect due to the HS-20 vehicles. To be compatible with the calculations performed with NONBAN, equation B-4 uses the unfactored values of R and D. Also, the value of DF_1 $LL_{HS\text{-}20}$ is obtained directly from a linear elastic grid analysis of the bridge using NONBAN. DF_1 $LL_{HS\text{-}20}$ is then obtained as the maximum linear elastic moment applied on any longitudinal girder under the effect of two side-by-side HS-20 trucks. To calculate DF_1 the sum of the moments from all the girders is divided by the largest girder moment. The DF_1 value used herein is thus obtained from NONBAN rather than using the LFD or the LRFD load distribution factors.

Using a linear elastic analysis, the moment due to the dead load at the midspan of a girder is obtained as 34200 kip-in. The external girder will carry a linear elastic moment equal to 13830 kip-in due to the two side-by-side HS-20 vehicles. The girder section has an ultimate girder capacity equal to 84993 kip-in. The 84993 kip-in value is obtained from the moment versus curvature relationship. A difference on the order of 2% in the ultimate girder capacity may be observed if equation B-3 is used instead of using the exact equilibrium equations with the stress-strain curves given in Figure B-3. The 34200 kip-in dead load moment and the 84993 kip-in ultimate girder capacity indicate that the live load margin (the amount available to carry the live load) is 50793 kip-in (84993 minus 34200 kip-in). The highest moment on any girder due to a set of HS-20 vehicles was found to be equal to 13830 kip-in. This highest moment is defined as DF_1 $LL_{HS\text{-}20}$. Using these values in equation B-4 we find that LF1 is equal to 3.67:

$$LF_1 = \frac{R - D}{DF_1 \quad LL_{HS\text{-}20}} = \frac{84993 - 34200}{13830} = 3.67 \tag{B-4}$$

This means that the bridge is capable of carrying 3.67 times the HS-20 trucks assuming linear elastic behavior before the first member failure is observed.

The external girder's distribution factor (DF_i x 2) obtained from this analysis is on the order of 0.76 times the weight of one truck. The value calculated herein is found to be higher than the 0.62 value used by Nowak during the calibration of the LRFD specifications [B-7]. It should be noted that Nowak's calibration assumes an interior girder. On the other hand, using the load distribution equation from the AASHTO LRFD code [B-9], we obtain a distribution factor for an interior girder equal to 0.69. According to the AASHTO LRFD specifications, the distribution factor for an exterior girder can be calculated from the distribution factor of an interior girder using the equation:

$$g_{exterior} = g_{interior}\left(0.77 + \frac{d_e}{2800}\right) \geq g_{interior} \qquad -300 \leq d_e \leq 1700 \qquad \text{(B-5)}$$

where d_e is the distance between the curb and the exterior girder in mm. The AASHTO code requires a clear distance greater than 0.6 m (2 ft) between the wheel load and the curb. Since the external wheel load is herein placed over the external girder this means that the clear distance between the external girder and the curb should be at least 0.6m (2 ft). For the 0.6 m (2 ft) distance, $g_{exterior}$ will be exactly equal to $g_{interior}$. To match the results of Equation (B-5) and the 0.76 factor obtained by NONBAN, the distance between the curb and the external girder should be 0.9 m (3 ft). In any case, the difference between the 0.69 value and the 0.76 value obtained herein is only 10% which is still acceptable. A portion of this difference is obviously due to the assumption of 0.6 m (2 ft) spacings between the adjacent HS-20 vehicles used in the calculations performed herein. This comparison concludes that the assumptions made herein on load placement are conservative and will provide a lower bound estimate on the safety of this bridge. It should be noted that since the final results of this study are presented in terms of the relative safety of the bridge i.e. as ratios of LFu/LF1, LF100/LF1 and LFd/LF1, then, the effect of load positioning and load configuration becomes less important.

As seen above, the bridge is capable of carrying 5.28 times the HS-20 vehicles if the nonlinear capacity is considered. Therefore, the redundancy ratio for the ultimate capacity, defined as LFu/LF1, is equal to 1.44 for this particular bridge. Similar calculations are performed for a variety of bridge configurations. These results are presented in the next paragraph.

Summary of Results

The results obtained from the analysis of all the prestressed concrete I-beam simple span bridges are given in Table B-3. The results of the continuous prestressed concrete I-beam bridges are given in Table B-4. Many previous nonlinear analyses of bridges assume that a simple span bridge formed by a system of parallel I-beams would collapse only when all its longitudinal members reach their ultimate capacities. When all the members reach their ultimate capacities, the bridge is no longer capable of carrying any additional load and the displacements

go to infinity and "a failure mechanism" is formed. For a mechanism to form each member of the bridge must be able to sustain a very high level of deflection without breaking. i.e. an infinite level of ductility is assumed. A comparison between the results of the analysis performed in this study and the results for a mechanism is shown in Table B-3. Specifically, Table B-3 shows LF300, LF200, LF100, LFu, LFd and LF1, and the values that would have been obtained if the loading were allowed to continue until a mechanism is formed. For the simple span bridges, the formation of the mechanism is approximated by taking the maximum moment capacity of each girder's section minus the dead load applied on the section, the difference is multiplied by the number of girders in the structure and then divided by the moment due two HS-20 trucks. This is represented by the equation:

$$mech. = \frac{n\ (\ R\ -\ D\ )}{LL_{HS20}} \qquad \text{(B-6)}$$

where n is the number of longitudinal girders, R is the member's resistance, D is the member's dead load and LL_{HS20} is the total moment effect on the bridge due to two HS-20 trucks. The values obtained from equation B-6 are shown in Table B-3 under the column labelled mech. (mechanism) and are given here to provide a rough comparison between the results of the analysis using the failure criteria used in this study and the values that would be obtained if infinite levels of ductility are assumed in each member. It is noted that the values for a mechanism could be more than 2.5 the value of LFu for large girder spacings.

Table B-3 also shows the ratios of LFu/LF1, LF100/LF1 and LFd/LF1 for the cases analyzed. It is observed that the ratio of LFu/LF1 may be as high as 1.57 showing up to 57% increase in system capacity compared to member capacity. Similarly LF100/LF1 may also reach a value on the order of 1.18. Even LFd/LF1 is shown to reach up to value of 1.02 indicating that some bridge configurations are still capable of carrying high levels of loads even when a girder is completely removed from the structural system.

The results show that for a given girder spacing the LFu/LF1 ratio increases as the number of girders is increased. It is noticed that the most optimum number of girders is six for a two-lane bridge and that increasing the number of girders beyond six does not improve the LFu/LF1 ratio. For a given number of girders, the LFu/LF1 ratio increases as the girder spacing increases from 4 to 8 ft. As the girder spacing increases beyond 8 ft there is a drop in the ratio. This behavior pattern is attributed to the fact that when the girders are closely spaced, all the girders will carry approximately equal percentage of the applied load. As the load is increased all the girders will tend to fail simultaneously thus the bridge has a low level of redundancy. As the spacing between the girders increase, the girders immediately below the applied load will tend to carry more of the load. The girders further away will carry less, as the load is increased and the girders below the load reach their ultimate capacity, the presence of ductility will allow the transfer the incremented load to the far girders. The transfer phenomenon will continue until all the girders

fail. The ability of the structure to transfer the load shows that a bridge configuration with moderately spaced girders has a higher level of redundancy than a structure with very closely spaced girders. When the spacing between the girders is too wide, the girders under the load will reach their crushing load before a full transfer of the load takes place. Thus, the level of redundancy of bridges with wide girder spacing will drop compared to bridges with moderate girder spacings.

The results show that the optimum bridge configuration for a two-lane bridge is a system formed by 6 beams with spacing around 6ft to 8 ft. It is interesting to note that this configuration is currently the most widely used for typical prestressed concrete I-girder bridges. The observations made herein are due to the fact that bridge failure is defined as the point at which one of the main longitudinal girders reaches its ductility limit rather than the point at which a mechanism form. The results also show that the LFu/LF1 ratio decreases slightly with the span length. This may due to the design details including the effect of member resistance to dead load, R/D, ratios.

The values for the LF100/LF1 ratio seem to follow the same trends observed above for the LFu/LF1 ratio. Actually, for each bridge configuration the LF100/LF1 value is only slightly lower than that of the corresponding LFu/LF1 value.

The LFd/LF1 ratio also follows the same trend. However, the tendencies are much more pronounced. In the sense that if the LFu/LF1 ratio decreases as the beam spacing is increased beyond 8 ft for a given number of beams, then the decrease in LFd/LF1 is even sharper. The only difference observed in the trend of the results is in the fact that there is no increase in the LFd/LF1 ratio as the spacing is increased from 4 ft to 8 ft as had been observed for LFu/LF1 and LF100/LF1.

The results of the 100, 120 and 150 ft continuous span prestressed concrete bridges with different number of beams and different beam spacings re shown in Table B-4. The analysis was performed assuming reinforced (non-prestressed) concrete sections in the negative bending regions as performed in the design example illustrated in section B-3 above. This type of designs is chosen herein because it is the most common design of continuous prestressed concrete bridges in the US. Three different loading conditions are considered for the continuous bridges. The first loading condition (case 1) assumes that only one lane is loaded by two side-by-side HS-20 trucks. This case corresponds to a failure in maximum positive bending, the vehicles are placed at 0.41 L of the span. Case 2 assumes that two spans are loaded each by one HS-20 vehicle. Case 3 assumes that the two spans are each loaded by two side-by-side HS-20 vehicles. Since cases 2 and 3 produce high levels of negative bending, the vehicles are placed at 0.57 L of each span.

The results show that for load case 1 and for the same bridge length and number of beams the LFu/LF1 ratio of continuous bridges is higher than that of the simple span bridges for small beam spacings. This means that the continuity at the middle support improves the redundancy of

the bridges with close beams. However, as the beam spacing increases, the LFu/LF1 of the continuous bridges becomes lower than that of the simple span bridges. This observation seems to reflect the different load transfer paths that the bridges have. For example, when the beams are closely spaced, as the external girder goes into the nonlinear range, the load seems to transfer transversely to the adjacent beams as well as longitudinally toward the support. On the other hand, when the beam spacing is wide, more load transfers longitudinally toward the support, and since the negative bending region has limited ductility because of the regular reinforcement, failure may occur at lower LFu/LF1 values than those of the simple span bridges. It is also noted that the LFu/LF1 ratio of load case1 is the most critical compared to the other load cases considered.

B-5. Sensitivity Analysis.

A parametric analysis is performed to study the sensitivity of the results to the assumptions made during the design of the bridge members as well as during the discretization and the nonlinear analysis of the bridge models. The simply-supported 30 m (100 ft) bridge with 6 beams at 240 cm (8 ft) and the 60 ft bridge with 8 beams at 6 ft spacings are used herein as the base cases for the sensitivity analysis. In addition, a continuous bridge with two 100 ft spans and 6 beams at 8 ft spacings is also used as the base case for the sensitivity analysis of continuous bridges. The sensitivity analysis described in this section looked at the effect of using a coarser mesh than the one proposed in the previous paragraph and the effect of changes in the points of application of the HS-20 vehicles. The effects of the presence of diaphragms at the supports, and the effect of using stiffer and stronger main elements and deck slabs were also investigated. The effect of deck skewness was checked by analyzing bridges with 15, 30 and 45 degree skews. Finally, the effect of errors in the estimate of the dead load, the maximum plastic hinge rotation and the length of the plastic hinge are also studied.

Simple span bridges

The results of the sensitivity analysis for the 100 ft simple span bridge with 6 beams are summarized in Table B-5. Table B-6 shows a similar sensitivity analysis performed on the 60 ft prestressed concrete I-beam bridge with 8 beams at 6 ft spacings. The following paragraphs present the observations made based on the results obtained in this study.

The results show that by increasing the longitudinal girder's torsional inertia of the 100 ft bridge by a factor of 4, the LFu/LF1 ratio does not change, while an 8% increase in the LF100/LF1 ratio and a 4% increase in the LFd/LF1 ratio are observed. If the slab's torsional inertia is increased by a factor of 4, then the LFu/LF1 ratio increase by about 18%, the LF100/LF1 ratio increases by 9% but the LFd/LF1 ratio increases by 74%. For the 60 ft bridge, the effect of changes in the torsional constant on the results are also insignificant while the effect of a four fold increase of the slab's torsional constant produces a change in LFU/LF1 of 20%,

LF100/LF1 increases by 11% and LFd/LF1 by 58%. These observations indicate that increasing the torsional rigidity of the slab may be an important factor in providing additional strength to damaged bridges. By doubling the torsional rigidity of the slab an improvement in LFd/LF1 on the order of 35% is expected. Such effect may be produced by the presence of diaphragms and in some cases by the presence of bracings.

Using a coarse mesh (with only 5 elements) reduces LFu/LF1 of the 100 ft bridge by 4% while LFd/LF1 reduces by 30%. The LF100/LF1 changes by about 10%. For the 60 ft bridge (shorter bridge), the rough mesh produces a change of 4% in the LFu/LF1 ratio, 5% for the LF100/LF1 ratio and only 6% for the LFd/LF1 ratio. This indicates that the meshing used in these analyses provides a reasonable level of stability in the results.

Using a spacing of 4 ft between the side-by-side trucks rather than 2 ft as was done in the base case reduces LFu/LF1 by 3% and LFd /LF1 by 2%. Moving the edge wheel line load 2 ft toward the interior of the bridge deck rather than placing it directly over the fascia girder increases the LFu/LF1 ratio by 1% and the LFd/LF1 ratio by 5% for the 100 ft bridge. The changes are 3% and 15% for the 60 ft bridge. Hence, the effect of the truck configuration and the load placement is in general not significant for the intact bridges. The lateral position of the vehicles however may be important for the damaged scenario because of the effect of the cantilever moment applied on the slab.

The effect of skews of 15, 30 and 45 degrees was investigated. The results show that having different angles of skewness did not practically affect the LFu/LF1 ratio, the LF100/LF1 ratio varies by about 5% and the LFd/LF1 ratio changes by a maximum value of 9% for the 100 ft bridge. The changes are respectively 9% and 18% for the 60 ft bridge. These results emphasize the importance of relatively "large skews" on the damage scenario of the shorter bridges. Moderate skews on the order of 35 degrees or less do not seem to produce any significant effect.

To study the effect of member capacities, the moment versus curvature curve is modified by increasing the values of the moments in the curve by 50% and effecting a similar increase in the slope of the moment-curvature curve. It is noticed that such a 50% increase in the longitudinal member capacities will decrease the LFu/LF1 ratio by about 13%. The LFd/LF1 ratio decreases by 8% for the 100 ft bridge. For the 60 ft bridge the change in LFu/LF1 is 11% and it is 16% for LFd/LF1. A 50% increase in the slab's strength (again effect by changing the ordinates of the moment-curvature curves of the slab members) increases LFu/LF1 by 4% and 3% for the 100 ft and the 60 ft bridges. The increase in LFd/LF1 is about 14% for both bridges. If the 50% increase in strength is also associated with a 50% increase in moments of inertia, negligible changes in the L/LF1 ratios are observed. Increasing the slab's inertias as well as the slab's strength by 50% produces an additional increase of 4% and 1% in LFu/LF1 and 10% and 7% in LFd/LF1 for the 100 ft and the 60 ft bridges respectively. If the 50% increase in the girder's inertias and strength is accompanied by a 50% increase in dead load, the LFu/LF1 ratio increases by 4% and 2% relative to the case where the girder's strength and inertias are increased without a corresponding increase in dead load. The LF100/LF1 decreases by 2% and 0%. On

the other hand, LFd/LF1 decreases by 19% and 6%. These results indicate that the effect of changes in the moments of inertias of the bridge members produces negligible change in the results. However, changes in the strength of the slab and the longitudinal members may produce some change in the final results. The effect of the slab's strength is only significant for the damaged scenario. On the other hand, the effect of changes in the longitudinal members' strength will affect the results of both the intact and damaged bridges.

Placing a diaphragm at the ends of the simple span, increases LFu/LF1 by only 2% to 3%, but increases LFd/LF1 by 19% for both the 100 ft and 60 ft bridges. These results are similar to the effects of increasing the strength of the slab.

To study the effect of member ductility on the results, the effect of the maximum plastic hinge rotations is analyzed. The maximum plastic hinge rotation as used in this study defines the point at which concrete crushing occurs in a longitudinal member. The maximum plastic hinge rotation is defined as the curvature at concrete crushing multiplied by the length of the plastic hinge. The higher the maximum plastic hinge rotation is, the higher is the load that can be carried by a member before it crushes. Thus, the maximum plastic hinge rotation models the effects of member ductility. In this analysis, a 50% increase in the maximum plastic hinge rotation is assumed but the length of the plastic hinge remains at its initial value. In this case, it is observed that the LFu/LF1 ratio increases by 10% and 14% (for the 100 ft and 60 ft bridges) while the LFd/LF1 ratio increases by 35% and 23%. Therefore, the effect of member ductility may be important especially for damaged bridges.

A 40% increase in the assumed length of the plastic hinge, without a corresponding change in the maximum plastic hinge rotation, reduces LFu/LF1 by 4% to 5% and LFd/LF1 by about 8% to 6%. This indicates that the results are insensitive to the effect of changes in the length of the plastic hinge if the maximum plastic hinge rotation remains unchanged.

To check the effect of the number of lane loaded, the 100 ft bridge was analyzed assuming that only one HS-20 vehicle is applied on the bridge. The one vehicle is placed such that its external wheel load is placed over the external girder. Another analysis looked at the effect of having three lanes loaded. In this case three side-by-side HS-20 were placed on the bridge and incremented. The results show that the LFu/LF1 ratio varies from 2.03 for one lane, to 1.69 for two lanes to 1.61 for three lanes. The LF100/LF1 ratio varies from 1.39 to 1.17 to 1.15. Finally the LFd/LF1 ratio varies from 0.83 to 0.65 to 0.68. These results show that although there is a noticeable difference between the results of one lane and those of two lanes, the maximum difference between the results for two and three lanes is less than 5%.

To study the effect of the number of beams, the same 100 ft bridge studied above is now assumed to be formed by two longitudinal beams. Each of the beams is assumed to have the same strength as three beams of the original bridge such that the sum of the strengths in the bridge remains constant. The analysis of NONBAN uses two side-by-side trucks located in the same location as for the 6-beam bridge. The value for LF1 obtained for the two-girder bridge is

equal to 3.44, LFu is 4.63, LF100 is 3.60 and LFd is 1.31. The load factor ratio LFu/LF1 becomes 1.35, the LF100/LF1 is 1.04 and LFd/LF1 is 0.38. These values are compared to LFu=5.28, LF100=3.63 and LFd=2.05 and LF1=3.67 with LFu/LF1=1.44, LF100/lF1=0.99 and LFd/LF1=0.56 for the six-beam bridge. This shows a drop in LFu/LF1 on the order of 7% and a drop in LFd/LF1 on the order of 32% for the two-beam bridge compared to the six-beam bridge. The calculations performed herein show that the slab (along with the contributions of cross beams, stringers and other secondary members) will permit the transfer of the load to only one beam of the bridge. Notice that the bridge analyzed herein would correspond to a bridge with two beams at 24 ft spacings. By comparing the results obtained for the two-beam bridge to the results of the four beam bridge at 12 ft spacings or the six-beam bridge at the 12 ft spacings (the largest spacings studied in Table B-3), it is observed that the LFu/LF1 and LFd/LF1 ratios from all these cases are somewhat similar. For example the LFu/LF1 for the 12 ft spacings is on the order of 1.37 to 1.39 versus 1.35 for the 24 ft spacing and the LFd/LF1 is 0.45 to 0.47 compared to 0.38. This confirms the observation made earlier that: As the spacing between beams increases, the effect of the number of beams becomes irrelevant and redundancy will solely depend on the spacing itself. The drop in the LFu/LF1 as the spacing goes from 12 ft to 24 ft is small but the effect on Lfd/LF1 is larger.

Finally, to check the effect of the damaged scenario on the results, different analyses were performed where the 100 ft bridge with 6 beams at 8 ft spacings was analyzed assuming that all the external girder is damaged (i.e. the external girder's moment of inertia is practically zero along the whole length of the girder), the middle 80% of the external girder is damaged (i.e. the middle 8 elements out of a total of ten elements representing the external girder have a moment of inertia practically equal to zero), the middle 60% is damaged, the middle 40% is damaged and the middle 20% is damaged. The results of the analysis represented by the load versus deformation plot are shown in Figure B-8. The label "2 elements" indicates that this scenario assumes that 2 out of ten elements are assumed to be damaged. Figure B-8 illustrates how the P-delta curve softens as the extent of damage increases. Due to errors in modeling the damaged scenario, the value of LFd are not always consistent. i.e. although the curve with 4 elements damaged is softer than the one with two elements damaged, the value of LFd for the former scenario is actually slightly lower than that of the latter. The errors are due to the discontinuities in the mesh introduced by the assumed damage, the effect of high torsional loads and cantilever moments introduced when the external girder (or a part of it) is damaged and errors in estimating the maximum plastic hinge rotation at which failure occurs. The LFd values range from about 2.1 to about 2.6. The deflection at which failure occurs ranges from about 34 in to about 47 in.

To check the robustness of the criteria chosen in this study to define bridge functionality (i.e. the L/100 criteria), the values obtained for the load factors corresponding to a maximum displacement of L/200 (LF200) are compared to the load factors corresponding to a maximum displacement of L/100 (designated as LF100 in the table) and the load factors corresponding to a maximum displacement of L/300 (designated as LF300 in table). The results indicate that the LF100/LF1 ratio remains reasonably stable throughout the sensitivity analysis. As a matter of fact the LF100/LF1 ratio remains between 0.95 and 1.08 for all the parametric changes

performed for simple span bridges. Thus, the LF100/LF1 ratio appears to provide a more robust measure of system redundancy than either the LF200/LF1 or even the LFu/LF1 ratios.

In summary, the results of the sensitivity analysis indicate that the mesh used provides reasonably stable results. Also, it is observed that the results are not affected by small changes in the lateral truck position. Similarly, the effect of small changes in the deck slab capacities are insignificant. The presence of a diaphragm at each support does not improve the results obtained for the intact bridges. However, the presence of the diaphragm improves the overall system capacity and redundancy of damaged bridges.

It is generally noticed that the observations made for the 100 ft bridge and the 60 ft bridge are consistent. The magnitude of the changes in the LFu/LF1 ratio of the two bridges for the sensitivity cases analyzed are also generally consistent for the two bridges. Although, showing similar trends, the magnitude of the changes in the LFd/LF1 ratios obtained as a result of the parametric changes are somewhat different for the 60 ft bridge compared to the 100 ft bridge. Some of these differences may be due to the effect of span to width ratios, the effect of resistance to dead load ratio and other design parameters. Also, the results of the damage scenario are generally more sensitive to the slab model used.

Continuous bridges

Results of the sensitivity analysis performed on the continuous bridges are shown in Table B-7. The continuous bridges analyzed are formed by two spans of 100 ft each. Each span is formed by 6 girders at 8 ft spacings. The continuous bridges are assumed to have regular (non-prestressed) reinforcements in the negative bending region which was designed to only carry the superimposed dead load and the AASHTO HS-20 live load.

The LFu/LF1 ratio of the 100 ft simple span bridge is 1.44 compared to the 1.41 value obtained for the continuous bridge. The LFd/LF1 ratio of the continuous bridge is 0.40 compared to 0.56 for the simple span bridge. This indicates that the effect of span continuity for prestressed concrete bridges will produce little change in the redundancy of intact bridges, but would reduce the redundancy for the damage scenario unless additional ductility is provided in the negative bending region as will be further discussed in this section.

If the maximum plastic hinge rotations of the positive bending region is increased by 50%, the value of LFu does not change but LFd increases by 6%. If the maximum plastic hinge rotation for the negative bending region is increased by 50%, LFu increases by about 11%. When both maximum plastic hinge rotations are increased by 50% the increase in LFu is of 11% while the increase in LFd is by 38%. Changes in the maximum plastic hinge rotations will not produce any change in LF1 because LF1 is calculated from the results of the linear elastic analysis. The observations made herein indicate that the effect of ductility in the negative bending region is a controlling factor for continuous bridges. Thus, bridges designed with high levels of ductility in

the section over the support will show improvement in redundancy. Bridges with low levels of ductility over the support will show lower levels of redundancy than simple span bridges especially for the damaged conditions.

Errors in the estimate of the length of the plastic hinge Lp of 40% will produce a change in LFu/LF1 on the order of 3%. The change in LFd/LF1 is on the order of 2% to 4% and LF100/LF1 changes by about 7%. This analysis is performed by changing Lp only without a corresponding change in the maximum plastic hinge rotation.

When the strength and stiffness of the slab is increased by 50%, the change in the LFu/LF1 value changes by about 4%. On the other hand, the LFd/LF1 ratio changes by up to 26% This is confirming the contribution of the slab (and by extension the presence of diaphragms) to the redundancy of heavily damaged bridges.

When the strength and stiffness of the longitudinal girders in both positive and negative bending is increased by 50%, the LFu/LF1 ratio decreases by about 9% for load case 1. For load case 3 the ratio increases by 8%. The effect of this change on the LFd/LF1 ratio is of 14% for load case 1 and 28% for load case3. If the girder's moments of inertia and only the positive bending strength is increased by 50% then the LFu/LF1 for load case 1 increases by only 2% and the LFd/LF1 increases by 23%. The change in LFd/LF1 is 23% for load case 1. The LFu/LF1 value for load cases 2 and 3 increase by up to 48% and LFd/LF1 increases by up to 68%.

If the negative bending strength is increased by 50% while the girder's stiffness is increased by 50%, then the LFu/LF1 ratios of load case 1 increases by 22% and LFd/LF1 by 41%. On the other hand, for load cases 2 and 3 LFu/LF1 decreases by 26% to 22% and the LFd/LF1 ratios decrease by 19% to 15%. The decrease in the ratios for load cases 2 and 3 is due to the fact that the increase in the stiffness and strength in the negative bending region is accompanied by an increase in LF1 as well as LFu and LFd. However, the increase in LF1 is much higher than that in LFu or LFd.

The presence of a 30 degree skew improves LFu by 4% for load case1. This is also associated with 2% increase in LF1 such that the LFu/LF1 ratio changes by about 2%. The other load cases produce a change in LFu of less than 2%. The largest observed change is 8% on LFd/LF1 of load case 2.

The analysis of the continuous bridges shows that the two-span continuous bridges produce lower system redundancy than simple span bridges except if the support is provided with additional ductility. This additional ductility is manifested by having sections with high maximum plastic hinge rotations. Additional ductility could be provided for example by placing sufficient shear reinforcement to increase the maximum allowable maximum plastic rotation compared to a section without shear reinforcement. Other factors of primary importance to the redundancy of continuous bridges are the strengths of the girders in both positive and negative bending.

B-6. Reliability Analysis and Calibration of Redundancy Factors.

Reliability Analysis

The calibration of the AASHTO LRFD code was performed by studying the reliability of bridge members assuming that bridges behave in a linear elastic manner. The purpose of the reliability analysis performed in this study is to obtain an objective estimate of the safety of the bridge systems analyzed accounting for their nonlinear behavior. By comparing the safety performance of a bridge system accounting for its nonlinear behavior to the performance of its most heavily loaded members assuming linear elastic behavior, a measure of the redundancy of the system is obtained. The reliability analysis undertaken in this study is performed using a Level II reliability program which accounts for different types of probability distributions. It should be noted that in previous reports, a lognormal model was used. With the lognormal model all the random variables are assumed to follow lognormal distributions. The Level II program used herein is capable of accounting for different types of probability distributions and thus the results will be more compatible with those of the LRFD calibration procedure. This section, and also as seen in Chapter 2, discusses the issue of using a lognormal versus a Gumbel distribution during the reliability analysis and demonstrates the lack of sensitivity of the results to the type of probability distribution used.

To illustrate how the reliability calculations are performed for the purposes of this study, the results of the base case of the 100 ft bridge with 6 beams at 8 ft are presented herein. The calculations of the linear elastic system indicate that the external member fails when the two HS-20 vehicles placed on the bridge are incremented by a factor LF1= 3.67. The nonlinear system's ultimate capacity on the other hand is reached when the weights of the HS-20 vehicles are incremented by a factor LFu=5.28.

To perform the reliability analysis, the statistical information on the loads applied on the bridge and the resistance of the system are required. As performed in this study, the resistance of the intact system is expressed in terms of the load multipliers LFu for the ultimate capacity, LF100 for the functionality criteria, and LF1 for first member failure assuming linear elastic behavior.

The load factors obtained from the nonlinear analysis express the capacity of the intact system to carry the live load. This capacity is obviously a function of the applied dead load and the member resistances. For prestressed concrete members, Nowak [B-7] suggests that the average member capacity is actually 1.05 the nominal design capacity (resistance bias =1.05). The member resistances are also associated with a coefficient of variation COV equal to 7.5%. The COV is defined as the ratio of the standard deviation and the mean of the variable. The COV gives a description of the statistical spread of the values that the random variable could take in comparison to the average value.

Nowak [B-7] assumes that the dead loads applied on the structure will have a bias that varies between 1.03 and 1.05 with a COV between 8% and 10% depending on whether we are considering factory-made members, cast in place members or other items. (Nowak also uses a COV of 25% for asphalt material and assumes that the average asphalt thickness is about 3.5 in). Based on these observations it is herein assumed that on the average, the total combined dead load effects will have a bias on the order of 1.05 and a COV on the order of 10%.

To calculate the bias and the COV of the load factor LF1, equation B-4 is used. The variable DF1 of equation B-4 gives the load distribution factor i.e. the percentage of the load carried by the most heavily member compared to the total load applied. This variable is not explicitly discussed by Nowak. However, field data taken in reference [B-10] suggest that the load distribution factor has a COV of about 8% if the traffic lanes are preset. Obviously, changing the lane positions will also change the load distribution factor. However, as explained earlier, the structural analysis performed in this study assumes that the vehicles are placed in one of the most critical lane positions. Therefore, to be consistent with Nowak's model, it is herein assumed that DF1 as calculated in this study is a deterministic variable with (i.e. the bias is equal to 1.0 and the COV is equal to 0.).

Keeping in mind the fact that the mean of the sum (or the difference) of two random variables is equal to the sum (or the difference) of their means, Equation B-4 is also valid to find the mean of LF1 given the means of R, D. (LLHS20 is a deterministic variable and as such has a COV of 0% and a bias equal to 1.0). Also, knowing that the COV of a random variable is the ratio of the standard deviation divided by the mean of the variable, the COV of the variable LF1 can also be calculated using equation B-4. The calculation is performed using the fact that the standard deviation of the sum or the difference of two random variables is equal to the square root of the sum of the squares of the standard deviations. For example, with R=84993 kip-in and D=34200 kip-in and LLHS20=13830 kip-in the value of LF1 is 3.67. To find LF1 the mean of R is obtained by multiplying R by the bias. For prestressed concrete the bias is 1.05, then, the mean of R R=84993x1.05=89243 kip-in. The mean of D is 34200x1.05=35910 kip-in. Using LLHS20 of 13830 kip-in and plugging in R mean and D mean in equation B-4 will yield a mean value of LF1 equal to 3.85. The bias in LF1 becomes 3.85/3.67=1.05. These calculations are illustrated in the following equations:

$$\overline{LF_1} = \frac{\overline{R} - \overline{D}}{DF_1 \quad LL_{HS\text{-}20}} = \frac{1.05 \times 84993 - 1.05 \times 34200}{13830} = 3.85 \qquad \text{(B-7)}$$

To find the standard deviation of LF1 we take the standard deviation of R (84993x1.05x7.5%) and the standard deviation of D (34200x1.05x10%), sum the square of each of these variables. Take the square root of the sum of the squares and then divide by 13830 kip-in. This will yield a

standard deviation equal to 0.549. The COV of LF1 is 0.549/3.85 which is 14.3%. This is illustrated as:

$$COV_{LF_1} = \frac{\sigma_{LF_1}}{\overline{LF_1}} = \frac{\dfrac{\sqrt{\sigma_R^2 + \sigma_D^2}}{DF_1 \quad LL_{HS\text{-}20}}}{\overline{LF_1}} \tag{B-8}$$

$$= \frac{\dfrac{\sqrt{(0.075x1.05x84993)^2+(0.1x1.05x34200)^2}}{13830}}{3.85} = 14.3\%$$

In his calibration process, Nowak [B-7] uses a maximum lifetime live load for a 75 year life span of the bridge. This produces a maximum moment for the 100-ft equivalent to that obtained by 1.89 times the effect of two HS-20 vehicles. The 1.89 factor accounts for the dynamic impact (1.10 for two lanes of traffic) as well as the static moment effect (1.72). Nowak also suggests that the applied live load (including impact effect) is associated with a coefficient of variation equal to 19% for the 100 ft bridge. If we assume that both LF1 and the 75 year maximum lifetime load follow lognormal distributions, then the safety index β_{member} can be calculated as:

$$\beta_{member} = \frac{\ln \dfrac{LF_1}{LL_{75}}}{\sqrt{v^2_{LL} + v^2_{LF}}} = \frac{\ln \dfrac{3.85}{1.89}}{\sqrt{0.14^2 + 0.19^2}} = 2.99 \tag{B-9}$$

Equation B-9 uses a lognormal model to illustrate the procedure followed. However, the reliability calculations performed herein use the statistical data given above but assume that the LF1 factor follows a lognormal distribution while the applied load follows a Gumbel distribution. Using a Gumbel distribution for the load rather than the lognormal distribution used in equation B-6 produces a safety index for member failure equal to 2.84 rather than 2.99. The 2.84 value is the safety index for a bridge member designed to satisfy the LFD criteria. The calculations performed herein use the load distribution factor obtained from the grid analysis using NONBAN and the loading conditions described above. The reliability calculations used herein are performed with a Level II reliability program. A Level II procedure calculates the reliability of a structural member or a structural system by transforming the probability distributions of the random variables into equivalent normal distributions.

To calculate the reliability of the whole system, it is herein assumed that LFu follows a lognormal distribution and is associated with the same bias as that of LF1 and the same COV. This assumption is somewhat subjective but is based on the assumption that the mean resistance of a system can be approximately equal to the system resistance obtained by using the means of the member resistances during the structural analysis. On the other hand, it is well known that the COV of the system is usually smaller than the COV of the individual members. However, this assumes that the structural model and system analysis process is exact. To account for the uncertainties in the structural modelling process while performing a nonlinear analysis, it is suggested to conservatively use a COV on LFu equal to the COV on the member resistances as represented by LF1. The same logic is followed while calculating the safety index for the functionality and the damaged limit states i.e. for LF100 and LFd.

The safety index obtained for system failure of the 100 ft prestressed concrete bridge is 4.08. This shows that the reliability of this bridge system produces a safety index higher than that of its most critical member by 1.24. As mentioned in Chapter 2 of this report, the difference between the reliability of the system and that of the first member to fail is used in this study as a probabilistic measure of redundancy. The calculations performed for the simple span prestressed concrete I-beam bridges studied in this project are shown in Table B-8.

All the reliability calculations performed herein use the statistical data given above and assume that the LF1 factor follows a lognormal distribution while the applied load follows a Gumbel distribution. The safety index for the first member failure is symbolized by β_{member}. The safety index for the ultimate limit state is defined as β_u. As mentioned earlier, β_u is calculated assuming that the LFu of the system follows a lognormal distribution with a bias equal to that of LF1 and a COV equal to that of LF1 (see Chapter 2). The same logic is herein followed to calculate the reliability index for the functionality, $\beta_{funct.}$, and the damaged limit states, β_d.

As mentioned in Chapter 2, the difference between the reliability of the ultimate capacity of the system and that of the first member to fail, $\Delta\beta_u$ (defined as β_u-β_{member}) is used in this study as a probabilistic measure of redundancy for the ultimate limit state. $\Delta\beta_f$ is defined as $\beta_{funct.}$ - β_{member}, and it gives the difference between the safety index of the system for the functionality limit state (i.e. for LF100) and that of the member. Finally, $\Delta\beta_d$ defined as $\beta_{damaged}$-β_{member}, and it gives the difference between the reliability of the damaged system (LFd) and that of the member of the intact system. These values are used herein as probabilistic measures of redundancy and are presented in Table B-8 for the simple span prestressed oncrete I-beam bridges analyzed in this study.

The results of the safety indices obtained for individual bridge members are somehow lower than those obtained by Nowak [B-7] because as explained above, the load (girder) distribution factors obtained in this study are more conservative than those used by Nowak. In any case, the actual values obtained here will not affect the final results of the study. This is because the reliability criteria used herein are normalized relative to the members indices. That is, the system

factors proposed in this study are calibrated based on the difference between the reliabilities of a system and those of the members.

Determination of Redundancy Criteria

Table B-8 gives the reliability indices obtained in this study for the simple span prestressed concrete bridges. The results show that for the ultimate limit state, the system reliability is on the average higher than the member reliability by 1.07 for all the simple span bridges considered. This means that $\Delta\beta u$ which was defined in the phase I report as a probabilistic measure of redundancy is on the average equal to 1.07. If one studies the performance of four beam bridges only, then the average value of $\Delta\beta u$ for these bridges is 0.79. Four beam bridges with spacings greater than 4 ft produce an average $\Delta\beta u$ equal to 0.97. Steel I-beam bridges with four beams with greater than 4 ft spacings produced an average $\Delta\beta u$ value equal to 0.72. In traditional bridge engineering practice all four beam bridges are considered to be redundant. Since 4 beam bridges with 4 ft are not normally used to carry two lanes of traffic, therefore, it is herein proposed to use a $\Delta\beta u$ value of 0.85 as the redundancy criterion for the ultimate limit state. That is, a bridge will be herein defined as sufficiently redundant if the reliability index of the system is higher than that of the member by at least 0.85. The 0.85 value is obtained as the average value of steel and prestressed concrete I-beam bridges with four beams spaced at more than 4ft center to center.

The average $\Delta\beta_f$ value obtained for all the simple span bridges studied for the functionality limit state is 0.08. The four beams with spacings greater than 4 ft produce an average $\Delta\beta u$ equal to 0.0. The steel bridges produced a $\Delta\beta_f$ with four beam at more than 4 ft of spacing. Therefore, the proposed redundancy criterion for the span length/100 limit state is 0.25.

For the damaged limit state, the average difference $\Delta\beta d$ between the damaged system's safety index and the member safety index of the intact system is -1.92. The four-beam bridges at spacings of 4 ft or more produce an average $\Delta\beta d$ equal to -2.40. This value is slightly lower than the -3.0 value obtained for steel bridges. The difference seems to be due to the effect of design details such as the effect of the dead loads. It is herein suggested to use a consistent value for both concrete and steel bridges. Therefore, it is herein proposed to use a value of -2.70 as the redundancy criterion for damaged bridges. The calculation for the damaged limit states uses a two-year return period rather than the 75 year return period. As mentioned in Chapter 2, a two-year period is chosen herein because it corresponds to the biennial inspection period. This two-year period implicitly accounts for the fact that if a bridge is so damaged that its external girders is knock out of service, it would be noticed and rehabilitate within the two-year period.

The redundancy criteria chosen herein will be used in the next paragraph to calibrate the proposed redundancy factors.

Calibration of Redundancy Factors

Redundancy factors are calibrated in this study such that bridges having configurations that do not provide sufficient levels of redundancy are penalized by requiring their individual members to provide higher levels of safety than those of bridges with sufficiently high levels of redundancy. On the other hand, bridges with high levels of redundancy are rewarded by allowing a lower level of member safety. This is performed by introducing redundancy factors in the design or safety-check equations. This study proposes to introduce a system redundancy factor on the resistance side of the design-check equation such that:

$$\phi_s \, \phi \, R = \gamma_d \, D + \gamma_l \, L \qquad \text{(B-10)}$$

where ϕ_s is the system redundancy factor, ϕ is the member resistance factor, R is the resistance capacity of the member, γ_d is the dead load factor, D is the dead load effect, γ_l is the live load factor, and L is the nominal (design) live load effect on an individual member (including dynamic impact). When ϕ_s is equal to 1.0 equation (B-7) becomes the same as the current design equation. If ϕ_s is greater than 1.0 this indicates that the system's configuration provides sufficient level of redundancy. When it is less than 1.0 then the level of redundancy is not sufficient.

The values obtained for $\Delta\beta u$, $\Delta\beta f$ and $\Delta\beta d$ can be used to calibrate redundancy factors for these three limit states for each bridge configuration analyzed in this study. For example, the procedure is illustrated using the results of the reliability analysis performed in the previous section for the 100 ft prestressed concrete I-beam bridge with 6 beams at 8 ft spacings. The results obtained for this particular bridge configuration shows that the difference between the safety indices of the ultimate limit state and the member is 1.24. Because 1.24 is greater than the 0.85 target value set in the previous paragraph, this bridge provides a sufficient level of redundancy for the ultimate limit state. Therefore, the safety index of this bridge's members could then be reduced by 0.39 while still satisfying the redundancy requirements. To lower the member safety index by 0.39 (from 2.84 to 2.45), it is sufficient to lower the LF1 factor down to a value of 3.24. The 3.24 was determined by trial and error using the reliability analysis program. It is herein suggested that a value of LF1 equal to 3.24 is sufficient to provide an adequate level of redundancy. Looking at Equation (B-4), it is noted that to reduce LF1 to a value of 3.24, assuming that D and DF_1 remain unchanged, the required moment capacity R should be reduced to 79050 kip-in. This value is 7% smaller than that required by the current LFD code. To achieve this 7% reduction, the system factor ϕ_s required in equation B-7 is equal to 1.07.

Values of ϕ_s factors for the simple span bridges are shown in Table B-9 for the three limit states studied. In addition ϕ_s factors for the LF100 limit state are also shown. The results show that for a given beam spacing, the ϕ_s factor (i.e. the bridge redundancy) increases as the number

of beams is increased. This increase however reaches a plateau at 6 beams, meaning that if the number of members is increased beyond 6 beams, no major improvement in bridge redundancy is observed.

On the other hand, for a given number of beams, the ϕ_s factor increases as the beam spacing is increased from 4ft to 8ft. But the factor decreases as the beam spacing is increased beyond 8 ft. This trend is explained by the fact that for narrow bridges, all the beams are almost equally heavily loaded and there is no reserve strength in the sense that if a beam fails all the beams will quickly follow suit. However, as the beam spacing is increased, some of the members that are less heavily loaded will pick up the load as some of the most heavily loaded members begin to fail. As the spacing becomes very large, the capacity of the slab to transfer the load decreases and very damage of the heavily loaded members occur before a complete transfer of the load is possible. This observation is evident because the nonlinear analysis performed herein does not allow for the formation of a full mechanism. Many previous studies on bridge system reliability and nonlinear behavior of bridges assume that bridge members have infinite levels of ductility and that system failure occurs when a mechanism is formed. In this study, system failure is assumed to occur when one of the longitudinal members exhibits very high level of damage represented by its reaching a maximum plastic hinge rotation. As discussed before this criterion is more consistent with laboratory and field experimental practice.

The results also show that in general, there is a tendency of the ϕ_s factors to decrease with span length. This is because the longer the span, the more evenly distributed is the load to all the bridge members. The changes in the ϕ_s factors with number of beams and beam spacings are observed to be similar whether we look at the ultimate limit state, the functionality limit state or the damaged limit state tables.

From the results it seems that the most optimum design for two-lane bridge as far as redundancy is concerned is 6 beams at 8 ft spacings. It is interesting to note that this configuration is currently the most widely used configuration for two-lane bridges.

Tables B-10,B-11, and B-12 give the reliability indices and the system factors for the simple span prestressed concrete bridges analyzed as part of the sensitivity analysis and for the prestressed continuous bridges. The results confirm the observations made above for the LFu/LF1, LF100/LF1 and LFd/LF1 ratios. In fact, if one looks at equation B-6, one notices that the $\Delta\beta$ values are directly related to the L/LF1 ratios. Although a second level reliability analysis is performed herein, the example illustrated in the paragraph on Reliability analysis of this section shows that the results of equation B-6 and the second level reliability analysis are similar.

B-7. Conclusions

This appendix gives a detailed description of the analysis and calibration of redundancy factors for prestressed concrete I-beam bridges. The factors are calibrated using a reliability procedure such that bridges that do not have sufficient levels of redundancy are penalized by requiring their members to have higher levels of safety than comparable redundant designs. On the other hand, bridges with high levels of redundancy are rewarded by allowing their members to have lower safety factors than normally required by current design and evaluation methods.

B-8. References

B-1. West R., "C&CA/CIRIA Recommendations on the Use of Grillage Analysis for Slab and Pseudo-Slab Bridge Decks", London Cement & Concrete Association and Construction Industry Research and Information Association, 1973.

B-2. Jaegar, L.G. and Bakht, B., "The Grillage Analogy in Bridge Analysis", Canada Journal of Civil Engineering, Vol. 9, National Research Council of Canada, 1982.

B-3. Hambly, E.C., "Bridge Deck Behaviour", Chapman and Hall, Ltd., London, 1976.

B-4. Zokaie T., Osterkamp, T.A., and Imbsen R.A., "Distribution of Wheel Loads on Highway Bridges", Final Report, NCHRP project 12-26/1, March 1991.

B-5. Gosbell K.B. and Stevens L.K., "Test Loading of a Full Scale Bridge", Australian Research Board, Proceedings, Vol. 4, Part 2, 1968 pages 2018-2041.

B-6. Burdette E.G. and Goodpasture, D.W., "Full Scale Bridge Testing - An Evaluation of Bridge Design Criteria", University of Tennessee, December 1971.

B-7. Nowak, A.S., "Calibration of LRFD Bridge Design Code", NCHRP project 12-33, May 1992.

B-8. Ghosn M. and Moses F., "Redundancy in Highway Bridge Superstructures", Report NCHRP 12-36, TRB, Washington DC, March 1994.

B-9. AASHTO, LRFD Bridge Design Specifications, First Edition, Washington DC, 1994.

B-10 Ghosn M. and Moses F., "Bridge Load Modeling and Reliability Analysis", Case Western Reserve University, Cleveland, Ohio, 1984

B-11 Cornell, C. A., "Risk-Based Structural Design", Proceedings of a Symposium on Risk Analysis, Department of Civil Engineering, University of Michigan, Ann Arbor, MI, August 1994.

B-12 Nilson, A.H., Winter, G. Design of Concrete Structures, 11 th. Edition, Mc Graw Hill, 1991.

B-13 Park, R. and Pauley, T., Reinforced Concrete Structures, Wiley & Sons, New York, 1975.

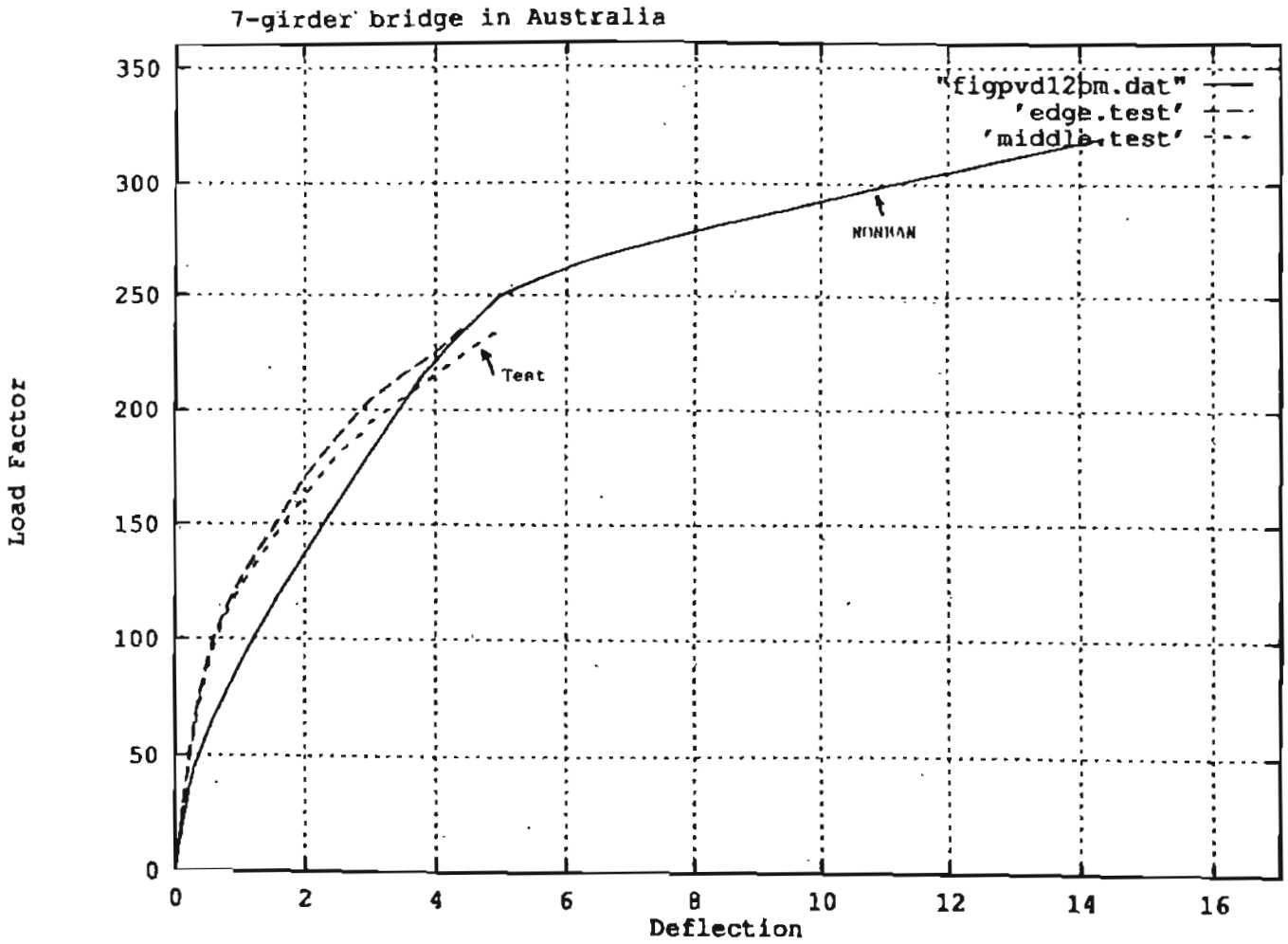

Figure B.1 Comparison of NONBAN to Experimental Results of Gosbell and Stevens [B-5]
(Lp = d and all dead load on composite section)

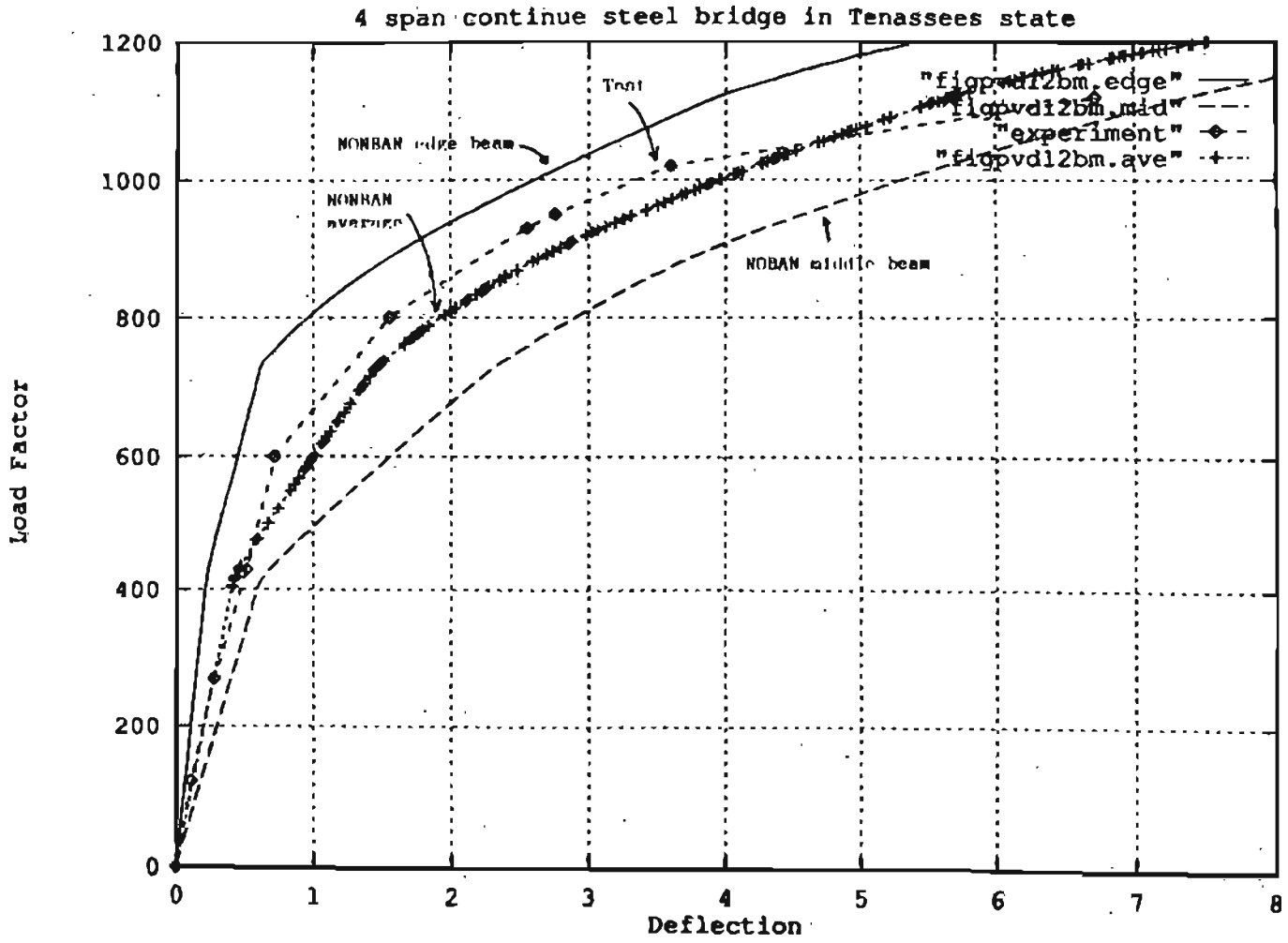

Figure B-2 Comparison of NONBAN Results to Experimental Results of Burdette and Goodpasture. [B-6]
(M-phi curve from reference B-6)

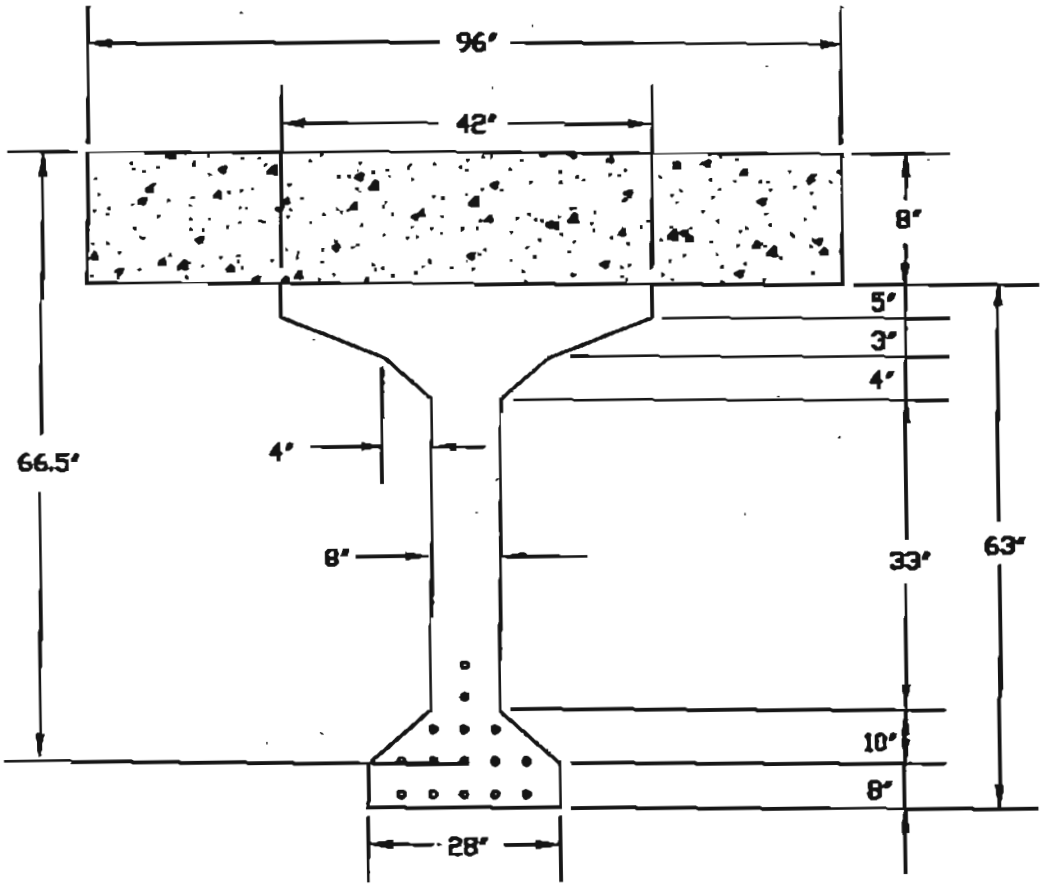

Figure B-3 Cross Section of Example 100 ft Simple Span Bridge with 6 beams at 8ft.

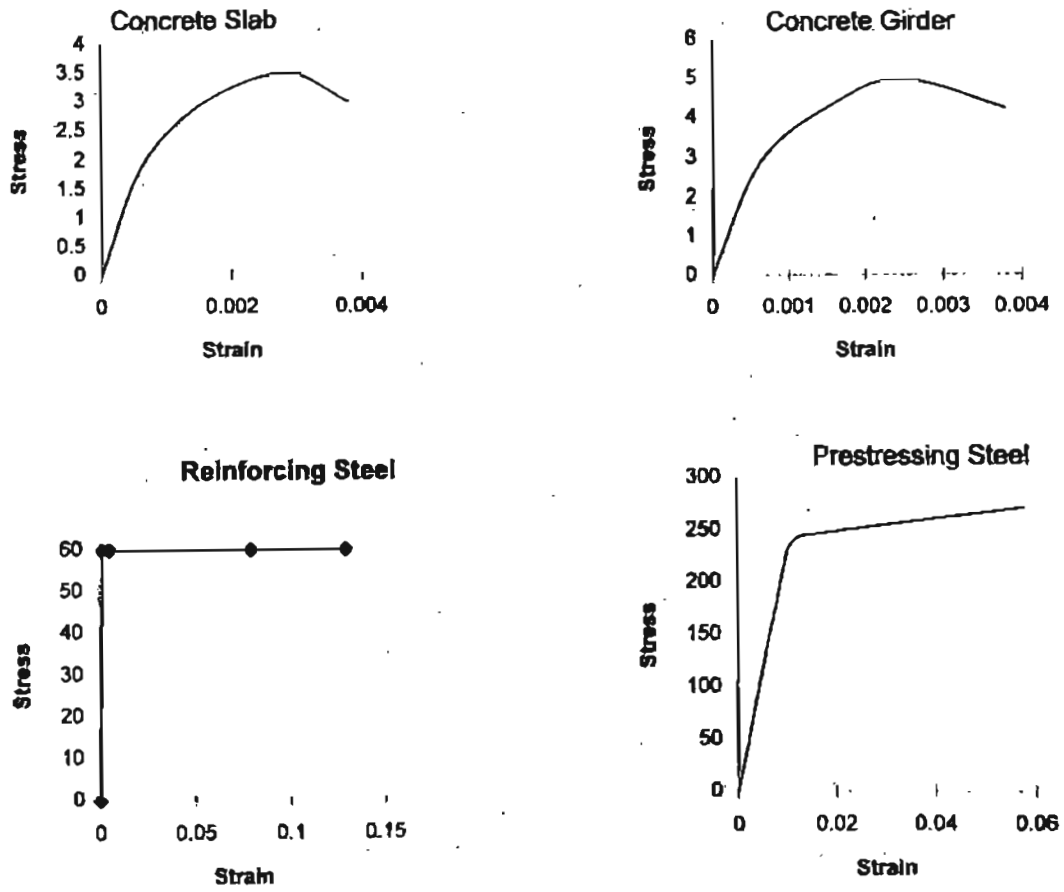

Figure B-4. Stress-strain diagrams of materials

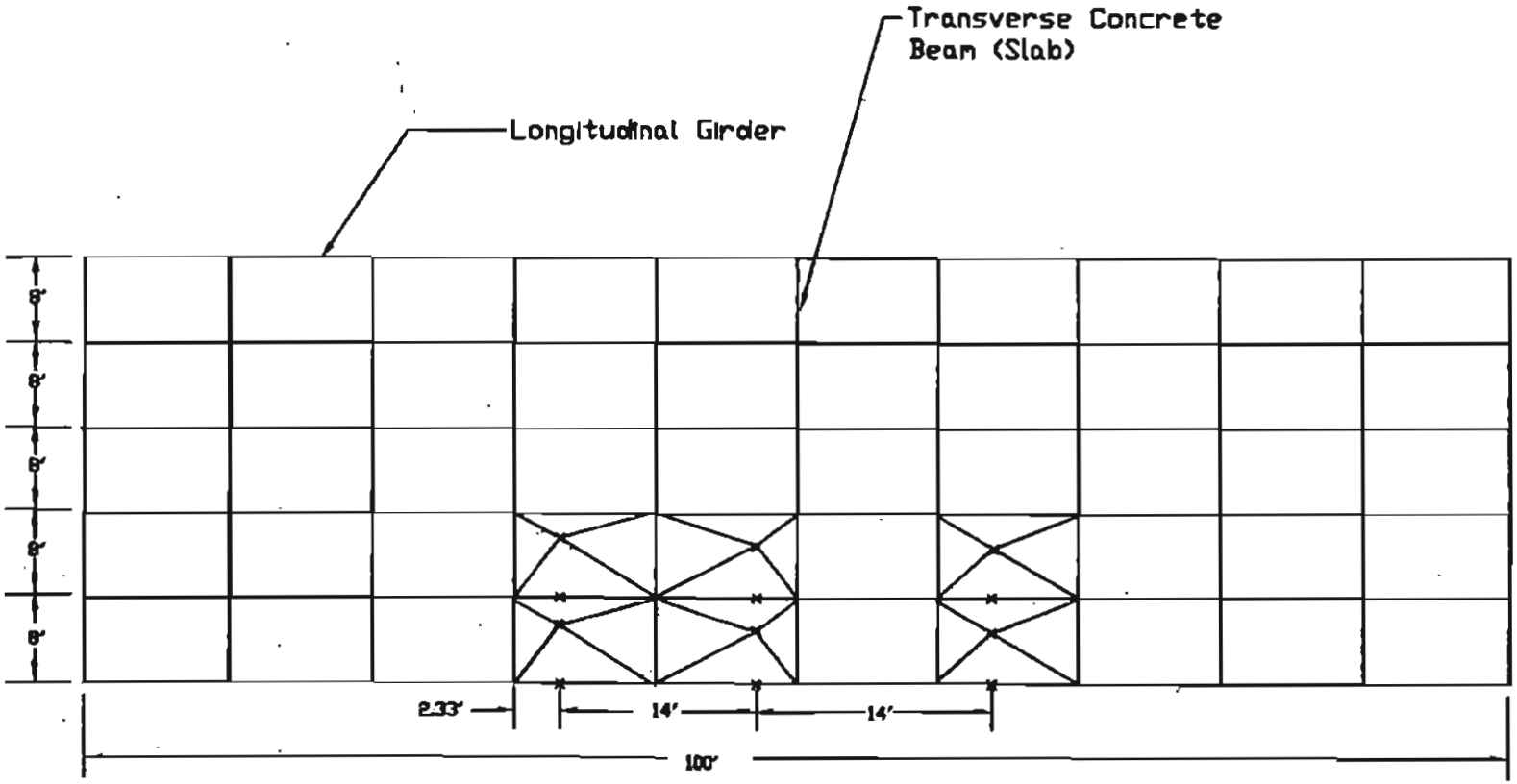

Figure B.5 Plan View of Mesh used in the Analysis of 100 ft Bridge.

Composite Prestressed Concrete Section

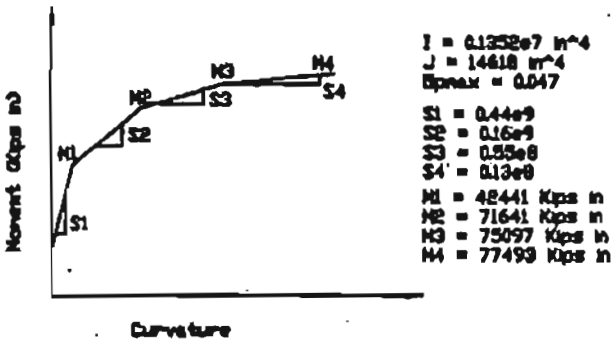

Transverse-Concrete Edge Beam (Slab)

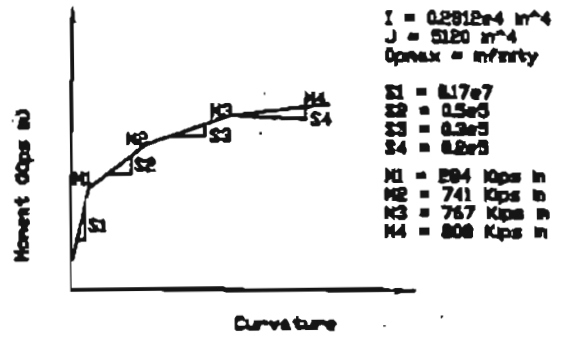

Transverse Concrete Interior Beam (Slab)

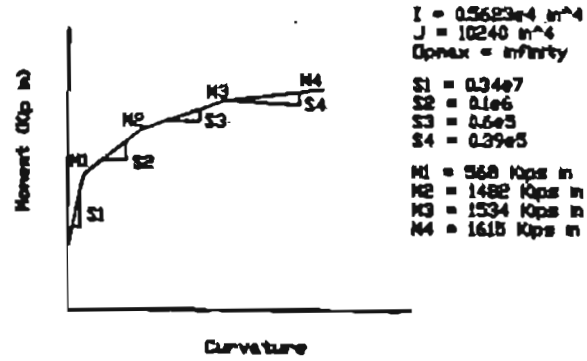

Figure B.6 Material Properties of Prestressed Concrete Members of 100 ft Bridge

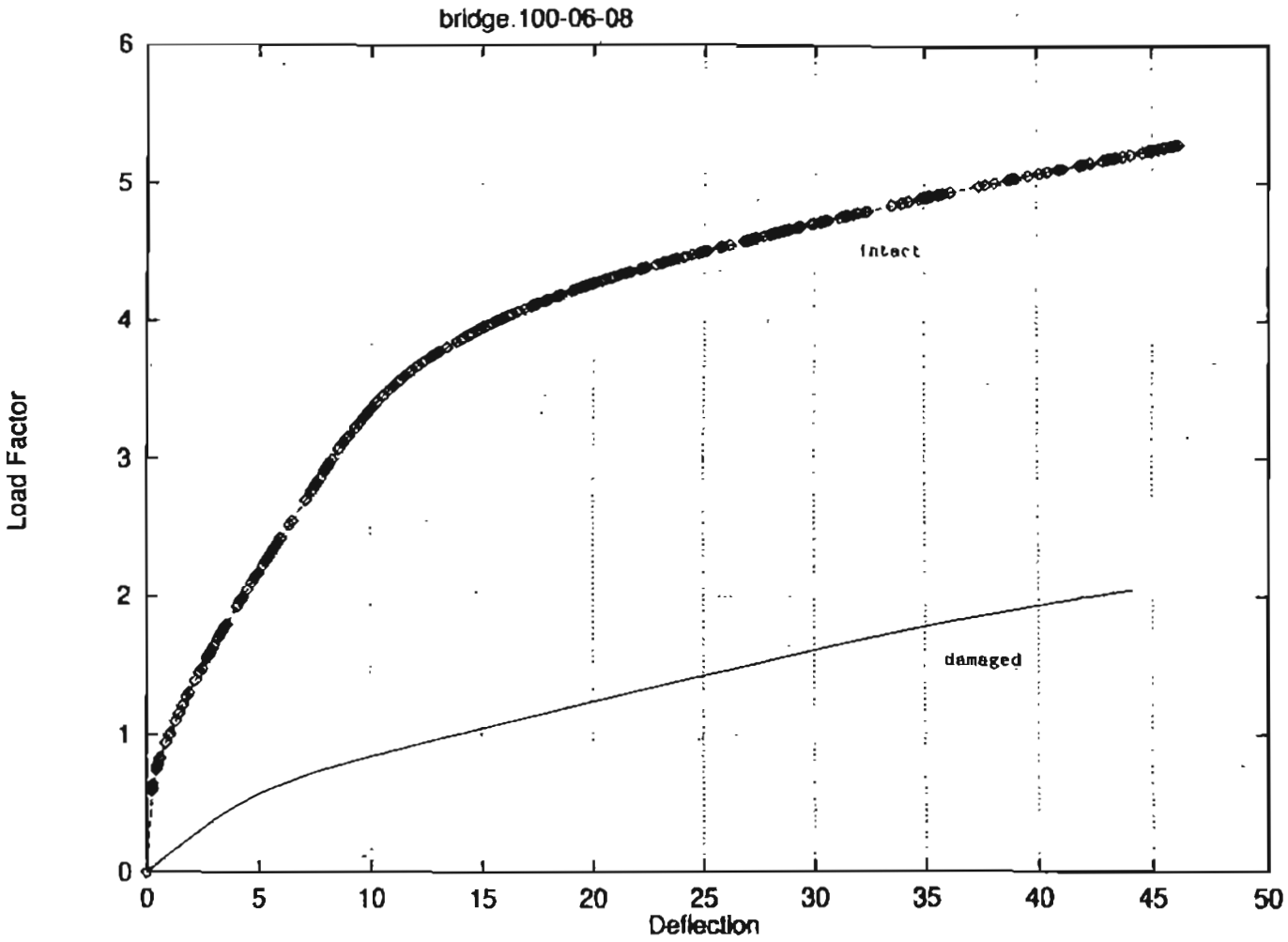

Figure B.7 Results of incremental analysis

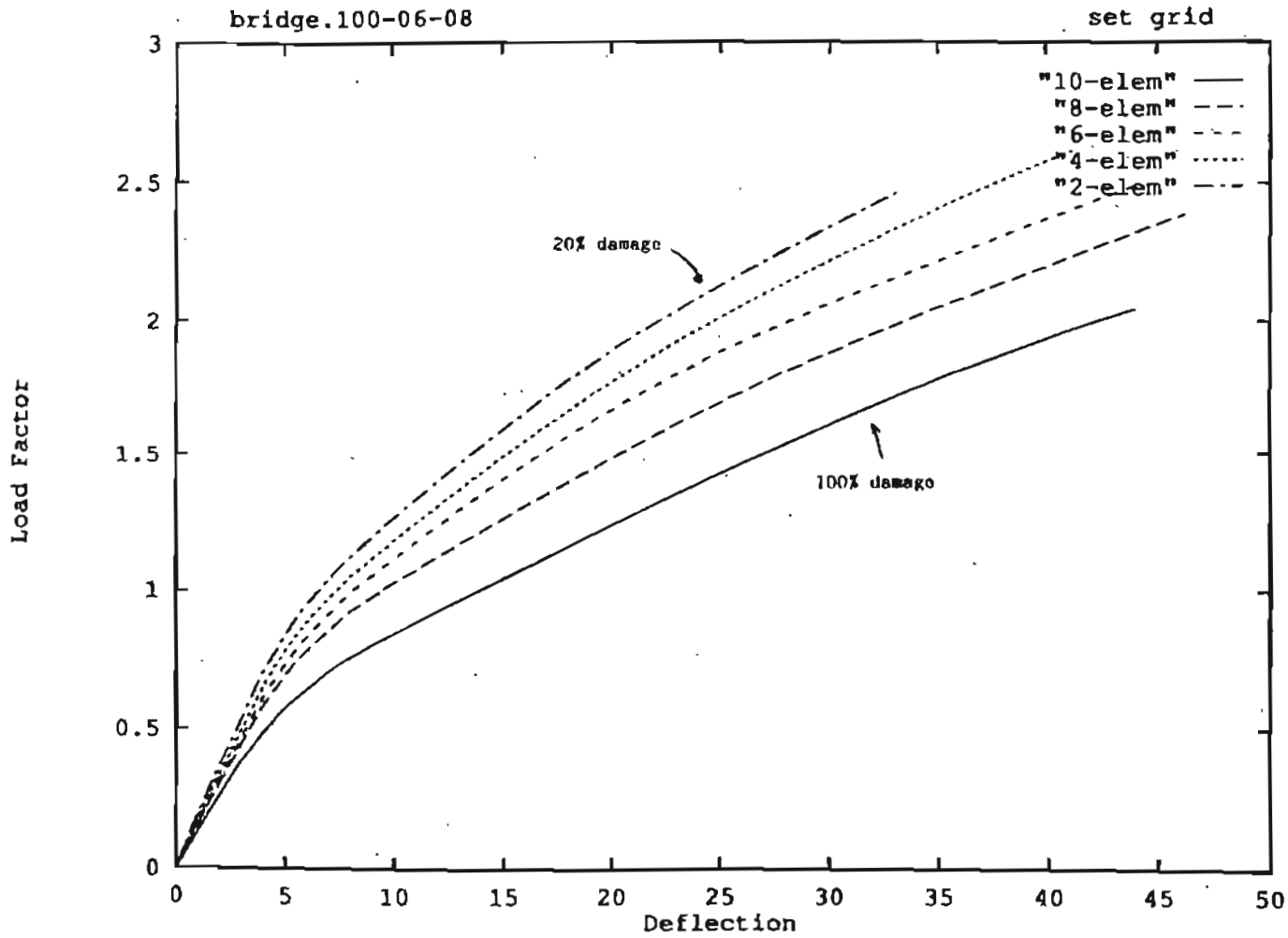

FigureB.8 Load-Deflection Curves for different damage scenarios.

Table B.1 Section Properties of Simple Span Bridges

The bridge span is 45.0

Spac	Type	Hf	Bf	Mub	As*	Fas	d
4.	1.	7.5	48.0	833.1	1.36	205.4	31.0
6.	1.	7.5	72.0	1202.3	1.95	295.5	31.0
8.	2.	8.0	96.0	1619.9	2.01	303.4	39.5
10.	2.	8.5	114.0	2013.8	2.47	372.9	40.0
12.	2.	8.5	114.0	2391.3	2.95	446.8	40.0

The bridge span is 60.0

Spac	Type	Hf	Bf	Mub	As*	Fas	d
4.	3.	7.5	48.0	1484.8	1.53	231.5	48.0
6.	3.	7.5	72.0	2056.6	2.11	319.2	48.0
8.	3.	8.0	96.0	2657.6	2.69	407.1	48.5
10.	3.	8.5	118.0	3273.3	3.28	495.8	49.0
12.	3.	8.5	118.0	3859.7	3.90	590.0	49.0

The bridge span is 80.0

Spac	Type	Hf	Bf	Mub	As*	Fas	d
4.	3.	7.5	48.0	2346.3	2.51	379.2	48.0
6.	3.	7.5	72.0	3216.1	3.41	515.3	48.0
8.	4.	8.0	96.0	4386.1	3.82	577.5	57.0
10.	4.	8.5	120.0	5333.9	4.59	694.3	57.5
12.	4.	8.5	122.0	6229.7	5.41	818.2	57.5

The bridge span is 100.0

Spac	Type	Hf	Bf	Mub	As*	Fas	d
4.	4.	7.5	48.0	3737.4	3.45	521.2	56.5
6.	4.	7.5	72.0	4938.3	4.49	679.0	56.5
8.	5.	8.0	96.0	6599.7	5.00	756.3	66.0
10.	5.	8.5	120.0	7922.5	5.94	897.6	66.5
12.	5.	8.5	144.0	9164.0	6.85	1035.8	66.5

The bridge span is 120.0

Spac	Type	Hf	Bf	Mub	As*	Fas	d
4.	5.	7.5	48.0	5601.3	4.51	681.3	65.5
6.	5.	7.5	72.0	7167.3	5.67	857.2	65.5
8.	6.	8.0	96.0	9025.9	6.05	914.2	75.0
10.	6.	8.5	120.0	10757.4	7.13	1078.5	75.5
12.	6.	8.5	144.0	12392.0	8.19	1237.6	75.5

The bridge span is 150.0

Spac	Type	Hf	Bf	Mub	As*	Fas	d
4.	5.	7.5	48.0	8539.2	6.16	930.7	74.5
6.	6.	7.5	72.0	10742.7	7.58	1145.7	74.5
8.	6.	8.0	96.0	13128.9	9.10	1376.4	75.0
10.	6.	8.5	120.0	15606.6	10.69	1616.2	75.5
12.	6.	8.5	144.0	17901.4	12.20	1844.8	75.5

(1) (2) (3) (4) (5) (6) (7) (8)

(1) beam spacing in feet
(2) AASHTO Beam type
(3) Slab thickness(in)
(4) Effective slab width(in)
(5) Factored moment (kip-in)
(6) Area of pres. steel(in^2)
(7) Prestressing force (kip)
(8) Effective depth (in)

Table B.2 Section Properties of Continuous Prestressed Concrete Bridges

The bridge span is 100.0

Spac	Type	Hf	Bf	Mub	As*	Fas	d	Mut	As	d
4.	4.	7.5	48.0	3309.9	3.01	455.3	56.5	1429.0	5.63	58.0
6.	4.	7.5	72.0	4297.0	3.86	583.0	56.5	2143.6	8.56	58.0
8.	5.	8.0	96.0	5744.6	4.31	652.3	66.0	2858.1	9.77	67.5
10.	5.	8.5	120.0	6853.6	5.09	769.6	66.5	3572.6	12.24	68.0
12.	5.	8.5	144.0	7881.4	5.84	882.9	66.5	4287.1	14.84	68.0

The bridge span is 120.0

Spac	Type	Hf	Bf	Mub	As*	Fas	d	Mut	As	d
4.	5.	7.5	48.0	5054.0	4.02	608.4	65.5	1955.3	6.66	67.0
6.	5.	7.5	72.0	6346.5	4.96	749.3	65.5	2933.0	10.12	67.0
8.	6.	8.0	96.0	7931.4	5.26	795.9	75.0	3910.7	11.83	76.5
10.	6.	8.5	120.0	9399.3	6.17	933.0	75.5	4888.3	14.84	77.0
12.	6.	8.5	144.0	10750.2	7.04	1064.1	75.5	5866.0	18.01	77.0

The bridge span is 150.0

Spac	Type	Hf	Bf	Mub	As*	Fas	d	Mut	As	d
4.	6.	7.5	48.0	7743.9	5.51	832.9	74.5	2892.2	8.71	76.0
6.	6.	7.5	72.0	9549.8	6.65	1005.2	74.5	4336.9	13.28	76.0
8.	6.	8.0	96.0	11538.4	7.90	1194.4	75.0	5782.5	17.87	76.5
10.	6.	8.5	120.0	13618.4	9.20	1390.7	75.5	7228.1	22.56	77.0
12.	6.	8.5	144.0	15515.6	10.43	1577.0	75.5	8673.7	27.57	77.0

(1) (2) (3) (4) (5) (6) (7) (8) (9) (10) (11)

(1) beam spacing in feet (2) AASHTO Beam type (3) Slab thickness(in)
(4) Effective slab width(in) (5) Positive moment (kip-in) (6) Area of pres. steel(in^2)
(7) Prestressing force (kip) (8) Effective depth (in) (9) Negative moment
(10) Area of reinforcing steel(in^2) (11) Effective depth in negative bending (in)

Table B.3 Summary of Results for Simple Span Bridges.

span	No. of beams	spac.	LF300	LF200	LF100	LFU	LFD	LF1	mech.	R	D	LL
(ft)		(ft)								kip-in	kip-in	kip-in
45	4	4	1.49	1.78	2.25	2.48	1.63	2.44	2.52	10685	2552	3339
45	4	6	1.89	2.25	3.00	3.53	2.10	2.86	3.68	15383	3499	4153
45	4	8	2.36	2.87	3.47	4.29	2.11	3.49	5.00	20909	4739	4835
45	4	10	2.64	3.19	3.79	4.74	2.06	3.39	6.24	26088	5914	5947
45	4	12	2.82	3.40	4.06	5.00	1.95	3.86	7.48	31047	6883	6272
45	6	4	1.75	2.12	2.91	3.57	2.56	2.63	3.77	10685	2552	3096
45	6	6	1.96	2.34	3.16	3.97	2.23	2.92	5.52	15383	3499	4070
45	6	8	2.42	2.95	3.57	4.39	2.19	3.02	7.50	20909	4739	5348
45	6	10	2.66	3.21	3.86	4.80	2.09	3.41	9.36	26088	5914	5910
45	6	12	2.98	3.57	4.26	5.19	2.11	3.86	11.22	31047	6883	6264
45	8	4	1.80	2.18	3.00	3.81	2.67	2.64	5.03	10685	2552	3084
45	8	6	1.97	2.35	3.17	4.00	2.24	2.93	7.35	15383	3499	4058
45	8	8	2.42	2.95	3.57	4.39	2.19	3.02	10.01	20909	4739	5348
45	8	10	2.66	3.21	3.86	4.80	2.09	3.41	12.48	26088	5914	5909
45	10	4	1.81	2.19	3.02	3.83	2.68	2.64	6.29	10685	2552	3085
45	10	6	1.97	2.35	3.17	4.00	2.24	2.93	9.19	15383	3499	4058
45	10	8	2.42	2.95	3.57	4.39	2.19	3.02	12.51	20909	4739	5348
60	4	4	1.40	1.74	2.24	2.46	1.48	2.40	2.52	18660	6480	5085
60	4	6	1.86	2.27	3.04	3.65	2.00	2.87	3.82	26254	7776	6441
60	4	8	2.06	2.51	3.37	4.54	2.13	3.17	5.10	34413	9720	7788
60	4	10	2.36	2.84	3.72	5.00	2.11	3.62	6.35	42401	11660	8502
60	4	12	2.57	3.09	4.00	5.25	1.59	4.10	7.63	50210	13276	8998
60	6	4	1.62	2.03	2.87	3.53	2.34	2.60	3.78	18660	6480	4882
60	6	6	1.94	2.37	3.20	4.16	2.13	2.93	5.73	26254	7776	6308
60	6	8	2.14	2.61	3.50	4.68	2.22	3.24	7.65	34413	9720	7612
60	6	10	2.40	2.90	3.81	5.06	2.17	3.66	9.53	42401	11660	8396
60	6	12	2.58	3.11	4.05	4.89	1.86	4.08	11.46	50210	13276	9059
60	8	4	1.67	2.09	2.97	3.77	2.45	2.61	5.03	18660	6480	4662
60	8	6	1.95	2.39	3.23	4.20	2.17	2.94	7.64	26254	7776	6292
60	8	8	2.14	2.61	3.49	4.69	2.26	3.24	10.21	34413	9720	7612
60	8	10	2.40	2.90	3.81	5.06	2.17	3.66	12.71	42401	11660	8395
60	10	4	1.69	2.12	3.00	3.79	2.47	2.61	6.29	18660	6480	4667
60	10	6	1.95	2.39	3.23	4.20	2.17	2.94	9.55	26254	7776	6292
60	10	8	2.14	2.61	3.49	4.69	2.26	3.24	12.76	34413	9720	7612
80	4	4	1.19	1.52	2.26	2.58	1.49	2.54	2.63	29912	11520	7236
80	4	6	1.63	1.99	2.92	3.74	2.04	3.03	3.90	41062	13820	8993
80	4	8	1.94	2.44	3.42	4.77	2.02	3.48	5.37	56950	19410	10780
80	4	10	2.24	2.78	3.78	5.26	1.99	3.87	8.65	69393	22890	12030
80	4	12	2.47	3.03	4.06	5.32	1.63	4.10	7.80	80378	25890	13280
80	6	4	1.38	1.77	2.75	3.70	2.45	2.63	3.95	29912	11520	7003
80	6	6	1.71	2.09	3.06	4.28	2.17	3.04	5.85	41062	13820	8952
80	6	8	2.03	2.56	3.59	4.94	2.13	3.58	8.06	56950	19410	10500
80	6	10	2.31	2.87	3.92	5.36	2.03	3.88	9.98	69393	22890	11980

Table B.3 (ct'd 2/3) Summary of Results for Simple Span Bridges.

80	6	12	2.49	3.07	4.14	5.40	1.66	4.11	11.69	80379	25890	13270
80	8	4	1.43	1.82	2.83	4.00	2.40	2.65	5.26	29912	11520	6935
80	8	6	1.74	2.13	3.13	4.33	2.20	3.06	7.80	41062	13820	8913
80	8	8	2.05	2.58	3.60	4.96	2.14	3.58	10.74	56950	19410	10500
80	8	10	2.31	2.88	3.92	5.36	2.06	3.88	13.31	69393	22890	11980
80	10	4	1.47	1.87	2.89	4.04	2.23	2.67	6.58	29912	11520	6898
80	10	6	1.74	2.13	3.13	4.34	2.20	3.06	9.74	41062	13820	8916
80	10	8	2.05	2.58	3.60	4.96	2.14	3.58	13.43	56950	19410	10500
100	4	4	1.01	1.37	2.35	2.80	1.48	2.73	2.83	47463	21600	9462
100	4	6	1.55	1.95	3.07	3.95	1.98	3.19	4.11	62818	26200	11780
100	4	8	1.79	2.28	3.47	5.06	1.96	3.80	5.55	84993	34200	14110
100	4	10	2.08	2.60	3.80	5.55	1.89	3.95	6.88	102489	39600	15940
100	4	12	2.35	2.89	4.08	5.86	1.91	4.28	8.19	118811	43920	17510
100	6	4	1.22	1.65	2.89	4.05	2.54	2.83	4.24	47463	21600	9141
100	6	6	1.61	2.04	3.20	4.60	2.14	3.20	6.17	62818	26200	11770
100	6	8	1.91	2.42	3.65	5.28	2.05	3.67	8.33	84993	34200	13830
100	6	10	2.17	2.72	3.97	5.70	1.97	3.99	10.32	102489	39600	15780
100	6	12	2.43	2.99	4.24	6.04	2.05	4.33	12.40	118811	43200	17450
100	8	4	1.25	1.70	2.98	4.45	2.49	2.86	5.66	47463	21600	9066
100	8	6	1.67	2.12	3.30	4.83	2.17	3.22	8.23	62818	26200	11670
100	8	8	1.91	2.44	3.66	5.32	2.07	3.67	11.11	84993	34200	13850
100	8	10	2.17	2.72	3.97	5.71	1.97	3.99	13.76	102489	39600	15780
100	10	4	1.29	1.75	3.04	4.52	2.21	2.88	7.07	47463	21600	8984
100	10	6	1.67	2.12	3.31	4.86	2.17	3.22	10.28	62818	26200	11670
100	10	8	1.97	2.43	4.25	5.32	2.07	3.67	13.89	84993	34200	13850
120	4	4	1.09	1.52	2.84	3.12	1.51	3.06	3.17	71042	35250	11690
120	4	6	1.64	2.01	3.27	4.22	1.85	3.39	4.39	91058	41470	14620
120	4	8	1.79	2.32	3.60	5.26	1.86	3.71	5.81	115980	50280	17710
120	4	10	2.14	2.70	3.98	5.82	1.79	4.09	7.23	138742	57020	19970
120	4	12	2.36	2.94	4.13	5.50	1.51	4.35	8.44	160219	64800	21920
120	6	4	1.29	1.80	3.21	4.43	2.48	3.16	4.75	71042	35250	11360
120	6	6	1.60	2.09	3.40	4.79	2.00	3.39	6.68	91058	41470	14640
120	6	8	1.92	2.48	3.81	5.50	2.00	3.81	8.72	115980	50280	17230
120	6	10	2.26	2.87	4.22	5.98	1.90	4.17	10.85	138742	57020	19610
120	6	12	2.43	3.05	4.32	5.64	1.61	4.39	12.67	160219	64800	21730
120	8	4	1.32	1.84	3.30	4.64	2.29	3.18	6.33	71042	35250	11270
120	8	6	1.67	2.18	3.51	4.86	2.05	3.43	8.78	91058	41470	14450
120	8	8	1.94	2.51	3.85	6.52	2.00	3.82	11.63	115980	50280	17220
120	8	10	2.27	2.88	4.22	6.00	1.90	4.17	14.46	138742	57020	19610
120	10	4	1.36	1.90	3.37	4.76	2.02	3.22	7.92	71042	35250	11120
120	10	6	1.68	2.20	3.52	4.86	2.05	3.43	10.97	91058	41470	14450
120	10	8	1.94	2.51	3.84	5.52	2.00	3.82	14.64	115980	50280	17220
150	4	4	1.15	1.63	2.91	3.43	1.39	3.41	3.40	108252	57710	14840
150	4	6	1.57	2.08	3.48	4.49	1.84	3.63	4.61	135664	67230	18850
150	4	8	1.83	2.39	3.80	5.13	1.35	3.82	5.91	166316	78570	23000
150	4	10	2.21	2.81	4.25	5.79	1.26	4.22	7.38	198446	89100	25920

Table B.3 (ct'd 3/3) Summary of Results for Simple Span Bridges.

150	4	12	2.40	3.01	4.40	5.81	1.23	4.49	8.52	227721	101200	28190
150	6	4	1.29	1.82	3.34	4.65	1.87	3.52	5.11	108252	57710	14340
150	6	6	1.61	2.15	3.59	4.97	1.77	3.61	6.91	135684	67230	18970
150	6	8	1.97	2.56	4.03	5.46	1.61	3.96	8.86	166316	78570	22140
150	6	10	2.37	3.02	4.54	6.01	1.38	4.38	11.04	198446	89100	24990
150	6	12	2.50	3.16	4.64	6.23	1.35	4.73	13.18	227721	97200	27570
150	8	4	1.30	1.84	3.39	4.84	1.93	3.53	6.61	108252	57710	14320
150	8	6	1.70	2.27	3.76	5.07	1.83	3.70	9.22	135684	67230	18510
150	8	8	2.02	2.63	4.10	5.50	1.52	4.00	11.82	166316	78570	21950
150	8	10	2.38	3.04	4.56	6.02	1.36	4.39	14.73	198446	89100	24910
150	10	4	1.36	1.93	3.52	4.91	1.95	3.51	8.51	108252	57710	14380
150	10	6	1.72	2.30	3.77	5.08	1.84	3.71	11.52	135684	67230	18460
150	10	8	2.02	2.63	4.11	5.50	1.53	4.00	14.77	166316	78570	21950

Table B.3 (b) LF/LF1 ratios for Simple Span Bridges.

span	No. of beams	spac.	LFU/LF1	LF100/LF1	LFD/LF1
(ft)		(ft)			
45	4	4	1.02	0.92	0.67
45	4	6	1.23	1.05	0.73
45	4	8	1.23	0.99	0.60
45	4	10	1.40	1.12	0.61
45	4	12	1.30	1.05	0.51
45	6	4	1.36	1.11	0.97
45	6	6	1.38	1.08	0.76
45	6	8	1.45	1.18	0.73
45	6	10	1.41	1.13	0.61
45	6	12	1.34	1.10	0.55
45	8	4	1.44	1.14	1.01
45	8	6	1.37	1.08	0.76
45	8	8	1.45	1.18	0.73
45	8	10	1.41	1.13	0.61
45	10	4	1.45	1.14	1.02
45	10	6	1.37	1.08	0.76
45	10	8	1.45	1.18	0.73
60	4	4	1.03	0.93	0.62
60	4	6	1.27	1.06	0.70
60	4	8	1.43	1.06	0.67
60	4	10	1.38	1.03	0.58
60	4	12	1.28	0.98	0.39
60	6	4	1.36	1.10	0.90
60	6	6	1.42	1.09	0.73
60	6	8	1.44	1.08	0.69
60	6	10	1.38	1.04	0.59
60	6	12	1.20	0.99	0.46
60	8	4	1.44	1.14	0.94
60	8	6	1.43	1.10	0.74
60	8	8	1.45	1.08	0.70
60	8	10	1.38	1.04	0.59
60	10	4	1.45	1.15	0.95
60	10	6	1.43	1.10	0.74
60	10	8	1.45	1.08	0.70
80	4	4	1.02	0.89	0.59
80	4	6	1.23	0.96	0.67
80	4	8	1.37	0.98	0.58
80	4	10	1.36	0.98	0.51
80	4	12	1.30	0.99	0.40
80	6	4	1.41	1.05	0.93
80	6	6	1.41	1.01	0.71
80	6	8	1.38	1.00	0.60
80	6	10	1.38	1.01	0.52

Table B.3 (b) (ct'd 2/3) LF/LF1 Ratios for Simple Span Bridges.

80	6	12	1.31	1.01	0.40
80	8	4	1.51	1.07	0.91
80	8	6	1.42	1.02	0.72
80	8	8	1.39	1.01	0.60
80	8	10	1.38	1.01	0.53
80	10	4	1.51	1.08	0.84
80	10	6	1.42	1.02	0.72
80	10	8	1.39	1.01	0.60
100	4	4	1.03	0.86	0.54
100	4	6	1.24	0.96	0.62
100	4	8	1.41	0.96	0.54
100	4	10	1.41	0.96	0.48
100	4	12	1.37	0.95	0.45
100	6	4	1.43	1.02	0.90
100	6	6	1.44	1.00	0.67
100	6	8	1.44	0.99	0.56
100	6	10	1.43	0.99	0.49
100	6	12	1.39	0.98	0.47
100	8	4	1.56	1.05	0.87
100	8	6	1.44	1.02	0.67
100	8	8	1.45	1.00	0.56
100	8	10	1.43	0.99	0.49
100	10	4	1.57	1.06	0.77
100	10	6	1.45	1.03	0.67
100	10	8	1.45	1.16	0.56
120	4	4	1.02	0.86	0.49
120	4	6	1.24	0.96	0.55
120	4	8	1.42	0.97	0.50
120	4	10	1.42	0.97	0.44
120	4	12	1.26	0.95	0.35
120	6	4	1.41	1.02	0.78
120	6	6	1.41	1.00	0.59
120	6	8	1.44	1.00	0.52
120	6	10	1.43	1.01	0.46
120	6	12	1.28	0.98	0.37
120	8	4	1.46	1.04	0.72
120	8	6	1.42	1.02	0.60
120	8	8	1.45	1.01	0.52
120	8	10	1.44	1.01	0.46
120	10	4	1.48	1.05	0.63
120	10	6	1.42	1.03	0.60
120	10	8	1.45	1.01	0.52
150	4	4	1.01	0.85	0.41
150	4	6	1.24	0.96	0.45
150	4	8	1.34	0.99	0.35
150	4	10	1.37	1.01	0.30

Table B.3 (b) (ct'd 3/3) LF/LF1 Ratios for Simple Span Bridges.

150	4	12	1.29	0.98	0.27
150	6	4	1.32	0.95	0.53
150	6	6	1.38	0.99	0.49
150	6	8	1.38	1.02	0.38
150	6	10	1.37	1.04	0.32
150	6	12	1.32	0.98	0.29
150	8	4	1.37	0.98	0.65
150	8	6	1.37	1.02	0.49
150	8	8	1.38	1.03	0.38
150	8	10	1.37	1.04	0.31
150	10	4	1.40	1.00	0.56
150	10	6	1.37	1.02	0.50
150	10	8	1.38	1.03	0.38

Table B-4. Summary of Results of Continuous Birdges.

	Span	100ft	no. of beams	4		beam spacing = 4ft					
	LFU	LF100	LFD	LF1+	FL1-	R+	D+	L+	R-	D-	L-
Case1	3.35	2.937	1.851	2.976114	4.211446	42126	19628	7559.112	19159	3060	3822.471
Case2	6.492	4.6	2.904	4.14241		42126	19628	5430.788	19159	3060	
Case3	3.383	2.955	1.837	3.606686	2.254779	42126	19628	6237.603	19159	3060	7139.656
	Span	100ft	no. of beams	4		beam spacing = 6ft					
	LFU	LF100	LFD	LF1+	FL1-	R+	D+	L+	R-	D-	L-
Case1	4.788	3.722	1.784	3.511625	6.024377	54947	22382	9275.27	28775	4500	4832.267
Case2	6.872	5.564	2.266	5.777531	2.861684	54947	22382	5500.896	28775	4500	8484.848
Case3	4.546	3.781	1.639	4.815027	2.398737	54947	22382	6599.261	28775	4500	10120.48
	Span	100ft	no. of beams	4		beam spacing = 8ft					
	LFU	LF100	LFD	LF1+	FL1-	R+	D+	L+	R-	D-	L-
Case1	5.443	4.194	1.573	3.862475	5.596332	74839	31165	11255.54	38371	5940	5795.08
Case2	8.05	6.672	2.51	6.999531	3.412403	74839	31165	8211.348	38371	5940	9504.32
Case3	5.161	4.269	1.586	5.219409	2.545587	74839	31165	8331.866	38371	5940	12743.9
	Span	100ft	no. of beams	4		beam spacing = 10ft					
	LFU	LF100	LFD	LF1+	FL1-	R+	D+	L+	R-	D-	L-
Case1	5.729	4.634	1.43	4.288241	6.349176	89087	35835	12416.61	47980	7560	6365.394
Case2	8.635	7.556	2.533	7.902401	3.920264	89087	35835	6737.893	47980	7560	3.920264
Case3	5.289	4.72	1.495	5.853618	2.875542	89087	35835	9094.924	47980	7560	14052.84

Table B-4 (ct'd 2/13) Summary of Results of Continuous Birdges.

	Span	100ft	no. of beams	4		beam spacing = 12ft					
	LFU	LF100	LFD	LF1+	FL1-	R+	D+	L+	R-	D-	L-
Case1	5.837	4.987	1.285	4.561961	6.929757	102306	39866.4	13689.84	57530	9000	7004.579
Case2	9.026	8.212	2.466	8.668861	4.408578	102306	39866.4	7202.527	57530	9000	11007.75
Case3	5.559	5.113	1.381	6.493851	3.253348	102306	39866.4	9814.559	57530	9000	14915.97
	Span	100ft	no. of beams	6		beam spacing = 4ft					
	LFU	LF100	LFD	LF1+	FL1-	R+	D+	L+	R-	D-	L-
Case1	4.836	3.597	2.738	3.105894	4.313379	42126	19628	7242.571	19159	3060	3731.788
Case2	6.986	5.251	3.464	4.968506	2.33	42126	19628	4528.625	19159	3060	6917.511
Case3	3.656	4.844	2.68	4.428554	2.115111	42126	19628	5080.247	19159	3060	7611.465
	Span	100ft	no. of beams	6		beam spacing = 6ft					
	LFU	LF100	LFD	LF1+	FL1-	R+	D+	L+	R-	D-	L-
Case1	5.144	3.881	1.953	3.445735	5.072452	54947	23173.2	9224.19	28775	4500	4785.702
Case2	7.061	5.861	2.413	5.9418	2.931934	54947	23173.2	5346.899	28775	4500	8276.561
Case3	4.79	3.956	1.763	4.911835	2.452043	54947	23173.2	6469.796	28775	4500	9697.679
	Span	100ft	no. of beams	6		beam spacing = 8ft					
	LFU	LF100	LFD	LF1+	FL1-	R+	D+	L+	R-	D-	L-
Case1	5.591	4.407	1.665	3.969663	5.773418	74639	31164.8	10952.65	38371	5940	5617.804
Case2	8.186	6.798	2.596	7.026161	3.421641	74639	31164.8	6187.673	38371	5940	9478.458
Case3	5.335	4.491	1.678	5.342542	2.607674	74639	31164.8	8134.991	38371	5940	12433.08

Table B-4 (ct'd 3/13) Summary of Results of Continuous Birdges.

	Span	100ft	no. of beams	6		beam spacing = 10ft					
	LFU	LF100	LFD	LF1+	FL1-	R+	D+	L+	R-	D-	L-
Case1	5.863	4.821	1.467	4.313047	6.349114	89087	35835	12345.44	47980	7660	6365.584
Case2	8.686	7.686	2.572	7.906686	3.920972	89087	35835	6735.46	47980	7560	10309.28
Case3	5.564	4.91	1.523	5.937275	2.915551	89087	35835	8970.516	47980	7560	13865.78
	Span	100ft	no. of beams	6		beam spacing = 12ft					
	LFU	LF100	LFD	LF1+	FL1-	R+	D+	L+	R-	D-	L-
Case1	5.905	5.069	1.298	4.566354	6.924098	102306	39866.4	13674.35	57530	9000	7009.119
Case2	9.034	8.227	2.475	8.669201	4.408453	102306	39866.4	7202.043	57530	9000	11007.75
Case3	5.637	5.191	1.391	6.527991	3.268691	102306	39866.4	9564.171	57530	9000	23839.5
	Span	100ft	no. of beams	8		beam spacing = 4ft					
	LFU	LF100	LFD	LF1+	FL1-	R+	D+	L+	R-	D-	L-
Case1	5.179	3.72	2.785	3.136259	4.356447	42126	19628	7174.651	19159	3060	3696.028
Case2	6.617	5.109	3.508	5.041952	2.357047	42126	19628	4461.129	19159	3060	6828.571
Case3	4.668	3.783	2.755	4.470692	2.132349	42126	19628	4954.313	19159	3060	7551.343
	Span	100ft	no. of beams	8		beam spacing = 6ft					
	LFU	LF100	LFD	LF1+	FL1-	R+	D+	L+	R-	D-	L-
Case1	5.155	3.937	1.957	3.459512	5.068143	54947	23173.2	9186.855	28775	4500	4790.962
Case2	7.069	5.867	2.426	5.94539	2.931944	54947	23173.2	5345.368	28775	4500	8278.581
Case3	4.806	3.994	1.775	4.939987	2.466143	54947	23173.2	6432.25	28775	4500	9843.75

Table B-4 (ct'd 4/13) Summary of Results of Continuous Birdges.

	Span	100ft	no. of beams	8		beam spacing = 8ft					
	LFU	LF100	LFD	LF1+	FL1-	R+	D+	L+	R-	D-	L-
Case1	5.594	4.41	1.666	3.975118	5.774242	74639	31164.6	10935.63	38371	5940	5615.98
Case2	8.186	6.799	2.596	7.02665	3.421873	74639	31164.6	6187.66	38371	5940	9478.458
Case3	5.338	4.492	1.678	5.34375	2.607969	74639	31164.6	8134.075	38371	5940	12433.08
	Span	100ft	no. of beams	8		beam spacing = 10ft					
	LFU	LF100	LFD	LF1+	FL1-	R+	D+	L+	R-	D-	L-
Case1	5.863	4.821	1.467	4.312843	6.349293	89087	35835	12349.02	47980	7560	6366.943
Case2	8.686	7.586	2.572	7.906895	3.921056	89087	35835	6735.423	47980	7560	10309.28
Case3	5.564	4.911	1.523	5.937637	2.915707	89087	35835	8970.449	47980	7560	13865.78
	Span	100ft	no. of beams	10		beam spacing = 4ft					
	LFU	LF100	LFD	LF1+	FL1-	R+	D+	L+	R-	D-	L-
Case1	5.192	3.738	2.785	3.152701	4.354922	42126	19628	7137.586	19159	3060	3697.502
Case2	6.4	5.309	3.507	5.044242	2.35731	42126	19628	4459.6	19159	3060	6828.571
Case3	4.418	3.801	2.644	4.472953	2.13184	42126	19628	5029.558	19159	3060	7551.343
	Span	100ft	no. of beams	10		beam spacing = 6ft					
	LFU	LF100	LFD	LF1+	FL1-	R+	D+	L+	R-	D-	L-
Case1	5.156	3.937	1.956	5.943915	2.932131	54947	23173.2	5345.355	28775	4500	8278.581
Case2	7.069	5.847	2.427	5.943915	2.932131	54947	23173.2	5345.355	28775	4500	8278.581
Case3	4.806	3.993	1.775	4.939573	2.486192	54947	23173.2	6432.914	28775	4500	9843.75

Table B-4 (ct'd 5/13) Summary of Results of Continuous Birdges.

	Span	100ft	no. of beams	10		beam spacing = 8ft					
	LFU	LF100	LFD	LF1+	FL1-	R+	D+	L+	R-	D-	L-
Case1	5.594	4.41	1.666	3.975233	5.774358	74639	31164.6	10935.91	38371	5940	5816.174
Case2	8.186	6.799	2.596	7.026697	3.421873	74639	31164.6	6187.646	38371	5940	9478.458
Case3	5.338	4.492	1.678	5.343835	2.608009	74639	31164.6	8134.069	38371	5940	12433.08
	Span	120ft	no. of beams	4		beam spacing = 4ft					
	LFU	LF100	LFD	LF1+	FL1-	R+	D+	L+	R-	D-	L-
Case1	3.71	3.225	1.887	3.295018	4.772482	64115	33287	9362.89	26214	4406.4	4569.892
Case2	6.625	4.957	3.147			64115	33287	6938.972	26214	4406.4	
Case3	3.715	3.313	2.129	4.574201	2.220636	64115	33287	6743.264	26214	4406.4	9619.495
	Span	120ft	no. of beams	4		beam spacing = 6ft					
	LFU	LF100	LFD	LF1+	FL1-	R+	D+	L+	R-	D-	L-
Case1	5.059	3.953	1.496	3.645951	5.530705	80887	38553	11609.07	39387	6480	5948.786
Case2	7.409	5.905	1.949	6.098948	3.180763	80887	38553	6939.266	39387	6480	10342.75
Case3	4.875	4.018	1.409	5.04106	2.707176	80887	38553	8397.837	39387	6480	12155.48
	Span	120ft	no. of beams	4		beam spacing = 8t					
	LFU	LF100	LFD	LF1+	FL1-	R+	D+	L+	R-	D-	L-
Case1	5.627	4.241	1.329	4.050472	6.284576	102593	48432.6	13862.39	52523	8553.6	6995.005
Case2	8.23	4.749	2.076	7.193382	3.819099	102593	48432.6	7805.532	52523	8553.6	11510.46
Case3	5.248	4.319	1.312	5.39129	2.963933	102593	48432.6	10419.67	52523	8553.6	14838.71

Table B-4 (ct'd 6/13) Summary of Results of Continuous Birdges.

	Span	120ft	no. of beams	4		beam spacing = 10ft					
	LFU	LF100	LFD	LF1+	FL1-	R+	D+	L+	R-	D-	L-
Case1	5.869	4.628	1.141	4.398703	6.953769	122222	53416.8	34398.43	85688	10886.4	7881.151
Case2	8.719	7.602	2	8.13049	4.400798	122222	53416.8	8483.366	65688	10886.4	12453.76
Case3	5.38	4.71	1.173	5.080867	3.358485	122222	53416.8	11314.53	65688	10886.4	16316.64
	Span	120ft	no. of beams	4		beam spacing = 12ft					
	LFU	LF100	LFD	LF1+	FL1-	R+	D+	L+	R-	D-	L-
Case1	5.995	4.998	1.001	4.709765	7.636024	1398535	58962.8	17167.79	78704	12960	8608.019
Case2	9.138	8.346	1.902	8.939712	4.946841	1398535	58962.8	9047.774	78704	12960	13292.12
Case3	5.565	5.144	1.068	5.693108	3.688942	1398535	58962.8	12084.21	78704	12960	17823.83
	Span	120ft	no. of beams	6		beam spacing = 4ft					
	LFU	LF100	LFD	LF1+	FL1-	R+	D+	L+	R-	D-	L-
Case1	5.235	3.91	2.649	3.404463	4.758182	64115	33267	9060.493	26214	4406.4	4582.898
Case2	7.472	5.823	3.779	5.510611	2.647585	64115	33267	5598.365	26214	4406.4	8237.432
Case3	5.103	3.974	2.802	4.842043	2.315644	64115	33267	6371.385	26214	4406.4	9418.283
	Span	120ft	no. of beams	6		beam spacing = 6ft					
	LFU	LF100	LFD	LF1+	FL1-	R+	D+	L+	R-	D-	L-
Case1	5.543	4.123	1.679	3.66009	5.587077	80887	38553	11568.06	39387	6480	5890.692
Case2	7.668	6.301	2.129	6.311468	3.2949	80887	38553	6708.235	39387	6480	9988.386
Case3	5.159	4.203	1.556	5.127435	2.729116	80887	38553	8259.081	39387	6480	12061.71

Table B-4 (ct'd 7/13) Summary of Results of Continuous Birdges.

	Span	120ft	no. of beams	6		beam spacing = 8ft					
	LFU	LF100	LFD	LF1+	FL1-	R+	D+	L+	R-	D-	L-
Case1	5.813	4.496	1.429	4.138376	6.370659	102593	46432.3	13573.25	52523	8553.6	6903.153
Case2	8.402	6.996	2.207	7.250944	3.847193	102593	46432.3	7744.18	52523	8553.6	11427.28
Case3	5.471	4.588	1.416	5.528324	3.050318	102593	46432.3	10159.61	52523	8553.6	14415.95
	Span	120ft	no. of beams	6		beam spacing = 10ft					
	LFU	LF100	LFD	LF1+	FL1-	R+	D+	L+	R-	D-	L-
Case1	6.059	4.853	1.203	4.450181	6.978056	122222	53416.8	15458.19	65688	10886.4	7851.885
Case2	8.821	7.723	2.098	8.146327	4.40716	122222	53416.8	8445.244	65688	10886.4	12433.32
Case3	5.616	4.951	1.238	6.196195	3.39427	122222	53416.8	11102.67	65688	10886.4	16142.78
	Span	120ft	no. of beams	6		beam spacing = 12ft					
	LFU	LF100	LFD	LF1+	FL1-	R+	D+	L+	R-	D-	L-
Case1	6.09	5.138	1.049	4.726156	7.632296	139835	58962.8	17113.32	78704	12960	8614.777
Case2	9.158	8.396	1.987	8.941596	4.946913	139835	58962.8	9046.001	78704	12960	13292.12
Case3	5.706	5.287	1.112	6.693749	3.687658	139835	58962.8	12078.85	78704	12960	17823.83
	Span	120ft	no. of beams	8		beam spacing = 4ft					
	LFU	LF100	LFD	LF1+	FL1-	R+	D+	L+	R-	D-	L-
Case1	5.467	4.044	2.709	3.442381	4.819595	64115	33267	8960.42	626214	4406.4	4524.368
Case2	7.286	5.907	3.838	5.634889	2.703062	64115	33267	5473.577	626214	4406.4	8066.429
Case3	5.251	4.107	2.888	4.906038	2.341917	64115	33267	8285.881	626214	4406.4	2.341917

Table B-4 (ct'd 8/13) Summary of Results of Continuous Birdges.

	Span	120ft	no. of beams	8		beam spacing = 6ft					
	LFU	LF100	LFD	LF1+	FL1-	R+	D+	L+	R-	D-	L-
Case1	5.563	4.214	1.706	3.690678	5.592877	80887	38553	11469.23	39387	6480	5883.069
Case2	7.684	6.31		6.317736	3.296892	80887	38553	6701.393	39387	6480	9982.589
Case3	5.186	4.274	1.568	5.172908	2.730982	80887	38553	8186.335	39387	6480	12053.26
	Span	120ft	no. of beams	8		beam spacing = 8ft					
	LFU	LF100	LFD	LF1+	FL1-	R+	D+	L+	R-	D-	L-
Case1	5.818	4.51	1.431	4.138377	6.367492	102593	46432.3	31643.26	52523	8553.6	8904.503
Case2	8.405	8.996	2.209	7.251449	3.847452	102593	46432.3	7744.142	52523	8553.6	11427.28
Case3	5.477	4.597	1.419	5.532507	3.052184	102593	46432.3	10152.35	52523	8553.6	14407.74
	Span	120ft	no. of beams	8		beam spacing = 10ft					
	LFU	LF100	LFD	LF1+	FL1-	R+	D+	L+	R-	D-	L-
Case1	6.06	4.858	6.06	4.449961	6.978166	122222	53416.8	15464.25	65688	10886.4	7853.821
Case2	8.822	7.724	8.821	8.146785	4.40743	122222	53416.8	8445.285	65688	10886.4	12433.32
Case3	5.616	4.952	5.614	6.196745	3.394336	122222	53416.8	11101.91	65688	10886.4	16142.78
	Span	120ft	no. of beams	10		beam spacing = 4ft					
	LFU	LF100	LFD	LF1+	FL1-	R+	D+	L+	R-	D-	L-
Case1	5.484	4.083	2.714	3.471883	4.830805	64115	33267	8883.629	26214	4406.4	4513.533
Case2	7.248	5.907	3.839	5.628012	2.703345	64115	33267	5480.836	26214	4406.4	8068.429
Case3	6.067	4.142	2.902	4.902412	2.343556	64115	33267	6290.369	26214	4406.4	9302.326

Table B-4 (ct'd 9/13) Summary of Results of Continuous Birdges.

	Span	120ft	no. of beams	10		beam spacing = 6ft					
	LFU	LF100	LFD	LF1+	FL1-	R+	D+	L+	R-	D-	L-
Case1	5.564	4.214	1.701	3.690073	5.591246	80887	38553	11474.1	39387	6480	5886.324
Case2	7.683	6.311	2.145	6.31824	3.296984	80887	38553	6701.393	39387	6480	9982.589
Case3	5.186	4.272	1.668	5.172908	2.730982	80887	38553	8186.335	39387	6480	12053.26
	Span	120ft	no. of beams	10		beam spacing = 8ft					
	LFU	LF100	LFD	LF1+	FL1-	R+	D+	L+	R-	D-	L-
Case1	5.818	4.51	1.434	4.138428	6.367576	102593	46432.3	13569.51	52523	8553.6	6904.678
Case2	8.405	6.998	2.211	7.25152	3.847476	102593	46432.3	7744.115	52523	8553.6	11427.28
Case3	5.477	4.597	1.421	5.532687	3.052297	102593	46432.3	10152.4	52523	8553.6	
	Span	150ft	no. of beams	4		beam spacing = 4ft					
	LFU	LF100	LFD	LF1+	FL1-	R+	D+	L+	R-	D-	L-
Case1	4.16	3.644	1.928	3.623868	5.610567	98014	54409	12033.91	38764	6885	18700
Case2	7.164	5.534	3.075	4.916532	2.480667	98014	54409	8865.723	38764	6885	12846.15
Case3	4.181	3.77	2.167	5.035251	2.59014	98014	54409	8659.049	38764	6885	12306.56
	Span	150ft	no. of beams	4		beam spacing = 6ft					
	LFU	LF100	LFD	LF1+	FL1-	R+	D+	L+	R-	D-	L-
Case1	5.508	4.414	1.204	3.848003	6.29958	120980	62669.7	15156.19	58261	10125	7642.553
Case2	7.867	6.62	1.614	6.53577	3.679987	120980	62669.7	8922.219	58261	10125	13081.22
Case3	5.248	4.524	1.149		3.036061	120980	62669.7	10609.95	58261	10125	15852.74

Table B-4 (ct'd 10/13) Summary of Results of Continuous Birdges.

	Span	150ft	no. of beams	4		beam spacing = 8ft					
	LFU	LF100	LFD	LF1+	FL1-	R+	D+	L+	R-	D-	L-
Case1	5.744	4.647	0.919	4.02734	6.928002	146757	72550.4	18422.2	77591	13365	9268.732
Case2	8.126	7.507	1.419	7.520001	4.46996	146757	72550.4	9870.567	77591	13365	14372.25
Case3	5.165	4.785	0.907	5.790506	3.349716	146757	72550.4	12817.56	77591	13365	19177.08
	Span	150ft	no. of beams	4		beam spacing = 10ft					
	LFU	LF100	LFD	LF1+	FL1-	R+	D+	L+	R-	D-	L-
Case1	6.039	4.94	0.698	4.327681	7.765396	173125	86463.7	44127.67	97284	17010	10336.96
Case2	8.483	8.346	1.204	8.490969	5.209977	173125	86463.7	10632.6	97284	17010	15411.13
Case3	5.207	5.142	0.712	6.233395	3.73046	173125	86463.7	14475.9	97284	17010	21512.03
	Span	150ft	no. of beams	4		beam spacing = 12ft					
	LFU	LF100	LFD	LF1+	FL1-	R+	D+	L+	R-	D-	L-
Case1	6.152	5.223	0.58	4.698603	8.63987	198276	92129.4	22593.77	116714	20250	11168.3
Case2	8.463	?	1.052	9.352219	5.882516	198276	92129.4	11350.08	116714	20250	16398.71
Case3	5.185	?	0.589	6.687678	4.123085	198276	92129.4	15870.9	116714	20250	23394.5
	Span	150ft	no. of beams	6		beam spacing = 4ft					
	LFU	LF100	LFD	LF1+	FL1-	R+	D+	L+	R-	D-	L-
Case1	5.843	4.369	2.609	3.688852	5.403139	98014	54409	11819.94	38764	6885	14548.62
Case2	8.119	6.532	3.792	6.131219	3.105147	98014	54409	7110.43	38764	6885	10264.29
Case3	5.588	4.458	2.812	4.033636	2.599435	98014	54409	8329.537	38764	6885	12261.38

Table B-4 (ct'd 11/13) Summary of Results of Continuous Birdges.

	Span	150ft	no. of beams	6		beam spacing = 6ft						
	LFU	LF100	LFD	LF1+	FL1-	R+	D+	L+	R-	D-	L-	
Case1	6.073	4.608	1.382	3.843974	6.3384	120980	62669.7	15167.83	58261	10125	7593.626	
Case2	8.257	7.122	1.825	6.885721	3.897664	120980	62669.7	8465.851	58261	10125	12346.4	
Case3	5.546	4.76	1.322	5.521197	3.05322	120980	62669.7	14134.57	58261	10125	15769.81	
	Span	150ft	no. of beams	6		beam spacing = 8ft						
	LFU	LF100	LFD	LF1+	FL1-	R+	D+	L+	R-	D-	L-	
Case1	6.044	4.955	0.994	4.172718	7.170633	146757	72550.4	17785.7	77591	13365	8957.788	
Case2	8.409	7.859	1.53	7.723755	4.596771	146757	72550.4	9607.703	77591	13365	13972.18	
Case3	5.509	5.136	0.986	5.942319	3.44151	146757	72550.4	12483.82	77591	13365	18856.18	
	Span	150ft	no. of beams	6		beam spacing =10ft						
	LFU	LF100	LFD	LF1+	FL1-	R+	D+	L+	R-	D-	L-	
Case1	6.33	5.234	0.785	4.485176	7.925381	173725	83463.7	47274.61	97284	17010	10129.26	
Case2	6.878	8.553	1.346	8.590088	5.270921	173725	83463.7	10508.68	97284	17010	15231.14	
Case3	5.539	5.474	0.796	6.335786	3.791853	173725	83463.7	14251.08	97284	17010	21177.27	
	Span	150ft	no. of beams	6		beam spacing = 12ft						
	LFU	LF100	LFD	LF1+	FL1-	R+	D+	L+	R-	D-	L-	
Case1	6.342	5.436	0.622	4.771129	8.696237	198276	92129.4	22249.75	1167174	20250	11093.64	
Case2	8.67	x	1.116	9.383303	5.899939	198276	92129.4	11314.81	1167174	20250	16353.64	
Case3	5.378	x	0.627	6.726161	4.144901	198276	92129.4	15780.85	1167174	20250	23272.49	

Table B-4 (ct'd 12/13) Summary of Results of Continuous Birdges.

	Span	150ft	no. of beams	8		beam spacing = 4ft					
	LFU	LF100	LFD	LF1+	FL1-	R+	D+	L+	R-	D-	L-
Case1	6.007	4.518	2.625	3.726927	5.490182	98014	54409	11700.48	38764	6885	5806.791
Case2	8.22	5.657	3.852	6.348537	3.226415	98014	54409	6869.225	38764	6885	9881.657
Case3	5.777	4.618	2.908	5.294719	2.632331	98014	54409	8235.337	38764	6885	12110.22
	Span	150ft	no. of beams	8		beam spacing = 6ft					
	LFU	LF100	LFD	LF1+	FL1-	R+	D+	L+	R-	D-	L-
Case1	6.093	4.747	1.391	3.914128	6.39588	120980	62669.7	14897.8	58261	10125	17302.97
Case2	5.272	7.138	1.843	6.918192	3.914441	120980	62669.7	8427.867	58261	10125	12296.04
Case3	5.596	4.864	1.341	5.564428	3.075586	120980	62669.7	10480.33	58261	10125	15652.82
	Span	150ft	no. of beams	8		beam spacing = 8ft					
	LFU	LF100	LFD	LF1+	FL1-	R+	D+	L+	R-	D-	L-
Case1	6.051	4.999	1.002	4.193217	7.167986	146757	72550.4	17697.72	77591	13365	8960.576
Case2	8.422	7.871	1.548	7.726919	4.598738	146757	72550.4	9802.739	77591	13365	13964.69
Case3	5.523	5.157	0.994	5.946814	3.442447	146757	72550.4	12477.78	77591	13365	18656.18
	Span	150ft	no. of beams	8		beam spacing = 10ft					
	LFU	LF100	LFD	LF1+	FL1-	R+	D+	L+	R-	D-	L-
Case1	6.331	5.254	0.782	4.488474	7.922432	173725	83463.7	20112.71	97284	17010	23825.21
Case2	8.68	8.656	1.339	8.590881	5.271298	173725	83463.7	10508.46	97284	17010	15231.14
Case3	5.545	5.479	0.791	7.038615	3.790835	173725	83463.7	1481.942	97284	17010	21177.27

Table B-4 (ct'd 13/13) Summary of Results of Continuous Birdges.

	Span	150ft	no. of beams	10		beam spacing = 4ft					
	LFU	LF100	LFD	LF1+	FL1-	R+	D+	L+	R-	D-	L-
Case1	6.105	4.593	2.635	3.791518	5.54778	98014	54409	11500.42	38764	6885	5746.14
Case2	8.166	6.68	3.865	6.384625	3.244057	98014	54409	6831.371	38764	6885	9629.311
Case3	5.8	4.678	2.927	5.339759	2.654285	98014	54409	8168.82	38764	6885	12014.39
	Span	150ft	no. of beams	10		beam spacing = 6ft					
	LFU	LF100	LFD	LF1+	FL1-	R+	D+	L+	R-	D-	L-
Case1	6.093	4.75	1.393	3.918985	6.391456	120980	62669.7	14875.87	58261	10125	7529.752
Case2	8.273	7.139	1.842	6.918817	3.914534	120961	62669.7	8506.765	58261	10125	12296.04
Case3	5.595	4.863	1.337	5.56261	3.073964	120980	62669.7	10486.01	58261	10125	15664.44
	Span	150ft	no. of beams	10		beam spacing = 8ft					
	LFU	LF100	LFD	LF1+	FL1-	R+	D+	L+	R-	D-	L-
Case1	6.051	5	1.018	4.192859	7.168097	146757	72550.4	17699.79	77591	13365	8960.716
Case2	8.422	7.872	1.538	7.727533	4.599156	146757	72550.4	9602.852	77591	13365	13964.69
Case3	5.523	5.157	1.007	5.946888	3.44252	146757	72550.4	12477.89	77591	13365	18656.18

Table B-5 Results of Sensitivity Analysis of 100 ft Simple Span Bridges.

span	beam	spac.	LF300	LF200	LF100	LFU	LFD	LF1	LFu/LF1	LF100/LF	LFd/LF1	comments
100	6	8	1.91	2.42	3.63	5.28	2.05	3.67	1.44	0.99	0.56	Base case
100	6	8	2.11	2.70	4.00	5.40	2.18	3.76	1.44	1.06	0.58	J = 4x J of original girder
100	6	8	1.99	2.54	3.82	5.41	2.12	3.70	1.46	1.03	0.57	J= 2 xJ of original girder
100	6	8	2.05	2.63	4.02	6.32	3.62	3.73	1.69	1.08	0.97	J of slab = 4 x original J
100	6	8	1.96	2.49	3.78	5.67	2.66	3.69	1.54	1.02	0.72	J of slab = 2 x original J
100	6	8	2.52	3.32	4.17	5.33	1.64	3.85	1.38	1.08	0.43	very coarse mesh
100	6	8	2.02	2.55	3.85	5.54	2.17	3.98	1.39	0.97	0.55	4 feet bteween trucks
100	6	8	2.29	2.90	4.34	5.98	2.46	4.18	1.43	1.04	0.59	4 feet between trucks and 2 ft to edge
100	6	8	2.17	2.74	4.12	5.84	2.27	3.87	1.48	1.06	0.59	2 feet between trucks and 2 feet from edge
100	6	8	1.93	2.44	3.68	5.27	1.93	3.68	1.43	1.00	0.52	15 deg. skew
100	6	8	1.97	2.49	3.74	5.27	2.09	3.69	1.43	1.01	0.57	30 deg. skew
100	6	8	2.06	2.61	3.86	5.37	2.27	3.72	1.44	1.04	0.61	45 deg. skew
100	6	8	2.72	3.34	4.78	6.83	2.69	4.90	1.35	0.98	0.55	girder strength = 1.2 original strength
100	6	8	1.91	2.43	3.67	5.38	2.17	3.67	1.47	1.00	0.59	slab strength = 1.2 original strength
100	6	8	3.82	4.58	6.40	8.56	3.48	6.75	1.27	0.95	0.51	girder strength =1.5 original strength
100	6	8	1.91	2.43	3.67	5.48	2.34	3.67	1.49	1.00	0.64	slab strength =1.5 original strength
100	6	8	2.79	3.42	4.86	6.67	2.70	4.93	1.35	0.99	0.55	girder strength & stiffness = 1.2 original values
100	6	8	1.93	2.45	3.70	5.46	2.27	3.65	1.50	1.01	0.62	slab strength & stiffness =1.2 original values
100	6	8	4.07	4.86	6.63	8.62	3.50	6.81	1.27	0.97	0.51	girder strength & stiffness = 1.5 original values
100	6	8	1.96	2.48	3.75	5.67	2.57	3.64	1.56	1.03	0.71	slab strength & stiffness =1.5 original values
100	6	8	2.24	2.85	4.29	6.12	2.21	4.41	1.39	0.97	0.50	girder strength, stiff & dead load =1.2 original values
100	6	8	2.73	3.48	5.23	7.26	2.31	5.50	1.32	0.95	0.42	girder strength, stiff & dead load = 1.5 original values
100	6	8	1.91	2.43	3.67	5.40	2.44	3.67	1.47	1.00	0.67	diaphragm
100	6	8	1.91	2.42	3.65	5.62	2.31	3.67	1.53	1.00	0.63	qmax = 1.2 original max. plast. hinge rotation
100	6	8	1.91	2.42	3.65	5.78	2.76	3.67	1.58	1.00	0.75	qmax = 1.5 original max. plast. hinge rotation
100	6	8	2.08	2.68	3.83	5.55	2.17	3.67	1.51	1.04	0.59	Lp = 0.8 original Lp
100	6	8	1.79	2.25	3.46	5.11	1.96	3.67	1.39	0.94	0.53	Lp= 1.2 original Lp
100	6	8	1.69	2.11	3.24	5.00	1.90	3.67	1.36	0.88	0.52	Lp = 1.4 original Lp

Table B-6 Results of Sensitivity Analysis of 60 ft Simple Span Bridges.

span	beam	spac.	LF300	LF200	LF100	LFU	LFD	LF1	LFu/LF1	LF100/LF	LFd/LF1	comments
60	8	6	1.95	2.39	3.23	4.20	2.17	2.94	1.43	1.10	0.74	Base case
60	8	6	2.12	2.61	3.50	4.35	2.22	2.99	1.46	1.17	0.74	J = 4x J of original girder
60	8	6	2.02	2.48	3.37	4.31	2.19	2.96	1.46	1.14	0.74	J= 2 xJ of original girder
60	8	6	2.11	2.62	3.65	5.12	3.49	2.98	1.72	1.22	1.17	J of slab = 4 x original J
60	8	6	2.01	2.47	3.38	4.54	2.71	2.95	1.54	1.15	0.92	J of slab = 2 x original J
60	8	6	2.40	2.85	3.35	3.98	2.01	2.89	1.38	1.16	0.70	very coarse mesh
60	8	6	2.09	2.55	3.45	4.46	2.33	3.26	1.37	1.06	0.72	4 feet bteween trucks
60	8	6	2.48	3.02	3.97	4.95	2.83	3.43	1.44	1.16	0.82	4 feet between trucks and 2 ft to edge
60	8	6	2.32	2.83	3.73	4.66	2.68	3.17	1.47	1.18	0.85	2 feet between trucks and 2 feet from edge
60	8	6	1.99	2.43	3.27	4.19	2.22	2.98	1.41	1.10	0.75	15 deg. skew
60	8	6	2.08	2.53	3.41	4.29	2.34	3.08	1.39	1.11	0.76	30 deg. skew
60	8	6	2.25	2.75	3.66	4.56	2.54	2.93	1.56	1.25	0.87	45 deg. skew
60	8	6	2.53	3.05	4.05	5.12	2.68	3.77	1.36	1.07	0.68	girder strength = 1.2 original strength
60	8	6	1.95	2.39	3.25	4.26	2.30	2.94	1.45	1.11	0.78	slab strength = 1.2 original strength
60	8	6	3.38	4.01	5.24	6.45	3.20	5.02	1.29	1.04	0.64	girder strength =1.5 original strength
60	8	6	1.96	2.40	3.27	4.33	2.46	2.94	1.47	1.11	0.84	slab strength =1.5 original strength
60	8	6	2.59	3.11	4.09	5.16	2.59	3.72	1.39	1.10	0.70	girder strength & stiffness = 1.2 original values
60	8	6	1.97	2.42	3.29	4.33	2.41	2.98	1.45	1.10	0.81	slab strength & stiffness =1.2 original values
60	8	6	3.54	4.19	5.36	6.50	3.20	4.87	1.34	1.10	0.66	girder strength & stiffness = 1.5 original values
60	8	6	2.00	2.46	3.37	4.51	2.72	3.03	1.49	1.11	0.90	slab strength & stiffness =1.5 original values
60	8	6	2.32	2.84	3.82	4.89	2.34	3.48	1.40	1.10	0.67	girder strength, stiff & dead load =1.2 original values
60	8	6	2.88	3.51	4.68	5.86	2.63	4.27	1.37	1.10	0.62	girder strength, stiff & dead load = 1.5 original values
60	8	6	1.97	2.42	3.29	4.33	2.59	2.94	1.47	1.12	0.88	diaphragm
60	8	6	1.95	2.39	3.23	4.43	2.45	2.94	1.51	1.10	0.83	qmax = 1.2 original max. plast. hinge rotation
60	8	6	1.95	2.39	3.23	4.79	2.67	2.94	1.63	1.10	0.91	qmax = 1.5 original max. plast. hinge rotation
60	8	6	2.10	2.60	3.33	4.34	2.22	2.94	1.48	1.13	0.75	Lp = 0.8 original Lp
60	8	6	1.84	2.24	3.14	4.10	2.09	2.94	1.40	1.07	0.71	Lp= 1.2 original Lp
60	8	6	1.76	2.12	3.02	4.03	2.06	2.94	1.37	1.03	0.70	Lp = 1.4 original Lp

Table B-7 Results of Sensitivity Analysis of Continuous Bridges

	LFU	LF100	LF200	LF300	LFD	LF1+	LF1-	R+	D+	L+	R-	D-	L-
Basic Case													
Case1	6.591	4.407	3.339	2.756	1.57	3.9696831	5.7734179	74639	31164.6	10952.649	38371	5940	5617.8042
Case2	8.186	6.798	5.242	4.399	2.594	7.0261606	3.4216413	74639	31164.6	6187.6735	38371	5940	9478.458
Case3	5.335	4.491	3.449	2.921	1.677	5.3425416	2.6076739	74639	31164.6	8134.9911	38371	5940	12433.076
Omax=1.2Θmax													
Case1	6.637	4.407	3.339	2.759	1.671	3.9693045	5.7728961	74639	31164.6	10952.649	38371	5940	5617.8042
Case2	8.537	6.798	5.242	4.399	2.879	7.0259687	3.4215481	74639	31164.6	6187.6735	38371	5940	9478.458
Case3	5.539	4.491	3.449	2.921	1.847	5.3441239	2.6084455	74639	31164.6	8134.9911	38371	5940	12433.076
Omax=1.5Θmax													
Case1	6.181	4.407	3.339	2.759	2.159	3.9696831	5.773418	74639	31164.6	10952.649	38371	5940	5617.8042
Case2	9.01	6.798	5.242	4.399	3.289	7.0261606	3.4216413	74639	31164.6	6187.6735	38371	5940	9478.458
Case3	6.807	4.491	3.449	2.921	2.082	5.3425416	2.6076739	74639	31164.6	8134.9911	38371	5940	12433.076
(Omax=1.2pos)													
Case1	5.591	4.407	3.339	2.756	1.665	3.9696831	5.773418	74639	31164.6	10952.649	38371	5940	5617.8042
Case2	8.186	6.798	5.242	4.399	2.594	7.0261606	3.4216413	74639	31164.6	6187.6735	38371	5940	9478.458
Case3	5.335	4.491	3.449	2.921	1.677	5.3425416	2.6076739	74639	31164.6	8134.9911	38371	5940	12433.076
(Omax=1.5pos)													
Case1	5.591	4.407	3.339	2.756	1.665	3.9696831	5.773418	74639	31164.6	10952.649	38371	5940	5617.8042
Case2	8.186	6.798	5.242	4.399	2.594	7.0261606	3.4216413	74639	31164.6	6187.6735	38371	5940	9478.458
Case3	5.335	4.491	3.449	2.921	1.677	5.3425416	2.6076739	74639	31164.6	8134.9911	38371	5940	12433.076

Table B-7 (ct'd 2/6) Results of Sensitivity Analysis of Continuous Bridges

(Θmax=1.2neg)													
Case1	5.837	4.407	3.339	2.756	1.871	3.9696631	5.773418	74639	31164.6	10952.649	38371	5940	5617.8042
Case2	8.537	6.798	5.242	4.399	2.879	7.0261606	3.4216413	74639	31164.6	6187.6735	38371	5940	9478.458
Case3	5.539	4.491	3.449	2.921	1.847	5.3425416	2.6076739	74639	31164.6	8134.9911	38371	5940	12433.076
(Θmax=1.5neg)													
Case1	6.181	4.407	3.339	2.756	2.159	3.9696631	5.773418	74639	31164.6	10952.649	38371	5940	5617.8042
Case2	9.01	6.798	5.242	4.399	3.289	7.0261606	3.4216413	74639	31164.6	6187.6735	38371	5940	9478.458
Case3	5.807	4.491	3.449	2.921	2.082	5.3425416	2.6076739	74639	31164.6	8134.9911	38371	5940	12433.076
Lp=0.8Lp													
Case1	5.744	4.536	3.614	2.964	1.724	3.9696631	5.773418	74639	31164.6	10952.649	38371	5940	5617.8042
Case2	8.333	6.979	5.6	4.658	2.664	7.0261606	3.4216413	74639	31164.6	6187.6735	38371	5940	9478.458
Case3	5.448	4.615	3.713	3.103	1.722	5.3425416	2.6076739	74639	31164.6	8134.9911	38371	5940	12433.076
Lp=1.2Lp													
Case1	5.494	4.268	3.143	2.603	1.621	3.9696631	5.773418	74639	31164.6	10952.649	38371	5940	5617.8042
Case2	8.06	6 596	4.966	4.2	2.539	7.0261606	3.4216413	74639	31164.6	6187.6735	38371	5940	9478.458
Case3	5.236	4.342	3.259	2.794	1.638	5.3425416	2.6076739	74639	31164.6	8134.9911	38371	5940	12433.076
Lp=1.4Lp													
Case1	5.415	4.107	2.998	2.486	1.596	3.9696631	5.773418	74639	31164.6	10952.649	38371	5940	5617.8042
Case2	7.943	6.402	4.783	4.083	2.489	7.0261606	3.4216413	74639	31164.6	6187.6735	38371	5940	9478.458
Case3	5.147	4.178	3.119	2.687	1.612	5.3425416	2.6076739	74639	31164.6	8134.9911	38371	5940	12433.076

Table B-7 (ct'd) 3/6 Results of Sensitivity Analysis of Continuous Bridges

	LFU	LF100	LF200	LF300	LFD	LF1+	LF1-	R+	D+	L+	R-	D-	L-
(=15)													
Case1	5.587	4.455	3.37	2.744	1.648	3.9899882	5.6197924	74639	31164.6	10895.872	38371	5940	5770.8536
Case2	8.061	6.766	5.206	4.358	2.682	7.0027454	3.427755	74639	31164.6	6208.1938	38371	5940	9461.2947
Case3	5.215	4.484	3.419	2.877	1.725	5.1806821	2.6383785	74639	31164.6	8391.6363	38371	5940	12301.354
(=30)													
Case1	5.797	4.53	3.442	2.824	1.628	4.0358949	5.4815254	74639	31164.6	10771.936	38371	5940	5816.4189
Case2	8.169	6.71	5.171	4.337	2.823	6.9832991	3.4479274	74639	31164.6	6225.4815	38371	5940	9405.9406
Case3	5.366	4.458	3.418	2.852	1.815	5.0351436	2.6806868	74639	31164.6	8634.1928	38371	5940	12053.057

Table B-7 (ct'd 4/6) Results of Sensitivity Analysis of Continuous Bridges

	LFU	LF100	LF200	LF300	LFD	LF1+	LF1-	R+	D+	L+	R-	D-	L-
(1.2Spos)													
Case1	5.665	4.439	3.383	2.771	1.783	3.9944173	5.7515792	74639	31164.6	10883.79	38371	5940	5638.6253
Case2	8.35	6.89	5.304	4.484	2.783	7.0625527	3.4339619	74639	31164.6	8155.6213	38371	5940	9444.1934
Case3	5.401	4.525	3472	2.942	1.78	5.4415022	2.6627558	74639	31164.6	7969.4114	38371	5940	12179.487
(1.5Spos)													
Case1	5.772	4.487	3.396	2.794	1.974	3.9645116	5.6730908	74639	31164.6	10965.891	38371	5940	5716.6368
Case2	8.582	7.012	5.384	4.536	3.051	7.1188561	3.4541343	74639	31164.6	8106.9362	38371	5940	9389.0386
Case3	5.495	4.574	3.504	2.971	1.927	5.5665611	2.7325833	74639	31164.6	7809.9205	38371	5940	11868.257
(1.2Sneg)													
Case1	5.71	4.485	3.375	2.781	1.832	3.9950457	5.7524844	74639	31164.6	10882.078	38371	5940	5637.738
Case2	8.482	7.026	5.397	4.496	2.861	7.0625527	3.4339619	74639	31164.6	8155.6213	38371	5940	9444.1934
Case3	5.452	4.575	3.492	2.953	1.823	5.4415022	2.6627558	74639	31164.6	7969.4114	38371	5940	12179.487
(1.5Sneg)													
Case1	5.886	4.587	3.426	2.817	2.119	3.9645116	5.6730908	74639	31164.6	10965.891	38371	5940	5716.6368
Case2	8.892	7.34	5.594	4.635	3.219	7.1188561	3.4541343	74639	31164.6	8106.9362	38371	5940	9389.0386
Case3	5.618	4.683	3.55	2.996	2.062	5.5665611	2.7325833	74639	31164.6	7809.9205	38371	5940	11868.257

Table B-7 (ct'd 5/6) Results of Sensitivity Analysis of Continuous Bridges

	LFU	LF100	LF200	LF300	LFD	LF1+	LF1-	R+	D+	L+	R-	D-	L-
(1.2Gpos)													
Case1	6.728	5.432	4.192	3.543	2.158	5.2416074	5.6373471	89566.8	31164.6	11142.04	38371	5940	5752.8833
Case2	9.692	8.184	6.384	5.439	3.357	9.398739	3.4122378	89566.8	31164.6	6213.6336	38371	5940	9504.3201
Case3	8.439	6.51	4.289	3.673	2.185	7.0426865	2.5525835	89566.8	31164.6	8292.6281	38371	5940	12705.167
(1.5Gpos)													
Case1	8.284	6.684	4.927	4.06	2.799	7.0953143	5.4730229	111958.5	31164.6	11388.937	38371	5940	5825.6101
Case2	11.65	9.764	7.329	6.13	4.339	12.94478	3.4029274	111958.5	31164.6	6241.4273	38371	5940	9530.3238
Case3	7.904	6.751	4.969	4.175	2.819	9.5217057	2.4874111	111958.5	31164.6	8485.2339	38371	5940	13038.054
(1.2Gneg)													
Case1	5.991	4.729	3.673	3.039	1.861	3.9018348	6.9712869	74639	31164.6	11142.04	46045	5940	5752.8833
Case2	8.744	7.293	5.736	4.876	2.897	6.996643	4.2196129	74639	31164.6	6213.6085	46045	5940	9503.9758
Case3	5.727	4.844	3.807	3.263	1.881	5.2436865	3.1572701	74639	31164.6	8290.8401	46045	5940	12702.429
(1.5Gneg)													
Case1	6.543	5.182	4.142	3.448	2.125	3.8179186	8.7106329	74639	31164.6	11388.937	57557	5940	5825.6101
Case2	9.538	7.994	6.452	5.57	3.322	6.9658942	5.4184973	74639	31164.6	6240.9469	57557	5940	9529.5803
Case3	6.287	5.354	4.326	3.755	2.187	5.1228246	3.9583892	74639	31164.6	8488.412	57557	5940	13039.867
(1.2G)													
Case1	7.072	5.716	4.466	3.78	2.323	5.250657	6.9712869	89567	31164.6	11122.875	46045	5940	5752.8833
Case2	10.15	8.559	6.795	5.849	3.617	9.2502534	4.2196129	89567	31164.6	6313.6	46045	5940	9503.9758
Case3	6.779	5.818	4.6	3.98	2.367	7.0442078	3.1572701	89567	31164.6	8290.8401	46045	5940	12702.429

Table B-7 (ct'd 6/6) Results of Sensitivity Analysis of Continuous Bridges

(1.5G)													
Case1	9.136	7.412	5.637	4.705	3.193	7.0953582	8.7106329	111959	31164.6	11386.837	57557	5940	5825.6101
Case2	12.79	10.791	8.384	7.155	4.998	12.945856	5.4184973	111959	31164.6	6240.9469	57557	5940	9529.5903
Case3	8.754	7.53	5.795	4.948	3.259	9.5204428	3.9583992	111959	31164.6	8486.412	57557	5940	13039.667

Table B-8 Safety Indices for Simple Span Bridges.

			SAFETY INDICES						
SPAN	BEAMS	SPAC.	MEMBER	ULTIMATE	DELTA beta	LF100	DELTA beta	DAMAGED	DELTA beta
45	4	4	1.99	2.05	0.06	1.67	-0.32	0.63	-1.35
45	4	6	2.60	3.37	0.77	2.78	0.18	1.72	-0.88
45	4	8	3.33	4.07	0.75	3.31	-0.02	1.74	-1.59
45	4	10	3.22	4.44	1.21	3.63	0.40	1.65	-1.58
45	4	12	3.69	4.63	0.94	3.87	0.18	1.42	-2.27
45	6	4	2.27	3.40	1.12	2.65	0.38	2.47	0.20
45	6	6	2.68	3.79	1.11	2.97	0.29	1.96	-0.72
45	6	8	2.81	4.16	1.35	3.41	0.61	1.89	-0.91
45	6	10	3.25	4.48	1.24	3.69	0.45	1.71	-1.54
45	6	12	3.70	4.78	1.08	4.05	0.36	1.74	-1.95
45	8	4	2.29	3.63	1.34	2.76	0.47	2.63	0.34
45	8	6	2.69	3.82	1.13	2.98	0.29	1.97	-0.71
45	8	8	2.81	4.16	1.35	3.41	0.61	1.89	-0.91
45	8	10	3.25	4.49	1.24	3.70	0.45	1.71	-1.54
45	10	4	2.29	3.65	1.36	2.79	0.50	2.64	0.35
45	10	6	2.69	3.82	1.13	2.98	0.29	1.97	-0.71
45	10	8	2.81	4.16	1.35	3.41	0.61	1.89	-0.91
60	4	4	1.71	1.81	0.09	1.44	-0.27	-0.01	-1.72
60	4	6	2.44	3.30	0.87	2.65	0.21	1.33	-1.10
60	4	8	2.82	4.10	1.28	3.04	0.22	1.60	-1.22
60	4	10	3.29	4.45	1.16	3.39	0.10	1.56	-1.73
60	4	12	3.76	4.65	0.89	3.67	-0.09	0.36	-3.40
60	6	4	2.03	3.13	1.10	2.39	0.36	1.91	-0.11
60	6	6	2.51	3.77	1.25	2.83	0.32	1.59	-0.93
60	6	8	2.90	4.21	1.31	3.18	0.28	1.77	-1.13
60	6	10	3.34	4.50	1.16	3.48	0.14	1.68	-1.66
60	6	12	3.73	4.38	0.65	3.71	-0.03	1.05	-2.69
60	8	4	2.04	3.36	1.32	2.52	0.47	2.09	0.05
60	8	6	2.52	3.80	1.28	2.87	0.34	1.66	-0.86
60	8	8	2.90	4.22	1.32	3.17	0.27	1.84	-1.06
60	8	10	3.34	4.50	1.16	3.48	0.14	1.68	-1.66
60	10	4	2.04	3.37	1.34	2.55	0.51	2.11	0.08

Table B-8 (ct'd 2/3) Safety Indices for Simple Span Bridges.

60	10	6	2.52	3.80	1.28	2.87	0.34	1.66	-0.86
60	10	8	2.90	4.22	1.32	3.17	0.27	1.84	-1.06
80	4	4	1.71	1.77	0.06	1.26	-0.45	-0.20	-1.91
80	4	6	2.41	3.17	0.75	2.28	-0.14	1.18	-1.23
80	4	8	2.91	4.01	1.10	2.85	-0.06	1.14	-1.77
80	4	10	3.29	4.37	1.08	3.21	-0.08	1.08	-2.21
80	4	12	3.51	4.43	0.92	3.48	-0.03	0.22	-3.29
80	6	4	1.83	3.05	1.22	2.00	0.17	1.85	0.01
80	6	6	2.43	3.64	1.21	2.46	0.02	1.44	-1.00
80	6	8	3.00	4.13	1.13	3.01	0.01	1.35	-1.65
80	6	10	3.31	4.44	1.13	3.34	0.04	1.17	-2.14
80	6	12	3.51	4.48	0.96	3.54	0.03	0.29	-3.22
80	8	4	1.87	3.33	1.46	2.11	0.24	1.78	-0.09
80	8	6	2.45	3.68	1.23	2.53	0.08	1.48	-0.97
80	8	8	3.00	4.14	1.14	3.02	0.02	1.37	-1.64
80	8	10	3.31	4.44	1.13	3.34	0.04	1.23	-2.08
80	10	4	1.89	3.36	1.47	2.18	0.29	1.49	-0.40
80	10	6	2.45	3.68	1.24	2.53	0.08	1.48	-0.97
80	10	8	3.00	4.14	1.14	3.02	0.02	1.37	-1.64
100	4	4	1.71	1.80	0.09	1.15	-0.56	-0.42	-2.12
100	4	6	2.35	3.10	0.75	2.21	-0.14	0.84	-1.52
100	4	8	2.77	3.93	1.16	2.64	-0.13	0.79	-1.98
100	4	10	3.11	4.28	1.17	2.98	-0.13	0.64	-2.47
100	4	12	3.42	4.51	1.09	3.26	-0.17	0.70	-2.72
100	6	4	1.83	3.07	1.24	1.91	0.08	1.73	-0.11
100	6	6	2.35	3.61	1.26	2.35	0.00	1.14	-1.21
100	6	8	2.84	4.08	1.24	2.82	-0.02	0.98	-1.87
100	6	10	3.15	4.37	1.22	3.13	-0.02	0.82	-2.33
100	6	12	3.48	4.59	1.11	3.38	-0.10	1.01	-2.47
100	8	4	1.86	3.39	1.52	2.02	0.16	1.66	-0.20
100	8	6	2.38	3.64	1.26	2.47	0.09	1.21	-1.18
100	8	8	2.84	4.10	1.27	2.83	-0.01	1.01	-1.83
100	8	10	3.15	4.38	1.23	3.13	-0.02	0.82	-2.33
100	10	4	1.89	3.43	1.54	2.09	0.19	1.21	-0.69
100	10	8	2.38	3.66	1.28	2.48	0.10	1.21	-1.18

Table B-8 (ct'd 3/3) Safety Indices for Simple Span Bridges.

100	10	8	2.84	4.10	1.27	3.34	0.50	1.01	-1.83
120	4	4	1.87	1.94	0.07	1.35	-0.53	-0.53	-2.40
120	4	6	2.31	3.06	0.74	2.19	-0.13	0.32	-2.00
120	4	8	2.66	3.84	1.18	2.56	-0.10	0.35	-2.32
120	4	10	3.04	4.24	1.20	2.95	-0.09	0.20	-2.84
120	4	12	3.26	4.06	0.80	3.09	-0.18	-0.56	-3.82
120	6	4	1.97	3.11	1.14	2.04	0.07	1.37	-0.61
120	6	6	2.31	3.47	1.17	2.32	0.01	0.63	-1.68
120	6	8	2.76	3.99	1.23	2.76	0.00	0.65	-2.11
120	6	10	3.10	4.33	1.22	3.14	0.04	0.45	-2.66
120	6	12	3.29	4.15	0.85	3.24	-0.05	-0.27	-3.56
120	8	4	2.00	3.25	1.25	2.13	0.13	1.10	-0.90
120	8	6	2.35	3.52	1.17	2.43	0.08	0.73	-1.62
120	8	8	2.76	4.00	1.24	2.79	0.03	0.64	-2.12
120	8	10	3.10	4.34	1.23	3.14	0.04	0.45	-2.66
120	10	4	2.05	3.34	1.29	2.20	0.16	0.83	-1.42
120	10	6	2.35	3.52	1.17	2.44	0.09	0.73	-1.62
120	10	8	2.76	4.00	1.24	2.78	0.02	0.64	-2.12
150	4	4	2.09	2.11	0.02	1.55	-0.54	-0.91	-3.00
150	4	6	2.40	3.10	0.70	2.26	-0.14	-0.26	-2.66
150	4	8	2.62	3.60	0.97	2.60	-0.02	-1.10	-3.73
150	4	10	3.01	4.06	1.05	3.04	0.02	-1.44	-4.45
150	4	12	3.23	4.09	0.86	3.16	-0.07	-1.56	-4.79
150	6	4	2.20	3.10	0.89	2.03	-0.17	0.24	-1.96
150	6	6	2.38	3.43	1.05	2.36	-0.02	0.04	-2.34
150	6	8	2.75	3.81	1.06	2.81	0.06	-0.61	-3.36
150	6	10	3.13	4.18	1.05	3.25	0.12	-1.03	-4.16
150	6	12	3.45	4.37	0.92	3.38	-0.06	-1.14	-4.59
150	8	4	2.21	3.22	1.01	2.07	-0.13	0.35	-1.85
150	8	6	2.46	3.49	1.03	2.52	0.05	0.17	-2.29
150	8	8	2.78	3.83	1.05	2.86	0.08	-0.59	-3.37
150	8	10	3.15	4.19	1.05	3.27	0.13	-1.03	-4.17
150	10	4	2.19	3.27	1.07	2.20	0.01	0.40	-1.80
150	10	6	2.47	3.50	1.03	2.52	0.05	0.20	-2.27
150	10	8	2.78	3.83	1.05	2.87	0.09	-0.56	-3.34

Table B-9 System Factors for Simple Span Bridges.

			SYSTEM FACTORS		
SPAN	BEAMS	SPAC.	ULTIMATE	FUNCTION.	DAMAGED
45	4	4	0.85	0.89	1.26
45	4	6	0.98	0.99	1.39
45	4	8	0.98	0.94	1.25
45	4	10	1.08	1.03	1.25
45	4	12	1.02	0.98	1.09
45	6	4	1.05	1.02	1.58
45	6	6	1.06	1.01	1.43
45	6	8	1.11	1.08	1.39
45	6	10	1.09	1.04	1.26
45	6	12	1.05	1.02	1.17
45	8	4	1.10	1.04	1.60
45	8	6	1.06	1.01	1.43
45	8	8	1.11	1.08	1.39
45	8	10	1.09	1.04	1.26
45	10	4	1.10	1.05	1.61
45	10	6	1.06	1.01	1.43
45	10	8	1.11	1.08	1.39
60	4	4	0.87	0.91	1.16
60	4	6	1.00	0.99	1.30
60	4	8	1.09	0.99	1.30
60	4	10	1.06	0.97	1.20
60	4	12	1.01	0.93	0.86
60	6	4	1.04	1.02	1.42
60	6	6	1.08	1.01	1.34
60	6	8	1.09	1.01	1.32
60	6	10	1.06	0.98	1.22
60	6	12	0.96	0.94	1.00
60	8	4	1.08	1.04	1.45
60	8	6	1.08	1.02	1.35
60	8	8	1.10	1.00	1.33
60	8	10	1.06	0.98	1.22
60	10	4	1.08	1.05	1.45

Table B-9 (ct'd 2/3) System Factors for Simple Span Bridges.

60	10	6	1.08	1.02	1.35
60	10	8	1.10	1.00	1.33
80	4	4	0.87	0.89	1.13
80	4	6	0.98	0.93	1.26
80	4	8	1.05	0.94	1.18
80	4	10	1.04	0.94	1.09
80	4	12	1.01	0.95	0.89
80	6	4	1.06	0.99	1.41
80	6	6	1.07	0.96	1.31
80	6	8	1.05	0.95	1.20
80	6	10	1.06	0.96	1.11
80	6	12	1.02	0.96	0.90
80	8	4	1.10	1.00	1.40
80	8	6	1.07	0.97	1.31
80	8	8	1.05	0.96	1.20
80	8	10	1.06	0.96	1.12
80	10	4	1.10	1.01	1.35
80	10	6	1.07	0.97	1.31
80	10	8	1.05	0.96	1.20
100	4	4	0.89	0.88	1.09
100	4	6	0.98	0.94	1.19
100	4	8	1.05	0.94	1.12
100	4	10	1.06	0.93	1.04
100	4	12	1.04	0.92	1.00
100	6	4	1.06	0.97	1.35
100	6	6	1.07	0.96	1.24
100	6	8	1.07	0.95	1.14
100	6	10	1.07	0.95	1.06
100	6	12	1.06	0.94	1.04
100	8	4	1.10	0.99	1.34
100	8	6	1.07	0.97	1.25
100	8	8	1.07	0.95	1.15
100	8	10	1.07	0.95	1.06
100	10	4	1.10	0.99	1.28
100	10	6	1.07	0.98	1.25

Table B-9 (ct'd 3/3) System Factors for Simple Span Bridges.

100	10	8	1.07	1.04	1.15
120	4	4	0.88	0.89	1.04
120	4	6	0.98	0.94	1.11
120	4	8	1.05	0.94	1.06
120	4	10	1.06	0.94	0.98
120	4	12	0.99	0.93	0.81
120	6	4	1.04	0.97	1.28
120	6	6	1.05	0.96	1.15
120	6	8	1.06	0.96	1.10
120	6	10	1.06	0.96	1.01
120	6	12	1.00	0.95	0.85
120	8	4	1.06	0.98	1.24
120	8	6	1.05	0.97	1.16
120	8	8	1.06	0.96	1.09
120	8	10	1.07	0.96	1.01
120	10	4	1.06	0.99	1.18
120	10	6	1.05	0.98	1.16
120	10	8	1.06	0.96	1.09
150	4	4	0.88	0.89	0.96
150	4	6	0.98	0.94	1.01
150	4	8	1.02	0.96	0.84
150	4	10	1.03	0.96	0.72
150	4	12	1.00	0.95	0.67
150	6	4	1.01	0.94	1.10
150	6	6	1.03	0.96	1.05
150	6	8	1.03	0.97	0.90
150	6	10	1.03	0.98	0.77
150	6	12	1.01	0.95	0.70
150	8	4	1.02	0.94	1.11
150	8	6	1.03	0.97	1.06
150	8	8	1.03	0.97	0.89
150	8	10	1.03	0.98	0.76
150	10	4	1.03	0.97	1.12
150	10	6	1.03	0.97	1.06
150	10	8	1.03	0.97	0.90

Table B-10 Safety Indices and System Factors for Continuous Bridges.

Table B-10 Reliability of sensitivity cases for 100 ft bridge															
			SAFETY INDICES							SYSTEM FACTORS - PHI s			COMMENTS		
SPAN	BEAMS	SPAC.	BETAM	ultimate	delta beta	funct.	delta beta	damaged	delta beta	ultimate	funct.	damaged			
100	8	6	2.84	4.08	1.24	2.80	-0.04	0.97	-1.87	1.07	0.95	1.14	Base case		
100	8	6	2.92	4.15	1.23	3.14	0.22	1.21	-1.71	1.07	0.99	1.17	J = 4x J of original girder		
100	8	6	2.87	4.17	1.30	2.98	0.11	1.11	-1.76	1.08	0.98	1.16	J= 2 xJ of original girder		
100	8	6	2.90	4.69	1.80	3.15	0.25	3.06	0.17	1.18	1.00	1.46	J of slab = 4 x original J		
100	8	6	2.86	4.33	1.47	2.94	0.08	1.97	-0.89	1.11	0.97	1.30	J of slab = 2 x original J		
100	8	6	3.03	4.14	1.11	3.31	0.28	0.03	-3.00	1.05	1.00	0.95	very coarse mesh		
100	8	6	3.12	4.25	1.13	3.00	-0.12	1.21	-1.92	1.05	0.94	1.14	4 feet bteween trucks		
100	8	6	3.29	4.50	1.22	3.42	0.13	1.68	-1.61	1.06	0.98	1.19	4 feet between trucks and 2 ft to edge		
100	8	6	3.04	4.32	1.28	3.25	0.21	1.40	-1.64	1.08	1.00	1.19	2 feet between trucks and 2 feet from edge		
100	8	6	2.85	4.07	1.22	2.84	0.00	0.72	-2.13	1.06	0.96	1.10	15 deg. skew		
100	8	6	2.88	4.09	1.21	2.92	0.04	1.08	-1.80	1.07	0.97	1.16	30 deg. skew		
100	8	6	2.89	4.14	1.25	3.02	0.13	1.38	-1.50	1.07	0.98	1.20	45 deg. skew		
100	8	6	3.95	5.02	1.07	3.86	-0.09	2.09	-1.86	1.04	0.94	1.17	girder strength = 1.2 original strength		
100	8	6	2.84	4.15	1.31	2.84	0.00	1.21	-1.63	1.08	0.96	1.18	slab strength = 1.2 original strength		
100	8	6	5.20	6.09	0.90	5.00	-0.20	3.09	-2.11	1.01	0.91	1.12	girder strength =1.5 original strength		
100	8	6	2.84	4.21	1.37	2.84	0.00	1.50	-1.34	1.09	0.96	1.23	slab strength =1.5 original strength		
100	8	6	3.97	5.04	1.07	3.92	-0.05	2.10	-1.87	1.04	0.94	1.16	girder strength & stiffness = 1.2 original values		
100	8	6	2.82	4.20	1.38	2.87	0.05	1.38	-1.44	1.09	0.97	1.21	slab strength & stiffness =1.2 original values		
100	8	6	5.23	6.13	0.89	5.13	-0.10	3.12	-2.11	1.01	0.93	1.12	girder strength & stiffness = 1.5 original values		
100	8	6	2.81	4.32	1.52	2.91	0.11	1.85	-0.96	1.11	0.98	1.29	slab strength & stiffness =1.5 original values		
100	8	6	3.46	4.57	1.11	3.37	-0.09	1.26	-2.20	1.05	0.94	1.09	girder strength, stiff & dead load =1.2 original v		
100	8	6	4.20	5.15	0.95	4.03	-0.17	1.43	-2.76	1.02	0.93	0.99	girder strength, stiff & dead load = 1.5 original v		
100	8	6	2.84	4.16	1.32	2.84	0.00	1.66	-1.18	1.08	0.96	1.26	diaphragm		
100	8	6	2.84	4.29	1.45	2.82	-0.02	1.45	-1.39	1.10	0.95	1.22	qmax = 1.2 original max. plast. hinge rotation		
100	8	6	2.84	4.39	1.55	2.82	-0.02	2.11	-0.73	1.12	0.95	1.33	qmax = 1.5 original max. plast. hinge rotation		
100	8	6	2.84	4.25	1.41	2.98	0.14	1.21	-1.63	1.10	0.98	1.18	Lp = 0.8 original Lp		
100	8	6	2.84	3.97	1.13	2.63	-0.21	0.79	-2.05	1.05	0.92	1.11	Lp= 1.2 original Lp		
100	8	6	2.84	3.89	1.05	2.41	-0.43	0.66	-2.18	1.04	0.88	1.09	Lp = 1.4 original Lp		

Table B-11 Safety Indices and System Factors for Sensitivity of 60 ft Bridges.

			SAFETY INDICES							SYSTEM FACTORS - PHI s			COMMENTS
SPAN	BEAMS	SPAC.	BETAM	ultimate	delta beta	funct.	delta beta	damaged	delta beta	ultimate	funct.	damaged	
60	8	6	2.52	3.80	1.28	2.87	0.34	1.66	-0.86	1.08	1.02	1.35	Base case
60	8	6	2.59	3.93	1.34	3.16	0.57	1.76	-0.84	1.10	1.06	1.36	J = 4x J of original girder
60	8	6	2.55	3.89	1.34	3.02	0.47	1.70	-0.85	1.09	1.04	1.35	J= 2 xJ of original girder
60	8	6	2.58	4.51	1.93	3.31	0.73	3.42	0.84	1.21	1.09	1.65	J of slab = 4 x original J
60	8	6	2.54	4.08	1.54	3.03	0.49	2.51	-0.03	1.13	1.05	1.50	J of slab = 2 x original J
60	8	6	2.47	3.62	1.15	3.00	0.54	1.36	-1.11	1.08	1.08	1.30	very coarse mesh
60	8	6	2.90	4.02	1.11	3.10	0.20	1.94	-0.96	1.05	0.99	1.35	4 feet bteween trucks
60	8	6	3.09	4.39	1.30	3.61	0.52	2.67	-0.42	1.09	1.05	1.46	4 feet between trucks and 2 ft to edge
60	8	6	2.81	4.18	1.37	3.39	0.58	2.47	-0.34	1.10	1.07	1.46	2 feet between trucks and 2 feet from edge
60	8	6	2.57	3.79	1.22	2.91	0.34	1.75	-0.82	1.07	1.02	1.36	15 deg. skew
60	8	6	2.69	3.87	1.18	3.06	0.37	1.95	-0.74	1.06	1.02	1.38	30 deg. skew
60	8	6	2.51	4.09	1.58	3.31	0.80	2.26	-0.25	1.14	1.11	1.46	45 deg. skew
60	8	6	3.47	4.58	1.10	3.73	0.26	2.36	-1.11	1.05	1.00	1.36	girder strength = 1.2 original strength
60	8	6	2.52	3.85	1.33	2.89	0.36	1.89	-0.64	1.09	1.02	1.39	slab strength = 1.2 original strength
60	8	6	4.56	5.50	0.94	4.72	0.16	3.19	-1.37	1.02	0.98	1.33	girder strength =1.5 original strength
60	8	6	2.52	3.91	1.38	2.91	0.39	2.14	-0.38	1.10	1.03	1.44	slab strength =1.5 original strength
60	8	6	3.42	4.60	1.18	3.76	0.34	2.38	-1.05	1.07	1.02	1.37	girder strength & stiffness = 1.2 original valu
60	8	6	2.57	3.91	1.33	2.93	0.36	2.07	-0.51	1.09	1.02	1.42	slab strength & stiffness =1.2 original values
60	8	6	4.44	5.53	1.08	4.80	0.35	3.19	-1.25	1.05	1.02	1.36	girder strength & stiffness = 1.5 original valu
60	8	6	2.63	4.05	1.42	3.02	0.38	2.51	-0.12	1.11	1.02	1.49	slab strength & stiffness =1.5 original values
60	8	6	3.13	4.34	1.21	3.46	0.33	1.95	-1.18	1.07	1.02	1.31	girder strength, stiff & dead load =1.2 origina
60	8	6	3.86	5.00	1.13	4.19	0.33	2.40	-1.47	1.06	1.02	1.26	girder strength, stiff & dead load = 1.5 origin
60	8	6	2.53	3.91	1.38	2.94	0.41	2.34	-0.19	1.10	1.03	1.47	diaphragm
60	8	6	2.52	3.99	1.46	2.87	0.34	2.13	-0.40	1.12	1.02	1.43	qmax = 1.2 original max. plast. hinge rotatio
60	8	6	2.52	4.27	1.74	2.87	0.34	2.45	-0.08	1.17	1.02	1.49	qmax = 1.5 original max. plast. hinge rotatio
60	8	6	2.52	3.92	1.39	2.97	0.45	1.75	-0.78	1.10	1.04	1.37	Lp = 0.8 original Lp
60	8	6	2.52	3.71	1.19	2.76	0.24	1.51	-1.01	1.07	1.00	1.32	Lp= 1.2 original Lp
60	8	6	2.52	3.65	1.13	2.62	0.10	1.45	-1.07	1.05	0.97	1.31	Lp = 1.4 original Lp

Table B-12 Safety Indices and System Factors of Continuous Birgdes

Table B-12 Reliability and system factors for continuous bridges.

				SAFETY INDICES (beta)							SYSTEM FACTORS (Phi)		
SPAN	BEAM	SPAC	oad ca	member	ultimate	delta beta	LF100	delta beta	damage	delat beta	ultimate	funct.	damage
100	4	4	1	1.99	2.41	0.41	1.95	-0.05	0.51	-1.49	0.93	0.95	1.17
100	4	4	2	0.16	5.00	4.84	3.73	3.56	2.18	2.02	1.70	1.58	1.83
100	4	4	3	1.50	3.07	1.56	2.57	1.06	0.81	-0.69	1.15	1.17	1.41
100	4	6	1	2.68	3.74	1.06	2.88	0.20	0.39	-2.29	1.04	0.99	1.07
100	4	6	2	1.95	5.22	3.27	4.43	2.47	1.18	-0.78	1.53	1.49	1.42
100	4	6	3	1.76	4.15	2.39	3.48	1.72	0.27	-1.48	1.33	1.31	1.26
100	4	8	1	2.99	4.15	1.16	3.27	0.28	-0.16	-3.14	1.05	1.01	0.92
100	4	8	2	2.63	5.83	3.21	5.11	2.48	1.61	-1.02	1.57	1.54	1.40
100	4	8	3	1.99	4.62	2.63	3.92	1.93	0.11	-1.88	1.39	1.37	1.18
100	4	10	1	3.37	4.36	0.98	3.64	0.26	-0.59	-3.96	1.02	1.00	0.79
100	4	10	2	3.14	6.11	2.97	5.58	2.44	1.64	-1.50	1.54	1.56	1.30
100	4	10	3	2.46	4.71	2.25	4.29	1.83	-0.19	-2.65	1.33	1.37	1.01
100	4	12	1	3.61	4.45	0.84	3.91	0.30	-1.11	-4.71	1.00	1.01	0.67
100	4	12	2	3.57	6.29	2.72	5.91	2.34	1.53	-2.04	1.49	1.55	1.16
100	4	12	3	2.92	4.90	1.97	4.59	1.66	-0.61	-3.53	1.27	1.35	0.82
100	6	4	1	2.14	3.63	1.49	2.65	0.50	1.98	-0.17	1.10	1.04	1.35
100	6	4	2	1.10	6.08	4.99	4.98	3.88	3.61	2.51	2.08	1.97	2.31
100	6	4	3	1.23	3.35	2.12	4.38	3.15	2.36	1.13	1.25	1.57	1.76
100	6	6	1	2.59	3.95	1.36	3.00	0.41	0.78	-1.83	1.08	1.03	1.14
100	6	6	2	2.05	5.32	3.27	4.62	2.57	1.44	-0.81	1.54	1.52	1.47
100	6	6	3	1.85	4.34	2.50	3.64	1.80	0.62	-1.22	1.36	1.33	1.32
100	6	8	1	3.08	4.24	1.16	3.44	0.3[illegible]	0.09	-2.99	1.05	1.02	0.95
100	6	8	2	2.64	5.90	3.26	5.18	2.54	1.74	-0.90	1.58	1.55	1.44
100	6	8	3	2.09	4.75	2.66	4.11	2.02	0.39	-1.70	1.41	1.40	1.22
100	6	10	1	3.39	4.44	1.04	3.77	0.38	-0.47	-3.87	1.03	1.02	0.80
100	6	10	2	3.14	6.13	2.99	5.60	2.46	1.71	-1.44	1.55	1.56	1.31
100	6	10	3	2.51	4.90	2.39	4.43	1.92	-0.09	-2.61	1.36	1.39	1.02
100	6	12	1	3.61	4.49	0.88	3.97	0.36	-1.06	-4.67	1.01	1.02	0.68
100	6	12	2	3.57	6.29	2.72	5.92	2.35	1.55	-2.02	1.49	1.56	1.17
100	6	12	3	1.07	3.20	2.14	2.90	1.83	-3.45	-4.52	0.84	0.88	0.43

Table B-12 (ct'd 2/6) Safety Indices and System Factors for Continuous Bridges.

				SAFETY INDICES (beta)							SYSTEM FACTORS (Phi)		
SPAN	BEAM	SPAC	oad ca	member	ultimate	delta beta	LF100	delta beta	damage	delat beta	ultimate	funct.	damage
100	8	4	1	2.18	3.85	1.68	2.76	0.58	2.04	-0.14	1.12	1.05	1.35
100	8	4	2	1.15	5.07	3.92	4.11	2.96	2.90	1.74	1.60	1.53	1.87
100	8	4	3	1.27	4.25	2.98	3.48	2.21	2.47	1.20	1.42	1.39	1.77
100	8	6	1	2.60	3.95	1.35	3.04	0.44	0.77	-1.83	1.08	1.03	1.14
100	8	6	2	2.05	5.33	3.28	4.62	2.57	1.47	-0.58	1.54	1.52	1.47
100	8	6	3	1.87	4.36	2.49	3.68	1.81	0.65	-1.22	1.36	1.34	1.32
100	8	8	1	3.09	4.24	1.15	3.44	0.35	0.09	-2.99	1.05	1.02	0.95
100	8	8	2	2.64	5.90	3.26	5.18	2.54	1.74	-0.90	1.58	1.55	1.44
100	8	8	3	2.09	4.75	2.66	4.11	2.02	0.39	-1.70	1.41	1.40	1.22
100	8	10	1	3.39	4.44	1.04	3.77	0.38	-0.47	-3.87	1.03	1.02	0.80
100	8	10	2	3.14	6.13	2.99	5.60	2.46	1.71	-1.44	1.55	1.58	1.31
100	8	10	3	2.51	4.90	2.39	4.43	1.92	-0.09	-2.61	1.36	1.39	1.02
100	10	4	1	2.19	3.86	1.67	2.78	0.58	2.04	-0.16	1.12	1.05	1.35
100	10	4	2	1.15	4.95	3.79	4.25	3.10	2.90	1.74	1.57	1.56	1.87
100	10	4	3	1.27	4.04	2.78	3.49	2.23	2.31	1.05	1.38	1.39	1.74
100	10	6	1	4.43	3.95	-0.48	3.04	-1.39	0.77	-3.67	0.79	0.74	0.84
100	10	6	2	2.05	5.33	3.28	4.61	2.56	1.47	-0.58	1.54	1.52	1.47
100	10	6	3	1.87	4.36	2.49	3.68	1.81	0.65	-1.22	1.36	1.34	1.32
100	10	8	1	3.09	4.24	1.15	3.44	0.35	0.09	-2.99	1.05	1.02	0.95
100	10	8	2	2.64	5.90	3.26	5.18	2.54	1.74	-0.90	1.58	1.55	1.44
100	10	8	3	2.09	4.75	2.66	4.11	2.02	0.39	-1.70	1.41	1.40	1.22

Table B-12 (ct'd 3/6) Safety Indices and System Factors for Continuous Bridges.

				SAFETY INDICES (beta)							SYSTEM FACTOR (phi)		
SPAN	BEAM	SPAC	load ca	member	ultimate	delat beta	LF100	delta beta	damage	delat beta	ultimate	funct.	damage
120	4	4	1	2.07	2.47	0.39	2.00	-0.07	0.35	-1.72	0.93	0.95	1.13
120	4	4	2	0.36	4.81	4.45	3.74	3.38	2.22	1.86	1.63	1.55	1.81
120	4	4	3	1.15	3.15	2.01	2.73	1.59	1.14	0.00	1.22	1.26	1.52
120	4	6	1	2.52	3.60	1.08	2.79	0.27	-0.58	-3.09	1.04	1.00	0.94
120	4	6	2	2.10	5.24	3.14	4.39	2.29	0.15	-1.95	1.51	1.45	1.17
120	4	6	3	1.96	4.15	2.19	3.44	1.48	-0.89	-2.85	1.29	1.27	0.97
120	4	8	1	2.92	4.01	1.09	3.08	0.15	-1.11	-4.04	1.04	0.98	0.79
120	4	8	2	2.79	5.65	2.85	3.59	0.80	0.46	-2.34	1.49	1.13	1.08
120	4	8	3	2.31	4.42	2.11	3.71	1.39	-1.30	-3.61	1.29	1.26	0.81
120	4	10	1	0.33	1.48	1.14	0.54	0.21	-5.83	-6.16	0.63	0.59	0.27
120	4	10	2	3.31	5.87	2.56	5.34	2.03	0.28	-3.04	1.43	1.45	0.93
120	4	10	3	2.78	4.51	1.73	4.02	1.24	-1.96	-4.74	1.21	1.23	0.62
120	4	12	1	3.50	4.31	0.81	3.70	0.20	-2.52	-6.02	0.99	0.99	0.52
120	4	12	2	3.74	6.06	2.32	5.70	1.96	0.03	-3.71	1.38	1.44	0.79
120	4	12	3	3.13	4.64	1.51	4.35	1.22	-2.54	-5.67	1.16	1.23	0.50
120	6	4	1	2.18	3.57	1.39	2.64	0.46	1.59	-0.60	1.08	1.03	1.27
120	6	4	2	1.36	5.27	3.91	4.34	2.98	2.91	1.55	1.61	1.54	1.84
120	6	4	3	1.32	4.31	2.99	3.40	2.08	2.26	0.93	1.42	1.36	1.71
120	6	6	1	2.53	3.89	1.37	2.93	0.40	-0.09	-2.62	1.08	1.02	1.01
120	6	6	2	2.24	5.37	3.14	4.63	2.40	0.58	-1.68	1.52	1.48	1.23
120	6	6	3	1.99	4.36	2.36	3.61	1.61	-0.35	-2.35	1.33	1.30	1.08
120	6	8	1	2.99	4.12	1.13	3.27	0.28	-0.79	-3.78	1.04	1.00	0.83
120	6	8	2	2.82	5.73	2.91	5.03	2.20	0.74	-2.08	1.50	1.48	1.15
120	6	8	3	2.42	4.58	2.15	3.93	1.50	-0.86	-3.29	1.30	1.29	0.88
120	6	10	1	3.27	4.30	1.03	3.56	0.29	-1.59	-4.87	1.03	1.01	0.66
120	6	10	2	3.32	5.92	2.60	5.40	2.08	0.51	-2.81	1.44	1.46	0.98
120	6	10	3	2.82	4.67	1.85	4.21	1.38	-1.63	-4.46	1.24	1.27	0.66
120	6	12	1	3.51	4.36	0.85	3.79	0.28	-2.29	-5.80	1.00	1.01	0.54
120	6	12	2	3.74	6.06	2.33	5.72	1.98	0.25	-3.49	1.38	1.45	0.83
120	6	12	3	3.13	4.73	1.60	4.45	1.32	-2.29	-5.42	1.16	1.26	0.53

Table B-12 (ct'd 4/6) Safety Indices and System Factors for Continuous Bridges.

				SAFETY INDICES (beta)							SYSTEM FACTOR (phi)		
SPAN	BEAM	SPAC	load ca	member	ultimate	delat beta	LF100	delta beta	damage	delat beta	ultimate	funct.	damage
120	8	4	1	2.22	3.71	1.49	2.75	0.53	1.66	-0.56	1.09	1.04	1.28
120	8	4	2	1.44	5.17	3.73	4.39	2.94	2.96	1.52	1.58	1.54	1.84
120	8	4	3	1.37	4.42	3.05	3.52	2.15	2.37	1.00	1.44	1.38	1.73
120	8	6	1	2.56	3.91	1.35	3.00	0.44	-0.03	-2.58	1.08	1.03	1.02
120	8	6	2	2.24	5.38	3.14	4.84	2.40	-3.31	-5.55	1.52	1.49	0.51
120	8	6	3	2.00	4.38	2.38	3.67	1.67	-0.31	-2.31	1.33	1.31	1.08
120	8	8	1	-0.18	1.20	1.38	0.19	0.36	-4.84	-4.67	0.63	0.59	0.39
120	8	8	2	2.82	5.73	2.91	5.03	2.21	0.75	-2.07	1.50	1.48	1.15
120	8	8	3	2.43	4.58	2.15	3.93	1.51	-0.85	-3.28	1.30	1.29	0.88
120	8	10	1	3.27	4.30	1.03	3.57	0.29	4.58	1.28	1.03	1.01	1.57
120	8	10	2	3.32	5.92	2.60	5.40	2.08	6.08	2.76	1.44	1.48	2.38
120	8	10	3	2.82	4.67	1.85	4.21	1.38	4.83	2.00	1.24	1.27	2.13
120	10	4	1	2.25	3.72	1.47	2.78	0.53	1.67	-0.58	1.09	1.04	1.27
120	10	4	2	1.44	5.15	3.71	4.39	2.94	2.96	1.52	1.57	1.54	1.84
120	10	4	3	1.38	4.96	3.58	3.55	2.18	2.39	1.02	1.54	1.38	1.74
120	10	6	1	2.56	3.91	1.35	3.00	0.44	-0.04	-2.60	1.08	1.03	1.02
120	10	6	2	2.24	5.38	3.14	4.84	2.40	0.81	-1.63	1.52	1.49	1.24
120	10	6	3	2.00	4.38	2.38	3.66	1.67	-0.31	-2.31	1.33	1.31	1.08
120	10	8	1	3.00	4.12	1.13	3.28	0.29	-0.77	-3.77	1.05	1.01	0.83
120	10	8	2	2.82	5.73	2.91	5.03	2.21	0.75	-2.07	1.50	1.48	1.15
120	10	8	3	2.43	4.58	2.15	3.93	1.51	-0.84	-3.27	1.30	1.29	0.88

Table B-12 (ct'd 5/6) Safety Indices and System Factors for Continuous Bridges.

				SAFETY INDICES (beta)							SYSTEM FACTOR (phi)		
SPAN	BEAM	SPAC	load ca	member	ultimate	delat beta	LF100	delta beta	damage	delat beta	ultimate	funct.	damage
150	4	4	1	2.23	2.67	0.44	2.25	0.02	0.33	-1.90	0.94	0.97	1.11
150	4	4	2	0.65	4.75	4.09	3.80	3.14	1.77	1.11	1.58	1.52	1.68
150	4	4	3	1.40	3.23	1.84	2.85	1.46	0.81	-0.58	1.20	1.24	1.42
150	4	6	1	2.53	3.68	1.15	2.98	0.44	-1.52	-4.05	1.04	1.03	0.80
150	4	6	2	2.29	5.10	2.81	4.46	2.16	-1.35	-3.64	1.44	1.43	0.81
150	4	6	3	2.04	4.07	2.03	3.52	1.49	-2.65	-4.69	1.26	1.27	0.63
150	4	8	1	2.75	3.90	1.15	3.22	0.47	-2.76	-5.51	1.05	1.03	0.59
150	4	8	2	3.02	5.23	2.21	4.93	1.91	-2.12	-5.14	1.33	1.40	0.56
150	4	8	3	2.42	4.01	1.59	3.73	1.31	-4.21	-6.63	1.17	1.24	0.40
150	4	10	1	0.16	1.42	1.26	0.67	0.51	-7.70	-7.86	0.67	0.65	0.18
150	4	10	2	3.58	5.39	1.81	5.32	1.75	-3.16	-6.74	1.23	1.38	0.40
150	4	10	3	2.82	4.04	1.22	3.99	1.17	-5.90	-8.72	1.08	1.22	0.25
150	4	12	1	3.33	4.22	0.88	3.68	0.35	-5.12	-8.45	1.01	1.02	0.30
150	4	12	2	4.02	5.38	1.36	0.00	0.00	-4.06	-8.08	1.12	0.00	0.31
150	4	12	3	3.19	4.02	0.84	0.00	0.00	-7.29	-10.48	1.00	0.00	0.19
150	6	4	1	2.29	3.71	1.43	2.82	0.53	1.39	-0.89	1.08	1.04	1.23
150	6	4	2	1.62	5.22	3.59	4.41	2.78	2.57	0.95	1.56	1.51	1.74
150	6	4	3	1.41	4.29	2.88	3.47	2.06	1.91	0.50	1.40	1.38	1.63
150	6	6	1	2.53	3.99	1.46	3.12	0.58	-0.95	-3.48	1.09	1.05	0.88
150	6	6	2	2.51	5.29	2.77	4.73	2.22	-0.68	-3.17	1.44	1.45	0.90
150	6	6	3	2.06	4.27	2.21	3.71	1.65	-1.79	-3.84	1.30	1.30	0.77
150	6	8	1	2.86	4.06	1.19	3.42	0.56	-2.41	-5.27	1.05	1.05	0.62
150	6	8	2	3.12	5.36	2.23	5.10	1.98	-1.88	-4.79	1.34	1.43	0.61
150	6	8	3	2.52	4.25	1.73	3.99	1.47	-3.65	-6.17	1.20	1.28	0.44
150	6	10	1	0.05	1.39	1.33	0.67	0.61	-7.70	-7.76	0.64	0.63	0.17
150	6	10	2	3.62	4.49	0.87	5.42	1.80	-2.44	-6.07	1.00	1.39	0.46
150	6	10	3	2.88	4.26	1.39	4.22	1.34	-5.11	-7.99	1.12	1.26	0.30
150	6	12	1	3.38	4.32	0.93	3.81	0.43	-4.77	-8.16	1.01	1.03	0.32
150	6	12	2	4.03	5.47	1.44	0.00	0.00	-3.66	-7.69	1.14	0.00	0.33
150	6	12	3	3.21	4.16	0.95	0.00	0.00	-6.83	-10.04	1.02	0.00	0.20

Table B-12 (ct'd 6/6) Safety Indices and System Factors for Continuous Bridges.

				SAFETY INDICES (beta)							SYSTEM FACTOR (phi)		
SPAN	BEAM	SPAC	load ca	member	ultimate	delat beta	LF100	delta beta	damage	delat beta	ultimate	funct.	damage
150	8	4	1	2.32	3.79	1.48	2.92	0.61	1.41	-0.91	1.08	1.05	1.22
150	8	4	2	1.78	5.26	3.49	3.88	2.10	2.63	0.85	1.55	1.38	1.73
150	8	4	3	1.46	4.42	2.95	3.60	2.13	2.04	0.58	1.42	1.38	1.65
150	8	6	1	2.59	4.00	1.41	3.21	0.62	-0.92	-3.51	1.08	1.05	0.88
150	8	6	2	2.53	3.62	1.10	4.74	2.21	-0.61	-3.14	1.05	1.45	0.91
150	8	6	3	2.09	4.30	2.21	3.79	1.70	-1.70	-3.79	1.30	1.32	0.78
150	8	8	1	2.88	4.06	1.18	3.45	0.57	-2.37	-5.25	1.05	1.05	0.62
150	8	8	2	3.13	5.36	2.24	5.11	1.98	-1.59	-4.72	1.34	1.43	0.62
150	8	8	3	2.52	4.25	1.74	4.00	1.48	-3.59	-6.11	1.20	1.28	0.45
150	8	10	1	3.14	4.26	1.12	3.65	0.51	-3.57	-6.71	1.04	1.04	0.45
150	8	10	2	3.62	5.48	1.85	5.42	1.80	-2.48	-6.10	1.25	1.39	0.46
150	8	10	3	2.88	4.27	1.39	4.22	1.35	-5.16	-8.03	1.12	1.28	0.29
150	10	4	1	2.37	3.84	1.47	2.97	0.60	1.43	-0.95	1.08	1.05	1.22
150	10	4	2	1.80	5.24	3.44	4.49	2.69	2.64	0.84	1.54	1.51	1.73
150	10	4	3	1.50	4.43	2.93	3.64	2.15	2.07	0.57	1.42	1.38	1.65
150	10	6	1	2.59	4.00	1.40	3.21	0.62	-0.91	-3.51	1.08	1.05	0.88
150	10	6	2	2.53	5.29	2.77	4.74	2.21	-0.61	-3.14	1.44	1.45	0.91
150	10	6	3	2.08	4.30	2.22	3.79	1.70	-1.72	-3.80	1.30	1.32	0.78
150	10	8	1	2.88	4.06	1.18	3.45	0.57	-2.30	-5.18	1.05	1.05	0.63
150	10	8	2	3.13	5.36	2.24	5.11	1.98	-1.63	-4.76	1.34	1.43	0.62
150	10	8	3	2.52	4.25	1.74	4.00	1.48	-3.51	-6.03	1.20	1.28	0.46

Table B-13 Safety Indices and System Factors for Sensitivity Analysis of Continuous Bridges.

				SAFETY INDICES = Beta							SYSTEM FACTORS = PHI s		
SPAN	BEAMS	SPAC.	Load case	member	ultimate	delta beta	funct.	delta beta	damage	delat beta	ultimate	funct.	damage
Base case													
100	6	8	1	3.08	4.24	1.16	3.44	0.35	-0.17	-3.25	1.05	1.02	0.91
100	6	8	2	2.64	5.90	3.26	5.18	2.54	1.74	-0.90	1.58	1.55	1.43
100	6	8	3	2.09	4.75	2.66	4.11	2.02	0.39	-1.70	1.41	1.40	1.22
Effect of ductility													
Θmax=1.2 original value for both negative and positive bending													
100	6	8	1	3.08	4.38	1.30	3.44	0.35	0.59	-2.50	1.08	1.02	1.04
100	6	8	2	2.64	6.07	3.43	5.18	2.54	2.15	-0.49	1.62	1.55	1.54
100	6	8	3	2.09	4.89	2.80	4.11	2.02	0.84	-1.25	1.44	1.40	1.32
Θmax=1.5 original value for both negative and positive bending													
100	6	8	1	3.08	4.58	1.50	3.44	0.35	1.16	-1.92	1.11	1.02	1.13
100	6	8	2	2.64	6.28	3.64	5.18	2.54	2.64	0.00	1.68	1.55	1.65
100	6	8	3	2.09	5.07	2.98	4.11	2.02	1.36	-0.73	1.48	1.40	1.44
Θmax=1.2 original value for positive bending													
100	6	8	1	3.08	4.24	1.16	3.44	0.35	0.09	-2.99	1.05	1.02	0.95
100	6	8	2	2.64	5.90	3.26	5.18	2.54	1.74	-0.90	1.58	1.55	1.43
100	6	8	3	2.09	4.75	2.66	4.11	2.02	0.39	-1.70	1.41	1.40	1.22
Θmax=1.5 original value for positive bending													
100	6	8	1	3.08	4.24	1.16	3.44	0.35	0.09	-2.99	1.05	1.02	0.95
100	6	8	2	2.64	5.90	3.26	5.18	2.54	1.74	-0.90	1.58	1.55	1.43
100	6	8	3	2.09	4.75	2.66	4.11	2.02	0.39	-1.70	1.41	1.40	1.22
Θmax=1.2 original value for negative bending													
100	6	8	1	3.08	4.38	1.30	3.44	0.35	0.59	-2.50	1.08	1.02	1.03
100	6	8	2	2.64	6.07	3.43	5.18	2.54	2.15	-0.49	1.62	1.55	1.54
100	6	8	3	2.09	4.89	2.80	4.11	2.02	0.84	-1.25	1.44	1.40	1.32
Θmax=1.5 original value for negative bending													
100	6	8	1	3.08	4.58	1.50	3.44	0.35	1.16	-1.92	1.11	1.02	1.13
100	6	8	2	2.64	6.28	3.64	5.18	2.54	2.64	0.00	1.68	1.55	1.65
100	6	8	3	2.09	5.07	2.98	4.11	2.02	1.36	-0.73	1.48	1.40	1.44

Table B-13 (ct'd 2/3) Safety Indices and System Factors for Sensitivity Analysis of Continuous Bridges.

Effect of plastic hinge length												
Lp=0.8 original value												
100	6	8	1	3.08	4.33	1.25	3.53	0.45	0.24	-2.84	1.07	1.03	0.98
100	6	8	2	2.64	5.97	3.33	5.28	2.64	1.85	-0.79	1.60	1.58	1.46
100	6	8	3	2.09	4.83	2.73	4.21	2.12	0.51	-1.58	1.42	1.42	1.25
Lp=1.2 original value													
100	6	8	1	3.08	4.18	1.10	3.33	0.24	-0.03	-3.11	1.04	1.00	0.93
100	6	8	2	2.64	5.84	3.20	5.07	2.43	1.65	-0.99	1.57	1.53	1.41
100	6	8	3	2.09	4.68	2.59	3.98	1.89	0.27	-1.82	1.39	1.37	1.20
Lp=1.4 original value													
100	6	8	1	3.08	4.13	1.05	3.20	0.12	-0.09	-3.17	1.03	0.98	0.92
100	6	8	2	2.64	5.78	3.14	4.95	2.31	1.59	-1.05	1.56	1.50	1.40
100	6	8	3	2.09	4.61	2.52	3.84	1.75	0.19	-1.90	1.38	1.34	1.18
Effect of skew													
15 degree skew													
100	6	8	1	3.10	4.24	1.14	3.47	0.37	0.05	-3.05	1.05	1.02	0.94
100	6	8	2	2.65	5.84	3.19	5.16	2.52	1.87	-0.77	1.57	1.55	1.47
100	6	8	3	2.13	4.66	2.53	4.08	1.95	0.52	-1.61	1.38	1.38	1.24
30 degree skew													
100	6	8	1	3.14	4.36	1.22	3.53	0.39	-0.01	-3.14	1.06	1.02	0.92
100	6	8	2	2.67	5.69	3.22	5.13	2.46	2.08	-0.59	1.58	1.54	1.51
100	6	8	3	2.21	4.77	2.56	4.08	1.87	0.76	-1.45	1.39	1.37	1.28

Table B-13 (ct'd 3/3) Safety Indices and System Factors for Sensitivity Analysis of Continuous Bridges.

Effect of slab strength and stiffness													
Slab stiffness and positive strength=1.2 original values													
100	6	8	1	3.10	4.28	1.18	3.46	0.36	0.41	-2.69	1.06	1.02	1.00
100	6	8	2	2.65	5.98	3.33	5.23	2.58	2.02	-0.63	1.60	1.57	1.50
100	6	8	3	2.17	4.79	2.62	4.13	1.96	0.67	-1.50	1.40	1.39	1.27
slab stiffness and positive strength = 1.5 original value													
100	6	8	1	3.08	4.35	1.27	3.50	0.42	0.81	-2.27	1.07	1.03	1.07
100	6	8	2	2.67	6.09	3.41	5.30	2.62	2.38	-0.30	1.62	1.58	1.58
100	6	8	3	2.27	4.86	2.59	4.17	1.90	1.03	-1.24	1.40	1.38	1.33
slab stiffness and negative strength = 1.2 original value													
100	6	8	1	3.10	4.31	1.21	3.49	0.39	0.50	-2.60	1.06	1.02	1.02
100	6	8	2	2.65	6.04	3.39	5.31	2.65	2.13	-0.52	1.62	1.58	1.53
100	6	8	3	2.17	4.83	2.66	4.18	2.00	0.78	-1.39	1.41	1.40	1.30
slab stiffness and negative strength = 1.5 original value													
100	6	8	1	3.08	4.41	1.33	3.57	0.49	1.09	-1.99	1.08	1.04	1.12
100	6	8	2	2.67	6.23	3.56	5.47	2.80	2.58	-0.10	1.66	1.62	1.63
100	6	8	3	2.27	4.94	2.67	4.26	1.99	1.32	-0.95	1.42	1.40	1.40

Table B-13 (ct'd 4/4) Safety Indices and System Factors for Sensitivity Analysis of Continuous Bridges.

Effect of girder strength and stiffness													
girder stiffness and positive strength = 1.2 original values													
100	6	8	1	4.16	5.04	0.88	4.29	0.12	1.22	-2.94	1.01	0.98	0.96
100	6	8	2	2.63	6.58	3.95	5.89	3.26	2.74	0.11	1.75	1.73	1.68
100	6	8	3	2.01	5.46	3.45	4.87	2.86	1.56	-0.45	1.58	1.58	1.50
girder stiffness and positive strength = 1.5 original values													
100	6	8	1	5.37	5.95	0.58	5.15	-0.22	2.29	-3.08	0.95	0.91	0.93
100	6	8	2	2.62	7.35	4.73	6.61	3.99	3.68	1.06	1.93	1.90	1.90
100	6	8	3	1.90	6.27	4.36	5.64	3.74	2.56	0.65	1.77	1.76	1.73
girder stiffness and negative strength = 1.2 original values													
100	6	8	1	3.02	4.47	1.45	3.67	0.65	0.56	-2.46	1.10	1.07	1.04
100	6	8	2	3.43	6.19	2.77	5.47	2.05	2.19	-1.24	1.52	1.49	1.39
100	6	8	3	2.83	5.03	2.21	4.40	1.58	0.92	-1.90	1.34	1.34	1.20
girder stiffness and negative strength = 1.5 original values													
100	6	8	1	2.95	4.77	1.82	3.98	1.03	1.10	-1.85	1.16	1.13	1.14
100	6	8	2	4.36	6.58	2.21	5.86	1.50	2.72	-1.64	1.38	1.35	1.29
100	6	8	3	3.67	5.41	1.74	4.80	1.12	1.54	-2.13	1.24	1.23	1.15
girder stiffness and positive and negative strength = 1.2 original values													
100	6	8	1	4.17	5.22	1.05	4.47	0.30	1.52	-2.65	1.04	1.01	1.01
100	6	8	2	3.43	6.80	3.38	6.11	2.68	3.02	-0.40	1.70	1.67	1.63
100	6	8	3	2.83	5.69	2.86	5.09	2.27	1.89	-0.93	1.52	1.52	1.45
girder stiffness and positive and negative strength = 1.5 original values													
100	6	8	1	5.37	6.33	0.96	5.53	0.16	2.78	-2.59	1.02	0.98	1.02
100	6	8	2	4.36	7.83	3.47	7.09	2.73	4.23	-0.13	1.82	1.77	1.80
100	6	8	3	3.67	6.75	3.08	6.13	2.46	3.12	-0.55	1.65	1.65	1.63

APPENDIX C

RELIABILITY AND REDUNDANCY OF STEEL I-BEAM BRIDGES

This appendix gives a detailed discussion on the findings made in this study on the redundancy of steel I-beam bridges. The observations made herein are based on the results of the nonlinear analysis of over 120 bridge configurations designed to satisfy the AASHTO LFD specifications. In addition to analyzing different bridge configurations, a sensitivity analysis is performed to study the effect of various design and analysis assumptions.

This appendix is divided into six sections. Section 1 describes the structural model used with NONBAN to analyze the steel I-beam bridges. In Section 2, the modeling procedure proposed in Section 1 is verified by comparing the results obtained by NONBAN to the results of field and laboratory tests on two full-scale and one model steel I-beam bridges. Section 3 describes the bridges that are designed for the purposes of this study. This section also gives the assumptions made during the design process. Section 4 describes the results of the nonlinear analysis performed for the bridges described in Section 3. The nonlinear analysis is performed using NONBAN and the bridges are discretized using the procedure described in Section 1. Results of the sensitivity analysis are presented in Section 5. Section 6 presents the results of the reliability analysis and the calibration of the redundancy factors. Tables and figures for this appendix are given at the end.

C-1. Modeling of Steel I-Beam Bridges.

In this study, the behavior of steel I-beam bridges is analyzed using the Nonlinear Bridge Analysis program NONBAN. As mentioned in Appendix F, the program uses a modified grillage analysis method to study the nonlinear behavior of typical bridge configurations. The validity of the program was verified by comparing its results to the published results of various beams, bridge models and full scale bridge tests and theoretical analyses as described in Appendix F. This section describes the structural model adopted in this study to analyze typical steel I-beam bridges using NONBAN.

C-1.1 Mesh Discretization

To use NONBAN, the bridge superstructure is discretized as longitudinal and transverse beam elements laying in the plane of the superstructure. This discretization procedure is typical for the grillage analysis method as described in several references on structural analysis including

the references by West, Jaegar, Bakht, Hambly or Zokaie and Imbsen which address the modeling of bridge superstructures [C-1,2,3,4].

The discretization procedure used in this study follows the recommendations made by Zokaie, Osterkamp and Imbsen [C-4] for discretizing a bridge superstructure into equivalent longitudinal and transverse members laying in the plane of the roadway surface. Specifically, longitudinal members are placed along girder centerlines. The longitudinal members' properties are taken to be those of the composite deck-member cross section if the beam is designed for composite action. For bridges that are built for non-composite action, longitudinal member properties are those of the girder alone. Thus, for noncomposite sections, the slab acts as a one way slab such that its contribution is only to the transverse distribution of the load without any contributions in the longitudinal direction.

The contributing slab width for composite sections is taken to be half the girder spacing on each side of the girder. For the case of very wide spacings, Zokaie et al [C-4] recommend that the shear lag effect be considered. They do not however, specify how this should be carried out, neither do they specify which spacings should be considered wide. To remain on the conservative side, this study uses the procedure proposed in the AASHTO specifications to determine the effective flange width of composite sections. In this sense, the effective flange width of a composite section is taken to be the minimum of half the girder spacing between adjacent beams, or one third the span length, or twelve times the slab thickness plus the width of the girder. For most cases considered in this study, the half girder spacing criterion governs. Even for the cases where the girders are so widely spaced that one of the other criteria governs, the parametric analysis performed in this study shows that the final recommendations are not sensitive to the effect of the different effective flange widths criteria.

For the edge beams, reference [C-4] recommends to"use judgment" to determine how to account for the effect of compositely designed curbs and parapets. For the purposes of this study, the effect of curbs and parapets is generally ignored except for the specific cases where a comparison between field tests and analytical results warrant their consideration. In the cases where the effect of the curbs and parapets is not known, and to partially account for their contributions, the longitudinal edge beams of a bridge are assumed to have the same moment capacities as the interior beams even if the effective flange width is actually smaller.

Transverse beams represent the contribution of the slab and diaphragms to the transverse distribution of the load. Zokaie et al. [C-4] recommend to use transverse beam spacings equal to about 1/10 of the effective span length to account for the slab's contribution in the transverse direction. This span/10 division is generally applied in this study. However, in order to minimize the mesh generation effort, and since we are using the same girder spacings and bridge configurations for steel and prestressed concrete bridges, the same meshes used for the prestressed concrete I-beam bridges are also used for the steel I-beam bridges. Thus, in certain instances, coarse meshes with divisions greater than span/10 are used. As in the case of prestressed concrete I-beam bridges, a transverse beam is applied for steel bridges wherever a

diaphragm exists. Properties of the transverse beams representing the deck slab are taken to be the properties of the tributary section of the deck slab. In the case where the diaphragm acts compositely with the deck, the properties of the composite section must be used. Otherwise, transverse beams representing the diaphragms are used independently of the beams representing the slab contribution.

This proposed grillage modeling technique ignores the coupling between the bending and rotation of the deck slab about the main axes of the bridge. Also, since the grillage model uses only beam elements, the effects of the membrane action and arching of the slab are ignored. Therefore, the proposed scheme may not be accurate enough to analyze possible failures in the deck slab itself. On the other hand, Zokaie et al [C-4] as well as Hambly [C-3] suggest that a grillage model may be conservatively used for the analysis of a bridge slab for design purposes. This, however, would require that the slab be discretized as an extremely fine grid of longitudinal and transverse beam elements. This project is concerned with the behavior of the main members of the superstructure and the analysis of the behavior of deck slabs is beyond the scope of this study. Therefore, an exact modeling of the deck slab is not carried out in this analysis. Despite the stated limitations in the slab model, section C-2 of this appendix will demonstrate that the proposed modeling scheme is sufficiently accurate to study the distribution of the load to the main longitudinal members of steel I-beam bridges which is the main purpose of this project.

C-1.2 Section properties

Elastic properties

To analyze steel I-beam bridges, the program NONBAN requires the same input data that is required by any commercial structural analysis program. For example, to describe the linear elastic properties of the bridge, the program requires that the following properties be defined for each beam element: a) The modulus of elasticity, E, b) the moment of inertia, I, c) the shear modulus, G, and d) the torsional constant J. This assumes that the contribution of shear deformations to the response of I-beam bridges can be ignored.

The moments of inertia and the torsional constants of the longitudinal as well as the transverse beams are calculated using the basic principles of structural mechanics. For the transverse beams representing the contribution of the slab, Zokaie et al. [C-4] and Hambly [C-3] recommend to use a torsional constant, J calculated as:

$$J = t^3/6 \qquad \text{per unit length of slab.} \qquad \text{(C.1)}$$

Inelastic properties

In addition to the typical elastic properties listed above, the program NONBAN requires information on the nonlinear section properties of each beam element. In particular, the program requires a moment versus plastic rotation curve for each beam element.

In this project, the moment versus plastic rotation curve of a steel I-beam member is obtained by first calculating the moment versus curvature relationship. The linear elastic part of the curve was already considered through the modulus of elasticity and the moment of inertia entered as part of the elastic properties data. Therefore, only the portion of the moment-curvature curve which corresponds to moments higher than the elastic limit is needed at this stage. Realizing that the curvature is the derivative of the rotation with respect to the length, the moment versus plastic rotation curve is obtained by multiplying the curvature by the length of the plastic hinge (see section C.3.1 of the phase I report for further detail [C-5]). This multiplication implicitly assumes that the moment (and thus the curvature) is constant within the section of the beam element that is inelastic.

For a steel I-beam member, the moment versus plastic curvature curve is obtained using the experimental data assembled by Schilling [C-6]. An experimentally derived curve rather than an analytical curve is used for the steel members because experimental data would more accurately reflect the true behavior of steel members. The experimental data used, as stated by Schilling [C-6], accounts for steel yielding including: the effect of residual stresses; the spread of yielding along the length of the beam as the loading progresses; cracking or local crushing of the slab; permanent distortion of the cross sectional shape; and any other factor that causes permanent rotations. The curves proposed by Schilling give a lower bound on the results of experimental investigations of typical steel bridge members. These curves gave excellent results when compared to experimental tests on full scale bridges as will be demonstrated further below.

The experimental data provided by Schilling [C-6] are similar to the curves recommended for use in the AASHTO Auto-stress design procedure [C-7]. The data give curves of moment versus plastic rotation for single (simple span or continuous) steel beams. The data provided in Reference [C-6] assume that the plastic rotation is concentrated in a small region of the steel girder "representing an angular discontinuity and that the rest of the girder is otherwise assumed to remain elastic". This assumption is valid for the case where a beam is analyzed under a particular loading condition that produces a plastic hinge at only one point of the beam. The mesh discretization scheme and loading conditions used in this study could produce situations where plastic hinges may form at different locations along the length of a particular beam. For this reason, it is herein suggested to reduce Schilling's experimental moments versus rotation curves to equivalent moment versus curvature curves. This is based on the realization that the curvature is the derivative of the rotation and thus gives a local (point) description of the nonlinear behavior as opposed to the rotation which gives a global (whole beam) description.

Figure C.1, gives the moment versus plastic rotation plots proposed by Schilling for: a) the positive bending of composite sections; b) the positive bending of non-composite sections, this same curve is also valid for negative bending of compact sections; and c) negative bending of non-compact sections. The corresponding moment versus curvature relationships are obtained by differentiating the moment rotations curves. This is done by discretizing a hypothetical beam loaded by one concentrated load, into small elements and insuring that the sum of the curvatures of each element add up to the total rotation of the beam. This approximate approach produces moment versus curvature plots that may include large oscillations (depending on the differentiation scheme and the accuracy of the original moment rotation curves). These curves are then smoothed to produce the moment-curvature relationships shown in Figure C.2. A program was written to perform these calculations and produce the moment curvature plots used in this appendix.

Since the program NONBAN requires moment versus rotations plots for each beam element, the moment versus curvature plots of Figure C.2 are then converted back to moment versus rotation curves assuming that the moment and thus the curvature is constant over half the element's length. This is equivalent to assuming that the plastic hinge length is equal to the element length/2. The approach followed in this study was found to produce excellent results as will be demonstrated further below.

Member ductility and failure criteria

Composite steel I-beam sections in positive bending will exhibit plastic deformations until the concrete on top of a composite section crushes or when the steel ruptures. Concrete crushing occurs when the maximum compressive strain in the concrete slab reaches a value of 0.0038. This is the same value used during the analysis of prestressed concrete I-beam bridges. Steel rupture occurs when the plastic hinge rotation is 65 mrad. This value is obtained from Schilling's curves for naked (noncomposite) steel sections (see Figure C.1-b). It should be noted that the contribution of the slab to the moment capacity in the negative bending region of continuous spans is generally ignored for steel bridges.

Based on the ductility criteria stated above, composite and noncomposite steel I-beam bridges with compact sections in the negative bending regions (if any exist) will reach their ultimate capacity when the ductility limit of any one member is exhausted. Bridge members with non-compact sections in negative bending, will unload gradually as shown in Figure C.2- c. In such cases, the ultimate capacity is reached when the global structural system begins to unload. i.e. when the load-deflection curve of the whole structure reaches a point where the slope turns negative.

Many previous nonlinear analyses of steel bridges assumed that steel bridge members have an infinite level of ductility. This would imply that bridge ultimate capacity will be reached as the result of a formation of a collapse mechanism. Since in this study the bridge is assumed to fail

when concrete crushing of the composite section occurs, then the ultimate capacity will be reached at levels lower than those that induce the formation of a mechanism.

It should be noted that the modeling scheme proposed herein accounts for nonlinearity only in the bending moment about the main (horizontal) axis of each (longitudinal or transverse) member . The torsional moments are assumed to remain in the linear elastic range. Also, as mentioned earlier, shear deformations are ignored for steel I-beam bridges. This assumes that the primary load effects produced in the bridge system are bending moments and that the torsional moments are relatively small. This assumption is consistent with the modeling assumptions made by other researchers as mentioned in Appendix A.

The program NONBAN is also set up to account for axial member deformations and for bending about the secondary (vertical) axis. These two factors, however, do not affect the behavior of the grid and these properties are assumed to remain in the linear elastic range.

Construction sequence

The latest version of NONBAN accounts for the bridge construction sequence in the sense that the dead load is divided into two types. The first type, the permanent dead load, is applied on the noncomposite section of the longitudinal members while the second type, the superimposed dead load, is applied on the composite section.

To accommodate this new option, two moment versus rotation curves and two sets of elastic properties are entered as part of the input data for the longitudinal beams only. The first moment versus rotation curve and set of elastic properties are those of the noncomposite section of the longitudinal beams. The second moment versus rotation curve and set of elastic properties are those of the composite section of the longitudinal beams. For continuous steel bridges, the construction sequence assumes that the permanent dead load is applied on the naked continuous steel members and that the superimposed dead load and the live load will act on the continuous composite sections.

A sensitivity analysis performed in section C.5 shows that the effect of including the construction sequence in the analysis does not affect the ultimate capacity although some softening in the load deflection curve is observed in the early loading stages.

C-1.3 Support conditions

In this study, it is always assumed that the supports are totally free to rotate. It should be noted however, that the slab discretization scheme adopted in section C-1.1 above will place a transverse beam element at the end of each span. This end transverse beam will often produce some limited rotational constraints at the supports. The rotations will be further constrained if large transverse diaphragms exist at the support.

C-1.4 Loading

The program NONBAN requires that the dead load data and the live load data be entered separately. The dead load is defined as the load that will remain constant throughout the incremental analysis. In general, the dead load is entered as a distributed load over the longitudinal beam elements and is divided into two types: the permanent dead load and the superimposed dead load. The analysis first calculates the internal moment in each beam element for the permanent dead load applied on the naked section. In the second step, the internal moments are adjusted to account for the composite action of the slab. The effect of the superimposed dead load is taken into consideration using composite section properties. Finally, the live load applied on the structure is incremented.

The live load data is defined as the load that will be incremented. This load is entered as point loads at the nodes. In this study, all the live loads are assumed to be due to vehicular traffic. If the location of a vehicle is chosen such that the wheels do not coincide with any of the mesh nodes, then, nominal (artificial) beam elements are created to join the wheels of the vehicle to the adjacent nodes. The purpose of these nominal elements is only to distribute the wheel loads to the adjacent nodes and they do not contribute to the strength or the stiffness of the structure. Therefore, these nominal beam elements are assumed to remain elastic and they are chosen to have extremely small moments of inertia and modulus of elasticity.

In order to use a consistent loading condition for the different bridge configurations analyzed in this study, the bridges are assumed to be loaded by trucks having the configuration of AASHTO's HS-20 vehicles. The trucks are placed on the bridge such that the external wheel line of the main vehicle is directly over one of the edge girders. The other vehicles are placed either behind or ahead of the main vehicle in the same line or to the side of the main vehicle. This loading pattern normally gives the most adverse condition except when the bridge has large overhangs. It should be noted that redundancy, as defined in this study, is in essence a comparison between the capacity of the structure to resist first member failure and the ultimate capacity. The results will be presented as ratios of these two values. Therefore, the final results are not dependent on the loading position or the magnitude of the truck loads used in the incremental analysis.

Only bridges with one simple span or bridges with two continuous spans are considered in this study. For simple span bridges, only one vehicle is placed in each lane. For continuous span bridges, three different loading scenarios are used. For load case 1, side-by-side vehicles are placed in one span. This load case studies the behavior of the bridge when the primary failure mechanism is in positive bending. Load case 2, places two vehicles in the edge lane of the bridge such that the vehicles are in separate spans. Only one lane is loaded. This load case studies the behavior of the bridge when the primary failure mechanism is in negative bending. Load case 3, places two vehicles in each lane of the bridge one vehicle in each span but allows the loading of two side-by-side lanes. This load case also studies the effect of primary failure in

negative bending. Load cases 2 and 3 are considered separately because load case 2 has a higher probability of occurrence in the lifetime of the structure than load case 3, although load case 3 is obviously the most critical of the two in a deterministic sense.

For simple span bridges, the vehicles are placed such that the drive axle of the HS-20 truck coincides with the bridge's mid-span. For continuous spans, two different loading positions are considered: When only one span is loaded, the HS-20 vehicles are placed such that the drive axle is at a distance of 0.41 the span length from the end (noncontinuous) support. When two spans are loaded, the vehicles are placed such that the drive axle is at 0.58 the span length from the end support. These two different positions are chosen herein because they correspond to the most critical design positions respectively for positive and negative bending.

It should be noted that the HS-20 configurations do not correspond to actual vehicular configurations. The HS-20 vehicles are used herein because most engineers are familiar with them and also because the maximum lifetime load effects used during the LRFD calibration are given in function of the effects of these HS-20 design trucks [C-8].

C-2. Model Verification.

The validity of the program NONBAN and the modeling scheme used to study the behavior of steel I-beam bridges is verified by comparing the results of NONBAN to those of two full-scale tests and one bridge model test. One of these was a field test conducted on a continuous four-span bridge in Tennessse [C-9], the other full scale bridge was built and tested in the laboratory of the University of Nebraska [C-10]. In addition, a model test performed as part of a study supported by the Ontario Ministry of Transportation [C-11] is also studied.

C-2.1 Tennessee field test

The Tennessee field test was performed on a four-span continuous bridge with span lengths of 70 ft, 90 ft, 90 ft and 70 ft. The bridge consists of four steel W36x170 rolled I-beams at 8.25 ft spacings supporting a 7 in deck slab. Sections over the piers had 10"x1/2"x1" cover plates. The loads were placed to simulate an HS truck in each lane of the second span. Reference [C-9] gives a more complete description of the tested bridge. Core samples were used to estimate the strength of the concrete in the deck and the steel of the beams. The beams and the slab were built to act as composite sections.

Tests to determine the ultimate load capacity of the bridge were performed by anchoring a rod into the rock below the bridge and jacking. The loads were then increased until the ultimate capacity is reached. The researchers observed that: "The first evidence of distress was related to the diaphragms when a noticeable and audible slip occurred between the diaphragm and the steel girders... The behavior of the bridge was almost linear elastic up to yielding of the section under

the applied loads... At a load of about 650 kips, a crack occurred between the curb and slab near the first pier and tension cracks were visible in the deck over the pier... After yielding, the bridge "lifted off" the abutment... Eventually, plastic hinges developed near the center pier and the web of the exterior girder buckled at the formation of the hinge..." Shortly after, compression failure occurred at one of the curbs and the test was terminated at a load of 1265 kips.

The program NONBAN is run assuming that the contribution of the curbs and overhang to the properties of the longitudinal edge beams is similar to the effect of half the slab in the interior beams. Thus, all four longitudinal girders are assumed to have the same properties. Since the diaphragms broke at an early stage of the loading process, and since no information was provided about the properties of the diaphragms, the NONBAN model ignored their presence. To prepare the mesh for the NONBAN analysis, each span is divided into ten equal segments. The NONBAN analysis used the composite properties of the longitudinal beams for regions of positive bending. In the negative bending regions, the beam properties assume non-composite section but includes the effect of the cover plates and the reinforcing steel of the slab. Since the amount of reinforcing steel was not provided in the reference, typical values were used. In this case it is assumed that the area of reinforcing steel is 3226 mm^2. The longitudinal beams are connected by forty-one transverse beams representing the transverse capacity of the slab. The possibility of having shear failures is not considered in this example.

Figure C.3 shows a comparison between the field results published in reference [C-9] and the results of NONBAN. Excellent agreement is observed in the figure for the whole range of the loading process. This includes the prediction of the yielding load and the ultimate load. In this analysis, bridge members are assumed to have an infinite level of ductility thus, the ultimate capacity is reached when a mechanism forms which is manifested by obtaining large levels of deformation for a very small increment of load. This example illustrates the validity of the program NONBAN to perform the nonlinear analysis of typical continuous steel bridges.

C-2.2 Nebraska Laboratory Test

The Nebraska laboratory test was performed on a full scale simple span (70 ft) bridge. The bridge was designed according to Nebraska Department of transportation standards. Construction procedures and testing methods were very carefully controlled. The bridge consists of three steel plate girders at 10 ft spacings supporting a 7.5 in deck slab. The loads were placed to simulate two side-by-side HS trucks. Reference [C-10] gives a more complete description of the tested bridge. Samples were used to estimate the strength of the concrete in the deck and the steel of the beams. The beams and the slab were built to act as composite sections. Although diaphragms were built as part of the structure and tested for working loads, all diaphragms except the end ones were removed when performing the ultimate load test.

Tests to determine the ultimate load capacity of the bridge were performed by jacking. The loads were then increased until punching shear failure occurred in the slab under one of the load

pads. The researchers observed that: " The girders remained elastic until a load level of 12 times HS-20 trucks... The location of the neutral axis did not change throughout the loading process indicating that composite action remained at very high load levels...". The punching shear failure in the slab occurred at a load level corresponding to 16 times HS-20 trucks. The deflection at that load level was measured to be approximately 7.1 in. Although the load deflection curve was beginning to flatten out at that point, it was evident that the ultimate capacity of the bridge was not reached.

The program NONBAN is run assuming that the sections are composite and accounting for the different properties of the edge beams and the interior beams. For the edge beams however, the effect of the railings was ignored. Since the middle diaphragms were removed before the ultimate load test, the NONBAN model ignored their presence. Also, the model ignored the presence of the edge diaphragms since their contribution at this point is mainly for stability of the loaded structure. The NONBAN model used the moment curvature plots corresponding to composite compact sections as recommended by Schilling for positive bending. To prepare the mesh for the NONBAN analysis, the span is divided into ten equal segments. The presence of reinforcing steel in slab was not considered. The longitudinal beams are connected by eleven transverse beams representing the transverse capacity of the slab.

Figure C.4 shows a comparison between the laboratory results published in reference [C-10] and the results of NONBAN. Excellent agreement is observed in the figure for the whole range of the loading process including the prediction of the yielding load and the maximum load. The results show that the ultimate capacity was not reached in the test although the slab punching shear failure occurred at a load level slightly lower than ultimate. Infinite level of member ductility is assumed. Hence, ultimate load is reached at a load factor corresponding to 17.21 times the two HS-20 trucks. This corresponds to the formation of a mechanism which is manifested by obtaining large levels of deformation for a very small increment of load. This example illustrates the validity of the program NONBAN to perform the nonlinear analysis of typical bridge simple span steel plate girder bridges.

C-2.3 Canada's Bridge Model Test

The Canadian laboratory test [C-11] was performed on a model of a simple span bridge with a span length equal to 6m. The bridge consists of three steel W250x39 rolled I-beams at 620 mm spacings supporting a 70 mm deck slab. Concrete and steel samples were used to estimate the strength of the concrete in the deck and the steel of the beams. The beams and the slab were built to act as composite sections.

Tests to determine the ultimate load capacity of the bridge were performed by using an actuator. The loads simulated a three-axle truck configuration. The loads were applied at three points above the middle girder as described in reference [C-11]. The loads were then increased

until the ultimate capacity was reached. The bridge was loaded up to a value of 766 kN (172.2 kips). At this load level the actuators' capacity was exhausted and the test was stopped. At that point a visible plastic hinge was formed in the middle beam. Longitudinal and diagonal cracks were observed on the bottom side of the slab near the central portion of the bridge. It was also observed that punching shear failure occurred under the load such that the loading platten was resting on the top surface of the steel beam. The researchers predicted that the bridge could have still taken up to 40 kN (9.5 kips) additional load if the actuators were still operational. In actuality however, the bridge unloaded to a value cloe to 720 kN.

The program NONBAN is run using the composite section properties. To prepare the mesh for the NONBAN analysis, the length of the bridge is divided into ten equal segments. The longitudinal beams are connected by eleven transverse beams representing the transverse capacity of the slab.

Figure C.5 shows a comparison between the laboratory results published in reference [C-11] and the results of NONBAN. Excellent agreement is observed in the figure for the whole range of loading including the prediction of the yielding load and the maximum load. It is observed that the NONBAN results produced an ultimate load of 719.5 kN. This value is similar to the maximum load measured in the laboratory. This indicates that the bridge could not sustain the additional 40 kN that the researchers predicted through their analysis. An infinite level of ductility is assumed for the bridge members, thus, NONBAN predicted that the ultimate capacity is reached when a mechanism forms which is manifested by obtaining large levels of deformation for a very small increment of load. This example gives another illustration of the validity of the program NONBAN to perform the nonlinear analysis of typical steel bridges.

C-2.3 Summary

The comparisons between the results of the two full scale bridge tests, the bridge model test and NONBAN illustrate the validity of the program and the modelling scheme used in this study. The comparisons confirm that the moment-rotation curves developed in this study based on the experimental data proposed by Schilling [C-6] provide an excellent representation of the actual behavior of steel bridge members. It is also observed that the bridges analyzed in this section are relatively narrow and thus superstructure failure would normally occur due to the formation of a plastic hinge mechanism. In two of the experiments, the full plastic mechanism did not actually develop because of the punching shear failure of the slab at the point of application of the load. In addition, the experiments reviewed herein demonstrate that the diaphragms break (in the Nebraska test they are just removed) at early loading stages, thus their contributions to the transverse distribution of the load is often negligible.

C-3. Bridge Configurations.

Design Considerations

To study the behavior of typical steel I-beam bridge configurations, 120 steel bridges are designed to cover typical span lengths and cross-sectional configurations. Simple span bridges as well as continuous two-span bridges with individual span lengths varying between 14 and 46 m (45 and 150 ft) are designed assuming that the deck is supported by 4, 6, 8 or 10 beams with beam spacings varying between 122 and 366 cm (4 and 12 ft). The concrete bridge decks are assumed to vary in depth between 19 and 22 cm (7.5 and 8.5 in) depending on the beam spacing. For each bridge configuration, section dimensions were chosen based on the span length and beam spacings to satisfy AASHTO' s requirements for beam depths (depth between span length/20 and span length/30) . The beams are assumed to be A-36 steel while the deck's strength is equal to 24 MPa (3.5 ksi).

The bridges are designed for strength to satisfy the AASHTO LFD criteria for HS-20 loading. LFD criteria are chosen herein as the base case in order to match the designs performed by Nowak [C-8] during the calibration of the LRFD code. Since the LRFD code was calibrated to match the average performance of the LFD criteria, the choice of codes followed in this study becomes insignificant. In addition, the object of this project is to study the redundancy for all types of bridges irrespective of the code used for their design. Therefore the choice of the design criteria is not of primary importance especially that the sensitivity analysis will specifically address cases when bridges do not satisfy the LFD design criteria.

During the design process, a resistance factor of 1.0 is used to select the required sections. The serviceability requirements were not checked because this study is concerned with the strength capacity of bridge systems and not member serviceability. The effect of using sections with higher or lower strengths than those that exactly satisfy the LFD strength criteria is studied separately in the parametric analysis described in section C-5 below.

For simple span and continuous bridges, the total depth of the section is assumed to be constant. To account for different required moments of inertia and ultimate section capacities in the negative region, the design uses steel cover plates.

Design Example

The design of an example simple span (150 ft) composite steel I-beam bridge is presented in this section to illustrate the assumptions made in this study. This bridge example is assumed to be formed by parallel beams at 8 ft spacings. The steel beams are assumed to have a moment of inertia equal to 75990 in^4.

The dead weight of the beam is assumed to be 0.26 kip/ft given that the cross sectional area of

the beam is 76.4 in^2. Assuming a slab thickness of 8.0 in, the dead weight of the tributary area of the slab becomes 0.8 kip/ft. The superimposed dead weight is assumed to be equal to 0.4 kip/ft. It is herein assumed that the beam's weight and the slab's weight are carried by the non-composite section (the continuous beam is used for multiple spans). On the other hand, the superimposed dead weight is carried by the (continuous) composite beams. These produce a total maximum positive dead load moment at the mid-span of the beam equal to 4106 kip-ft.

The live loads are applied on the composite (continuous) section. The AASHTO HS-20 truck produces a maximum positive bending moment equal to 2475 kip-ft.

The impact factor for this 150-ft span length is 1.18. The girder distribution factor for this 8-ft girder spacing is 1.45 of a wheel's load. The LFD load factors of 1.3 for the dead loads and 1.3 times 5/3 for the live loads produce a factored maximum positive bending moment equal to 9933 kip-ft. In order to simplify the design process, the maximum positive bending moments from the dead weights and the live load are added together even though, they may not be occurring at exactly the same section.

For this design example, it is assumed that the concrete strength is 3.5 ksi for the slab and A36 steel is used for the I-beams. The effective flange width is 8 ft.

Using a resistance factor equal to 1.0, the capacity of the section is found by equilibrium assuming that the steel is in the plastic range and using Witney's rectangular block to model the stress in the concrete. The calculated nominal moment capacity for the composite beam section chosen is 10150 kip-ft which is slightly (2%) above the required moment (9933 kip-ft). In the design calculations, it is assumed that the section in positive bending is always compact. Failure of the section is assumed to occur when the concrete crushes or when the steel ruptures. For the section used herein concrete crushing is assumed to occur when the strain in the concrete reaches a value equal to 0.0038. This occurs at a level of curvature equal to 0.000461. The maximum plastic hinge rotation associated with this level of curvature is compared to the maximum plastic hinge rotation of the naked steel section to ascertain that section failure occurs due to concrete crushing and not steel rupture. Steel rupture is assumed to occur at a plastic hinge rotation equal to 65 mrad as proposed by Schilling [C-6]. The comparison shows that all the sections designed in this study would fail due to crushing before steel rupture is reached.

Summary of Designs

All the composite steel I-beam bridges designed in this study follow the procedure illustrated in the example detailed above. Table C-1 gives a summary of the designs for the simple span composite steel I-beam bridge members. Table C-2 gives the summary for the two-span continuous bridges.

C-4. Results of Nonlinear Analysis.

The nonlinear analysis of the steel I-beam bridge systems designed as described in the previous section is performed using the program NONBAN. This section illustrates how the bridges are modeled and summarizes the results of the analysis.

Preparation of Input Data.

The mesh discretization and modeling procedure used in this study follow the general guidelines given by Zokaie, Osterkamp and Imbsen [C-4] and the procedure outlined in section C-1 of this appendix. The beams in the longitudinal direction account for the composite action between the slab and the I-beams. In addition, it is herein assumed that the bridges have no transverse diaphragms. This means that the lateral distribution of the load is only effected by the transverse properties of the deck slab. The sensitivity analysis performed further below demonstrates that the presence of the diaphragms does not change the results significantly if the diaphragms are assumed to have low torsional rigidities. However, it is observed that the presence of transverse members with high torsional inertias will improve the transverse distribution of the load.

It should be noted that available methods for estimating the torsional rigidities of the slab and transverse members are very approximate because of the discretization of the slab into mesh elements. Also, the model used ignores the interaction between torsion and the two directional bending moments in the deck slab. This interaction may be significant especially in the inelastic range. However, the comparisons of the model used to the experimental results (section C-2) show that the modeling scheme used is sufficiently accurate for the purposes of this study. Different methods have been suggested to account for the torsional capacity of the longitudinal and transverse beams. For example, Hambly [C-3] suggests to use a torsional constant equal to twice the bending moment of inertia for the slab elements.

In this study, it is assumed that the transverse beam elements representing the contribution of the slab have a torsional constant J calculated as given in equation (C-1). For the beams in the longitudinal directions, the torsional constant of the steel is negligible compared to that of the concrete slab. The torsional constant of the slab is also calculated as given in equation (C-1).

The discretization of the bridge superstructures for the base cases studied herein divides every longitudinal beam into equal segments. For a given bridge configuration, steel bridges were divided into a mesh following the same divisions as those of the corresponding prestressed concrete bridges.

The moment-rotation curves for the longitudinal members are calculated based on their section moment capacities using the curves shown in Figure C-3. For the transverse members representing the contribution of the concrete slab to the transverse distribution of the load, the moment-rotation curves are calculated as explained in Appendix B.

The dead load is assumed to be uniformly distributed along the length of each longitudinal member. All the longitudinal members are assumed to carry the same dead load. The live load is formed by HS-20 vehicles placed longitudinally in the most critical design points. In general, the outside wheel of the end vehicle is placed over the web of the exterior beam. The spacing between side-by-side trucks is conservatively chosen to be 0.6 m (2 ft). The base case assumes two side-by-side HS-20 vehicles. As mentioned in section C-1, the analysis of the continuous spans assumes three different load combinations.

The nonlinear incremental analysis is performed using the program NONBAN. No safety factors are applied on the resistances. Similarly, no safety factors or impact factors are applied on the loads during the analysis. This is because the purpose of the incremental analysis is to evaluate the capacity of the bridge (not its loading). The capacity is herein expressed in terms of how many HS-20 trucks it can carry before it fails. The effect of the dynamic impact will be included on the loading side of the safety check equation that will be performed further below during the reliability analysis.

The AASHTO HS-20 vehicles are incremented until bridge system failure occurs. The load factor at which the system fails is defined as LFu. LFu gives the factor by which the weights of the initial HS-20 vehicles should be multiplied to produce system failure. Failure of the bridge is assumed to occur when one main longitudinal member reaches a plastic hinge rotation equal to the maximum allowable plastic rotation. This maximum allowable plastic rotation is obtained from the moment-rotation curves and it corresponds to the value at which the concrete crushes or the steel ruptures. It is herein assumed that concrete crushing under transverse bending or in secondary members will only produce local failures. Therefore, yielding in transverse direction is considered but concrete crushing is not checked.

In addition to calculating the load factor corresponding to the ultimate capacity of the bridge system (LFu), the load factor corresponding to the level at which the bridge becomes non-functional is recorded. At this point, it is assumed that a bridge becomes non-functional when the maximum live load displacement under a main longitudinal member reaches a value corresponding to the span length/100. The load factor corresponding to this displacement level is expressed by the variable LF100. The L/100 value is chosen herein because it is similar to the values at which many bridge field tests were stopped when the researchers observed potentially high and dangerous deflections. This criterion was changed from the span/200 criterion used in the Phase I report because it was found that the L/200 criterion occurred at points of the load deflection curve where the curve is still ascending steeply. This would then produce load factors for functionality that are very sensitive to the design and modeling assumptions. For example at the early loading stages the values of the load factor are very sensitive to the moment of inertias of the sections, they are also very sensitive to the estimate of the plastic hinge length and to the construction sequence. The L/100 criterion occurs at points where the slope of the load deflection curve is flattening out thus it would give more stable results. It should be noted that the reliability calibration process accounts for the different criteria used by using different safety index target values. Therefore, whether we use L/100 with a large safety index target or L/200

with a small target the final redundancy factors will be similar. However, the L/100 will give more consistent results which would be less sensitive to the modeling assumptions.

Following the calculation of the ultimate capacity of the intact structure, a similar analysis is performed assuming damaged conditions. In this study, a bridge's damaged condition assumes that the external girder is so heavily damaged that it can no longer carry any load. This would simulate a situation where the external girder is knocked out of service due to a collision or severe damage. The incremental nonlinear analysis of bridge structures where the external member is assumed to be totally damaged is executed using the same assumptions stated above for the intact structures. The ultimate load capacity for a damaged bridge scenario is designated by the variable LFd. In the NONBAN model, damaged members are represented by very low moments of inertia. The live load positions used for the damaged cases are the same as those used for the intact bridges. This means that the external wheel load of the HS-20 vehicle lies directly above the damaged external girder. In this analysis, failure is assumed to occur when one of the intact longitudinal girders reaches its maximum plastic hinge rotation. Although the nonlinearity of the transverse members is accounted for, no failures in the transverse direction are considered i.e. crushing of the concrete in the slab is not checked. This assumption may be unconservative because there is a possibility that the cantilevered portion of the slab would break under the effect of the extruding wheel load. However, it is herein assumed that the parapet and the railing will provide enough support so that the slab will still be able to transfer the load laterally to the adjacent intact girder. This assumption is used herein because this project is concerned with studying the distribution of the load to the longitudinal members and not in the analysis of the capacity of the slabs.

To provide a measure of a bridge's level of redundancy, the load factor at which the intact bridge system fails (LFu) , the load factor at which the bridge becomes non-functional (LF100) as well as the load factor for the damaged bridge scenario (LFd) are compared to the load factor corresponding to the first member failure LF1. LF1 in this case is calculated assuming linear elastic behavior of the bridge members. A linear elastic behavior is assumed in order to be consistent with current member oriented design and analysis procedures. Thus, the LF1 factor represents the estimated bridge member capacity using current traditional member checking methods without consideration of the code-specified safety factors. The calculation of LF1 is illustrated further below.

Because redundancy is essentially a comparison between the system capacity and that of the individual bridge members, the ratios of LFu/LF1, LF100/LF1 and LFd/LF1 are used as objective deterministic measures of bridge redundancy. Section C-6 of this appendix proposes a probabilistic measure of redundancy as expressed in terms of the reliability indices.

Detailed Example

The analysis of a 150 ft simple span bridge is presented in this section to illustrate the structural model used in the calculations performed on the composite steel I-beam bridges. The bridge is assumed to have 6 beams spaced 8 ft center to center. The slab is assumed to be 8 in thick acting compositely with the girder. The slab has a concrete strength equal to 3.5 ksi while the girder's nominal yielding stress is 36 ksi. The member's cross section is shown in Figure C.6.

The bridge is discretized as shown in Figure C.7. The longitudinal beams represent the contributions of the composite slab-girder section. These beams are placed at the centerline of the girders. The spacings between the longitudinal beams are thus 96 in. The transverse beams represent the contribution of the slab to the transverse distribution of the loads. Transverse beams are placed each at 1/10 of the girders length. Thus, the spacing between the transverse beams is 180 in. It is herein assumed that the slab is reinforced in the transverse direction on the top and the bottom by an equal amount of steel and thus the slab will have equal moment capacities for both negative and positive bending.

The dead load on the longitudinal beams is assumed to equal 0.088 kip/in acting on the noncomposite steel section. The superimposed dead load is 0.033 kip/in acting on the composite steel-concrete section.

Two side-by-side AASHTO HS-20 trucks are used for the live load. The location of the tire loads are indicated by X in Figure C-7. The external wheel line coincides with the external girder. Nominal beams connect the tire loads to the adjacent mesh nodes as shown in the figure.

For the elastic material properties, the modulus of elasticity of the longitudinal members is taken as 29000 ksi. The shear modulus for the steel is 11153 ksi. The modulus of elasticity of the (concrete) transverse members is 3372 ksi and the shear modulus is 1405 ksi.

The elastic properties of the noncomposite and the composite longitudinal beams are given in Figure C-8 a & b. All the longitudinal beams are assumed to have the same properties.

The elastic properties of the interior transverse beams are given in Figure C-9. The elastic properties of the transverse end beams are also given in Figure C.9. As can be seen, the end transverse beams are assumed to have properties equal to 1/2 those of the middle transverse beams.

Figures C-8 and C-9 also show the moment versus curvature plots obtained for the longitudinal and transverse beams. To obtain the moment versus plastic rotation curves, the slopes of the moment versus curvature plots are divided by L_p (the length of the plastic hinge). For steel members, the plastic hinge length is assumed to be equal to half the length of the element. For this example, the value of L_p used is 90 in.

The maximum plastic hinge rotation for the longitudinal beams is taken as the maximum curvature obtained from the moment-curvature plot and multiplied by L_p. The transverse beams representing the slab are assumed to have an infinitely high maximum plastic hinge rotation. This means that failure of the bridge system occurs only due to failures in the longitudinal members although the model accounts for the material nonlinearity of the slab.

The supports at the ends of each longitudinal beam are free to rotate in all directions but their displacements are fixed in all directions.

The damage scenario assumes that the external girder immediately below the external wheel line can no longer carry any load. The program accounts for this scenario by using a negligibly small moment of inertia for the elements representing the external girder.

The results of the nonlinear analysis for the intact structure and the damaged condition of the example bridge are shown in Figure C-10. The results show that the ultimate capacity is reached when the HS-20 vehicles are incremented by a factor, LFu equal to 4.43. A displacement equal to span length/300 (6 in) is reached when the load factor, LF300 is equal to 2.61. A displacement equal to span length/200 is reached when the loads are incremented by a factor, LF200, equal to 3.18. A displacement equal to span length/100 is reached when the load factor reaches a value, LF100, equal to 4.03. The analysis of the damaged bridge reveals that the ultimate capacity of the damaged bridge is reached when the HS-20 vehicles are incremented by a factor LFd equal to 1.79. LFu and LFd correspond to the load increment at which the concrete in any longitudinal girder reaches crushing.

The calculation of the elastic load factor LF1 is effected using the equation:

$$LF_1 = \frac{R - D}{DF_1 \; LL_{HS\text{-}20}} \qquad \text{(C-2)}$$

where R is the member's unfactored moment capacity, D is the member's unfactored dead load, DF_1 is the linear elastic distribution factor for the member as calculated from NONBAN assuming linear elastic behavior, $LL_{HS\text{-}20}$ is the total live load moment effect due to the HS-20 vehicles. The product $DF_1\ LL_{HS\text{-}20}$ is obtained from the linear elastic results of NONBAN as the highest live load moment effect for any longitudinal member.

Using a linear elastic analysis, the moment due to the dead load at the midspan of a girder is obtained as 49005 kip-in. The external girder will carry a linear elastic moment equal to 22331 kip-in due to the two side-by-side HS-20 vehicles. The girder section has an ultimate girder capacity equal to 121804 kip-in. The 49005 kip-in dead load moment and the 121804 kip-in ultimate girder capacity indicate that the live load margin (the amount available to carry the live load) is 72799 kip-in (121804 minus 49005 kip-in). Since one set of HS-20 vehicles produces a

moment equal to 22331 kip-in on the external girder ($DF_1\ LL_{HS\text{-}20}$), then the bridge is capable of carrying 3.26 times the HS-20 trucks assuming linear elastic behavior. Hence LF1 is equal to 3.26.

The external girder's distribution factor obtained from this analysis is on the order of 0.75 times the weight of one truck. The value calculated herein is found to be higher than the 0.58 value used by Nowak during the calibration of the LRFD specifications [C-8]. But closer to the (S/5.5) value of the AASHTO standard specifications. It should be noted that Nowak's calibration assumes an interior girder, while the calculations performed herein are for an exterior girder.

As seen above, the bridge is capable of carrying 4.43 times the HS-20 vehicles before the concrete in a longitudinal girder reaches crushing. The calculations account for the nonlinear behavior of the structure. Therefore, the redundancy ratio for the ultimate capacity, defined as LFu/LF1, is equal to 1.36 for this particular bridge. Similar calculations are performed for a variety of bridge configurations. These results are presented in the next paragraph.

Summary of Results

The results obtained from the analysis of all the steel I-beam simple span bridges are given in Table C-3. In addition to giving the values of LF300, LF200, LF100, LFu, LFd and LF1 Table C-3 gives the value that would have been obtained if the loading were allowed to continue until a mechanism is formed. For the simple span bridges, the formation of the mechanism is approximated by taking the maximum moment capacity of each girder's section minus the dead load applied on the section, the difference is multiplied by the number of girders in the structure and then divided by the moment due two HS-20 trucks. This is represented by the equation:

$$mech. = \frac{n\ (\ R\ -\ D\ )}{LL_{HS20}} \qquad \text{(C-3)}$$

where n is the number of longitudinal girders, R is the member's resistance, D is the member's dead load and LL_{HS20} is the total moment effect on the bridge due to two HS-20 trucks. The values obtained from equation C-3 are shown under the column labelled mech. (mechanism) and are given here to provide a rough comparison between the results of the analysis using the failure criteria described above and the values that would be obtained if infinite levels of ductility are assumed in each member. The results show that the values of LFu and mech. are fairly close for narrow bridges. As the bridge width increases, the difference becomes large. In fact mech. could be as high as 3 times the value of LFu for large girder spacings.

Table C.3 also shows the ratios of LFu/LF1, LF100/LF1 and LFd/LF1 for the cases analyzed. It is observed that the ratio of LFu/LF1 may be as high as 1.46 showing a 46% increase in system capacity compared to member capacity. Similarly LF100/LF1 may also reach a value on the order of 1.38. Even LFd/LF1 is shown to reach up to value of 0.90 indicating that some bridge configurations are still capable of carrying high levels of loads even when a girder is completely removed from the structural system.

The results show that, for a given girder spacing, the LFu/LF1 ratio increases as the number of girders is increased. It is noticed that the most optimum number of girders is six for a two-lane bridge and that increasing the number of girders beyond six does not significantly improve the LFu/LF1 ratio. For a given number of girders, the LFu/LF1 ratio increases as the girder spacing increases from 4 to 8 ft. As the girder spacing increases beyond 8 ft there is a drop in the ratio. This observation is due to the fact that for narrow bridges, all the girders are almost equally loaded under the effect of two side-by-side trucks. In this case if one girder fails, the other members do not have enough reserve strength to carry the additional load and will also fail. As the girder spacing increases, some of the girders which may be far from the load will carry less moment than those immediately under the load. If the girder under the load fails, the other girders will have some reserve strength and will help carry some of the additional load. As the girder spacings increases further, the slab will not be able to transfer the load to the far members and crushing of the girder under the load will occur before the transfer to the other girders takes full effect.

The results show that the optimum bridge configuration for a two-lane bridge is a system formed by 6 beams with spacing around 6ft to 8 ft. It is interesting to note that this configuration is currently the most widely used for typical steel I-girder bridges. The observations made above are due to the fact that bridge failure is defined as the point at which one of the main longitudinal girders reaches its ductility limit rather than the point at which a mechanism form. The results also show that the LFu/LF1 ratio increases slightly with the span length but it is believed that this slight increase is mostly due to the design details and the effect of the resistance to dead load ratios.

The values for the LF100/LF1 ratio seem to follow the same trends mentioned above for the LFu/LF1 ratio. Actually, for each bridge configuration the LF100/LF1 are only slightly lower than those of the corresponding LFu/LF1 values.

The LFd/LF1 ratio also follows the same trend. However, the tendencies are much more pronounced. In the sense that if the LFu/LF1 ratio decreases as the beam spacing is increased beyond 8 ft for a given number of beams, then the decrease in LFd/LF1 is even sharper. The only difference observed in the trend of the results is in the fact that there is no increase in the LFd/LF1 ratio as the spacing is increased from 4 ft to 8 ft as had been observed for LFu/LF1 and LF100/LF1.

The results of the 120 ft continuous span steel bridges with different number of beams and different beam spacings re shown in Table C-4. The analysis was performed for both compact and noncompact sections in the negative bending regions. Three different loading conditions are considered for the continuous bridges. The first loading condition (case 1) assumes that only one lane is loaded by two side-by-side HS-20 trucks. This case corresponds to a failure in maximum positive bending, the vehicles are placed at 0.41 L of the span. Case 2 assumes that two spans are loaded each by one HS-20 vehicle. Case 3 assumes that the two spans are each loaded by two side-by-side HS-20 vehicles. Since cases 2 and 3 produce high levels of negative bending, the vehicles are placed at 0.57 L of each span. The results show that bridges with noncompact sections are highly nonredundant, giving LFu/LF1 ratios less than 1.0 for load cases 1 and 2. Also, notice that many of the bridges with noncompact sections fail even before the span length/100 value is reached (these cases are symbolized by the X in the table). This indicates that the bridges would fail in a brittle fashion with very little warning. On the other hand, the results show that span continuity improves the redundancy of the bridges compared to simple span bridges if the sections in negative bending are compact.

C-5. Sensitivity Analysis.

Sensitivity of simple span bridges

A parametric analysis is performed to study the sensitivity of the results to the assumptions made during the design of the bridge members as well as during the discretization and the nonlinear analysis of the bridge structural models. The simply-supported 45 m (150 ft) bridge with 6 beams at 240 cm (8 ft) is used as the base case for the sensitivity analysis. The sensitivity analysis looks at the effects of changes in the properties of the bridge members. For example, the effects of the presence of diaphragms at the supports, and the effect of using stiffer and stronger main elements and deck slabs were investigated. The effect of deck skewness was checked by analyzing the 45 m (150 ft) bridge with a 30 degree skew. In addition, the effect of errors in the estimate of the dead load and the maximum plastic hinge rotation are also studied. Below is a detailed discussion on the results obtained. The results are also shown in Table C-5.

The first parametric analysis looked at the effect of including the construction sequence during the structural analysis. The results of the base case (case 0 in Table C-5) for the intact bridge analyzed above assumed that the permanent dead load was applied on the naked steel section while the superimposed dead load was applied on the composite section. In this example, the calculations are repeated assuming that the permanent and the superimposed dead loads are applied on the composite section. This simulates a shored construction of the bridge. The results obtained for LFu, LF100, LF200, LF300 and LF1 are shown under case 1 of Table C-5. The values obtained are respectively 4.42, 4.03, 3.22, 2.65 and 3.26. These values are compared to 4.43, 4.03, 3.18, 2.61 and 3.26 for the base case. It is obvious that the dead load application sequence does not affect the results of the intact bridge as the load factor increases beyond first yielding. The analysis of the damaged condition should account for a more complicated loading

sequence. For example, the permanent dead load is first applied on each naked girder. Subsequently, the superimposed dead load is applied. Finally, the dead load of the damaged girder is applied on the remaining composite girders. The program NONBAN is not set to accept a three-phased loading sequences. However, a special case is studied in order to study the effect of the three-phased application of the dead load. In this special case, we assume that the damaged girder will distribute its dead load to the other girders after the composite action takes effect. i.e. the undamaged girders will carry their permanent dead loads on the non-composite sections, then carry the superimposed loads plus the weight of the damaged girder on the composite sections. In this case, the damaged scenario will produce an LFd value equal to 1.77. This value is reasonably close to the 1.79 value obtained if all the dead loads are applied on the composite sections. For this reason, this study assumes that all the dead loads are applied on the composite section for the damaged cases.

This study assumes that a damaged bridge has lost the load carrying capacity of the external girder under the applied load. To study the effect of this extreme damage scenario, several other scenarios are analyzed. These additional scenarios assume first that only the middle 80% of the external girder is damaged, then 60%, then 40 % and finally that only 20% of the girder is damaged. The results show that LFd increases from 1.79 to 1.85, 1.91, 1.98 and finally to 2.02 as the damaged zone is decreased. Notice that the maximum difference between total damage and 20% damage is about 13%. These cases are not presented in Table C-5.

Next, we looked at the effect of the torsional constant. If the torsional constant of the longitudinal beams is doubled (case 2 in Table C-5), the results obtained for LFu, LF100, LF200, LF300 and LF1 are respectively 4.59, 4.17, 3.30, 2.71 and 3.30. The damaged scenario produced an LFd value equal to 1.91. It is observed that doubling the torsional constant produces a slight increase in all the load factors (less than 4% for the intact and 7% for the damaged). However, it is also observed that the ratio of LFu/LF1, LF100/LF1, LF200/LF1 and LF300/LF1 is even less sensitive to this change producing a difference of less than 3%.

Doubling the torsional constant of the transverse beams (case 3 in Table C-5) produced LFu, LF100, LF200, LF300 and LF1 values of 4.69, 4.16, 3.29, 2.70 and 3.30 respectively. The damaged scenario produces an LFd value equal to 2.11. It is herein observed that the effect of the torsional constant of the transverse beams (including the slab) produces higher load factor values. The most significant effect is observed in the ultimate load factor LFu that changes by about 6% for the intact bridge. The damaged bridge improvement in LFd is about 18%.

When the moment of inertia of the longitudinal beams is doubled (case 4), the LFu, LF100, LF200, LF300 and LF1 obtained are respectively 4.41, 4.13, 3.56, 3.04 and 3.250. Notice that this change does not affect LFu nor LF1 significantly but increases the values of the other factors relative to the base case. It is noticed that the effect decreases as the load factors increase beyond first yield. This is because the change in the moment of inertia affects the linear elastic portion of the curve but not the plastic range. The LFd value on the other hand changes very slightly to 1.76.

When the moment of inertia of the transverse beams are doubled (case 5), the NONBAN analysis produces LFu, LF100, LF200, LF300 and LF1 respectively as 4.43, 4.06, 3.24, 2.66 and 3.24. The LFd value is 1.77. The effects are similar but even less pronounced than those observed when the longitudinal stiffness is increased.

Another case looked at the effect of doubling the nonlinear moments of the longitudinal beams (case 6). In this case, the ordinates of the moment curvature relationship and the corresponding slopes are doubled. The LFu, LF100, LF200, LF300 become respectively 10.23, 8.90, 5.69 and 3.94 with LF1 equal to 8.72. The LFd value is 4.104. In this case as expected the change in the factors is significant. It is also observed that the ratios LFu/LF1, LF100/LF1, LF200/LF1, LF300/LF1 and LFd/LF1 are reduced. For example, LFu/LF1 and LFd/LF1 are reduced by about 14%.

When the nonlinear moments of the transverse beams are doubled, case 7, the ordinates and slopes of the moment curvature plots are doubled. The LFu, LF100, LF200, LF300 and LF1 become 4.51, 4.08, 3.23, 2.65 and 3.26. The maximum difference between these values and those of the base case is less than 2%. The value for LFd however becomes 2.02 representing a change of 13%.

If the nonlinear moments of the transverse beams are halved (case 8), LFu, LF100, LF200, LF300 and LF1 become respectively 4.22, 3.90, 3.19, 2.65 and 3.26. The difference between these values and those of the base case are less than 4.5%. The value of LFd becomes 1.35 i.e. about 25% lower than that of the base case.

When the value of the dead load is doubled (increased by 100% see case 9 in Table C-5), LFu, LF100, LF200, LF300 and LF1 are respectively 1.71, 1.51, 1.20, .085 and 1.07. It is observed that LFu/LF1, LF100/LF1, LF200/LF1 and LF300/LF1 increase. The increase is about 17% for LFu/LF1. It is also noticed that when the dead load is doubled the bridge collapses under its own dead load when the external girder is damaged (LFd=0.)

Assuming that the maximum plastic hinge rotation i.e. the rotation that produces crushing in the concrete and subsequently defines the maximum loading on the bridge is doubled to a value of 0.0864 radian (case 10). The corresponding LFu value becomes 4.86 representing an increase of about 10%. The values of LF100, LF200, and LF300 are not affected. The increase in LFu is partially due to the fact that the moment-curvature curves used herein have a small slope representing some strain hardening in the material properties. Also, by allowing a higher rotation on the most heavily load member, more of the load is distributed to the other members allowing a higher LFu value for the system as a whole. The effect of improving the ductility of the longitudinal members is most noticeable for the damage scenario where the LFd value increases to 2.31 representing an increase of about 30%.

If a skew of 30 degrees is introduced on the deck (case 11), LFu, LF100, LF200, LF300 and LF1 values are respectively 4.49, 4.08, 3.25, 2.67 and 3.30. These values are quite similar (slightly higher) to the base case values of 4.43, 4.03, 3.18, 2.61 and 3.26. More importantly, the ratios LFu/LF1, LF100/LF1, LF200/LF1 and LF300/LF1 are practically unchanged. The skew however decreases the value of LFd to 1.69 a change of about 6%.

When the size of the mesh used for the analysis is doubled (case 12), LFu, LF100, LF200, LF300 and LF1 values are respectively 4.41, 4.19, 3.28, 2.68 and 3.26. The differences between these results and those of the base case are on the order of 3 to 4%.

In case 13 of Table C-5, a diaphragm is introduced on the ends of the superstructure. The diaphragm is chosen such that it has the property of the longitudinal beams. The LFu, LF100, LF200, LF300 obtained in this case are respectively 4.42, 4.04, 3.22, 2.65 and LF1 is 3.26. LFd becomes 1.82. This case shows practically no changes compared to the base case where no diaphragms are assumed. If in addition, the same diaphragm is placed at the midspan as well as at the ends (case 14), the results for LFu, LF100, LF200, LF300 are respectively 4.50, 4.12, 3.27 and 2.68. The value of LF1 becomes 3.30. LFd becomes 2.05. Notice that the difference in LFu is less than 2% and that the ratio of LFU/LF1 is 1.36 which is unchanged from the base case. On the other hand the improvement in LFd is about 14%.

Summary for simple span bridges

The results of the sensitivity analysis for the 150 ft bridge with 6 beams at 8 ft are summarized in Table C-5 for the simple span bridge. The results indicate that the mesh used provides reasonably stable results. Also, it is observed that the effect of changes in the deck slab capacities are insignificant for the intact bridge. Similarly, the presence of diaphragms at each support and the midpoint does not improve the results obtained for the intact bridges. However, the presence of the diaphragm and the strengthening of the deck slab improve the overall system capacity and redundancy of damaged bridges.

Due to the difficulty of estimating the true torsional rigidity of bridge members, a sensitivity is performed to study the importance of this factor on the final results. It is noted that, although a high increase in the assumed torsional rigidity of the longitudinal beams does not affect the results of the analysis significantly, an increase in the torsional rigidity of the members representing the deck slab produce a noticeable improvement in the LF/LF1 ratio especially for the damaged case.

Other results show that increasing the bridge skew does not produce any significant change in the LFu/LF1 ratio of the intact bridge although a reduction in the ratio of damaged bridges is observed. It is also noted that an increase in the longitudinal member capacities will decrease the LF/LF1 ratios.

Continuous bridges

The results of the simple span bridge are also compared to those of a continuous two-span bridge with 6 beams at 8ft. The two spans have equal lengths of 150 ft each. The bridge is designed according to the LFD criteria. The moment capacity of the bridge elements in positive bending is 82132 kip-in. The moment capacity of the sections in negative bending is 126806 kip-in. Each span is divided into ten equal longitudinal beam elements. The maximum plastic hinge rotation of the beam elements in positive bending is calculated as 0.0464 radian. This rotation corresponds to the point at which the concrete of the composite longitudinal girders crushes and is calculated based on an assumed geometry of a typical composite bridge girder cross section. On the other hand, the maximum plastic hinge rotation for the members in negative bending is 0.0315 radian. This rotation corresponds to the point at which the steel ruptures. This value is obtained from the curves provided by Schilling for compact non-composite steel sections. The permanent dead load is assumed to be equal to 0.088 k/in and the superimposed dead load is 0.033 k/in. In the calculations of the intact bridge it is assumed that the permanent dead load is applied on the continuous naked steel section. On the other hand the superimposed dead load is applied on the continuous composite girders. Due to the difficulty of accounting for the construction sequence for the damaged scenario, it is assumed that all the dead load is applied on the composite section when analyzing the damaged cases.

Three different loading conditions are considered for the continuous bridges. The first loading condition (case 1) assumes that only one lane is loaded by two side-by-side HS-20 trucks. This case corresponds to a failure in maximum positive bending, the vehicles are placed at 0.41 L of the span. Case 2 assumes that two spans are loaded each by one HS-20 vehicle. Case 3 assumes that the two spans are each loaded by two side-by-side HS-20 vehicles. Since cases 2 and 3 produce high levels of negative bending, the vehicles are placed at 0.57 L of each span. The results of the analysis are summarized in Table C-6. The data labelled "Sens. 0" in Table C-6 gives the results of the simple span bridge. "Sens. 1" gives the results of the continuous bridge using traditional design.

The results of the continuous bridge (Sens. 1) shows that the two-span continuous bridges produce higher LFu/LF1, LF100/LF1 and LFd/LF1 ratios for case 1, than the corresponding simple span bridge (Sens.0) as long as the section in negative bending is compact. Case 3 on the other hand gives similar results to those of the simple span bridge for the LFu/LF1, and LFd/LF1 ratios, the LF100/LF1 ratio is about 5% higher than that of the simple span bridge. If the section in negative bending is assumed to be noncompact, then the ratios decrease considerably for all the load cases considered especially for the damaged cases where the LFd/LF1 ratio decreases to about 0.26 from 0.55 for load case 3. It is noticed that even the LFu/LF1 ratio decreases to slightly below 1.0. The intact bridge reaches it maximum plastic hinge rotation without showing a high level of deformations (a deflection of span length/100 was never reached). This indicates that a continuous bridge with noncompact sections at the support is nonredundant and will fail in a brittle mode with little warning.

Increasing the level of ductility of the section in positive bending by doubling the maximum plastic hinge rotation (Sens. 2) improves the LFu/LF1 ratio of load case 1 when compact negative bending sections are used. None of the other ratios is affected. If the ductility of the compact negative section is improved by doubling the maximum plastic hinge rotation (Sens. 3), the LFd/LF1 ratios for load cases 2 and 3 improve with little noticeable change in any other ratio.

The last effect studied for continuous bridges is the sensitivity to changes in the moment capacity of the sections. For example, if the moment capacity of the section in positive bending is doubled from 82132 kip-in to 164264 kip-in (Sens. 4), accompanied by a doubling of the slopes of the moment curvature curves, then, all the failure modes are drastically changed. This change produced a decrease in the LF/LF1 ratios for load case 1 but drastically improved the ratios for load cases 2 and 3. This observation is found to be valid for both compact and noncompact negative bending sections.

By doubling the moment capacity of the section in negative bending (Sens. 5), we observe again that the changes in the failure modes produce increases in all the LF/LF1 ratios. The least affected ratio is the LF100/LF1 for load case 1.

The results of the sensitivity analysis for the continuous bridges show the importance of the ductility at the continuous end and the importance of the mode that causes the failure of the bridge. The failure mode is primarily due to the relative values of the moments capacities in positive bending and negative bending.

C-6. Reliability Analysis and Calibration of Redundancy Factors.

Reliability Analysis

The calibration of the AASHTO LRFD code was performed by studying the reliability of bridge members assuming that bridges behave in a linear elastic manner. The purpose of the reliability analysis performed in this study is to obtain an objective estimate of the safety of the bridge systems analyzed accounting for their nonlinear behavior. By comparing the safety performance of a bridge system accounting for its nonlinear behavior to the performance of its most heavily loaded member assuming linear elastic behavior, a measure of the redundancy of the system is obtained. The reliability analysis undertaken in this study is performed using a Level II reliability program which accounts for different types of probability distributions. It should be noted that in the Phase I report, a lognormal model was used. With the lognormal model all the random variables are assumed to follow lognormal distributions. The Level II program used herein is capable of accounting for different types of probability distributions and thus the results will be more compatible with those of the LRFD calibration procedure [C-8]. The reliability analysis performed herein is used to calibrate the system factors that will be used

as part of the deterministic design and evaluation equations. A typical engineer will not need to perform such reliability calculations on a routine basis.

To illustrate how the reliability calculations are performed for the purposes of this study, the results of the base case of the 150 ft bridge with 6 beams at 8 ft are presented herein. The calculations of the linear elastic system indicate that the external member fails when the two HS-20 vehicles placed on the bridge are incremented by a factor LF1= 3.26. The nonlinear system's ultimate capacity on the other hand is reached when the weights of the HS-20 vehicles are incremented by a factor LFu=4.43.

To perform the reliability analysis, the statistical information on the loads applied on the bridge and the resistance of the system are required. As performed in this study, the resistance of the intact system is expressed in terms of the load multipliers LFu for the ultimate capacity, LF100 for the functionality criteria, and LF1 for first member failure assuming linear elastic behavior.

The load factors obtained from the nonlinear analysis express the capacity of the intact system to carry the live load. This capacity is obviously a function of the applied dead load and the member resistances. For steel I-girder members, Nowak [C-8] suggests that the average member capacity is actually 1.12 the nominal design capacity (resistance bias =1.12). The member resistances are also associated with a coefficient of variation COV equal to 10%.

In addition, Nowak [C-8] assumes that the dead loads applied on the structure will have a bias that varies between 1.03 and 1.05 with a COV between 8% and 10% depending on whether we are considering factory-made members, cast in place members or other items. (Nowak also uses a COV of 25% for asphalt material and assumes that the average asphalt thickness is about 3.5 in). Based on these observations it is herein assumed that on the average, the total combined dead load effects will have a bias on the order of 1.05 and a COV on the order of 10%.

To calculate the bias and the COV of the load factor LF1, equation C-2 is used. The variable DF1 of equation C-2 gives the load distribution factor i.e. the percentage of the load carried by the most heavily member compared to the total load applied. This variable is not explicitly discussed by Nowak. However, field data taken in reference [C-12] suggest that the load distribution factor has a COV of about 8% if the traffic lanes are preset. Obviously, changing the lane positions will also change the load distribution factor. This implies that the COV is even higher than 8%. Also, as explained earlier, the structural analysis performed in this study assumes that the external wheel of the edge vehicle is placed immediately over the external girder. In most instances, except for large overhangs, this position produces the most critical loading condition. In order to be consistent with the LRFD calibration procedure, it is herein assumed that DF1 as calculated in this study is a deterministic value.

Keeping in mind that the mean of the sum (or the difference) of two random variables is equal to the sum (or the difference) of their means, Equation C-2 is also valid to find the mean

of LF1 given the means of R, D. (LLHS20 is a deterministic variable and a such has a COV of 0% and a bias equal to 1.0). Using equation C-2 with the mean of R and D, it is found that the mean value of LF1 is equal to 3.81 resulting in a bias on LF1 on the order of 1.17 for the 150 ft simple span bridge with 6 beam at 8ft. This is illustrated as:

$$\overline{LF_1} = \frac{\overline{R} - \overline{D}}{DF_1 \quad L.L_{HS\text{-}20}} = \frac{1.12 \; x \; 121804 \; - \; 1.05 \; x \; 49005}{22331} = 3.81 \qquad \text{(C-4)}$$

Also, knowing that the COV of a random variable is the ratio of the standard deviation divided by the mean of the variable, the COV of the variable LF1 can also be calculated using equation C-2. The calculation is performed using the fact that the standard deviation of the sum or the difference of two random variables is equal to the square root of the sum of the squares of the standard deviations. This will produce a COV for LF1 equal to 17% for the 150 ft simple bridge with 6 beams at 8ft. This is illustrated as:

$$COV_{LF_1} = \frac{\sigma_{LF_1}}{\overline{LF_1}} = \frac{\dfrac{\sqrt{\sigma_R^2 + \sigma_D^2}}{DF_1 \quad L.L_{HS\text{-}20}}}{\overline{LF_1}} \qquad \text{(C-5)}$$

$$= \frac{\dfrac{\sqrt{(0.1x1.12x121804)^2+(0.1x1.05x49005)^2}}{22331}}{3.81} = 17\%$$

In his calibration process, Nowak [C-8] assumes that the maximum lifetime load in 75 years produces a maximum moment for a 150-ft simple span bridge equivalent to that obtained by 2.01 times the effect of two HS-20 vehicles. The 2.01 factor accounts for the dynamic impact as well as the static moment effect. Nowak also assumes that the applied live load (including impact effect) is associated with a coefficient of variation equal to 19% for the 150 ft bridge. Similar values are also given for a two-year return period. It is herein suggested that for the ultimate limit state described by LFu, and the functionality limit state described by the variable LF100, the maximum lifetime (75-year) load be used. For the damaged condition it is proposed to use a two-year return period. A two-year period is chosen because it corresponds to the required biennial inspection period. This two-year return period implies that the inspection process will detect any bridge deficiencies due to high structural damage (equivalent to the loss in the load carrying capacity of one member).

The reliability calculations performed herein use the statistical data given above and assume that the LF1 factor follows a lognormal distribution while the applied load follows a Gumbel distribution. Chapter 2 of this report gives a brief description of the reliability analysis performed herein and gives a definition of the safety index, β. The safety index obtained for member failure, β_{member}, of the 150 ft bridge with 6 beams at 8 ft spacing, is 2.43. If one uses a lognormal format to calculate the member reliability of that bridge the safety index obtained becomes 2.49. As mentioned earlier, the lognormal format assumes that both LF1 and the 75 year maximum load follow lognormal distributions.

To calculate the reliability of the whole system, it is herein assumed that LFu follows a lognormal distribution and is associated with the same bias as that of LF1 and the same COV. This assumption is somewhat subjective but is based on the observation made by Cornell [C-13] that the mean resistance of a system subjected to loads with high levels of uncertainty can be approximated as equal to the system resistance obtained by using the means of the member resistances during the structural analysis. On the other hand, it is well known that the COV of the system is usually smaller than the COV of the individual members. However, this assumes that the structural model and system analysis process is exact. To account for the uncertainties in the structural modelling process while performing a nonlinear analysis, it is herein suggested to use a COV on LFu equal to the COV on the member resistances as represented by LF1. The safety index for the first member failure is symbolized by β_{member}. The safety index for the ultimate limit state is defined as β_u. The same logic is herein followed to calculate the reliability index for the functionality, $\beta_{funct.}$, and the damaged limit states,β_d.

The safety index obtained for system failure, β_u, of the 150 ft simple span I-girder bridge is 3.44. This shows that the reliability of this bridge system produces a safety index higher than that of its most critical member by 1.01. i.e. $\Delta\beta u$ (defined asβ_u-β_{member}) is equal to 1.01. As mentioned in Chapter 2, the difference between the reliability of the system and that of the first member to fail, $\Delta\beta_u$, is used in this study as a probabilistic measure of redundancy. The calculations performed for all the simple span steel I-beam bridges studied in this project are shown in Table C-7. The results of the safety indices obtained for individual bridge members are somewhat lower than those obtained by Nowak [C-8] because as explained above, the load (girder) distribution factors obtained in this study are for the exterior girder rather than those of the interior girders used by Nowak. $\Delta\beta_f$ defined as $\beta_{funct.}$ - β_{member}, and $\Delta\beta_d$ defined asβ_u-β_{member}, are also calculated and listed in Table C-7.

Determination of Redundancy Criteria

Table C-7 gives the reliability indices obtained in this study for the simple span steel bridges. The results show that for the ultimate limit state, the system reliability is on the average higher than the member reliability by 0.81 for all the simple span bridges considered. This means that $\Delta\beta_u$ which was defined in Chapter 2 as a probabilistic measure of redundancy is on the average

equal to 0.81. If one studies only the performance of four beam bridges with spacings greater than 4 ft only, then the average value of $\Delta\beta_u$ for these bridges is 0.72. In traditional bridge engineering practice all four beam bridges are considered redundant. It should be noted that the prestressed concrete bridges produced a $\Delta\beta_u$ of 0.82 for four beam bridges, and about 0.97 for bridges with four beams spaced at more than 4 ft. .the 0.75 value is close to the average value obtained from steel and concrete. Therefore, it is herein proposed to use a $\Delta\beta_u$ value of 0.85 as the redundancy criterion for the ultimate limit state. That is, a bridge will be herein defined as sufficiently redundant if the reliability index of the system is higher than that of the member by at least 0.85. The 0.85 value is the average value for both concrete and steel 4-beam bridges with spacings greater than 4 ft.

The average $\Delta\beta_f$ value obtained for all the simple span steel bridges with 4 beams and spacings greater than 4 ft for the functionality limit state is 0.53 for a 75-year return period. The same bridge configurations using prestressed concrete girders produce an average $\Delta\beta_f$ value of 0.0. Therefore, it is herein proposed to use a $\Delta\beta_f$ value of 0.25 as the redundancy criterion for the functionality limit state with a 75-year return period. This is average for all the prestressed concrete and steel bridges considered.

For the damaged limit state, the average difference $\Delta\beta_d$ between the damaged system's safety index and the member safety index of the intact system is -2.1 using a two-year return period on the live load. The four-beam bridges with spacing greater than 4 ft produce an average $\Delta\beta_d$ equal to -2.96. The prestressed concrete bridges produce an average $\Delta\beta_d$ = -2.40 for four beam bridges with spacings greater than 4 ft. Therefore, it is herein proposed to use a value of -2.70 using a two-year return period as the redundancy criterion for damaged bridges.

The redundancy criteria chosen herein will be used in the next paragraph to calibrate the proposed redundancy factors.

Calibration of Redundancy Factors

Redundancy factors are calibrated in this study such that bridges having configurations that do not provide sufficient levels of redundancy are penalized by requiring their individual members to provide higher levels of safety than those of bridges with sufficiently high levels of redundancy. On the other hand, bridges with high levels of redundancy are rewarded by allowing a lower level of member safety. This is performed by introducing redundancy factors in the design or safety-check equations. The proposed format includes a redundancy factor on the resistance side of the equation such that:

$$\phi_s \, \phi \, R = \gamma_d \, D + \gamma_l \, L \qquad \text{(C-6)}$$

where ϕ_s is the system redundancy factor, ϕ is the member resistance factor, R is the resistance capacity of the member, γ_d is the dead load factor, D is the dead load effect, γ_l is the live load factor, and L is the live load effect on an individual member (including dynamic impact). When ϕ_s is equal to 1.0 equation (C-6) becomes the same as the current design equation. If ϕ_s is greater than 1.0 this indicates that the system's configuration provides sufficient level of redundancy. When it is less than 1.0 then the level of redundancy is not sufficient.

The values obtained for $\Delta\beta_u$, $\Delta\beta_f$ and $\Delta\beta_d$ can be used to calibrate redundancy factors for the three system limit states of each bridge configuration analyzed in this study. As an example, the procedure is illustrated using the results of the reliability analysis performed in the previous section for the 150 ft steel I-beam bridge with 6 beams at 8 ft spacings. The results obtained for this particular bridge configuration show that the difference between the safety indices of the ultimate limit state and the member is 1.01. Because 1.01 is greater than the 0.85 target value set in the previous paragraph, this bridge provides a sufficient level of redundancy for the ultimate limit state. Therefore, the safety index of this bridge's members could be reduced by 0.16 while still satisfying the redundancy requirements. To lower the member safety index by 0.16 (from 2.43 to 2.27), it is sufficient to lower the LF1 factor from 3.26 down to a value of 3.12. The 3.12 was determined by trial and error using the reliability analysis program. It is herein suggested that a value of LF1 equal to 3.12 is sufficient to provide an adequate level of redundancy. Looking at Equation (C-2), it is noted that to reduce LF1 to a value of 3.12, assuming that D and DF_1 remain unchanged, the required moment capacity R should be reduced to 118700 kip-in. This value is 3% smaller than that required by the current LFD code. To achieve this 3% reduction, the system factor ϕ_s required in equation C-6 is equal to 1.03. Similar calculations are performed for all the cases studied herein. The results are shown in Table C-8 for the simple span bridges.

From the results it appears that the most optimum design for two-lane bridge as far as redundancy is concerned is 6 beams at 8 ft spacings. It is interesting to note that this configuration is currently the most widely used configuration for two-lane bridges. The results also show that, for a given number of beams, the ϕ_s factor increases as the beam spacing is increased from 1.2 m to 2.4 m (4 ft to 8 ft). However, the factor decreases as the beam spacing is increased beyond 2.4 m. This trend is explained by the fact that, for narrow bridges, all the beams are almost equally loaded and there is no reserve strength available. Hence, if one beam fails all the beams will quickly follow suit. However, as the beam spacing is increased, the load distribution is uneven and the least loaded members will pick up the load as the most heavily loaded member fails. As the spacing becomes very large, the capacity of the slab to transfer the load decreases and damage to the members under the applied load occur before a complete transfer to the other members is possible. This observation is evident because the nonlinear analysis performed herein considers the possibility of system damage before the formation of a plastic mechanism. Similar trends are observed for the ultimate limit state, the functionality limit state, or the damaged limit state. The trends are however the sharpest for the damaged limit state.

Table C-9 gives the results obtained for the sensitivity analysis. Table C-10 gives the results obtained for the continuous bridges.

C-7. Conclusions

This appendix gives a detailed description of the analysis and calibration of redundancy factors for steel I-beam bridges. The factors are calibrated using a reliability procedure such that bridges that do not have sufficient levels of redundancy are penalized by requiring their members to have higher levels of safety than comparable redundant designs. On the other hand, bridges with high levels of redundancy are rewarded by allowing their members to have lower safety factors than normally required by current design and evaluation methods.

References

C-1. West R., "C&CA/CIRIA Recommendations on the Use of Grillage Analysis for Slab and Pseudo-Slab Bridge Decks", London Cement & Concrete Association and Construction Industry Research and Information Association, 1973.

C-2. Jaegar, L.G. and Bakht, B., "The Grillage Analogy in Bridge Analysis", Canada Journal of Civil Engineering, Vol. 9, National Research Council of Canada, 1982.

C-3. Hambly, E.C., "Bridge Deck Behaviour", Chapman and Hall, Ltd., London, 1976.

C-4. Zokaie T., Osterkamp, T.A., and Imbsen R.A., "Distribution of Wheel Loads on Highway Bridges", Final Report, NCHRP project 12-26/1, March 1991.

C-5. Ghosn M. and Moses F., "Redundancy in Highway Bridge Superstructures" Report NCHRP 12-36, TRB, Washington DC, March 1994.

C-6. Schilling C.G., "A Unified Autostress Method", Project 51, Development of Design Specifications for Continuous Composite Plate-Girder Bridges, American Iron and Steel Institute, November 1989.

C-7. Haaijer, G. Carskaddan, P.S. and Grubb, M.A., "Autostress Design of Steel Bridges", Journal of Structural Engineering, ASCE, Vol. 109, No. 12, Jan. 1983.

C-8. Nowak, A.S., "Calibration of LRFD Bridge Design Code", NCHRP 12-33, May 1992.

C-9. Burdette E.G. and Goodpasture, D.W., "Full Scale Bridge Testing - An Evaluation of Bridge Design Criteria", University of Tennessee, December 1971.

C-10. KATHOL S., AZIZINAMINI, A. and, LUEDKE, J., "Strength Capacity of Steel Girder Bridges", NDOR Research Project No. RES1 (0099) P469, Nebraska Department of Roads, February 1995.

C-11. Razaqpur, A.G. and Nofal M., "Transverse Load Distribution at Ultimate Limit States in Single Span Slab-on-Girder Bridges with Compact Steel Girders", Ontario Ministry of Transportation, MISC-88-01, September 1988.

C-12. Ghosn M. and Moses F., "Bridge Load Modeling and Reliability Analysis", Case Western Reserve University, Cleveland, Ohio, 1984

C-13. Cornell, C. A., "Risk-Based Structural Design", Proceedings of a Symposium on Risk Analysis, Department of Civil Engineering, University of Michigan, Ann Arbor, MI, August 1994.

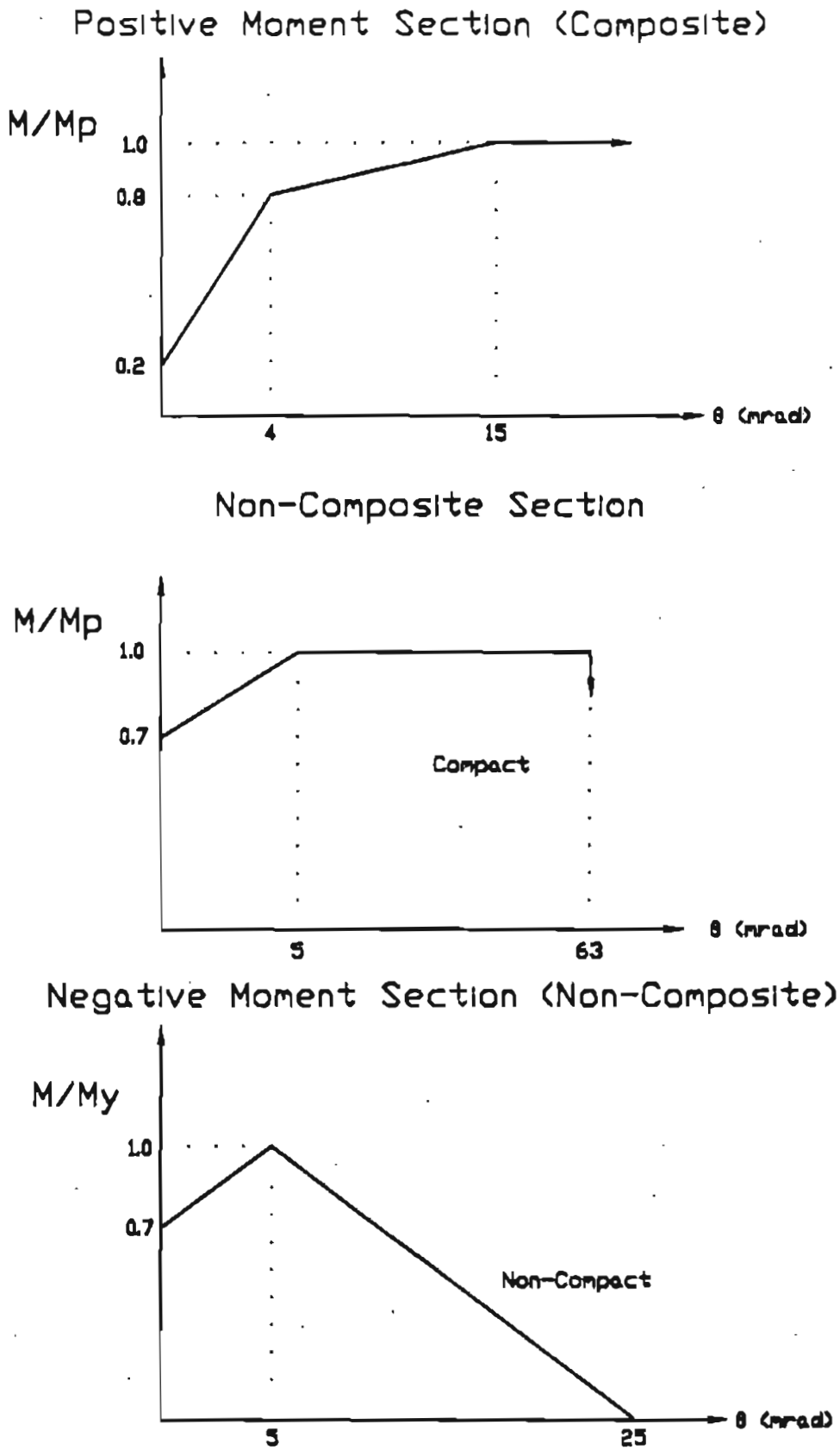

Figure C.1 Typical Moment versus Plastic Rotation Curves for Steel I-beams.

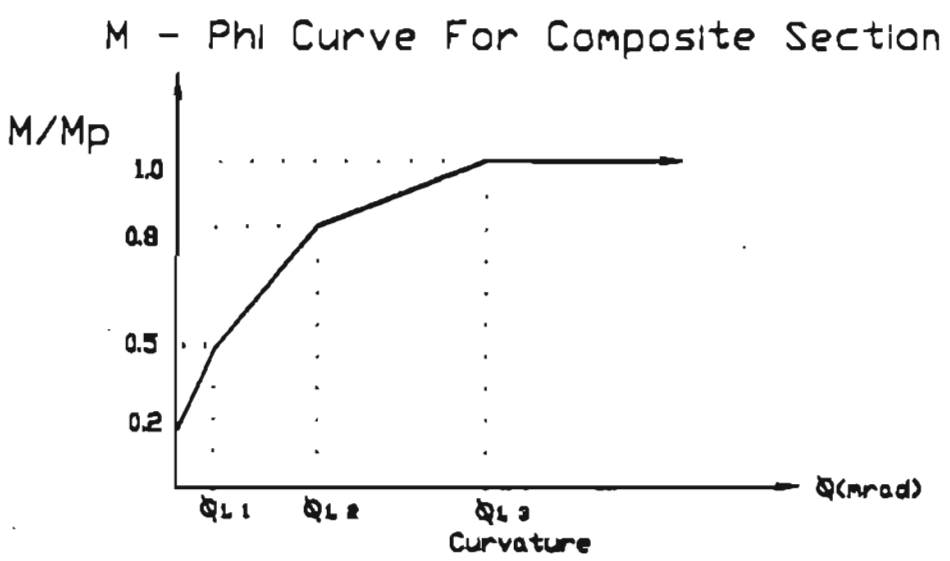

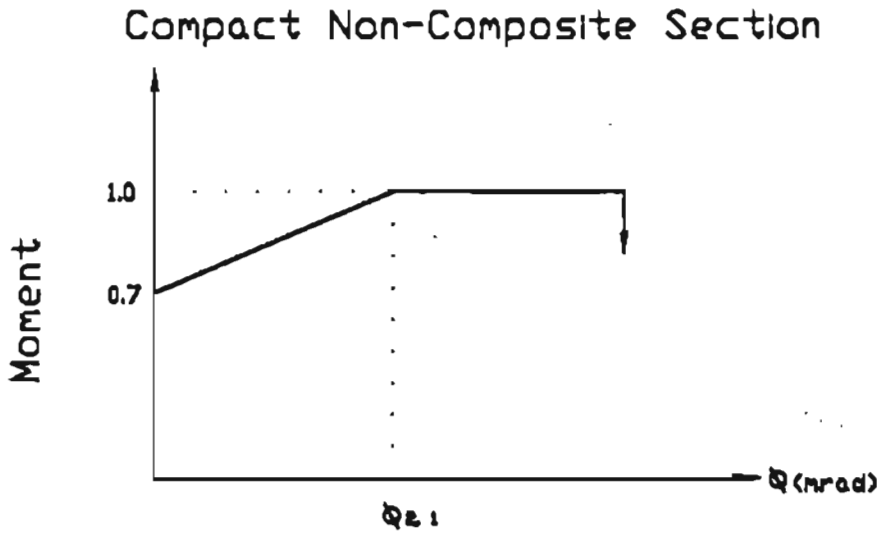

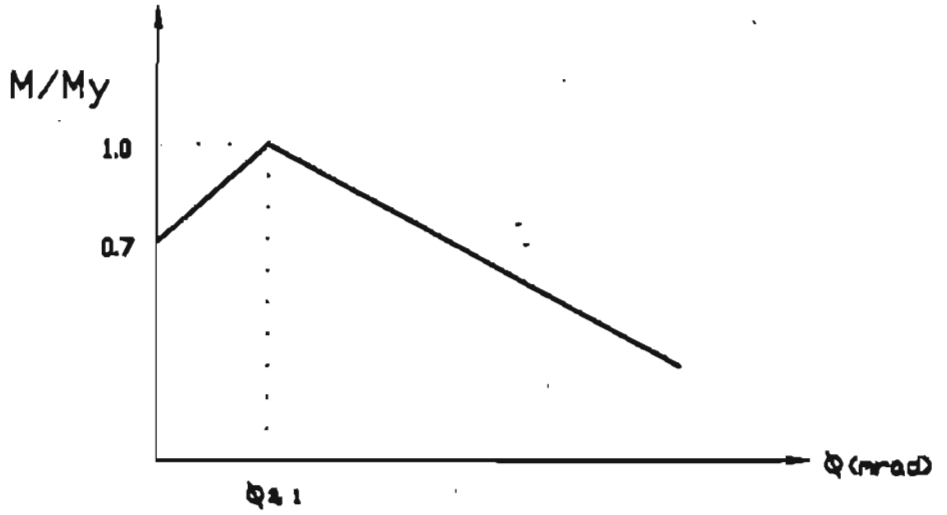

Figure C.2 Typical Moment versus Plastic Curvature Relationships for Steel I-beams.

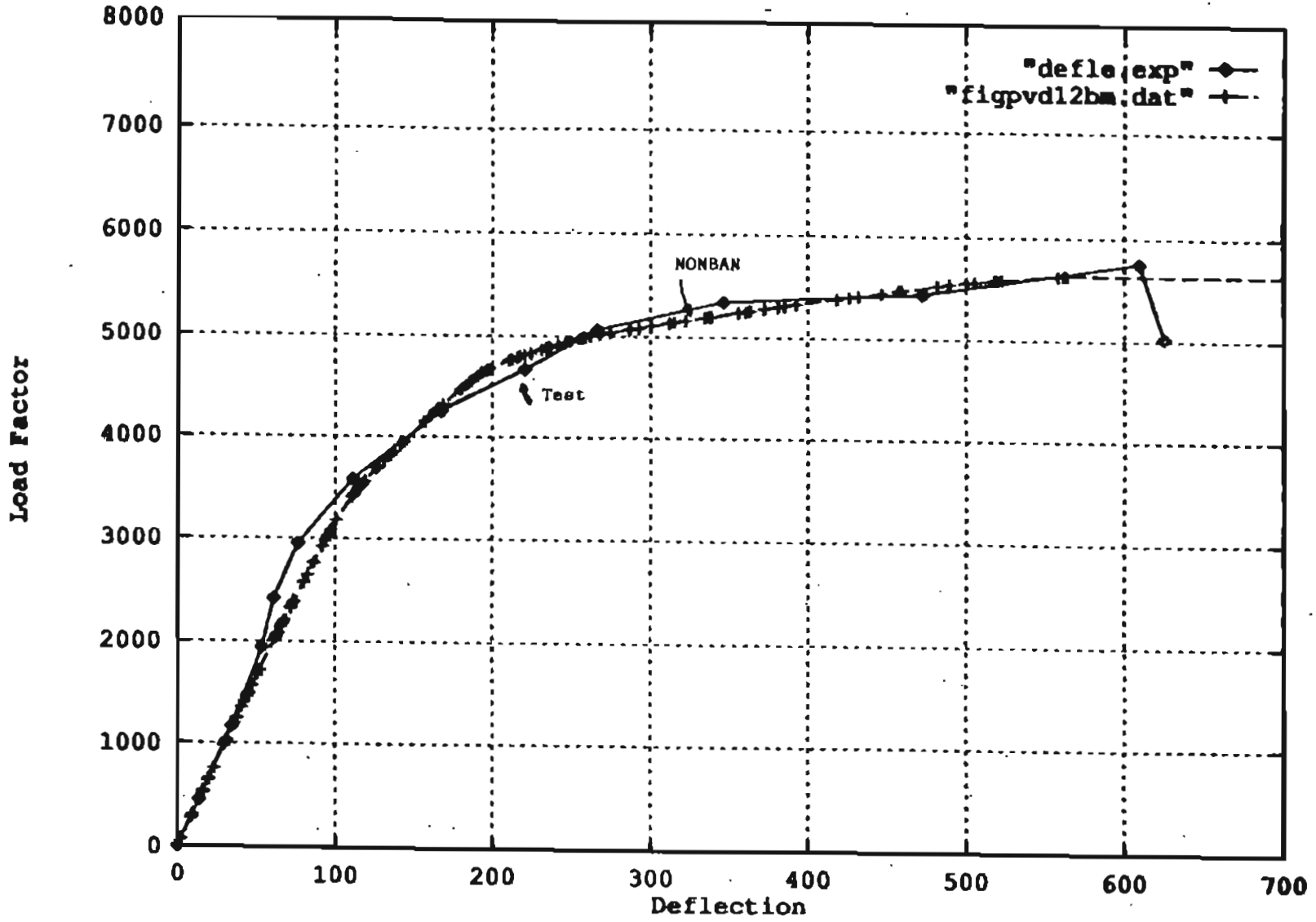

Figure C.3 Comparison of NONBAN Results to Experimental Results of Burdette and Goodpasture [C-9]

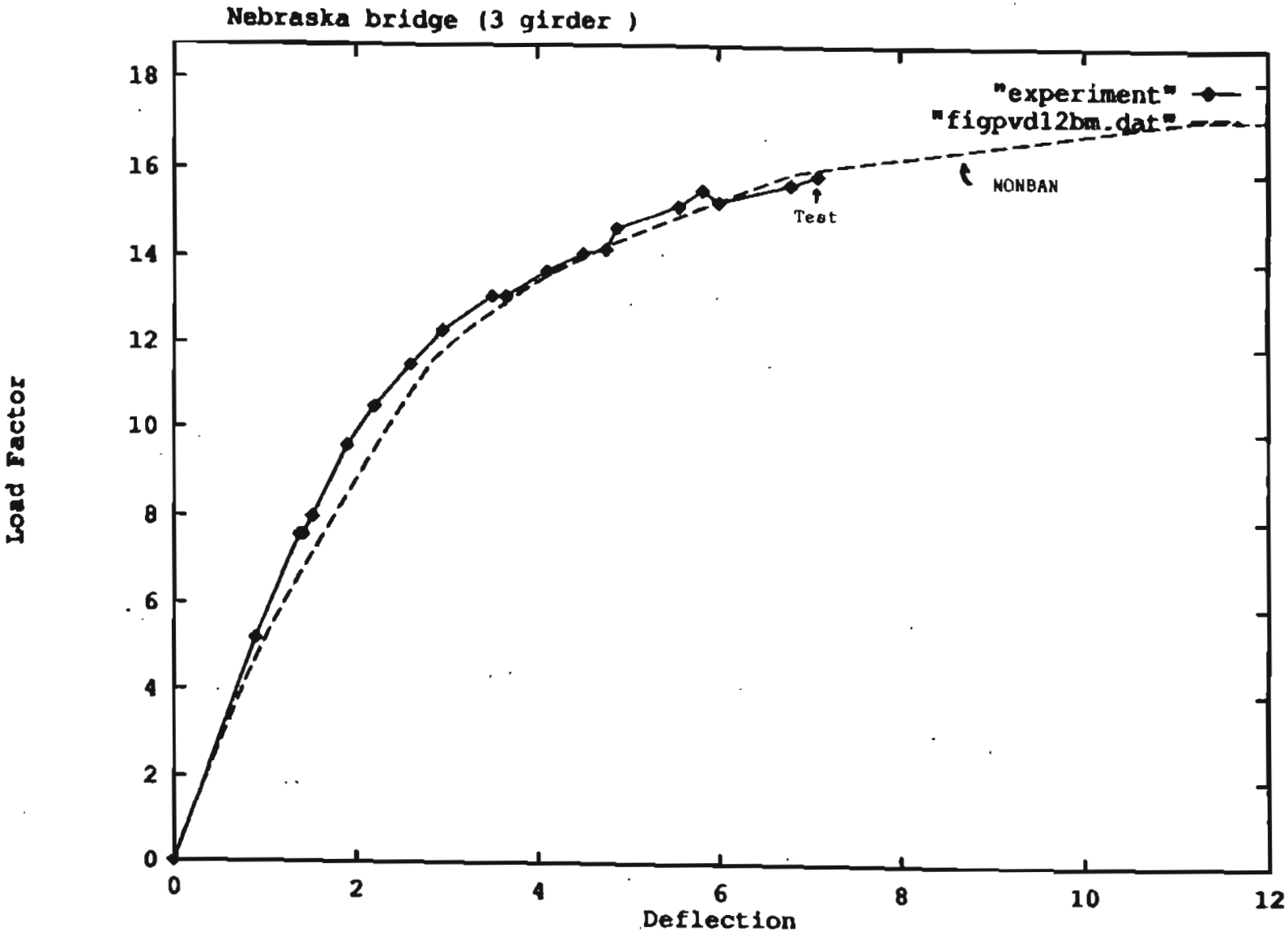

Figure C.4 Comparison of NONBAN Results to Experimental Results of Kathol et. al. [C-10]

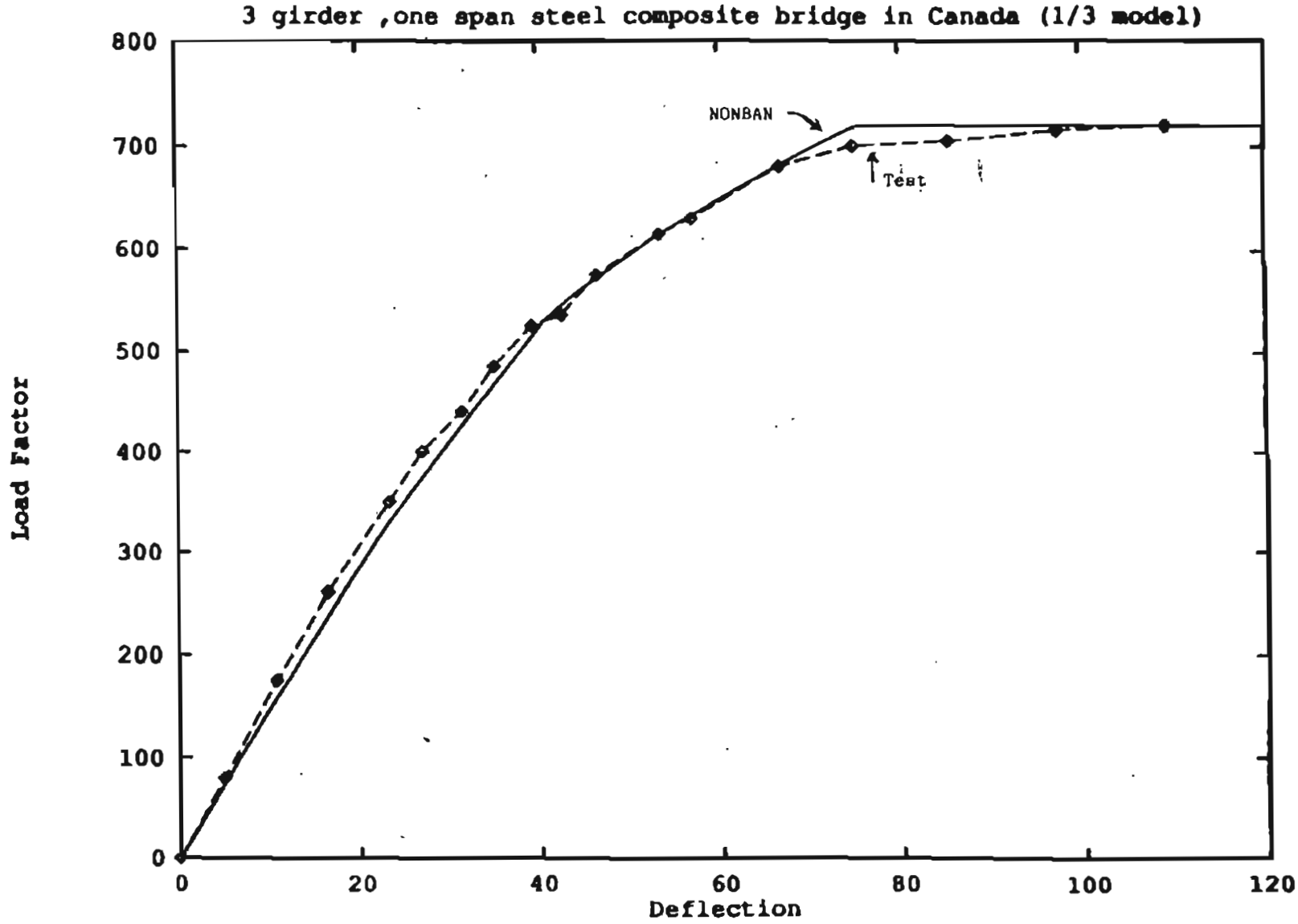

Figure C.5 Comparison of NONBAN Results to Experimental Results of Razaqpur and Nofal [C-11]

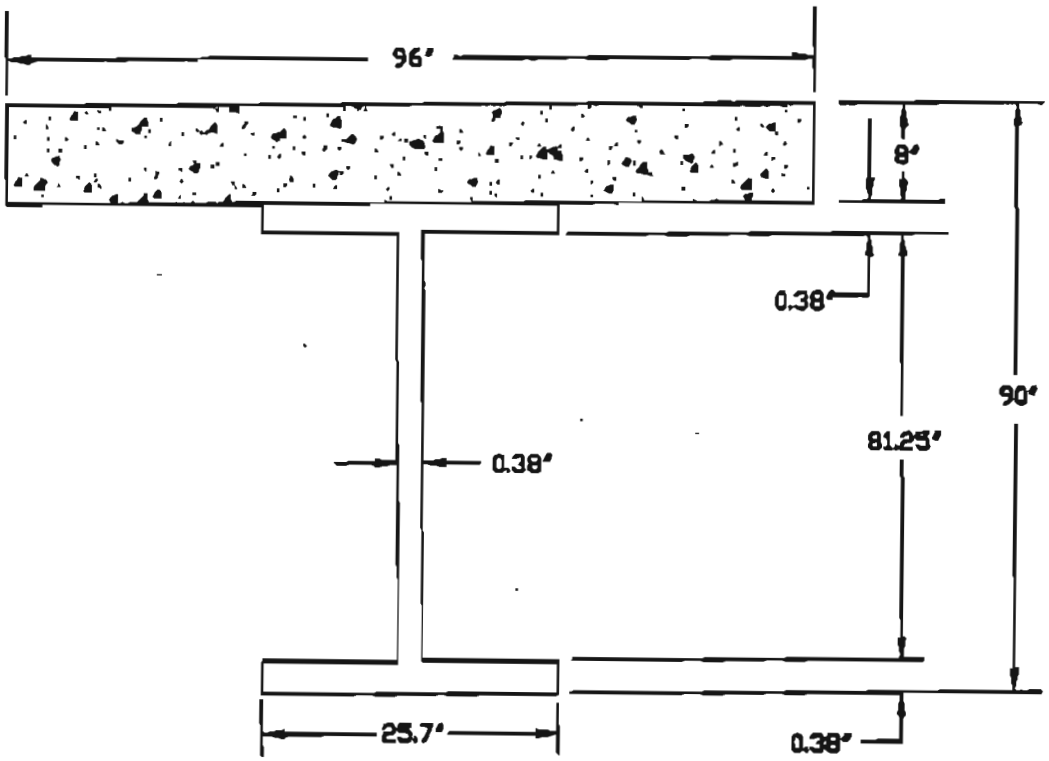

Figure C.6 Cross Section of Example 150 ft Simple Span Bridge with 6 beams at 8ft.

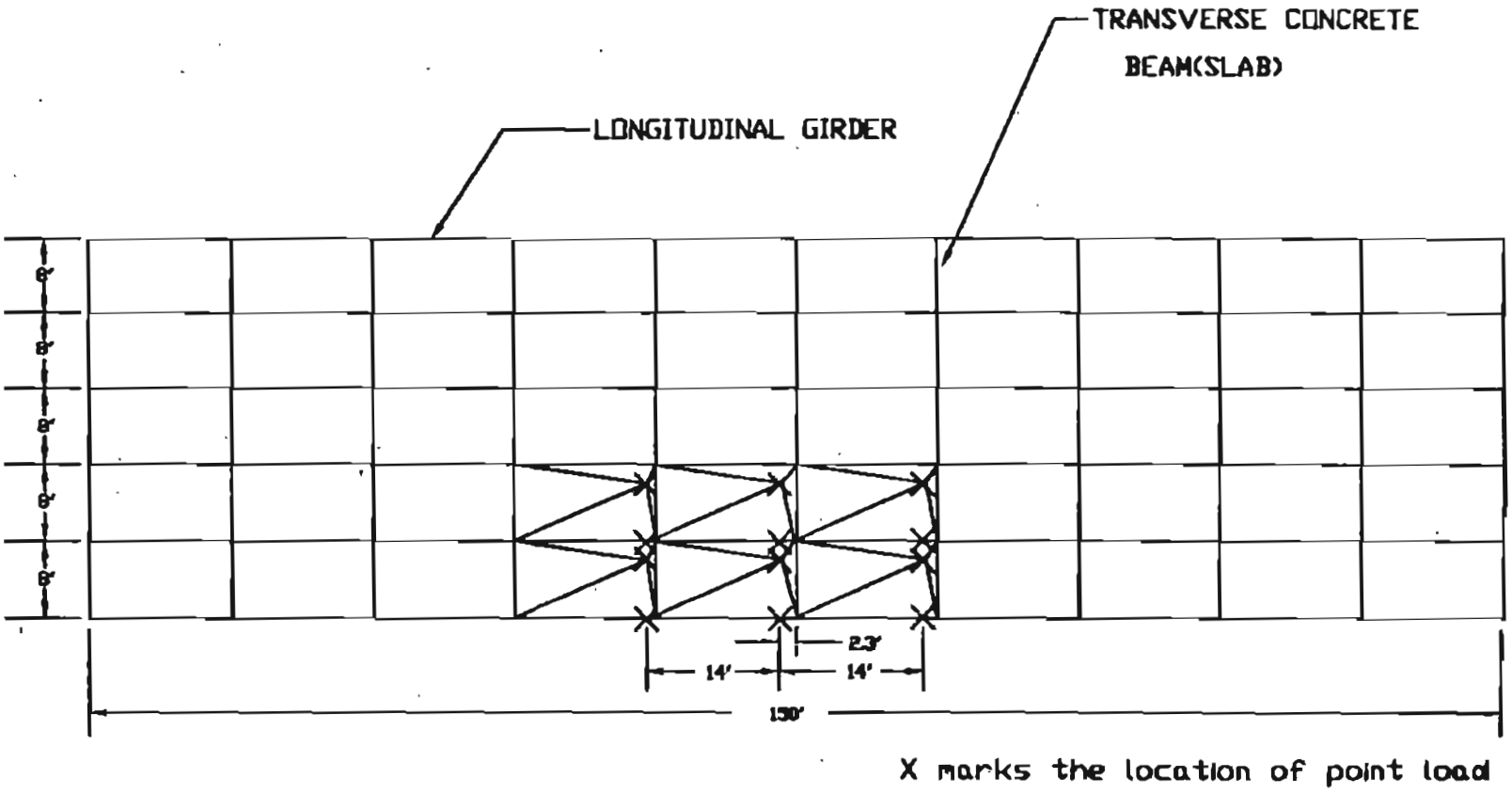

Figure C.7 Plan View of Mesh used in the Analysis of 150 ft Bridge.

Table C.1 Section Properties of Steel Bridges[1]

The bridge span is 45.0

Spac	Hf	Mu	section	d	A	Iz	Iy	Ir	S	phi	Mn
4.	7.5	9161.	compt	27.0	61.8	3318.	8662.	423.	169.	0.000762	9161.
			steel	18.5	16.8	876.	22.	1.	90.	1000.	3926.
6.	7.5	13733.	compt	27.0	92.7	4987.	29205.	635.	255.	0.000762	13733.
			steel	18.0	25.2	1326.	45.	3.	136.	1000.	5942.
8.	8.0	18415.	compt	32.4	123.7	8529.	73803.	1026.	344.	0.000924	18415.
			steel	23.0	27.7	2371.	75.	2.	194.	1000.	8356.
10.	8.5	23220.	compt	35.1	140.8	11610.	94056.	1308.	433.	0.000839	23220.
			steel	25.1	32.5	3266.	95.	3.	246.	1000.	10594.
12.	8.5	27812.	compt	37.8	145.2	14850.	94088.	1309.	516.	0.000739	27812.
			steel	27.9	36.9	4374.	126.	4.	299.	1000.	12997.

The bridge span is 60.0

Spac	Hf	Mu	section	d	A	Iz	Iy	Ir	S	phi	Mn
4.	7.5	14385.	compt	36.0	65.9	7116.	8692.	423.	268.	0.000613	14385.
			steel	27.8	20.9	2280.	52.	1.	160.	1000.	7023.
6.	7.5	21538.	compt	36.0	98.8	10842.	29266.	635.	408.	0.000614	21538.
			steel	27.3	31.3	3598.	106.	2.	253.	1000.	10894.
8.	8.0	28847.	compt	43.2	130.2	18195.	73869.	1026.	543.	0.000750	28847.
			steel	34.1	34.2	5924.	141.	2.	337.	1000.	14561.
10.	8.5	36395.	compt	46.8	148.4	24733.	94160.	1308.	682.	0.000681	36395.
			steel	37.2	40.0	8084.	199.	3.	422.	1000.	18358.
12.	8.5	43559.	compt	50.4	153.6	32106.	94236.	1308.	829.	0.000602	43559.
			steel	40.6	45.2	11198.	275.	3.	534.	1000.	23044.

---

[1] Spac. = Spacing between beams in feet.
Hf = Thickness of slab (in)
Mu = Required member capacity (kip-in)
compt = Composite section
steel = Naked steel section
d = Depth of section (in)
A = Area of Cross section (in^2)
Iz = Moment of inertia about horizontal axis (in^4)
Iy = Moment of inertia about vertical axis (in^4)
Ir = Polar moment of inertia (in^4)
S = Section elastic modulus (in^3)
phi = Curvature at crushing
Mn = Actual moment capacity (kip-in)

Table C.1 (ct'd) Section Properties of Steel Bridges

The bridge span is 80.0

Spac	Hf	Mu	section	d	A	Iz	Iy	Ir	S	phi	Mn
4.	7.5	22397.	compt	43.2	73.6	13601.	8759.	423.	438.	0.000507	2239
			steel	34.7	28.6	5230.	119.	1.	293.	1000.	1255
6.	7.5	33492.	compt	43.2	110.3	20273.	29378.	637.	652.	0.000507	3349
			steel	34.3	42.8	7744.	218.	4.	434.	1000.	1867
8.	8.0	45039.	compt	48.0	146.4	30798.	74033.	1029.	862.	0.000508	4503
			steel	38.6	50.4	11250.	305.	5.	562.	1000.	2436
10.	8.5	56757.	compt	52.8	166.3	43255.	94423.	1311.	1099.	0.000470	5675
			steel	42.8	57.9	16290.	462.	6.	735.	1000.	3155
12.	8.5	67764.	compt	57.6	172.8	56494.	94594.	1312.	1326.	0.000447	6776
			steel	47.6	64.4	22336.	632.	7.	910.	1000.	3895

The bridge span is 100.0

Spac	Hf	Mu	section	d	A	Iz	Iy	Ir	S	phi	Mn
4.	7.5	31659.	compt	54.0	78.0	24495.	8883.	423.	631.	0.000499	3165
			steel	45.6	33.0	10397.	243.	1.	447.	1000.	1903
6.	7.5	47205.	compt	54.0	116.7	35924.	29546.	636.	924.	0.000497	4720
			steel	45.4	49.2	14859.	386.	3.	639.	1000.	2763
8.	8.0	63429.	compt	60.0	154.1	55827.	74285.	1029.	1249.	0.000475	6342
			steel	50.6	58.1	22750.	557.	5.	875.	1000.	3734
10.	8.5	79887.	compt	66.0	175.0	76497.	94743.	1311.	1555.	0.000447	7988
			steel	56.3	66.6	30904.	782.	6.	1075.	1000.	4639
12.	8.5	95216.	compt	72.0	182.1	99301.	95016.	1311.	1867.	0.000445	9521
			steel	62.3	73.7	41789.	1055.	6.	1316.	1000.	5674

The bridge span is 120.0

Spac	Hf	Mu	section	d	A	Iz	Iy	Ir	S	phi	Mn
4.	7.5	42395.	compt	64.8	82.2	38321.	8930.	423.	826.	0.000492	4239
			steel	56.6	37.2	16719.	290.	1.	584.	1000.	2539
6.	7.5	62963.	compt	64.8	122.8	57664.	29700.	636.	1241.	0.000487	6296
			steel	56.2	55.3	25450.	540.	3.	888.	1000.	3833
8.	8.0	84299.	compt	72.0	161.2	89856.	74669.	1028.	1682.	0.000472	8429
			steel	62.8	65.2	39002.	941.	4.	1219.	1000.	5183
10.	8.5	106111.	compt	79.2	183.1	122459.	95250.	1310.	2083.	0.000444	10611
			steel	69.6	74.8	52423.	1289.	5.	1483.	1000.	6395
12.	8.5	126267.	compt	86.4	190.6	157927.	95649.	1311.	2487.	0.000437	12626
			steel	76.8	82.3	70002.	1688.	6.	1797.	1000.	7750

The bridge span is 150.0

Spac	Hf	Mu	section	d	A	Iz	Iy	Ir	S	phi	Mn
4.	7.5	61762.	compt	81.0	88.7	70567.	9297.	423.	1232.	0.000486	6175
			steel	72.8	43.7	33989.	657.	1.	925.	1000.	3948
6.	7.5	91326.	compt	81.0	132.1	104039.	30286.	636.	1811.	0.000480	9132
			steel	72.5	64.6	49584.	1126.	3.	1349.	1000.	5789
8.	8.0	121804.	compt	90.0	172.4	162631.	75667.	1028.	2462.	0.000461	12180
			steel	80.9	76.4	75990.	1939.	4.	1853.	1000.	7837
10.	8.5	153150.	compt	99.0	195.7	219983.	96016.	1310.	3028.	0.000433	15315
			steel	89.4	87.3	100832.	2055.	5.	2228.	1000.	9588
12.	8.5	181839.	compt	108.0	203.9	281519.	96555.	1311.	3588.	0.000427	18183
			steel	98.4	95.5	132832.	2594.	6.	2670.	1000.	11501

Table C.2 Section Properties of Continuous Steel Bridges[2]

The bridge span is 120

spac	Hf	Mu	section	d	A	Iz	Iy	Ir	S	Phi/Angl	Mn
4	7.5	29450	compt	64.8	69.8	27452	8715	422	554	0.000517	29450
		47328	pier	57.9	54.7	34917	5804	1	1206	0.0315	47328
			steel	57.3	24.8	10471	75	0	365	1000	16273
6	7.5	43829	compt	64.8	104.3	41740	29532	634	841	0.000522	43829
		64324	pier	57.9	74.8	47371	12011	2	1636	0.0315	64324
			steel	57.3	36.8	16409	372	1	573	1000	24994
8	8.0	58523	compt	72.0	139.6	64783	74332	1025	1142	0.000587	58523
		83673	pier	64.8	86.5	68991	12245	2	2131	0.0315	83673
			steel	64.0	43.6	25388	604	1	793	1000	34042
10	8.5	73450	compt	79.2	158.3	90523	94750	1307	1449	0.000546	73450
		102776	pier	71.6	96.1	93620	11495	3	2616	0.0315	102776
			steel	70.7	49.9	36292	789	2	1027	1000	43668
12	8.5	87446	compt	86.4	163.3	117285	95009	1307	1735	0.000495	87446
		120475	pier	78.8	102.8	120739	12964	3	3065	0.0315	120475
			steel	77.9	55.0	48570	1048	2	1247	1000	53019

The bridge span is 150

spac	Hf	Mu	section	d	A	Iz	Iy	Ir	S	Phi/Angl	Mn
4	7.5	41620	compt	81.0	73.4	46440	8679	422	754	0.000507	41620
		73463	pier	74.1	66.9	69351	12159	1	1871	0.0315	73463
			steel	73.5	28.4	17652	39	0	480	1000	22387
6	7.5	61705	compt	81.0	109.6	74724	29848	634	1211	0.000507	61705
		99037	pier	74.1	88.5	94280	22002	2	2544	0.0315	99037
			steel	73.5	42.1	31878	688	1	867	1000	37386
8	8.0	82132	compt	90.0	145.7	115727	74789	1025	1638	0.000515	82132
		126804	pier	82.8	101.1	134867	21173	2	3260	0.0315	126804
			steel	82.0	49.7	48865	1061	1	1192	1000	50598
10	8.5	102991	compt	99.0	165.2	153929	95098	1307	1980	0.000479	102991
		155669	pier	91.1	115.2	181209	43698	2	3977	0.0315	155669
			steel	90.5	56.8	61978	1137	2	1370	1000	60155
12	8.5	122356	compt	108.0	170.7	198087	95435	1307	2357	0.000447	122356
		182340	pier	100.1	123.4	232931	50232	3	4653	0.0315	182340
			steel	99.5	62.3	82079	1474	2	1650	1000	72493

[2] Notation similar to that used in Table C-1.
pier = Section at pier (negative bending properties).

Table C.3 Summary of Results for Simple Span Bridges.

span	No. of beams	spac.	LF300	LF200	LF100	LFU	LFD	LF1	mech.	LFU/LF1	LF100/LF1	LFD/LF1
(ft)		(ft)										
45	4	4	1.44	1.82	2.21	2.21	1.50	2.19	2.24	1.01	1.01	0.68
45	4	6	1.79	2.31	3.03	3.15	1.59	2.70	3.36	1.17	1.12	0.59
45	4	8	2.25	2.69	3.41	3.51	1.46	2.97	4.48	1.18	1.15	0.49
45	4	10	2.55	3.01	3.78	3.85	1.39	3.28	5.61	1.17	1.15	0.42
45	4	12	2.80	3.27	4.03	4.09	0.98	3.58	6.72	1.14	1.13	0.27
45	6	4	1.59	2.10	2.85	2.99	1.99	2.36	3.35	1.27	1.21	0.84
45	6	6	1.81	2.36	3.16	3.31	1.67	2.71	5.04	1.22	1.17	0.62
45	6	8	2.29	2.74	3.49	3.60	1.48	3.00	6.72	1.20	1.17	0.49
45	6	10	2.79	3.37	4.03	4.07	1.40	3.29	8.41	1.24	1.22	0.42
45	6	12	2.80	3.28	4.04	4.10	1.34	3.57	10.08	1.15	1.13	0.37
45	8	4	1.61	2.12	2.92	3.09	2.03	2.37	4.47	1.31	1.24	0.86
45	8	6	1.81	2.37	3.18	3.34	1.67	2.72	6.72	1.23	1.17	0.61
45	8	8	2.29	2.74	3.50	3.60	1.48	3.00	8.96	1.20	1.17	0.49
45	8	10	2.58	3.04	3.84	3.91	1.40	3.29	11.21	1.19	1.17	0.43
45	10	4	1.62	2.14	2.94	3.10	2.03	2.38	5.59	1.30	1.24	0.85
45	10	6	1.82	2.37	3.18	3.33	1.73	2.72	8.39	1.23	1.17	0.64
45	10	8	2.29	2.74	3.50	3.60	1.48	3.00	11.20	1.20	1.17	0.49
60	4	4	1.51	1.82	2.21	2.21	1.46	2.18	2.25	1.01	1.01	0.67
60	4	6	1.86	2.31	3.00	3.19	1.81	2.64	3.37	1.21	1.14	0.68
60	4	8	2.27	2.71	3.42	3.68	1.60	2.93	4.50	1.26	1.17	0.54
60	4	10	2.58	3.03	3.80	4.01	1.48	3.25	5.63	1.23	1.17	0.45
60	4	12	2.84	3.30	4.06	4.23	1.32	3.53	6.74	1.20	1.15	0.37
60	6	4	1.64	2.09	2.80	3.04	2.04	2.30	3.37	1.32	1.22	0.89
60	6	6	1.88	2.36	3.13	3.39	1.81	2.64	5.05	1.28	1.19	0.68
60	6	8	2.33	2.79	3.55	3.82	1.65	2.98	6.75	1.28	1.19	0.55
60	6	10	2.62	3.08	3.89	4.11	1.47	3.28	8.45	1.25	1.18	0.45
60	6	12	2.85	3.33	4.10	4.27	1.32	3.54	10.11	1.21	1.16	0.37
60	8	4	1.66	2.12	2.88	3.14	2.11	2.31	4.50	1.36	1.25	0.91
60	8	6	1.90	2.39	3.17	3.42	1.82	2.66	6.73	1.29	1.19	0.68
60	8	8	2.33	2.79	3.55	3.83	1.65	2.98	9.00	1.28	1.19	0.55
60	8	10	2.62	3.08	3.89	4.11	1.46	3.28	0.00	1.25	1.19	0.45
60	10	4	1.68	2.15	2.91	3.17	2.11	2.33	5.62	1.36	1.25	0.91
60	10	6	1.90	2.39	3.18	3.43	1.82	2.66	8.42	1.29	1.19	0.68
60	10	8	2.33	2.79	3.55	3.83	1.48	2.98	11.25	1.28	1.19	0.50

Table C.3 (ct'd 2/3) Summary of Results for Simple Span Bridges.

span	No. of	spac.		LF300	LF200	LF100	LFU	LFD	LF1	mech.		LFU/LF1	LF100/LF1	LFD/LF1
	beams													
(ft)		(ft)												
80	4	4		1.58	1.93	2.37	2.37	1.53	2.34	2.41		1.01	1.01	0.65
80	4	6		1.84	2.30	3.03	3.20	1.60	2.65	3.41		1.21	1.14	0.60
80	4	8		2.15	2.62	3.42	3.68	1.51	2.91	4.56		1.26	1.17	0.52
80	4	10		2.48	2.96	3.81	4.00	1.34	3.23	5.70		1.24	1.18	0.41
80	4	12		2.77	3.26	4.07	4.26	1.19	3.53	6.81		1.21	1.15	0.34
80	6	4		1.87	2.16	2.96	3.20	2.05	2.44	3.81		1.31	1.21	0.84
80	6	6		1.85	2.35	3.16	3.40	1.73	2.64	5.11		1.28	1.20	0.65
80	6	8		2.24	2.74	3.60	3.87	1.61	3.01	6.87		1.28	1.19	0.53
80	6	10		2.54	3.04	3.94	4.16	1.36	3.29	8.55		1.26	1.20	0.41
80	6	12		2.80	3.30	4.13	4.33	1.20	3.55	10.22		1.22	1.16	0.34
80	8	4		1.69	2.20	3.04	3.32	2.13	2.45	4.82		1.35	1.24	0.87
80	8	6		1.89	2.40	3.24	3.47	1.76	2.69	6.81		1.29	1.20	0.65
80	8	8		2.24	2.74	3.59	3.86	1.59	3.00	9.13		1.28	1.20	0.53
80	8	10		2.55	3.05	3.94	4.15	1.34	3.29	11.40		1.26	1.20	0.41
80	10	4		1.73	2.25	3.10	3.37	2.16	2.50	6.02		1.35	1.24	0.86
80	10	6		1.9	2.41	3.24	3.47	1.76	2.69	3.22		1.29	1.20	0.65
80	10	8		2.00	2.45	3.23	3.47	1.20	2.65	10.05		1.31	1.22	0.45
100	4	4		2.08	2.28	2.28	2.28	1.42	2.26	2.32		1.01	1.01	0.63
100	4	6		1.93	2.36	3.08	3.28	1.59	2.68	3.47		1.22	1.15	0.59
100	4	8		2.25	2.70	3.50	3.71	1.38	2.95	4.65		1.26	1.19	0.47
100	4	10		2.56	3.04	3.89	4.04	1.20	3.26	5.80		1.24	1.19	0.37
100	4	12		2.86	3.35	4.19	4.35	1.07	3.57	6.93		1.22	1.17	0.30
100	6	4		2.16	2.64	2.99	3.06	1.99	2.32	3.48		1.32	1.28	0.86
100	6	6		1.94	2.41	3.22	3.50	1.81	2.66	5.20		1.32	1.21	0.68
100	6	8		2.35	2.85	3.69	3.91	1.48	3.05	6.98		1.28	1.21	0.49
100	6	10		2.65	3.15	4.07	4.23	1.22	3.35	8.70		1.26	1.21	0.36
100	6	12		2.89	3.40	4.28	4.45	1.07	3.61	10.39		1.23	1.19	0.30
100	8	4		2.21	2.73	3.12	3.21	2.09	2.33	4.64		1.38	1.34	0.90
100	8	6		2.00	2.49	3.33	3.59	1.84	2.73	6.94		1.31	1.22	0.67
100	8	8		2.37	2.87	3.71	3.92	1.51	3.07	9.31		1.28	1.21	0.49
100	8	10		2.66	3.16	4.08	4.23	1.22	3.35	11.60		1.26	1.22	0.37
100	10	4		1.81	2.27	3.05	3.27	2.13	2.39	5.80		1.37	1.28	0.89
100	10	6		2.01	2.50	3.34	3.56	1.84	2.74	8.67		1.30	1.22	0.67
100	10	8		2.36	2.87	3.58	3.92	1.53	3.07	11.63		1.28	1.17	0.60

Table C.3 (ct'd 3/3) Summary of Results for Simple Span Bridges.

span	No. of beams	spac.	LF300	LF200	LF100	LFU	LFD	LF1	mech.	LFU/LF1	LF100/LF1	LFD/LF1
(ft)		(ft)										
120	4	4	1.88	1.97	2.38	2.38	1.42	2.33	2.40	1.01	1.01	0.61
120	4	6	2.01	2.43	3.16	3.38	1.56	2.73	3.55	1.24	1.16	0.57
120	4	8	2.32	2.78	3.56	3.83	1.33	2.98	4.75	1.28	1.19	0.45
120	4	10	2.62	3.11	3.95	4.15	1.18	3.29	5.90	1.26	1.20	0.36
120	4	12	2.91	3.43	4.30	4.46	1.07	3.59	7.05	1.24	1.20	0.30
120	6	4	1.79	2.22	2.96	3.26	1.99	2.39	3.60	1.37	1.24	0.83
120	6	6	2.02	2.49	3.31	3.61	1.75	2.71	5.33	1.33	1.22	0.65
120	6	8	2.44	2.96	3.79	4.07	1.48	3.1	7.13	1.31	1.22	0.48
120	6	10	2.74	3.27	4.18	4.39	1.27	3.4	8.86	1.29	1.23	0.37
120	6	12	2.99	3.54	4.45	4.63	1.11	3.66	10.57	1.27	1.22	0.30
120	8	4	1.81	2.27	3.06	3.38	2.10	2.39	4.80	1.41	1.28	0.88
120	8	6	2.10	2.60	3.43	3.71	1.80	2.79	7.11	1.33	1.23	0.64
120	8	8	2.47	3.00	3.83	4.10	1.49	3.13	9.51	1.31	1.22	0.47
120	8	10	2.75	3.28	4.19	4.39	1.27	3.41	11.81	1.29	1.23	0.37
120	10	4	1.88	2.36	3.14	3.45	2.13	2.47	6.00	1.40	1.27	0.86
120	10	6	2.12	2.62	3.44	3.72	1.81	2.81	8.88	1.32	1.22	0.64
120	10	8	2.47	3.00	3.83	4.10	1.47	3.13	11.88	1.31	1.22	0.47
150	4	4	1.82	2.13	2.51	2.51	1.45	2.48	2.50	1.01	1.01	0.59
150	4	6	2.15	2.80	3.34	3.65	1.61	2.88	3.70	1.27	1.16	0.56
150	4	8	2.45	2.95	3.74	4.14	1.47	3.12	4.90	1.33	1.20	0.47
150	4	10	2.75	3.29	4.14	4.46	1.23	3.43	6.09	1.30	1.21	0.36
150	4	12	3.07	3.64	4.52	4.80	1.06	3.77	7.25	1.27	1.20	0.28
150	6	4	1.93	2.37	3.13	3.55	2.16	2.52	3.74	1.41	1.25	0.86
150	6	6	2.16	2.67	3.51	3.90	1.88	2.85	5.54	1.37	1.23	0.66
150	6	8	2.61	3.18	4.03	4.42	1.79	3.26	7.35	1.35	1.23	0.55
150	6	10	2.93	3.53	4.45	4.78	1.39	3.59	9.13	1.33	1.24	0.39
150	6	12	3.18	3.79	4.74	5.00	1.21	3.85	10.88	1.30	1.23	0.31
150	8	4	1.96	2.44	3.25	3.69	2.27	2.52	4.99	1.46	1.29	0.90
150	8	6	2.28	2.81	3.68	4.03	1.95	2.97	7.39	1.36	1.24	0.66
150	8	8	2.66	3.24	4.09	4.46	1.78	3.31	9.80	1.35	1.24	0.54
150	8	10	2.94	3.55	4.47	4.79	1.38	3.59	12.17	1.33	1.24	0.38
150	10	4	2.06	2.56	3.36	3.76	2.29	2.62	6.24	1.44	1.29	0.87
150	10	6	2.31	2.85	3.70	4.05	1.95	3.00	9.24	1.35	1.23	0.65
150	10	8	2.66	3.25	4.09	4.47	1.73	3.31	12.26	1.35	1.24	0.52

Table C-4. Summary of Results of Continuous Birdges[3].

	span	120	ft	no. of beams	4		beam spacing =	4	ft							
	LFU	LF100			LFD	LF1+	LF1-	R+	D+	L+	R-	D-	L-	LFu/LF1	LF100/LF	LFd/LF1
compact																
Case1	3.018	2.811			1.875	2.409	7.268	29450	7128	9266	47330	14256	4551	1.25	1.17	0.78
case 2	5.71	5.092			3.032	3.52	3.457	29450	7128	6342	47330	14256	9588	1.65	1.47	0.88
case 3	3.41	3.41			2.334	3.358	3.422	29450	7128	6651	47330	14256	9665	1.02	1.02	0.70
noncompact																
case 1	3.02	2.81			1.40	2.41	7.27	29450	7128	9266	47330	14256	4551	1.25	1.17	0.58
case 2	3.45	x			1.42	3.52	3.46	29450	7128	6342	47330	14256	9568	1.00	X	0.41
case 3	3.10	x			1.15	3.36	3.42	29450	7128	6651	47330	14256	9665	0.92	X	0.34
	span	120	ft	no. of beams	4		beam spacing =	6	ft							
	LFU	LF100			LFD	LF1+	LF1-	R+	D+	L+	R-	D-	L-	LFu/LF1	LF100/LF	LFd/LF1
compact																
Case1	4.098	3.707			2.207	2.849	7.02	43829	10627	11653	64326	21254	6135	1.44	1.30	0.77
case 2	6.781	6.332			3.095	4.944	4.273	43829	10627	6716	64326	21254	10079	1.59	1.48	0.72
case 3	4.547	4.309			2.192	3.98	3.399	43829	10627	8343	64326	21254	12673	1.34	1.27	0.64
noncompact																
case 1	3.963	3.707			1.198	2.849	7.02	43829	10627	11653	64326	21254	6135	1.39	1.30	0.42
case 2	4.246	x			1.421	4.944	4.273	43829	10627	6716	64326	21254	10079	0.99	X	0.33
case 3	3.228	x			0.981	3.98	3.398	43829	10627	8343	64326	21254	12673	0.95	X	0.29

[3] LF1+ = LF1 for positive bending
LF1- = LF1 for negative bending
R+ = R for positive bending (kip-in)
R- = R for negative bending (kip-in)
D+ = Dead load for postive bending (kip-in)
D- = Dead load for negative bending (kip-in)
L+ = Maximum positive live load on one girder (kip-in)
L- = Maximum negative live load on one girder (kip-in)

Table C-4 (ct'd 2/9) Summary of Results of Continuous Birdges.

	span	120	ft	no. of beams		4		beam spacing =		8	ft					
	LFU	LF100			LFD	LF1+	LF1-	R+	D+	L+	R-	D-	L-	LFu/LF1	LF100/LF	LFd/LF1
compact																
Case1	4.678	4.212			2.04	3.097	7.331	58523	14515	14209	83675	29030	7454	1.51	1.36	0.66
case 2	7.873	7.355			3.251	5.846	4.894	58523	14515	7527	83675	29030	11165	1.61	1.50	0.66
case 3	5.036	4.739			2.117	4.367	3.579	58523	14515	10076	83675	29030	15268	1.41	1.32	0.59
noncompact																
case 1	4.294	4.212			1.02	3.097	7.331	58523	14515	14209	83675	29030	7454	1.39	1.36	0.33
case 2	4.859	x			1.441	5.846	4.894	58523	14515	7527	83675	29030	11165	0.99	X	0.29
case 3	3.428	x			0.876	4.367	3.579	58523	14515	10076	83675	29030	15268	0.96	X	0.24
	span	120	ft	no. of beams		4		beam spacing =		10	ft					
	LFU	LF100			LFD	LF1+	LF1-	R+	D+	L+	R-	D-	L-	LFu/LF1	LF100/LF	LFd/LF1
compact																
Case1	5.054	4.692			1.796	3.416	7.884	73450	18792	15998	102778	37584	8269	1.48	1.37	0.53
case 2	8.687	8.243			3.224	6.676	5.394	73450	18792	8188	102778	37584	12087	1.61	1.53	0.60
case 3	5.417	5.202			1.956	4.82	3.836	73450	18792	11341	102778	37584	16995	1.41	1.36	0.51
noncompact																
case 1	4.627	x			0.889	3.416	7.884	73450	18792	15998	102778	37584	8269	1.35	#VALUE!	0.26
case 2	5.354	x			1.394	6.676	5.394	73450	18792	8188	102778	37584	12087	0.99	X	0.26
case 3	3.67	x			0.808	4.82	3.836	73450	18792	11341	102778	37584	16995	0.96	X	0.21

Table C-4 (ct'd 3/9) Summary of Results of Continuous Birdges.

	span	120	ft	no. of beams		4		beam spacing =		12	ft					
	LFU	LF100			LFD	LF1+	LF1-	R+	D+	L+	R-	D-	L-	LFu/LF1	LF100/LF	LFd/LF1
compact																
Case1								87446	22291		120477	44582				
case 2	9.319	8.871			3.11	7.382	5.842	87446	22291	8826	120477	44582	12990	1.60	1.52	0.53
case 3	5.739	5.559			1.812	5.272	4.13	87446	22291	12359	120477	44582	18377	1.39	1.35	0.44
noncompact																
case 1								87446	22291		120477	44582				
case 2	5.783	x			1.363	7.382	5.842	87446	22291	8826	120477	44582	12990	0.99	X	0.23
case 3	3.937	x			0.759	5.272	4.13	87446	22291	12359	120477	44582	18377	0.95	X	0.18
	span	120	ft	no. of beams		6		beam spacing =		4	ft					
	LFU	LF100			LFD	LF1+	LF1-	R+	D+	L+	R-	D-	L-	LFu/LF1	LF100/LF	LFd/LF1
compact																
Case1	3.942	3.44			2.888	2.487	6.941	29450	7128	8974	47330	14256	4765	1.59	1.38	1.08
case 2	6.533	6.017			3.777	4.279	4.274	29450	7128	5216	47330	14256	7737	1.53	1.41	0.88
case 3	4.491	4.231			2.887	3.435	3.362	29450	7128	6499	47330	14256	9837	1.34	1.26	0.86
noncompact																
case 1	3.915	3.44			1.893	2.487	6.941	29450	7128	8974	47330	14256	4765	1.57	1.38	0.76
case 2	4.252	x			2.012	4.279	4.274	29450	7128	5216	47330	14256	7737	0.99	X	0.47
case 3	3.187	x			1.52	3.435	3.362	29450	7128	6499	47330	14256	9837	0.95	X	0.45

Table C-4 (ct'd 4/9) Summary of Results of Continuous Birdges.

	span	120	ft	no. of beams	6		beam spacing =	6	ft							
	LFU	LF100			LFD	LF1+	LF1-	R+	D+	L+	R-	D-	L-	LFu/LF1	LF100/LF	LFd/LF1
compact																
Case1	4.32	3.862			2.449	2.831		43829	10627	11730	64326	21254	6164	1.53	1.36	0.87
case 2	7.092	6.628			3.244	5.268	4.61	43829	10627	6279	64326	21254	9343	1.54	1.44	0.70
case 3	4.817	4.576			2.427	3.972	3.392	43829	10627	8359	64326	21254	12694	1.42	1.35	0.72
noncompact																
case 1	4.177	3.862			1.471	2.831		43829	10627	11730	64326	21254	6164	1.48	1.36	0.52
case 2	4.593	x			1.697	5.268	4.61	43829	10627	6279	64326	21254	9343	1.00	X	0.37
case 3	3.271	x			1.231	3.972	3.392	43829	10627	8359	64326	21254	12694	0.98	X	0.36
	span	120	ft	no. of beams	6		beam spacing =	8	ft							
	LFU	LF100			LFD	LF1+	LF1-	R+	D+	L+	R-	D-	L-	LFu/LF1	LF100/LF	LFd/LF1
compact																
Case1	4.898	4.443			2.191	3.212	7.614	58523	14515	13703	83675	29030	7177	1.52	1.38	0.68
case 2	8.065	7.482				6.058	5.08	58523	14515	7264	83675	29030	10756	1.59	1.47	0.00
case 3	5.286	5.004			2.254	4.499	3.691	58523	14515	9782	83675	29030	14803	1.43	1.36	0.61
noncompact																
case 1	4.533	4.443			1.201	3.212	7.614	58523	14515	13703	83675	29030	7177	1.41	1.38	0.37
case 2	5.052	x				6.058	5.08	58523	14515	7264	83675	29030	10756	0.99	X	0.00
case 3	3.551	x			1.07	4.499	3.691	58523	14515	9782	83675	29030	14803	0.98	X	0.29

Table C-4 (ct'd 5/9) Summary of Results of Continuous Birdges.

	span	120	ft	no. of beams	6		beam spacing =	10	ft							
	LFU	LF100			LFD	LF1+	LF1-	R+	D+	L+	R-	D-	L-	LFu/LF1	LF100/LF	LFd/LF1
compact																
Case1	5.268	4.902			1.931	3.521	8.056	73450	18792	15526	102778	37585	8093	1.50	1.39	0.55
case 2	8.774	8.332			3.319	6.766	5.465	73450	18792	8078	102778	37585	11930	1.61	1.52	0.61
case 3	5.639	5.415			2.026	4.906	3.904	73450	18792	11140	102778	37585	16700	1.44	1.39	0.52
noncompact																
case 1	4.622	x			0.993	3.521	8.056	73450	18792	15526	102778	37585	8093	1.37		0.28
case 2	5.444	x			1.567	6.766	5.465	73450	18792	8078	102778	37585	11930	1.00	X	0.29
case 3	3.754	x			0.932	4.906	3.904	73450	18792	11140	102778	37585	16700	0.96	X	0.24
	span	120	ft	no. of beams	6		beam spacing =	12	ft							
	LFU	LF100			LFD	LF1+	LF1-	R+	D+	L+	R-	D-	L-	LFu/LF1	LF100/LF	LFd/LF1
compact																
Case1	5.435	5.178			1.646	3.783	8.578	87446	22291	17223	120477	44582	8847	1.44	1.37	0.44
case 2	9.364	8.933			3.138	7.402	5.855	87446	22291	8802	120477	44582	12962	1.60	1.53	0.54
case 3	5.81	5.639			1.834	5.297	4.147	87446	22291	12299	120477	44582	18303	1.40	1.36	0.44
noncompact																
case 1	5.029	x			0.845	3.783	8.578	87446	22291	17223	120477	44582	8847	1.33		0.22
case 2	5.804	x			1.422	7.402	5.855	87446	22291	8802	120477	44582	12962	0.99	X	0.24
case 3	3.963	x			0.812	5.297	4.147	87446	22291	12299	120477	44582	18303	0.96	X	0.20

Table C-4 (ct'd 6/9) Summary of Results of Continuous Birdges.

	span	120	ft	no. of beams		8		beam spacing =		4	ft					
	LFU	LF100			LFD	LF1+	LF1-	R+	D+	L+	R-	D-	L-	LFu/LF1	LF100/LF	LFd/LF1
compact																
Case1	4.061	3.543			2.751	2.497	7.011	29450	7128	8939	47330	14256	4717	1.63	1.42	1.10
case 2	6.624	6.111			3.832	4.584	4.582	29450	7128	4869	47330	14256	7218	1.45	1.33	0.84
case 3	4.837	4.391			2.975	3.473	3.397	29450	7128	6427	47330	14256	9735	1.37	1.29	0.88
noncompact																
case 1	4.054	3.543			2.018	2.497	7.011	29450	7128	8939	47330	14256	4717	1.62	1.42	0.81
case 2	4.494	x			2.071	4.584	4.582	29450	7128	4869	47330	14256	7218	0.98	X	0.45
case 3	3.244	x			1.636	3.473	3.397	29450	7128	6427	47330	14256	9735	0.95	X	0.48
	span	120	ft	no. of beams		8		beam spacing =		6	ft					
	LFU	LF100			LFD	LF1+	LF1-	R+	D+	L+	R-	D-	L-	LFu/LF1	LF100/LF	LFd/LF1
compact																
Case1	4.382	3.966			2.466	2.912	7.146	43829	10627	11402	64326	21254	6027	1.50	1.36	0.85
case 2	7.114	6.646			3.249	5.369	4.68	43829	10627	6183	64326	21254	9204	1.52	1.42	0.69
case 3	4.87	4.641			2.442	4.045	3.455	43829	10627	8207	64326	21254	12466	1.41	1.34	0.71
noncompact																
case 1	4.232	3.966			1.486	2.912	7.146	43829	10627	11402	64326	21254	6027	1.45	1.36	0.51
case 2	4.649	x			1.711	5.369	4.68	43829	10627	6183	64326	21254	9204	0.99	X	0.37
case 3	3.345	x			1.259	4.045	3.455	43829	10627	8207	64326	21254	12466	0.97	X	0.36

Table C-4 (ct'd 7/9) Summary of Results of Continuous Birdges.

	span	120	ft	no. of beams	8		beam spacing =	8	ft							
	LFU	LF100			LFD	LF1+	LF1-	R+	D+	L+	R-	D-	L-	LFu/LF1	LF100/LF	LFd/LF1
compact																
Case1	4.925	4.477			2.194	3.239	7.627	58523	14515	13586	83675	29030	7165	1.52	1.38	0.68
case 2	8.042	7.536			3.4	6.066	5.085	58523	14515	7255	83675	29030	10747	1.58	1.48	0.67
case 3	5.302	5.017			2.257	4.509	3.697	58523	14515	9760	83675	29030	14781	1.43	1.36	0.61
noncompact																
case 1	4.549	4.477			1.204	3.239	7.627	58523	14515	13586	83675	29030	7165	1.40	1.38	0.37
case 2	5.065	x			1.67	6.066	5.085	58523	14515	7255	83675	29030	10747	1.00	X	0.33
case 3	3.57	x			1.081	4.509	3.697	58523	14515	9760	83675	29030	14781	0.97	X	0.29
	span	120	ft	no. of beams	8		beam spacing =	10	ft							
	LFU	LF100			LFD	LF1+	LF1-	R+	D+	L+	R-	D-	L-	LFu/LF1	LF100/LF	LFd/LF1
compact																
Case1	5.274	4.912			1.898	3.524	8.053	73450	18792	15508	102778	37584	8096	1.50	1.39	0.54
case 2	8.771	8.332			3.32	6.767	5.465	73450	18792	8077	102778	37584	11930	1.60	1.52	0.61
case 3	5.843	5.419			2.027	4.906	3.903	73450	18792	11141	102778	37584	16704	1.45	1.39	0.52
noncompact																
case 1	4.829	x			0.993	3.524	8.053	73450	18792	15508	102778	37584	8096	1.37		0.28
case 2	5.444	x			1.564	6.767	5.465	73450	18792	8077	102778	37584	11930	1.00	X	0.29
case 3	3.755	x			0.929	4.906	3.903	73450	18792	11141	102778	37584	16704	0.96	X	0.24

Table C-4 (ct'd 8/9) Summary of Results of Continuous Birdges.

	span	120	ft	no. of beams	10		beam spacing =	4	ft							
	LFU	LF100			LFD	LF1+	LF1-	R+	D+	L+	R-	D-	L-	LFu/LF1	LF100/LF	LFd/LF1
compact																
Case1	4.102	3.613			2.782	2.567	7.198	29450	7128	8697	47330	14256	4595	1.60	1.41	1.08
case 2	6.637	6.112			3.853	4.627	4.668	29450	7128	4824	47330	14256	7086	1.43	1.32	0.83
case 3	4.667	4.421			2.998	3.533	3.467	29450	7128	6318	47330	14256	9540	1.35	1.28	0.86
noncompact																
case 1	4.089	3.613			2.039	2.567	7.198	29450	7128	8697	47330	14256	4595	1.59	1.41	0.79
case 2	4.516	x			2.109	4.627	4.668	29450	7128	4824	47330	14256	7086	0.98	X	0.48
case 3	3.333	x			1.69	3.533	3.467	29450	7128	6318	47330	14256	9540	0.96	X	0.49
	span	120	ft	no. of beams	10		beam spacing =	6	ft							
	LFU	LF100			LFD	LF1+	LF1-	R+	D+	L+	R-	D-	L-	LFu/LF1	LF100/LF	LFd/LF1
compact																
Case1	4.396	3.978			2.477	2.93	7.152	43829	10627	11330	64326	21254	6022	1.50	1.36	0.85
case 2	7.111	6.644			3.256	5.373	4.682	43829	10627	6179	64326	21254	9200	1.52	1.42	0.70
case 3	4.671	4.64			2.447	4.051	3.457	43829	10627	8197	64326	21254	12458	1.41	1.34	0.71
noncompact																
case 1	4.242	3.978			1.496	2.93	7.152	43829	10627	11330	64326	21254	6022	1.45	1.36	0.51
case 2	4.648	x			1.724	5.373	4.682	43829	10627	6179	64326	21254	9200	0.99	X	0.37
case 3	3.348	x			1.262	4.051	3.457	43829	10627	8197	64326	21254	12458	0.97	X	0.37

Table C-4 (ct'd 9/9) Summary of Results of Continuous Birdges.

	span	120	ft	no. of beams	10		beam spacing =		8	ft						
	LFU	LF100			LFD	LF1+	LF1-	R+	D+	L+	R-	D-	L-	LFu/LF1	LF100/LF	LFd/LF1
compact																
Case1	4.917	4.475			2.195	3.24	7.626	58523	14515	13584	83675	29030	7165	1.52	1.38	0.68
case 2	8.043	7.537			3.399	6.067	5.085	58523	14515	7254	83675	29030	10748	1.58	1.48	0.67
case 3	5.3	5.015			2.257	4.509	3.697	58523	14515	9761	83675	29030	14782	1.43	1.36	0.61
noncompact																
case 1	4.543	4.475			1.204	3.24	7.626	58523	14515	13584	83675	29030	7165	1.40	1.38	0.37
case 2	5.066	x			1.67	6.067	5.085	58523	14515	7254	83675	29030	10748	1.00	X	0.33
case 3	3.562	x			1.08	4.509	3.697	58523	14515	9761	83675	29030	14782	0.96	X	0.29

Table C-5 Results of Sensitivity Analysis of Simple Span Bridges.

case #	comment	LFu	LF100	LF200	LF300	LFd	LF1	R	D	L	LFu/LF1	LF100/LF1	LFd/LF1
								kip-in	kip-in	kip-in			
case 0	Base case	4.43	4.03	3.18	2.61	1.79	3.26	121804	49005	22319	1.36	1.24	0.55
case 1	Fully composite	4.42	4.03	3.22	2.65	1.79	3.26	121804	49005	22035	1.35	1.24	0.55
case 2	Long. tors. const.	4.59	4.17	2.30	2.71	1.91	3.30	121804	49005	22060	1.39	1.26	0.58
case 3	Trans. tors. const.	4.69	4.16	3.29	2.70	2.11	3.30	121804	49005	22401	1.42	1.26	0.64
case 4	Long. mom. inert.	4.41	3.56	3.56	3.04	1.76	3.25	121804	49005	22442	1.36	1.09	0.54
case 5	Trans. mom. inert.	4.43	4.07	3.24	2.66	1.77	3.24	121804	49005	22319	1.36	1.25	0.55
case 6	Long. mom. curve	10.23	8.90	5.69	3.94	4.10	8.72	243608	49005	22319	1.17	1.02	0.47
case 7	Trans. mom. curve	4.51	4.08	3.23	2.65	2.02	3.26	121804	49005	22319	1.38	1.25	0.62
case 8	Trans. mom. curve	4.22	3.90	3.19	2.65	1.35	3.26	121804	49005	22319	1.29	1.20	0.41
case 9	Dead load	1.71	1.51	1.20	0.85	0.00	1.07	121804	98010	22319	1.60	1.42	0.00
case 10	Max. hinge	4.86	4.03	3.22	2.65	2.31	3.26	121804	49005	22319	1.49	1.24	0.71
case 11	skew	4.49	4.08	3.25	2.67	1.69	3.30	121804	49005	22074	1.36	1.24	0.51
case 12	mesh	4.41	4.19	3.28	2.68		3.26	121804	49005	21890	1.35	1.29	
case 13	diaphragm at ends	4.42	4.04	3.22	2.65	1.82	3.26	121804	49005	22313	1.36	1.24	0.56
case 14	diaphragm at 3 poi	4.50	4.12	3.27	2.68	2.05	3.30	121804	49005	22061	1.36	1.25	0.62

Table C-6 Results of Sensitivity Analysis of Continuous Bridges

	LFU	LF100	LF200	LF300	LFD	LF1+	LF1-	R+	D+	L+	R-	D-	L-	LFu/LF1	LF100/LF1	LFd/LF1
sens0																
simple	4.43	4.03	3.18	2.61	1.79	3.76		121804	49005	22061				1.36	1.24	0.55
sens1																
base case continuous																
compact																
Case1	5.29	4.71	3.63	2.91	2.31	3.32	8.92	82132	23085	17788	126806	46170	9037	1.59	1.42	0.70
case 2	8.95	8.27	7.45	6.43	3.54	6.38	6.01	82132	23085	9255	126806	46170	13425	1.49	1.38	0.59
case 3	5.80	5.49	4.93	4.31	2.35	4.68	4.25	82132	23085	12628	126806	46170	18965	1.36	1.29	0.55
noncompact																
case 1	4.92	4.71	3.63	2.91	1.23	3.32	8.92	82132	23085	17788	126806	46170	9037	1.48	1.42	0.37
case 2	5.85	x	x	x	1.69	6.38	6.01	82132	23085	9255	126806	46170	13425	0.97	X	0.28
case 3	4.01	x	x	x	1.11	4.68	4.25	82132	23085	12628	126806	46170	18965	0.94	X	0.26
sens2																
ductility +																
compact																
case 1	5.87	4.71	3.63	2.91	2.31	3.32	8.92	82132	23085	17788	126806	46170	9037	1.77	1.42	0.70
case 2	8.99	8.27	7.45	6.43	3.54	6.38	6.01	82132	23085	9255	126806	46170	13425	1.50	1.38	0.59
case 3	5.83	5.49	4.93	4.31	2.35	4.68	4.25	82132	23085	12628	126806	46170	18965	1.37	1.29	0.55
noncompact																
case 1	4.92	4.71	3.63	2.91	1.23	3.32	8.92	82132	23085	17788	126806	46170	9037	1.48	1.42	0.37
case 2	5.85	x	x	x	1.69	6.38	6.01	82132	23085	9255	126806	46170	13425	0.97	X	0.28
case 3	4.01	x	x	x	1.11	4.68	4.25	82132	23085	12628	126806	46170	18965	0.94	X	0.26
sens3																
ductility -																
compact																
case 1	5.29	4.71	3.63	2.91	2.35	3.32	8.92	82132	23085	17788	126806	46170	9037	1.59	1.42	0.71
case 2	8.95	8.27	7.45	6.43	4.62	6.38	6.01	82132	23085	9255	126806	46170	13425	1.49	1.38	0.77
case 3	5.80	5.49	4.93	4.31	2.99	4.68	4.25	82132	23085	12628	126806	46170	18965	1.36	1.29	0.70

Table C-6 (ct'd 2/2) Results of Sensitivity Analysis of Continuous Bridges

	LFU	LF100	LF200	LF300	LFD	LF1+	LF1-	R+	D+	L+	R-	D-	L-	LFu/LF1	LF100/LF1	LFd/LF1
sens4																
moment +																
compact																
case 1	9.59	8.68	5.76	4.00	3.80	7.94	8.92	164264	23085	17788	126806	46170	9037	1.21	1.09	0.48
case 2	13.80	12.90	9.98	8.07	5.57	15.25	6.01	164264	23085	9255	126806	46170	13425	2.30	2.15	0.93
case 3	9.47	8.99	6.88	5.49	3.72	11.18	4.25	164264	23085	12628	126806	46170	18965	2.23	2.12	0.88
noncompact																
case 1	8.05	x		5.76	4.00	1.93	7.94	8.92	164264	23085	17788	126806	46170	9037	1.01	X	0.24
case 2	6.35	x		x	x	2.12	15.25	6.01	164264	23085	9255	126806	46170	13425	1.06	X	0.35
case 3	4.40	x		x	x	1.37	11.18	4.25	164264	23085	12628	126806	46170	18965	1.04	X	0.32
sens5																
moment -																
compact																
case 1	5.59	4.79	3.64	2.91	2.95	3.32	22.95	82132	23085	17788	253608	46170	9037	1.68	1.44	0.89
case 2	12.47	11.37	8.85	7.14	6.24	6.38	15.45	82132	23085	9255	253608	46170	13425	1.95	1.78	0.98
case 3	8.49	7.71	6.10	4.78	4.12	4.68	10.94	82132	23085	12628	253608	46170	18965	1.82	1.65	0.88
noncompact																
case 1	5.59	4.79	3.64	2.91	2.95	3.32	22.95	82132	23085	17788	253608	46170	9037	1.68	1.44	0.89
case 2	11.49	11.37	8.85	7.14	4.87	6.38	15.45	82132	23085	9255	253608	46170	13425	1.80	1.78	0.76
case 3	7.98	7.71	6.10	4.78	3.24	4.68	10.94	82132	23085	12628	253608	46170	18965	1.71	1.65	0.69

Table C-7 Safety Indices for Simple Span Bridges.

			SAFETY INDICES						
SPAN	BEAMS	SPAC.	MEMBER	ULTIMATE	DELTA beta	LF100	DELTA beta	DAMAGED	DELTA beta
45	4	4	1.80	1.84	0.03	1.84	0.03	0.59	-1.22
45	4	6	2.58	3.13	0.55	2.99	0.41	0.84	-1.74
45	4	8	2.91	3.49	0.58	3.39	0.48	0.46	-2.45
45	4	10	3.26	3.82	0.56	3.75	0.49	0.25	-3.01
45	4	12	3.56	4.02	0.46	3.97	0.41	-1.44	-5.00
45	6	4	2.08	2.93	0.85	2.76	0.68	1.73	-0.35
45	6	6	2.59	3.30	0.71	3.13	0.54	1.04	-1.55
45	6	8	2.94	3.58	0.64	3.47	0.53	0.52	-2.42
45	6	10	3.27	4.01	0.74	3.98	0.70	0.29	-2.99
45	6	12	3.55	4.03	0.48	3.98	0.43	0.08	-3.47
45	8	4	2.09	3.05	0.96	2.85	0.76	1.81	-0.28
45	8	6	2.60	3.33	0.73	3.16	0.55	1.04	-1.56
45	8	8	2.94	3.58	0.64	3.48	0.54	0.52	-2.42
45	8	10	3.27	3.87	0.60	3.81	0.54	0.29	-2.99
45	10	4	2.11	3.06	0.95	2.88	0.76	1.81	-0.30
45	10	6	2.60	3.32	0.71	3.15	0.55	1.18	-1.42
45	10	8	2.94	3.58	0.64	3.48	0.54	0.52	-2.42
60	4	4	1.66	1.71	0.05	1.71	0.05	0.32	-1.34
60	4	6	2.36	3.03	0.67	2.82	0.46	1.21	-1.15
60	4	8	2.73	3.53	0.79	3.27	0.54	0.71	-2.03
60	4	10	3.10	3.82	0.72	3.64	0.54	0.32	-2.78
60	4	12	3.38	4.00	0.62	3.86	0.48	-0.13	-3.52
60	6	4	1.85	2.86	1.01	2.57	0.72	1.68	-0.17
60	6	6	2.36	3.24	0.88	2.97	0.60	1.22	-1.15
60	6	8	2.80	3.66	0.86	3.41	0.61	0.84	-1.96
60	6	10	3.12	3.90	0.78	3.71	0.59	0.34	-2.78
60	6	12	3.39	4.03	0.65	3.89	0.51	-0.14	-3.53
60	8	4	1.87	2.97	1.11	2.67	0.80	1.81	-0.06
60	8	6	2.39	3.28	0.88	3.01	0.62	1.24	-1.15
60	8	8	2.80	3.67	0.87	3.41	0.61	0.84	-1.96
60	8	10	3.12	3.90	0.78	3.71	0.59	0.31	-2.81
60	10	4	1.91	3.02	1.11	2.71	0.81	1.82	-0.09
60	10	6	2.39	3.29	0.90	3.02	0.63	1.24	-1.15
60	10	8	2.80	3.67	0.87	3.41	0.61	0.38	-2.42

Table C-7 (ct'd 2/3) Safety Indices for Simple Span Bridges.

			SAFETY INDICES						
SPAN	BEAMS	SPAC.	MEMBER	ULTIMATE	DELTA beta	LF100	DELTA beta	DAMAGED	DELTA beta
80	4	4	1.72	1.77	0.05	1.77	0.05	0.31	-1.41
80	4	6	2.18	2.85	0.67	2.66	0.48	0.50	-1.68
80	4	8	2.51	3.32	0.81	3.07	0.56	0.26	-2.26
80	4	10	2.86	3.59	0.73	3.43	0.57	-0.28	-3.14
80	4	12	3.17	3.81	0.64	3.65	0.48	-0.82	-3.99
80	6	4	1.88	2.85	0.97	2.56	0.69	1.50	-0.38
80	6	6	2.17	3.06	0.89	2.80	0.64	0.83	-1.34
80	6	8	2.63	3.50	0.87	3.25	0.62	0.53	-2.10
80	6	10	2.93	3.73	0.80	3.54	0.62	-0.21	-3.14
80	6	12	3.19	3.86	0.67	3.70	0.51	-0.79	-3.97
80	8	4	1.89	2.97	1.08	2.67	0.78	1.64	-0.25
80	8	6	2.23	3.12	0.89	2.88	0.66	0.89	-1.33
80	8	8	2.62	3.49	0.87	3.24	0.62	0.48	-2.14
80	8	10	2.93	3.72	0.79	3.54	0.62	-0.28	-3.20
80	10	4	1.96	3.02	1.06	2.73	0.77	1.69	-0.27
80	10	6	2.23	3.12	0.89	2.89	0.66	0.90	-1.33
80	10	8	2.11	3.03	0.92	2.79	0.68	-0.71	-2.82
100	4	4	1.38	1.41	0.03	1.41	0.03	-0.20	-1.58
100	4	6	2.02	2.73	0.71	2.51	0.49	0.29	-1.73
100	4	8	2.36	3.15	0.79	2.95	0.59	-0.32	-2.68
100	4	10	2.71	3.43	0.73	3.31	0.60	-0.94	-3.64
100	4	12	3.02	3.68	0.66	3.56	0.54	-1.47	-4.49
100	6	4	1.49	2.49	1.00	2.41	0.92	1.21	-0.28
100	6	6	2.00	2.96	0.96	2.67	0.67	0.83	-1.17
100	6	8	2.48	3.33	0.85	3.13	0.65	-0.01	-2.49
100	6	10	2.80	3.58	0.79	3.45	0.66	-0.87	-3.66
100	6	12	3.05	3.75	0.70	3.62	0.57	-1.48	-4.53
100	8	4	1.51	2.66	1.15	2.56	1.05	1.39	-0.11
100	8	6	2.09	3.04	0.95	2.78	0.70	0.89	-1.19
100	8	8	2.50	3.33	0.83	3.15	0.65	0.07	-2.43
100	8	10	2.80	3.58	0.79	3.46	0.67	-0.86	-3.66
100	10	4	1.60	2.72	1.12	2.48	0.88	1.47	-0.14
100	10	6	2.10	3.01	0.91	2.79	0.69	0.89	-1.21
100	10	8	2.50	3.33	0.83	3.02	0.53	0.12	-2.37

Table C-7 (ct'd 3/3) Safety Indices for Simple Span Bridges.

			SAFETY INDICES						
SPAN	BEAMS	SPAC.	MEMBER	ULTIMATE	DELTA beta	LF100	DELTA beta	DAMAGED	DELTA beta
120	4	4	1.32	1.37	0.04	1.37	0.04	-0.38	-1.71
120	4	6	1.90	2.65	0.74	2.42	0.51	0.02	-1.88
120	4	8	2.22	3.07	0.85	2.82	0.61	-0.67	-2.88
120	4	10	2.55	3.33	0.78	3.16	0.62	-1.19	-3.73
120	4	12	2.85	3.57	0.72	3.45	0.60	-1.64	-4.48
120	6	4	1.41	2.53	1.12	2.19	0.78	1.01	-0.40
120	6	6	1.87	2.87	1.00	2.58	0.71	0.50	-1.38
120	6	8	2.35	3.27	0.92	3.03	0.68	-0.20	-2.56
120	6	10	2.66	3.51	0.85	3.35	0.69	-0.86	-3.52
120	6	12	2.91	3.69	0.78	3.56	0.65	-1.47	-4.38
120	8	4	1.42	2.65	1.23	2.31	0.89	1.21	-0.21
120	8	6	1.98	2.96	0.98	2.70	0.71	0.61	-1.38
120	8	8	2.38	3.30	0.91	3.07	0.68	-0.17	-2.56
120	8	10	2.66	3.51	0.85	3.36	0.69	-0.86	-3.52
120	10	4	1.53	2.72	1.18	2.40	0.86	1.27	-0.27
120	10	6	2.01	2.97	0.97	2.71	0.70	0.63	-1.37
120	10	8	2.38	3.30	0.91	3.07	0.69	-0.23	-2.61
150	4	4	1.47	1.51	0.04	1.51	0.04	-0.34	-1.81
150	4	6	2.01	2.81	0.81	2.51	0.51	0.09	-1.91
150	4	8	2.28	3.22	0.94	2.89	0.61	-0.28	-2.56
150	4	10	2.59	3.45	0.86	3.21	0.62	-1.02	-3.61
150	4	12	2.91	3.69	0.79	3.50	0.59	-1.68	-4.58
150	6	4	1.53	2.72	1.19	2.29	0.76	1.24	-0.29
150	6	6	1.97	3.03	1.06	2.68	0.71	0.71	-1.26
150	6	8	2.43	3.44	1.01	3.13	0.71	0.52	-1.91
150	6	10	2.74	3.68	0.93	3.45	0.70	-0.50	-3.25
150	6	12	2.98	3.83	0.85	3.65	0.68	-1.10	-4.07
150	8	4	1.53	2.85	1.32	2.42	0.89	1.42	-0.11
150	8	6	2.11	3.14	1.03	2.84	0.73	0.85	-1.26
150	8	8	2.48	3.46	0.98	3.18	0.70	0.50	-1.98
150	8	10	2.74	3.68	0.94	3.46	0.72	-0.53	-3.28
150	10	4	1.67	2.91	1.24	2.53	0.86	1.45	-0.22
150	10	6	2.15	3.15	1.01	2.86	0.71	0.85	-1.30
150	10	8	2.48	3.47	0.99	3.18	0.70	0.38	-2.10

Table C-8 System Factors for Simple Span Bridges.

			SYSTEM FACTORS		STEEL
SPAN	BEAMS	SPAC.	ULTIMATE	FUNCTION.	DAMAGED
45	4	4	0.84	0.96	1.31
45	4	6	0.93	1.04	1.22
45	4	8	0.94	1.05	1.06
45	4	10	0.94	1.06	0.93
45	4	12	0.91	1.04	0.58
45	6	4	1.00	1.09	1.51
45	6	6	0.97	1.07	1.26
45	6	8	0.95	1.06	1.06
45	6	10	0.98	1.11	0.94
45	6	12	0.92	1.04	0.84
45	8	4	1.02	1.11	1.53
45	8	6	0.97	1.07	1.26
45	8	8	0.95	1.06	1.06
45	8	10	0.95	1.07	0.94
45	10	4	1.02	1.11	1.52
45	10	6	0.97	1.07	1.29
45	10	8	0.95	1.06	1.06
60	4	4	0.85	0.96	1.27
60	4	6	0.96	1.04	1.33
60	4	8	0.99	1.06	1.15
60	4	10	0.97	1.06	0.98
60	4	12	0.95	1.05	0.83
60	6	4	1.03	1.09	1.51
60	6	6	1.01	1.07	1.33
60	6	8	1.00	1.08	1.16
60	6	10	0.98	1.07	0.98
60	6	12	0.96	1.06	0.83
60	8	4	1.05	1.11	1.53
60	8	6	1.01	1.08	1.33
60	8	8	1.01	1.08	1.16
60	8	10	0.98	1.07	0.98
60	10	4	1.05	1.11	1.53
60	10	6	1.01	1.08	1.33
60	10	8	1.01	1.08	1.06

Table C-8 (ct'd 2/3) System Factors for Simple Span Bridges.

			SYSTEM FACTORS		STEEL
SPAN	BEAMS	SPAC.	ULTIMATE	FUNCTION.	DAMAGED
80	4	4	0.85	0.96	1.25
80	4	6	0.96	1.05	1.20
80	4	8	0.99	1.06	1.09
80	4	10	0.98	1.06	0.91
80	4	12	0.96	1.05	0.75
80	6	4	1.02	1.08	1.45
80	6	6	1.01	1.08	1.27
80	6	8	1.00	1.08	1.12
80	6	10	0.99	1.08	0.91
80	6	12	0.96	1.05	0.76
80	8	4	1.05	1.10	1.47
80	8	6	1.01	1.08	1.27
80	8	8	1.00	1.08	1.12
80	8	10	0.99	1.07	0.90
80	10	4	1.04	1.10	1.47
80	10	6	1.01	1.08	1.27
80	10	8	1.01	1.08	0.98
100	4	4	0.86	0.96	1.19
100	4	6	0.97	1.05	1.18
100	4	8	0.99	1.06	1.00
100	4	10	0.98	1.07	0.82
100	4	12	0.96	1.06	0.68
100	6	4	1.03	1.12	1.42
100	6	6	1.02	1.08	1.28
100	6	8	1.00	1.08	1.04
100	6	10	0.99	1.08	0.82
100	6	12	0.97	1.06	0.67
100	8	4	1.05	1.14	1.44
100	8	6	1.02	1.08	1.28
100	8	8	1.00	1.08	1.05
100	8	10	0.99	1.08	0.82
100	10	4	1.05	1.11	1.44
100	10	6	1.01	1.08	1.28
100	10	8	1.00	1.05	1.06

Table C-8 (ct'd 3/3) System Factors for Simple Span Bridges.

			SYSTEM FACTORS		STEEL
SPAN	BEAMS	SPAC.	ULTIMATE	FUNCTION.	DAMAGED
120	4	4	0.86	0.97	1.17
120	4	6	0.98	1.05	1.14
120	4	8	1.00	1.06	0.97
120	4	10	0.99	1.07	0.81
120	4	12	0.98	1.07	0.69
120	6	4	1.05	1.09	1.38
120	6	6	1.03	1.08	1.23
120	6	8	1.01	1.08	1.03
120	6	10	1.00	1.08	0.85
120	6	12	0.99	1.08	0.71
120	8	4	1.06	1.11	1.41
120	8	6	1.02	1.08	1.23
120	8	8	1.01	1.08	1.03
120	8	10	1.00	1.08	0.85
120	10	4	1.06	1.10	1.40
120	10	6	1.02	1.08	1.23
120	10	8	1.01	1.08	1.02
150	4	4	0.87	0.97	1.14
150	4	6	0.99	1.04	1.13
150	4	8	1.02	1.06	1.03
150	4	10	1.00	1.07	0.84
150	4	12	0.99	1.06	0.68
150	6	4	1.06	1.08	1.37
150	6	6	1.04	1.08	1.24
150	6	8	1.03	1.08	1.14
150	6	10	1.01	1.08	0.90
150	6	12	1.00	1.08	0.76
150	8	4	1.08	1.10	1.40
150	8	6	1.03	1.08	1.24
150	8	8	1.02	1.08	1.13
150	8	10	1.02	1.08	0.90
150	10	4	1.06	1.10	1.39
150	10	6	1.03	1.08	1.24
150	10	8	1.03	1.08	1.11

Table C-9 Safety Indices and System Factors for Continuous Bridges.

	span	120	ft	no. of beams		4		beam spacing =		4 ft
	βu	βf	βd	βm	Δβu	Δβf	Δβ d	ϕ	ϕ (funct.)	ϕ (damage)
compact										
Case1	2.33	2.07	0.78	1.48	0.85	0.59	-0.71	1.00	1.07	1.39
case 2	4.24	3.85	2.21	2.53	1.71	1.33	-0.32	1.17	1.22	1.47
case 3	2.98	2.92	1.71	2.93	0.05	-0.01	-1.22	0.83	0.95	1.31
noncompact										
case 1	2.33	2.07	-0.53	1.48	0.85	0.58	-2.02	1.00	1.06	1.13
case 2	2.52	x	-0.92	2.53	-0.01	x	-3.45	0.83	x	0.86
case 3	2.65	x	-1.32	2.93	-0.28	x	-4.24	0.77	x	0.71
	span	120	ft	no. of beams		4		beam spacing =		6 ft
	βu	βf	βd	βm	Δβu	Δβf	Δβ d	ϕ	ϕ (funct.)	ϕ (damage)
compact										
Case1	3.41	3.06	1.44	2.12	1.29	0.94	-0.68	1.09	1.14	1.42
case 2	4.78	4.55	2.26	3.23	1.55	1.32	-0.97	1.14	1.22	1.35
case 3	3.86	3.68	1.46	2.88	0.98	0.8	-1.42	1.03	1.11	1.25
noncompact										
case 1	3.29	3.06	-1.29	2.12	1.17	0.94	-3.41	1.07	1.14	0.86
case 2	3.21	x	-0.88	3.23	-0.02	x	-4.11	0.83	x	0.74
case 3	2.71	x	-2.03	2.88	-0.18	x	-4.91	0.81	x	0.62

Table C-9 (ct'd 2/9) Safety Indices and System Factors for Continuous Bridges.

	span	120	ft	no. of beams		4		beam spacing =		8 ft.
	βu	βf	βd	βm	Δβu	Δβf	Δβ d	ϕ	ϕ (funct.)	ϕ (damage)
compact										
Case1	3.86	3.5	1.12	2.42	1.44	1.08	-1.3	1.13	1.18	1.30
case 2	5.25	5.02	2.42	3.67	1.59	1.36	-1.24	1.15	1.22	1.30
case 3	4.18	3.98	1.33	3.04	1.14	0.94	-1.72	1.06	1.13	1.19
noncompact										
case 1	3.56	3.5	-2.11	2.42	1.14	1.08	-4.53	1.06	1.18	0.66
case 2	3.64	x	-0.8	3.67	-0.02	x	-4.46	0.84	x	0.69
case 3	2.9	x	-2.54	3.04	-0.15	x	-5.58	0.81	x	0.53
	span	120	ft	no. of beams		4 ft		beam spacing =		10 ft.
	βu	βf	βd	βm	Δβu	Δβf	Δβ d	ϕ	ϕ (funct.)	ϕ (damage)
compact										
Case1	4.12	3.86	0.6	2.77	1.35	1.1	-2.17	1.11	1.18	1.11
case 2	5.55	5.37	2.38	3.96	1.58	1.41	-1.58	1.14	1.23	1.22
case 3	4.39	4.26	1.02	3.25	1.14	1.01	-2.24	1.06	1.15	1.09
noncompact										
case 1	3.82	x	-2.82	2.77	1.05	x	-5.58	1.04	x	0.51
case 2	3.94	x	-0.92	3.96	-0.02	x	-4.89	0.84	x	0.63
case 3	3.11	x	-2.88	3.25	-0.15	x	-6.13	0.82	x	0.47

Table C-9 (ct'd 3/9) Safety Indices and System Factors for Continuous Bridges.

	span	120	ft	no. of beams		4 ft		beam spacing =		12 ft.
	βu	βf	βd	βm	Δβu	Δβf	Δβ d	ϕ	ϕ (funct.)	ϕ (damage)
compact										
Case1	x	x	x	x	x	x	x	x	x	x
case 2	5.77	5.61	2.25	4.22	1.56	1.39	-1.97	1.14	1.23	1.14
case 3	4.57	4.47	0.72	3.49	1.08	0.98	-2.78	1.04	1.14	0.99
noncompact										
case 1	x	x	x	x	x	x	x	x	x	x
case 2	4.18	x	-1.02	4.22	-0.03	x	-5.24	0.84	x	0.59
case 3	3.33	x	-3.16	3.49	-0.16	x	-6.65	0.82	x	0.42
	span	120	ft	no. of beams		6		beam spacing =		4 ft.
	βu	βf	βd	βm	Δβu	Δβf	Δβ d	ϕ	ϕ (funct.)	ϕ (damage)
compact										
Case1	3.27	2.8	2.19	1.61	1.66	1.19	0.58	1.16	1.19	1.65
case 2	4.7	4.42	2.98	3.26	1.44	1.16	-0.28	1.12	1.19	1.51
case 3	3.85	3.65	2.48	2.87	0.99	0.78	-0.39	1.03	1.11	1.47
noncompact										
case 1	3.25	2.8	0.82	1.61	1.64	1.19	-0.79	1.16	1.19	1.38
case 2	3.24	x	0.63	3.26	-0.02	x	-2.63	0.83	x	1.01
case 3	2.68	x	-0.03	2.87	-0.19	x	-2.9	0.80	x	0.96

Table C-9 (cl'd 4/9) Safety Indices and System Factors for Continuous Bridges.

	span	120	ft	no. of beams		6		beam spacing =		6 ft.
	βu	βf	βd	βm	Δβu	Δβf	Δβ d	ϕ	ϕ (funct.)	ϕ (damage)
compact										
Case1	3.59	3.2	1.84	2.1	1.49	1.11	-0.26	1.13	1.18	1.51
case 2	4.93	4.7	2.43	3.48	1.45	1.22	-1.06	1.12	1.2	1.34
case 3	4.06	3.88	1.84	2.88	1.18	1.01	-1.03	1.07	1.15	1.33
noncompact										
case 1	3.47	3.2	-0.3	2.1	1.38	1.11	-2.4	1.11	1.18	1.06
case 2	3.47	x	-0.09	3.48	-0.01	x	-3.57	0.84	x	0.83
case 3	2.75	x	-0.96	2.88	-0.12	x	-3.83	0.82	x	0.79
	span	120	ft	no. of beams		6		beam spacing =		8 ft.
	βu	βf	βd	βm	Δβu	Δβf	Δβ d	ϕ	ϕ (funct.)	ϕ (damage)
compact										
Case1	4.02	3.68	1.41	2.55	1.47	1.13	-1.14	1.13	1.19	1.34
case 2	5.34	5.08	x	3.79	1.55	1.29	x	1.14	1.21	x
case 3	4.34	4.16	1.56	3.15	1.2	1.01	-1.58	1.07	1.15	1.22
noncompact										
case 1	3.75	6.68	-1.28	2.55	1.2	1.13	-3.83	1.07	1.19	0.78
case 2	3.77	x	x	3.79	-0.02	x	x	0.84	x	x
case 3	3.01	x	-1.59	3.15	-0.13	x	-4.73	0.82	x	0.65

Table C-9 (ct'd 5/9) Safety Indices and System Factors for Continuous Bridges.

	span	120	ft	no. of beams		6		beam spacing =		10 ft.
	βu	βf	βd	βm	Δβu	Δβf	Δβ d	ϕ	ϕ (funct.)	ϕ (damage)
compact										
Case1	4.26	4.01	0.9	2.87	1.39	1.14	-1.97	1.12	1.2	1.16
case 2	5.58	5.4	2.48	4	1.57	1.4	-1.52	1.14	1.23	1.23
case 3	4.52	4.39	1.15	3.31	1.21	1.08	-2.16	1.07	1.16	1.10
noncompact										
case 1	3.96	x	-2.23	2.87	1.09	x	-5.1	1.05	x	0.57
case 2	3.99	x	-0.41	4	-0.01	x	-4.41	0.84	x	0.70
case 3	3.18	x	-2.19	3.31	-0.13	x	-5.51	0.82	x	0.54
	span	120	ft	no. of beams		6		beam spacing =		12 ft.
	βu	βf	βd	βm	Δβu	Δβf	Δβ d	ϕ	ϕ (funct.)	ϕ (damage)
compact										
Case1	4.37	4.2	0.22	3.12	1.25	1.08	-2.91	1.09	1.19	0.96
case 2	5.79	5.63	2.28	4.22	1.56	1.41	-1.94	1.14	1.23	1.15
case 3	4.61	4.52	0.76	3.5	1.11	1.01	-2.74	1.05	1.15	0.99
noncompact										
case 1	4.1	x	-3.09	3.12	0.98	x	-6.21	1.03	x	0.44
case 2	4.2	x	-0.83	4.22	-0.03	x	-5.05	0.84	x	0.61
case 3	3.35	x	-2.84	3.5	-0.15	x	-6.34	0.82	x	0.45

Table C-9 (ct'd 6/9) Safety Indices and System Factors for Continuous Bridges.

	span	120	ft	no. of beams		8		beam spacing =		4 ft.
	βu	βf	βd	βm	Δβu	Δβf	Δβ d	ϕ	ϕ (funct.)	ϕ (damage)
compact										
Case1	3.38	2.96	2.27	1.62	1.75	1.28	0.65	1.18	1.2	1.66
case 2	4.74	4.47	3.03	3.49	1.25	0.98	-0.47	1.08	1.15	1.48
case 3	3.96	3.78	2.59	2.9	1.06	0.87	-0.32	1.04	1.13	1.49
noncompact										
case 1	3.37	1.62	1.08	1.62	1.75	1.28	-0.54	1.18	1.2	1.43
case 2	3.43	x	0.75	3.49	-0.07	x	-2.75	0.82	x	0.99
case 3	2.75	x	0.29	2.9	-0.16	x	-2.62	0.81	x	1.02
	span	120	ft	no. of beams		8		beam spacing =		6 ft.
	βu	βf	βd	βm	Δβu	Δβf	Δβ d	ϕ	ϕ (funct.)	ϕ (damage)
compact										
Case1	3.64	3.29	1.87	2.2	1.44	1.09	-0.34	1.12	1.18	1.50
case 2	4.94	4.71	2.43	3.54	1.41	1.18	-1.1	1.11	1.19	1.33
case 3	4.09	3.93	1.87	2.94	1.15	0.99	-1.07	1.06	1.15	1.32
noncompact										
case 1	3.52	3.29	-0.25	2.2	1.32	1.09	-2.45	1.10	1.18	1.05
case 2	3.51	x	-0.05	3.54	-0.02	x	-3.59	0.83	x	0.83
case 3	2.83	x	-0.86	2.94	-0.11	x	-3.79	0.82	x	0.80

Table C-9 (ct'd 7/9) Safety Indices and System Factors for Continuous Bridges.

	span	120	ft	no. of beams		8				8 ft.
	βu	βf	βd	βm	Δβu	Δβf	Δβ d	ϕ	ϕ (funct.)	ϕ (damage)
compact										
Case1	4.04	3.71	1.41	2.58	1.46	1.13	-1.17	1.13	1.19	1.33
case 2	5.33	5.11	2.58	3.79	1.53	1.31	-1.21	1.14	1.22	1.30
case 3	4.35	4.17	1.57	3.15	1.2	1.02	-1.58	1.07	1.15	1.22
noncompact										
case 1	3.76	3.71	-1.26	2.58	1.18	1.13	-3.84	1.07	1.19	0.77
case 2	3.78	x	-0.15	3.79	-0.01	x	-3.94	0.84	x	0.77
case 3	3.03	x	-1.54	3.15	-0.12	x	-4.69	0.82	x	0.65
	span	120	ft	no. of beams		8				10 ft.
	βu	βf	βd	βm	Δβu	Δβf	Δβ d	ϕ	ϕ (funct.)	ϕ (damage)
compact										
Case1	4.27	4.02	0.83	2.87	1.39	1.15	-2.05	1.12	1.2	1.14
case 2	5.58	5.4	2.48	4	1.57	1.4	-1.52	1.14	1.23	1.23
case 3	4.53	4.39	1.15	3.31	1.22	1.08	-2.16	1.07	1.16	1.00
noncompact										
case 1	3.96	x	-2.23	2.87	1.09	x	-5.11	1.05	x	0.57
case 2	3.99	x	-0.42	4	-0.01	x	-4.42	0.84	x	0.70
case 3	3.18	x	-2.21	3.31	-0.13	x	-5.52	0.82	x	0.54

Table C-9 (ct'd 8/9) Safety Indices and System Factors for Continuous Bridges.

	span	120	ft	no. of beams		10				4 ft.
	βu	βf	βd	βm	Δβu	Δβf	Δβ d	ϕ	ϕ (funct.)	ϕ (damage)
compact										
Case1	3.41	2.97	2.31	1.73	1.68	1.24	0.58	1.17	1.2	1.65
case 2	4.78	4.47	3.05	3.56	1.22	0.91	-0.51	1.07	1.14	1.47
case 3	3.98	3.8	2.62	2.97	1.01	0.83	-0.36	1.03	1.12	1.48
noncompact										
case 1	3.4	2.97	1.12	1.73	1.67	1.24	-0.61	1.16	1.2	1.42
case 2	3.47	x	0.82	3.56	-0.08	x	-2.73	0.81	x	0.99
case 3	2.84	x	0.43	2.97	-0.14	x	-2.55	0.81	x	1.03
	span	120	ft	no. of beams		10				6 ft.
	βu	βf	βd	βm	Δβu	Δβf	Δβ d	ϕ	ϕ (funct.)	ϕ (damage)
compact										
Case1	3.65	3.3	1.88	2.22	1.43	1.08	-0.34	1.12	1.18	1.50
case 2	4.94	4.71	2.44	3.54	1.4	1.17	-1.1	1.11	1.19	1.33
case 3	4.09	3.93	1.87	2.94	1.15	0.99	-1.07	1.06	1.15	1.32
noncompact										
case 1	3.53	3.3	-0.22	2.22	1.3	1.08	-2.44	1.10	1.18	1.05
case 2	3.51	x	-0.02	3.54	-0.02	x	-3.56	0.83	x	0.84
case 3	2.83	x	-0.85	2.94	-0.11	x	-3.78	0.82	x	0.80

Table C-9 (ct'd 9/9) Safety Indices and System Factors for Continuous Bridges.

	span	120	ft	no. of beams		10				8 ft.
	βu	βf	βd	βm	Δβu	Δβf	Δβ d	ϕ	ϕ (funct.)	ϕ (damage)
compact										
Case1	4.03	3.71	1.42	2.58	1.45	1.12	-1.17	1.13	1.19	1.33
case 2	5.33	5.11	2.58	3.79	1.53	1.31	-1.21	1.14	1.22	1.30
case 3	4.35	4.17	1.67	3.15	1.2	1.02	-1.58	1.07	1.15	1.22
noncompact										
case 1	3.76	3.71	-1.26	2.58	1.18	1.12	-3.84	1.07	1.19	0.77
case 2	3.78	x	-0.15	3.79	-0.01	x	-3.94	0.84	x	0.77
case 3	3.02	x	-1.54	3.15	-0.13	x	-4.69	0.82	x	0.65

Table C-10 Sensitivity of Calibration of Continuous Bridges.

	span	150.00	ft	no. of beams		6.00			spacing =	8 ft.
sens1	βu	βf	βd	βm	Δβu	Δβf	Δβ d	ϕ	ϕ (funct.)	ϕ (damage)
compact										
Case1	4.19	3.80	1.54	2.59	1.60	1.20	-1.05	1.16	1.20	1.34
case 2	5.33	5.06	2.39	4.01	1.32	1.06	-1.62	1.09	1.16	1.21
case 3	4.31	4.13	1.37	3.28	1.03	0.85	-1.91	1.03	1.12	1.15
noncompact										
case 1	3.94	3.80	-1.20	2.59	1.35	1.20	-3.79	1.10	1.20	0.79
case 2	3.92	x	-0.48	4.01	-0.09	x	-4.49	0.83	x	0.69
case 3	3.09	x	-1.81	3.28	-0.19	x	-5.09	0.81	x	0.60
sens2	span	150.00	ft	no. of beams		6.00			spacing =	8 ft.
ductility +	βu	βf	βd	βm	Δβu	Δβf	Δβ d	ϕ	ϕ (funct.)	ϕ (damage)
compact										
case 1	4.55	3.80	1.54	2.59	1.96	1.20	-1.05	1.23	1.20	1.34
case 2	5.34	5.06	2.39	4.01	1.34	1.06	-1.62	1.10	1.16	1.21
case 3	4.33	4.13	1.37	3.28	1.04	0.85	-1.91	1.04	1.12	1.15
noncompact										
case 1	3.94	3.80	-1.20	2.59	1.35	1.20	-3.79	1.10	1.20	0.79
case 2	3.92	x	-0.48	4.01	-0.09	x	-4.49	0.83	x	0.69
case 3	3.09	x	-1.81	3.28	-0.19	x	-5.09	0.81	x	0.60
sens3	span	150.00	ft	no. of beams		6.00			spacing =	8 ft.
ductility -	βu	βf	βd	βm	Δβu	Δβf	Δβ d	ϕ	ϕ (funct.)	ϕ (damage)
compact										
case 1	4.19	3.80	1.60	2.59	1.60	1.20	-0.99	1.16	1.20	1.36
case 2	5.33	5.06	3.29	4.01	1.32	1.06	-0.72	1.09	1.16	1.39
case 3	4.31	4.13	2.24	3.28	1.03	0.85	-1.04	1.03	1.12	1.32

Table C-10 (ct'd 2/2) Sensitivity of Calibration of Continuous Bridges.

sens4	span	150.00	ft	no. of beams		6.00			spacing =	8 ft.
moment +	βu	βf	βd	βm	Δβu	Δβf	Δβ d	ϕ	ϕ (funct.)	ϕ (damage)
compact										
case 1	6.50	6.12	3.40	5.79	0.72	0.34	-2.38	0.97	1.02	1.08
case 2	6.82	6.58	3.90	4.01	2.81	2.58	-0.10	1.39	1.46	1.51
case 3	5.95	5.77	2.99	3.28	2.67	2.49	-0.30	1.35	1.43	1.45
noncompact										
case 1	5.84	x	0.82	5.79	0.05	x	-4.97	0.83	x	0.60
case 2	4.19	x	0.47	4.01	0.18	x	-3.54	0.87	x	0.84
case 3	3.40	x	-0.85	3.28	0.12	x	-4.13	0.86	x	0.74
sens5	span	150.00	ft	no. of beams		6.00			spacing =	8 ft.
moment -	βu	βf	βd	βm	Δβu	Δβf	Δβ d	ϕ	ϕ (funct.)	ϕ (damage)
compact										
case 1	4.38	3.85	2.44	2.59	1.79	1.26	-0.15	1.19	1.21	1.52
case 2	10.61	6.53	4.50	7.73	2.89	-1.20	-3.23	0.71	0.75	0.90
case 3	9.29	5.55	3.48	6.86	2.43	-1.31	-3.38	0.68	0.72	0.87
noncompact										
case 1	4.38	3.85	2.44	2.59	1.79	1.26	-0.15	1.19	1.21	1.52
case 2	10.23	6.53	3.62	7.73	2.51	-1.20	-4.10	0.67	0.75	0.75
case 3	9.02	5.55	2.63	6.86	2.16	-1.31	-4.23	0.65	0.72	0.72

APPENDIX D

RELIABILITY AND REDUNDANCY OF PRESTRESSED CONCRETE BOX GIRDER BRIDGES

This appendix presents the technical findings obtained in the study on the redundancy of simple span prestressed concrete box girder bridges. Spread box bridges as well as multi-box beam bridges are considered. Fifty bridges have been designed following AASHTO specifications. The nonlinear analyses are carried out using the program NONBAN. The reliability evaluation of the structural systems are performed using a computer program based on the Level II reliability approach. The analytical models, assumptions and computational procedures are discussed in this appendix.

This appendix consists of five sections. Section 1 describes the structural model applied in the analysis of prestressed concrete box girder bridges. The model is verified by comparing the output of NONBAN to the experimental results of a model spread box girder bridge as shown in Section 2. Section 3 explains the method used in designing the bridges. A design example is given to illustrate the assumptions and the design procedure. Section 4 lists the analytical results using NONBAN. Reliability and redundancy calculations are described in Section 5.

D.1. Modeling of Prestressed Concrete Box Girder Bridges

Detailed nonlinear bridge structural analysis using a general finite element computer program may be used to study the nonlinear behavior of prestressed box girder bridges. However, expensive computational costs and tedious input data preparation curb the application of a general finite element program for the nonlinear analysis of bridges for the purposes of this study. The program NONBAN is used herein with the superstructure modeled as a grillage. A major advantage of NONBAN is that shear and moment values for girders are directly obtained and integration of stress is not necessary. The guidelines for modeling box girder bridges with NONBAN along with a sample problem illustrating their application are given below.

D.1.1 Mesh Discretization

The grillage mesh is generated in the plane of the bridge superstructure following the guidelines presented by Hambly [D.1] and Zokaie [D.2]. The mesh consists of longitudinal and transverse beams.

For spread boxes, longitudinal grillage beams are placed to coincide with the centerline of each web of the box . The bending and torsional inertias are lumped at this location. It is assumed that bridges are constructed compositely. The inertia is taken to be the composite inertia of a half box section with the contributing slab. The concrete in the prestressed box may be different from that in the slab. Thus, the modulus of elasticity of the box is converted to that of the slab using the modular ratio, n. Since the AASHTO code specifies that the entire slab width in a box girder bridge shall be assumed effective for compression, the shear lag effect is not considered. Thus, the effective slab width is taken to be half of the girder spacing.

The torsional constant of the prototype composite box section ,C_t , is determined by the following expression which accounts for the effect of the slab directly above the top of the box:

$$C_t = 4A^2/\text{sum}(S_i/t_i) \qquad (D.1)$$

t_i and Si (i=1,2,3,4) are the geometrical parameters shown in Fig.D.1 while A is the area of the box enclosed by the center-line of the webs and flanges. Half of C_t is used for each longitudinal grillage beam.

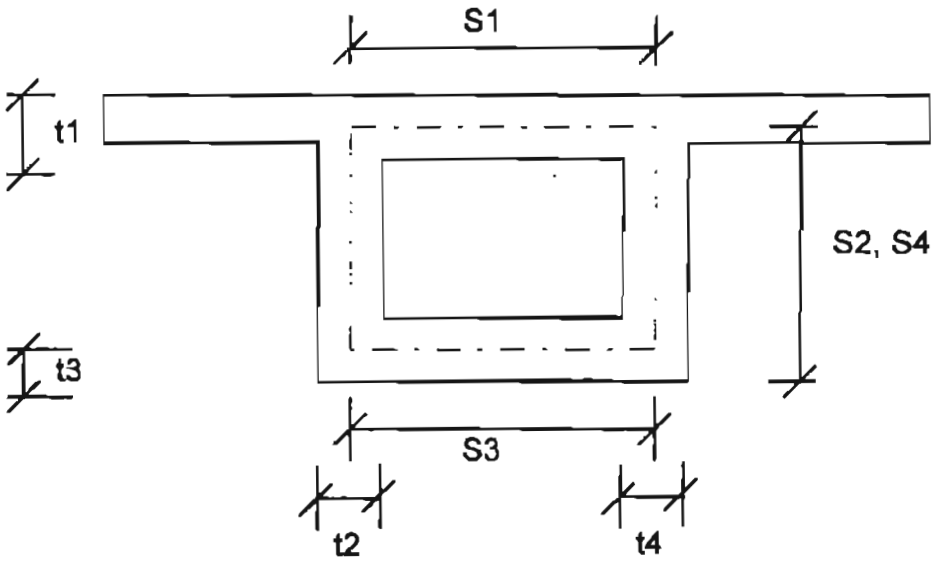

Fig. D.1 Geometrical parameters corresponding to torsional constant

For the edge beams, to be conservative, the structural effect of curbs and parapets is ignored. However, the edge beams are considered to have the same structural resistance as the interior ones.

No intermediate diaphragms are used in the box girder bridges in this study. The absence of diaphragms is compatible with the specification requirements. Zokaie's suggestion is applied in order to represent the contribution of the slab to the transverse distribution of the load. That is, transverse beams modeling the behavior of the slab are placed at spacings of at least 1/10 the effective span length. The transverse beams are of two types. The first type is used for the section between adjacent box girders. In this case, the transverse beam properties are based only on the slab thickness and corresponding material behavior as described in the appendix for I-beam bridges. The second type of transverse beams is used to model the box beam section along with the slab. The transverse properties are based on the transverse bending inertia of the box and an equivalent shear area to account for the in-plane distortions of the box. The properties of the transverse element are proportional to the element width. To include the effect of the in-plane deformations in the analysis model, a transverse shear area per unit width [D.1] is calculated as:

$$A_s = \frac{(T_t)^3 + (T_b)^3}{S \cdot G} \cdot \frac{2 \cdot (T_w)^3 \cdot E}{(T_w)^3 \cdot S - \left[(T_t)^3 + (T_b)^3\right] \cdot d} \qquad \text{(D.2)}$$

where

T_t = top thickness of the box section including the slab
T_b = bottom thickness of the box section
T_w = web thickness
S = width of the box
d = bridge depth measured from the top to the midpoint at the bottom of the box
E = the modulus of elasticity
G = the shear modulus of elasticity.

Equation (D.2) is obtained from [D.1] by assuming that the horizontal shear force is shared between the top and bottom slabs in proportion to their individual flexural stiffnesses and that there are points of contraflexure midway between the webs.

Other factors such as the effect of membrane action, arching effect of the slab and the effect of the coupling between the bending and rotation of the deck about the main axes of the bridge are ignored.

Multi-box beam bridges connected by shear keys are represented by a grillage with longitudinal members coincident with the center lines of the beams. These members are associated with the total moment of inertia of the box and the total torsional constant. Transverse beam properties are calculated for the top and the bottom slabs of the boxes and a shear area, A_s, is calculated as given in Equation (D.2). The shear keys are represented by short flexible members as recommended by Hambly [D.1].

D.1.2 Section Properties

Elastic properties

The elastic properties required in the program NONBAN are similar to those used with any structural analysis program. They are: The moment of inertia, the torsional constant, the shear area (required to account for in-plane bending of the boxes), the modulus of elasticity, and the shear modulus. The calculation of the section geometrical properties follows the conventional methods used in structural analysis.

The shear effect of the box webs is ignored in calculating the shear area of longitudinal beams. The equivalent area A_S is used as the shear area of the transverse beams representing the transverse properties of the box section. The shear area for the transverse beam elements between the box sections is the equivalent shear area of a section of the slab of rectangular cross section. The corresponding torsional constant per unit length of the slab is:

$$J = T^3/6 \qquad \text{(D.3)}$$

The calculation of the rest of the elastic properties for concrete members has been described in Appendix B (Section B.1).

Bending Inelastic properties

The nonlinear behavior in bending about the horizontal axis as well as the shearing nonlinearity of the beam elements are considered in the analysis of the box girder bridges. The axial member deformations and the bending about the vertical axis are assumed to be insignificant. These are assumed to remain in the linear elastic range. Also, the torsional nonlinearity of the beam elements is not considered in this study. Comparisons between the results of such models and experimental and theoretical studies have been reported in Appendix F. These comparisons have shown that the proposed model is sufficiently accurate to represent the behavior of typical box girder bridges. One additional comparison is performed in section D.2 of this appendix.

In this study, the effect of material nonlinearities on the behavior of a beam element is represented by rotational springs attached to the ends of the beam elements. A modified stiffness matrix that accounts for possible flexural and shear nonlinearity has thus been included in program NONBAN (see Appendix F). The nonlinear behavior is expressed by a multilinear relationship between the member resistance and its deformation.

The nonlinear relationship between the moment and section curvature is obtained through the iteration procedure described in Section B.1 of Appendix B. The nonlinear

stress-strain behavior of steel (either prestressed or reinforced) and concrete is used as the input data along with the sectional geometry of the beam elements. The output relationship of moment vs. curvature is approximately divided into 4-linear segments such that the four segments form the M-Phi curve. The slopes and the critical moment values of the segments of the M-Phi curve are used as input data in NONBAN.

The moment versus plastic rotation relationship is obtained by multiplying the curvature by the plastic hinge length Lp. This assumes a constant plastic curvature within a length Lp of the beam element. This assumption is fully explained by Park and Pauley [D.3]. From the results of tests on simply supported beams, Corley [D.4] proposed the following empirical equation for the equivalent length of the plastic hinge:

$$Lp = \frac{d}{2} - \frac{0.1 \cdot L}{\sqrt{d}} \qquad (D.4)$$

where d is the effective depth of the section and L is the length of the beam. In addition, because of the mesh discretization procedure, Lp should not be larger than half of the length of the beam element. Equation (D.4) is used herein because it gives a reasonable approximation of the plastic hinge length of box girder bridges as will be shown in section D.2. Equation (D.4) is used for box girder bridges because it provides better results for deep box members than the simple Lp=d formula used for I-beam bridges.

The bridge system is assumed to have reached its maximum capacity when any point in the longitudinal beam reaches its maximum plastic hinge rotation. At this point, the program NONBAN stops the nonlinear incremental analysis. The maximum plastic hinge rotation is determined following the empirical equations described in the final Phase I report for NCHRP Project 12-36/1 [D.5]. Similar results can be obtained by taking the maximum curvature at concrete crushing (or steel rupture if it occurs before crushing) times the length of the plastic hinge.

Shearing Inelastic properties

In addition to bending nonlinearity, concrete box girders may exhibit shearing nonlinearity. When the beam is in the linear elastic range, the initial shear stiffness is given by the shearing modulus G multiplying the shear area A_V. This gives the slope of the first segment of the shear deformation curve.

The shearing deformation curve is straight until the concrete cracks at a load V_{CR}. There are two types of cracks in the concrete beams. The web crack occurs under a cracking shear load V_{CRw}, and the inclined crack occurs under the load of V_{CRi}. Both V_{CRi} and V_{CRw} are determined following the 1996 AASHTO standard specifications. The lower value of V_{CRi} and V_{CRw}, is chosen as the final cracking shear load, V_{CR}. When the load

increases above V_{CR} , the shearing deformation curve is approximated as another straight line with a slope of K_{vt}. The slope is calculated using equation [D.5]:

$$K_{vt} = [\rho_v / (1+4n\rho_v)]E_s T_w d \qquad (D.5)$$

where ρ_v is the shear steel reinforcement ratio, n is the modulus ratio and E_s is the elastic modulus of the reinforcing steel.

The ultimate shear resistance is the summation of the cracking capacity V_{CR} and the reinforcing steel capacity V_s. V_s is determined by :

$$V_s = A_t f_y d / s \qquad (D.6)$$

where V_s is the area of shear reinforcement within a distance s, and f_y is the reinforcing steel yielding stress.

For transverse beam elements, the ultimate shear capacity is considered to be the same as the cracking shear load.

D.1.3 Support conditions

All the ends of the girders are considered as simply-supported, and rotational moments in all 3 directions are released. However, there are transverse beam elements linking the supports at the ends of the girders, which would partially restrain the girder torsion about the longitudinal axis as well as the bending about the member's horizontal axis.

D.1.4 Loading

The dead load on the bridge is applied as a distributed load over the length of the longitudinal beams. Dead load is the load that is not changed during the incremental analysis. It consists of the self-weight of the boxes, the weight of the slab, and the weight of the wearing surface, curbs and parapets. All these loads are assumed to be uniformly distributed over the girders. Shored construction is assumed and the dead load is applied on the composite section. Appendix B demonstrated that, for most cases, there is little difference in the final results whether we assume shored construction or whether some permanent dead loads are applied on the non-composite sections.

It is assumed that all the live load comes from vehicular traffic. AASHTO HS-20 truck load configuration is used in this study. Concentrated point loads are used for the live load. The magnitude of the load is incremented as the nonlinear analysis proceeds. The

HS-20 trucks are placed to produce maximum moment in the external web of the edge girder. In most cases, the external wheel line of the truck coincides with one of the exterior girder webs. Longitudinally, the drive axle of the truck is located at the midspan of the bridge since this location produces a moment very close to the maximum bending moment. To be conservative, each traffic lane is assumed to have one truck on it. The trucks are placed side by side with a minimum side clearance of 4 ft between the vehicles.

If the location of a wheel load coincides with a mesh node, then the load is applied at that node. If the wheel location does not coincide with a node of the mesh, the wheel's load is equivalently distributed to the 4 nodes adjacent to the wheel. The tributary area approach is used for this purpose. As an illustration, let us assume that a point load of magnitude W is applied at point G which happens to lie between nodes A,B, C and D of a mesh as shown in Fig. D.2. The load W can then be distributed to the four adjacent nodes A, B, C and D. The equivalent load P_B distributed to Point B would be equal to:

$$P_B = W \text{ (Area of EGCF) / (Area of ABCD)} \qquad \text{(D.7)}$$

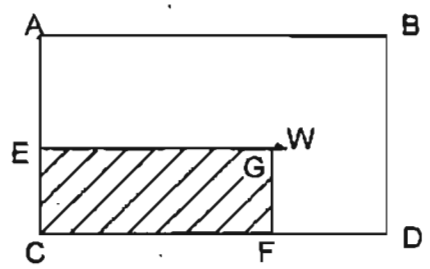

Fig. D.2 Determination of nodal equivalent load

Similar logic is used to calculated P_A, P_C and P_D.

D.2. Verification of the Nonlinear Analysis Model.

The analysis model and the validity of the program NONBAN are verified by comparing the results obtained by NONBAN to those of available laboratory tests. A 2-box spread simply-supported 1/7-scale model bridge was tested by Mirza et al. at McGill University [D.6]. They studied the overall static response at different levels of load up to collapse. The geometry and structural details of the tested bridge are shown in Fig. D.3. The depth of the prestressing steel varies along the length of the girders. In addition the shear reinforcement in the girder varies along the length of the girders. Point loads simulating the configuration of the design truck of the Ontario Highway Bridge Design Code are applied on the prototype bridge.

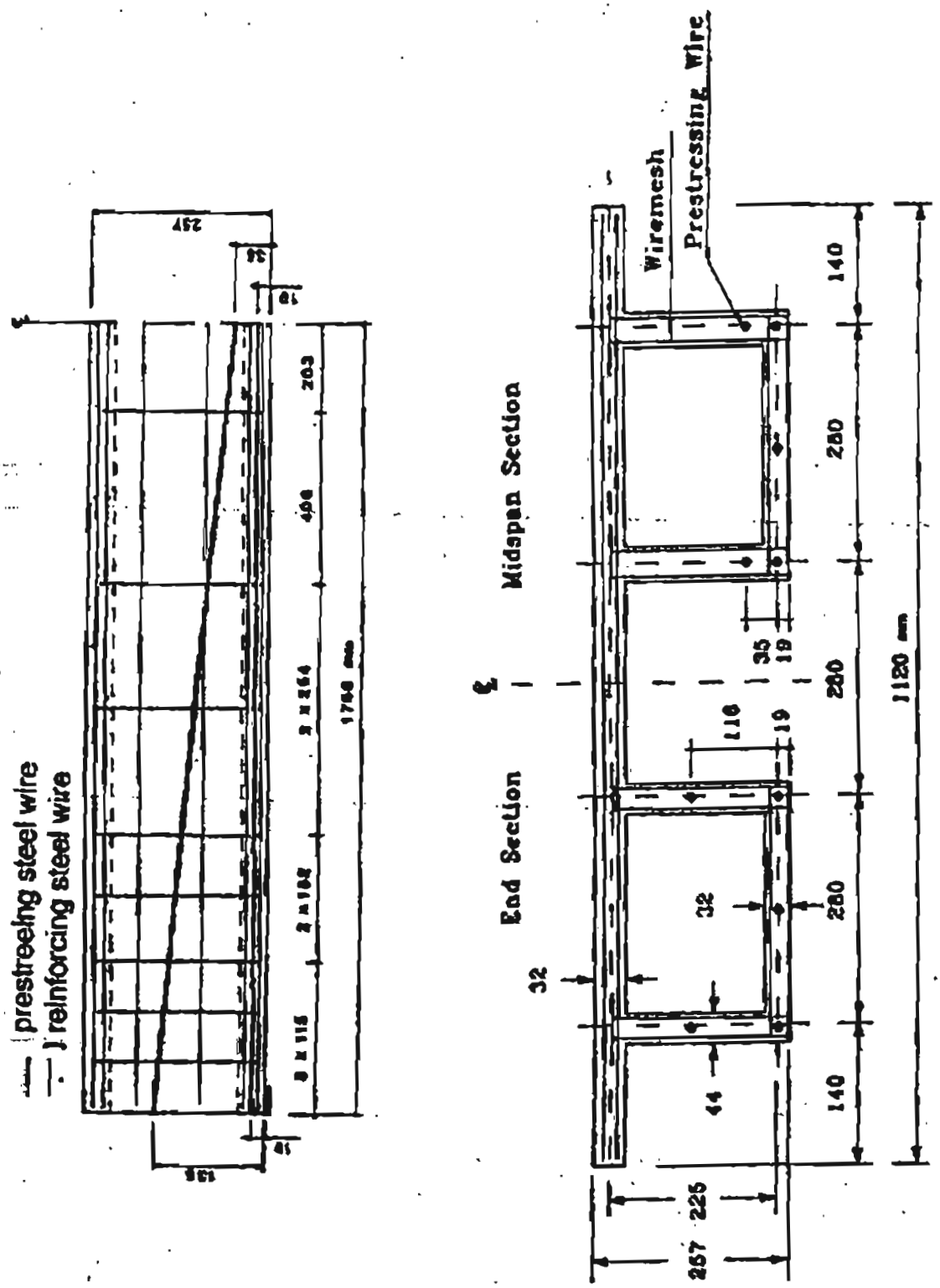

Fig. D.3 Geometry and structural details of model bridge

To model the tendon of variable depth in the box, each longitudinal beam is discretized into 4 types of elements. 12 types of transverse beam elements are used to account for different element widths. The mesh was chosen such that the loading points coincide with the nodes in the mesh as shown in Fig. D.4. The bridge model is analyzed by NONBAN following the approach described above. The nonlinear bending behavior of each type of longitudinal beam element is represented by a 4-segment moment versus plastic curvature relationship while the nonlinear shearing behavior of longitudinal beams is characterized by a bilinear shear versus shear strain curve. Each web of the box is assumed to be simply-supported at both ends of the bridge.

The results from running NONBAN for this model bridge are compared to the experimental results as shown in Fig. D.5. NONBAN predicts that ultimate failure occurs under 5.63 truck loading at a mid-span deflection of 1.5 in. compared to the experimental value of 5.4 truck loading at the mid-span deflection of 1.3 in. The relative error for ultimate loading is only about four percent. Also, NONBAN gives satisfactory agreement for the loading at the onset of cracking.

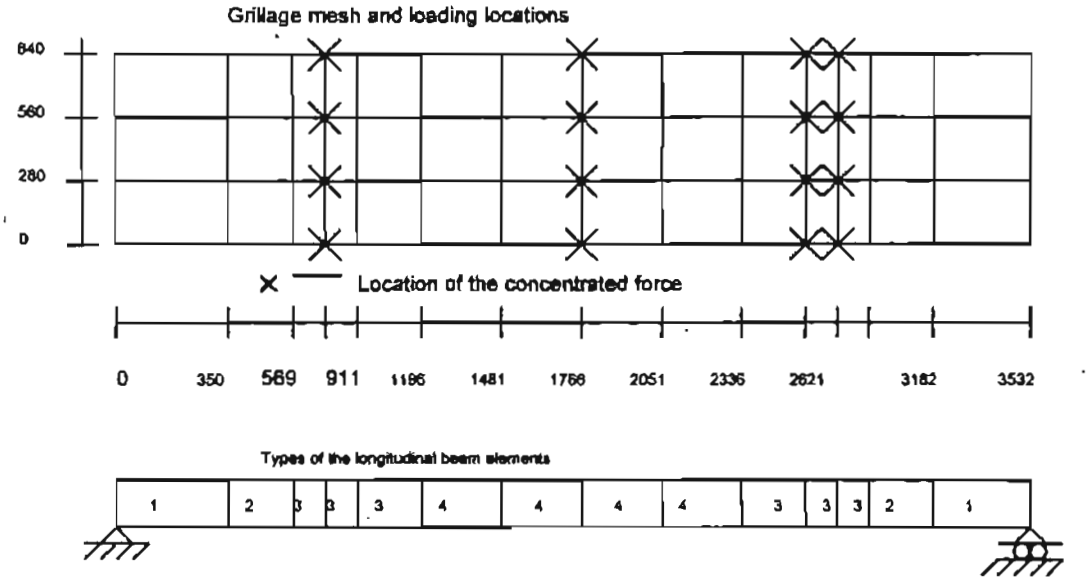

Fig. D.4 Mesh discretization for the model bridge

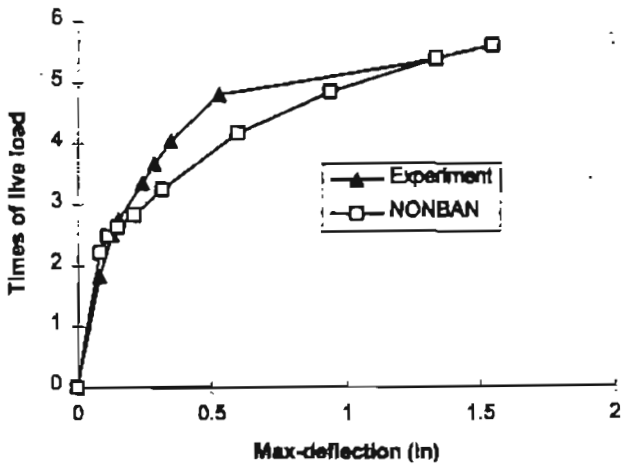

Fig. D.5 Comparison of NONBAN's results to experimental results.

Due to the assumption of a constant plastic hinge length, there is a discrepancy between the experimental values and grillage analysis results in the early stages of nonlinearity. However, there is no significant effect on the prediction of ultimate loading, and on the redundancy analysis.

D.3. Design of Bridges

D.3.1 Bridge Configurations

To investigate the behavior of typical prestressed concrete spread box girder bridges, 45 bridges have been designed. The bridges have spans of 60 ft , 100 ft and 150 ft. The number of girders varies from 2, 3, to 5. The depth of a bridge is assumed to be 0.065 span. The girder spacings are 8 ft , 15 ft and 25 ft . The bridge decks are 8 in thick for 8 ft spacing, 9 in for 15 ft spacing and 10 in for 25 spacing. The number of traffic lanes varies depending on the combination of number of girders and spacings. For example, the bridge with 5 box beams at 15 ft is designed for both 5 lanes and 6 lanes.

Three multi-box beam bridges are also designed. The base case is a 70 ft bridge with 10 adjacent boxes. The box's width is 4 ft and is 33 deep. The slab thickness is 5.5 inches. The section is assumed to be noncomposite. The other two bridges assume 8 adjacent boxes and 11 adjacent boxes. The shear keys are assumed to carry all the required shear. The possibility of shear key failures are considered in the damaged scenario when the external box is assumed to be totally damaged.

D.3.2 Load and Load effect

Dead load consists of the box self weight, slab weight, weights of curbs and parapets, and the weight of the wearing surface. 1996 AASHTO design criteria are used during the design process with:

Impact load = 50 / (span +125)
Live load: The HS-20 live load configuration has been used in the design process
The reduction factor of live load = 1 if number of lanes is less than 3
= 0.9 if number of lanes is 3
= 0.75 if number of lanes is greater than 3
The live load distribution factor is determined following Article 3.28 of the AASHTO design manual.

Using LFD criteria, the live load effect for the purposes of design is 2.17 times the load distribution factor times the reduction factor times the impact factor times the static load effect of a line of truck wheel on a simply-supported beam.

D.3.3 Primary Data

A Mathcad algorithm is developed to perform the design. The span length, spacing of box girders, number of traffic lanes, and the number of boxes are required as basic input data.

The assumed data are:
the slab concrete strength fcs'= 3.5 ksi
the box concrete strength fcb' =5 ksi
prestressing steel strength fps = 270 ksi
the reinforcing steel yielding strength fy = 60 ksi
initial prestress fsi =0.75 fps
effective prestress fse = 0.6 fps
rupture modulus for box beam fr =0.53 ksi

The initial prestressing stress is taken as 0.75fps. To simpify the calculation of the effective prestressing stress, 0.8 times the initial prestressing stress is used as the effective prestressing stress [D.7].

The design bending strength with a resistance factor of 0.95 must be greater than 1.2 times the cracking moment. The reinforcing index is limited to less than 0.3.

D.3.4 Design example

As an illustration of the procedure followed, the design of a 3 box girder bridge with a 100 ft span and with girder spacings of 8 ft is detailed.

Step 1: Define the geometry

Horizontal clearance of the bridge = 24 ft, width of the curb = 1.5 ft, width of the parapet = 1.25, width of box = 4 ft, thickness of box web = 5 in, thickness of box flange = 5.5 in, depth of bridge = 78 in, thickness of the slab = 8 in. The girder is assumed to be composite. Using this data, the following section properties are obtained:

- Moment of inertia for the longitudinal grillage beam =741700 in^4
- The distance from the bottom fiber to the neutral axis =52.36 in

Step 2: Determine the load effect on the longitudinal beams

The dead load applied on the longitudinal beam is determined as 0.117 kips/in. Two traffic lanes are used in this design. The live load distribution factor for the interior beam is evaluated as 1.442 while that for the exterior beam is found to be 1.5, which is defined as the live load distribution factor. The impact load factor is 1.222. Thus, the maximum moment and maximum shear for the live load in the grillage beam are determined as 8382 kips-in and 29.9 kips. The required moment and shear are evaluated as 45520 kips-in and 156 kips.

Step 3: Calculate the prestressing force

In this step, the entire slab width shall be assumed effective for compression as stipulated in the 1996 AASHTO specifications.

For the final condition, the AASHTO Code permits a concrete tensile stress of 424 psi in the prestressed tension zone. The member is assumed to be bonded, the pretensioned strands be 4 in above the bottom face of the girder. Therefore, prestressing steel area of 2.72 in^2 and effective pretressing force of 440 kips are obtained using the preceding data. The available longitudinal beam resistance is 48410 kips-in which is greater than required 45520 kip-in. The bottom fiber stress of 416 psi is lower than 424 psi. The reinforcing index is 0.041 while the ratio of member strength to cracking moment is calculated as 1.56. All these satisfy the requirements established by the AASHTO Code.

Since the 0.065 is used here for the ratio of the bridge depth to span, the deflection check for the bridge design is not necessary, according to AASHTO specification.

Step 4: Chose the shear reinforcement in the box

For the inclined cracking, the critical shear strength of the grillage beam can be found using AASHTO's criteria to be 115.8 kips. Notice that a constant prestressing eccentricity is used here. The web's critical shear resistance is 179.1 kips. Thus, we define the smaller value as the cracking shear strength of the longitudinal beam element. Number 4 double-legged stirrups used in the girder produced a required stirrup spacing equal to 20 in.

The spacing of the stirrups does not exceed 3/4 of the depth of the beam, nor is it lower than the amount required for the minimum web reinforcement set by the AASHTO Code. The stirrups not only act to provide shear reinforcement for the web of the girder but also provide reinforcement across the girder-slab interface horizontal shear and ensure composite action. The AASHTO Code states that full transfer of horizontal shearing forces may be assumed when contact surfaces are clean and intentionally roughened and when vertical ties with an area at least 0.22 in^2/ft are provided. Therefore, the spacing of 20 in also meets this requirement.

Step 5: Design the slab

The dead load for the slab consists of the slab's self-weight and the weight of the wearing surface. It is assumed that the main reinforcement is perpendicular to the traffic. Thus, the live load effect is determined by the equation from AASHTO specification:

$$LLs = (span+2)*0.5 \text{ (kips)} \qquad (D.7)$$

The impact factor is chosen as 1.3. Viewing the slab as continuous beam on the girder, the reinforcements in the positive bending zone and negative bending zone are found to be 0.312 in^2 / ft and 0.372 in^2 / ft, respectively.

D.3.5 Summary of designs

The section details of the spread box girder bridges designed in this study are summarized below. Table D.1 gives the definition of the mathematical symbols. Table D.2 shows the bridge geometry and Table D.3 lists the design details.

Table D.1. Notation:

d----- effective depth of the composite section (in)
S------ spacing of the girders (ft)
Nl----- number of the lanes
As----- Area of the prestressing steel (in^2)
Pe---- effective prestressing force (kips)
PhiMn-----bending strength (in-kips)
Mcr---- cracking moment of the section (in-kips)
Av----- area of the web reinforcement (in^2)
ss----- longitudinal spacing of the web reinforcement (in)
Vn----- nominal shear strength of the box girder (kips)
Ast---- area of reinforcement per feet width of the slab (in^2/ft)
dt----- effective depth of the slab (in)
Mnt---- nominal bending strength per feet width of the slab (in-kips/ft)
Vnt---- nominal shear strength per feet width of the slab (kips/ft)

Table D.2. Section geometries:

	8 ft spacing	15 ft spacing	25 ft spacing
thickness of slab (in)	8	9	10
width of box girder (ft)	4	7	10
thickness of web (in)	5	7	9
thickness of the flanges (in)	5.5	7.5	10

Table D.3. Design details

1. Span 60 ft with 2 boxes

S	Nl	d	As	Pe	PhiMn	Mcr	Av	ss	Vn	Ast	dt	Mnt	Vnt
8	1	43	3.77	610	38480	25400	1.24	22	223	0.372	5.44	114	7.6
15	2	43	6.32	1022	65080	42500	1.24	13	372	0.540	6.44	193	8.5
25	3	43	9.43	1528	97820	60900	1.24	7	551	0.948	7.44	376	9.5

2. Span 60 ft with 3 boxes

S	Nl	d	As	Pe	PhiMn	Mcr	Av	ss	Vn	Ast	dt	Mnt	Vnt
8	2	43	3.8	614	38680	25480	1.24	22	224	0.372	5.44	114	7.6
15	3	43	5.86	949	60620	39880	1.24	14	347	0.540	6.44	193	8.5
15	4	43	6.55	1061	67300	43540	1.24	12	392	0.540	6.44	193	8.5
25	5	43	9.16	1484	95160	59140	1.24	7	547	0.948	7.44	376	9.5
25	6	43	10.3	1666	106140	65120	1.24	6	601	0.948	7.44	376	9.5

3. Span 60 ft with 5 boxes

S	Nl	d	As	Pe	PhiMn	Mcr	Av	ss	Vn	Ast	dt	Mnt	Vnt
8	3	43	3.34	540	34380	22900	1.24	25	199	0.372	5.44	114	7.6
8	4	43	4.27	692	42320	28500	1.24	18	254	0.372	5.44	114	7.6
15	5	43	5.24	849	54620	36320	1.24	17	307	0.540	6.44	193	8.5
15	6	43	5.90	955	61020	39980	1.24	14	350	0.540	6.44	193	8.5
25	8	43	8.34	1351	87100	54600	1.24	9	485	0.948	7.44	376	9.5
25	9	43	8.76	1420	91300	56620	1.24	8	513	0.948	7.44	376	9.5
25	10	43	9.28	1504	96360	59180	1.24	7	549	0.948	7.44	376	9.5

4. Span 100 ft with 2 boxes

S	Nl	d	As	Pe	PhiMn	Mcr	Av	ss	Vn	Ast	dt	Mnt	Vnt
8	1	74	5.33	863	94920	60960	0.8	20	320	0.372	5.44	114	7.6
15	2	74	8.90	1441	159660	104680	0.8	12	528	0.540	6.44	193	8.5
25	3	74	12.8	2106	235000	153800	0.8	9	744	0.948	7.44	376	9.5

5. Span 100 ft with 3 boxes

S	Nl	d	As	Pe	PhiMn	Mcr	Av	ss	Vn	Ast	dt	Mnt	Vnt
8	2	74	5.44	881	96820	62100	0.8	20	320	0.372	5.44	114	7.6
15	3	74	8.04	1303	145100	95980	0.8	20	440	0.540	6.44	193	8.5
15	4	74	9.20	1491	164820	107220	0.8	12	542	0.540	6.44	193	8.5
25	5	74	12.5	2028	226800	148580	0.8	9	736	0.948	7.44	376	9.5
25	6	74	14.0	2264	251600	162560	0.8	7	845	0.948	7.44	376	9.5

Table D.3. (Ct'd) Design details

6. Span 100 ft with 5 boxes

S	Nl	d	As	Pe	PhiMn	Mcr	Av	ss	Vn	Ast	dt	Mnt	Vnt
8	3	74	4.74	768	85140	55080	0.8	20	298	0.372	5.44	114	7.6
8	4	74	5.86	950	103880	66680	0.8	20	345	0.372	5.44	114	7.6
15	5	74	7.32	1186	132680	88640	0.8	18	424	0.540	6.44	193	8.5
15	6	74	8.30	1345	149520	98400	0.8	14	485	0.540	6.44	193	8.5
25	8	74	11.9	1928	216000	142700	0.8	10	386	0.948	7.44	376	9.5
25	9	74	12.7	2060	230000	150560	0.8	9	732	0.948	7.44	376	9.5
25	10	74	13.7	2220	247000	160120	0.8	8	790	0.948	7.44	376	9.5

7. Span 150 ft with 2 boxes

S	Nl	d	As	Pe	PhiMn	Mcr	Av	ss	Vn	Ast	dt	Mnt	Vnt
8	1	113	7.58	1228	207200	125380	0.8	26	458	0.372	5.44	114	7.6
15	2	113	12.5	2030	344800	216200	0.8	15	755	0.540	6.44	193	8.5
25	3	113	18.0	2916	499000	318200	1.24	16	1085	0.948	7.44	376	9.5

8. Span 150 ft with 3 boxes

S	Nl	d	As	Pe	PhiMn	Mcr	Av	ss	Vn	Ast	dt	Mnt	Vnt
8	2	113	7.60	1229	207400	125160	1.24	30	595	0.372	5.44	114	7.6
15	3	113	11.5	1858	317000	199720	1.24	28	685	0.540	6.44	193	8.5
15	4	113	13.0	2106	357200	222200	1.24	23	778	0.540	6.44	193	8.5
25	5	113	17.6	2846	487600	311000	1.24	17	1056	0.948	7.44	376	9.5
25	6	113	19.4	3142	535800	337800	1.24	15	1160	0.948	7.44	376	9.5

9. Span 150 ft with 5 boxes

S	Nl	d	As	Pe	PhiMn	Mcr	Av	ss	Vn	Ast	dt	Mnt	Vnt
8	3	113	6.82	1105	187560	113920	0.8	30	414	0.372	5.44	114	7.6
8	4	113	8.14	1320	221600	134180	0.8	22	494	0.372	5.44	114	7.6
15	5	113	10.5	1705	292200	185220	0.8	21	630	0.540	6.44	193	8.5
15	6	113	11.8	1907	325000	203800	0.8	17	707	0.540	6.44	193	8.5
25	8	113	16.6	2690	462000	296800	0.8	12	998	0.948	7.44	376	9.5
25	9	113	17.6	2850	488000	311000	0.8	11	1057	0.948	7.44	376	9.5
25	10	113	18.8	3040	519400	328400	0.8	10	1127	0.948	7.44	376	9.5

Details of the multi-box beam sections designed in this study are presented below.

Table D.4 Notation

Nb= # of boxes
Nl = # of lanes
Bw=Box width (ft)
Tt=Thickness of top flange (in)
Tb=Thickness of bottom flange (in)
Tw=Thickness of web (in)
De=depth of box (in)
Ac=area of concrete box section (in^2)
I=moment of inertia (in^4)
d=Effective depth of prestressing steel (in)
As = Area of prestressing steel (in^2)
Pe=Effective prestressing force (kips)
Mcr= Cracking moment (kip-in)
Mu=Ultimate moment (kip-in)
Av=Area of shearing reinforcement (in^2)
ss=Spacing of stirrups (in)
Vn=Shearing strength of the box (kips)

f'c=Concrete strength=5 ksi
fy=Shearing reinforcement strength=60 ksi
fps=Prestressing steel strength=270 ksi

Table D.5 Design details of multi-box beam bridges

Span	Nb	Nl	Bw	Tt	Tb	Tw	De	Ac	I	d	As	Pe	Mcr	Mu	Av
70'	10	3	4'	5.5	5.5	5	33	753	110450	24.7	4.07	659	14759	22030	0.8
70'	8	2	4'	5.5	5.5	5	33	753	110450	24.7	4.07	659	14773	22050	0.8
100'	10	3	4'	5.5	5.5	5	54	963	380000	41.1	4.43	718	28000	42700	0.8
70'	11	3	4'	5.5	5.5	5	33	753	110450	24.7	4.09	663	14840	22160	0.8
40'	10	3	4'	5.5	5.5	5	21	624	33590	14.8	2.73	443	5846	8705	0.8

D.4. Results of Nonlinear Analysis

The nonlinear analysis of the prestressed box girder bridges designed as described in the previous section is performed using the program NONBAN. This section explains the preparation of input data along with an illustration of the analysis of a sample spread box beam bridge.

D.4.1 Preparation of Input Data

As described in the previous section, the superstructure of the spread box bridge is discretized as a grillage mesh. The mesh is formed by 5 types of beam elements. Element Type I is used for the longitudinal grillage beams. Each beam represents half of the composite box girder section. It is assigned half of the characteristic values for the entire section such as the moment of inertia, equivalent shearing area and the torsional constant. Element Type V represents the transverse effect of the portion of the slab which is between two adjacent boxes. It is assumed that no diaphragms exist in the bridge. The interaction between torsion and bending moment is not considered herein. The slab is divided into 11 transverse beams. The evaluation of the structural properties for element Type V is similar to that described in Appendix B for I-beam bridges. Element Type IV models the transverse effect of the composite box section which consists of the top and bottom slabs of the box. Since the concrete strength of the slab is different than that of the box, the elastic material constants are converted to those of the slab. The moment of inertia for element Type IV is easy to find, using traditional structural analysis principles. The equivalent shearing area is calculated as described in equation (D.2) to account for the distortion of the boxes. The grillage members at the support ends are represented by elements of Type II and Type III. Their member properties have half the values of those of Type IV and V, respectively. It is noted that beam elements Type II and IV are much stronger than Type III and V elements. It is assumed that no local failure would occur in elements of Type II and IV.

It should be noted that when a grillage is subjected to a torque, the longitudinal member carries a part of the total torque applied on the cross-section, while the other half is carried by the shear forces in the deck. Therefore, as Hambly suggests [D.1], the torsional constant used with element Type I (representing one web) is actually 1/2 that of a box section, but, simultaneously, the torsional constant per unit width for element Type IV (slab of the box) is equal to 1/2 the torsional constant per unit width of the box. The torsional constant for element Type V (slab between boxes) has a value calculated as given in Equation (D.3).

While determining the moment-rotation relationships for all types of elements, typical stress-strain curves for concrete, reinforcing steel and prestressing steel are used and the tensile capacity of the concrete is ignored. These stress-strain diagrams are shown in Appendix B. The cracking moment is independently calculated as the moment which will produce a stress equal to the modulus of rupture in the outer surface of the tension part

of the beam. Nonlinear behavior initiates when the moment in a beam exceeds the cracking moment. The transverse beam element is assumed to have an infinitely high maximum plastic hinge rotation. Thus, NONBAN will not stop the incremental analysis unless one longitudinal member reaches its maximum plastic hinge rotation.

The dead load is assumed to be carried equally by each girder. The live load is placed transversely such that the edge web of the bridge would be the most heavily loaded member. Thus, the transverse placement of the load depends on the number of girders, the spacing between the box girders and the number of traffic lanes on the bridge. For example, the transverse load configuration for a 5-girder bridge with spacing 15 ft and 5 lanes has its exterior wheel immediately above the edge web. On the other hand, the transverse load configuration for the same bridge with 6 lanes places the exterior wheel on the overhang 2.5 ft away from the edge web. In most cases, the exterior wheel line of the HS20 vehicle coincides with one of the edge webs of the bridge.

The AASHTO HS-20 truck load is incremented during the nonlinear analysis. The program stops the iteration process when one of the longitudinal beams reaches its maximum plastic hinge rotation. Transverse beams are assumed to have an infinite level of ductility and thus would not break although they may exhibit nonlinear behavior. This means that transverse failures in the slab or a box girder are considered as local failures. The live load factor LFu is obtained at the failure of the whole system as was explained in Appendix B for I-girder bridges. The critical member load factor LF_1 assuming linear elastic behavior, as well as the load factors when the nonlinear bridge reaches a displacement equal to span length/100, LF_{100}, span length/200, LF_{200}, and a span length/300, LF_{300}, are also determined by NONBAN.

The damaged bridge scenario assumes that one edge web has been totally damaged and can no longer carry any load. In NONBAN, this web is replaced by a very flexible beam while the rest of the bridge structure sustains the incremental loading. It is herein assumed that although the external web is damaged and its moment of inertias goes to zero, the box's torsional coefficient does not change. This scenario simulates a case where the prestressing tendons rupture but the boxes' integrity and shearing capacity remain intact.

Detailed Example

As an illustration of the procedure followed, the analysis of a 100 ft spread box girder bridge is given here. This bridge is designed to have 3 box girders spaced at 8 ft with two traffic lanes. The following design parameters are used:

bridge horizontal clearance = 28 ft
bridge depth = 78 in.
thickness of slab = 8 in
box width = 48 in
thickness of both top and bottom box flange = 5.5 in
web = 5 in
prestressing steel area = 5.44 in^2 with an effective depth of 74 in
effective prestressing force = 881 kips
slab concrete strength =3.5 ksi
box concrete strength = 5 ksi
Poisson's ratio = 0.2
reinforcement steel yielding stress = 60 ksi
#4 bar double-legged stirrups spacing 20 in are used as the shear reinforcement
a distribution reinforcement of 0.37 in^2 per ft is used in the top of the slab with an effective depth of 5.4 in

The sketch of the cross section for this bridge is shown in Fig. D.6a.

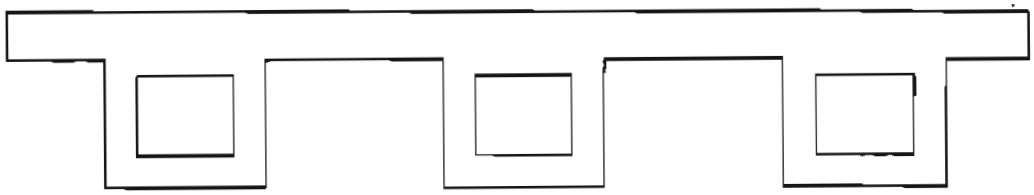

Fig. D.6a Cross section of the sample bridge.

The grillage mesh, which is shown in Fig. D.6b, consists of 115 elements with 66 nodes. The 60 longitudinal beam elements are placed 48 inches apart while 55 transverse elements are spaced at 120 inches. There are 6 elements of type II, and 4 elements of type III. Type IV constitutes a total of 27 elements and type V, 18 elements. The dead load on the longitudinal beams is 0.117 kips/in. The live load configuration is shown in Fig. D.5 indicated by the symbol x. The external wheel line coincides with an edge web where a line of the longitudinal grillage beams is located.

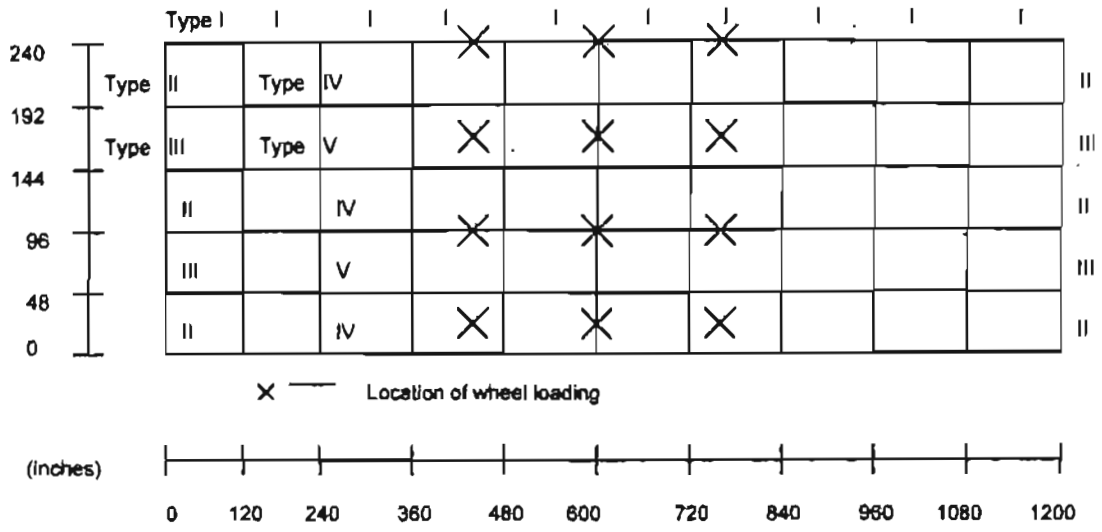

Fig. D.6b Structural discretization of the 100 ft bridge.

The elastic properties of the composite longitudinal grillage beam (half of the box section) are given in Table D.6. The elastic properties for element Type IV and V are also listed in Table D.6. The concrete of the girders has a strength of 5 ksi and has been converted to that of 3.5 ksi for slab.

Table D.6 Elastic properties of beam elements

	Type I	Type IV	Type V
Axial area (in^2)	1204	2538	960
Moment of inertia (in^4)	886500	2558000	5120
Torsional constant (in^4)	267600	479400	10240
Shearing area (in^2)	466	23.7	640

The moment versus plastic curvature relationship for each Type is represented as a 4-linear curve. The curve for a longitudinal beam element is as shown in Fig. D.7. The cracking moment for this element is 31000 in-kips The plastic hinge length is evaluated to be 51 in. The shear-shear force relationship, with nominal shear strength of 160 kips, is plotted in Fig. D.8. The moment versus plastic curvature relationship for element Type V is plotted in Fig. D.9 while its shearing nonlinear behavior is modeled as shown in Fig. D.10.

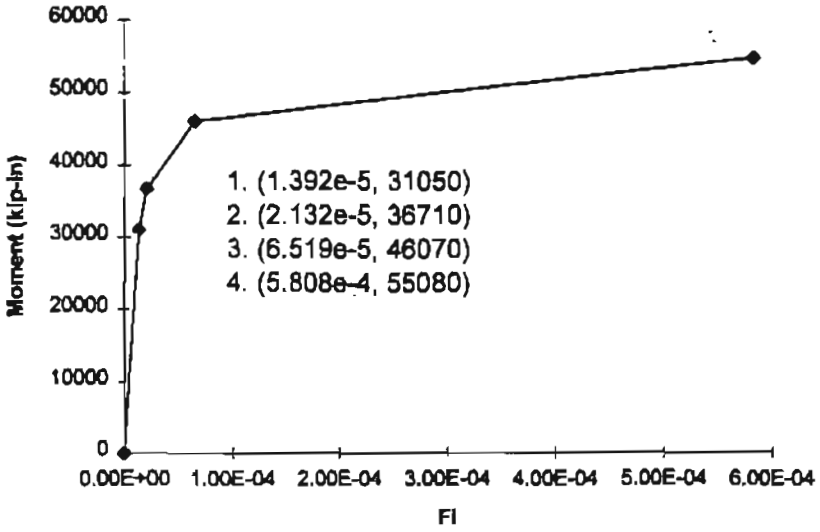

Fig.D.7 Moment-curvature relationship for Type I elements

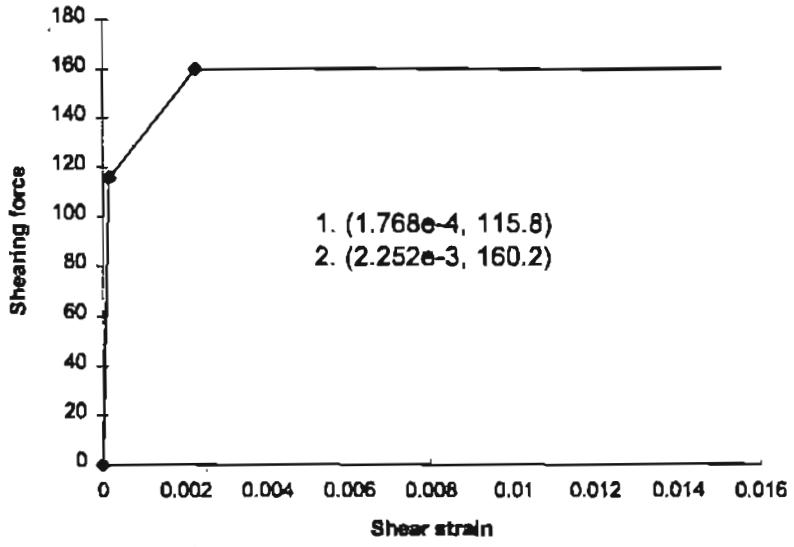

Fig. D.8 Shear-strain relationship for elements of Type I.

For the damaged bridge scenario, the external beam element where the exterior traffic wheel line is located is assigned a negligibly small moment of inertia. The maximum plastic hinge rotation is checked for the other longitudinal beam elements. This scenario assumes that the capacity of the box to contribute to the transverse distribution of

the load is not affected by the damage. Also, this damage model assumes that the torsional capacity of the box remains intact. A sensitivity analysis performed below studies the effect of losing the torsional capacity of the whole box as well as the bending capacity of the external web.

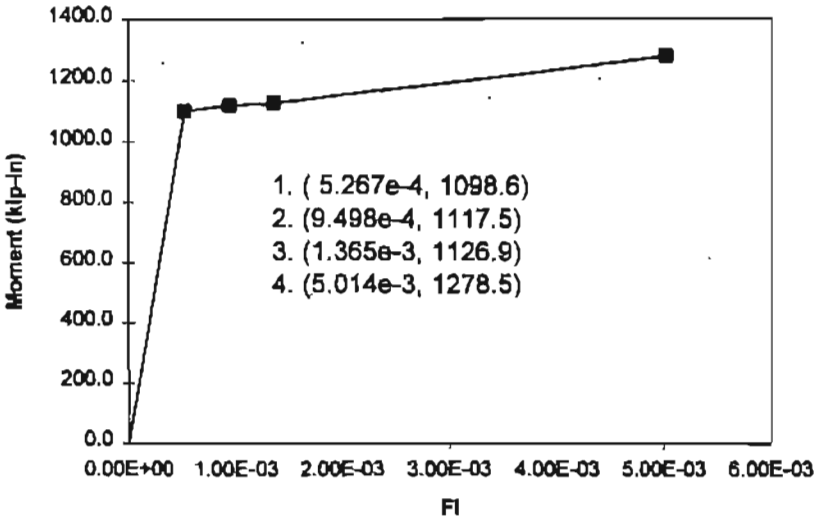

Fig. D.9 Moment-curvature relationship for Type V elements

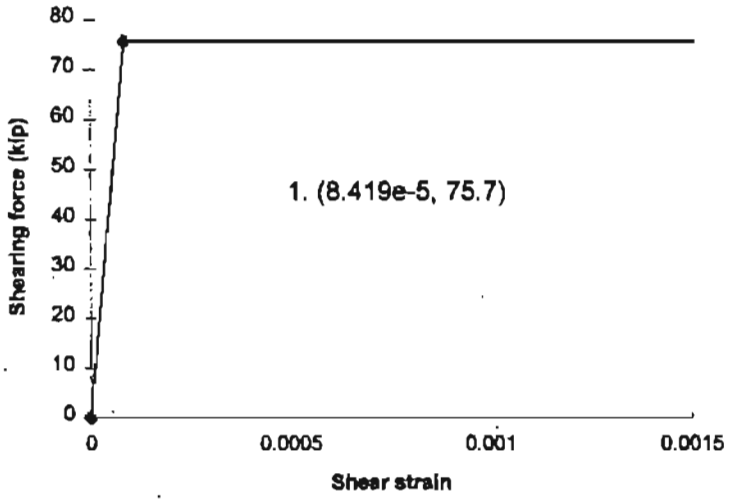

Fig. D.10 Shear-strain relationship for elements of Type V.

Using a linear elastic analysis of the grillage model, the moment due to dead load at the mid-span of the bridge in the external beam element is found to be 21060 kip-in. The corresponding live load moment due to the side-by-side HS-20 truck is equal to 6714 kip-in. The ultimate capacity of the beam element gives a value of 48850 kip-in. Therefore, we obtain a load factor LF_1 of 4.14 for critical member failure assuming linear elastic behavior.

The results of the nonlinear analysis for this sample bridge are given in Fig. D.11. The LFu for ultimate limit state is 5.24 with LF_{100} of 4.15, LF_1 of 4.14. For the damaged scenario (external web loses bending capacity), LF_d is found to be 3.74. Therefore, the redundancy ratios LF_u/LF_1, , LF_{100}/LF_1, and LF_d/LF_1 for the ultimate limit state, functionality limit state and damaged condition are 1.27, 1.00 and 0.90, respectively.

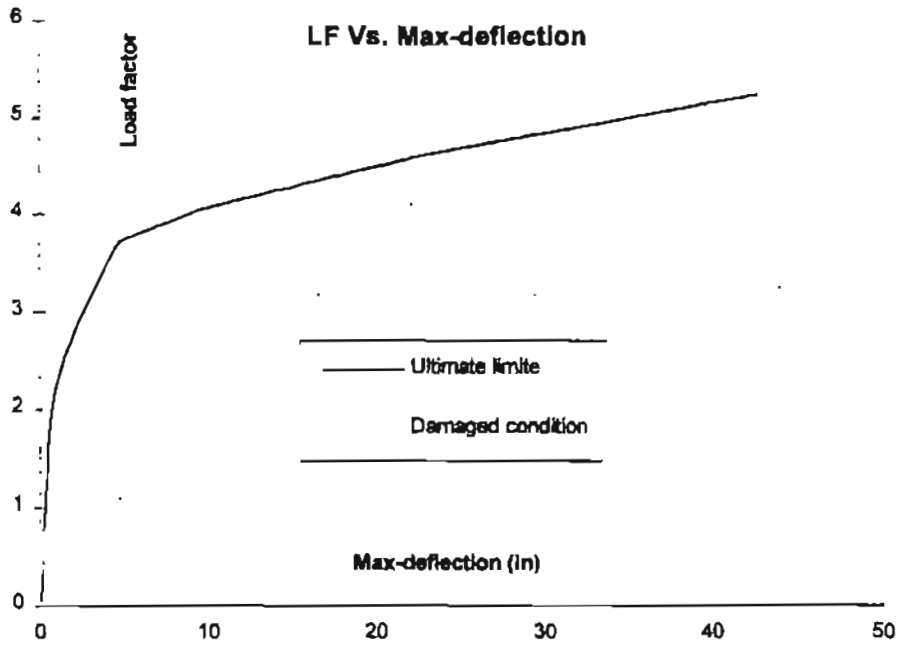

Fig. D.11 Load capacity for the sample bridge

Summary of Results

Calculations similar to those illustrated in the previous paragraph are performed for the 50 bridges designed in this Appendix. The corresponding LF ratios for these bridges with different spans and number of girders are given in Table D.7 for the spread box girder bridges. The calculations reported herein are for the cases where each bridge is fully loaded carrying as many lanes as it can fit. i.e. number of lanes = total width/12 ft. Table D.7 gives the average value obtained for each bridge configuration. For example, if two bridges with 3 beams at 15 ft are designed (one for 3 lanes and one for 4 lanes of traffic) then Table D.5 gives the average of the results of the analysis of these two bridges.

Table D.7 Results of nonlinear analysis for spread box girder bridges.

Table D.7.1 Load Factor Ratios for ultimate state (LFu/LF1)

Span	60 ft			100 ft			150 ft		
Beam spacing	8 ft	15 ft	25 ft	8 ft	15 ft	25 ft	8 ft	15 ft	25 ft
2 beams	1.27	1.20	1.17	1.24	1.15	1.13	1.21	1.17	1.17
3 beams	1.31	1.25	1.20	1.27	1.17	1.15	1.24	1.19	1.18
5 beams	1.34	1.28	1.22	1.36	1.34	1.21	1.27	1.26	1.19

Table D.7.2 Load Factor Ratios for damaged state (LFd/LF1)

Span	60 ft			100 ft			150 ft		
Beam spacing	8 ft	15 ft	25 ft	8 ft	15 ft	25 ft	8 ft	15 ft	25 ft
2 beams	0.76	0.68	0.61	0.71	0.63	0.55	0.62	0.57	0.50
3 beams	0.96	0.70	0.65	0.90	0.73	0.62	0.70	0.65	0.59
5 beams	0.98	0.85	0.82	0.92	0.82	0.77	0.95	0.83	0.71

Table D.7.3 Load Factor Ratios for functionality (LF100/LF1)

Span	60 ft			100 ft			150 ft		
Beam spacing	8 ft	15 ft	25 ft	8 ft	15 ft	25 ft	8 ft	15 ft	25 ft
2 beams	1.07	0.98	0.94	0.99	0.92	0.86	0.95	0.91	0.88
3 beams	1.07	1.00	0.97	1.00	0.92	0.90	0.96	0.91	0.89
5 beams	1.10	0.98	0.96	1.05	0.94	0.96	1.00	0.91	0.92

The results given in Table D.7 show that the LFu/LF1 varies within a relatively narrow range of 1.36 to 1.17. For a given spacing, some increase in LFu/LF1 is observed when the number of box girders is increased from two to five. The maximum increase is equal to 0.08. There is tendency for the LFu/LF1 ratio to decrease slightly as the span length increases. The maximum difference in LFu/LF1 due to changes in span length is 0.07.

The LFd/LF1 ratio varies within a range of 0.50 to 0.98. This ratio changes due to changes in the span length, number of beams and beam spacing. The LFd/LF1 ratio tabulated above assumes that the box does not lose its torsional rigidity when the external web of the external box is damaged. The values of LFd/LF1 shown above would decrease by 30% to 50% if we assume that the torsional rigidity of the box is also affected by the damage.

The change in LF100/LF1 with the number of beams is small. The difference is normally less than 0.04 except for one case where it is 0.06. Similarly, a change in the span length produces a maximum difference in LF100/LF1 of less than 0.10

If the 100 ft span bridge with 3 box girders at 15 ft is analyzed using three lanes of HS-20 trucks, then the results as shown in Table D.7 are produced by a value of LFu=5.37, LF100 =4.23, LFd =3.41 and LF1=4.70. The ratios become LFu/LF1= 1.14, LF100/LF1= 0.90 and LFd/LF1= 0.73. If the same bridge is loaded by only two lanes of traffic, then LFu is 6.85, LF100=5.53. and LF1 =5.08. Using a damage scenario where the torsion constant is set to zero then LFd is 3.25. The ratios become LFu/LF1= 1.24, LF100/LF1=1.09 and LFd/LF1= 0.64. The observation made herein is that loading the bridge by three lanes of traffic or two lanes of traffic produces a change in LFu/LF1 on the order of 9%. The change in LF100/LF1 is on the order of 20%. Notice that the LFd for the fully loaded bridge with full torsional capacity of the box maintained is still 5% higher than the LFd of the bridge with only two lanes if the torsional capacity is lost. The change in LFd/LF1 is of 12%.

If the 100 ft bridge with 3 box girders at 25 ft spacings with 5 lanes is fully loaded the LFu obtained is 5.77, LF100 is 4.55, LFd is 3.27 and LF1 is 5.00. The ratios are LFu/LF1=1.15, LF100/LF1=0.91 and LFd/LF1= 0.65. Loading the bridge with only two lanes of traffic produces LFu=7.87, LF100=5.95 and LF1=5.59. The ratios become LFu/LF1=1.41, LF100/LF1=1.06. The LFd/LF1 ratio obtained assuming that the torsion coefficient goes to zero becomes LFd/LF1=0.45. These ratios are respectively 23%, 17% and 30% different than the base case scenarios. These calculations illustrate the effect of the number of loaded lanes on the results of the nonlinear analysis. It should be noted however, that having 3 or more lanes equally heavily loaded is associated with a low probability of occurrence during the life of the bridge structure.

Results of the multi-box beam bridges (or adjacent boxes) are given in Table D.8. The results indicate that the ratio of LFu/LF1 ranges from 1.41 to 1.54 with an average of 1.49 for the bridges with 10 and 11 boxes. Similarly, the average LF100/LF1 value for the 100 and 11 box bridges is about 1.25 and the range varies from 1.19 to 1.32. The average of LFd/LF1 for the case where one exterior box is totally damaged is 1.20 for the 10 and 11 boxes. The value of LFd/LF1 decreases to 1.02 for the 8 box system.

Table D.8 Results for multi-box beam bridges

Span	boxes	lanes	LFu	LF100	LFd	LF1	LFu/LF1	LF100/LF1	LFd/LF1
70'	10	3	6.63	5.38	5.37	4.50	1.47	1.19	1.19
70'	11	3	6.98	5.74	5.60	4.57	1.53	1.26	1.23
70'	8	2	4.93	4.14	3.96	3.87	1.27	1.07	1.02
100'	10	3	7.99	6.85	6.47	5.66	1.41	1.21	1.14
40'	10	3	5.99	5.14	4.73	3.88	1.54	1.32	1.22

D.5. Reliability Analysis and Calibration of System Factors

Reliability Analysis

To perform the reliability analysis, the structural safety margin, Z, is defined as

$$Z = LF - LL \qquad (D.8)$$

where LF is the load factor corresponding to the capacity of a structure to carry live load, and equals R-D. R is the system resistance and D is dead load effect. LL is the maximum lifetime traffic live load effect. LL is a function of the sum of the static truck load effect L and the dynamic effect I. Both LF and LL are normalized herein and are given as multipliers of the static load effect of the standard HS-20 AASHTO truck load.

Redundancy in this study relates to the capacity of a bridge system to support load under a variety of defined limit states discussed above. The differences between the safety indices of the system and the safety index of the most critical member, namely,

$$\Delta\beta_u = \beta_{ult} - \beta_{member}$$
$$\Delta\beta_f = \beta_{funct.} - \beta_{member}$$
$$\Delta\beta_d = \beta_{damaged} - \beta_{member} \qquad (D.9)$$

are used to describe the redundancy of a bridge structure, where β_{member}, $\beta_{ult.}$, $\beta_{funct.}$ and $\beta_{damaged}$ are respectively the safety indices corresponding to critical member (i.e. the safety index corresponding to LF1), ultimate (i.e. the safety index corresponding to LFu), functionality (i.e. the safety index corresponding to LF100) and damage (i.e. the safety index corresponding to LFd) limit state conditions. $\Delta\beta_u$, $\Delta\beta_f$ and $\Delta\beta_d$ are therefore the corresponding measures of structural redundancy.

The reliability analysis is carried out on a Level II reliability program that can account for different types of probability distributions. The nonlinear behavior of the bridge system under all types of limit states are compared to the performance of its most heavily loaded members assuming linear elastic behavior. It is assumed that LL follows an extreme type I distribution with the coefficient of variation (COV) 0.19 while LF follows a lognormal distribution. The biases and COV's for the LF random variables are calculated for each design as explained in Appendix B.

As an illustration, the results of the 100 ft bridge with 3 box girders at 8 ft span are given here. The elastic analysis gives the critical member load factor of 4.14. The nonlinear ultimate capacity load factor is 5.24. Thus, the safety index for critical member failure is 3.20 while the safety index for ultimate limit state is 3.99. The difference between them is 0.79. Similarly, the differences in safety indices for functionality limit and damaged condition are 0.0 and -0.08.

The differences in reliability indices for the bridges designed and analyzed are listed in Tables D.9.1-D.9.3. These values shown are average values for each configuration.

Table D.9.1 Relative safety indices for span of 60 ft

Spacing	8 ft			15 ft			25 ft		
Indices	$\Delta\beta_u$	$\Delta\beta_d$	$\Delta\beta_f$	$\Delta\beta_u$	$\Delta\beta_d$	$\Delta\beta_f$	$\Delta\beta_u$	$\Delta\beta_d$	$\Delta\beta_f$
2 beams	0.85	-0.72	0.22	0.63	-1.08	-0.06	0.57	-1.49	-0.23
3 beams	0.93	0.12	0.25	0.78	-0.99	0.01	0.66	-1.25	-0.11
5 beams	1.05	0.18	0.39	0.91	-0.32	-0.10	0.68	-0.52	-0.13

Table D.9.2 Relative safety indices for span of 100 ft

Spacing	8 ft			15 ft			25 ft		
Indices	$\Delta\beta_u$	$\Delta\beta_d$	$\Delta\beta_f$	$\Delta\beta_u$	$\Delta\beta_d$	$\Delta\beta_f$	$\Delta\beta_u$	$\Delta\beta_d$	$\Delta\beta_f$
2 beams	0.72	-0.92	-0.04	0.46	-1.29	-0.28	0.42	-1.78	-0.50
3 beams	0.79	-0.08	0.01	0.52	-0.80	-0.30	0.47	-1.32	-0.36
5 beams	1.04	-0.08	0.16	0.98	-0.40	-0.22	0.65	-0.68	-0.17

Table D.9.3 Relative safety indices for span of 150 ft

Spacing	8 ft			15 ft			25 ft		
Indices	$\Delta\beta_u$	$\Delta\beta_d$	$\Delta\beta_f$	$\Delta\beta_u$	$\Delta\beta_d$	$\Delta\beta_f$	$\Delta\beta_u$	$\Delta\beta_d$	$\Delta\beta_f$
2 beams	0.60	-1.34	-0.16	0.51	-1.56	-0.30	0.50	-1.93	-0.39
3 beams	0.67	-0.90	-0.15	0.55	-1.13	-0.30	0.52	-1.43	-0.38
5 beams	0.78	0.07	0.00	0.73	0.35	-0.30	0.55	-0.87	-0.30

Based on studies of steel and concrete I-beam bridges (see Appendices B and C), it was observed that bridge systems that are recognized to have adequate levels of redundancy produced a relative system index $\Delta\beta_u$ equal to 0.85 or higher; $\Delta\beta_d$ equal to -2.70 or higher; $\Delta\beta_f$ equal to 0.25 or higher. These target β's were extracted from typical four-girder systems accepted by bridge engineers as "adequately redundant". It can be seen that most of the design examples for the spread box concrete girder bridges in Table 9 cannot meet the requirements for redundancy for the ultimate and functionality limit states. This is because the relative stiffness of the boxes causes less reserve capacity for the system compared to I-beam system of the same span and geometry. Another casue of the difference is the fact that the tables herein assume that the whole width of the bridge is fully loaded while the results shown in Appendices B and C assume only two lanes of traffic. The damage scenario seems to satisfy the redundancy requirements because it is herein assumed that the damage to the outer web of the external box girder does not produce a reduction in the torsional stiffness of the box. This would simulate a situation where the cables of the outer web snapped without heavily damaging the concrete of the box or the shearing reinforcement. Thus, the torional coefficient of the box remains is not reduced.

In general, bridges will have high levels of redundancy when main members are more closely spaced. Also, the level of redundancy decreases as the span length increases. In the present approach, the presence of high redundancy as evidenced by large $\Delta\beta$ is used to justify the reduction of the member dimensions. Low redundancy as evidenced by small $\Delta\beta$ requires that members be strengthened to increase system reliability.

Results of the multi-box beam bridges are shown in Table D.10 below. The results indicate that in general the multi-box beam bridges satisfy the preset requirements for redundancy even in the damage situations. This is because the large number of tightly spaced boxes used in such designs ensures a relatively high level of bridge safety even when one box is fully damaged.

Table D.10 Results for multi-box beam bridges

Span	boxes	lanes	$\Delta\beta_u$	$\Delta\beta_f$	$\Delta\beta_d$
70'	10	3	1.37	0.63	0.89
70'	11	3	1.51	0.80	0.99
70'	8	2	0.85	0.24	0.35
100'	10	3	1.19	0.65	0.73

Development of the Redundancy Factors

To reward redundant designs and penalize nonredundant designs, a system factor is proposed to be included in the LRFD member check equation such that:

$$\phi_s \phi R = \gamma_D D + \gamma_L L(1+I) \qquad (D.10)$$

where ϕ_s is the system factor, ϕ is the resistance factor, γ_D is the dead load partial coefficient and γ_L is the live load partial coefficient.

The system factors for the cases analyzed in this Appendix are listed in Tables D.11 for spread box beam bridges and in Table D.12 for multi-box (adjacent) beam bridges.

Table D.11.1 System factors for span of 60 ft

Spacing	8 ft			15 ft			25 ft		
ϕ_s	ult.	funct.	dam.	ult.	funct.	dam.	ult.	funct	dam.
2 beams	1.00	0.99	1.38	0.96	0.94	1.32	0.95	0.91	1.24
3 beams	1.01	1.00	1.52	0.99	0.96	1.34	0.97	0.94	1.27
5 beams	1.04	1.02	1.60	1.01	0.94	1.47	0.97	0.93	1.41

Table D.11.2 System factors for span of 100 ft

Spacing	8 ft			15 ft			25 ft		
ϕ_s	ult.	funct.	dam.	ult.	funct.	dam.	ult.	funct	dam.
2 beams	0.98	0.95	1.30	0.93	0.91	1.24	0.93	0.88	1.16
3 beams	0.99	0.96	1.41	0.95	0.91	1.32	0.94	0.90	1.23
5 beams	1.04	0.99	1.45	1.02	0.93	1.37	0.97	0.93	1.33

Table D.11.3 System factors for span of 150 ft

Spacing	8 ft			15 ft			25 ft		
ϕ_s	ult.	funct.	dam.	ult.	funct.	dam.	ult.	funct	dam.
2 beams	0.96	0.94	1.21	0.95	0.92	1.17	0.95	0.90	1.12
3 beams	0.97	0.94	1.26	0.95	0.92	1.24	0.95	0.91	1.19
5 beams	0.99	0.96	1.41	0.98	0.92	1.33	0.96	0.92	1.26

Table D.12 System factors for multi-box beam bridges

Span	boxes	lanes	ultimate	functionality	damaged
70'	10	3	1.10	1.07	1.69
70'	11	3	1.13	1.11	1.71
70'	8	2	1.00	1.00	1.60
100'	10	3	1.21	1.23	1.68

It is seen that bridges have higher redundancy when the girders are closely spaced and when the system has more girders. A system factor above 1.0 indicates that the system has sufficient level of redundancy and is "rewarded" by allowing a lower safety factor than normally allowed.

D.6. References

D.1. Hambly, E. C., "Bridge Deck Behaviour", Chapman and Hall, Ltd., London, 1976.

D.2. Zokaie, T., Osterkamp, T. A., and Imbsen R. A., "Distribution of Wheel Loads on Highway Bridges", Final Report, NCHRP project 12-26/1, March 1991.

D.3. Park, R., and Pauley, T., "Reinforced Concrete Structures", Wiley and Sons, New York, 1975.

D.4. Corley, W. G. "Rotational Capacity of Reinforced Concrete Beams", J. Struct. Div., ASCE, **92**(5), 121-146, 1966.

D.5. Ghosn, M., and Moses, F., "Redundancy in Highway Bridge Superstructures", NCHRP 12-36, TRB, Washington, DC, March, 1994.

D.6. Mirza, M. et al. "An Experimental Study of Static And Dynamic Response of Prestressed Concrete Box Girder Bridges." *Can. J. Civ. Engrg.*, Ottawa, Canada, **17**(3), 481-493, 1990.

D.7. Lin T. Y., and Burns N. H., "Design of Prestressed Concrete Structures", Wiley and Sons, New York, 1981.

APPENDIX E

REDUNDANCY IN BRIDGE SUBSTRUCTURES

Many bridge failures occur due to failures in substructure elements. Such failures occur due to scour, earthquakes and accidents such as collision by trucks, ships and debris with bridge supporting elements. Redundancy of substructural elements is currently considered in the AASHTO Standard Specifications for Highway Bridges under the provisions for seismic design. For example, the specifications recommend different response modification factors depending on the type of the substructure and the number of columns in a bent. The basis of these recommendations is not, however, clear. In addition, the specification does not require the consideration of redundancy for other than seismic design.

The AASHTO LRFD Bridge Specifications recommend the consideration of member ductility and the presence of redundancy while checking the strength limit state of all bridge members including substructure elements. The specifications' recommendations, however, are clearly subjective and the specifications recognize the importance of continued research to provide improved quantification of ductility and redundancy and their interaction in bridge structural systems.

The other parts of this report focus on the behavior of bridge superstructures. In this study, bridge superstructures are classified based on their material properties and their topology in order to propose redundancy factors that give an objective measure of their levels of redundancy. System modification factors are then added to the member design-check equations to penalize superstructures that do not provide adequate levels of system redundancy. These factors are calibrated using reliability-techniques to ensure that bridges provide adequate levels of superstructure system safety.

Research is needed to extend the approach proposed for bridge superstructures to also include substructures. The proposed research will develop a systematic approach for considering substructure redundancy and ductility during the design and load capacity evaluation of highway bridges. The proposed criteria should be based on the consequences of a failure of a substructural element to the structural integrity and the functionality of the complete bridge system. Element failures could be brittle such as those produced by a sudden failure due to scour and collisions, or they could be ductile such as those that may occur under the effect of seismic loads.

The issue of substructural redundancy has not been addressed in this project which was only concerned with bridge superstructures. The general concepts developed herein, however, can be easily extended to study the effect of damage to substructural elements on the load carrying capacity of the complete bridge system.

This appendix is based on the MS thesis of Mr. J. Oliver of the Department of Civil Engineering of the University of Pittsburgh [E-1]. The object of this appendix is to study the factors affecting substructural redundancy by showing the effects of removing center supports from a continuous bridge system. The procedure is illustrated by looking at a particular two-span, four-girder bridge configuration and studying the changes in member loading and bridge response following hypothetical failure incidents of the loss of interior supports. The residual capacity expressed in terms of the bridge live load capacity remaining following such a failure incident is analyzed. The results are compared for different substructure configurations. Example of substructure configurations studied include individual piers under each interior support, two piers each carrying a pair of interior supports, and a single pier supporting all four interior supports. The analyses performed in this section assume linear-elastic behavior of the structure, although nonlinear behavior can be used in the future. Also, only a grid model is assumed although a 3-dimensional analysis could be used in the future to more accurately model the piers and the interaction between piers, caps and superstructure. Finally, the loadings used in

this example are the same as the AASHTO design loads (i.e. either the HS-20 truck or the distributed lane load). These loads do not correspond to actual truck configurations and could in the future be replaced by more realistic configurations or by configurations that would produce the same effects as the maximum lifetime loads.

The bridge will be analyzed using the program GRIDPROG which was developed for this research project. GRIDPROG is a general purpose grid analysis program which can perform an elastic analysis to solve for deflections and member bending moments. GRIDPROG can simultaneously solve a grid system for different load cases. Such cases may consist of joint loads, distributed member loads, and moving loads. These load cases can be enveloped and combined to find the effects of support failures. Unlike NONBAN, GRIDPROG is only capable of performing a linear elastic of a grid model.

E.1 BRIDGE AND LOADING LAYOUT

E.1.1 Bridge Profile

The bridge analyzed is example II/3A taken from the Highway Structures Design Handbook [E-2]. A typical section of this bridge can been seen in Figure E-1. The bridge is formed by two composite continuous spans of 70 ft. each. There are four W30x108 50 ksi main girders with 1"x12" bottom cover plates spanning 11 ft. and 3/8"x8" top cover plates spanning 4 ft. from either side of the center support. The concrete deck is 7" thick with a compressive strength of 4 ksi and a modular ratio (n=8). In the negative moment region there are 14 No. 6 longitudinal bars at 6-in spacing.

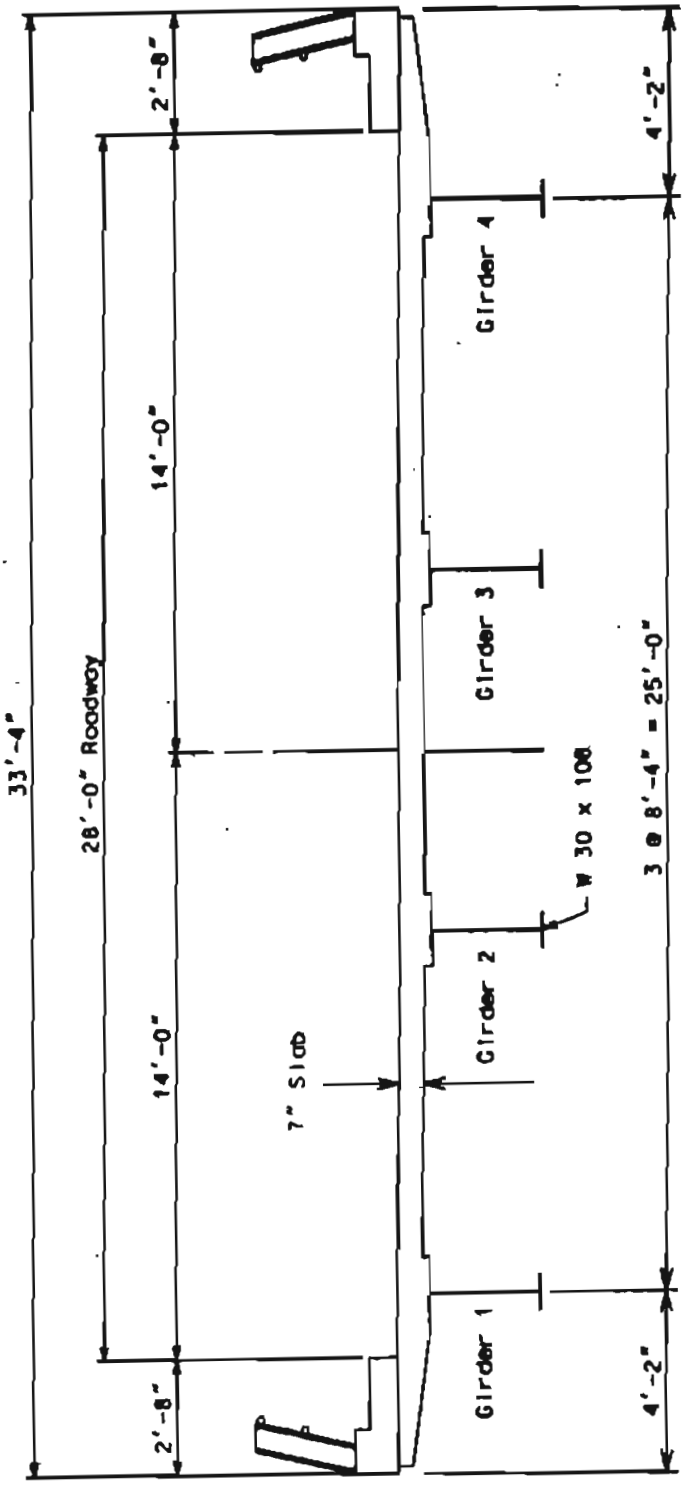

Figure E-1 Example Bridge Cross Section

Figure E-2 shows one beam's profile with the cover plates. The beam cross sectional properties are presented in reference [E-1].

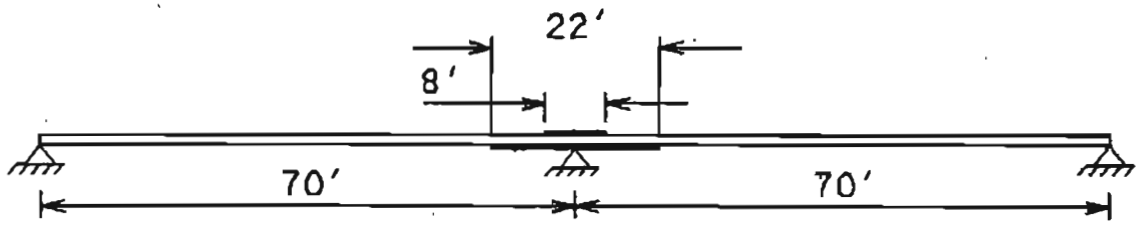

Figure E-2 Two-Span Beam Model

E.1.2 One-Dimensional Analysis.

The following results were obtained from analyzing the bridge system as a single beam. Analyzing the beam for Dead Load, the moment diagram in Figure E-3 is obtained using the program GRIDPROG.

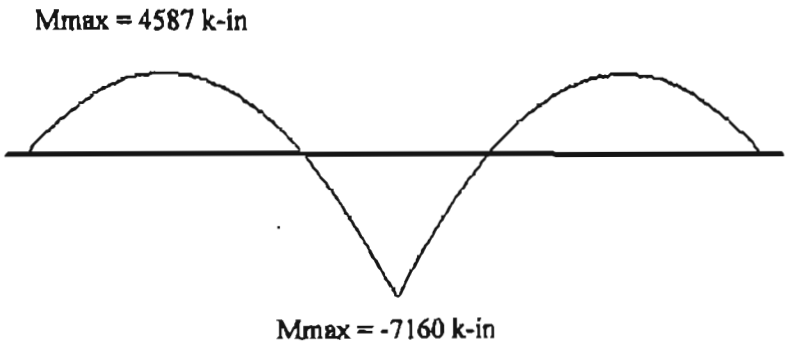

Figure E-3 Dead Load Moment Diagram

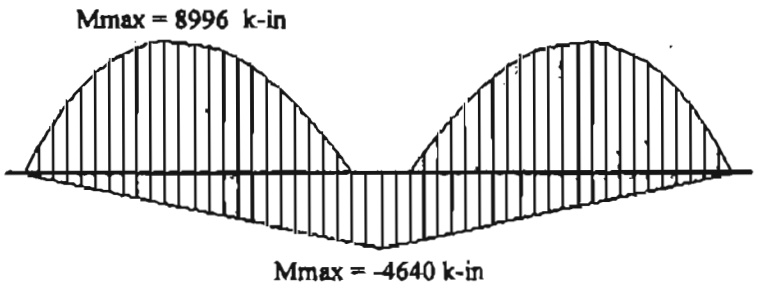

Figure E-4 Live Load Moment Envelope due to Truck Loading

The moment envelope for the beam due to the AASHTO HS-20 truck loading including impact and the load distribution factor is shown in Figure E-4. Figure E-5 shows the moment envelope due the AASHTO equivalent lane loading including impact and distribution factors.

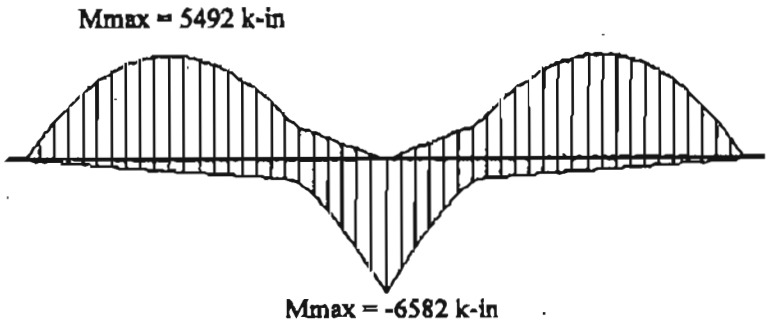

Figure E-5 Live Load Moment Envelope due to Lane Load

Combining Figures E-4 and E-5, the total live load moment envelope is obtained as shown in Figure E-6.

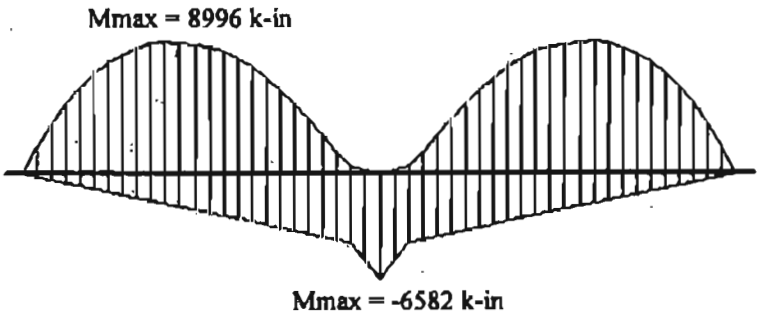

Figure E-6 Live Load Moment Envelope Diagram

The maximum positive moment for Figure E-6 occurs at 28 ft from the end supports with a value of 8996 kip-in and is due to the truck loading. The maximum negative moment occurs at the interior support with a value of -6582 k-in. and is due to the lane loading and its associated point load in each span.

During the analysis performed in reference [E-2] a prismatic beam model is assumed. The maximum positive moment was found to be 750 k-ft (or 9000 k-in) and the maximum negative moment was found to be -601 k - ft (or 7212 k-in). The positive moments are almost identical but they differ for the negative moment region. The negative moment shown in Figure E-6 is smaller than the negative moment taken from design example II/3A. This is because the negative moment from Figure E-6 is obtained from a non-prismatic beam with cover plates over the negative moment region. In the negative moment region, the deck does not contribute to the stiffness of the beam. If a prismatic beam is assumed as was done in reference [E-2], more moment is transmitted to the prismatic beam's negative moment region causing a larger negative moment than for the actual beam with different cross-section properties.

E.1.3 Grid Analysis and Loading Placements

Grid Layout

The grid model used and analyzed by GRIDPROG is shown in Figure E-7. The model has 80 joints and 121 members. The joint numbers are circled. There are 12 support joints all supported in the positive Z direction. When placing the loadings, it was necessary to identify extra joints at the locations of the loads so that joint loads could be used.

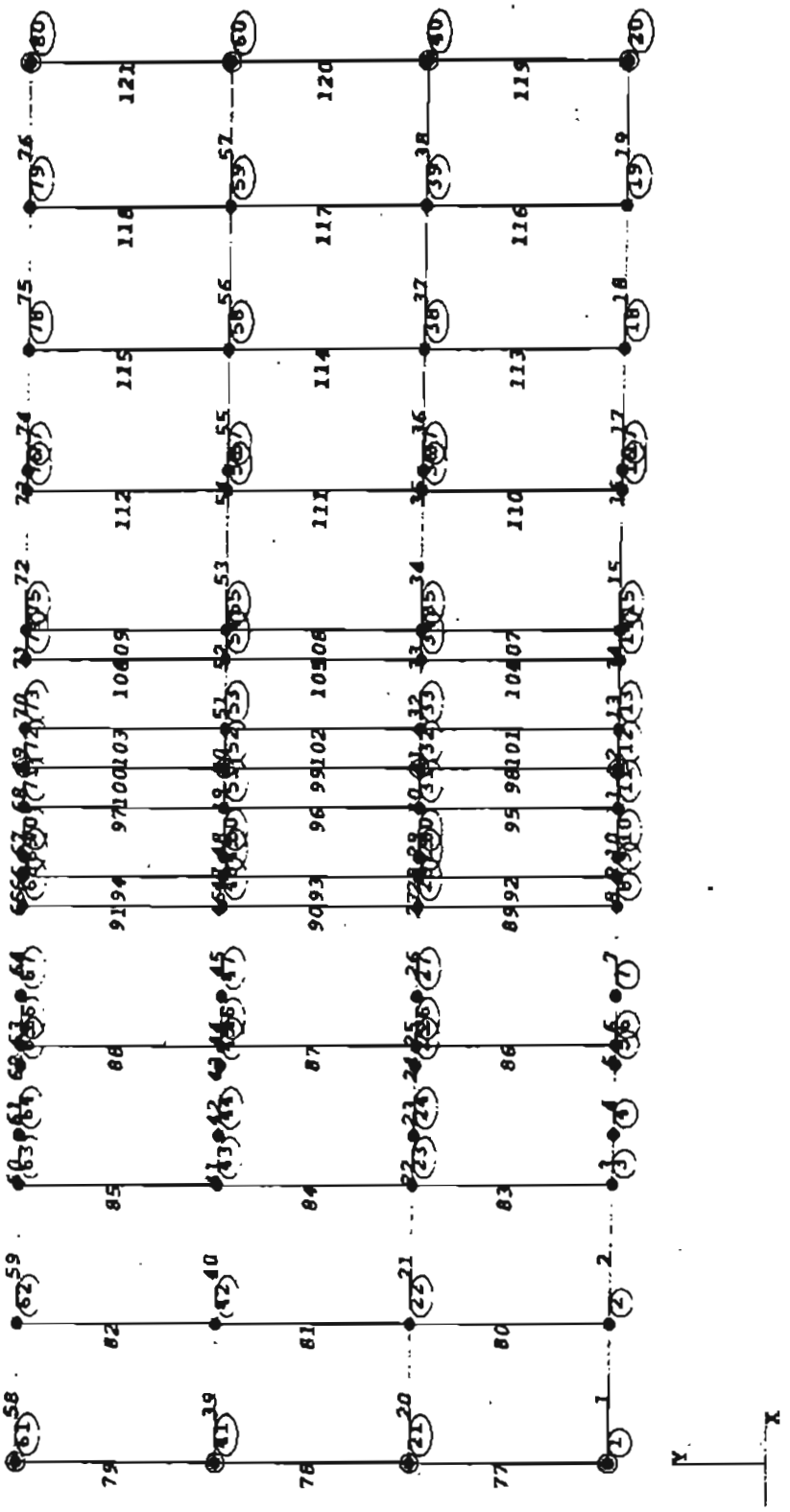

Figure E-7 Intact Grid Model

Section Properties

Each longitudinal girder is made up of 3 different cross sectional properties and 1 material property. Figures E-8 and E-9 show two typical cross sections of the longitudinal girders. In addition to the properties of the main girders, properties of the transverse beams representing the contribution of the slab to transverse distribution of the loads are also calculated. For the transverse properties, studies[E-3] have been done trying to determine the best approximation for the effective width. Here, the effective slab width will be assumed to be 1/2 the sums of the widths of the adjacent sections.

$$b = \frac{(S1 + S2)}{2} \qquad (E.1)$$

where S1 is one width of an adjacent section, and S2 is the other adjacent width.

Grid Loading Placements

The final step, in preparing the design model to be analyzed, is to determine the placement of the loadings to obtain maximum moment. The most critical design points for the bridge using traditional design methodology are the point at 28 ft from the end support for positive bending and the point above the interior support for negative bending. For the damaged scenarios, the point of maximum positive moment will vary for each girder. However, to simplify the analysis procedure and to reduce the effort required to find the most critical points for the damaged scenarios, it is herein assumed that a position of 28 ft. from the end support will be a good representation for the bridge system and this will be the only point considered for the positive moment region. For the grid model, the applied loadings must also be transversely

positioned to produce maximum bending moment. In this analysis, the loads will be positioned transversely so that girder 1 has its maximum possible loading.

Figure E-10 shows the plan view of the grid system including the sidewalk area. Figure E-11 shows the placement of the AASHTO Truck Loading on the grid system to produce maximum bending moment for the intact structure. The upper picture shows the load positioning to produce maximum positive moment and the bottom shows the positioning to produce maximum negative moment due to the AASHTO Truck Loading. The adjacent trucks are positioned 48" apart with a minimum distance of 24" to the curb in a 12 foot wide design lane as interpreted from AASHTO [E-4].

Figure E-12 shows the positioning of the AASHTO Lane Loading and its associated point loads to produce maximum bending moment on the grid system. The lane load is positioned such that its edge is against the sidewalk and there is a 24" spacing between the two lane loadings. The upper picture shows the load positioning to produce maximum positive moment and the bottom shows the positioning to produce maximum negative moment due to the AASHTO Lane Loading and its associated point loads. For positive moment, only one point load is considered. One in each span is considered for negative moment. The following assumptions were made when placing the lane loading. These are the assumptions normally used in engineering practice as interpreted from the AASHTO code [E-4]:

- The 10 foot wide load lane is assumed to be placed inside a 12 foot wide design lane.
- There is no minimum distance between the lane load and the curb.
- There is a minimum distance between adjacent lane loadings of 2 feet.
- The associated point loading is assumed to be a line load perpendicular to the longitudinal direction.
- The line load is equal to the point load divided by the load lane width.

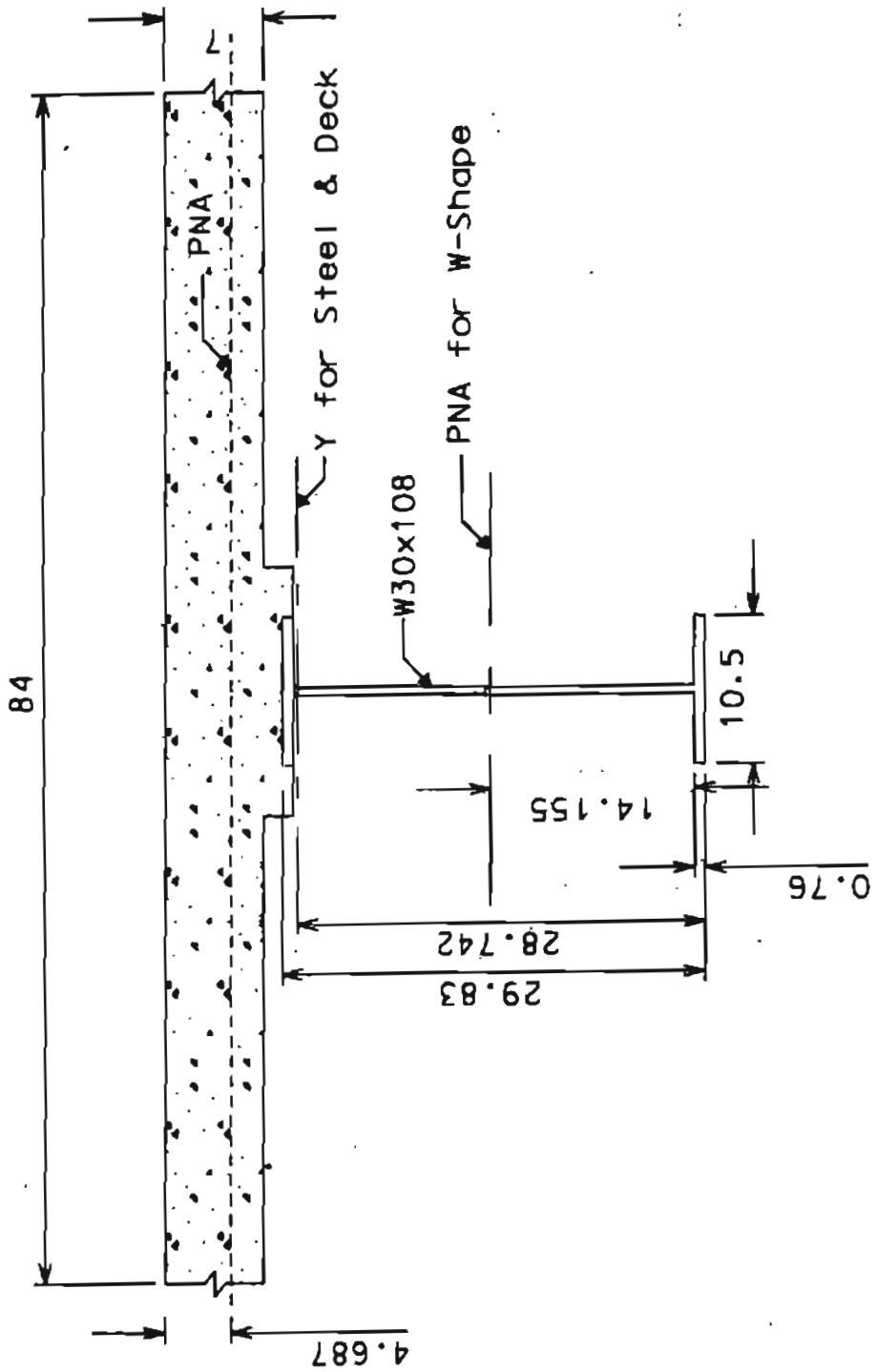

Figure E-8 Positive Moment Region Section 28 ft. from End Support.

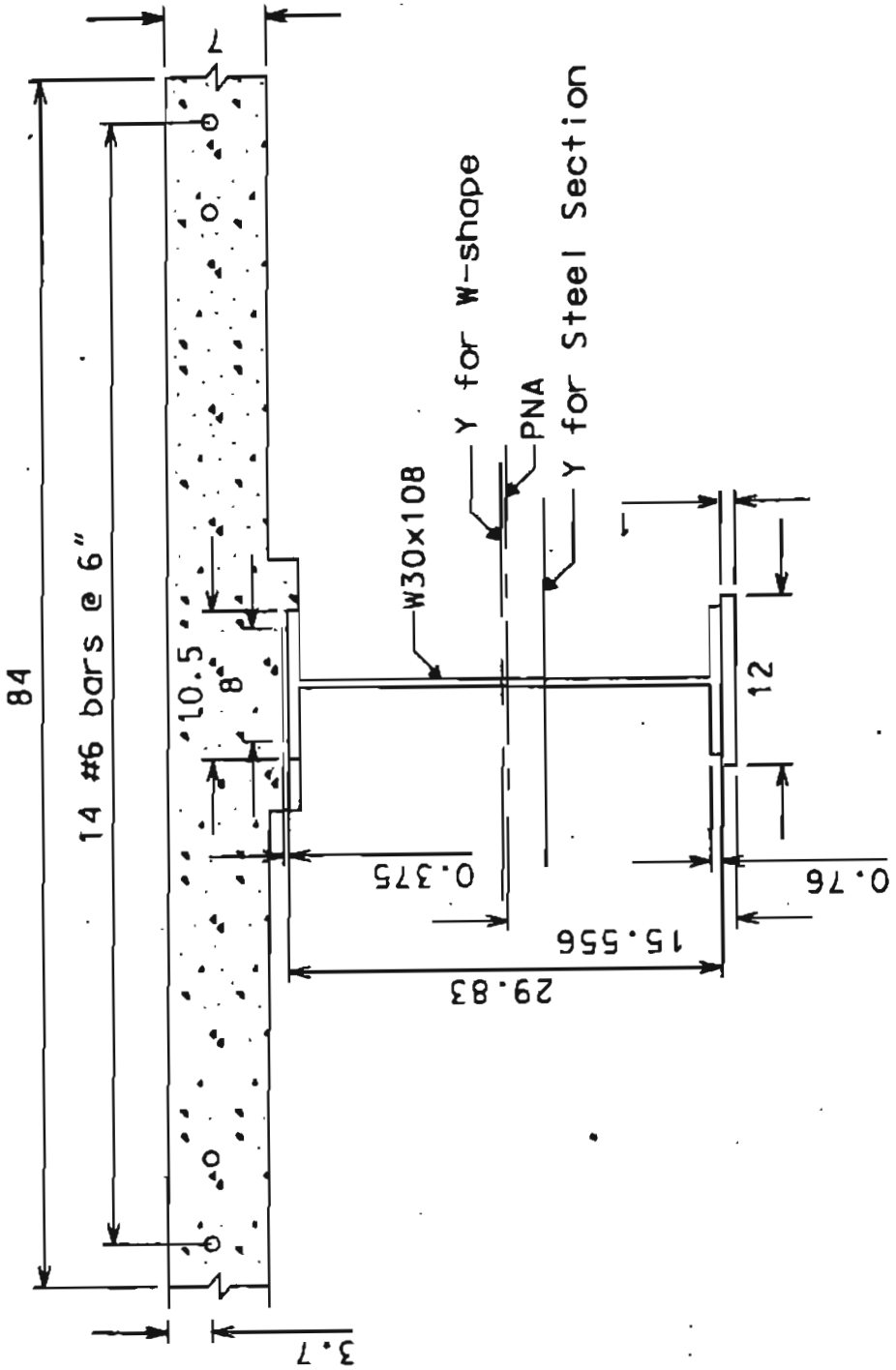

Figure E-9 Negative Moment Region Section 4 ft from the Interior Support

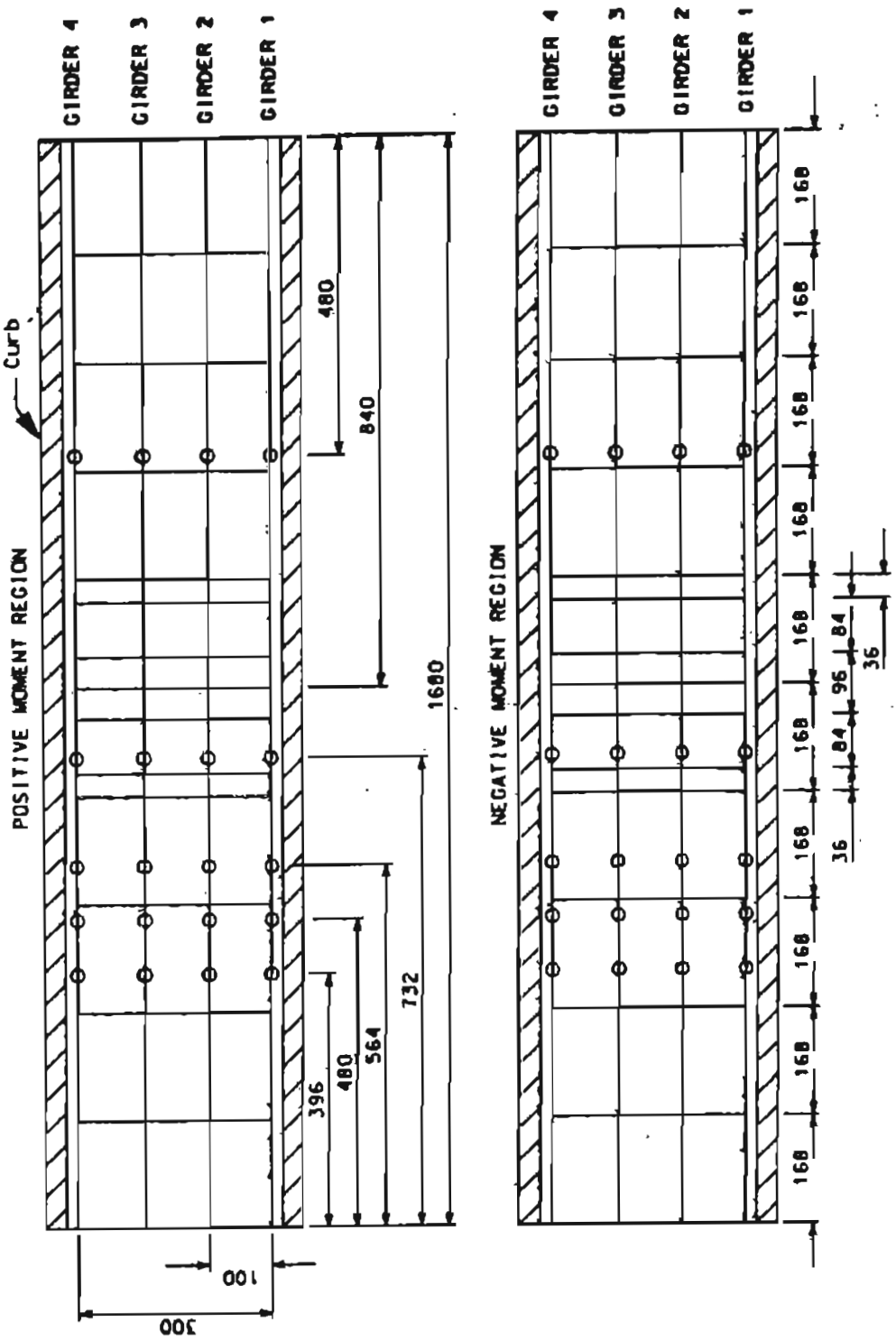

Figure E-10 Plan View of Grid Layout

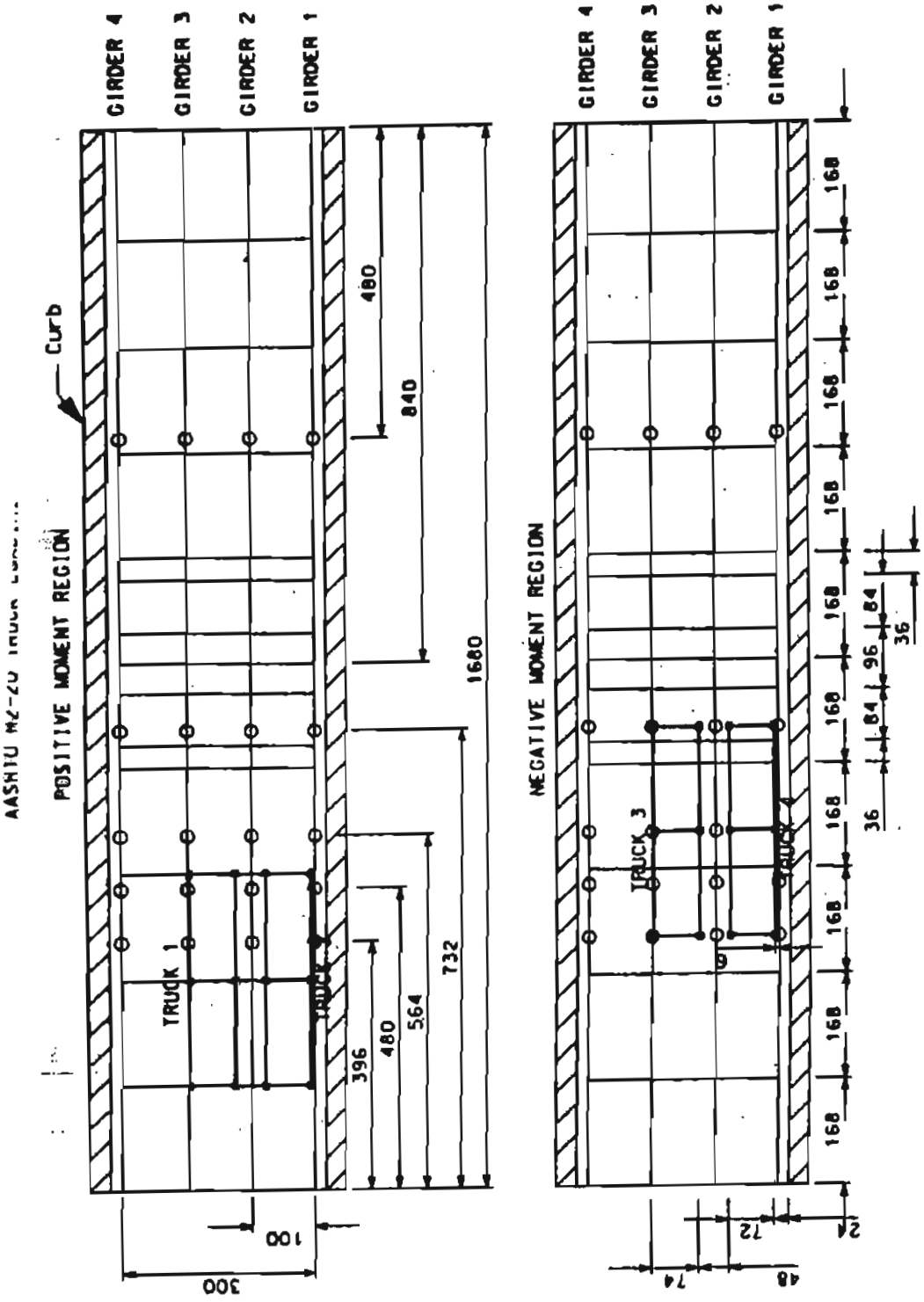

Figure E-11 AASHTO Truck Loading Layout

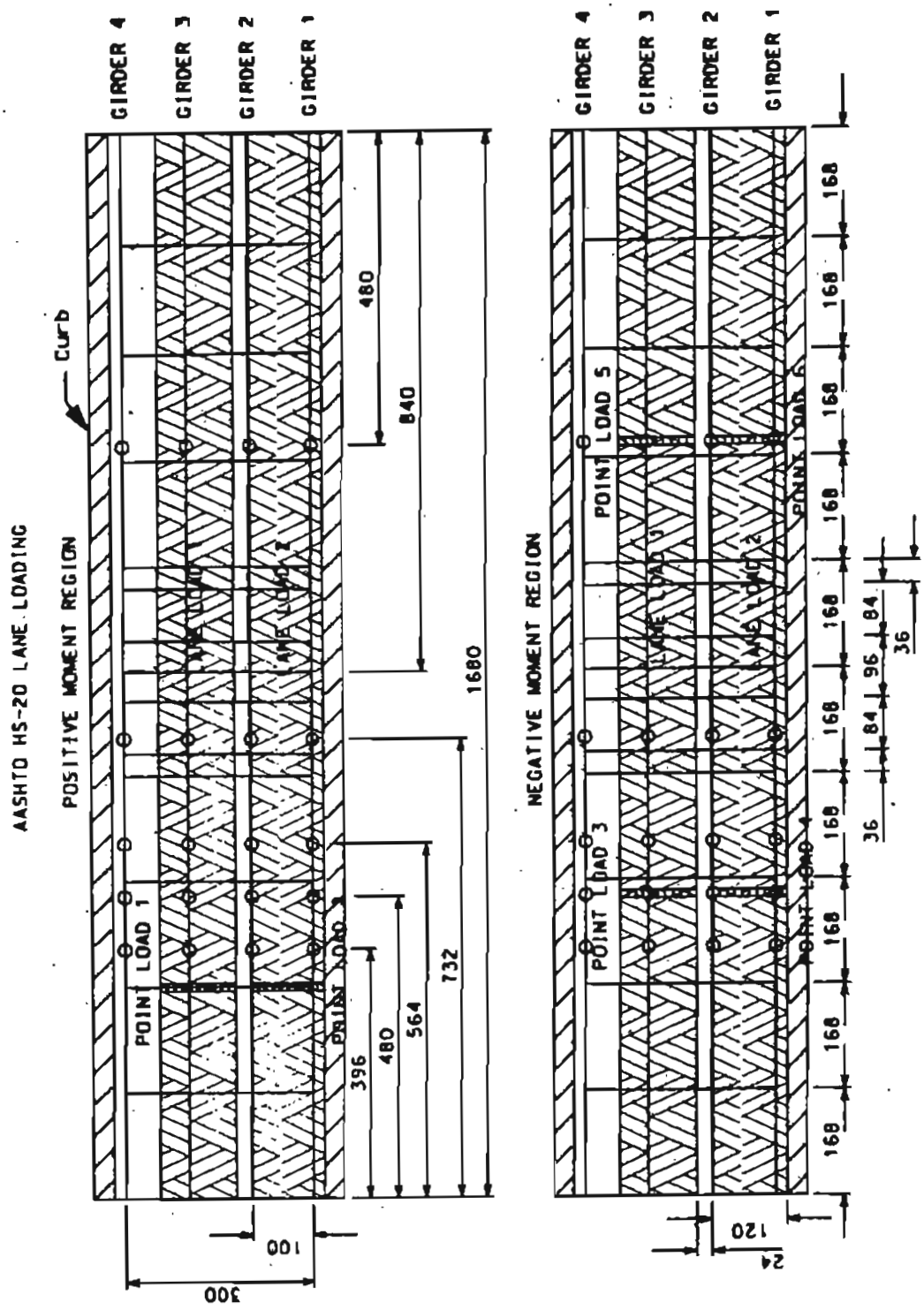

Figure E-12 AASHTO Lane Loading Layout

E.2 EFFECT OF SUPPORT FAILURES BY ELASTIC ANALYSIS

E.2.1 Unfactored Moments

To illustrate the effects of removing center supports from the bridge described in section E.1, the resulting unfactored dead plus live load bending moments from the various failure scenarios will be presented in Tables E-1 and E-2. The following support failures are considered: a) failure of the interior support under girder 1, b) failure of the interior support under girder 2, c) failure of the interior supports under girders 1 and 2, d) failure of the interior supports under all girders.

Table E-1 gives the bending moments at 28 ft. from the end support in the positive moment region are presented for the various scenarios. Table E-2 gives the bending moments at the interior support for the various failure scenarios. In Table E-1a and E-2a, the dead load moments for the positive and negative moment regions respectively are presented. Tables E-1b and E-2b present the live load moments and Table E-1c and E-2c present the combined dead and live load moments for the positive and negative moment regions respectively. In Tables E-1 and E-2, column 2 represents the initial intact moments which are denoted as Mo.

From Table E-1 and Table E-2, it can be seen that girder 1 and girder 2 are the most critical girders since they have the highest moments due to the applied loading conditions and induced support failures. Also, one can see that removing all the supports produces the greatest change in the bending moments. These results will be discussed further in Section E.2.4.

Table E-1 Bending Moments at 28 ft. from the End Support

Table E-1a Dead Load Bending Moments at 28 ft. from the End Support

Unfactored Dead Load Moments (k-in)

Girder	Intact, Mo	Support 1 removed	Support 2 removed	Support 1&2 removed	All removed
1	4655	4600	4841	6410	20050
2	4655	5621	4459	7695	20050
3	4655	5026	4712	7277	20050
4	4655	4058	4755	2547	20050

Table E-1b Live Load Bending Moments at 28 ft. from the End Support

Unfactored Live Load Moments Including Impact (k-in)

Girder	Intact, Mo	Support 1 removed	Support 2 removed	Support 1&2 removed	All removed
1	8439	8415	8515	9180	14671
2	7882	8297	7802	9174	12975
3	5805	5964	5828	6915	10039
4	2216	1961	2258	1322	5530

Table E-1c Dead + Live Load Bending Moments at 28 ft. from the End Support

Unfactored Dead + Live Load Moments Including Impact (k-in)

Girder	Intact, Mo	Support 1 removed	Support 2 removed	Support 1&2 removed	All removed
1	13093	13016	13356	15590	34721
2	12537	13918	12261	16869	33025
3	10460	10990	10540	14193	30089
4	6871	6019	7012	3869	25580

Table E-2 Bending Moments at Interior Support

Table E-2a Dead Load Bending Moments at Interior Support

Unfactored Dead Load Moments (k-in)

Girder	Intact, Mo	Support 1 removed	Support 2 removed	Support 1&2 removed	All removed
1	-7160	-1915	-8466	6678	31329
2	-7160	-13442	-3650	-2303	31329
3	-7160	-5052	-9411	-20603	31329
4	-7160	-6515	-6747	862	31329

Table E-2b Live Load Bending Moments at Interior Support

Unfactored Live Load Moments Including Impact (k-in)

Girder	Intact, Mo	Support 1 removed	Support 2 removed	Support 1&2 removed	All removed
1	-5481	-1836	-6440	4255	21488
2	-5623	-9988	-3045	-2093	18580
3	-4739	-3273	-6393	-14296	15703
4	-1594	-1146	-1290	4084	13208

Table E-2c Dead + Live Load Bending Moments at Interior Support

Unfactored Dead + Live Load Moments Including Impact (k-in)

Girder	Intact, Mo	Support 1 removed	Support 2 removed	Support 1&2 removed	All removed
1	-12641	-3751	-14906	10932	52817
2	-12783	-23430	-6695	-4396	49908
3	-11899	-8325	-15804	-34899	47032
4	-8754	-7661	-8037	4945	44536

E.2.2 Deflections

The effects of the various support failures on the deflections are also calculated. The effects will be illustrated in terms of the ratio of span length to deflections. Before proceeding with the deflection results, a discussion of the procedure used in the Highway Structures Design Handbook [E-2] will be discussed. The procedure presented is for finding the deflections of continuous beams.

From the Highway Structures Design Handbook [E-2], the following procedure for finding the dead load deflections is presented. The dead load deflections must be computed in two steps. The first step involves the deflections caused from the weight of the concrete slab along with the weight from the stringer and framing details. Since there is no composite action from the deck until it is dry, the slab, framing, and stringer details act on the steel section alone. Therefore, the dead load deflections from this initial case are calculated based on the moment of inertia of the steel section only. After the deck stiffens, the deck and steel section act together compositely. Therefore, when calculating the deflections caused by the weight of the curb, parapets, railing and wearing surface, an increased moment of inertia from the composite section must be used. When calculating the increased moment of inertia, a modular ratio of $3n$ [E-2] is used to allow for creep.

When calculating deflections from live load, the Highway Structures Design Handbook uses the following procedure. The live load will consist of two lanes of truck loading which are evenly distributed among the four girders. The deflections will be found for live load plus impact. No distribution factors will be used. Since the deck is composite, it is assumed that the deflections in all four girders will be equal.

The maximum live load deflection from design example II/3A is 0.902 in at 28 ft. from the end support. The deflection-span ratio is 1/930 which is well within the allowable 1/800 value.

The deflections from the grid analysis are presented next. Since the dead load deflections are accounted for by the camber in the girders, only the deflections for the unfactored live load on the grid structure will be presented. The dead load is uniform for each girder in both the grid and beam analysis. Therefore, the same deflections will result from a grid analysis as resulted from a beam analysis.

The grid analysis for live load deflections will provide the actual distribution factors. The beam analysis of reference [E-2], calculated the deflections by assuming that each girder received equal live load. This will not produce the same results as those of the grid analysis. The grid system will be loaded just as was done to obtain the results for the live load moments.

The ratio of $\frac{\text{Span Length}}{\text{Deflections}}$ will be shown for the critical points as determined from the grid analysis just as was done for the analysis of the moments. Table E-3 shows this ratio in the positive moment region for the unfactored live load at 28 ft. from the end supports. Table E-4 shows this ratio in the negative moment region for the unfactored live load at the interior support. In Table E-4, a value of "-----" means that there was no deflection for that point.

Table E-3 Span Length over Deflections at 28 ft. from the End Support using Unfactored Live Load Deflections

Girder	Intact	Support 1 removed	Support 2 removed	Support 1&2 removed	All removed
1	628	527	619	288	104
2	685	633	671	411	121
3	931	929	910	735	151
4	2230	2451	2219	3889	212

Table E-4 Span Length over Deflections at the Interior Support using Unfactored Live Load Deflections

Girder	Intact	Support 1 removed	Support 2 removed	Support 1&2 removed	All removed
1	------	1020	------	187	45
2	------	------	4515	425	52
3	------	------	------	------	61
4	------	------	------	------	76

AASHTO limits the deflection-span ratio to 1/800 the span for non pedestrian bridges. The values for girders 1 and 2 in Table E-3 exceed this ratio for each scenario, including the intact scenario. Section E.2.4 will further discuss these results.

E.2.3 Overload Condition

To check the overload condition of a bridge, we will:

1. Compare the induced member moments to the ultimate moment capacity of the section and denote it by Ω in equation (E-2) , and

2. Express the residual capacity of the bridge in terms of the live load capacity equation (E-3).

Member Moments vs. Ultimate Capacity

When comparing the induced member moments, M_i, to the ultimate moment capacity, Mu, of the section, equation (E-2) is used:

$$\Omega = \frac{M_i}{M_u} \qquad \text{(E-2)}$$

When using (E-2), ignore any signs associated with M_i and M_u. Always use their positive values. Therefore, from reviewing (E-2), it can be seen that an unfactored $\frac{M_i}{M_u} > 1$ means that the member's bending moment is greater than the ultimate moment capacity of the section and the member's capacity has been exceeded. $\frac{M_i}{M_u} \leq 1$ means that the bending moment of this girder is less than or equal to its ultimate moment capacity so the structure has not reached its ultimate moment capacity. Whenever M_i is positive, the positive ultimate moment capacity of the section is used and if M_i is negative, the negative ultimate moment capacity is used. For the negative moment region, both a positive and negative ultimate moment capacity is needed since the moments shown in Table E-2 switch from negative to positive after supports are removed. In the positive moment region, only a positive ultimate moment capacity is needed.

The bridge being considered has a positive ultimate moment capacity of 32,866 k-in for girders 1 through 4 at 28 ft. from the end support. Refer to references [E-1 and E-2] for detailed

calculations of the ultimate moment capacity. This bridge is overdesigned when compared to the required moment capacity according to the AASHTO LFD criteria if one uses the exact load distribution obtained from the grid analysis rather than using the distribution factors of AASHTO. For example, considering a dead load factor, $\gamma_D = 1.3$, and a live load factor, γ_L=2.167, the LFD criteria would produce a moment of 1.3(4655) + 2.167(8439) = 24,335 k – in for girder 1. Refer to Table E-1 for the dead and live load moments when calculating the total factored moments.

Using equation E-2 for girder 1, which is the bridge's positive moment region design girder, we get a $\frac{M_i}{M_u} = \frac{24,335}{32,866} = 0.74 < 1$; therefore the structure has not reached its ultimate moment capacity.

To help better reflect the effects of the support failures, the ultimate moment capacities have been re-adjusted by a factor so that the maximum moment capacity is equal to the largest factored member bending moment obtained in each support failure scenario $\left(\gamma_D \cdot M_D + \gamma_L \cdot M_L(1+I) = M_u\right)$. As a result, these values will better reflect the structure's behavior as if the intact girders were loaded to their ultimate moment capacity. Therefore, any ratio over 1 means the girder has exceeded its capacity under the adjusted conditions.

For the positive moment region, the ultimate moment capacity has been adjusted by the following amount: $\frac{32,866 - 24,335}{24,335} = 35.06\%$. Therefore, for the positive moment region with $\gamma_D = 1.3$ and γ_L=2.167, the results obtained are shown in Table E-5 for the ratio of moment to ultimate moment adjusted by 35.06% at 28 ft. from the end support.

Table E-5 Mi/Mu Ratios at 28 ft. from End Support using $\gamma_D = 1.3$ & γ_L=2.167 for the Moments

Girder	Intact	Support 1 removed	Support 2 removed	Support 1&2 removed	All removed
1	1.00	1.00	1.02	1.16	2.38
2	0.95	1.04	0.93	1.23	2.23
3	0.77	0.80	0.77	1.00	1.96
4	0.45	0.39	0.46	0.25	1.56

The same re-adjustment is performed for the moment capacity at the interior support. For example, considering a dead load factor, $\gamma_D = 1.3$, and a live load factor, γ_L=2.167, we get a moment of $1.3(-7160) + 2.167(-5623) = -21{,}493$ k – in for girder 2 at the interior support. This value is lower than the actual moment capacity. The negative moment region has an negative ultimate moment capacity of -33,268 k - in and a positive ultimate moment capacity of 52,821 k-in. (For the positive ultimate moment capacity, the contribution of the deck is included since there are shear studs used in the negative moment region). Whenever the negative moments become positive, the positive ultimate moment capacity must be used. For the negative moment region, the positive and negative ultimate moment capacities have been adjusted by $\frac{33{,}268 - 21{,}493}{21{,}493} = 54.79\%$ with $\gamma_D = 1.3$ and γ_L=2.167. The positive ultimate moment capacity has been adjusted by the same amount as was the negative ultimate moment capacity. This rough approximation is based on the assumption that the added capacity for the positive ultimate moment capacity is gained by the deck only. The steel area does not change. The results obtained are given in Table E-6 for the ratio of moment to ultimate moment at the interior support. By adjusting the positive ultimate moment capacity at the interior support, it will be assumed to be (52,821 / 15479) = 34,123 k - in instead of 52,821 k-in.

Table E-6 Mi/Mu ratios at the interior support using
$\gamma_D = 1.3$ & $\gamma_L = 2.167$ for the Moments

Girder	Intact	Support 1 removed	Support 2 removed	Support 1&2 removed	All removed
1	0.99	0.30	1.16	0.53*	2.56*
2	1.00	1.82	0.53	0.35	2.38*
3	0.91	0.64	1.21	2.69	2.19*
4	0.59	0.51	0.54	0.29*	2.03*

Since Tables E-5 and E-6 deal with factored loads, a bridge with a $\frac{M_i}{M_u} > 1$ has not reached its ultimate capacity since safety margins are still included

Live Load Capacity

In this section, we will perform the same analysis of the residual capacity however we will be using the unfactored loads. i.e. we will express the residual capacity of a bridge in terms of the live load capacity to see how much live load the bridge can carry under the induced support failures when no safety factors are included. We will define the loaf factor for substructure as LF_{sub}

$$LF_{sub} = \frac{Mu - DLM}{LLM} \qquad \text{(E-3)}$$

* These values use a positive ultimate moment capacity of 52,821 k-in for the negative moment region which has been adjusted to reflect a design at ultimate capacity.

where, DLM is the dead load moment, and

LLM is the live load moment including impact

This definition is similar to the definition of the load factor LF as used in the rest of this report. In this analysis we assume that the live load moment includes the effect of impact. In the future the effect of impact could be easily taken out in order to be consistent with the other sections of this report. If following an induced support failure, $LF_{sub} \geq 1.0$, the structure has not reached its ultimate moment capacity. The structure therefore has a live load capacity greater than 1. If $0 \leq LF_{sub} < 1.0$ then the member live load bending moment is greater than the ultimate moment capacity and the structure can only carry a fraction of the live loading even without safety factors. If $LF_{sub} < 0$, then the resulting dead load moment alone is greater than the ultimate moment capacity and the structure cannot carry any live load.

The resulting live load factors for the various support failure scenarios are presented in Tables E-7 and E-8. Table E-7 shows the live load factors at 28 ft from the end support in the positive moment region obtained by using equation (E-3). The ultimate moment capacity is again adjusted here to help better reflect a bridge which has been designed to its ultimate moment capacity.

Table E-7 LF_{sub} at 28 ft. in from end support

Girder	Intact	Support 1 removed	Support 2 removed	Support 1&2 removed	All removed
1	2.33	2.35	2.29	1.95	0.29
2	2.50	2.26	2.55	1.81	0.33
3	3.39	3.24	3.37	2.47	0.43
4	8.88	10.34	8.67	16.48	0.77

The negative moment region live load factor at the interior support using equation (E-3) is presented in Table E-8. The negative and positive ultimate moment capacities have once again been adjusted to help better reflect a bridge designed to its ultimate moment capacity. The results shown will be discussed further in Section E.2.4.

Table E-8 LF_{sub} at the interior support[1]

Girder	Intact	Support 1 removed	Support 2 removed	Support 1&2 removed	All removed
1	2.61	10.66	2.02	6.45*	0.13*
2	2.55	0.81	5.86	9.17	0.15*
3	3.02	5.02	1.89	0.06	0.18*
4	8.99	13.07	11.43	8.15*	0.21*

Tables E-9 and E-10 show a summary of the original and adjusted ultimate moment capacities which are used in Tables E-5, E-6, E-7, and E-8.

Table E-9 Ultimate Moment Capacities at 28 ft. from the End Support

Girder	Actual Positive M_u	Adjusted Positive M_u
1	32,866 k-in	24,335 k-in
2	32,866 k-in	24,335 k-in
3	32,866 k-in	24,335 k-in
4	32,866 k-in	24,335 k-in

[1] The values denoted with * use a positive ultimate moment capacity of 52,821 k-in for the negative moment region which has been adjusted to reflect a design at ultimate capacity.

Table E-10 Ultimate Moment Capacities at the Interior Support

Girder	Actual Negative M_u	Adjusted Negative M_u	Actual Positive M_u	Adjusted Positive M_u
1	-33,269 k-in	-21,493 k-in	52,821 k-in	34,123 k-in
2	-33,269 k-in	-21,493 k-in	52,821 k-in	34,123 k-in
3	-33,269 k-in	-21,493 k-in	52,821 k-in	34,123 k-in
4	-33,269 k-in	-21,493 k-in	52,821 k-in	34,123 k-in

Reviewing the LF_{sub} values obtained in Table E-8 when supports 1 and 2 were removed, we notice that the live load capacity for girder 1 and girder 4 is calculated using the positive ultimate moment capacity at the interior support. This means that the moments at these points are positive. Due to the support failures, the moment in girder 1 is positive while the moment in girder 2 is increasing positively. At the same time, the moment in girder 3 becomes even more negative while the moment in girder 4 becomes positive.

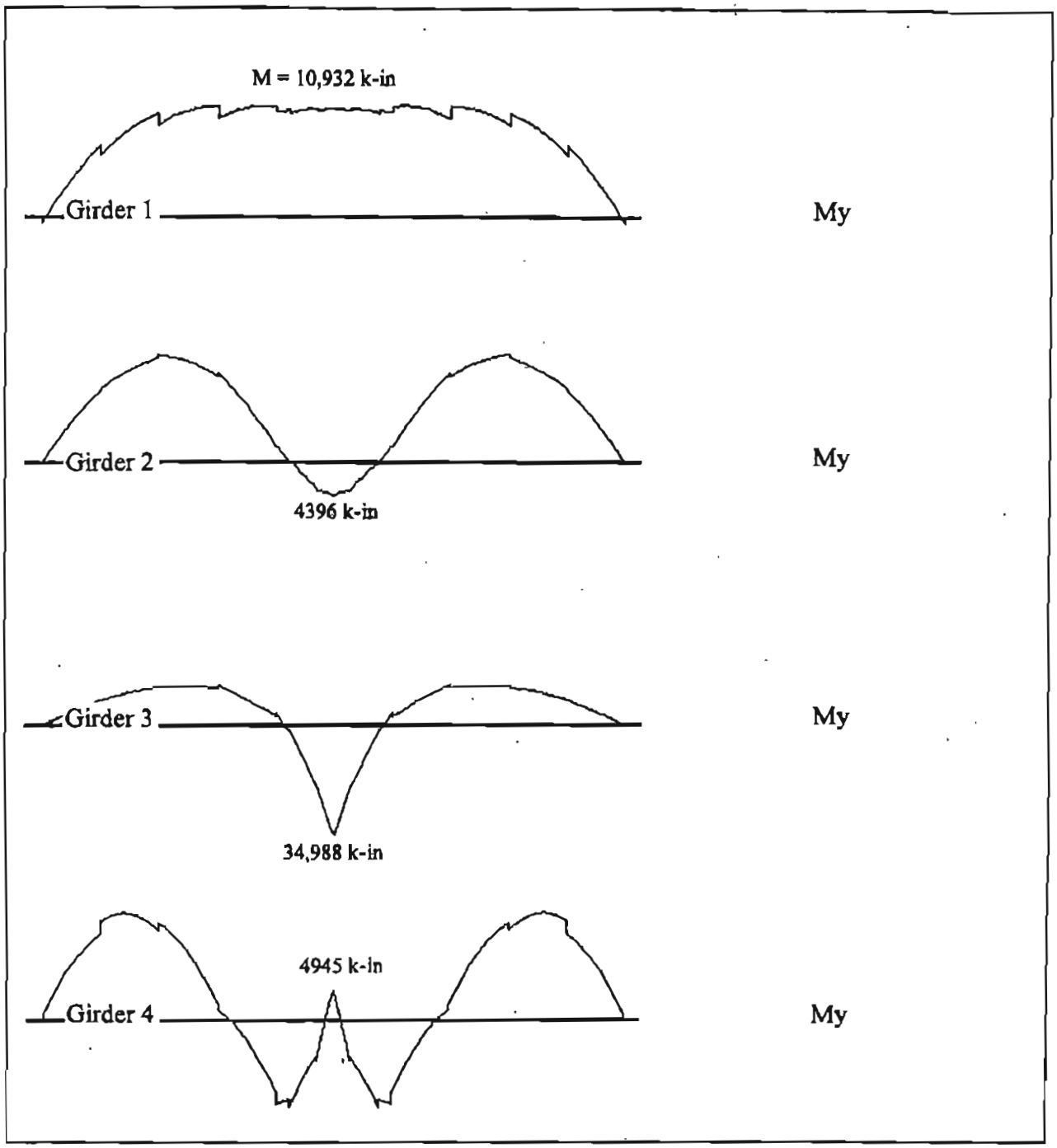

Figure E-13 Dead plus Live Load Moment Diagrams at the Interior Support for Failure of Supports 1 & 2

E.2.4 Discussion of Results

The unfactored dead, live, and dead + live load moments were presented in Tables E-1 and E-2 for the positive and negative moment regions respectively. By reviewing Table E-1c, we can see that removing a single support such as support 1 or support 2 for the positive moment region results in a decrease in moment at these points, but increases the adjacent girder's moment. When removing support 1, the moment in girder 1 goes from 13,093 k-in to 13,016 k-in while the moment in girder 2 goes from 12,537 k-in to 13,918 k-in. When removing support 2, the moment in girder 2 goes from 12,537 k-in to 12,261 k-in while the moment in girder 1 goes from 13,093 k-in to 13,356 k-in. The moment in girder 3 goes from 10,460 k-in to 10,540 k-in. In both cases, the moments in the girder which experiences the support failure decreases while the adjacent girder's moments increase.

Also, from Table E-1c in the positive moment region, we see that removing supports 1 and 2 simultaneously causes their adjacent member, girder 3, to increase in moment by the greatest amount from 10,460 k-in to 14,193 k-in. Girder 2 has the second greatest increase and the greatest moment of 16,869 k-in since it must now carry some of the load of girder 1.

Table E-2c shows a similar correlation for the negative moment region. Here again, the moments at the interior supports which experiences a support failure increase, while the moments at the adjacent supports decrease with respect to the original moments. For instance, when removing girder 1, the moment in girder 1 goes from -12,641 k-in to -3751 k-in while the moment in girder 2 goes from -12,783 k-in to -23430 k-in. When removing girder 2, the moment in girder 2 goes from -12,783 to -6695 k-in while the moment in girder 1 goes from -12,641 k-in to -14,906 k-in. The moment in girder 3 also increases negatively.

Also, in the negative moment region, when removing supports 1 and 2, the unfactored moment in girder 1 goes from -12641 k-in to +10932 k-in. Girder 1 has switched from double curvature to positive single curvature thus increasing the moments in girders 1 and 2. Girder 2 goes from -12,783 k-in to -4396 k-in. It still has a negative moment, but the moment is becoming more positive. Girder 3 remains negative, but changes in moment by the largest amount from -11,899 k-in to -34,899 k-in as seen in Table E-2c. For this scenario, girder 3 is now being the adjacent support to girder 1 and 2 so it must support them both. The moment here increases negatively due to the added loading induced by the support failures. Girder's 4 moment increased into positive curvature from -8754 k-in to +4945 k-in with this scenario.

Removing all of the center supports in the negative moment region causes the entire structure to bend in single positive curvature thus greatly increasing the moments all from negative to positive values as seen in Table E-2c. Girder 1 changes from –12,641k-in to 52,817 k-in. The positive moment region's moments, from Table E-1c, have also greatly increased. Girder 1 increases from 13,093 k-in to 34,721 k-in. These effects will be further discussed below.

These results, just presented, give an indication of the behavior of this bridge under hypothetical support failures. To further the investigation, the factored moments compared to their adjusted ultimate moment capacity were presented in Tables E-5 and E-6. For the positive moment region, girders 1, 2, and 3 all have a M_f/M_u ratio greater than 1.0 when supports 1 and 2 are removed. Girder 2 has the greatest ratio of 1.23 which means that the factored moments have exceeded their adjusted ultimate moment capacity.

For the negative moment region, girder 3 has a ratio of 2.69 when supports 1 and 2 removed. The ultimate moment capacity of this girder has been exceeded for this scenario. Girders 1, 2, and 4 all have ratios under 1.0 when using the adjusted ultimate moment capacity. The ultimate moment capacities for these girders have not been exceeded. When removing all

supports, girder 1 has the largest ratio of 2.38 for the positive moment region. For the negative moment region, girder 1, with all supports removed, has a ratio of 2.56. This bridge under these two scenarios for the adjusted states has exceeded its ultimate moment capacity.

Using these results shows the effects of the induced support failures on the moments as they compare to their ultimate capacity. Given a failure scenario, it can be determined if the bridge under factored loads has exceeded its ultimate capacity.

Another critical factor when examining a damaged bridge, is how much live load, (LF_{sub}) can the structure carry under these damaged conditions. These are shown in Tables E-7 and E-8 . Here, the calculations are performed with no safety factors, but including the impact factor. For the positive moment region, the bridge does not experience a LF_{sub} <1.0 for the presented scenarios until all supports are removed. This means that at the point of 28 ft. from the end support, the moments here will allow for the bridge to be overloaded with 226% of the live load when support 1 is removed. With support 2 removed, the bridge can carry 229% of the live load. With support 1 & 2, 181% of the live load can be carried without reaching its ultimate moment capacity. This is a result of the negative moment region after induced support failure, switching from negative to positive curvature. In order for the positive moments to continually increase, the moments at the interior support must first become positive. Since the moments at the interior support do not all become positive until all interior supports fail, the positive moments do not greatly increase until then. When all the interior supports are removed only 29% of the live load can be carried.

Let us examine the negative moment region next. Here, as shown in Table E-8, the bridge experiences a LF_{sub} <1.0 in girder 2 when support 1 is removed. Here, 81% of the live load can be carried. Notice that LF_{sub} in girders 1 and 3 decreases when support 2 is removed, but they are still greater that 1.0. This is due to girder 2 being an interior girder and its moments are being redistributed among the remaining girders, primarily, the adjacent girders, 1 and 3. For

this case, 189% of the live load can be carried without reaching its ultimate moment capacity. Girder 3 under support 1 and 2 failures experiences similar conditions as did girder 2 when support 1 was failed. Its LF_{sub} equals 0.06. This means that only 6% of the live load can by carried without reaching its ultimate capacity. This is because girder 3 is picking up the distributed loading of the adjacent girders 1 and 2 and it is now acting as an exterior support girder.

When all supports are removed, $LF_{sub} < 1.0$ for the negative moment region at the interior support. For this case, the structure has only 13% of the live load capacity remaining and no live loading is recommended. The structure here is again being compared to the positive ultimate moment capacity at the interior support.

Tables E-3 and E-4 show the span length over the deflections due to the induced support failures. As shown, the larger the value, the smaller the deflection. A 1 in. deflection would result in a value of 840 i.e. the span length/840 is equivalent to 1in of deflection. The girders suffering the support failures have the greatest deflections. Table E-4 show that the AASHTO limit is not exceeded until supports 1 and 2 are removed.

E.3 CONCLUSIONS

Elastic Analysis Conclusions

This appendix illustrated how the analysis of substructural redundancy of highway bridges can be performed. The procedure is illustrated using a typical bridge example using a linear elastic analysis and assuming different support failure scenarios. It has been shown that a failure of a support under an interior girder has less of an effect on the bending moments and deflections of the structure than does a failure of a support under an exterior girder. It has also

been shown that the critical points of interest of a two span bridge are the section of the girders immediately over the supports. It has been found that after the loss of the support of an exterior girder (support 1), the structure can carry 81% of the live load without exceeding its ultimate moment capacity. When losing one support of an interior girder (support 2), the structure can still carry 189% of its live load without exceeding its ultimate moment capacity. With the loss of one exterior girder's support and its adjacent support (supports 1 & 2), the structure can carry only 6% of its live load without exceeding its ultimate moment capacity. However, the adjacent girders (girders 2 and 4) still have considerable capacity remaining. For the last scenario (all interior supports lost), only 13% of the design live load can be carried by the structure. In addition to this, we see that a removal of all center supports would result in a deflection-span ratio of 1/45 causing large changes in the shape of the bridge. These results are based on the assumption that the adjusted ultimate moment capacity just satisfies the intact design requirements.

Based on the analysis performed in this appendix, we notice that there are two desirable substructural configurations to guard against catastrophic bridge failures after possible failure of the supports of a two-span bridge. The first configuration consists separate piers under each support. This configuration has been chosen based on the good performance of the bridge when support 1 or support 2 were separately removed. This however, may not be the most efficient, esthetically pleasing, or cost effective arrangement. Also, it is possible that all four piers may be damaged at once due to their smaller design requirements. The extent of the damage may be a function of the type of damage and the size of the pier.

The other desirable substructure configuration would consist of a double pier arrangement where each pier would support two girders. For this configuration, the loss of one pier would produce the loss of supports 1 & 2. In this case, girder 3 would carry only 6% of its live load (see Table E-8), but girders 2 and 4 would have a considerable amount of capacity remaining. Normally, as a results of this failure, the structure will become inelastic and there

will be an inelastic redistribution from girder 3 to girders 2 and 4. This inelastic redistribution will make this pier arrangement more desirable than a single pier arrangement. Also, the improbability of the structure receiving the full live load which produces maximum moment at the time of failure makes this two-pier arrangement a desirable configuration. This arrangement would also have a larger pier design making it more resistant to impacts while making constructability easier. Additional pier protection to avoid against possible damage from impacts would also aid each arrangement

Recommendations for Further Study

Additional bridges of various sizes and spans need to be analyzed for induced support failures as was done in this appendix. The behavior of the girder moments under these support failure conditions need to be looked at and appropriate conclusions need to be drawn. Nonlinear behavior should be considered as part of the analysis procedure. Besides material nonlinearity, the complete change in modes of failures must be accounted for. For example, as the moments become positive at the interior supports, the section properties as well as the ultimate moment capacity change. Research is needed to study how to account for this change during the analysis process. Other issues in need of further study include the positioning of the vehicles on the roadway surface in order to create the worst loading scenarios. These may be different for different assumed failure sequences.

The results of such detailed analyses should be incorporated in a general framework for considering substructure redundancy in the design and load capacity evaluation of highway bridges. The proposed framework should be compatible with current research on redundancy in bridge superstructures and should be applicable for implementation in the AASHTO LRFD Specifications for Highway Bridges. It is anticipated that the research will include the following tasks:

Task 1. Review and assess relevant current practice and research findings. This information would be assembled from the technical literature and the experience of bridge engineers.

Task 2. Identify common substructure configurations that will be addressed. Also, identify possible substructure failure scenarios that are relevant to this study. These scenarios should include the possibility of one column failure in single and multi-column bents as well as failures at the supports and bearings. Both brittle and ductile failures in substructural elements must be considered. In addition, identify the bridge system strength and functionality limit states that will be considered.

Task 3. Outline a framework for consideration of substructure redundancy in the design and load capacity evaluation of highway bridge structural systems. Develop a reliability model to analyze the safety of bridges and their substructures. Outline the calibration process that will be followed to implement the proposed framework. Also, identify the statistical data requirements to perform the reliability analysis and to perform the calibration.

Task 4. Extend NONBAN to include substructure behavior. Verify the validity of proposed analytical models with field investigations and/or laboratory and theoretical studies.

Task 5. Analyze a range of typical bridge configurations using the models developed. Perform the calibration of redundancy factors and finalize the proposed framework. The framework must be applicable for inclusion in the AASHTO LRFD Specifications for Highway Bridges.

REFERENCES

E-1 Oliver, J. M., "Reanalysis of Bridges with Support Failures", M.S. Thesis, Department of Civil Engineering, University of Pittsburgh, December 1996.

E-2 Highway Structures Design Handbook, November 1976.

E-3 Hambly, E. C., "Bridge Deck Behavior", Second edition, Chapman & Hall, New York, NY, 1991.

E-4 AASHTO Standard Specifications for Highway Bridges, 15 th. edition, Washington , DC 1992.

NCHRP Report 406 Appendix F

12-36

Copy No. 13

REDUNDANCY IN HIGHWAY BRIDGE SUPERSTRUCTURES

VOLUME II

APPENDIX F: Documentation of Program NONBAN

Prepared for

National Cooperative Highway Research Program
Transportation Research Board
National Research Council

TRANSPORTATION RESEARCH BOARD

NAS-NRC
PRIVILEGED DOCUMENT

Michel Ghosn, Linzhong Deng, Jian Ming Xu,
Y. Liu and Fred Moses

Department of Civil Engineering
The City College
of The City University of New York
New York, New York

May 1997

Acknowledgement

This work was sponsored by the American Association of State Highway and Transportation Officials, in co-operation with the Federal Highway Administration, and was conducted in the National Cooperative Highway Research Program which is administered by the Transportation research Board of the National Research Council.

Table of Contents

ACKNOWLEDGEMENT

This report was written by Prof. Michel Ghosn, Mr. Linzhong Deng, Mr. Jian Ming Xu, Dr. Y. Liu and Prof. Fred Moses. The original version of the program NONBAN was developed by Dr. Y. Liu formerly a research associate at Case Western Reserve University. The contributions of Mr. Charles Schilling in helping to develop the original framework of the program are gratefully acknowledged.

PREFACE

The objective of this appendix is to provide a preliminary documentation for the program NONBAN. The program was developed to study the nonlinear behavior of bridge systems using a grillage analysis. The program as presented herein is ONLY intended for use by the research team involved in the study on the redundancy of bridge superstructures. Therefore, the reader may find that the program is not user friendly nor efficiently written. Several sections written for the original version of the program may still be listed in the current version although they are not currently used.

The first section of this document gives an introduction to the program NONBAN including the hardware and software requirements and the required technical expertise for using the program. Section 2 summarizes the theoretical background used in the development of the program. The third section gives the program's logic and flow chart. Section 4 presents examples and comparisons to validate the results of the program. Section 5 explains how to prepare the input data file. Finally, section 6 gives the program listing. The program is divided into 50 blocks (number 0 to 49) and several subroutines. Comment cards provide a brief explanation of each block and subroutine as well as give the definition of the variables used in each block.

APPENDIX F
NONLINEAR BRIDGE ANALYSIS PROGRAM "NONBAN"

F.1 INTRODUCTION

F.1.1 General Background

Bridge system capacity is defined as the capability of a bridge to carry heavy loads due to the interaction of its members in a complete system. The study of the nonlinear behavior of bridge systems in the nonlinear range prior to the occurrence of ultimate capacity requires the investigation of member performance as well as transverse and longitudinal load redistribution. To calculate this system capacity, the nonlinear analysis of a bridge system is required. Many computer programs are available to perform the linear elastic analysis of bridge systems. For example, reference[F.1] by Zokaie, et al, gives a list of some of these programs such as GENDEK [F.2], CURVBRG [F.3] and MUPDI [F.4] . These programs, however, are specialized for the analysis of specific bridge types and are capable of performing only linear elastic analyses. Therefore, they are not suitable for studying the nonlinear behavior of bridge systems.

Specialized nonlinear bridge analysis programs are also available. For example, Kostem and his co-workers developed programs BOVA [F.5] and BOVAS [F.6] to perform the nonlinear analysis of concrete and steel slab on girder bridge systems. Idriss and White [F.7] also developed a program to perform the nonlinear analysis of steel I-girder bridge systems. Similarly, Maheu [F.8] developed a program to perform the nonlinear elasto-plastic analysis of steel girder bridge systems. Scordelis and his co-workers developed programs for the nonlinear analysis of box type bridges. For example, the program NOBOX [F.9] is used for the nonlinear analysis and ultimate strength of multi-cell reinforced concrete box girder bridges. The program NAPBOX [F.10] is used for the analysis of rectangular single-cell reinforced and prestressed concrete box girder bridges. Kostem and Hand also developed a program for the inelastic analysis of spread box-beam bridges [F.11] . Each one of these programs was, however, designed to analyze one particular type of bridges. An engineer who is interested in studying the behavior of different types of bridges must therefore be familiar with the requirements and limitations of several such programs.

General purpose nonlinear finite element packages can also be used for the nonlinear analysis of any structure and in particular bridge structures. For example, FINITE [F.12] was used in reference [F.1] to analyze a variety of bridge structures but was only used to study the behavior in the linear elastic range although the program is capable of performing nonlinear analyses. The program ABAQUS [F.13] is an especially powerful program that can be adapted to perform the analysis of any type of structure. For example, ABAQUS [F.13] was used by Helba and Kennedy [F.14] to analyze the collapse loads of continuous skewed composite steel bridges. Other commercially

available programs with similar capabilities include ANSYS [F.15] , NONSAP [F.16] , DYN3D [F.17] and many others.

The programs listed in the previous paragraph are theoretically usable for any type-of bridge structure. The problem with such general purpose commercial packages, especially for use in the nonlinear range, is the complexity of the required input data and the specialized training required before an engineer becomes familiar with their use, capabilities and limitations. For example, if the nonlinear behavior is studied using the basic principles of 3-dimensional plasticity, the program requires complete input information on the type of plastic flow model to be used and the definitions of failures in 3 dimensions. For composite bridge systems, complications also may occur in modeling the shear connections between the different materials. Difficulties also arise when the effect of the construction sequence needs to be considered.

Because of the difficulty of adapting the general purpose programs for large scale analysis of many bridge types, this study developed a general nonlinear bridge analysis program NONBAN (**NON**linear **B**ridge **AN**alysis). The objective is to develop a program that can be routinely used to analyze the nonlinear behavior of common type bridge structures. The requirements set by the research team during the development of the program were:

1. The program requires simple input information such that it could be used on a routine basis by the research team to analyze many bridge models without requiring lengthy preparation of input data.

2. The program should be applicable for studying the nonlinear behavior of common type bridge structures including slab on I- beam bridges as well as box girder bridges.

3. The program gives an accurate representation of the global nonlinear response of bridge systems.

NONBAN as developed herein satisfies all these three requirement. NONBAN is also designed to account for the effect of the construction sequence.

F.1.2 GENERAL DESCRIPTION OF THE PROGRAM NONBAN

The program NONBAN developed in this study uses a grillage (grid) analysis procedure where the bridge system is discretized as longitudinal and transverse beam elements. The longitudinal elements model the behavior of the main longitudinal members while the transverse elements represent the behavior of the slab and diaphragms.

The grillage model used in NONBAN is similar to models used by Zokaie, et al, [F.1] to produce the load distribution factors for the AASHTO LRFD specifications. Despite the proven accuracy of available grillage programs, it was necessary for the research team to

develop NONBAN in order to extend the grillage concepts to the nonlinear behavior range which was not reported by neither Zokaie [F.1] nor Bakht [F.18] .

The program NONBAN performs a nonlinear analysis of bridge systems using a modified stiffness matrix that accounts for material nonlinearity. In this program, the linear elastic stiffness matrices of the beam elements are modified to account for possible flexural and shear nonlinearities. This is achieved by assuming that nonlinearity due to bending is concentrated at the ends of a beam element and that its effect can be represented by rotational springs attached to the ends of the elements. Shear nonlinearity is also considered by updating the shear stiffness, Kv. In the linear elastic range, Kv is equal to GA_v, where G is the shear modulus and A_v is the shear area. As the shear forces exceed their elastic limits, the shear stiffness is updated as will be seen further below. The stiffness of the rotational springs are obtained from moment versus rotation curves as explained in section F.2 of this Appendix. The validity of the proposed models for including shear as well as flexural nonlinearity in the analysis of structural members is verified in Section F.4.

To study the behavior of typical bridge systems, NONBAN is based on a nonlinear incremental analysis. With this approach, the loads are incremented and the behavior of every element in the grid is continuously monitored and updated until system failure occurs. Section F.3 of this appendix gives a more complete description of the program logic and structure including a program flow chart.

Grillage analyses of slab on I-beam bridges is routinely performed by many engineers to study the linear- elastic response of bridge systems. Phase I of this study [F.19] demonstrated that the grillage analysis can also be used to study the nonlinear behavior of such systems. The analysis of box-girder bridges is, however, more complicated because it requires an accurate representation of the high torsional capacity of these systems. Hambly in reference [F.20] has shown that the grillage analysis can be used for box-girder bridges if the torsional stiffness is properly modeled. Zokaie in reference [F.1] used the Hambly approach to develop the load distribution factors of the AASHTO LRFD code [F.21] . Section F.2, briefly describes the modeling scheme proposed by Hambly.

Several sensitivity analyses performed in Section F.4 of this report demonstrate that the discretization scheme proposed by Hambly [F.20] was sufficiently accurate to study the global nonlinear behavior of typical box beams as well as unicell and multicell concrete box girder bridges. The accuracy of NONBAN to account for the torsional capacity of bridge members was tested by comparing its results to analytical results and to experimental results. For example, Section F.4 of this report presents several examples that show the applicability of the program for the analysis of box beams under torsional loads. Also, Section F.4 demonstrates the applicability of NONBAN to analyze prestressed concrete unicell box girder bridges.

F.1.3 HARDWARE AND SOFTWARE REQUIREMENTS OF NONBAN

The program NONBAN was written in Fortran 77 version 5.9. Aside from the Fortran compiler, NONBAN is a stand alone program and does not require any special routines to run. The current version of NONBAN is developed for a Digital Equipment VAX-64420 computer system using a VMS 5.5-2 operating system. Although developed for the VAX, the program was also used on a standard PC, a DEC workstation as well as an ultra SPARC SUN workstation. The program needs little memory to run, at most 0.5 Mb. The required disk space usually is 200 kb depending on the scale of the analyzed structural model and the output option. In the current version, all the output is written to file. The sizes of the output files depend on the size of the bridge structural model used and on the number of iterations required until the structure exhibits failure. Similarly, the computation time varies depending on the structural model and the number of iterations needed as well as the capacity of the computer processor.

F.1.4 TECHNICAL EXPERTISE REQUIREMENTS FOR USING NONBAN

Section F.5 of this appendix provides a set of documentation for the program NONBAN. Section F.5 of also provides an example showing how to prepare NONBAN input data to perform the analysis of a typical steel I-beam bridge. In summary, to use the program NONBAN the following steps should be followed:

1. Discretize the structural model of the bridge into a grid. This is done by dividing it into beam elements connected by nodes .

2. Provide a geometric description of the bridge by entering the node coordinates, the way these nodes are connected by the beams (framing) and a description of the boundary conditions.

3. Enter the linear material properties of every beam element.

4. Enter the nonlinear material properties of every beam element.

5. Enter the locations, directions and magnitudes of the applied dead and live loads.

Except for item 4. concerned with the nonlinear material properties, the required NONBAN input data is similar to the input data required by any general purpose linear elastic structural analysis program. These linear elastic programs are routinely used by engineers to analyze all types of structures including bridges.

As explained in Section F.1.1, many available nonlinear analysis packages require complicated input information to model the nonlinear behavior of structural elements. NONBAN was designed to simplify such input information. For example, for modeling the nonlinear material behavior under bending moment, moment versus plastic rotation curves are required by NONBAN. These curves can be derived for steel I-beam and

concrete members using a combination of analytical and empirical equations (See appendix B and C of this final report.).

The moment versus rotation curves for steel I-beams used in this study are derived based on empirical curves provided by Schilling [F.22] . The curves of Schilling are in a generic form and were developed from experimental tests. Schilling points out that such curves do incorporate local buckling, residual stresses, etc. Different curves are given for composite and noncomposite beams with compact and noncompact sections. Therefore, depending on the section type, the curves are given in function of either the plastic section capacity M_p or the capacity of the section at first yield M_y. Schilling's curves are given for beams that exhibit the formation of a single hinge. There curves are adjusted in this study to account for the possible formation of many hinges. An explanation as to how this is done is given in Appendix C.

For concrete members (both reinforced and prestressed) the moment versus rotation curves are developed analytically using section equilibrium as explained in Appendix B. The analysis requires the section geometry, and the stress-strain curves of concrete and reinforced and/or prestressed steel. Since element rotation is related to section curvature, the moment-rotation curves are developed from the moment-curvature relationships. Moment versus curvature relationships for a given concrete section are obtained from the basic principles of equilibrium and are routinely used by engineers while calculating the ultimate capacity of reinforced concrete and prestressed concrete sections. To convert the moment curvature relationships to moment rotation curves, the curvatures are multiplied by the length of the plastic hinge, Lp. Empirical methods to calculate this plastic hinge length are available and can be calculated from basic information on beam properties.

The program NONBAN also accounts for shear nonlinearity. The program requires as input information a shear force versus shear deformation curve which can be obtained from empirical equations as explained in Section F.2 of this Appendix. The principles used to develop such curves are familiar.

Although engineers may not generally have calculated moment versus rotation curves for concrete or steel members, or developed shear versus shear deformation curves on a routine basis, the principles needed to develop such curves are clear and there should not be difficulty in preparing the input data for the program NONBAN. In this study, the researchers developed separate programs to perform such calculations based on section and material properties.

Although NONBAN is very simple to use, it should be noted that this program has been developed as a research tool and not as a commercial package. Hence, NONBAN does not contain the normal internal diagnostics which would permit it to detect operator input errors. For example, upon detecting input inconsistencies, NONBAN may simply crash without providing any indications as to where the error was detected. Therefore, the program operator must be experienced with structural analysis programs in order to detect such errors and be able to correct them with little feed back from the program.

The aim of NONBAN is to provide behavior information in the nonlinear range to model the reliability. There is no specialized training required for using NONBAN due to the nature of the program. Because it is not a commercial computer package engineers should be familiar with both structural analysis packages and with the behavior of bridge structures in order to use the program.

F.1.5 APPENDIX OUTLINE

The objective of this appendix is to provide a preliminary documentation for the program NONBAN. The program was developed to study the nonlinear behavior of bridge systems using a grillage analysis. The program as presented herein is ONLY intended for use by the research team involved in the study on the redundancy of bridge superstructures. Therefore, the reader may find that the program is not user friendly nor efficiently written. To help explain the theoretical background and logic of the program, this appendix is composed of six section.

Section F.1 gives an introduction to this appendix. It explains the purpose of the program NONBAN, and describes the software and hardware requirements for program installation and program running.

Section F.2 of this appendix provides the theoretical background for the program NONBAN. It briefly describes the derivation of the stiffness matrices used with NONBAN and explains the significance of the moment rotation curves and the shear deformation curves which are used to model the nonlinear material behavior of bridge members. Section F.2 also describes the incremental analysis technique used in the program.

Section F.3 provides a flow chart describing the structure and the logic of the program. Also, this section provides a more detailed description of the function of each block of the program.

Section F.4 demonstrates the accuracy and the validity of the program by comparing the results of NONBAN to exact results of simple beam examples, to the results of other programs for both the linear elastic range and the nonlinear range. It also compares the results obtained by NONBAN to the results of laboratory tests of beams, to experimental results on laboratory bridge models and finally to experimental results of full scale bridge tests. Several additional comparisons are also provided in Appendix B, C and D of this report and in the Phase I report.

Section F.5 explains in detail how to prepare the input data for the program. It also gives advice on how best to discretize the bridge models for analysis with NONBAN. These inputs will be illustrated by means of an example of an actual bridge analyzed in this study. In addition, explanations about how to interpret the NONBAN output are provided.

Section F.6 provides a listing of the program. The program listing also gives the definitions of the variables used in the program. A copy of the program is also provided to NCHRP.

SECTION F.2

THEORETICAL BACKGROUND

F.2.1 INTRODUCTION

The stiffness matrix method has been in use for several decades to perform the linear elastic analysis of structural frames. In Europe, where bridge design codes do not provide simplified analysis models as currently provided by AASHTO's distribution factors, the stiffness matrix approach is the most widely used method for the analysis and design of bridge systems. In this approach, the longitudinal members of a bridge system are modeled as longitudinal beam elements along the main axis of the bridge, while the slab and diaphragms are modeled as transverse beams. The axes of the bridge system are referred to as the "global axes", while the axes of a beam are known as the "local axes".

To properly model the interaction between the longitudinal and transverse members of a bridge system, the torsion as well as the bending of each member about its major local axes must be considered. The deflections of interest, however, are the displacements in the global vertical direction. The bending of the cross sections control the nonlinear behavior of each section of the bridge system. Such a structural model is known as a grid or grillage. Figure F.1 gives an example of how a bridge system can be modeled as a grid.

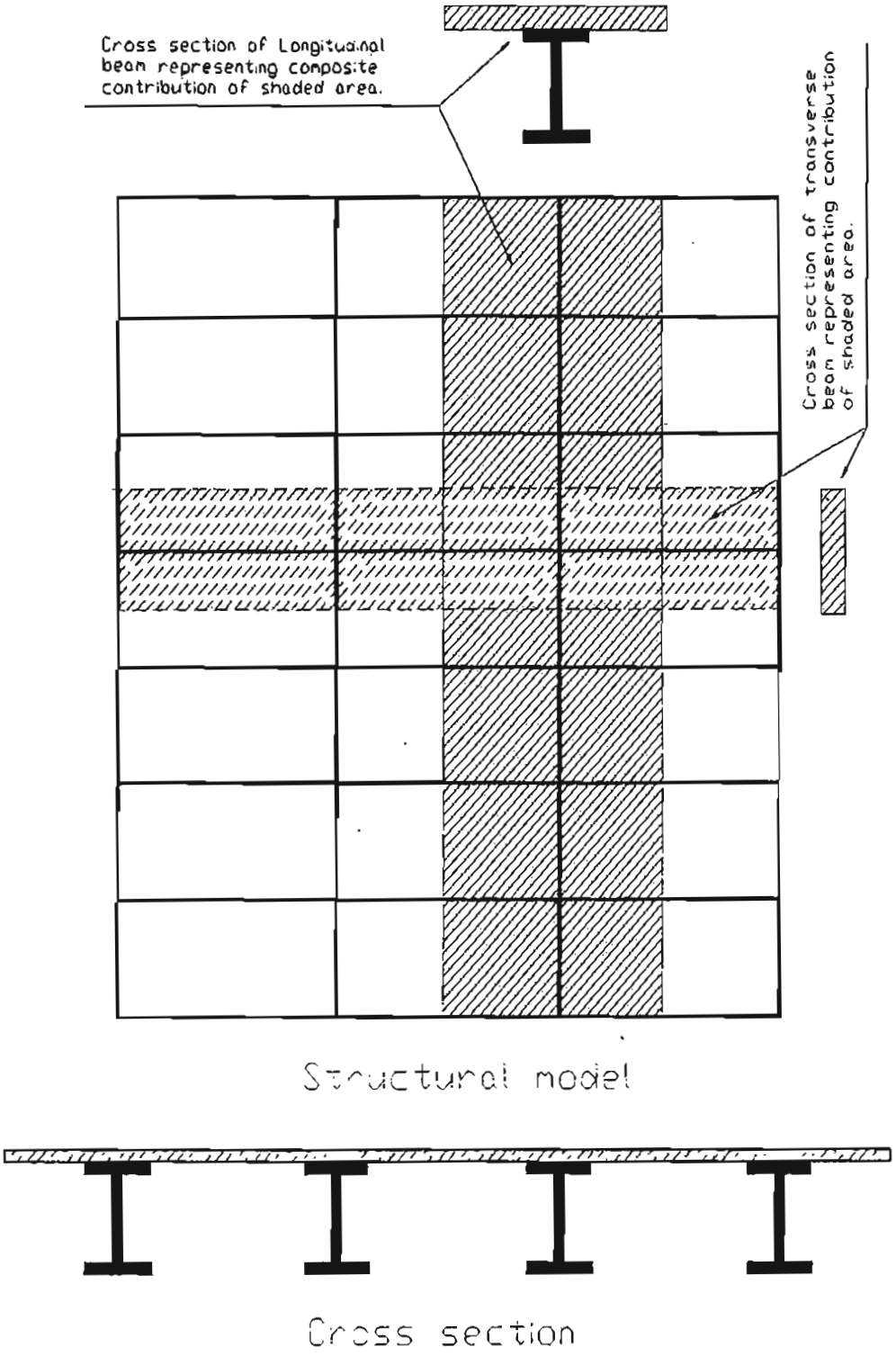

Figure F.1 Discretization of a bridge system as a grid.

The stiffness matrix of one beam element gives the exact relationship between the member's generalized internal forces (forces and moments) and generalized deformations (displacements and rotations). The stiffness matrix of one beam element in the linear elastic range in a three-dimensional space is given in figure F.2. The matrix is given in function of the beam's length L, its moments of inertia Iy and Iz, its torsional constant Ix, its cross sectional area A, its shear areas Ay and Az, its Modulus of elasticity E and its shear Modulus G. Each beam end can displace in the x,y and z directions as well as rotate about the x,y and z axes. Therefore, every point is associated with six degrees of freedom.

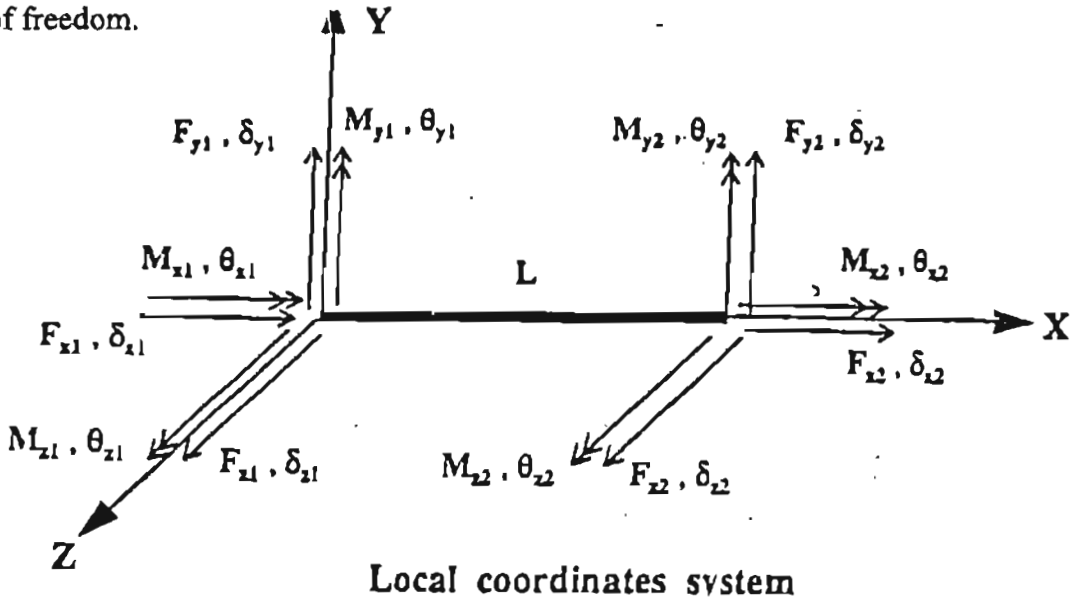

Local coordinates system

$$\begin{bmatrix} F_{x1} \\ F_{y1} \\ F_{z1} \\ M_{x1} \\ M_{y1} \\ M_{z1} \\ F_{x2} \\ F_{y2} \\ F_{z2} \\ M_{x2} \\ M_{y2} \\ M_{z2} \end{bmatrix} = \begin{bmatrix} K_{1,1} & \cdots & & & & & & & & & & K_{1,12} \\ & K_{2,2} & & & & K_{2,6} & & K_{2,8} & & & & K_{2,12} \\ & & \cdots & & & & & & & & & \\ & & & \cdots & & & & & & & & \\ & & & & \cdots & & & & & & & \\ & & & & & \cdots & & & & & & \\ & K_{6,2} & & & & K_{6,6} & & K_{6,8} & & & & K_{6,12} \\ & & & & & & \cdots & & & & & \\ & K_{8,2} & & & & K_{8,6} & & K_{8,8} & & & & K_{8,12} \\ & & & & & & & & \cdots & & & \\ & & & & & & & & & \cdots & & \\ & & & & & & & & & & \cdots & \\ & K_{12,2} & & & & K_{12,6} & & K_{12,8} & & & & K_{12,12} \end{bmatrix} \times \begin{bmatrix} \delta_{x1} \\ \delta_{y1} \\ \delta_{z1} \\ \theta_{x1} \\ \theta_{y1} \\ \theta_{z1} \\ \delta_{x2} \\ \delta_{y2} \\ \delta_{z2} \\ \theta_{x2} \\ \theta_{y2} \\ \theta_{z2} \end{bmatrix}$$

F.2 Stiffness matrix of one beam element.

The stiffness matrix is symmetric, in which:

$$K_{1,1} = \frac{EA}{L} \qquad K_{5,5} = \frac{4EI_y}{L} \qquad K_{9,3} = \frac{-12EI_y}{L^3} \qquad K_{11,3} = \frac{-6EI_y}{L^2}$$

$$K_{2,2} = \frac{12EI_z}{L^3} \qquad K_{6,2} = \frac{6EI_z}{L^2} \qquad K_{9,5} = \frac{-6EI_y}{L^2} \qquad K_{11,5} = \frac{2EI_y}{L}$$

$$K_{3,3} = \frac{12EI_y}{L^3} \qquad K_{6,6} = \frac{4EI_z}{L} \qquad K_{9,9} = \frac{12EI_y}{L^3} \qquad K_{11,9} = \frac{6EI_y}{L^2}$$

$$K_{4,4} = \frac{GI_x}{L} \qquad K_{7,1} = \frac{-EA}{L} \qquad K_{10,4} = \frac{-GI_x}{L} \qquad K_{11,11} = \frac{4EI_y}{L}$$

$$K_{5,3} = \frac{-6EI_y}{L^2} \qquad K_{7,7} = \frac{EA}{L} \qquad K_{10,10} = \frac{GI_x}{L} \qquad K_{12,2} = \frac{6EI_z}{L^2}$$

$$K_{8,2} = \frac{-12EI_z}{L^3} \qquad K_{12,6} = \frac{2EI_z}{L}$$

$$K_{8,6} = \frac{-6EI_z}{L^2} \qquad K_{12,8} = \frac{-6EI_z}{L^2}$$

$$K_{8,8} = \frac{12EI_z}{L^3} \qquad K_{12,12} = \frac{4EI_z}{L}$$

in which:

A	Cross sectional area;
Ay	Shear area in the Y direction;
Az	Shear area in the Z direction;
Ix	Torsional constant;
Iy	Moment of inertia about Y axis;
Iz	Moment of inertia about Z axis;
L	Length of beam element;
E	Modulus of elasticity;
G	Shear Modulus;

$$\lambda_y = \frac{12EI_z}{GAI_yL^2}$$

$$\lambda_y = \frac{12EI_y}{GAI_zL^2}$$

In the case where shear deformations should be included:

All the Ki,j terms in the stiffness matrix involving Iz are divided by $(1+\lambda y)$;

All the Ki,j terms in the stiffness matrix involving Iy are divided by $(1+\lambda z)$;

The term λz is added to the numerator of K5,5 and K11,11;

The term λy is added to the numerator of K12,12;

The term λz is subtracted from the numerator of K11,5;
The term λy is subtracted from the numerator of K12,6;

To analyze the behavior of a system formed by several beam elements, a global stiffness matrix is assembled. The global stiffness matrix gives the relationship between the forces applied on the system and the deformations at the ends of every beam element. The global stiffness matrix is assembled by superposing the coefficients of the elements' stiffness matrices using the principles of compatibility and equilibrium.

F.2.2 INCREMENTAL ANALYSIS OF NONLINEAR STRUCTURES

To consider the nonlinear behavior of structures, the incremental loading technique is often used. The technique assumes that the behavior of each element can be divided into several linear segments where each segment corresponds to different material properties. It is further assumed that the member behaves in a linear elastic manner within each segment. Figure F.3 shows a typical curve describing the nonlinear behavior of an element in bending. The points of transition between segments will be referred to as "subhinges".

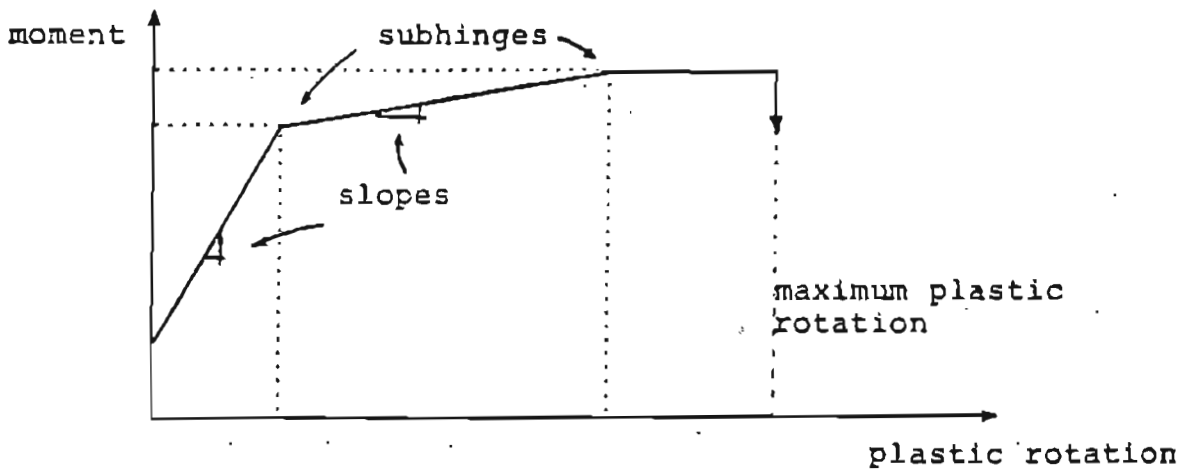

F.3 Typical moment versus rotation curve for nonlinear behavior of beams.

To perform the incremental analysis, it is first assumed that all beam elements are in their linear elastic range corresponding to the first segment of each element's curve. A load is then applied on the structure and the forces and deformations of each element are calculated. Each beam element is then checked to calculate the factor by which the initial load should be multiplied in order to reach the level at which the next subhinge will form. The load factor that is finally applied for the whole bridge system is the lowest factor obtained. The internal forces and deflections are calculated for the factored load. These are the final results of the first iteration.

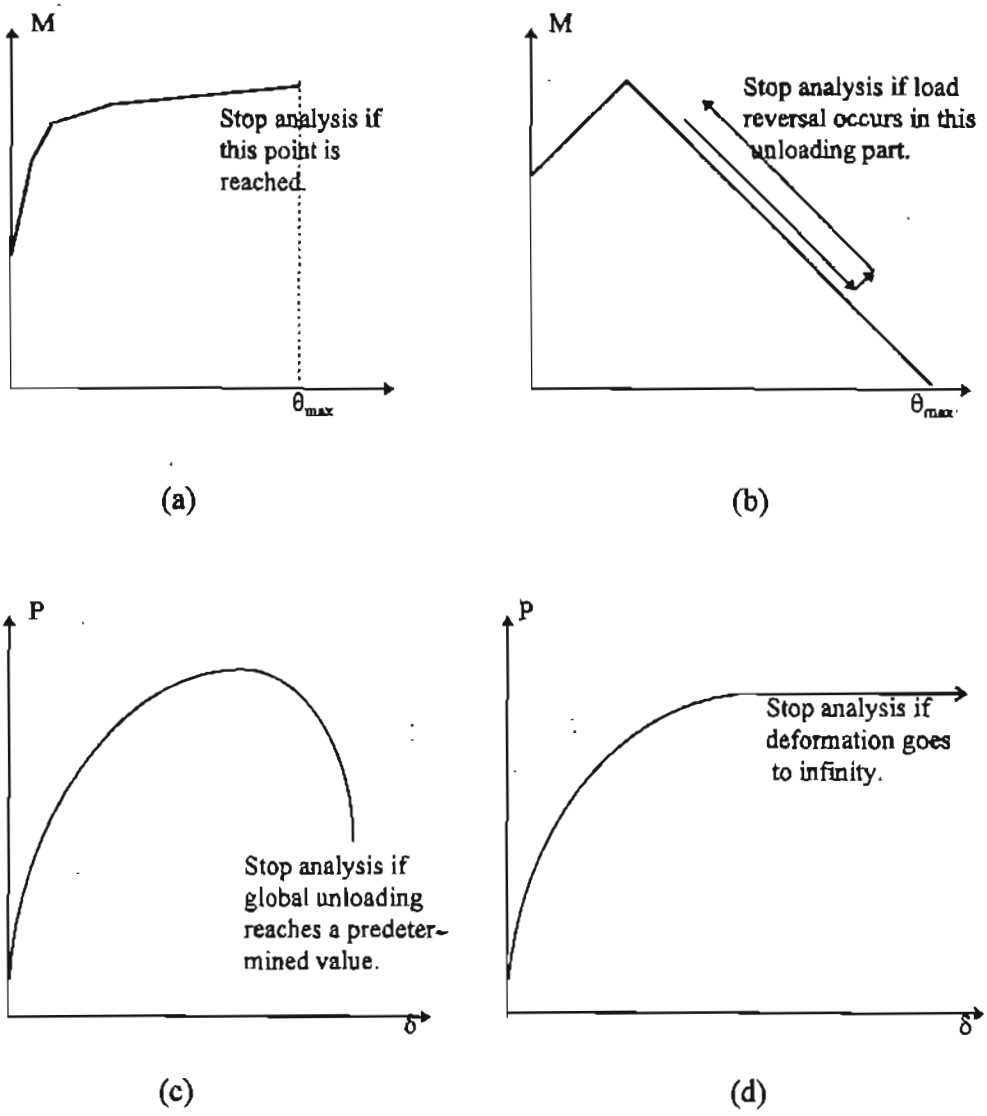

F. 4 Illustration of Typical Stopping criteria used in NONBAN

The stiffness of the element where a subhinge forms is updated to reflect the properties of the next segment. A second elastic analysis is then performed with the updated stiffness matrix and with the original load. Every element is checked to find the lowest possible load factor by which the results of the second analysis should be multiplied to produce a new subhinge. This load factor is the incremental load factor. The results of the second analysis are multiplied by the incremental load factor and then added to the results of the first iteration. These are the results of the second iteration. The total load factor at this stage is the incremental load factor added to the load factor obtained in the previous iteration. The process is thus repeated until the structure becomes unstable or until a predetermined stopping criterion is met. Typical stopping criteria include a total deflection limit, a total rotation limit, reversal of member unloading, or a large level of global unloading. Figure F.4 gives an illustration for these stopping criteria.

The results of the incremental analysis are typically presented in curves giving the load factor versus the response of interest. Common plots usually give the load factor versus maximum deflection.

F.2.3 NONBAN PROGRAM LOGIC

The program NONBAN is designed to perform the nonlinear analysis of multi-girder and box girder bridge systems using the incremental loading technique. The bridge is modeled as a grid with longitudinal beam elements modeling the behavior of the main girders and transverse beam elements modeling the behavior of the slab and the diaphragms. The behavior of each element in its elastic range is represented by its elastic Modulus and section properties. The element stiffness matrix used by NONBAN for the linear elastic range is the full three-dimensional matrix shown in figure F.2. The nonlinear behavior of each element is represented by a multi-linear moment versus plastic rotation curve (M-θ) as shown in figure F.3. The plastic rotation is defined as the total rotation minus the elastic rotation.

The incremental analysis technique is used by NONBAN as described earlier. As the load applied on the bridge system is incremented and a subhinge forms at the end of an element, a rotational spring is introduced at that end to model the change in the behavior of the element. The stiffness of the rotational spring is obtained from the slope of the appropriate segment of the M-θ curve. The stiffness matrix of the element is then changed to account for the rotational spring. Four different cases are thus considered: a) The element is in the elastic range without subhinges at neither end. b) A subhinge formed on the left end of the element. c) A subhinge formed at the right end of the element. d) Two subhinges formed at both ends of the beam element. Each case produces a different stiffness matrix as described in section [F.2.4] The

derivation of the stiffness coefficient for a beam element with rotational springs as its ends is given in section F.2.4.

F.2.4 DERIVATION OF MODIFIED STIFFNESS MATRICES

The coefficients of the stiffness matrix give the relationships between the forces and moments at the ends of a beam element and the displacements and rotations also at the ends of the element. For example, as shown in figure F.2, the coefficient K2,12 gives the relationship between the force in the second degree of freedom and the deformation in the 12 th. degree of freedom. As shown in figure F.2, the force in the second degree of freedom corresponds to the shear force in the y direction at end 1 of the beam, Fy1. The deformation of the 12 th. degree of freedom is the rotation about the Z axis at end 2, θ_{z2}. To find the coefficient K2,12 , the basic concepts of equilibrium are applied. For example, in the case where one subhinge has formed at end 1 of the beam element, the beam element can be modeled as shown in figure F.5. Where the length of the section undergoing inelastic deformations is assumed to be small compared to the length of the section still elastic. To find the coefficient K2,12 , a deformation θ_{z2} is applied on the 12 th degree of freedom and the force corresponding to the second degree of freedom, Fy1, is calculated.

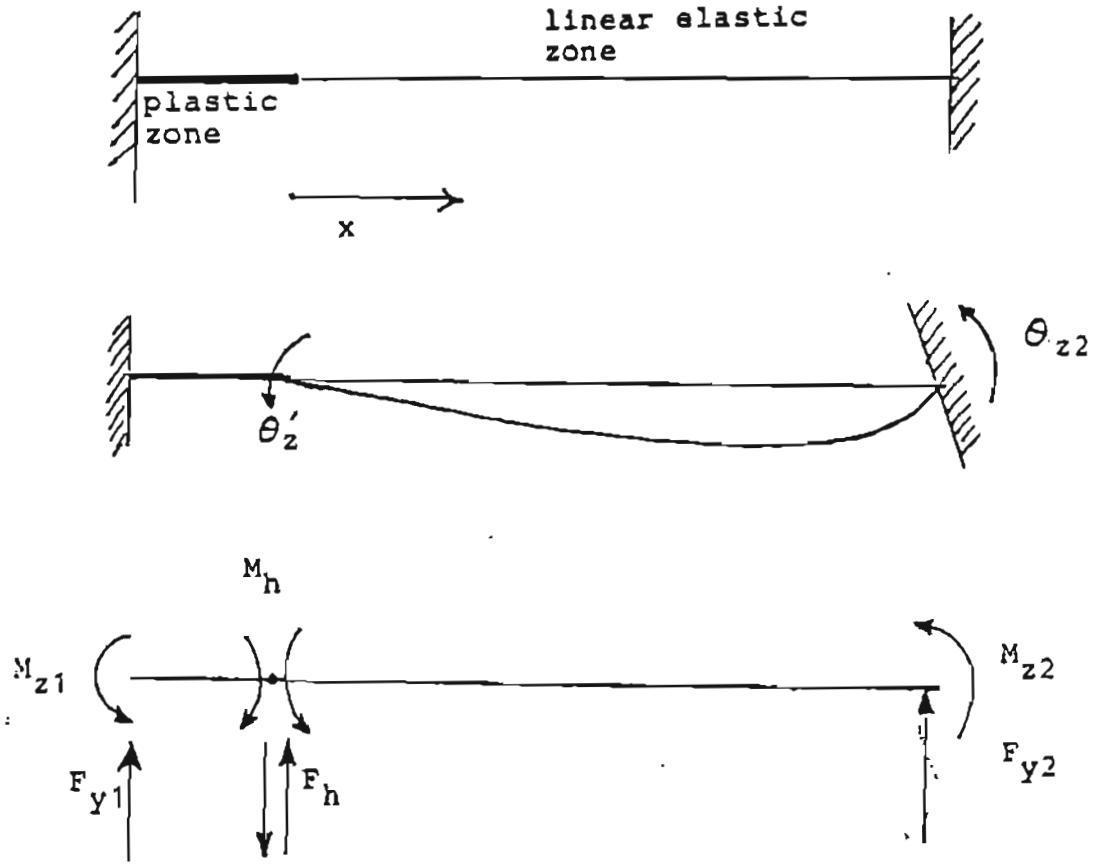

F.5 Model of nonlinear beam element.

Applying the rotation θ_{z2} while keeping the other degrees of freedom from deforming, produces the forces shown in figure F.5 c. From equilibrium it can be easily deduced that the force at end 1 Fy1 is equal to the force in the hinge Fh. Similarly, the moment at end 1, Mz1, is equal to the moment in the subhinge Mh.

Using the principle of equilibrium in the elastic section of the beam, one can write that:

$$E I_z Y'' = M_h - F_h X \qquad (F.1)$$

where E is the Modulus of elasticity, Iz is the moment of inertia about the z axis, y" is the second derivative of the displacement in the y direction about the x axis, M_h is the moment at the subhinge and F_h is the force at the subhinge.

The boundary conditions are given as:

$$\begin{aligned} y &= 0 \quad \text{at} \quad x = 0 \\ y &= 0 \quad \text{at} \quad x = L \\ y' &= \theta_z' \quad \text{at} \quad x = 0 \\ y' &= \theta_{z2}' \quad \text{at} \quad x = L \end{aligned} \qquad (F.2)$$

Also, in the inelastic part of the beam, the rotation θ'_z is related to the moment by:

$$M_h = KP_1 \theta'_z \qquad (F.3)$$

where KP1 is the slope of the M-θ curve.

By integrating equation (F.1) twice with respect to x and plugging in the boundary conditions, the force Fy1 = Fh is calculated as:

$$F_{y1} = F_h = \frac{2+\beta_1}{4+\beta_1} \frac{6 E I_z}{L^2} \theta_{z2} \qquad (F.4)$$

where β_1 is defined as (KP1 L)/EIz.

Hence, the coefficient K2,12 is the factor that multiplies θ_{z2} in equation (F.4) and is given as:

$$K_{2,12} = \frac{2+\beta_1}{4+\beta_1}\,\frac{6EI_z}{L^2} \qquad (F.5)$$

Similar calculations are performed for all the forces and moments and all the degrees of freedom. Different stiffness matrices are obtained for the four different cases of subhinge formations enumerated above. Figure F.2 shows the stiffness matrix for the elastic beam with no subhinges. Figure F.6 shows the stiffness coefficients for the nonlinear cases with: one subhinge on both ends of a beam element. Only the coefficients shown in figure F.6 are changed, the rest of the coefficients remain as shown in figure F.2. It is noted that if one end is in the linear elastic range one can use the coefficients given in figure F.6 with a slope KP= ∞ .

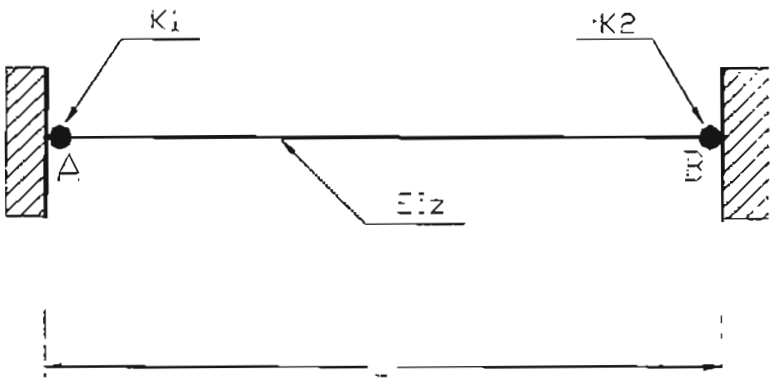

F.6 Plastic hinge at end A and end B.

$$K(2,2) = K(8,8) = 6*\left[-1+\frac{3(2+\beta_1)(2+\beta_2)}{\beta_1(4+\beta_2)+4(3+\beta_2)}\right]\frac{EI_z}{L^3}$$

$$K(2,6) = K(6,2) = \frac{6(2+\beta_2)}{\beta_1(4+\beta_2)+4(3+\beta_2)}\frac{K_1}{L}$$

$$K(2,8) = K(8,2) = 6*\left[1-\frac{3(2+\beta_1)(2+\beta_2)}{\beta_1(4+\beta_2)+4(3+\beta_2)}\right]\frac{EI_z}{L^3}$$

$$K(2,12) = K(12,2) = \frac{6\beta_2(2+\beta_1)}{\beta_1(4+\beta_2)+4(3+\beta_2)}\frac{EI_z}{L^2}$$

$$K(6,6) = \frac{4(3+\beta_2)K_1}{\beta_1(4+\beta_2)+4(3+\beta_2)}$$

$$K(6,8) = K(8,6) = \frac{-6\beta_1(2+\beta_2)}{\beta_1(4+\beta_2)+4(3+\beta_2)}\frac{EI_z}{L^2}$$

$$K(8,12) = K(12,8) = -K(2,12)$$

$$K(6,12) = K(12,6) = \frac{2\beta_1\beta_2}{\beta_1(4+\beta_2)+4(3+\beta_2)}\frac{EI_z}{L}$$

$$K(12,12) = \frac{4(3+\beta_1)K_{21}}{\beta_1(4+\beta_2)+4(3+\beta_2)}$$

Where: $\beta_1 = \frac{KP_1 L}{EI_z}$; $\beta_2 = \frac{KP_2 L}{EI_z}$

KP_1= K1 = slope of M-θ curve for end A.

KP_2= K2 = slope of M-θ curve for end B.

F.2.5 EFFECTS OF NONCOMPOSITE SECTIONS.

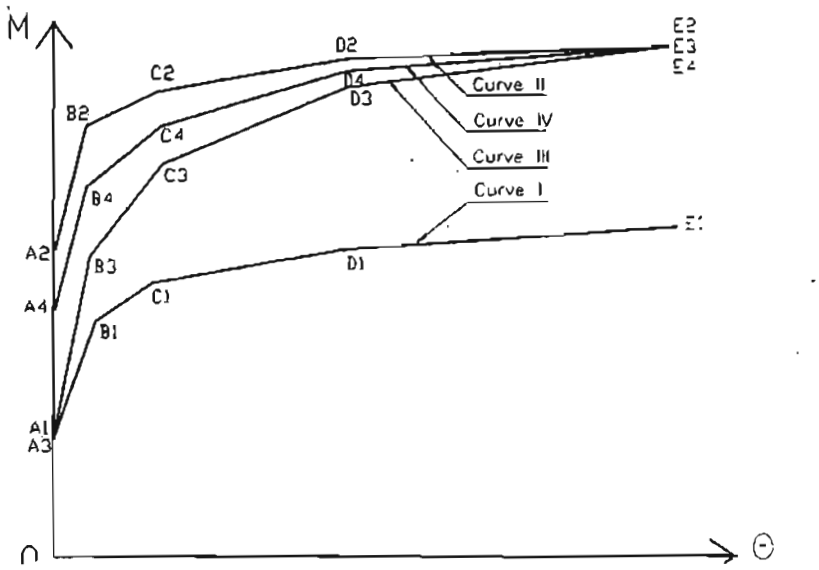

Fig. F.7 M-theta curves for noncomposite and composite sections.

The moment rotation curves used in NONBAN can be for either composite or noncomposite sections. However, a bridge's construction sequence may often result in some loads (permanent dead loads) being carried by the noncomposite section while other loads (superimposed dead loads and live loads) carried by the composite section. NONBAN accounts for this effect by considering the interaction between the moment rotation curves of the noncomposite and composite sections. For example, before the concrete deck hardens and reaches its final strength, only the noncomposite section of the girder resists the permanent dead loads. The permanent dead loads include the weights of the girders and the slab. The M-theta curve of the noncomposite section is represented by curve I: A1-B1-C1-D1-E1 in Fig. F.7. After the concrete hardens and reaches its final strength, the girder and the slab work together as a composite section. The M-theta curve of this composite section is represented by curve II: A2-B2-C2-D2-E2 in Fig.F.7. The loads resisted by the composite girders are the superimposed dead loads and live loads. The superimposed dead loads are the weight of the wearing surface, the attachments, etc. The live loads include the lane load, the truck loads, the seismic load, wind load, etc. The question is: how can the switch from the noncomposite moment rotation curve to the composite moment rotation curve be executed as the composite action takes effect. NONBAN accounts for this effect by assuming that the M-theta curve of this composite effect is represented by either curve III or curve IV depending on the intensity of the

permanent dead loads. Curves III and IV are derived from curves I and II by interpolation. Notice that the ultimate moment capacity of the composite section, M_{E2}, is not affected by the loading sequence. Therefore M_{E3} of curve III and M_{E4} of curve IV are equal to M_{E2} of curve II. When the moment caused by the permanent dead load is greater than M_{A1}, the M-theta curve of the combined effect is represented by curve III: A3-B3-C3-D3-E3 where M_{A3} is equal to M_{A1} and M_{E3} is equal to M_{E2}. The M_{B3}, M_{C3} and M_{D3} are increased proportionally from curve I as a function of M_{E2} -M_{A1} : When the moment caused by the permanent dead load is less than M_{A1}, The combined M-theta curve is represented by curve IV: A4-B4-C4-D4-E4. NONBAN assumes that the moment M_{A4} acting on the composite section causes the same stress at the bottom of the composite section as the stress at the bottom of noncomposite section caused by the moment M_{A1}. The M_{B4}, M_{C4} and M_{D4} points are increased proportionally from curve I as a function of M_{E2} -M_{A4} .

F.2.6. EFFECTS OF NONCOMPACT SECTIONS.

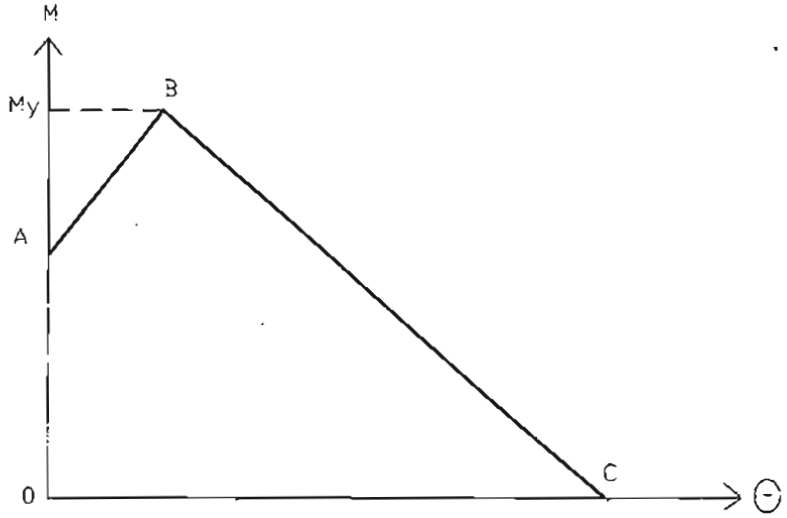

Fig. F.8 M-θ curve of noncomposite section.

NONBAN uses the M-theta curve of noncompact section derived from the empirical data provided by Schiling. In this section, unloading occurs when the moment reaches the yielding capacity My, i.e. point B on the curve shown in Figure F.8. NONBAN assumes that this section cannot undergo reloading once unloading begins, i.e. once structural equilibrium indicates that the noncompact section's moment has reached a value on leg BC of the curve shown. Because member reloading in segment BC is associated with numerical instability, the NONBAN analysis is stopped and the system is assumed to have reached its collapse loads. (See also figure F.4(b))

F.2.7. NONLINEAR ANALYSIS OF CONTINUOUS BRIDGES.

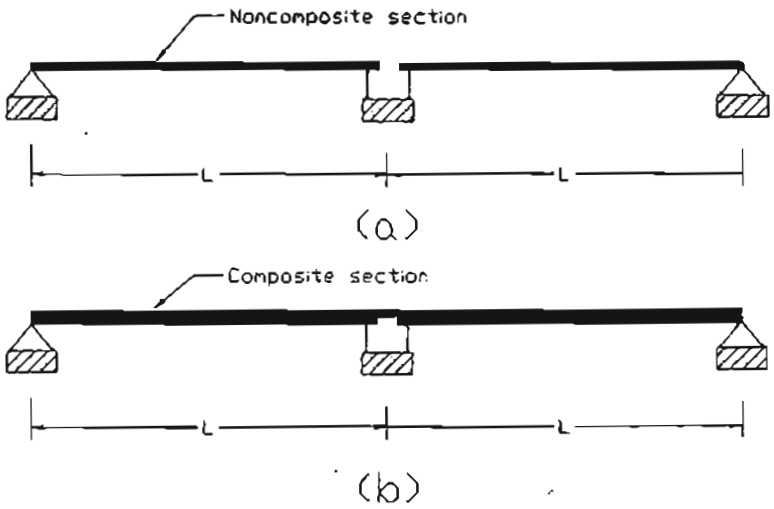

Fig. F.9 Continuous bridge with simply supported girders.

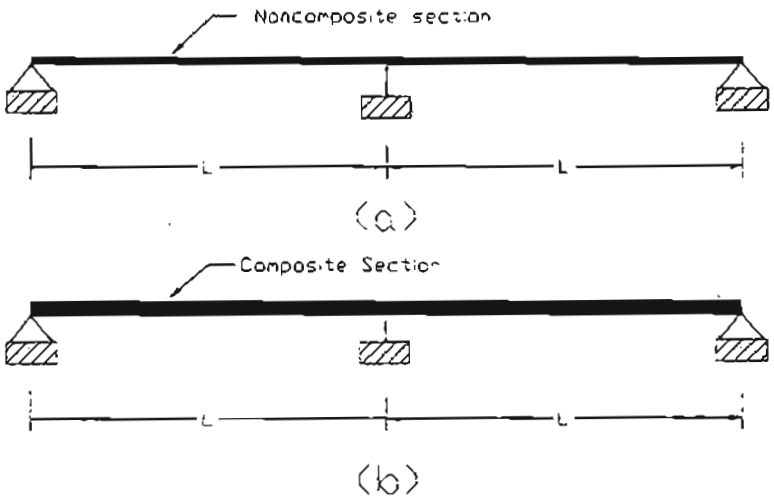

Fig.F.10 Continuous bridge with continuously supported girders.

NONBAN can distinguish between different construction sequences when it analyzes continuous bridges. In case I, shown in Fig. F.9, the girders with noncomposite sections work independently. They are simply supported at both ends in each span. The loads resisted by these noncomposite sections are the permanent dead loads. When the concrete hardens, the girders and the slab form composite sections that resist the superimposed dead loads and live

loads, as shown in case (b) in Fig. F.9. In case II, shown in Fig. F.10, the girders with noncomposite sections have continuity at the support. They carry the permanent dead loads. When the concrete hardens, the girders and the slab form composite sections that resist the superimposed dead loads and live loads, as shown in Figure 10.b). Except for the boundary conditions, NONBAN performs the nonlinear analysis of continuous bridges in the same manner as the nonlinear analysis of simply supported bridges, i.e. the interaction between the M-θ curves of the composite and noncomposite sections are as shown in figure F.7.

F.2.8 SHEAR NONLINEARITY OF CONCRETE MEMBERS.

In addition to nonlinearity under bending, concrete members exhibit nonlinear behavior due to shear. Shear behavior, however, is very difficult to model. Experimental results on the behavior of concrete members under shear show extremely wide scatter and the models available for predicting the ultimate shear capacity are extremely unreliable ([F.23] , [F.24] , [F.25]). Although bridge field tests and model tests have shown that shear failures in bridges under high loads are not usual, modeling the shear transfer mechanism seems to be an important factor for the analysis of concrete box-girder bridges [F.9] . In this study, modeling the shear behavior of concrete members uses a multilinear shear deformation curve as proposed in reference [F.9] . (see figure F.11).

When the beam is still in the linear elastic range, the initial shear stiffness is given as:

$$K_{v0} = GA_v \qquad \text{(F.6)}$$

where G is the shear modulus and Av is the shear area. Eq. F.6 gives the slope of the first segment of the shear deformation curve. In this range, the shear forces are assumed to be mostly carried by the concrete and the longitudinal reinforcing steel. The slope remains constant until the concrete cracks at a load V_{cr}. If no shear reinforcement is provided, the member will fail at that load level. V_{cr} can be calculated using the empirical equation proposed by Zsutty [F.25] (see also reference [F.23]) by:

$$V_{cr} = 59\,\{f'c\rho_w \frac{d}{a}\}^{1/3} b_w d \qquad \text{(F.7)}$$

where f'c is the concrete compressive strength in psi, ρ_w is the flexural shear reinforcement to shear area ratio and a/d is the shear span ratio. b_w is the web width and d is the effective depth.

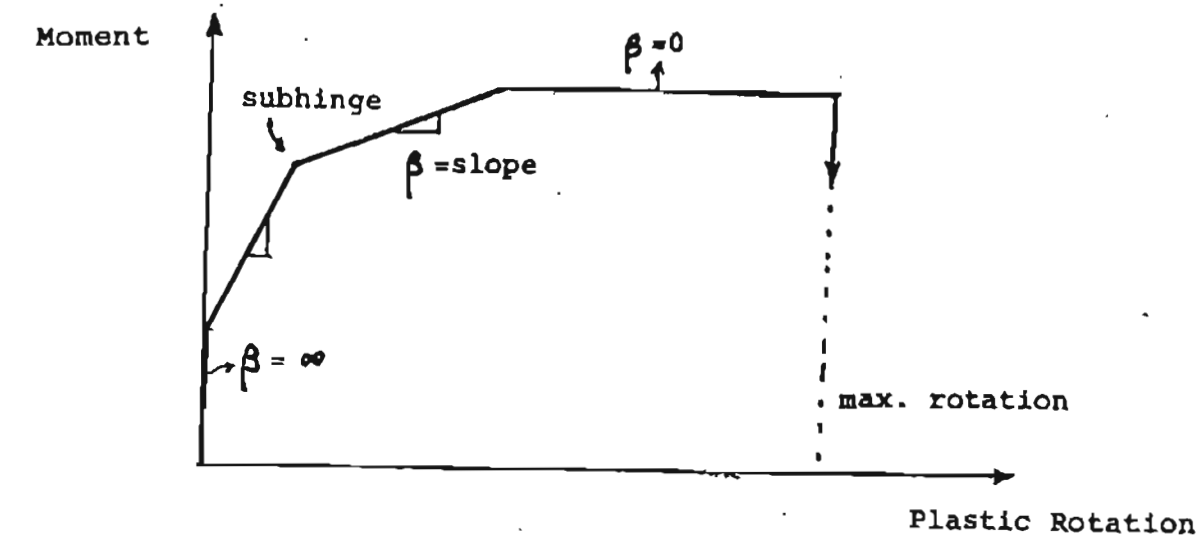

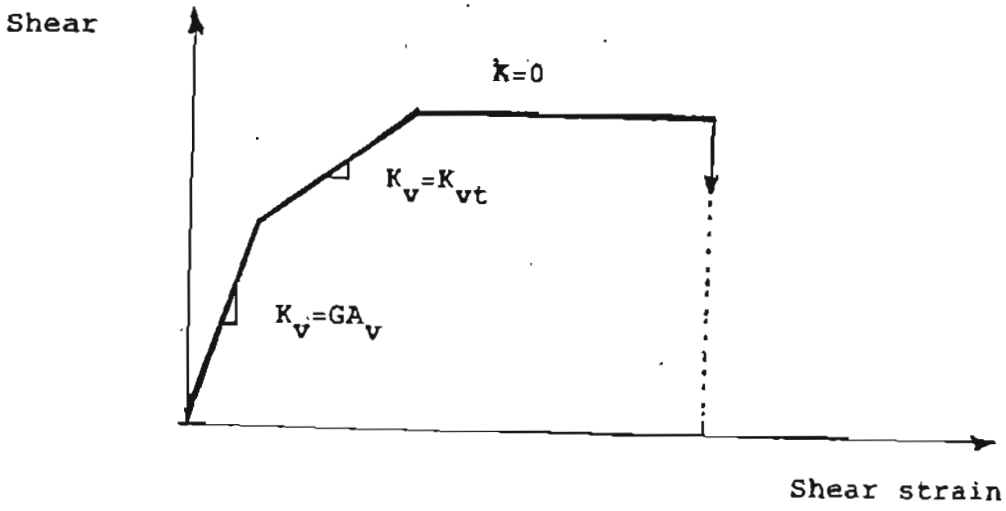

F.11 Material nonlinearity models for NONBAN.

If shear reinforcement is provided, it would produce additional strength and the ultimate shear capacity would be due to a combination of the concrete strength and the strength due to the vertical shear reinforcing bars. The slope of the shear--shear deformation curve above the cracking level can be obtained using the equation derived by Park and Pauley ([F.23]) which is given as:

$$K_{vt} = \frac{\rho_v}{1+4n\rho_v} E_s b_w d \qquad \text{(F.8)}$$

where E_s. is the elastic modulus of the reinforcing steel, b_w is the web thickness, d is the effective depth, and ρ_v is the shear reinforcement steel ratio and n is the modulus ratio.

Ultimate shear capacity is normally calculated by adding the capacity at cracking V_{cr} to the reinforcing steel capacity V_s such that:

$$V_u = V_{cr} + V_s \qquad \text{(F.9)}$$

where V_s is equal to:

$$V_s = \frac{A_t f_y d}{s} \qquad \text{(F.10)}$$

where A_t is the area of shear reinforcement within a distance s, f_y is the yield stress of steel, d is the effective depth of the section.

Reference [F.21] uses a variation on the model described above. For example, Eq. F.10 is corrected to account for the angle of inclination of the diagonal compressive stresses applied on the cross-section. This angle of inclination is calculated from tables as a function of the ratio of the applied shear stress to the compressive concrete stress capacity, f'c, and the strain in the longitudinal reinforcement

This model and similar models are widely used throughout the world although they are known to vastly underpredict the true shear capacity. This low prediction in the model is because it ignores many of the physical phenomena that help provide additional shear capacity such as arch action, aggregate interlock, etc.([F.23],[F.24], [F.25]). Many researchers are trying to develop better models based on the theory of fracture mechanics. These models however require further refinement before they can be used in actual practice [F.26]. Hall in reference [F.27] proposes a shear capacity model that is claimed to provide a better representation of the true shear capacity of concrete members.

In NONBAN , the effect of shear nonlinearity is modeled by a multilinear shear curve and it is up to the operator to decide the shape and magnitude of the points on this curve.

SECTION F.3

STRUCTURE OF THE PROGRAM NONBAN

The program NONBAN can be used to perform either a linear elastic analysis or a nonlinear incremental analysis of multi-girder bridge systems. The program is divided into 50 blocks (labeled from 0 to 49) and several subroutines. This section gives a brief description of the program's structure. The flow chart is given in figure F.12. For more details, the reader should consult the program listing given in Section F.5. The listing includes comment cards which give a more complete description of the program operation and definitions of the variables used.

As mentioned earlier, this program is designed as a research tool. Therefore, the reader may find that it is not user friendly nor efficiently written. The program contains many blocks and subroutines that are no longer used. For example, several subroutines were included to model the bridge deck using linear plate elements. These should not be used if the operator wishes to account for the nonlinear behavior of the deck. Also, two subroutines are used to perform an automatic generation of the mesh and input data. In addition, two other subroutines are used to prepare the output data for plotting. These routines are not necessary for understanding the program operation and the program can be executed without calling them. Therefore, the description of these specialized subroutines is not carried out in this report.

F.3.1 INPUT INFORMATION

This section gives a brief description of the required input information, Section F.5 of this Appendix gives a more detailed explanation of the input format.

F.3.1.1 System Information (Blocks 0 to 5)

After setting up the dimensions and the common blocks, the program expects the user to enter general information about the bridge model and the type of analysis that is required. Depending on the analysis option, this information requires two or three input lines.

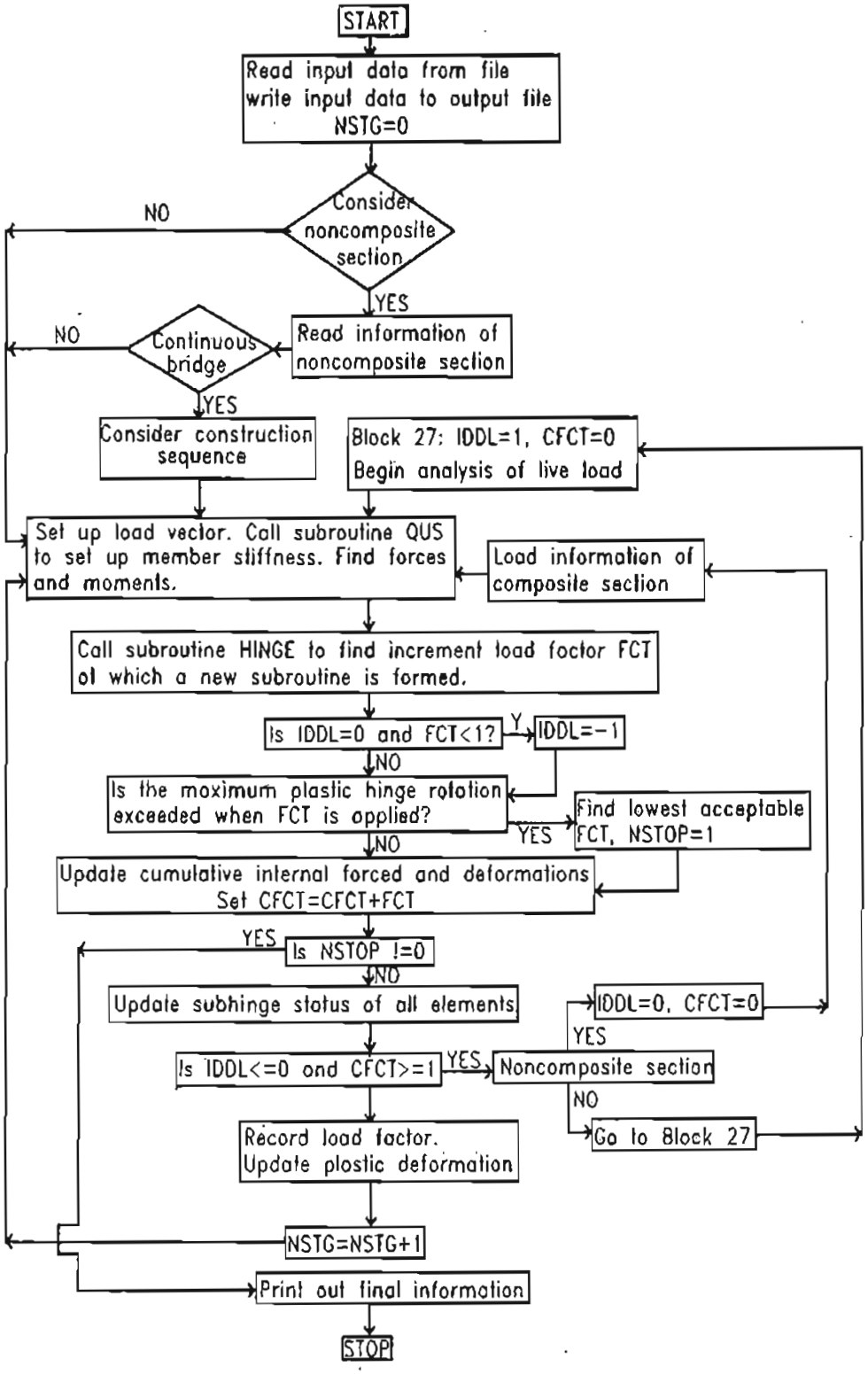

Fig. F.12. Flow chart of program NONBAN.

The first line includes three data entries: the analysis option, the Poison ratio and shear analysis indicator. The program assumes that all of the elements have the same Poison's ratio which is also entered in this stage. The second line includes the total number of nodes in this bridge, the total number of beam elements and the total number of beam elements that will undergo inelastic deformation. If the option number is great than 3, the third line is required. The data in the third line depends on the analysis option. Seven different analysis options are accepted: 1) Elastic analysis of the dead loads, 2) Nonlinear analysis of the dead loads, 3) Incremental analysis of live loads including dead load effects without considering the construction sequence. 4) Nonlinear analysis considering noncomposite sections for permanent load and accounting for continuity at support for all dead loads. 5) Nonlinear analysis considering noncomposite sections and assuming simple supports for permanent dead loads. 6) Same as 5 and accounting for effect of prestressing forces. 7) Option for calculation of elastic live load margin (LF1) and other redundancy information. (not completed yet).

The data in the third line are: a) the number of elements of girder beams if analysis option is 4 or 5, b) the number of elements of girder beams, the magnitude of prestressing force, the eccentricity of prestressing force and the allowed ultimate tension stress of the material in below the point of prestress if the analysis option equals 6, c) following the screen advece, put the analysis option of the input file NONBAN9.DAT if the analysis option equals 7.

F.3.1.2 Elastic Properties (Block 6)

The program divides the beam elements into categories based on their type of material. The cross sectional area, the moments of inertia about the two bending axes, the torsional constant, the section modulus of the principal bending, the elastic modulus, the shear modulus, the shear area in the vertical direction and shear area in the horizontal direction of each material type are required as input. The local x axis defines the longitudinal axis of the beam and the local z axis defines the primary bending axis.

F.3.1.3 Nonlinear Properties (Block 6)

If a nonlinear analysis is desired, the program expects the operator to enter information about the moment versus plastic rotation curve (M-θ) and shear deformation curve for each material type. Each curve must have four segments which are characterized by the moments or shear forces at which the subhinges are formed and the slope of each segment. In addition, the program requires for each material type a limiting maximum plastic hinge rotation

which is used as a stopping criterion. Three different curves are required for every material type: The first gives the behavior in positive bending and the second for the behavior in negative bending. The third gives the behavior of shear force. On the other hand, the operator can enter moment versus plastic curvature curves and the program will automatically convert these to moment rotation curves if the plastic hinge length is entered. If the M-θ curve is entered directly, then the length of the plastic hinge should be entered as 1.

F.3.1.4 Geometric Properties (Blocks 7-13)

The program expects to read the node coordinates in three dimensions. In addition, the connectivity of these nodes by beam elements is required. The properties of each beam element are identified by assigning to every element a material type number from the list of materials previously entered.

The program calculates the direction cosines of every element which are subsequently used to perform the rotation between the global and local coordinate systems. The boundary conditions are entered by identifying the nodes that are restrained. The restrained displacements and/or rotations are also identified and are always assigned a value of one.

F.3.1.5 Identification of the shape and size of the Global Stiffness Matrix (Block 14)

Using the beam connectivity information, the program calculates the size of the global stiffness matrix. The program also defines the address of every degree of freedom in the global stiffness matrix. In this program, the global stiffness matrix is a one dimensional array arranged such that it contains the data of the lower triangular portion of the global matrix with a variable bandwidth which depends on the size of the matrix.

F.3.1.6 Dead Load Data (Blocks 15 & 16)

Dead loads are defined herein as the loads that will not be incremented. The dead load data can be entered as either concentrated loads (and moments) at the nodes or as uniform loads along the beams. The intensity of the uniform dead load is in the local y direction. The numbers of the first and the last beam in the series of beams that carry uniform dead load should be entered. The program automatically converts the uniform load data into equivalent concentrated forces and moments applied at the ends of each beam. If the analysis option is greater than 3, NONBAN requires two dead loads. Dead load one is the permanent dead load which is supported by the noncomposite

section. The permanent dead load includes the weight of girder, slab and transverse diaphragms. Dead load two is the superimposed dead load which is applied on the bridge after composite action takes effect. The superimposed dead load includes the weight of wearing surface, sidewalks and other attachments.

F.3.1.7 Live Load Data (Block 17)

The live load data defines the loads that will be incremented during the course of the nonlinear analysis. The final results are given as load factors i.e. as multipliers of the original live load data entered at this point. Only concentrated loads (forces as well as moments) can be entered here.

F.3.1.8 Output Option (Block 18)

To minimize the amount of output obtained from the program, a listing of the nodes for which detailed information is required is entered at this stage.

F.3.1.9 Printing of Input Data (Block 19)

A summary of the input data is printed out by calling subroutine WRITDATA.

F.3.2 PREPROCESSING OF PERMANENT DEAD LOADS AND SUPERIMPOSED DEAD LOADS
(Blocks 20-23)

As a first step, the program performs the analysis of the dead loads separately. The load vector for the analysis of the dead loads is set up at this stage by superposing the concentrated dead load data and the uniform dead load data. The program initializes all the counters and the vectors where the results will be stored. If the analysis option is greater than 3, the program performs the analysis of the permanent dead loads first. Then the program uses the composite member properties and prepares the appropriate mesh for the analysis of the superimposed dead load. Except for the material properties and the mesh used, the analysis performed for the superimposed dead loads is similar to the analysis performed for the permanent dead loads.

F.3.3 ANALYSIS OF DEAD LOADS (Block 24)

The analysis of the dead loads is performed following the same approach used later for the incremental analysis with one exception. The load factor for the dead load analysis should never exceed 1.0. The analysis of the dead load is performed by going to block 28 (paragraph F.3.5).

F.3.4 INITIALIZE VARIABLES FOR INCREMENTAL ANALYSIS (Blocks 25-27)

The internal moments as well as the permanent rotations (if any) obtained from the analysis of the dead loads are saved for the incremental analysis. However, the deflections are initialized to zero. Therefore, zero deflections are hence defined as the deflections of the bridge under dead load alone. The live load vector is also set up at this stage and the live load factor is set to zero.

F.3.5 STRUCTURAL ANALYSIS (Block 28)

The structural analysis is performed by calling subroutine QUS. QUS initializes the global stiffness matrix and then calls subroutine RODJ which calculates the stiffness matrix for every beam element. Element stiffness matrix is derived from the modified flexibility matrix which accounts for the inelastic rotation when the element goes beyond the elastic range. Subroutine RODJ also rotates these stiffness matrices from the local coordinate system to the global coordinate system. After returning from RODJ, subroutine QUS calls subroutine K1PKJ that assembles the global stiffness matrix. The load vector is assembled in QUS. Subroutine SSSJC is then called to solve the system of simultaneous equations. The deformations of every degree of freedom are given in global coordinates. The maximum displacement is identified when the program returns to the main routine.

F.3.6 CALCULATION OF INTERNAL FORCES FOR ONE LOAD STEP (Blocks 29-31)

The program analyzes the results of each load step by first calculating the end moments for each element. This is performed by calling subroutine RODJ again to find the stiffness matrix. At this point the stiffness matrix calculated for the local axes (before rotation) is used. However, since the deformations were calculated in the global system, these will have to be rotated to the local system before multiplying them by the stiffness matrix. The matrix

multiplication yields the internal forces and moments at the ends of every beam element. If the user had asked for an elastic analysis, the program is stopped at this stage after printing out the results obtained.

F.3.7 BEGIN THE INCREMENTAL ANALYSIS (Blocks 32-34)

If this is the first iteration step, the program initializes the cumulative load factor and the cumulative moments. The program also identifies the members that are being loaded from those that are being unloaded. The next subhinge that could be formed at the ends of every element is identified. The moments at which these new subhinges would be formed are calculated by adjusting the M-θ curves to account for the internal moments due to the dead loads.

F.3.8 FIND THE LOAD FACTOR FOR ONE ITERATION (Block 35)

The program calls subroutine HINGE to perform a comparison between the moments at which the subhinges would form, the cumulative moments of every element accumulated from previous load steps and the internal moments obtained from the last load step as described in paragraph F.3.6. The factor that would cause each element to reach its next subhinge is calculated. The final load factor which will be used is the lowest factor. This factor is called the incremental load factor. The program also identifies the members where a subhinge would form if the incremental load factor is applied.

F.3.9 CHECK MAXIMUM PLASTIC HINGE ROTATION (Block [F.23])

The program verifies that by using the incremental load factor identified in block 35 (paragraph F.3.8), the maximum plastic hinge rotation limit is not exceeded for any element. Otherwise, the program calculates the maximum possible incremental load factor that can be used.

F.3.10 UPDATE CUMULATIVE FORCES AND DISPLACEMENTS (Blocks 37-45)

The program updates the total load factor by adding the incremental load factor calculated from the last iteration step to those found in previous steps. Also, if this is an analysis of dead loads, the program verifies that the total load factor including the incremental load factor does not exceed 1.0. The program then calculates the cumulative displacements and rotations for every node as well as the cumulative internal moments. This is done by multiplying the deformations and internal moments calculated in blocks 29 through 31

(paragraphs F.3.6) for one load step by the incremental load factor and then adding them to the cumulative moments and deformations calculated in previous iterations.

F.3.11 PREPARE FOR NEXT ITERATION STEP (Blocks 46-48)

The data is prepared for the next iteration. The next possible hinges that would form at the ends of every beam element are identified. The updated slopes of the M-θ curves are also identified for every element. The program then returns to block 28 (paragraph F.3.5) or to block 25 (paragraph F.3.4) if this is the end of the dead load analysis.

F.3.12 STOPPING (Block 49)

The program stops if one of the following criteria is met:

- Any section's total rotation equals the maximum plastic hinge rotation.
- The stiffness matrix is not solvable due to errors in the input data.
- A maximum number of 600 iterations has been performed.
- A very large displacement was calculated denoting that the structure became unstable.
- A large unloading in a member whose slope is still positive.
- A reloading in a noncomposite member whose slope has reached a negative value.
- After one iteration if elastic analysis only was requested.
- After calculating the internal moments due to the application of the dead loads if only a dead load analysis option had been indicated.

SECTION F.4

PROGRAM VALIDATION

To verify the accuracy of the program NONBAN, the analysis of several bridge models was performed. The results of NONBAN were compared to exact results, to the results of other programs and to results published by other researchers. This section gives a sample of the many tests and comparisons performed during the development of the program. As can be seen in this report, the comparisons show that NONBAN gives excellent agreement with exact and published results for both the elastic analysis and the elasto-plastic analysis of simple beam models as well as complete bridge models.

The proposed approach of using M-θ curves for performing a complete nonlinear analysis was further tested by comparing the results of NONBAN with the published results of full scale laboratory tests of beams as well as full scale field tests of bridges. Here again, excellent agreement was observed. In addition to the comparisons given in this section, many comparisons are presented in Appendices B, C and D of this report and in appendix D of the phase I report. Many of the comparisons reported there are not repeated in this appendix.

F.4.1 ELASTIC ANALYSIS OF BEAM MODELS

The analysis of five beam models has been performed under different loading conditions to verify the capability of the program to produce exact results in the linear elastic range. For these analyses each span was divided into four elements of equal lengths.

The models tested in this section are shown in figure F.13. Table F.1 compares the results obtained by NONBAN to the exact results. Perfect match is obtained with 0% error for most of the cases studied. The very small differences observed for the continuous beams are only due to round off errors.

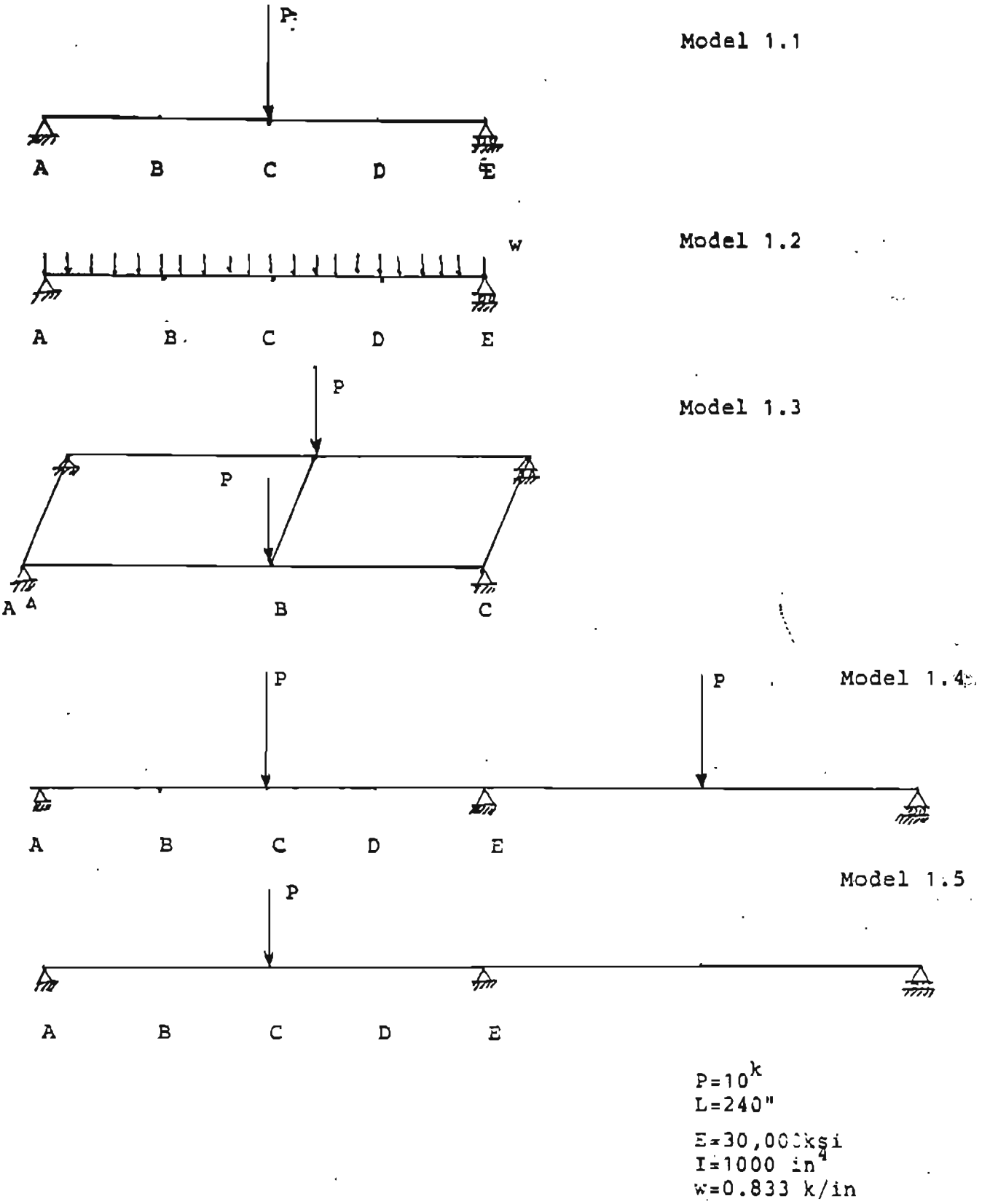

Figure F.13 Elastic beam models.

Table F.1 - Comparison of Results of NONBAN to Exact results of Beam Models (Linear-elastic)

Model	Response	Exact	NONBAN	Error
1.1	moment at C	600 kip-in	600 kip-in	0%
	moment at B	300 kip-in	300 kip-in	0%
	deflection at C	0.096 in	0.096 in	0%
	deflection at B	0.066 in	0.066 in	0%
	rotation at A	0.0012 rad	0.0012 rad	0%
	rotation at B	0.0009 rad	0.0009 rad	0%
1.2	moment at C	600 kip-in	600 kip-in	0%
	,moment at B	300 kip-in	300 kip-in	0%
	deflection at C	0.12 kip-in	0.12 kip-in	0%
	deflection at B	0.0855 in	0.0855 in	0%
	rotation at A	0.0016 rad	0.0016 rad	0%
1.3	moment at C	600 kip-in	600 kip-in	0%
	deflection at C	0.096 in	0.096 in	0%
	ratation at C	0.0012 rad	0.0012 rad	0%
1.4	moment at C	374.4 kip-in	370.0 kip-in	0.2%
	moment at E	451.2 kip-in	450.0 kip-in	0.3%
1.5	moment at C	243.6 kip-in	243.8 kip-in	0.1%
	moment at E	225.6 kip-in	225.0 kip-in	0.3%

F.4.2 ELASTO-PLASTIC ANALYSIS OF BEAM MODELS

Several beam models were also analyzed assuming that their material behavior was elasto-plastic. These models are shown in figure F.14. Models 2.6, 2.7 and 2.8 test the capability of NONBAN to consider hinges that form under the effect of the dead load alone. Table F.2 shows the comparisons between the results given by NONBAN and the exact results. Here again, excellent agreement is observed. The small differences observed for certain cases are only due to round off errors.

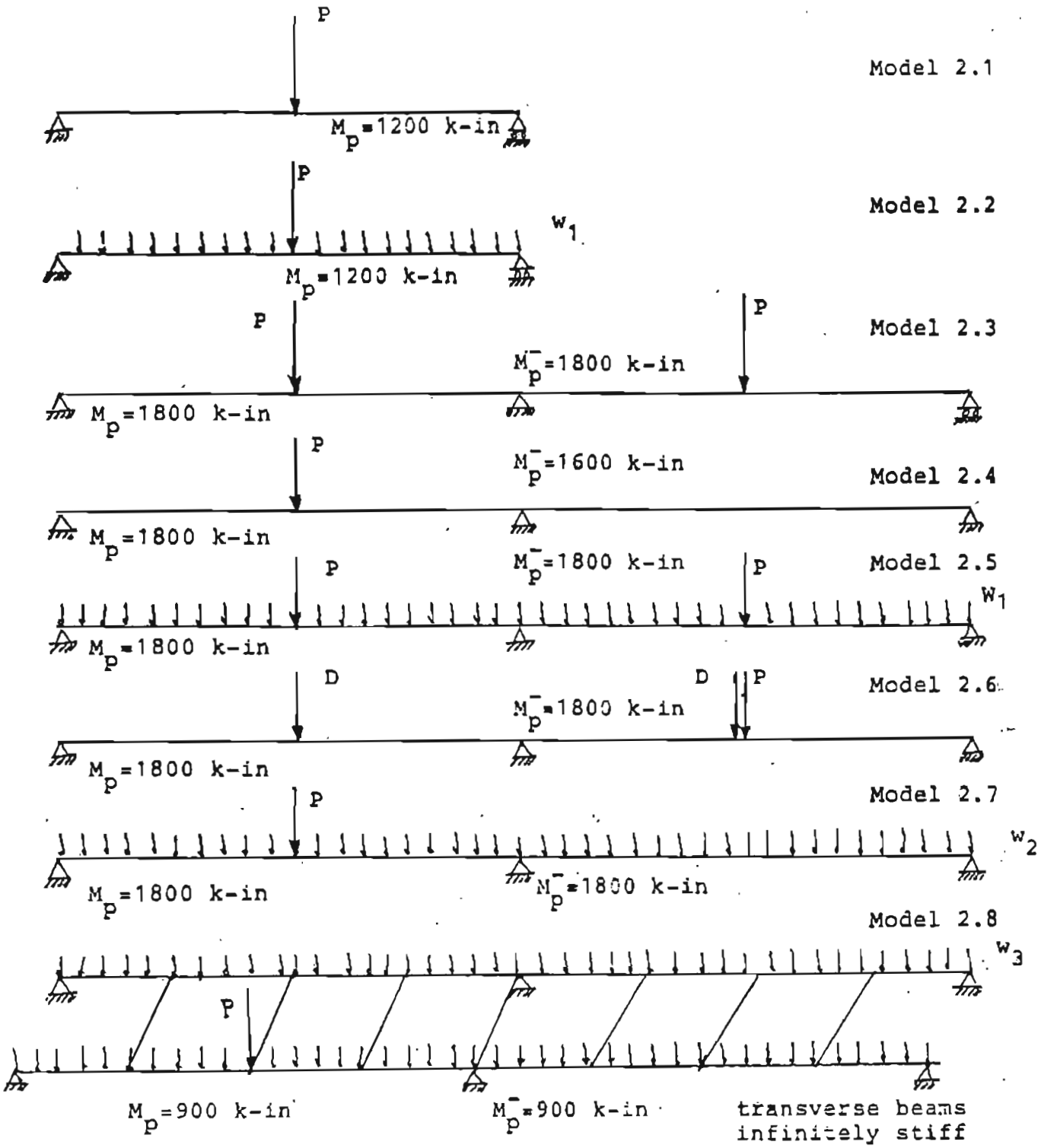

P=10 K
L=240 in
E=30000 ksi
I=1000 in^4

w_1=0.0833 k/in
w_2=0.260 k/in
w_3=0.130 k/in
D=42 kips

F.14 Elasto-Plastic beam models.

Table F.2 - Comparison of Results of Beam Models Assuming Elasto-Plastic Behavior

Model	Load Factor at	Exact	NONBAN	Error
2.1	Ultimate	2.00	2.00	0%
2.2	Ultimate	1.00	1.00	0%
2.3	1st hinge	3.99	4.00	0.3%
	Ultimate	4.50	4.50	0%
2.4	1st hinge	3.69	3.69	0%
	Ultimate	4.33	4.33	0%
2.5	1st hinge	2.67	2.67	0%
	Ultimate	3.50	3.50	0%
2.6	1st hinge	0.95	0.95	0%
	Ultimate	0.31	0.30	3%
2.7	1st hinge	0.96	0.96	0%
2.8	Ultimate	1.38	1.38	0%

F.4.3 NONLINEAR BEHAVIOR OF BEAM MODELS

The example illustrated in figure F.15 was designed to test the capability of the program to handle several segments on the moment versus plastic rotation curves. Also, this example tested the capability of NONBAN to include member softening (negative slopes). The continuous beam shown in figure F.15 was analyzed exactly and the results compared to those obtained from NONBAN. Table F.3 shows that the results of NONBAN give perfect agreement with the exact results.

Table F.3 - Comparisons of Results of Beam Model Assuming Nonlinear Behavior

Model	Load Factor at	Exact	NONBAN	Error
3.1	1st hinge	3.69	3.69	0%
	2nd hinge	4.50	4.50	0%
	Ultimate	3.08	3.08	0%

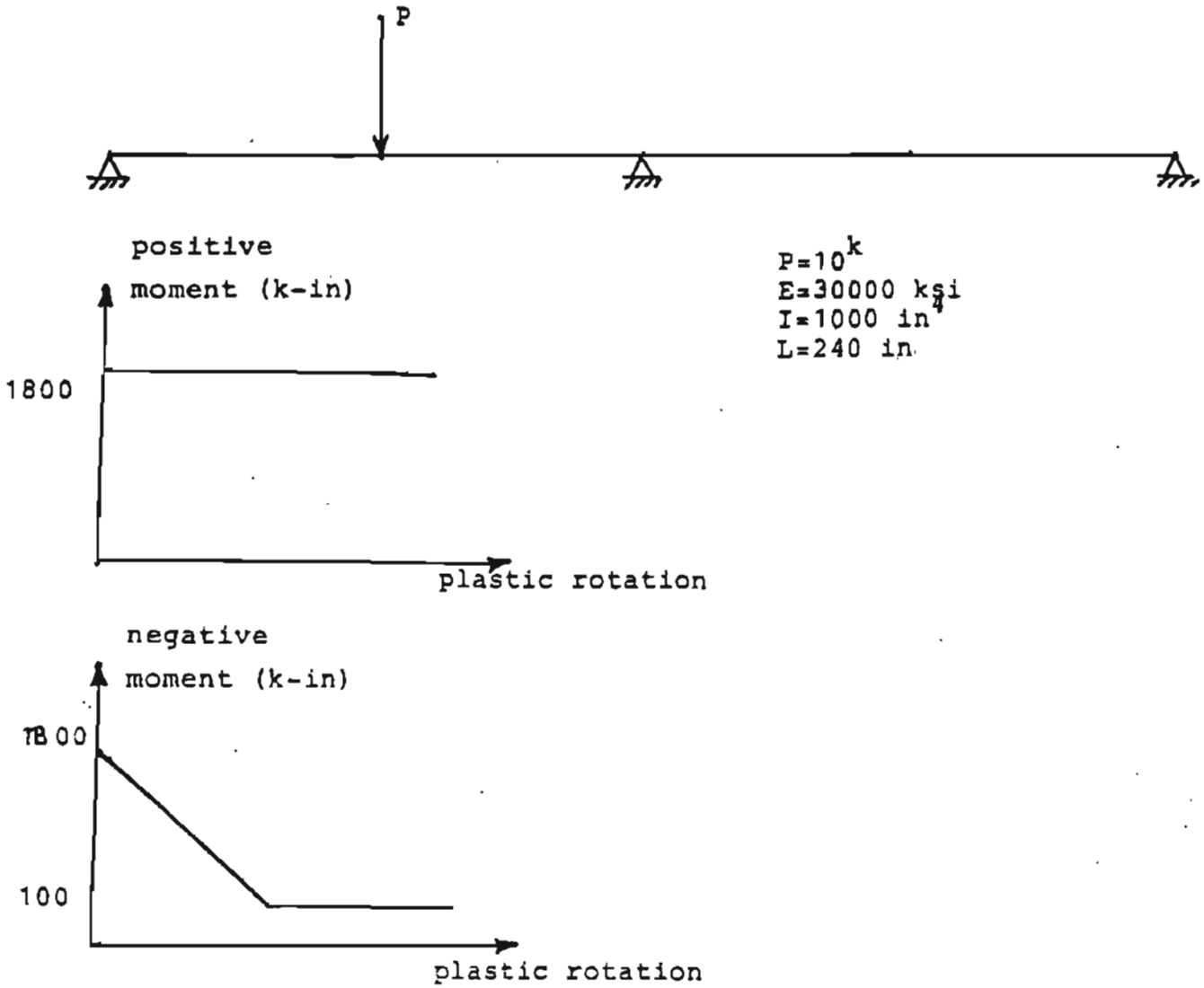

F.15 -Nonlinear beam model 3.1

To check the sensitivity of the results to different levels of mesh refinement, the model shown in figure F.16 was analyzed assuming that it is formed of a total of 8 beam elements, then assuming 16 beam elements and finally assuming 32 beam elements. The results are plotted in figure F.17. Figure F.17 confirms that the results are not sensitive to the mesh size unless the deformations become excessive. The difference for very large deformations is due to the assumption made during the derivation of the stiffness matrices which considered that the nonlinearity is concentrated at the ends of the beam elements. Fig. F.17 also confirms that the results do not influence the magnitude of the calculated ultimate load. For example, in the case analyzed in this section divergence in the load curves due to the different mesh sizes begins at a load level equal to 92% of the ultimate capacity. It is noted that at that load level the deformation is higher than span length over 100 (L/100). In our opinion, these differences at such a high level of load and deformation are acceptable for practical engineering purposes. The example given is for a hypothetical bridge formed by one single beam. For more realistic bridge models the effect of mesh size is shown to be negligible as will be further discussed in section F.4.6.

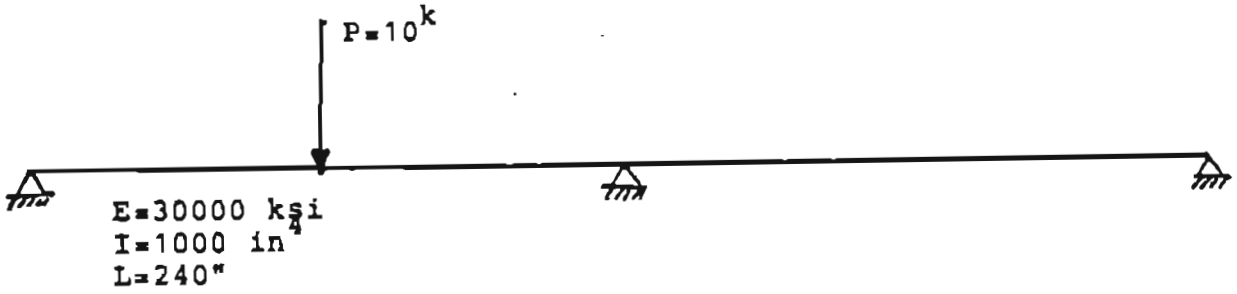

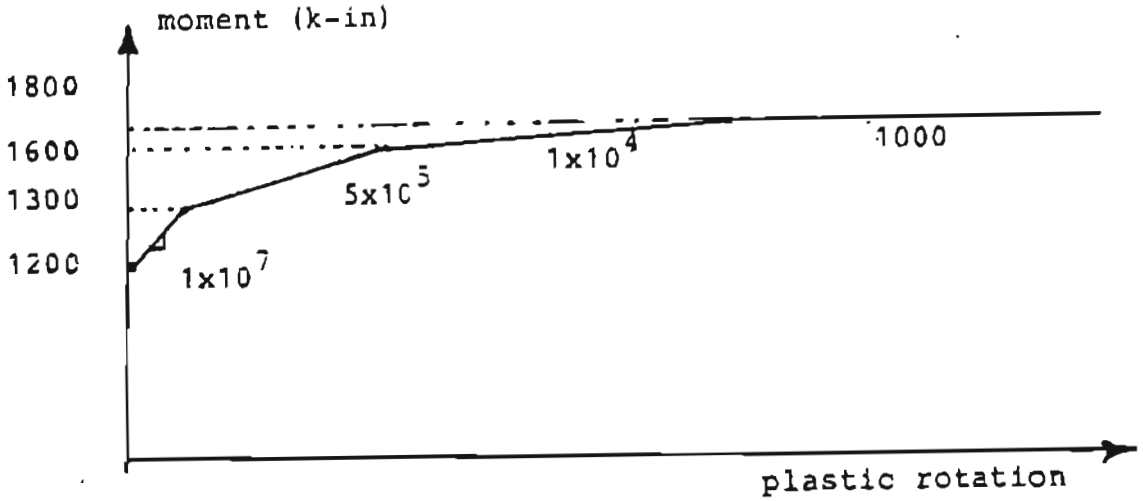

F.16 Nonlinear beam model 3.2

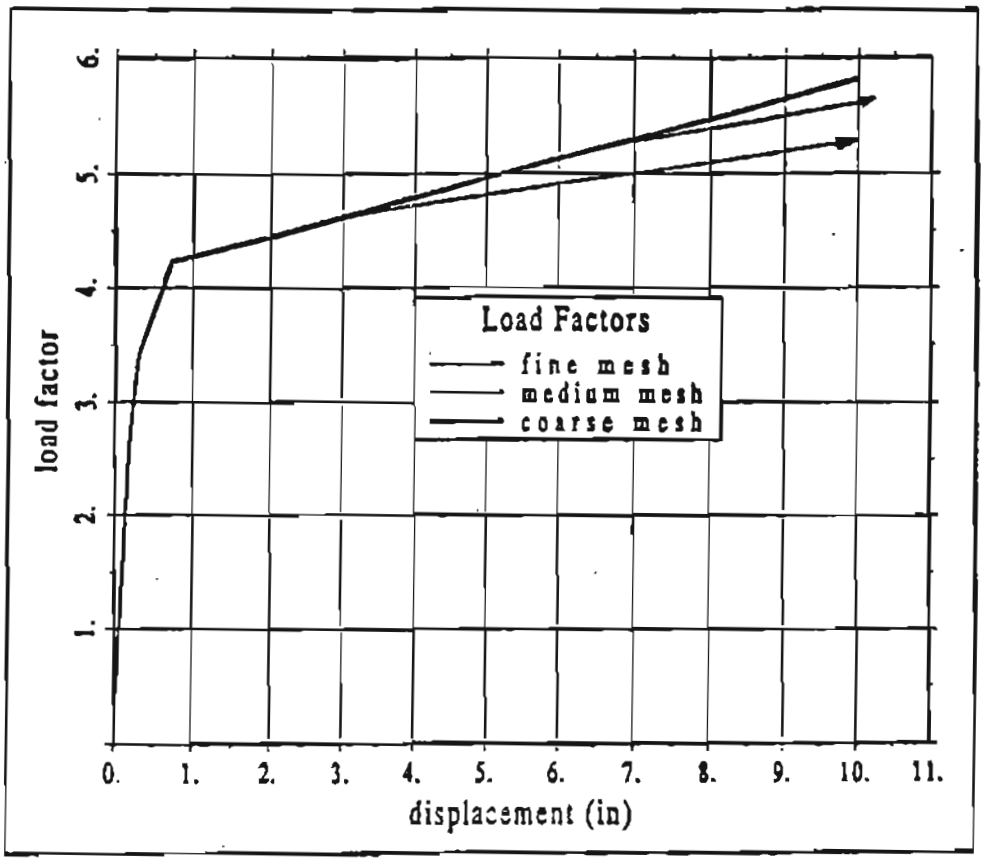

F.17 -Comparison of results for different mesh refinements.

F.4.4 ELASTIC ANALYSIS OF BRIDGE MODELS

To further verify the validity of NONBAN, the program was tested on a full scale bridge model. A linear elastic analysis was performed. In this example, the longitudinal girders were modeled as beam elements while the bridge deck was modeled as plate elements. The use of plate elements was later abandoned in order to better model the nonlinear behavior of the deck which the plate elements used with NONBAN did not consider. NONBAN can model the bridge deck as plate elements if only an elastic analysis is performed.

The four-girder 80-ft simple-span steel composite bridge shown in figure F.18 was analyzed using NONBAN and using SAP90. The bridge was first analyzed assuming dead load only. The analysis was then repeated assuming HS-20 loading. One vehicle was assumed to be on the bridge at the point causing the maximum moment effect in one beam. The analysis was performed for the dead load only and then for the dead load plus one vehicle load. Also, several damage scenarios were assumed: In the first case, the bridge was assumed to be intact, the second case considered a bridge where the outer girder was damaged at the point of maximum moment, and finally the third case considered a bridge where the inner girder was damaged at the point of maximum moment. In this example, member damage was simulated by removing a 10-ft element of the girder near the mid-point.

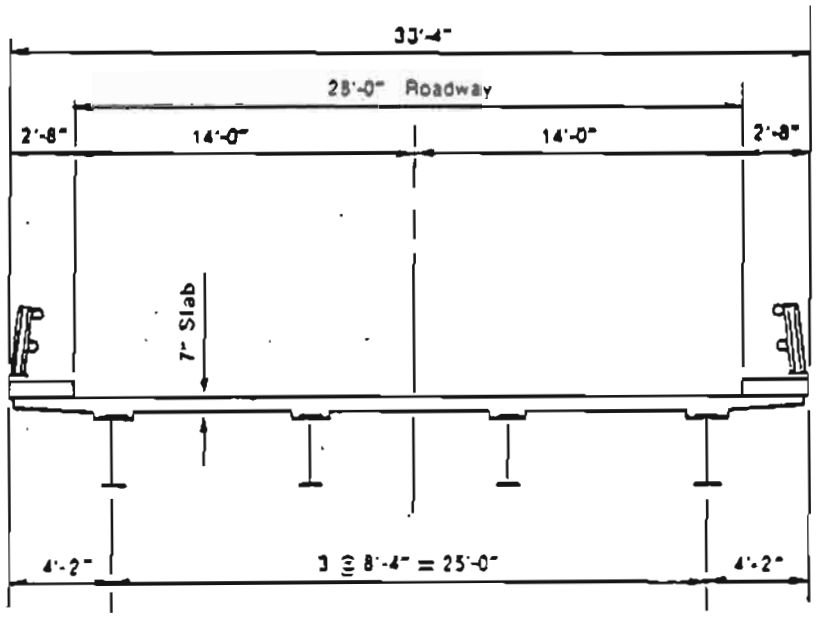

TYPICAL SECTION

F.18 -Cross section of steel bridge model.

Table F.4 gives the maximum displacements and the maximum moments for all the cases analyzed using NONBAN and SAP90. The comparisons shown in table F.4 illustrate that the maximum difference between NONBAN and SAP90 is less than 4% for the maximum displacement. The moments are found to be within 1.2%. These differences are very acceptable and are mostly due to the different types of plate elements used in NONBAN and in SAP90.

Table F.4 - Comparison of results of simple span steel bridge to results of SAP90 finite element package.

		Maximum Deflection (in)			Maximum Moment x 10^4		
Load	Case	NONBAN	SAP90	Error	NONBAN	SAP90	Error
DL	Intact	0.668	0.667	0.16%	0.1022	0.102	0.14%
DL	Outer Girder Damaged	2.022	2.016	0.30%	1.933	1.927	0.41%
DL	Inner Girder Damaged	1.138	1.101	3.25%	1.527	1.499	1.20%
LL	Intact	0.501	0.507	0.64%	0.822	0.828	0.70%
LL	Outer Girder Damaged	1.708	1.640	1.00%	1.339	1.332	0.50%
LL	Inner Girder Damaged	0.661	0.659	0.40%	1.115	1.110	0.45%

Another comparison with the results of SAP90 is performed for a four-girder continuous bridge with two 100 ft spans. The cross section of the bridge is the same as that shown in figure F.18. The results of the linear analysis using AASHTO vehicles as live load, are shown in table F.5. The loading conditions considered are: dead load alone, one lane loaded in one span or two spans and two lanes loaded in one span and two spans. The comparison between NONBAN and SAP90 shows good agreement for all the cases considered with a maximum difference on the order of 2% for the maximum negative moment under dead load.

Table F.5 - Comparison of results of two- span continuous steel bridge to results of SAP90 finite element package

		Max. Positive Moment (10^4 kip-in)		Max. Negative Moment (10^4 kip-in)		Max. Deflection (in)	
Span	Loading	NONBAN	SAP90	NONBAN	SAP90	NONBAN	SAP90
1 span	1 lane	0.74	0.74	0.33	0.33	0.87	0.86
	2 lanes	1.02	1.02	0.45	0.44	1.21	1.21
2 spans	1 lane	0.66	0.66	0.61	0.61	0.70	0.69
	2 lanes	0.89	0.88	0.83	0.83	0.94	0.94
	DL	1.00	1.00	1.32	0.30	1.14	1.13

Another example tested is a simple span prestressed concrete bridge with three box girder cells as shown in figure F.19. The results of NONBAN are compared to those of the program PGRIDVAX developed at the Polytechnic University of Catalonia for the design and analysis of bridges. The results show perfect agreement between the two packages. In this example, the box girders are modeled as beam elements but shear deformations are included to account for the stiffening effect of the box girder over its entire width. The deck is modeled as transverse beams and the load is applied as shown in figure F.19. Table F.6 shows a comparison between the results of NONBAN and those of PGRIDVAX.

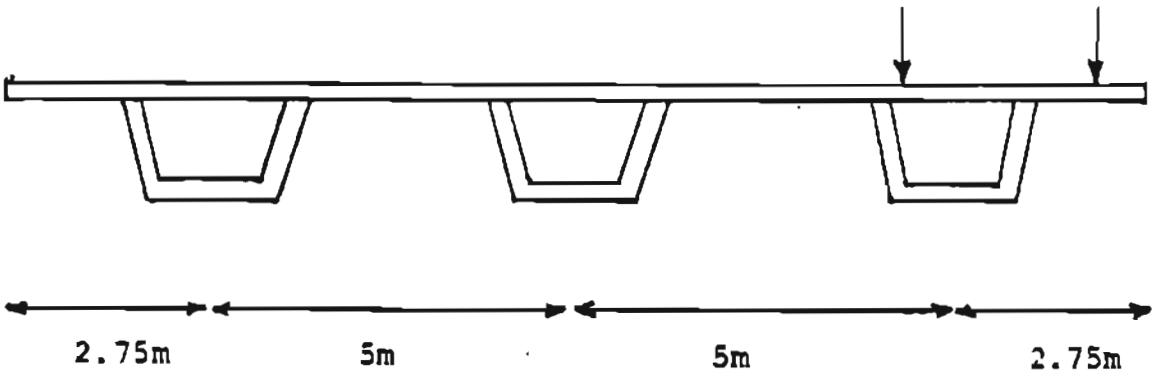

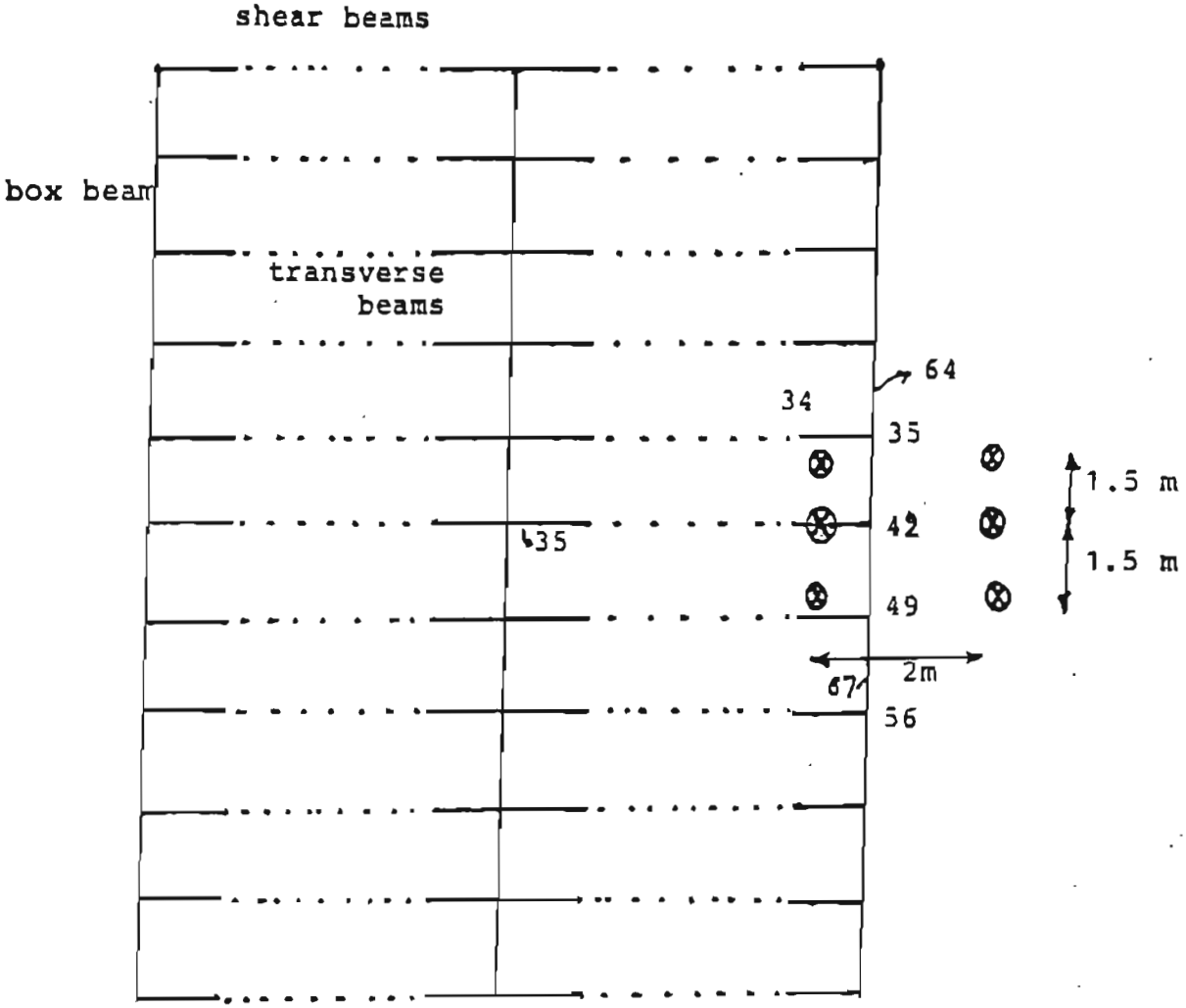

Box beam properties

$I=0.3244\ m^4$

$J=0.528\ m^4$

$E=3000000\ t/m^2$

shear beam $A_s=61.5\ cm^2$

F.19 -Model of prestressed concrete box girder bridge.

Table F.6 - Comparison of Results of Prestressed Concrete Bridge Model Assuming Elastic Behavior

Response	Location	PGRIDVAX	NONBAN	Error
Deflection	joint 34	0.0110 m	0.0110 m	0%
	joint 35	0.0126 m	0.0126 m	0%
	joint 42	0.0134 m	0.0134 m	0%
	joint 49	0.0126 m	0.0126 m	0%
	joint 56	0.0106 m	0.0106 m	0%
Rotations	joint 34	0.0015 rad	0.0015 rad	0%
	joint 35	0.0015 rad	0.0015 rad	0%
	joint 42	0.0015 rad	0.0015 rad	0%
	joint 49	0.0015 rad	0.0015 rad	0%
	joint 56	0.0014 rad	0.0014 rad	0%
Internal Moments				
	member 35	82.39 Kn-m	82.40 Kn-m	0%
	member 64	202.5 Kn-m	202.5 Kn-m	0%
	member 67	147.1 Kn-m	147.1 Kn-m	0%

F.4.5 NONLINEAR ANALYSIS OF BRIDGE MODEL.

NONBAN was also "tested" by analyzing one of the bridges used by Maheu in a study for the Ontario Ministry of Transportation (F.8). The bridge is a slab-on-girder steel structure composite in both the positive and negative bending regions. The five-girder two-lane bridge has two continuous spans of 12.8m each. The cross section and elevation of the bridge are given in Figure F.20. The bridge was modeled as a grid by Maheu (F.8) and the analysis was performed assuming elasto-plastic behavior of the longitudinal members and elastic behavior of the deck slab, i.e. no transverse hinges are included in the analysis. This assumption was based on the observation made by Maheu [F.8] that experimental tests have shown that deck slabs possess much greater strengths than their flexural resistance would suggest and thus failure of slabs in the transverse direction is unlikely. The steel sections were assumed to be compact and fully braced. The bridge was symmetrically loaded using four OHBDC vehicles as shown in figure F.20. The results of the analysis are presented in figure F.21. The figure shows the total applied live load in Kilo-Newtons versus maximum deflection in millimeters. The solid line gives the results as published in reference [F.8]; the dashed line gives the results obtained using the program NONBAN. The comparison indicate that the post-elastic behavior obtained using NONBAN is very close to the curve obtained by Maheu.

This page is Blank

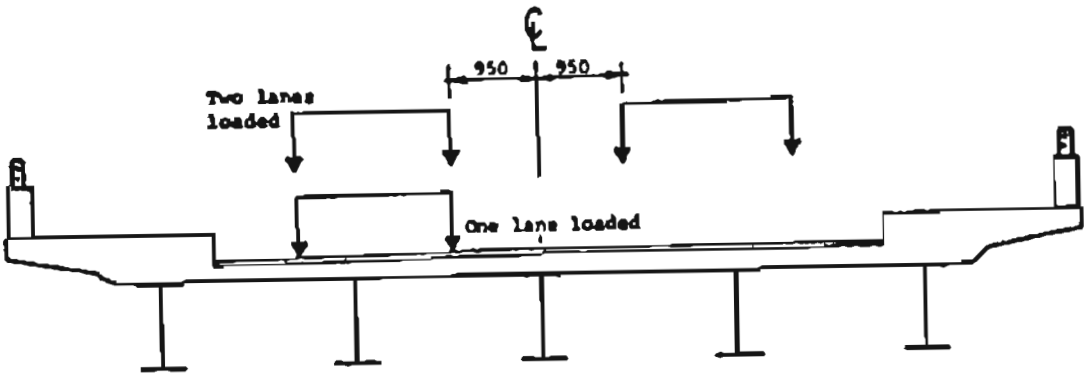

(a) Transverse positions of CHBD vehicle

All dimensions in mm

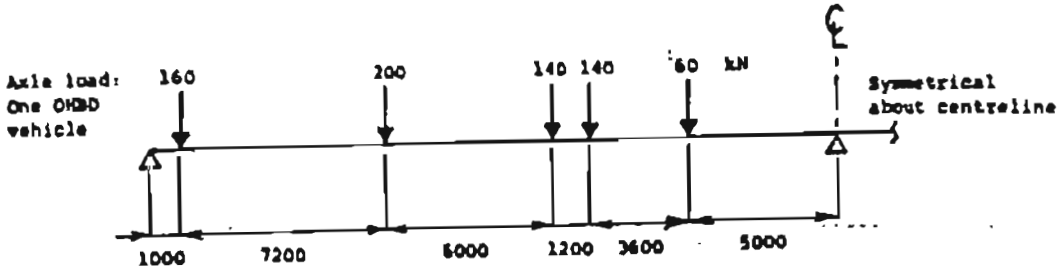

(b) Longitudinal position

F.20 Loading and Layout of bridge analyzed by Maheu (D-3).

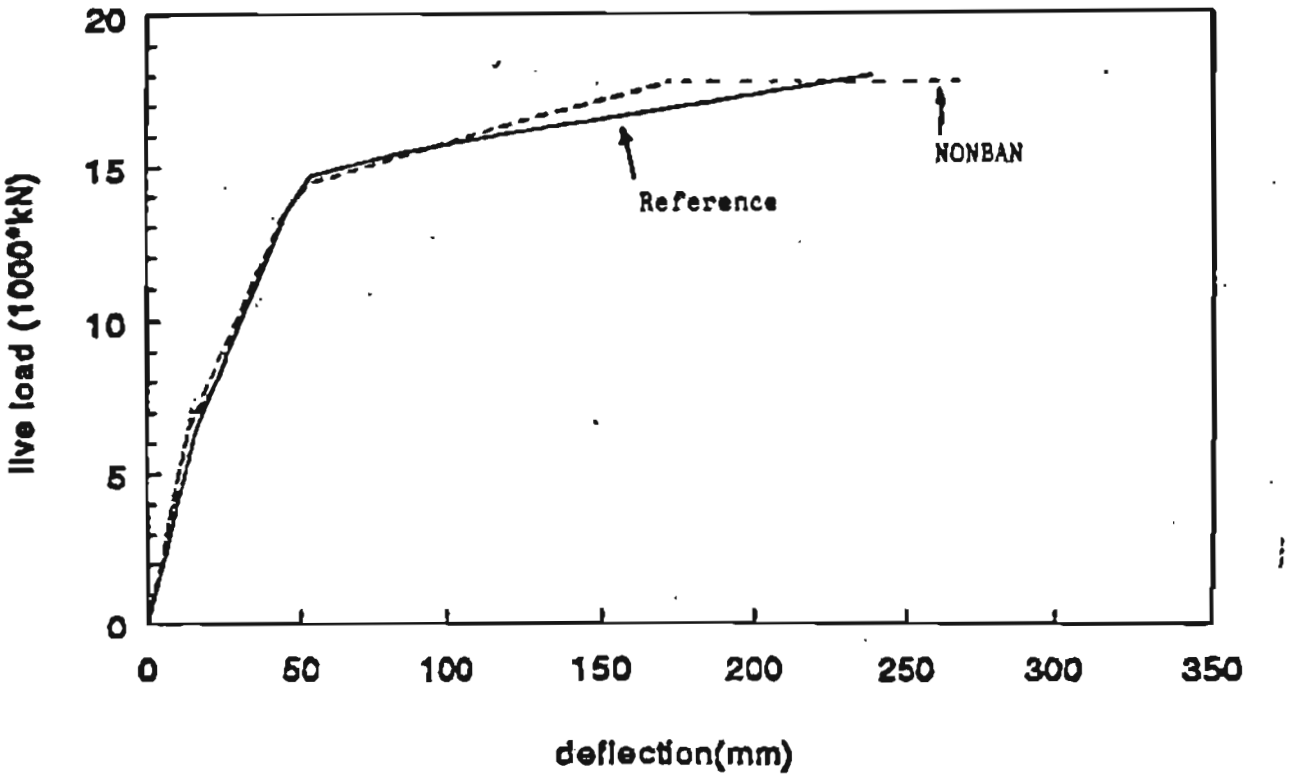

F.21 Compare is on of results between Maheu (F.8) and NONBAN.

This page is Blank

F.4.6 ANALYSIS OF BOX BEAMS UNDER TORSION

The program NONBAN is designed to model a bridge as a system of one dimensional beam elements. The program accounts for the torsional deformations of the beam elements in the linear elastic range using the torsional rigidity of each member represented by GI_x where G is the elastic shear modules and I_x is the torsional inertia. This approach can be used for the analysis of slab on I-beam type bridges where the torsional inertia of the longitudinal beams is relatively small and does not significantly contribute to the lateral distribution of the load. For box bridges, where the torsional properties of the members are extremely important, Hambly [F.20] proposes a model that accurately accounts for the torsional capacity as well as the in-plane deformations of the boxes. The model, however, does not account for out-of-plane deformations such as those due to warping. It should be noted that Hambly's behavior models were extensively used in the derivations of distribution factors by Zokaie, Osterkamp and Imbsen F.1.

The model proposed by Hambly can be summarized as follows:

1. To account for the flexural capacity of box girder bridges, each web of a box girder is assumed to act as a one dimensional beam element in the longitudinal direction with a moment of inertia equal to 1/n of the total moment of inertia of the box(where n is the number of webs). Another option involves the use of weighing factors where the weighing factors are functions of the location of the center of gravity of the whole girder and the tributary area of each web. Although more theoretically sound, Hambly suggests that the second option does not significantly improve the accuracy of the results.

2. To account for the torsional capacity of the box girder, the total torsional inertia of the box is divided to each longitudinal beam (representing the contribution of a web) and to the transverse beams (representing the contribution of the upper and lower flanges including the effect of the slab). Each web will carry 1/2n of the total torsional inertia and each transverse beam carries s/2b of the total torsional inertia (where s is the spacing between the transverse beams and b is the total width of the box girder).

3. To account for the in-plane deformations of the cross section (or cross-sectional distortions), Hambly assumes that the flange of the box acts in the transverse direction as a shear beam. The moment of inertia of this transverse beam is calculated from the moment of inertia of the top flange (including the deck slab for composite box girders) and the bottom flange. The equivalent shear area of this transverse beam is calculated as a function of the capacity of the box to resist in-plane forces applied on the whole box.

The scheme proposed by Hambly ignores the effect of out-of-plane deformations such as warping effects etc. In fact, Soliman et. al. [F.28] and Siddiqui [F.29] have

shown that out-of plane deformations are negligible for box girders with support diaphragms. Since normal bridge designs include diaphragms at the supports of box girder bridges, it is herein concluded that out-of-plane deformations can be ignored without significantly affecting the results.

The modeling scheme used herein is summarized in Figure F.22 Hambly [F.20] proposed this method to model the linear elastic behavior of bridges using a grillage analysis which is also the basic structural model used in NONBAN. The nonlinear torsional behavior of structural members is extremely difficult to model because of the interaction between the torsional capacity with the shear and moment capacities of structural members [F.30]. It is herein assumed that for a bridge system, torsional loads will remain in the linear elastic range and that the nonlinear behavior of the bridge is only due to bending and shear. The validity of this assumption for the nonlinear analysis of box bridges is verified in sections F.4.7 and F.4.8 by comparing the results obtained by NONBAN using the Hambly modeling scheme to experimental and analytical results obtained by other researchers.

To test the applicability of Hambly's approach for the linear elastic analysis of boxes, an example was taken from an analytical study by Calgaro J.A. and Virlogeux, M., [F.31]. The properties of the box example and the applied loading are shown in Figure F.23. The box is fixed at both ends and a uniformly distributed torsion is simulated by an antisymmetric distributed load applied on top of the webs. To solve this type of torsional problems, Calgaro and Virlogeux developed an analytical method based on the principles of equilibrium. The method they developed resulted in a differential equation similar to that obtained for beams on elastic foundations.

Closed-form solutions were possible for simple boundary conditions such as simple supports or fixed supports similar to those used in the example shown in figure F.23. The model ignores the effect of web shear deformations as well as the effect of out-of-plane deformations. The NONBAN input data prepared for the example problem solved in reference [F31] follow the scheme proposed by Hambly[F20]. The beam properties used in the NONBAN analysis are shown in figure F.23. The results obtained from NONBAN are compared to the theoretical results obtained by Calgaro and Virlogeux in table F.7.

For example, using NONBAN, the maximum bending moment in a longitudinal member was found to be equal to 18.9 kN.m resulting in a maximum stress of 6.10 MPa. The maximum stress calculated in the analytical model was found to be equal to 6.27 MPa. On the other hand, the maximum deflection calculated theoretically was found to be equal to 1.49×10^{-5} m while the grillage analysis yielded a deflection of 1.77×10^{-5} m. Using concentrated point loads at the mid-span rather than the uniform loads over the full length, yielded a maximum displacement of 6.93×10^{-7} m using the theoretical approach of Calgaro while

NONBAN yielded a maximum displacement equal to 7.0×10^{-7} m. The analytical approach proposed by Calgaro and Virlogeux does not account for out-plane deformations nor does it account for shear deformations in the webs of the boxes. To be consistent with the latter assumption, NONBAN was used assuming infinitely large web shear areas. NONBAN does not account for out-of-plane deformations

The modeling scheme proposed by Hambly was also tested by comparing the results of NONBAN to the results obtained by Seible[F.4] for the linear elastic analysis of boxes under torsion. Two concrete boxes one with a base of 3ft and the other with a base of 9 ft under loads producing high levels of torsion were analyzed by Seible and compared to previously published analytical results. The results obtained are summarized in figure F.24. For the 3 ft wide box, the model proposed by Hambly and used in NONBAN seems to overpredict the maximum deflection when NONBAN includes the shear deformations in the webs. The maximum deflection obtained with NONBAN is 4.2×10^{-5} ft compared to 2.93×10^{-5} ft reported by Seible. When the shear deformations are not included, then the maximum deflection calculated by NONBAN becomes 2.80×10^{-5} ft which is reasonably close to the analytical results

On the other hand, as shown in Figure F.24 for the box with the 9 ft base, Seible obtained a maximum deflection of 10.26×10^{-5} ft. compared to 8.70×10^{-5} ft with NONBAN including web shear deformations. For the case when the web shear deformations are not included, NONBAN produces a deflection of 5.93×10^{-5} ft. The theoretical model of Calgaro and Virlogeux for the box with the 9 ft base produced a maximum deflection of 5.58×10^{-5} ft.

The conclusions drawn from these examples indicate that:

1. The modeling scheme proposed by Hambly[F.20] produces deformations under high torsional loads similar to those obtained analytically by Calgaro et al. [F.31]. This ignores the effect of web shear and out-of-plane deformations such as warping.

2. The effect of warping and web shear deformations are negligible for torsionally rigid boxes under relatively small torsional loads such as the 3 ft box beam tested by Seible. Hence, Hambly's modeling scheme and Calgaro's analytical methods are valid.

3. Hambly's modeling scheme and Calgaro's method underpredict the deformations in box girders with low torsional rigidities under high torsional loads. This is because in such cases, the out-of-plane deformations and the web-shear deformations become more significant.

4. It is concluded that since the torsional loads applied on bridge structures are not normally the dominant loading conditions and since the presence of end diaphragms will reduce the effect of deformations due to warping, that Hambly's modeling scheme is accurate enough to account for the correct load distribution of box girder bridges. This assumption will be further verified in the examples analyzed in sections F.4.7 and F.4.8.

F.4.7 NONLINEAR ANALYSIS OF BOX GIRDER BRIDGES

Another verification of the validity of the analysis approach proposed in this study has been performed by comparing the results obtained by NONBAN to the results of Choudhury and Scordelis [F.10]. These authors developed a finite element model to perform the nonlinear analysis of box girder configurations. Although their program was compared in the linear elastic range against experimental results, it was not tested in the nonlinear range because of the "unavailability of experimental data". They used their program to study the behavior of one example bridge under CALTRANS special permit vehicles. The bridge is a unicell, three-span (160',200',160') continuous prestressed concrete curved box girder bridge designed to satisfy AASHTO's HS-20 and CALTRANS requirements.

The bridge geometry and material properties are as shown in Figures F.25 and F.26. For this example, the bridge model and member properties used with NONBAN follow the scheme outlined by Hambly [F.20]. The NONBAN output data is as shown in Figure F.27. In this example, it was assumed that material nonlinearities are only due to flexure. Also, to simplify the input data preparation, the moment versus rotation curves for each section was assumed to be bilinear i.e. elasto-plastic behavior of the members was assumed. Shear deformations are included in the NONBAN analysis but the shear is assumed to remain in the linear elastic range.

The results obtained from NONBAN are compared to the analytical results of Choudhury [F.10] as shown in Figure F.27. The results show good agreement between NONBAN and the published results. As expected, the curve produced with NONBAN is somewhat stiffer than the published curve because of the simplifications used in developing the moment-rotation curves used in NONBAN, i.e., the fact of using bilinear moment rotation curves. NONBAN somewhat underpredicts the ultimate load due to possible overestimation in the dead load effects and also due to minor changes in the loading conditions. (Figure F.26 shows the loading condition used in reference [F.10] and that used with NONBAN). The results of this example emphasize that even with a rough approximation of the moment rotation curves, NONBAN produces reasonably good agreement with the results of specialized finite element programs for the nonlinear analysis of box girder bridges. It should be noted herein, that if shear failure were included in the analysis, the ultimate capacity of the bridge would

have been highly underpredicted. This is because the shear strength model of Eq. F.9 used in this example underpredicts the shear capacity of the webs. This would have predicted a load factor at ultimate of only 1.2 rather than the value of 5.6 predicted in reference[F.10].

F.4.8 NONLINEAR ANALYSIS OF MULTI-CELL BOX BRIDGES

To test the validity of NONBAN and the approach proposed by Hambly [F.20} for modeling the behavior of multi-cell box bridges, the results of a model bridge tested by Scordelis et. al. [F.32] and analyzed by Seible [F.9] are compared to the results obtained using NONBAN. The bridge model is a reinforced concrete continuous (two spans) four-cell bridge. The bridge was symmetrically loaded with two point loads in each span.

The bridge geometry is as shown in Figure F.28. Figure F.29 shows the discretization used by Seible and Figure F.29 gives the section properties and the reinforcement of each element. In the NONBAN analysis the bridge model was discretized as done by Seible except for the element at the mid-support (No. 11) which was divided into two elements to better model the high flexural and shear rigidities of the support conditions. The moment versus rotation relationships for each element were obtained separately for positive and negative bending depending on the amount of reinforcement.

The results obtained for this case are compared to those obtained by Seible and to the experimental results in Figure F.30. It is observed that a very good match between the results is obtained for this bridge with the model used. It should be noted, however, that the results of NONBAN seem to be quite sensitive to the assumed length of the plastic hinge, Lp, used while deriving the moment versus rotation curves.

This sensitivity is believed to be caused by the scale effect due to the relatively deep thickness of the box compared to the total length of the bridge model and the length of the elements. Based on a sensitivity analysis performed as part of the analysis of this bridge, it appears that using moment versus rotation curves with an Lp value obtained from Park and Pauley [F.23] provides the best results with an additional condition that Lp be always less than 1/2 the length of the element.

It should also be noted that here again using Eq. F.9 to check the shear ultimate capacity of the bridge model would have underpredicted the observed failure load by about 50 percent.

Table F.7 Comparison the results of NOBAN and theoretical results.

Case	Calgaro, et al	NONBAN
Distributed load		
Max Stress	6.27 MPa	6.10 MPa
Max. Displacement	1.49 E -5 m	1.77 E -5m
Concentrate load		
Max. Displacement	6.93 E-7 m	7.00 E-7m

Table F.7 Comparison the results of NOBAN and theoretical results.

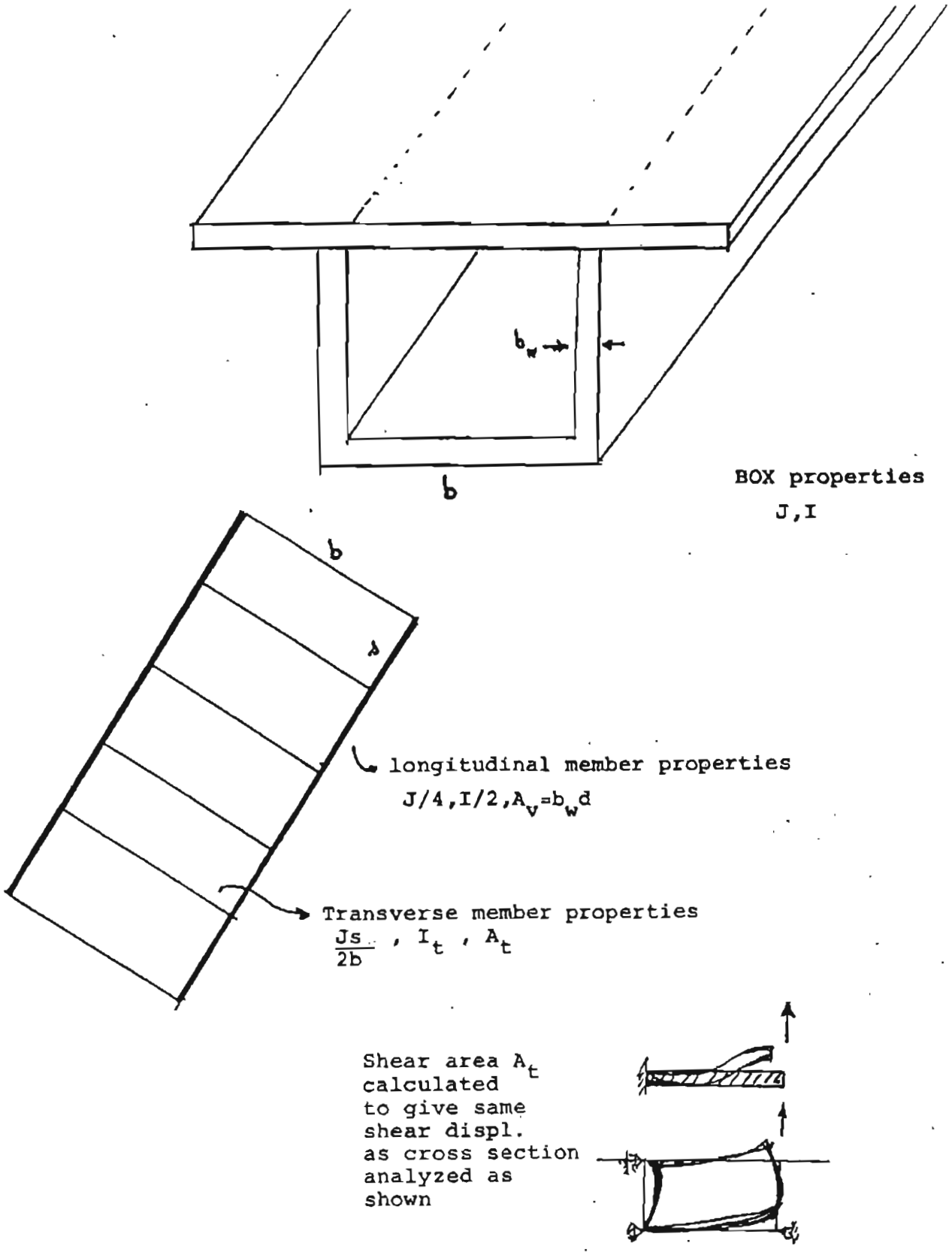

Figure F.22 Summary of Hambly's modeling scheme for box girder.

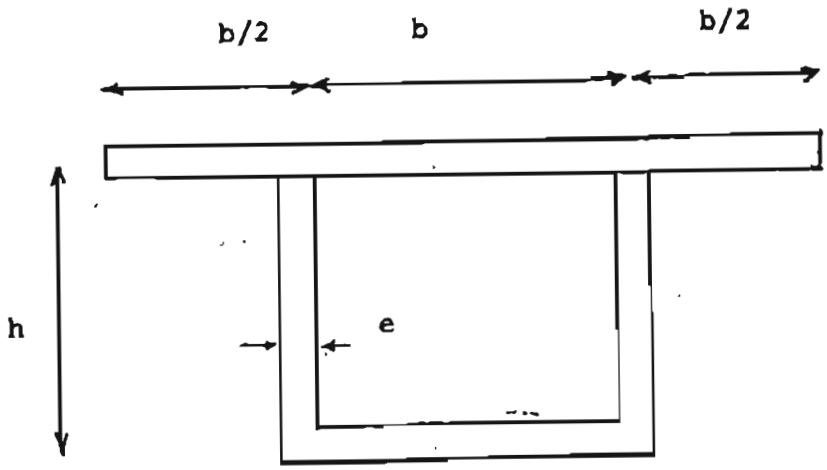

$E=4\ 10^4$ MPa
$\nu=0.2$
L=25 m
q=1 kN/m
b=5.5 m
h=3 m
e=0.3 m

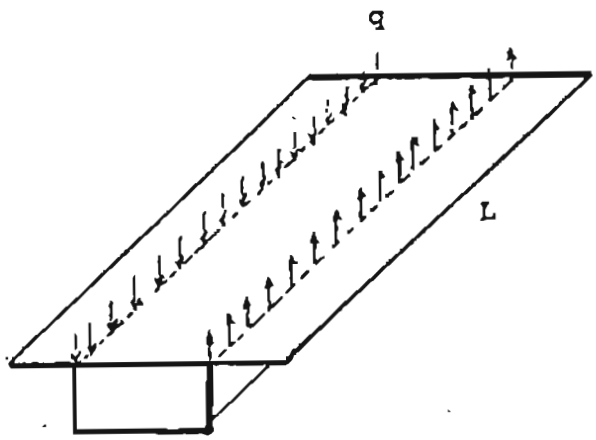

Figure F.23 Properties of box beam analyzed by Calgaro et al.

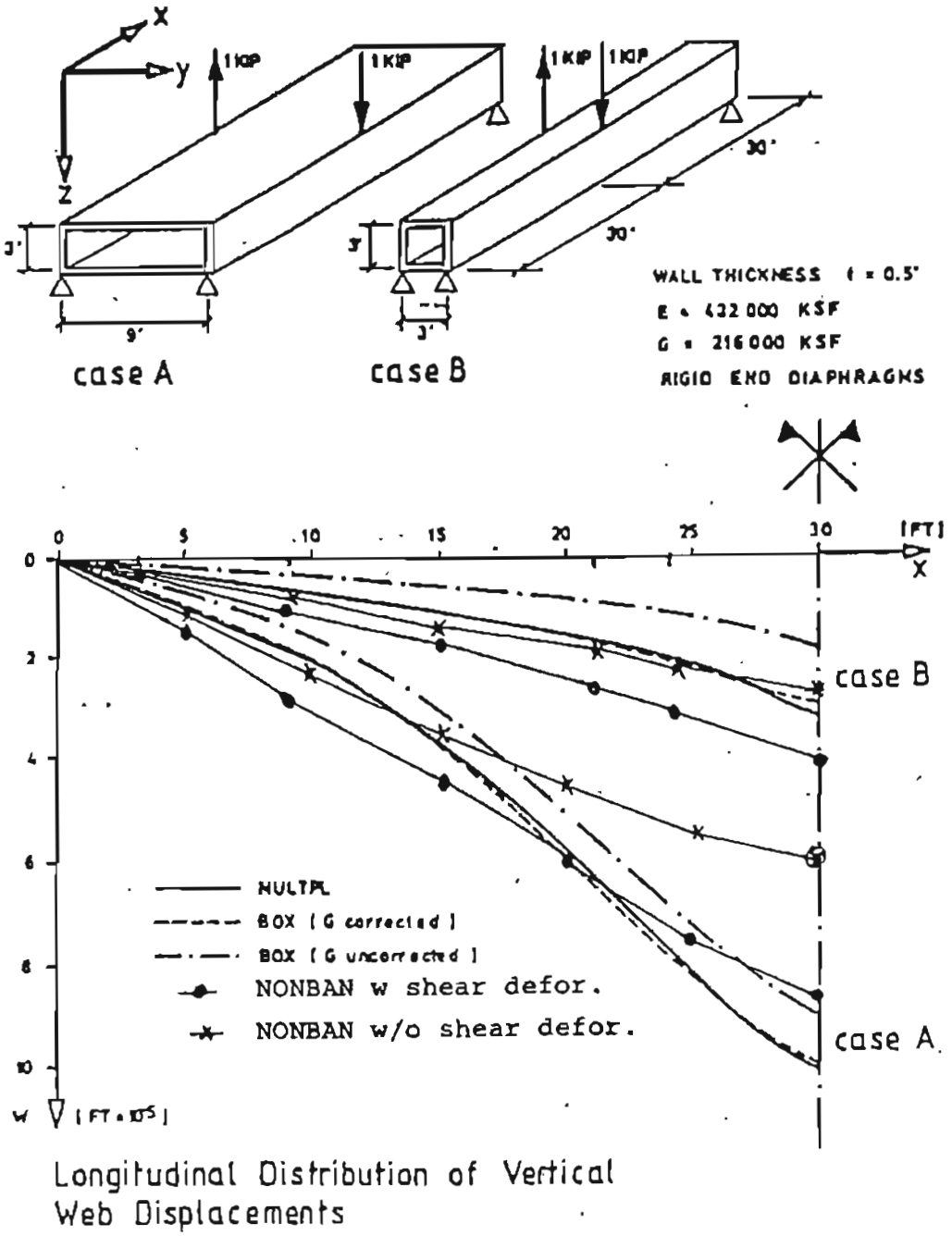

Longitudinal Distribution of Vertical Web Displacements

Figure F.24 Comparison of NONBAN to torsion examples of Seible.

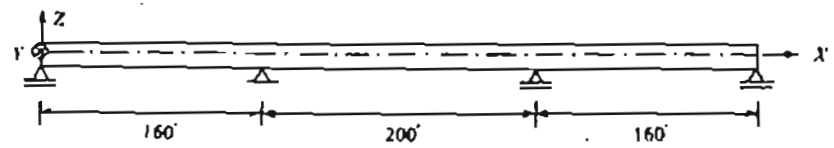

SPAN ARRANGEMENT

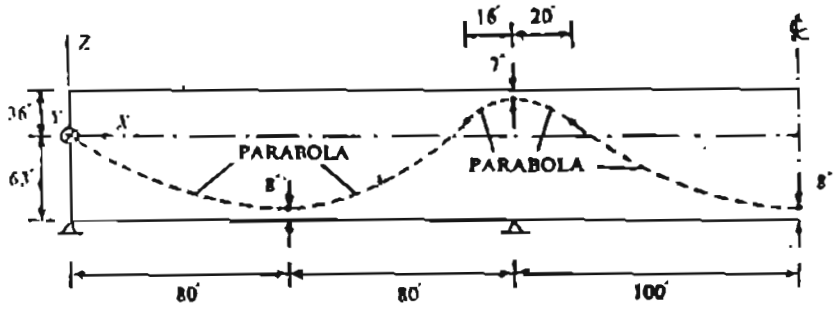

PRESTRESSING TENDON PROFILE

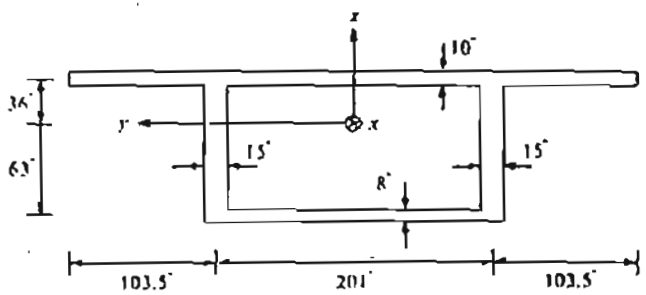

CROSS SECTION

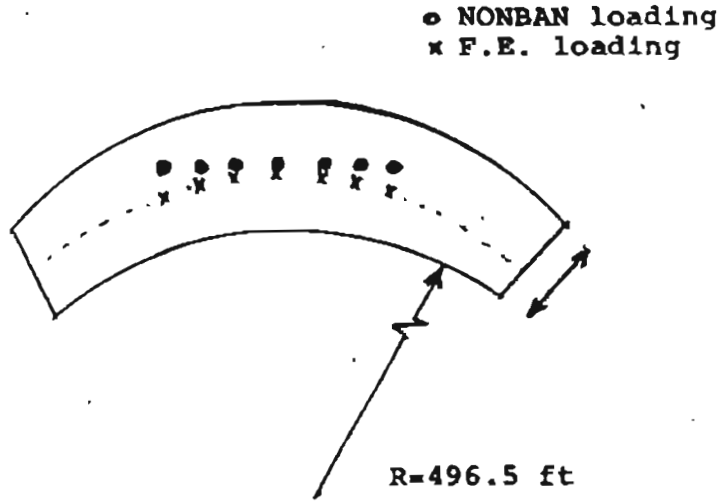

Figure F.25. Properties of box girder bridge.

Concrete:

f'_c = 4,000 psi
E_{ci} = 3.605×10^6 psi
f_t = 500 psi
ϵ_{cu} = 0.004
β = 0.85
ν = 0.20
τ_{cr} = 190 psi
β_1 = 0.85

Longitudinal reinforcing steel:

f_y = 60 ksi
E_{s1} = 29,000 ksi
E_{s2} = 0
ϵ_{su} = 0.03

Transverse reinforcing steel:

f_{yt} = 60 ksi
E_s = 29,000 ksi

Prestressing steel:

ϵ_1 = 0.00715 ; σ_1 = 196.6 ksi ; E_p = 27,500 ksi
ϵ_2 = 0.00900 ; σ_2 = 220.0 ksi
ϵ_3 = 0.01150 ; σ_3 = 240.0 ksi
ϵ_4 = 0.01350 ; σ_4 = 245.0 ksi
ϵ_5 = 0.05800 ; σ_5 = 270.0 ksi

Anchorage slip at each jacking end: Δ_a = 0.25 in.

Wobble friction coefficient: K = 0.0002/ft

Curvature friction coefficient: μ = 0.25/radian

Unit weight of composite structure: w = 155 pcf

Tension stiffening coefficient: k = 0

Figure F.26. Material properties of box girder bridge.

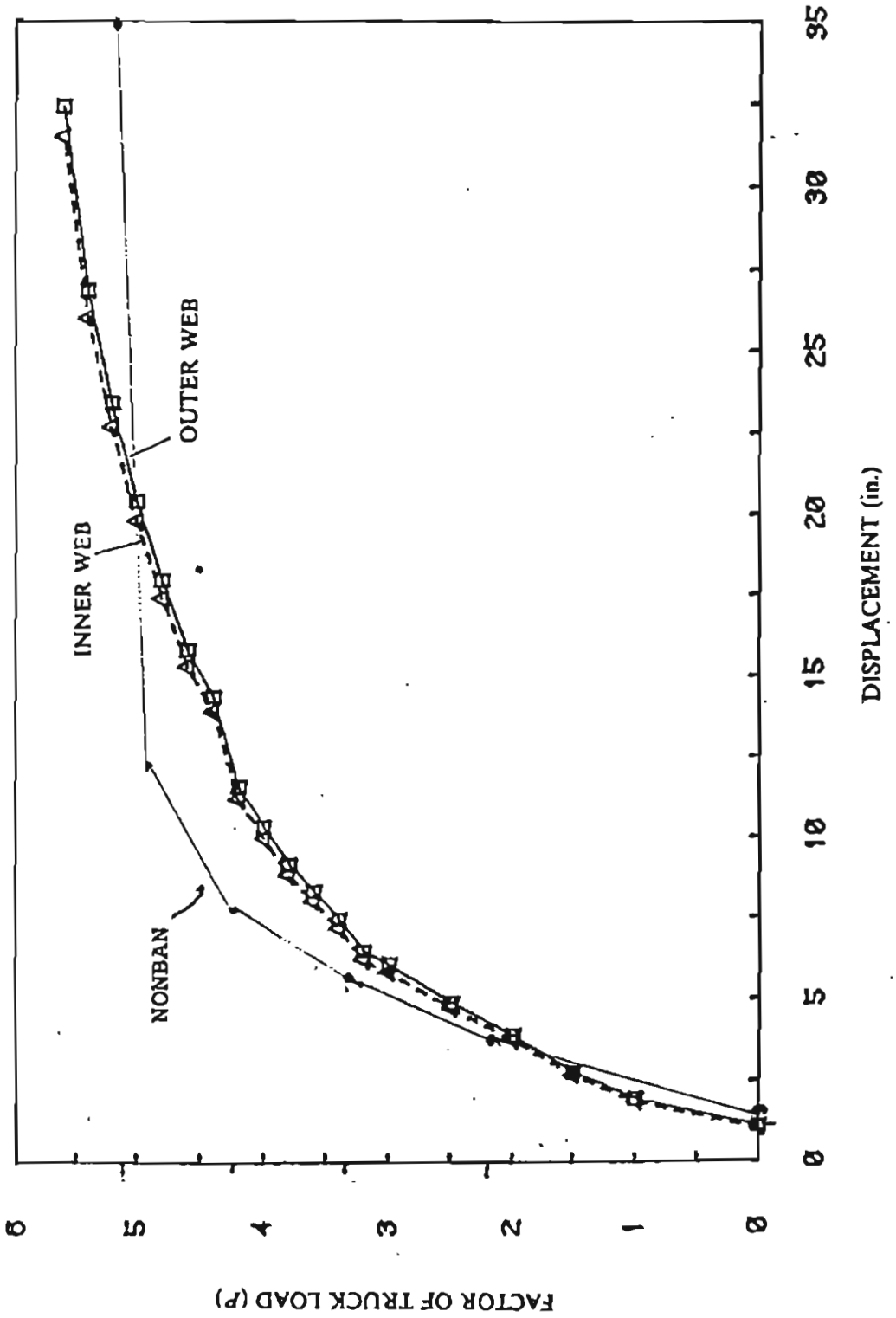

Figure F.27 Comparison between NONBAN and finite element analysis of box girder bridge.

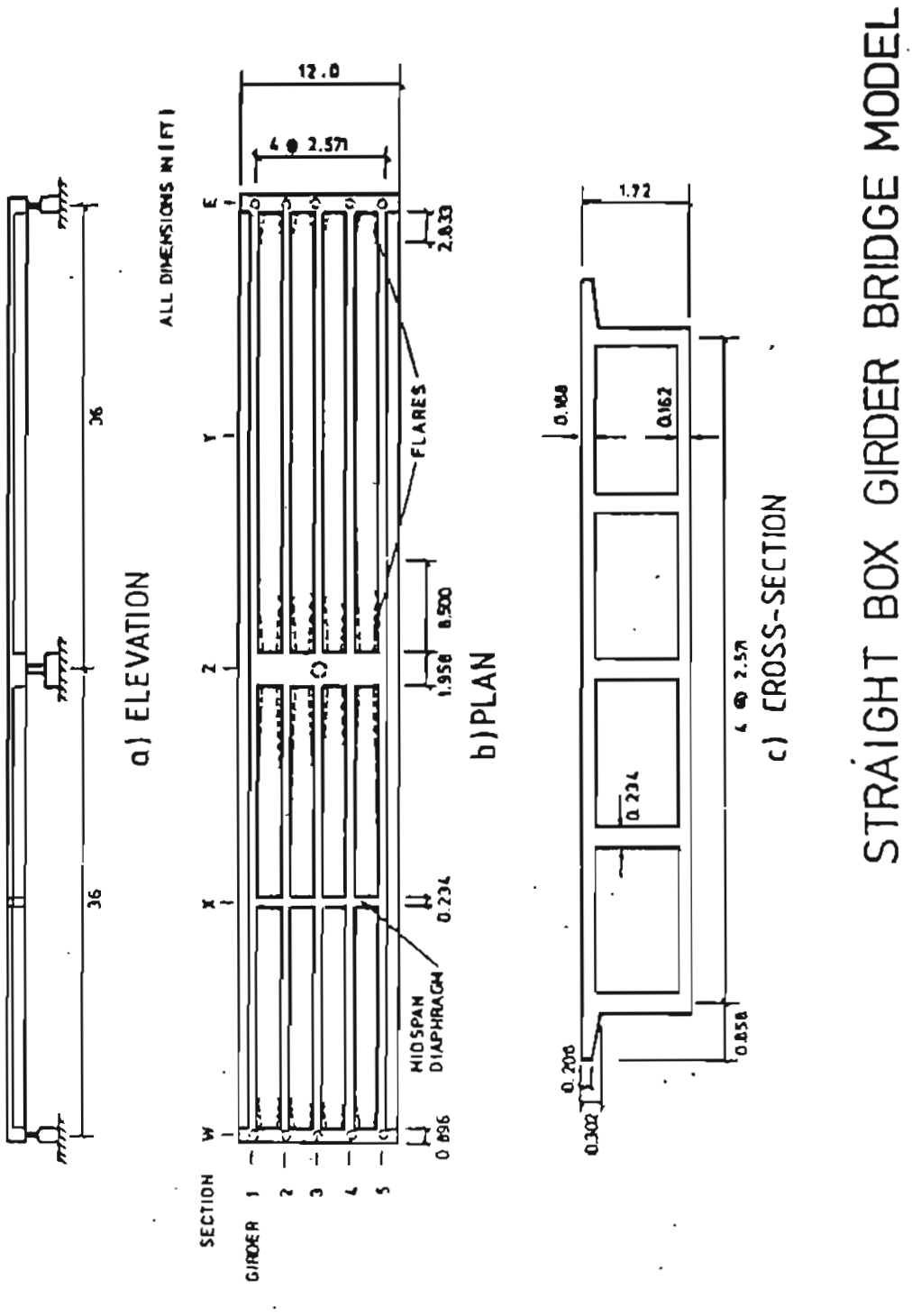

Figure F.28 Geometric properties of multi-cell concrete box girder bridge model.

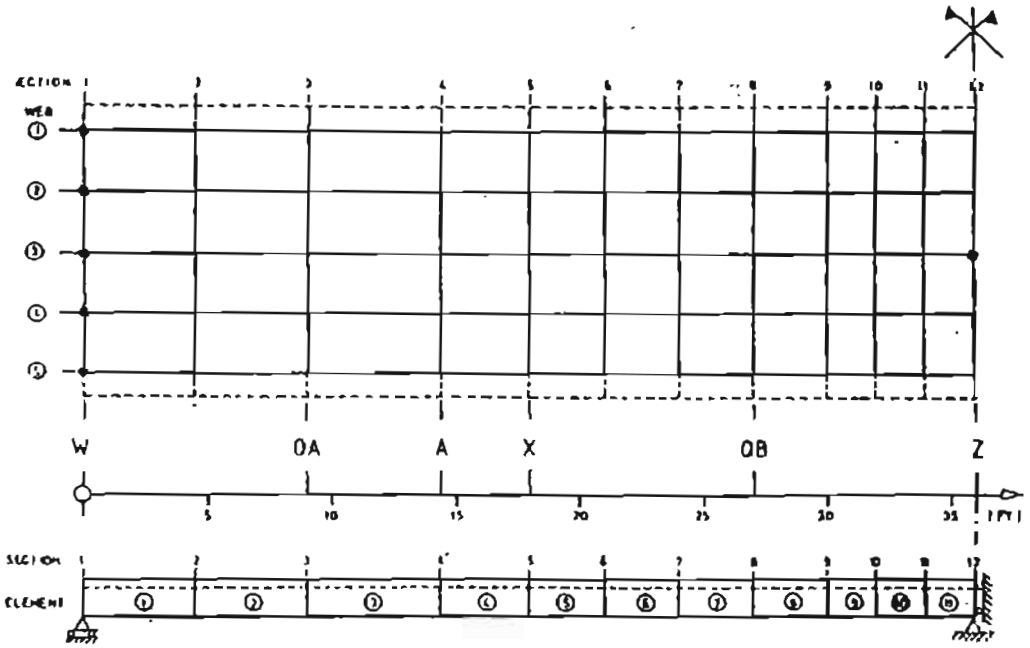

- DISCRETIZATION FOR GRILLAGE MODEL -

SLAB REINFORCEMENT AND WEB THICKNESS

FOR LONGITUDINAL BEAM ELEMENTS

BEAM ELEMENT NO.	LONGITUDINAL REINFORCEMENT AREA				WEB THICK-NESS	SHEAR STIRRUP REIN-FORCE-MENT AREA
	TOP SLAB		BOTTOM SLAB			
	INTERIOR GIRDER	EXTERIOR GIRDER	INTERIOR GIRDER	EXTERIOR GIRDER		
	[in.²]	[in.²]	[in.²]	[in.²]	[ft]	[in.²/in]
1	0.59	0.59	1.96	0.88	0.252	0.012
2	0.59	0.59	2.35	1.27	0.234	0.0077
3	0.59	0.59	2.74	1.47	0.234	0.0077
4	0.59	0.59	2.74	1.47	0.234	0.0077
5	0.59	0.59	2.74	1.47	0.234	0.0077
6	0.59	0.59	2.35	1.27	0.234	0.0077
7	0.59	0.59	1.42	0.79	0.234	0.012
8	2.55	1.87	1.37	0.64	0.279	0.014
9	3.19	2.60	0.80	0.59	0.324	0.018
10	3.53	2.75	0.80	0.59	0.354	0.015
11	5.00	4.00	0.80	0.59	1.286	0.018

*CENTER BENT ELEMENT

f'_c = 4500 psi $E_s = 2.9 \cdot 10^6$ 1 in. = 25.4 mm

E_c = 550 600 kip/ft² f_{sy} = 60 ksi 1 ft = 0.305 m

G = 220 200 kip/ft² 1 kip = 4.448 kN

Figure F. 29. Mesh and material properties of multi cell concrete girder bridge.

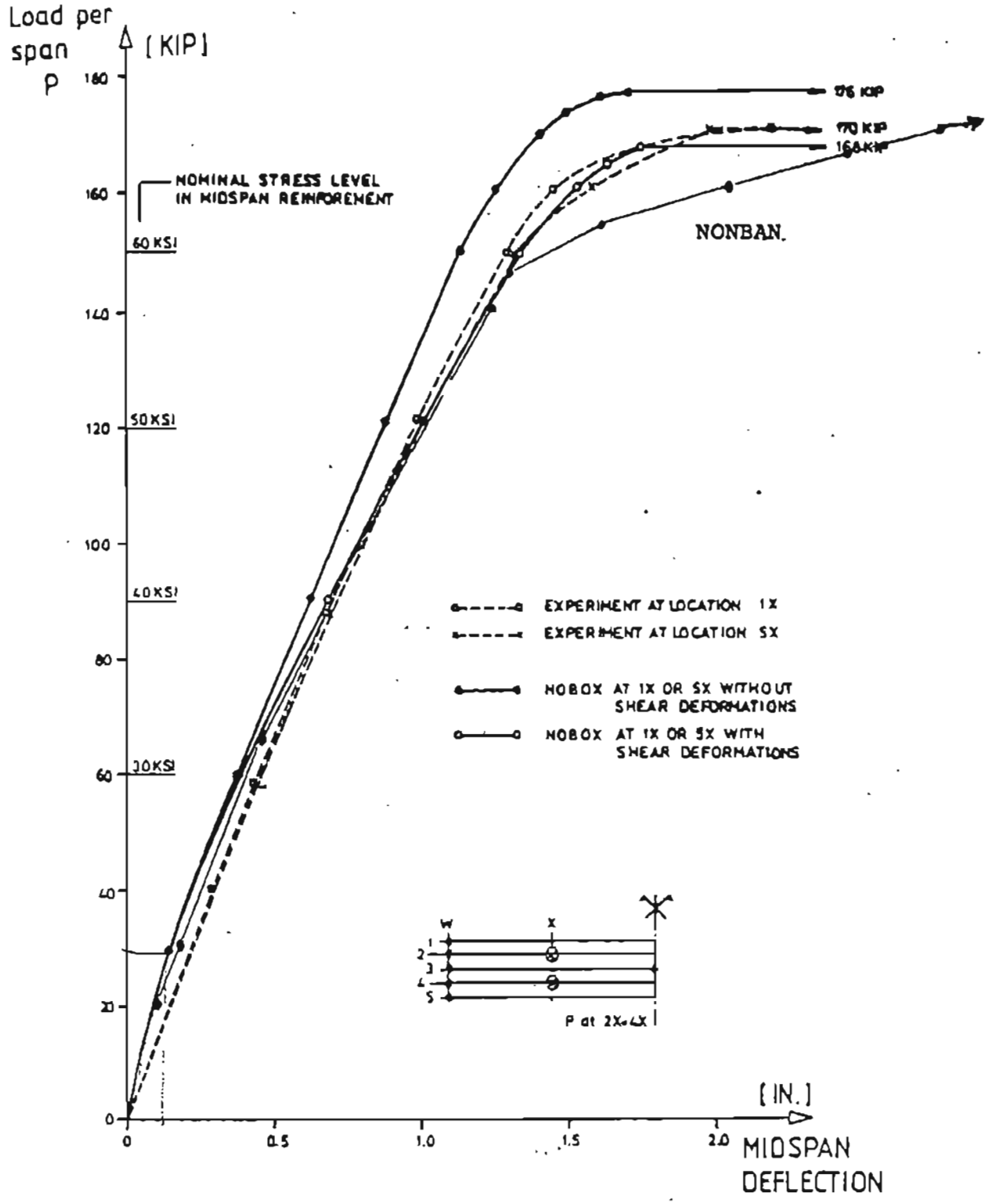

Figure F. 30. Comparison between NONBAN and results of Seible.

F.4.9 SENSITIVITY OF NONBAN TO MESH-SIZE

From experimentation with the program NONBAN it has been observed that there are two factors that affect the results of the nonlinear analysis. The first one is the stopping criterion. The second one is the stability of the mesh size. NONBAN's primary stopping criterion is based on the maximum plastic hinge rotation. This is calculated from the materials plastic properties. The methodology used to find the stopping criterion and to develop the mesh discretization procedure is based on successful comparisons between results of NONBAN and those of published experimental tests. Although several such comparisons were performed, their overall number is still limited. Nevertheless, due to the absence of contradictory information, it is herein suggested that the proposed mesh discretication procedure is valid for the purposes of this study and that the results are not sensitive to the mesh size. As an illustration of the analysis of the importance of the mesh size, the results of NONBAN using different mesh sizes are compared to those of the experimental data for the bridge test performed in Nebraska [F.33].

Figure F.31 shows the mesh of the base case which divided the longitudinal girders into ten equal beam elements. The results obtained show excellent agreement with the test results as illustrated in figure F.32. If the mesh is refined such that the longitudinal girder are divided into 5, 20, or 40 equal elements, the final results are as good as those of the base case as shown in figure F.33. It is noted however, that the mesh size did produce some difference in the final failure point. This difference is manifested by having different displacements at failure while the ultimate loads obtained from the different meshes show negligible differences.

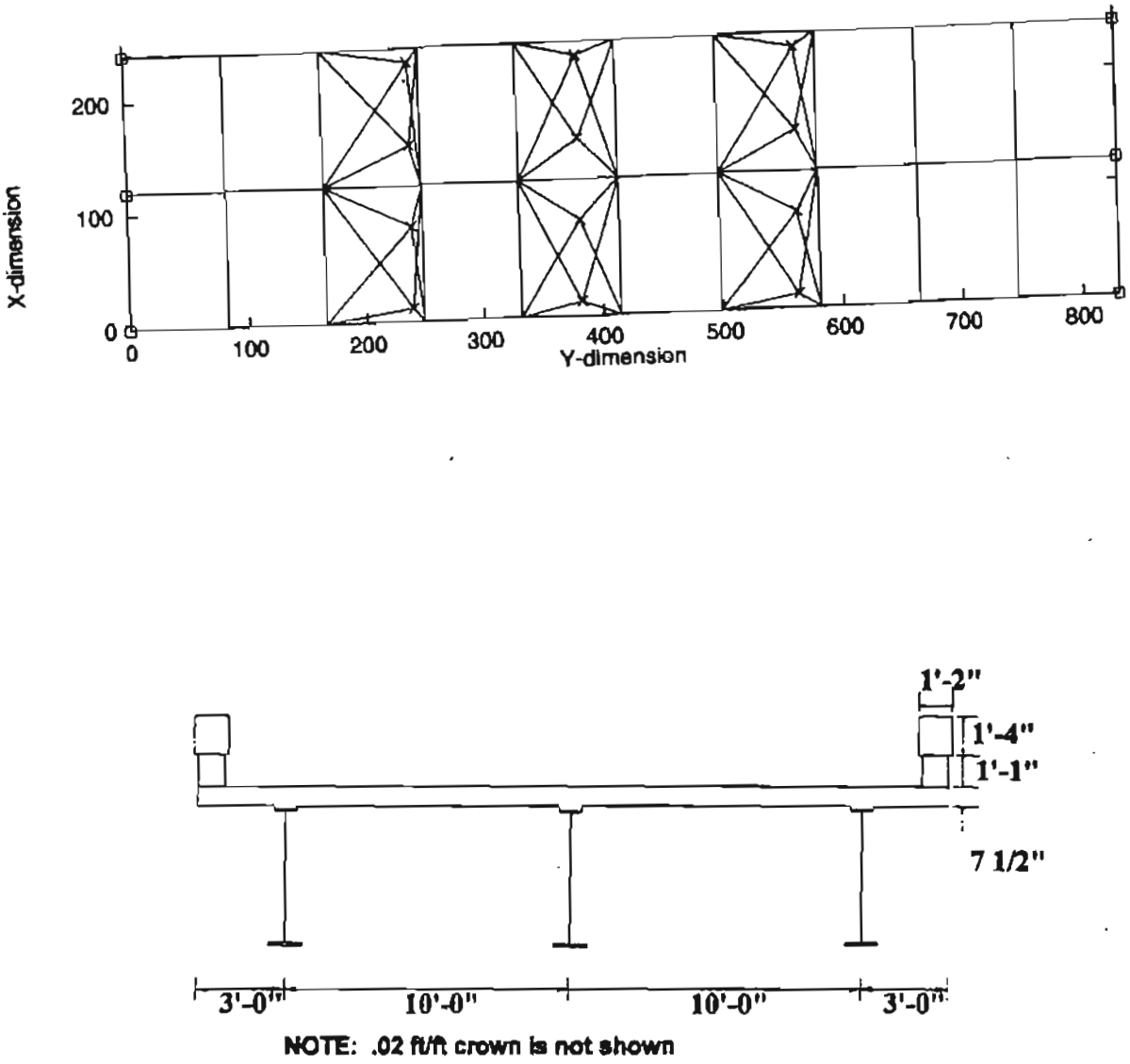

Figure F.31. The structural model of the base case of Nebraska bridge.

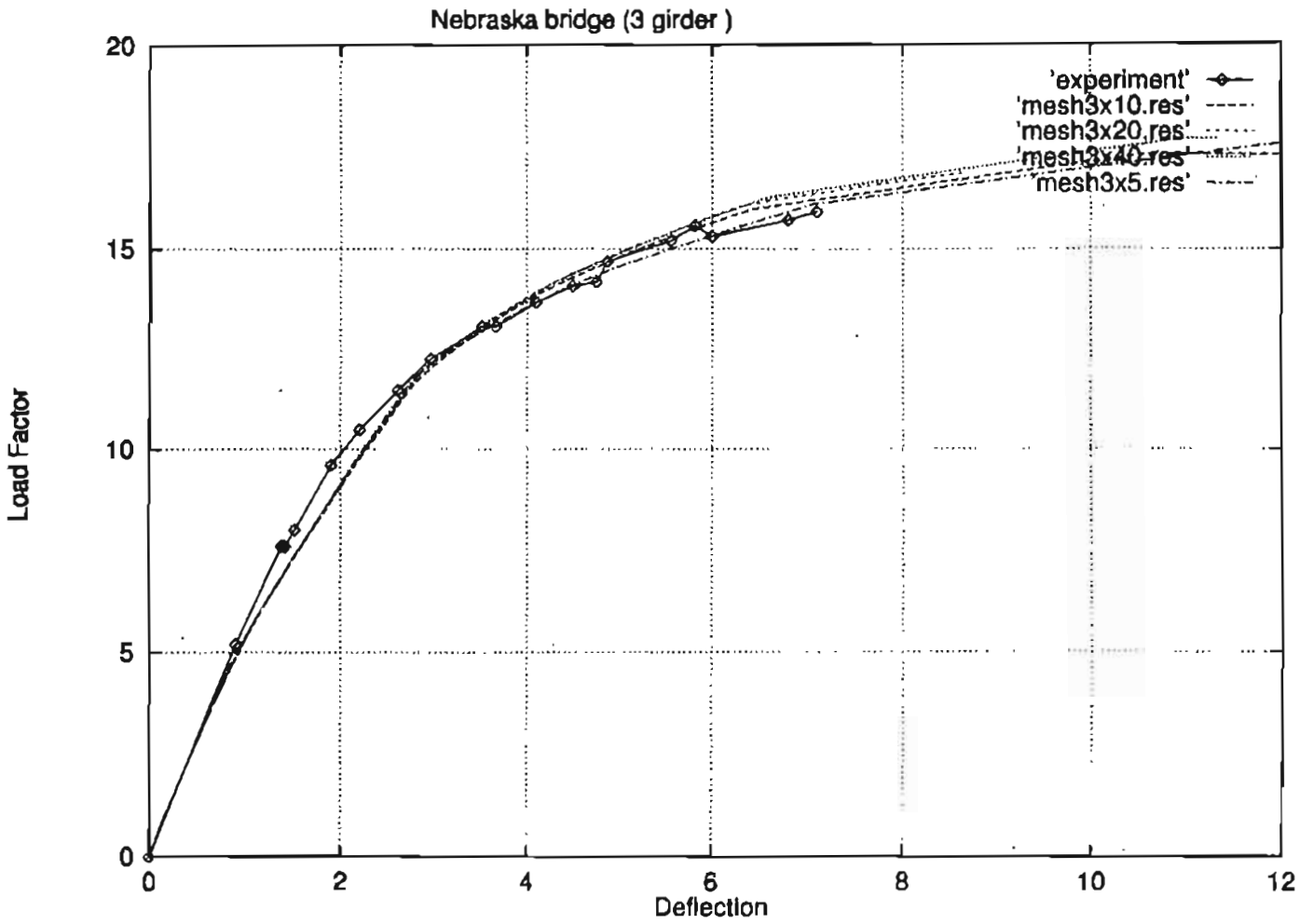

Figure F.32. Results of Nebraska bridge for different mesh sizes and from test.

F.4.10 CONCLUSIONS

This section illustrated a technique to study the nonlinear behavior of bridges using a grillage discretization based on the approach proposed by Hambly [F.20]. The method developed is valid for steel and concrete (prestressed and reinforced) slab on I-beam bridges as well as box girder bridges.

The nonlinear analysis program NONBAN can be used to perform such an analysis. In NONBAN, flexural nonlinearity is accounted for by using moment versus plastic rotation curves. In addition, multilinear shear deformation curves can also be used with NONBAN to account for the effect of shear nonlinearities. Several comparisons between the results obtained by NONBAN and other published numerical results as well as published experimental results of full scale and model bridges were performed. The results obtained verified the validity of NONBAN and the Hambly model for the nonlinear analysis of bridges subjected to truck traffic loads. The comparisons proved that NONBAN can model the global behavior of common type bridge structures including I-beam and box girder bridges with sufficient accuracy.

The proposed model is applicable to situations where the dominant loading condition is due to bending with relatively low levels of shearing and torsional loads. Because available shear strength models seem to significantly underpredict the shear capacity of typical bridge structures, the best correlation with other numerical and experimental results are obtained when shear failures are ignored.

SECTION F.5

PREPARATION OF INPUT DATA FILES

The input data required by program NONBAN has been described in section F.3 of this appendix. This section illustrates the preparation of the input data file and the input data format required by NONBAN. This is accomplished through a full scale steel girder bridge which is designed, constructed and tested by University of Nebraska-Lincoln and Nebraska Department of Road [F.33].

F.5.1 INPUT FILE FORMAT

NONBAN needs an input file "NONBAN9.DAT " to run. This file can be edited by any text editor and put in the directory where NONBAN will run. Table F.8 shows the NONBAN9.DAT's format. Each row in Table F.8 describes the line of input data required at this stage. The "*" designates a data entry. The data entry must be an integer number when the explanation says "number". The data entry is a real number (with or without a decimal point) in all other cases.

Table F.8. The formate of the NONBAN'S input file "NONBAN9.DAT"

1) TITLE Put the project title in the first line.
2) 0 Required.
3) Need a blank line here.
4) "GENERAL PROPERTY" This is a subtitle for this data block.
5) *, *, * Need three data entries in this line. 1st number is the analysis option. =1, elastic analysis of dead loads. =2, nonlinear analysis of dead loads. =3, incremental analysis of live loads including dead load effects without considering the construction sequence. =4, nonlinear analysis considering noncomposite sections for permanent load and accounting for continuity at support for all dead loads. =5, nonlinear analysis considering noncomposite sections and assuming simple

supports for permanent dead loads.
=6, same as 5 and accounting for effect of prestressing forces.
=7, option for calculation of elastic live load margin (LF1) and other redundancy information. Not completed yet.

2nd is the Poison ratio ν.

3rd is shear analysis indicator.
=1, include shear deformation.
=0, not include shear deformation.

6) *, *,*

Need three data entries in this line.
1st is the total number of nodes.
2nd is the number of elements
3rd is the number of elements which will undergo inelastic deformations.

7) * (if analysis option is 4 or 5)
or: *, *, *, * (if analysis option is 6)

This needs one or four data entry depending on the analysis option line.

If analysis option is 4 or 5, only need one entry in this line which is the number of longitudinal girder beam elements.

If analysis option is 6, need 4 entries in this line.
1st is number of longitudinal girder beam elements.
2nd is the amount of prestressing force acting on the girder's section.
3rd is eccentricity of prestressing force.
4th is the allowable tension stress of the material below the prestressing point.

8) Blank line

9) "Noncomposite section properties"

subtitle.

Note:
1. If Analysis option <=3, do not need this section, go to step 15 to put the composite section properties.
2. NONBAN assumes that all longitudinal girders have the dame noncomposite properties.

10) *, *, *, *, *, *, *, *, *

Nine data entry in this line to describe the noncomposite elastic section properties.
1st is the section's area A.

2nd is the moment inertia Iz. 3rd is the moment inertia Iy. 4th is the torsion inertia I_ρ. 5th is the section modules Sz. 6th is the elastic modules E. 7th is the shear modules G. 8th is shear area in y direction Ay. 9th is the shear area in z direction Az.
11) *, *, *, * These four data entries correspond to the moments at the subhinge points of M-Phi curve in positive bending for noncomposite section M1, M2, M3, M4 in the positive bending M-phi curve of noncomposite section. See Fig. 33.
12) *, *, *, * These four data entries give the slopes S1, S2, S3, S4 of M-Phi curve for the positive bending M-phi curve of noncomposite section. See Fig. 33.
13) *, * The first data is the plastic hinge length Lp of noncomposite section in positive bending . The second data is the maximum plastic hinge rotation of noncompetitive section in positive bending.
14) Blank line
15) "Composite section properties" Subtitle.
16) * Number of different section types.
17) *, *, *, *, *, *, *, *, * This line needs nine data entries to describe the elastic properties of section type 1. 1st is the section area A. 2nd is the moment inertia Iz. 3rd is the moment inertia Iy. 4th is the torsion inertia I_x. 5th is the section modules Sz. 6th is the elastic modules E. 7th is the shear modules G. 8th is the shear area in y direction Ay. 9th is the shear area in z direction Az.
18) *, *, *, * These four data correspond to the moments M1, M2, M3, M4 of M-Phi curve for the positive bending of section type 1. See Fig. 33.
19) *, *, *, *

These four data give the slopes S1, S2, S3, S4 of M-Phi curve for the positive bending of section type 1. See Fig. 33.
20) *, * The first data is the plastic hinge length of section type 1 in positive bending. The second data is the maximum plastic hinge rotation of section type 1 in positive bending.
21) *, *, *, * These four data correspond to the moments M1, M2, M3, M4 of M-Phi curve for the negative bending of section type 1. See Fig. 33.
22) *, *, *, * These four data give the slopes S1, S2, S3, S4 of M-Phi curve for the negative bending of section type 1. See Fig. 33.
23) *, * The first data is the plastic hinge length of section type 1 in negative bending. The second data is the maximum plastic hinge rotation of section type 1 in negative bending. See Fig. 33.
24) *, *, *, * These four data correspond to shear V1, V2, V3, V4 in the V-R curve of section type 1. See Fig. 33.
25) *, *, *, * These four data correspond to the slopes R1, R2, R3, R4 in the V-R curve of section type 1. See Fig. 33.
26) Repeat steps 17) to 25) to enter properties of the second section type.
27) Repeat steps 17) to 25) to enter properties of next section type until all of the section types given in step 16) are listed.
28) blank line
29) "X-Y-Z coordinates" Subtitle.
30) *, *, *, ... input all of the X coordinates of the nodes starting from node 1 to the last node.
31) *, *, *, ... input all of the Y coordinates of the nodes starting from node 1 to the last node.
32) *, *, *, ... input all of the Z coordinates of the nodes starting from node 1 to the last node.
33) Blank line.
34) " Beam connections and beam types"

Subtitle.
35) *, *, *, ... input the numbers corresponding to the left nodes of all beams from the first beam to the last beam. Girders are listed first. transferverse beams second. The lasts are the beams which do not go to plastic deformation.
36) *, *, *, ... input the numbers corresponding to the right nodes of all beams from the first beam to the last beam.
37) *, *, *, ... input the section type numbers defined in the block "composite section properties" for all beams starting from the first beam to the last beam.
38) Blank line.
39) "The number of plate elements" Subtitle.
40) * This number is the number of elements. put "0" here. The plate element option can only do elastic analysis at present.
41) blank line.
42) "Restraints" Subtitle.
43) * Number of nodes which are restrained.
44) *, *, *, *, *, *, *, * This line describes the restraint information of one node. 1st data is the number of the node which is restrained. 2nd data =0, means that the node is free to displace in X direction. =1, means that the node is restrained from displacement in the x directions. 3rd data =0, means that the node is free to displace in Y direction. =1, means restrained in Y direction's movement. 4th data =0, means. that the node is free to displace in Z direction. =1, means restrained in Z direction's movement. 5th data =0, means that the node is free to rotate about the X axis. =1, means restraint in X direction's rotation. 6th data =0, means that the node is free to rotate about the Y axis.

=1, means restraint in Y direction's rotation. 7th data =0, means that the node is free to rotate about the Z axis. =1, means restraint in Z direction's rotation.
45) Repeats 44) step to put the restraint information for the second point.
46) Repeats 44) step to put the restraint information for another point until all of the points which are restrained are listed.
47) blank line
48) "Concentrated dead load" subtitle.
49) * Put "0" here. This means no concentrated dead loads.
50) Blank line.
51) "Uniform dead loads" Subtitle.
52) * This is the number of lines which describe the uniformly distributed dead loads.
53) *, *, *, * input the information about the first type of dead load. 1st data is the beam number on which this type of dead load begins. 2nd data is the number of the last beam on which this type of dead load is applied. 3rd data is the dead load which acts on the noncomposite section. (permanent dead load). 4th data is the dead load which acts on the composite section section. (superimposed dead load).
54) Repeat 53) step to input the second type of dead load.
55) Repeat 53) step to input another type of dead load until all of types of dead load listed in step 52) are entered.
56) Blank line.
57) "Live load" Subtitle.
58) * This data is the number of concentrated live loads which must act on nodes.
59) *, *, *, *, *, *, * These seven data describe the information for the first load point. 1st data is the node number on which the first load is acting.

2nd data is the first load's component in X direction. 3rd data is the first load's component in Y direction. 4th data is the first load's component in Z direction. 5th data is the first load's moment about X axis. 6th data is the first load's moment about Y axis. 7th data is the first load's moment about Z axis.
60) Repeat step 59) to input the second live load information for the second load point.
61) Repeat step 59) to input another live load information until all of the live loads listed in step 58) are entered.
62) Blank line
63) * This is the number of nodes for which detailed output information is required. Note: Detailed output means that the displacements and rotations for these nodes will be listed with output file. Also it means that the moments and shearing forces for the beams connected by this nodes will be listed with output file. Finally, file figpve22bm.dat will list the maximum displacement from any of these nodes versus the load factor obtained for every load increment.
64) *, *, *, ... Input the nodes for which detailed output is required.
65) Blank line.
66) "END" This is the end of input file.

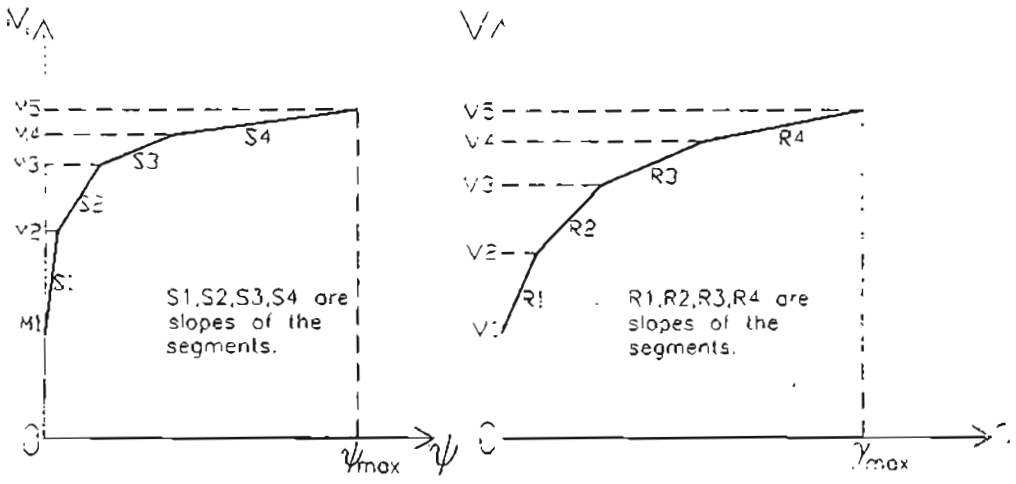

Figure F.33. Description of M-φ and M-γ curves required by NONBAN.

F.5.2 DESCRIPTION OF EXAMPLE BRIDGE ANALYZED USING NONBAN

To illustrate how the NONBAN input data is prepared, a typical bridge with three girders is used as an example. This example bridge is taken from reference [F.33]. The bridge was designed, constructed and tested in the Structural Laboratory of the University of Nebraska-Lincoln for a project sponsored by the Nebraska Department of Roads. The bridge is a full scale model with a span of 70 feet and is 26 feet wide. The superstructure consists of three welded plate girders built compositely with a 71/2 inch reinforced concrete deck. The girders are spaced 10 feet on center and the reinforced concrete deck has a 3-ft overhang. The concrete barrier is a typical Nebraska Department of Roads (NDOR) open concrete bridge rail, With 11x11 inch posts spaced 8 feet on center. The center girder is elevated 2 3/8 inches above the outside girders to produce a crown of 0.02 ft/ft. See Figs. F.34 and F.35 respectively, for the structural steel plan and bridge cross-section. The plates forming the girders consist of a 9x3/4 top flange, a 54x3/8 web, a 14x1 1/4 center bottom flange, and 14x3/4 end bottom flanges. Figure F. 36 shows the cross section of the interior girder at midspan with the effective concrete slab width. Figure F.37 shows the slab reinforcement detail. Intermediate web stiffeners consisting of a total of 4 5/16 in thick plates spaced at 39.5 inches and 10 plates at 67.2 inches. Shear studs 7/8 in diameter and 5 inches tall are spaced 18 at 7 inches, 14 at 9 inches, and 16 at 10 3/16 inches from left to right. The studs are placed symmetrically about the girder centerline. Fig. 38 shows a typical girder elevation.

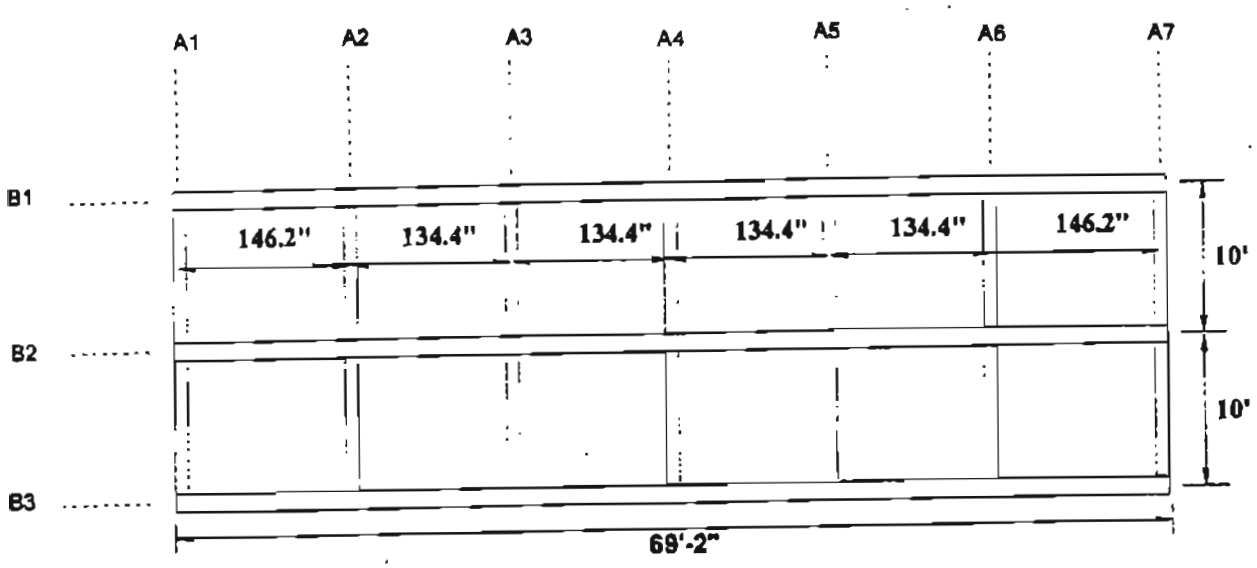

Figure F.34 Structural steel plan of model bridge.

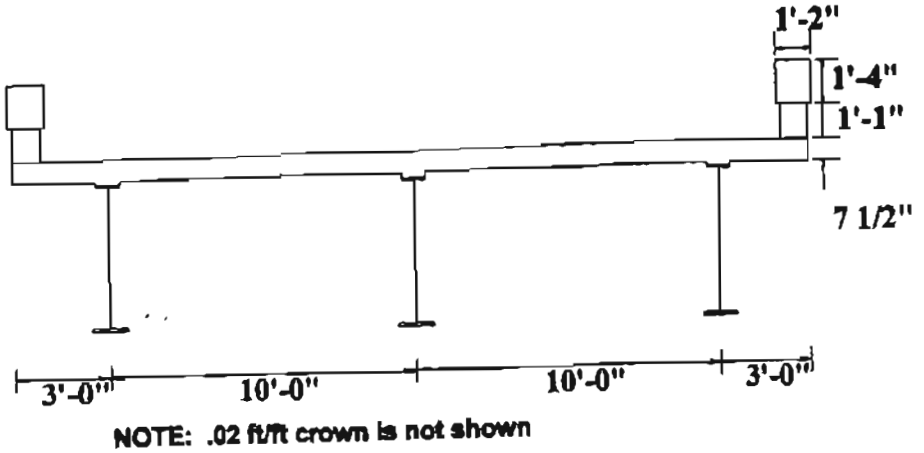

Figure F. 35. Cross section of modal bridge.

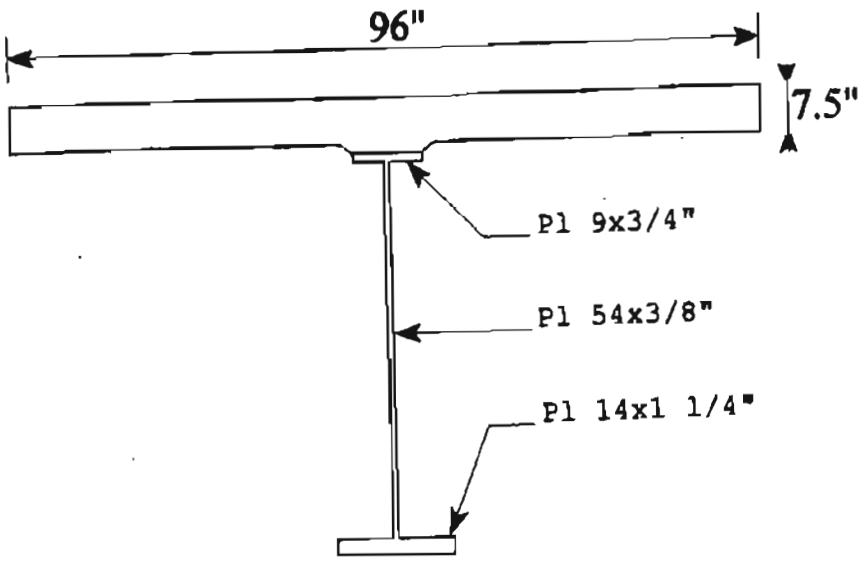

Figure F.36 Cross section of the interio girder at midspan with effective width of the concrete slab.

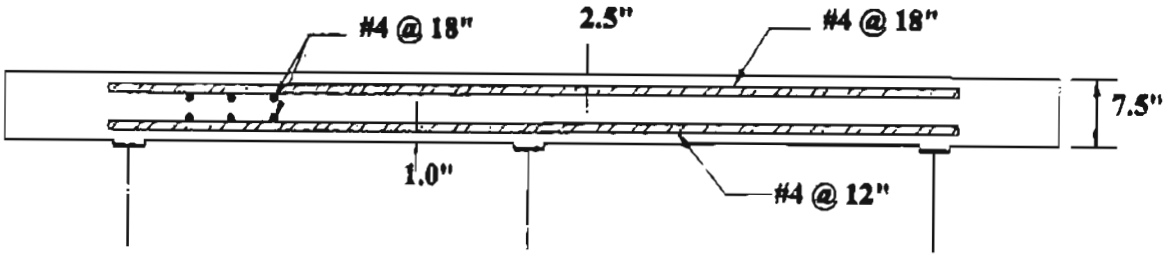

Figure F.37 Slab reinforcement detail.

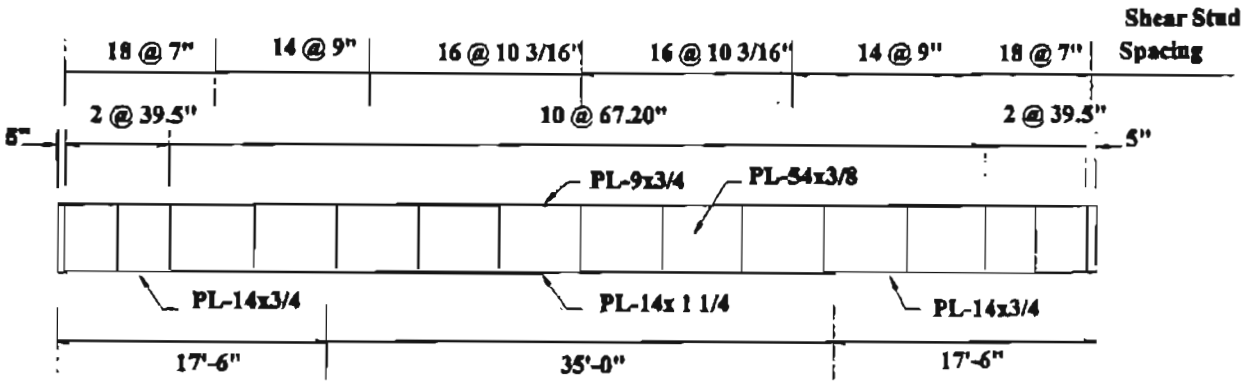

Figure F.38 Elevation for both interior and exterior girders.

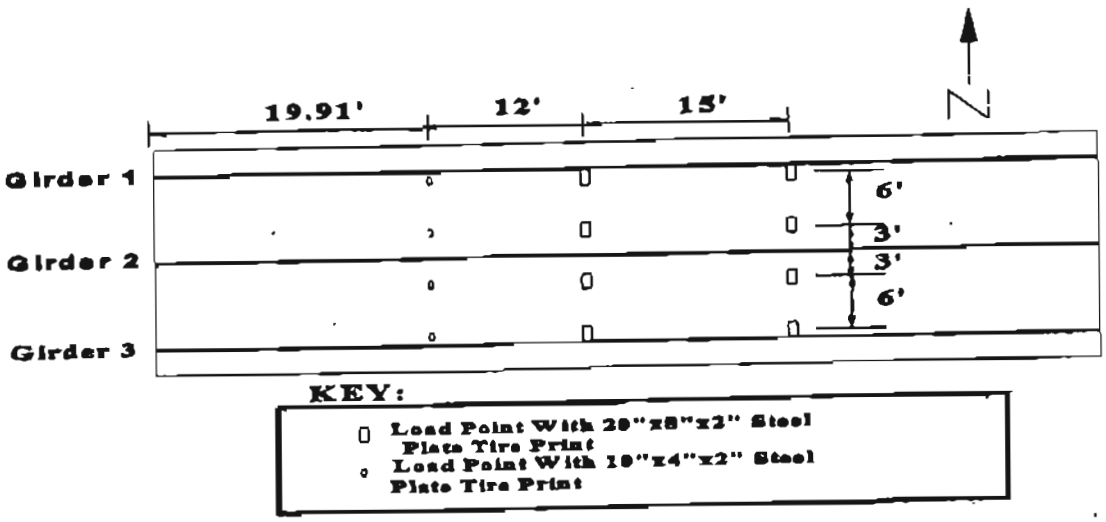

Figure F. 39. Loading configuration simulating one H20 truck on each lane.

During bridge construction cross-frames ("K-Frame" type) were placed at 11.2 feet spacings. For the ultimate load test, the cross frames were removed and the bridge was loaded in both lanes simultaneously until failure occurred. The bridge finally failed when shear punching accursed under one loading point in the slab. Figure F.39 shows the loading configuration used. These loads simulate two side-by-side vehicles having configurations similar to that of one HS-20 truck in each lane.

Strength tests were performed on steel samples and concrete cylinders. The average results of these tests are summarized in the Table F.9.

Table F.9. Summary of material strength

Material	Yield Strength f_y (ksi)	Ultimate Strength f_u (ksi)	Young's Modulus E (ksi)
Structural Steel	41.73	65.56	27,600
Rebar	72.6	119.35	27,550
Concrete		6.151	4,470

To perform the structural analysis, the bridge is modeled as a grid as shown in figure F.40. Each longitudinal girder is divided into 10 equal elements. The contribution of the slab to the longitudinal strength and stiffness are accounted for

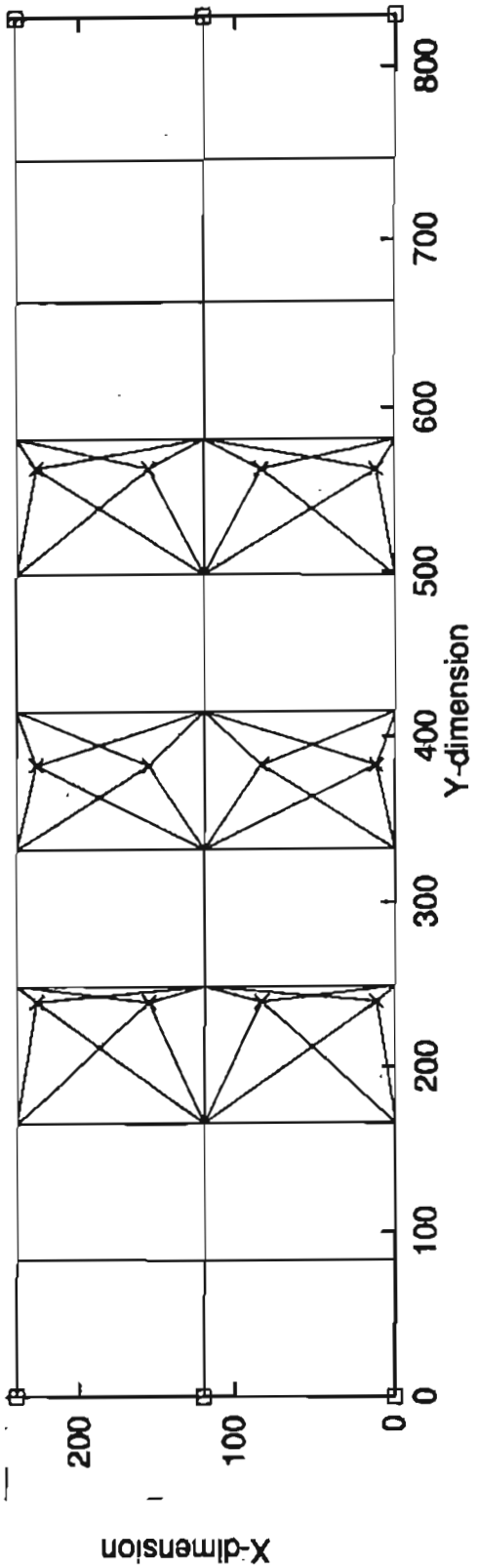

Figure F.40 The grid mesh used to model the Nebraska bridge.

by using the properties of the composite section. The contribution of the slab to the transverse distribution of the load is represented by 11 transverse beams. The points of application of the wheel loads is represented by the symbol X in figure F.40. Since these points do not correspond to actual nodes of the grid model, nominal (artificial) beams with negligible stiffnesses are used to connect these points to the adjacent nodes.

Elastic and inelastic member properties are calculated for each type of section. The longitudinal girders' moment of inertia is found to be 66955 in^4. The ultimate moment capacity is 77493 kip-in for positive bending. In negative bending, the ultimate capacity is 19931 kip-in. The naked steel's section produces a moment of inertia of 21332 in^4 and the ultimate moment capacity is 35988 kip-in. The middle transverse beam representing the contribution of a 83 in wide portion of the slab (see figure F.40) has a moment of inertia equal to 2980 in^4, the torsion coefficient, J, is 5840 in^4 and the ultimate moment capacity is 746 kip-in. The end transverse beams have moments of inertia and ultimate moment capacity equal to1/2 those of the middle beams. See Table F.10 for details of the moment curvature relationships used for each element type.

Table F.10.1 Section properties of Nebraska bridge.

Longitudinal Girder's Section Properties							
A=161.2 in^2, I=66955 in^4, J=1328 in^4							
Positive Bending				Negative Bending			
M1	15499	S1	7.390e9	M1	3986	S1	7.390e9
M2	30997	S2	2.065e9	M2	15945	S2	2.065e9
M3	61994	S3	1.871e8	M3	19930	S3	1.871e8
M4	77493	S4	100	M4	19931	S4	100

Table F.10.2 Section properties of Nebraska bridge.

Middle Transverse Beam's Section Properties							
A=639 in^2, I=2980 in^4, J=5840 in^4							
Positive Bending				Negative Bending			
M1	472	S1	.153e7	M1	304	S1	.462e5
M2	624	S2	.189e6	M2	330	S2	.358e5
M3	663	S3	.165e6	M3	389	S3	.162e5
M4	746	S4	.130e5	M4	403	S4	.880e3

Table F.10.3 Section properties of Nebraska bridge.

Edge Transverse Beam's Section Properties							
A=319 in^2, I=1490 in^4, J=2920 in^4							
Positive Bending				Negative Bending			
M1	236	S1	.763e6	M1	152	S1	.231e5
M2	312	S2	.946e5	M2	165	S2	.179e5
M3	332	S3	.827e5	M3	195	S3	.810e4
M4	373	S4	.652e4	M4	201	S4	.440e3

The dead load is divided into a permanent dead load and a superimposed load. The dead load applied on the naked section is equal to 0.092 kip/in. The superimposed dead load applied on the composite girders is 0.023 kip/in.

Since the results given in reference F.33 are presented in terms of the effect of one HS-20 truck. The point loads applied on the grid were chosen to have a total weight equal to that of one HS-20 truck. In that manner, each front tire is assumed to be 2 kips and all other tires are 8 kips each.

This data is used to prepare the input data file for NONBAN. Section F5.3 will describe the actual input format used for this bridge example.

F.5.3 LISTING OF INPUT DATA FILE

The information gathered in section F.5.2 for the bridge model is entered into the program NONBAN through a data file "NONBAN9.DAT". An example of a data file is given in Table F.11. The data is entered in blocks, each block is given a title and a blank line separates between the blocks. A free-format is used throughout the program so the operator can simply leave a blank space between each entry. Table F.11 gives a listing and explanation of "NONBAN9.DAT" for the example bridge described in F.5.2. The left-hand side column of the table is the original data of "NONBAN9.DAT". The right-hand side column gives some comments on the data entries. For detailed information refer to section F.5.1.

Table F.11 The list and explanation of file NONBAN9.DAT

Nebraska Bridge (3 girder) 0 General Information 4 .3 0 45 100 52 30	- Title - 0 means no shear deformations. - Consider the effect of noncomposite section by choosing option parameter=4.
Noncomposite Section Properties 44.5,21332,301.3,17,990,42,27600,10615,0,0 25890,35986,35987,35988 4438400,100,100,100 42,0.0459 Composite Section Properties 4 161.2,66955,3686,1328,1307.5,27600,10615,0,0 15499,30997,61994,77493 7.39e9,2.065e9,1.871e8,100 42,0.0459 3986,15945,19930.8,19931 7.39e9,2.065e9,1.871e8,100 42,0.0459 100000,1,1,1 100000,1,1,1 0.319E+03 0.149E+04 0.447E+05 0.292E+04 0.401E+03 4470 1862 0 0 0.236E+03 0.312E+03 0.332E+03 0.373E+03 0.763E+06 0.946E+05 0.827E+05 0.652E+04 6.25,1000 0.152E+03 0.165E+03 0.195E+03 .201e+3 0.231E+05 0.179E+05 0.810E+04 .44e3 4.75 1000 100000,1,1,1 100000,1,1,1 0.639E+03 0.298E+04 0.357E+06 0.584E+04 0.802E+03 4470 1862 0 0 0.472E+03 0.624E+03 0.663E+03 0.746E+03 0.153E+07 0.189E+06 0.165E+06 0.130E+05 6.25 1000 0.304E+03 0.330E+03 0.389E+03 .403e3 0.462E+05 0.358E+05 0.162E+05 .88e3 4.75 1000 100000,1,1,1 100000,1,1,1 .01,.01,.01,.01,.01,4470,1863,0,0 1e6,1e6,1e6,1e6	- Mu for noncomposite section is 35988 kip-in. - Properties of composite section. - Positive M-Phi. - Negative M-Phi - Shear V-R. - Properties of transverse beam representing the edge slab strip whose width is 60 in. - Properties of transverse beam representing the middle slab strip whose width is 120 in. - Properties of nominal beams

1e6,1e6,1e6,1e6 100,1000 1e6,1e6,1e6,1e6 1e6,1e6,1e6,1e6 100,1000 100000,1,1,1 100000,1,1,1	that transfer the truck's wheel loads to adjacent nodes.
x-y-z coordinate 0. 120. 240. 0. 120. 240. 0. 120. 240. 0. 120. 240. 0. 120. 240. 0. 120. 240. 0. 120. 240. 0. 120. 240. 0. 120. 240. 0. 120. 240. 0. 120. 240. 12. 12. 12. 84. 84. 84. 156. 156. 156. 228. 228. 228.	X coordinates of all nodes.
0. 0. 0. 83. 83. 83. 166. 166. 166. 249. 249. 249. 332. 332. 332. 415. 415. 415. 498. 498. 498. 581. 581. 581. 664. 664. 664. 747. 747. 747. 830. 830. 830. 239.8 382.9 562.9 239.8 382.9 562.9 239.8 382.9 562.9 239.8 382.9 562.9	Y coordinates of all nodes following same sequence as above.
0. 0. 0. 0. 0. 0. 0. 0. 0. 0. 0. 0. 0. 0. 0. 0. 0. 0. 0. 0. 0. 0. 0. 0. 0. 0. 0. 0. 0. 0. 0. 0. 0. 0. 0. 0. 0. 0. 0. 0. 0. 0. 0. 0. 0.	Z coordinates of all nodes following same sequence as above. (Always 0 for a grid).
beam connection and material type 1 4 7 10 13 16 19 22 25 28 2 5 8 11 14 17 20 23 26 29 3 6 9 12 15 18 21 24 27 30 1 2 4 5 7 8 10 11 13 14 16 17 19 20 22 23 25 26 28 29 31 32 7 10 8 11 13 16 14 17 19 22 20 23 7 10 8 11 13 16 14 17 19 22 20 23 8 11 9 12 14 17 15 18 20 23 21 24 8 11 9 12 14 17 15 18 20 23 21 24	Node numbers corresponding to the left end node of each beam. Start with the beams that undergo inelastic deformations (put girder member's nodes first, then those transverse beams).
4 7 10 13 16 19 22 25 28 31 5 8 11 14 17 20 23 26 29 32 6 9 12 15 18 21 24 27 30 33 2 3 5 6 8 9 11 12 14 15 17 18 20 21 23 24 26 27 29 30 32 33 34 34 34 34 35 35 35 35 36 36 36 36 37 37 37 37 38 38 38 38 39 39 39 39 40 40 40 40 41 41 41 41 42 42 42 42 43 43 43 43 44 44 44 44 45 45 45 45	Node numbers corresponding to the right end node of each beam. Follow the same numbering sequence as above.

1 1 1 1 1 1 1 1 1 1 1 1 1 1 1 1 1 1 1 1 1 1 1 1 1 1 1 1 1 1 2 2 3 3 3 3 3 3 3 3 3 3 3 3 3 3 3 3 3 3 2 2 4 4 4 4 4 4 4 4 4 4 4 4 4 4 4 4 4 4 4 4 4 4 4 4 4 4 4 4 4 4 4 4 4 4 4 4 4 4 4 4 4 4 4 4 4 4 4 4	Material type number for every beam element. Follow the same numbering sequence as above.
plates 0 restraints 6 1 1 1 1 0 0 0 2 1 1 1 0 0 0 3 1 1 1 0 0 0 31 1 1 1 0 0 0 32 1 1 1 0 0 0 33 1 1 1 0 0 0	No plate elements. Number of supports=6. Simple suports at ends.
concentrate dead load 0 unifirm dead load 1 1 30 0.092 0.023 live load 12 34 0 0 2 0 0 0 35 0 0 8 0 0 0 36 0 0 8 0 0 0 37 0 0 2 0 0 0 38 0 0 8 0 0 0 39 0 0 8 0 0 0 40 0 0 2 0 0 0 41 0 0 8 0 0 0 42 0 0 8 0 0 0 43 0 0 2 0 0 0 44 0 0 8 0 0 0 45 0 0 8 0 0 0 33 1 2 3 4 5 6 7 8 9 10 11 12 13 14 15 16 17 18 19 20 21 22 23 24 25 26 27 28 29 30 31 32 33 end	No concentrated dead loads. Dead loads applied on elements 1 through 30. Permanent dead load=0.092. Superimposed dead load=0.023 12 point loads of 2 or 8 kips each applied in the Z direction. Give output for 33 critical nodes Node numbers for detailed output.

F.5.4 OUTPUT DATA FILE

The output of the analysis is given in file NONBAN9.OUT. An example output file is shown in Table F.12. The output file is divided into three sections. Section 1 gives the input information starting with the general system information, followed by the material properties for each material type, the coordinates of every node, a listing of the beam elements with the nodes at the left end, the nodes at the right ends and the material type of every beam. The output file also gives a listing of the applied dead and live loads.

Section 2 of the output file contains the output of the dead load analysis. First it gives the internal moments at the ends of every beam element (RMA & RMB) obtained from the elastic analysis. It also gives the shear forces at the ends (RFA & RFB). If nonlinear deformations occur in the bridge under the effect of the dead load alone, the dead load output lists the displacements and rotations at every node for which a detailed output information is desired (U,V,W Rot. X, Rot. Y, Rot. Z) as well as the internal moments (RMAD, RMBD) and shear forces (RFA, RFB) and the plastic hinge rotations (SITADA, SITADB) at the ends of the beam elements for only the beams connected with nodes for which detailed output information is desired. If nonlinear deformations occur under the effect of the dead load , this output is repeated for every iteration until the dead load ratio reaches a maximum value of 1.0 at which point the final internal moments due to the dead load are listed.

Section 3 gives the output of the incremental analysis. For each iteration stage, the output includes the incremental load factor (FCT), the displacements and rotations at every node for which detailed output information is desired (U,V,W, Rot. X, Rot. Y, Rot. Z), the cumulative internal moments and shears at the ends of every element connected to the nodes identified for detailed output information (CMA & CMB, CFA & CFB), the plastic hinge rotations at the ends of every element (SITAA & SITAB), the node number at which the maximum displacement occurs (NODE), the maximum displacement (CUMAX), the maximum displacement in a primary beam element (CUMAXBEAM), the element where CUMAXBEAM occurred (MEMBER) and the total live load factor (FACTOR). The elements where subhinges formed (IR), the stage of loading of the element at the left end (JJK1) and the right end (JJK2) as well as the slopes of the moment versus plastic hinge rotation curves (RKT1 and RKT2) at the ends of these elements are also provided for each loading stage.

In addition to NONBAN9.OUT, a file named figpvd12bm.dat is produced giving a listing of the load factor and the maximum displacements in the primary beam elements. This file can be used to plot the final results of the analysis. For example, figure F.42, gives a plot of the results of the example analyzed in this

section. A file named figpvd22bm.dat gives the load factor and the maximum displacements for the nodes for which detailed output information is desired.

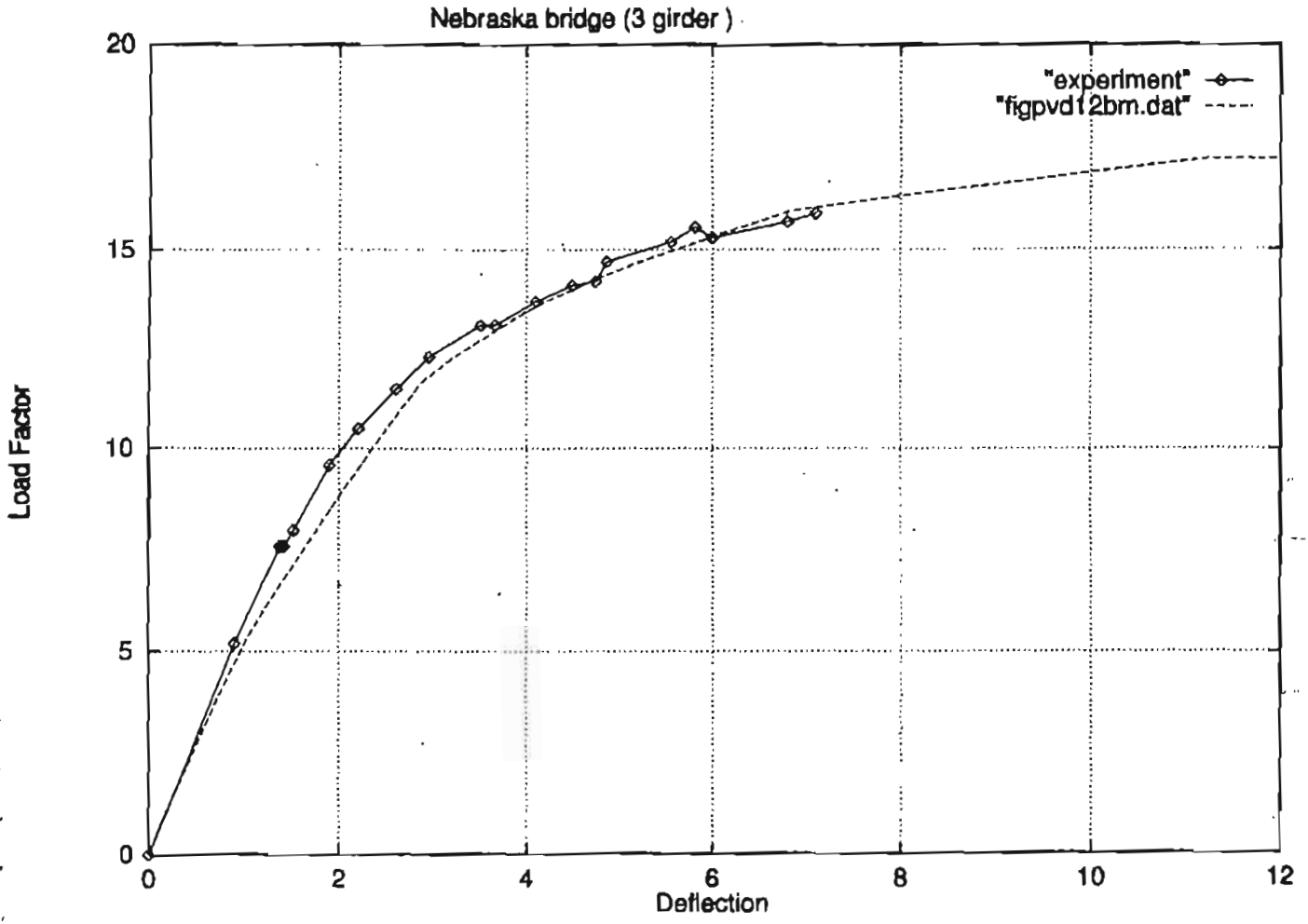

F.42 The Load-deflection curve plotted by NONBAN's out put file.

REFERENCES

F.1 Zokaie, T., Osterkamp, T.A., Imbsen, R.A., "Distribution of Wheel Loads on Highway Bridges", NCHRP project 12-26, TRB, Washington DC,March 1991.

F.2 Pail, G.H., and Buckle I.G., "Computer Programs for Bridge Deck Analysis", Report No. UC SESM 70-6, University of California, Berkeley, April, 1970.

F.3 Mondkar, D.P., and Pail, G.B., "CURVBRG-A Computer Program for Analysis of Curved Open Girder Bridges", Report No. UC SESM 74-17, University of California, Berkeley, December, 1974.

F.4 Lin, C.S., and Scordelis, A.C., "Computer Program for Bridges on Flexible Bents", Report, No. UC SESM 71-24, University of California, Berkeley, December, 1971.

F.5 Peterson, W.S., and Kostem, C.N., "User's Manual for Program BOVA", Fritz Engineering Laboratory Report No. 378B.6A, Lehigh Univ., Bethlehem, PA, 1975.

F.6 Hall, J.C., and Kostem, C.N., "User's Manual for Program BOVAS", Fritz Engineering Laboratory Report No. 435.3A, Lehigh Univ., Bethlehem, PA. 1981.

F.7 Idriss, R.L. and White, K.R., "Secondary Load Paths in Bridge Systems",Transportation Research Records No. 1290., TRB Bridge Engineering Conference March 1991.

F.8 Maheu J.M, "Redistribution of Moments in Slab on Girder Bridges", Ontario Ministry of Transportation.

F.9 Seibel, F., "Nonlinear Analysis and Ultimate Strength of Multi-Cell Reinforced Concrete Box Girder Bridges", UCB/SESM82/02, Department of Civil Engineering, University of California at Berkeley, Berkeley, CA, 1982.

F.10 Choudhury, D., "Analysis of Curved Nonprismatic Reinforced and Prestressed Concrete Box Girder Bridges", Report No. UCB/SEMM-86/13, Department of Civil Engineering, University of California, Berkeley, CA, December 1986.

F.11 Hand, T. and Rostem, C.N., "Inelastic Analysis of Prestressed Concrete Spread Box-Beam Bridges", Fritz Engineering Laboratory Report No. 432.8,Lehigh University, Bethlehem, PA, Oct. 1984.

F.12 Lopez, L.A., Rehak, D.R., Dodds, R.H., and Schmidt, R.J.,"POLO-FINITE, A Structural Mechanics System for Linear and Nonlinear, Static and Dynamic Analysis, Civil Engineering Systems Laboratory, University of Illinois at UrbanaChampaign.

F.13 Hibbitt, H.D., Karlsson, B.I., and Sorenson, J., "ABAQUS general purpose finite element code", Hibbitt, Karlsson and Sorensen Inc.Providence, R.I.

F.14 Helba, A. and Kennedy, J.B., "Collapse Loads of Continuous Skew Composite Bridges", ASCE Journal of Structural Engineering, Vol. 120, No. 5, May, 1994.

F.15 ANSYS User's Manual, Swanson Analysis Systems, Inc., Houston PA.

F.16 "NONSAP User Manual", Structural Mechanics Computer Laboratory,University of Southern California, Jan., 1981.

F.17 Hallquist, J.O., "DYNA3D User's Manual (Nonlinear Dynamic Analysis of Structures in Three Dimensions", Lawrence Livermore National Laboratory, April, 1988.

F.18 Jaegar, L.G. and Bakht, B., "The Grillage Analogy in Bridge Analysis", Canada Journal of Civil Engineering, Vol. 9, National Research Council of Canada, 1982.

F.19 Ghosn M. and Moses F., "Redundancy in Highway Bridge Superstructures" Report NCHRP 12-36, TRB, Washington DC, March 1994.

F.20 Hambly, E.,C., "Bridge Deck Behavior", Chapman and Hall, London, 1976.

F.21 Kulicki, J.M., "Development of Comprehensive Bridge Specification and Commentary", NCHRP 12-33, Draft Report, MarcSh 1993.

F.22 Schilling, C.G., "A Unified Autostress Method", Report 51,American Iron and Steel Institute, November 1989.

F.23 Park, R. and Pauley, T., Reinforced Concrete Structures, Wiley and Sons, New York, 1975.

F.24 Leonhardt, F. and Walther R. "The Stuttgart Shear Tests, 1961", Cement and Concrete Association, No. 111, London, 1962.

F.25 Zsutty, T.C., "Shear Strength Prediction for Separate Categories of Simple Beam Tests", ACI Journal, V. 68, No. 2, Feb. 1971

F.26 Bazant, Z, P. and Ozbolt, J., and Eligehausen, R.,"Fracture Size Effect: 1. Review of Evidence for Concrete Structures", ASCE Journal of Structural Engineering, 1992.

F.27 Hall, R.T., Discussion on: "Shear Strength of HighStrength Concrete Beams with Web Reinforcement, ACI Structural Journal, V. 87, No. 2, March-April, 1990.

F.28 Soliman, M.I., and Ghali,M.K., "Effect of Diaphragms on the Behavior of R.C. Box Girder Bridges", Fourth International Conference on Short and Medium Span Bridges, CSCE, Halifax, Nova Scotia, CA, Aug.1994.

F.29 Siddiqui, A.H., "Effects of Diaphragms on Stress Reduction in Box Girder Bridge Sections", Canadian Journal of Civil Engineering", Vol. 15, No.1, Feb. 1988.

.F.30 Chapman, J.C., "The Structural Behavior of Steel and Concrete Box Girder Bridges", Structural Engineer, Vol. 49, No. 3, 1971.

F.31 Calgaro, J.A., and Virlogeux, M. "Projet et Construction des Ponts: Analyse Structurale des Tabliers de Ponts",Presse de L'Ecole Nationale des Ponts et Chaussees, Paris 1 988.

F.32 Scordelis, A.C., Bouwkamp, J.G., and Wasti, S.T., "Structural Behavior of a Two Span Reinforced Concrete Box Girder Bridge Model",Vols. 1,2 and 3, Report Nos. UC SESM, 715, 71-6, 71-7, University of California, Berkeley, CA, 1971.

F.33 KATHOL S., AZIZINAMINI, A. and, LUEDKE, J., "Strength Capacity of Steel Girder Bridges", NDOR Research Project No. RES1 (0099) P469, Nebraska Department of Roads, February 1995.

TYPICAL PARTIAL OUTPUT

Nebraska bridge (3 girder)

N= 45 IRGJ=100 IRGJ1= 52 ISGJ= 0
NBE= 6 RMU= 0.2000 IG= 0

MATERIAL : 1

FJ= 161.2 IZ= 0.6696E+05 IY= 3686. IX= 1328. EBEAM= 0.2760E+05

MPP1= 0.1550E+05 MPP2= 0.3100E+05 MPP3= 0.6199E+05 MPP4= 0.7749E+05
KTP1= 0.1760E+09 KTP2= 0.4917E+08 KTP3= 0.4455E+07 KTP4= 2.381
RLP= 42.00 SITMAXP= 1.000

MPN1= 3986. MPN2= 0.1594E+05 MPN3= 0.1993E+05 MPN4= 0.1993E+05
KTN1= 0.1760E+09 KTN2= 0.4917E+08 KTN3= 0.4455E+07 KTN4= 2.381
RLN= 42.00 SITMAXN= 1.000

RV1 = 0.1000E+06 RV 2= 1.000 RV 3= 1.000 RV 4= 1.000
KB 1= 0.1000E+06 KB 2= 1.000 KB 3= 1.000 KB 4= 1.000

MATERIAL : 2

FJ= 319.0 IZ= 1490. IY= 0.4470E+05 IX= 2920. EBEAM= 4470.

MPP1= 236.0 MPP2= 312.0 MPP3= 332.0 MPP4= 373.0
KTP1= 0.1221E+06 KTP2= 0.1514E+05 KTP3= 0.1323E+05 KTP4= 1043.
RLP= 6.250 SITMAXP= 1000.

MPN1= 152.0 MPN2= 165.0 MPN3= 195.0 MPN4= 201.0
KTN1= 4863. KTN2= 3768. KTN3= 1705. KTN4= 92.63
RLN= 4.750 SITMAXN= 1000.

RV1 = 0.1000E+06 RV 2= 1.000 RV 3= 1.000 RV 4= 1.000
KB 1= 0.1000E+06 KB 2= 1.000 KB 3= 1.000 KB 4= 1.000

MATERIAL : 3

FJ= 639.0 IZ= 2980. IY= 0.3570E+06 IX= 5840. EBEAM= 4470.

MPP1= 472.0 MPP2= 624.0 MPP3= 663.0 MPP4= 746.0
KTP1= 0.2448E+06 KTP2= 0.3024E+05 KTP3= 0.2640E+05 KTP4= 2080.
RLP= 6.250 SITMAXP= 1000.

MPN1= 304.0 MPN2= 330.0 MPN3= 389.0 MPN4= 403.0
KTN1= 9726. KTN2= 7537. KTN3= 3411. KTN4= 185.3
RLN= 4.750 SITMAXN= 1000.

RV1 = 0.1000E+06 RV 2= 1.000 RV 3= 1.000 RV 4= 1.000
KB 1= 0.1000E+06 KB 2= 1.000 KB 3= 1.000 KB 4= 1.000

MATERIAL : 4

FJ= 0.1000E-01 IZ= 0.1000E-01 IY= 0.1000E-01 IX= 0.1000E-01 EBEAM= 4470.

MPP1= 0.1000E+07 MPP2= 0.1000E+07 MPP3= 0.1000E+07 MPP4= 0.1000E+07
KTP1= 0.1000E+05 KTP2= 0.1000E+05 KTP3= 0.1000E+05 KTP4= 0.1000E+05
RLP= 100.0 SITMAXP= 1000.

MPN1= 0.1000E+07 MPN2= 0.1000E+07 MPN3= 0.1000E+07 MPN4= 0.1000E+07
KTN1= 0.1000E+05 KTN2= 0.1000E+05 KTN3= 0.1000E+05 KTN4= 0.1000E+05
RLN= 100.0 SITMAXN= 1000.

RV1 = 0.1000E+06 RV 2= 1.000 RV 3= 1.000 RV 4= 1.000
KB 1= 0.1000E+06 KB 2= 1.000 KB 3= 1.000 KB 4= 1.000

NODE	X(i)	Y(i)	Z(i)
1	0.	0.	0.
2	120.0	0.	0.
3	240.0	0.	0.
4	0.	79.64	0.
5	120.0	79.64	0.
6	240.0	79.64	0.
7	0.	159.3	0.
8	120.0	159.3	0.
9	240.0	159.3	0.
10	0.	238.9	0.
11	120.0	238.9	0.
12	240.0	238.9	0.
13	0.	310.9	0.
14	120.0	310.9	0.
15	240.0	310.9	0.
16	0.	382.9	0.
17	120.0	382.9	0.
18	240.0	382.9	0.
19	0.	472.9	0.
20	120.0	472.9	0.
21	240.0	472.9	0.
22	0.	562.9	0.
23	120.0	562.9	0.
24	240.0	562.9	0.
25	0.	655.3	0.
26	120.0	655.3	0.
27	240.0	655.3	0.
28	0.	747.6	0.
29	120.0	747.6	0.
30	240.0	747.6	0.
31	0.	840.0	0.
32	120.0	840.0	0.
33	240.0	840.0	0.
34	12.00	239.8	0.
35	12.00	382.9	0.
36	12.00	562.9	0.
37	84.00	239.8	0.
38	84.00	382.9	0.
39	84.00	562.9	0.

40	156.0	239.8	0.
41	156.0	382.9	0.
42	156.0	562.9	0.
43	228.0	239.8	0.
44	228.0	382.9	0.
45	228.0	562.9	0.

IR	IAJ	IBJ	IRKT	IDK
1	1	4	1	0
2	4	7	1	0
3	7	10	1	0
4	10	13	1	0
5	13	16	1	0
6	16	19	1	0
7	19	22	1	0
8	22	25	1	0
9	25	28	1	0
10	28	31	1	0
11	2	5	1	0
12	5	8	1	0
13	8	11	1	0
14	11	14	1	0
15	14	17	1	0
16	17	20	1	0
17	20	23	1	0
18	23	26	1	0
19	26	29	1	0
20	29	32	1	0
21	3	6	1	0
22	6	9	1	0
23	9	12	1	0
24	12	15	1	0
25	15	18	1	0
26	18	21	1	0
27	21	24	1	0
28	24	27	1	0
29	27	30	1	0
30	30	33	1	0
31	1	2	2	0
32	2	3	2	0
33	4	5	3	0
34	5	6	3	0
35	7	8	3	0
36	8	9	3	0
37	10	11	3	0
38	11	12	3	0
39	13	14	3	0
40	14	15	3	0
41	16	17	3	0
42	17	18	3	0
43	19	20	3	0
44	20	21	3	0
45	22	23	3	0
46	23	24	3	0
47	25	26	3	0

48	26	27	3	0
49	28	29	3	0
50	29	30	3	0
51	31	32	2	0
52	32	33	2	0
53	10	34	4	0
54	13	34	4	0
55	11	34	4	0
56	14	34	4	0
57	13	35	4	0
58	16	35	4	0
59	14	35	4	0
60	17	35	4	0
61	19	36	4	0
62	22	36	4	0
63	20	36	4	0
64	23	36	4	0
65	10	37	4	0
66	13	37	4	0
67	11	37	4	0
68	14	37	4	0
69	13	38	4	0
70	16	38	4	0
71	14	38	4	0
72	17	38	4	0
73	19	39	4	0
74	22	39	4	0
75	20	39	4	0
76	23	39	4	0
77	11	40	4	0
78	14	40	4	0
79	12	40	4	0
80	15	40	4	0
81	14	41	4	0
82	17	41	4	0
83	15	41	4	0
84	18	41	4	0
85	20	42	4	0
86	23	42	4	0
87	21	42	4	0
88	24	42	4	0
89	11	43	4	0
90	14	43	4	0
91	12	43	4	0
92	15	43	4	0
93	14	44	4	0
94	17	44	4	0
95	15	44	4	0
96	18	44	4	0
97	20	45	4	0
98	23	45	4	0
99	21	45	4	0
100	24	45	4	0

IBB= 1 2 3 7 8 9 13 14 15 181

IBB= 182 183 187 188 189 193 194 195

UNIFORM DEAD LOAD:

From elem.	to elem.	VALUE
1	30	0.9200E-01

NO. LIVE LOAD= 12

NODE	PX	PY	PZ	RMX	RMY	RMZ
34	0.	0.	2.000	0.	0.	0.
35	0.	0.	8.000	0.	0.	0.
36	0.	0.	8.000	0.	0.	0.
37	0.	0.	2.000	0.	0.	0.
38	0.	0.	8.000	0.	0.	0.
39	0.	0.	8.000	0.	0.	0.
40	0.	0.	2.000	0.	0.	0.
41	0.	0.	8.000	0.	0.	0.
42	0.	0.	8.000	0.	0.	0.
43	0.	0.	2.000	0.	0.	0.
44	0.	0.	8.000	0.	0.	0.
45	0.	0.	8.000	0.	0.	0.

****

OUTPUT OF ANALYSIS

****

*** OUTPUT OF DEAD LOAD ANALYSIS ***

STAGE : 0

ELEMENT	RMA	RMB	RFA	RFB
1	-0.7409E-04	2786.	38.64	-31.32
2	2786.	4988.	31.31	-23.99
3	4988.	6606.	23.99	-16.66
4	6606.	7567.	16.65	-10.03
5	7567.	8051.	10.04	-3.419
6	8052.	7986.	3.411	4.869
7	7985.	7175.	-4.863	13.14
8	7175.	5568.	-13.15	21.65
9	5568.	3177.	-21.65	30.14
10	3177.	-0.7253E-04	-30.14	38.64
11	0.1482E-03	2785.	38.64	-31.31
12	2785.	4987.	31.31	-23.98
13	4987.	6605.	23.98	-16.66
14	6605.	7565.	16.65	-10.02
15	7565.	8050.	10.05	-3.422
16	8050.	7985.	3.412	4.868
17	7983.	7174.	-4.856	13.14
18	7174.	5567.	-13.15	21.64
19	5567.	3176.	-21.64	30.14
20	3176.	0.1451E-03	-30.14	38.64

21	-0.7409E-04	2786.	38.64	-31.32
22	2786.	4988.	31.31	-23.99
23	4988.	6606.	23.99	-16.66
24	6606.	7567.	16.65	-10.03
25	7567.	8051.	10.04	-3.419
26	8052.	7986.	3.411	4.869
27	7985.	7175.	-4.863	13.14
28	7175.	5568.	-13.15	21.65
29	5568.	3177.	-21.65	30.14
30	3177.	-0.7253E-04	-30.14	38.64
31	-0.1626E-01	0.8132E-02	0.2033E-03	-0.2033E-03
32	0.8132E-02	-0.1626E-01	-0.2033E-03	0.2033E-03
33	-0.1557E-01	0.7436E-02	0.1917E-03	-0.1917E-03
34	0.7436E-02	-0.1557E-01	-0.1917E-03	0.1917E-03
35	-0.1494E-01	0.6802E-02	0.1812E-03	-0.1812E-03
36	0.6802E-02	-0.1494E-01	-0.1812E-03	0.1812E-03
37	-0.1443E-01	0.6282E-02	0.1726E-03	-0.1726E-03
38	0.6282E-02	-0.1443E-01	-0.1726E-03	0.1726E-03
39	-0.1413E-01	0.5969E-02	0.1675E-03	-0.1675E-03
40	0.5969E-02	-0.1413E-01	-0.1675E-03	0.1675E-03
41	-0.1394E-01	0.5791E-02	0.1644E-03	-0.1644E-03
42	0.5791E-02	-0.1394E-01	-0.1644E-03	0.1644E-03
43	-0.1397E-01	0.5819E-02	0.1649E-03	-0.1649E-03
44	0.5819E-02	-0.1397E-01	-0.1649E-03	0.1649E-03
45	-0.1421E-01	0.6088E-02	0.1691E-03	-0.1691E-03
46	0.6088E-02	-0.1421E-01	-0.1691E-03	0.1691E-03
47	-0.1473E-01	0.6620E-02	0.1779E-03	-0.1779E-03
48	0.6620E-02	-0.1473E-01	-0.1779E-03	0.1779E-03
49	-0.1543E-01	0.7319E-02	0.1896E-03	-0.1896E-03
50	0.7319E-02	-0.1543E-01	-0.1896E-03	0.1896E-03
51	-0.1621E-01	0.8106E-02	0.2026E-03	-0.2026E-03
52	0.8106E-02	-0.1621E-01	-0.2026E-03	0.2026E-03
53	-0.5527E-01	0.1801E-01	0.6090E-02	-0.6090E-02
54	0.4792	0.9980E-01	-0.5261E-02	0.5261E-02
55	-0.2085E-02	0.3732E-02	0.5386E-04	-0.5386E-04
56	0.1480	0.3371E-01	-0.8836E-03	0.8836E-03
57	0.5036	0.1201	-0.5255E-02	0.5255E-02
58	-0.7291E-01	0.1330E-02	0.6186E-02	-0.6186E-02
59	0.1593	0.3777E-01	-0.9364E-03	0.9364E-03
60	-0.7484E-03	-0.1784E-03	0.5278E-05	-0.5278E-05
61	0.5098	0.1217	-0.4276E-02	0.4276E-02
62	-0.6690E-01	-0.1538E-02	0.5447E-02	-0.5447E-02
63	0.2130	0.5017E-01	-0.1158E-02	0.1158E-02
64	0.6243E-04	-0.1297E-02	-0.1259E-04	0.1259E-04
65	-0.5486E-01	0.5651E-01	0.1326E-02	-0.1326E-02
66	0.1954	0.3367E-01	-0.1470E-02	0.1470E-02
67	-0.1011	0.8195E-01	0.5084E-02	-0.5084E-02
68	0.4125	0.1869E-01	-0.4941E-02	0.4941E-02
69	0.2110	0.3819E-01	-0.1562E-02	0.1562E-02
70	-0.5652E-01	0.5737E-01	0.1356E-02	-0.1356E-02
71	0.4381	0.2577E-01	-0.5123E-02	0.5123E-02
72	-0.1103	0.8152E-01	0.5330E-02	-0.5330E-02
73	0.2761	0.4360E-01	-0.1889E-02	0.1889E-02
74	-0.5831E-01	0.6058E-01	0.1415E-02	-0.1415E-02
75	0.4744	0.3538E-01	-0.4530E-02	0.4530E-02
76	-0.1061	0.7404E-01	0.5004E-02	-0.5004E-02

77	-0.1011	0.8195E-01	0.5084E-02	-0.5084E-02
78	0.4125	0.1869E-01	-0.4941E-02	0.4941E-02
79	-0.5486E-01	0.5651E-01	0.1326E-02	-0.1326E-02
80	0.1954	0.3367E-01	-0.1470E-02	0.1470E-02
81	0.4381	0.2577E-01	-0.5123E-02	0.5123E-02
82	-0.1103	0.8152E-01	0.5330E-02	-0.5330E-02
83	0.2110	0.3819E-01	-0.1562E-02	0.1562E-02
84	-0.5652E-01	0.5737E-01	0.1356E-02	-0.1356E-02
85	0.4744	0.3538E-01	-0.4530E-02	0.4530E-02
86	-0.1061	0.7404E-01	0.5004E-02	-0.5004E-02
87	0.2761	0.4360E-01	-0.1889E-02	0.1889E-02
88	-0.5831E-01	0.6058E-01	0.1415E-02	-0.1415E-02
89	-0.2085E-02	0.3732E-02	0.5386E-04	-0.5386E-04
90	0.1480	0.3371E-01	-0.8836E-03	0.8836E-03
91	-0.5527E-01	0.1801E-01	0.6090E-02	-0.6090E-02
92	0.4792	0.9980E-01	-0.5261E-02	0.5261E-02
93	0.1593	0.3777E-01	-0.9364E-03	0.9364E-03
94	-0.7484E-03	-0.1784E-03	0.5278E-05	-0.5278E-05
95	0.5036	0.1201	-0.5255E-02	0.5255E-02
96	-0.7291E-01	0.1330E-02	0.6186E-02	-0.6186E-02
97	0.2130	0.5017E-01	-0.1158E-02	0.1158E-02
98	0.6243E-04	-0.1297E-02	-0.1259E-04	0.1259E-04
99	0.5098	0.1217	-0.4276E-02	0.4276E-02
100	-0.6690E-01	-0.1538E-02	0.5447E-02	-0.5447E-02

NODE	U(X)	V(Y)	W(Z)	Rot. X	Rot. Y	Rot. Z
1	0.	0.	0.3864E-48	2.536	0.1092E-01	0.
2	0.	0.	0.3864E-48	2.536	-0.1203E-12	0.
3	0.	0.	0.3864E-48	2.536	-0.1092E-01	0.
4	0.	0.	198.5	2.408	0.1092E-01	0.
5	0.	0.	198.5	2.407	-0.1203E-12	0.
6	0.	0.	198.5	2.408	-0.1092E-01	0.
7	0.	0.	377.6	2.058	0.1092E-01	0.
8	0.	0.	377.6	2.058	-0.1204E-12	0.
9	0.	0.	377.6	2.058	-0.1092E-01	0.
10	0.	0.	521.8	1.538	0.1093E-01	0.
11	0.	0.	521.7	1.538	-0.1205E-12	0.
12	0.	0.	521.8	1.538	-0.1093E-01	0.
13	0.	0.	612.4	0.9657	0.1096E-01	0.
14	0.	0.	612.3	0.9655	-0.1207E-12	0.
15	0.	0.	612.4	0.9657	-0.1096E-01	0.
16	0.	0.	659.5	0.3350	0.1094E-01	0.
17	0.	0.	659.4	0.3349	-0.1207E-12	0.
18	0.	0.	659.5	0.3350	-0.1094E-01	0.
19	0.	0.	653.0	-0.4768	0.1093E-01	0.
20	0.	0.	652.9	-0.4767	-0.1208E-12	0.
21	0.	0.	653.0	-0.4768	-0.1093E-01	0.
22	0.	0.	575.0	-1.244	0.1090E-01	0.
23	0.	0.	574.9	-1.244	-0.1207E-12	0.
24	0.	0.	575.0	-1.244	-0.1090E-01	0.
25	0.	0.	428.1	-1.908	0.1089E-01	0.
26	0.	0.	428.0	-1.908	-0.1207E-12	0.
27	0.	0.	428.1	-1.908	-0.1089E-01	0.
28	0.	0.	228.9	-2.366	0.1088E-01	0.
29	0.	0.	228.8	-2.365	-0.1206E-12	0.

30	0.	0.	228.9	-2.366	-0.1088E-01	0.
31	0.	0.	0.3864E-48	-2.536	0.1088E-01	0.
32	0.	0.	0.3864E-48	-2.536	-0.1206E-12	0.
33	0.	0.	0.3864E-48	-2.536	-0.1088E-01	0.

DEAD LOAD RATIO= 1.000 KA= 0 KB= 0 KBA= 0 KBB= 0

ELEMENT	RMAD	RMBD	SITADA	SITADB	RFAD	RFBD
1	-0.7409E-04	2786.	0.	0.	38.64	-31.32
2	2786.	4988.	0.	0.	31.31	-23.99
3	4988.	6606.	0.	0.	23.99	-16.66
4	6606.	7567.	0.	0.	16.65	-10.03
5	7567.	8051.	0.	0.	10.04	-3.419
6	8052.	7986.	0.	0.	3.411	4.869
7	7985.	7175.	0.	0.	-4.863	13.14
8	7175.	5568.	0.	0.	-13.15	21.65
9	5568.	3177.	0.	0.	-21.65	30.14
10	3177.	-0.7253E-04	0.	0.	-30.14	38.64
11	0.1482E-03	2785.	0.	0.	38.64	-31.31
12	2785.	4987.	0.	0.	31.31	-23.98
13	4987.	6605.	0.	0.	23.98	-16.66
14	6605.	7565.	0.	0.	16.65	-10.02
15	7565.	8050.	0.	0.	10.05	-3.422
16	8050.	7985.	0.	0.	3.412	4.868
17	7983.	7174.	0.	0.	-4.856	13.14
18	7174.	5567.	0.	0.	-13.15	21.64
19	5567.	3176.	0.	0.	-21.64	30.14
20	3176.	0.1451E-03	0.	0.	-30.14	38.64
21	-0.7409E-04	2786.	0.	0.	38.64	-31.32
22	2786.	4988.	0.	0.	31.31	-23.99
23	4988.	6606.	0.	0.	23.99	-16.66
24	6606.	7567.	0.	0.	16.65	-10.03
25	7567.	8051.	0.	0.	10.04	-3.419

26	8052.	7986.	0.	0.	3.411	4.869
27	7985.	7175.	0.	0.	-4.863	13.14
28	7175.	5568.	0.	0.	-13.15	21.65
29	5568.	3177.	0.	0.	-21.65	30.14
30	3177.	-0.7253E-04	0.	0.	-30.14	38.64
31	-0.1626E-01	0.8132E-02	0.	0.	0.2033E-03	-0.2033E-03
32	0.8132E-02	-0.1626E-01	0.	0.	-0.2033E-03	0.2033E-03
33	-0.1557E-01	0.7436E-02	0.	0.	0.1917E-03	-0.1917E-03
34	0.7436E-02	-0.1557E-01	0.	0.	-0.1917E-03	0.1917E-03
35	-0.1494E-01	0.6802E-02	0.	0.	0.1812E-03	-0.1812E-03
36	0.6802E-02	-0.1494E-01	0.	0.	-0.1812E-03	0.1812E-03
37	-0.1443E-01	0.6282E-02	0.	0.	0.1726E-03	-0.1726E-03
38	0.6282E-02	-0.1443E-01	0.	0.	-0.1726E-03	0.1726E-03
39	-0.1413E-01	0.5969E-02	0.	0.	0.1675E-03	-0.1675E-03
40	0.5969E-02	-0.1413E-01	0.	0.	-0.1675E-03	0.1675E-03
41	-0.1394E-01	0.5791E-02	0.	0.	0.1644E-03	-0.1644E-03
42	0.5791E-02	-0.1394E-01	0.	0.	-0.1644E-03	0.1644E-03
43	-0.1397E-01	0.5819E-02	0.	0.	0.1649E-03	-0.1649E-03
44	0.5819E-02	-0.1397E-01	0.	0.	-0.1649E-03	0.1649E-03
45	-0.1421E-01	0.6088E-02	0.	0.	0.1691E-03	-0.1691E-03
46	0.6088E-02	-0.1421E-01	0.	0.	-0.1691E-03	0.1691E-03

47	-0.1473E-01	0.6620E-02	0.	0.	0.1779E-03	-0.1779E-03
48	0.6620E-02	-0.1473E-01	0.	0.	-0.1779E-03	0.1779E-03
49	-0.1543E-01	0.7319E-02	0.	0.	0.1896E-03	-0.1896E-03
50	0.7319E-02	-0.1543E-01	0.	0.	-0.1896E-03	0.1896E-03
51	-0.1621E-01	0.8106E-02	0.	0.	0.2026E-03	-0.2026E-03
52	0.8106E-02	-0.1621E-01	0.	0.	-0.2026E-03	0.2026E-03
53	-0.5527E-01	0.1801E-01	0.	0.	0.6090E-02	-0.6090E-02
54	0.4792	0.9980E-01	0.	0.	-0.5261E-02	0.5261E-02
55	-0.2085E-02	0.3732E-02	0.	0.	0.5386E-04	-0.5386E-04
56	0.1480	0.3371E-01	0.	0.	-0.8836E-03	0.8836E-03
57	0.5036	0.1201	0.	0.	-0.5255E-02	0.5255E-02
58	-0.7291E-01	0.1330E-02	0.	0.	0.6186E-02	-0.6186E-02
59	0.1593	0.3777E-01	0.	0.	-0.9364E-03	0.9364E-03
60	-0.7484E-03	-0.1784E-03	0.	0.	0.5278E-05	-0.5278E-05
61	0.5098	0.1217	0.	0.	-0.4276E-02	0.4276E-02
62	-0.6690E-01	-0.1538E-02	0.	0.	0.5447E-02	-0.5447E-02
63	0.2130	0.5017E-01	0.	0.	-0.1158E-02	0.1158E-02
64	0.6243E-04	-0.1297E-02	0.	0.	-0.1259E-04	0.1259E-04
65	-0.5486E-01	0.5651E-01	0.	0.	0.1326E-02	-0.1326E-02
66	0.1954	0.3367E-01	0.	0.	-0.1470E-02	0.1470E-02
67	-0.1011	0.8195E-01	0.	0.	0.5084E-02	-0.5084E-02
68	0.4125	0.1869E-01	0.	0.	-0.4941E-02	0.4941E-02
69	0.2110	0.3819E-01	0.	0.	-0.1562E-02	0.1562E-02
70	-0.5652E-01	0.5737E-01	0.	0.	0.1356E-02	-0.1356E-02
71	0.4381	0.2577E-01	0.	0.	-0.5123E-02	0.5123E-02
72	-0.1103	0.8152E-01	0.	0.	0.5330E-02	-0.5330E-02
73	0.2761	0.4360E-01	0.	0.	-0.1889E-02	0.1889E-02
74	-0.5831E-01	0.6058E-01	0.	0.	0.1415E-02	-0.1415E-02
75	0.4744	0.3538E-01	0.	0.	-0.4530E-02	0.4530E-02
76	-0.1061	0.7404E-01	0.	0.	0.5004E-02	-0.5004E-02
77	-0.1011	0.8195E-01	0.	0.	0.5084E-02	-0.5084E-02

084E-02						
78	0.4125	0.1869E-01	0.	0.	-0.4941E-02	0.4
941E-02						
79	-0.5486E-01	0.5651E-01	0.	0.	0.1326E-02	-0.1
326E-02						
80	0.1954	0.3367E-01	0.	0.	-0.1470E-02	0.1
470E-02						
81	0.4381	0.2577E-01	0.	0.	-0.5123E-02	0.5
123E-02						
82	-0.1103	0.8152E-01	0.	0.	0.5330E-02	-0.5
330E-02						
83	0.2110	0.3819E-01	0.	0.	-0.1562E-02	0.1
562E-02						
84	-0.5652E-01	0.5737E-01	0.	0.	0.1356E-02	-0.1
356E-02						
85	0.4744	0.3538E-01	0.	0.	-0.4530E-02	0.4
530E-02						
86	-0.1061	0.7404E-01	0.	0.	0.5004E-02	-0.5
004E-02						
87	0.2761	0.4360E-01	0.	0.	-0.1889E-02	0.1
889E-02						
88	-0.5831E-01	0.6058E-01	0.	0.	0.1415E-02	-0.1
415E-02						
89	-0.2085E-02	0.3732E-02	0.	0.	0.5386E-04	-0.5
386E-04						
90	0.1480	0.3371E-01	0.	0.	-0.8836E-03	0.8
836E-03						
91	-0.5527E-01	0.1801E-01	0.	0.	0.6090E-02	-0.6
090E-02						
92	0.4792	0.9980E-01	0.	0.	-0.5261E-02	0.5
261E-02						
93	0.1593	0.3777E-01	0.	0.	-0.9364E-03	0.9
364E-03						
94	-0.7484E-03	-0.1784E-03	0.	0.	0.5278E-05	-0.5
278E-05						
95	0.5036	0.1201	0.	0.	-0.5255E-02	0.5
255E-02						
96	-0.7291E-01	0.1330E-02	0.	0.	0.6186E-02	-0.6
186E-02						
97	0.2130	0.5017E-01	0.	0.	-0.1158E-02	0.1
158E-02						
98	0.6243E-04	-0.1297E-02	0.	0.	-0.1259E-04	0.1
259E-04						
99	0.5098	0.1217	0.	0.	-0.4276E-02	0.4
276E-02						
100	-0.6690E-01	-0.1538E-02	0.	0.	0.5447E-02	-0.5
447E-02						

NODE : 41 CUMAX= 660.0 DEAD LOAD RATIO= 1.000

NODE OF MAX. DISPLACEMENT AMONG BEAMS : 18 CUMAXBEAM= 659.5

DEAD LOAD: ELEMENT	MOMENT A	MOMENT B	FORCE A	FORCE B
1	-0.7409E-04	2786.	38.64	-31.32
2	2786.	4988.	31.31	-23.99
3	4988.	6606.	23.99	-16.66
4	6606.	7567.	16.65	-10.03
5	7567.	8051.	10.04	-3.419
6	8052.	7986.	3.411	4.869
7	7985.	7175.	-4.863	13.14
8	7175.	5568.	-13.15	21.65
9	5568.	3177.	-21.65	30.14
10	3177.	-0.7253E-04	-30.14	38.64
11	0.1482E-03	2785.	38.64	-31.31
12	2785.	4987.	31.31	-23.98
13	4987.	6605.	23.98	-16.66
14	6605.	7565.	16.65	-10.02
15	7565.	8050.	10.05	-3.422
16	8050.	7985.	3.412	4.868
17	7983.	7174.	-4.856	13.14
18	7174.	5567.	-13.15	21.64
19	5567.	3176.	-21.64	30.14
20	3176.	0.1451E-03	-30.14	38.64
21	-0.7409E-04	2786.	38.64	-31.32
22	2786.	4988.	31.31	-23.99
23	4988.	6606.	23.99	-16.66
24	6606.	7567.	16.65	-10.03
25	7567.	8051.	10.04	-3.419
26	8052.	7986.	3.411	4.869
27	7985.	7175.	-4.863	13.14
28	7175.	5568.	-13.15	21.65
29	5568.	3177.	-21.65	30.14
30	3177.	-0.7253E-04	-30.14	38.64
31	-0.1626E-01	0.8132E-02	0.2033E-03	-0.2033E-03
32	0.8132E-02	-0.1626E-01	-0.2033E-03	0.2033E-03
33	-0.1557E-01	0.7436E-02	0.1917E-03	-0.1917E-03
34	0.7436E-02	-0.1557E-01	-0.1917E-03	0.1917E-03
35	-0.1494E-01	0.6802E-02	0.1812E-03	-0.1812E-03
36	0.6802E-02	-0.1494E-01	-0.1812E-03	0.1812E-03
37	-0.1443E-01	0.6282E-02	0.1726E-03	-0.1726E-03
38	0.6282E-02	-0.1443E-01	-0.1726E-03	0.1726E-03
39	-0.1413E-01	0.5969E-02	0.1675E-03	-0.1675E-03
40	0.5969E-02	-0.1413E-01	-0.1675E-03	0.1675E-03
41	-0.1394E-01	0.5791E-02	0.1644E-03	-0.1644E-03
42	0.5791E-02	-0.1394E-01	-0.1644E-03	0.1644E-03
43	-0.1397E-01	0.5819E-02	0.1649E-03	-0.1649E-03
44	0.5819E-02	-0.1397E-01	-0.1649E-03	0.1649E-03
45	-0.1421E-01	0.6088E-02	0.1691E-03	-0.1691E-03
46	0.6088E-02	-0.1421E-01	-0.1691E-03	0.1691E-03
47	-0.1473E-01	0.6620E-02	0.1779E-03	-0.1779E-03

48	0.6620E-02	-0.1473E-01	-0.1779E-03	0.1779E-03
49	-0.1543E-01	0.7319E-02	0.1896E-03	-0.1896E-03
50	0.7319E-02	-0.1543E-01	-0.1896E-03	0.1896E-03
51	-0.1621E-01	0.8106E-02	0.2026E-03	-0.2026E-03
52	0.8106E-02	-0.1621E-01	-0.2026E-03	0.2026E-03
53	-0.5527E-01	0.1801E-01	0.6090E-02	-0.6090E-02
54	0.4792	0.9980E-01	-0.5261E-02	0.5261E-02
55	-0.2085E-02	0.3732E-02	0.5386E-04	-0.5386E-04
56	0.1480	0.3371E-01	-0.8836E-03	0.8836E-03
57	0.5036	0.1201	-0.5255E-02	0.5255E-02
58	-0.7291E-01	0.1330E-02	0.6186E-02	-0.6186E-02
59	0.1593	0.3777E-01	-0.9364E-03	0.9364E-03
60	-0.7484E-03	-0.1784E-03	0.5278E-05	-0.5278E-05
61	0.5098	0.1217	-0.4276E-02	0.4276E-02
62	-0.6690E-01	-0.1538E-02	0.5447E-02	-0.5447E-02
63	0.2130	0.5017E-01	-0.1158E-02	0.1158E-02
64	0.6243E-04	-0.1297E-02	-0.1259E-04	0.1259E-04
65	-0.5486E-01	0.5651E-01	0.1326E-02	-0.1326E-02
66	0.1954	0.3367E-01	-0.1470E-02	0.1470E-02
67	-0.1011	0.8195E-01	0.5084E-02	-0.5084E-02
68	0.4125	0.1869E-01	-0.4941E-02	0.4941E-02
69	0.2110	0.3819E-01	-0.1562E-02	0.1562E-02
70	-0.5652E-01	0.5737E-01	0.1356E-02	-0.1356E-02
71	0.4381	0.2577E-01	-0.5123E-02	0.5123E-02
72	-0.1103	0.8152E-01	0.5330E-02	-0.5330E-02
73	0.2761	0.4360E-01	-0.1889E-02	0.1889E-02
74	-0.5831E-01	0.6058E-01	0.1415E-02	-0.1415E-02
75	0.4744	0.3538E-01	-0.4530E-02	0.4530E-02
76	-0.1061	0.7404E-01	0.5004E-02	-0.5004E-02
77	-0.1011	0.8195E-01	0.5084E-02	-0.5084E-02
78	0.4125	0.1869E-01	-0.4941E-02	0.4941E-02
79	-0.5486E-01	0.5651E-01	0.1326E-02	-0.1326E-02
80	0.1954	0.3367E-01	-0.1470E-02	0.1470E-02
81	0.4381	0.2577E-01	-0.5123E-02	0.5123E-02
82	-0.1103	0.8152E-01	0.5330E-02	-0.5330E-02
83	0.2110	0.3819E-01	-0.1562E-02	0.1562E-02
84	-0.5652E-01	0.5737E-01	0.1356E-02	-0.1356E-02
85	0.4744	0.3538E-01	-0.4530E-02	0.4530E-02
86	-0.1061	0.7404E-01	0.5004E-02	-0.5004E-02
87	0.2761	0.4360E-01	-0.1889E-02	0.1889E-02
88	-0.5831E-01	0.6058E-01	0.1415E-02	-0.1415E-02
89	-0.2085E-02	0.3732E-02	0.5386E-04	-0.5386E-04
90	0.1480	0.3371E-01	-0.8836E-03	0.8836E-03
91	-0.5527E-01	0.1801E-01	0.6090E-02	-0.6090E-02
92	0.4792	0.9980E-01	-0.5261E-02	0.5261E-02
93	0.1593	0.3777E-01	-0.9364E-03	0.9364E-03
94	-0.7484E-03	-0.1784E-03	0.5278E-05	-0.5278E-05
95	0.5036	0.1201	-0.5255E-02	0.5255E-02
96	-0.7291E-01	0.1330E-02	0.6186E-02	-0.6186E-02
97	0.2130	0.5017E-01	-0.1158E-02	0.1158E-02
98	0.6243E-04	-0.1297E-02	-0.1259E-04	0.1259E-04
99	0.5098	0.1217	-0.4276E-02	0.4276E-02
100	-0.6690E-01	-0.1538E-02	0.5447E-02	-0.5447E-02

***** END OF DEAD LOAD ANALYSIS *****

*** OUTPUT OF DEAD LOAD ANALYSIS ***

STAGE : 1

NODE	U(X)	V(Y)	W(Z)	Rot. X	Rot. Y	Rot. Z
1	0.	0.	0.4830E-48	2.536	0.1092E-01	0.
2	0.	0.	0.4830E-48	2.536	-0.1203E-12	0.
3	0.	0.	0.4830E-48	2.536	-0.1092E-01	0.
4	0.	0.	198.5	2.408	0.1092E-01	0.
5	0.	0.	198.5	2.408	-0.1203E-12	0.
6	0.	0.	198.5	2.408	-0.1092E-01	0.
7	0.	0.	377.7	2.058	0.1092E-01	0.
8	0.	0.	377.6	2.058	-0.1204E-12	0.
9	0.	0.	377.7	2.058	-0.1092E-01	0.
10	0.	0.	521.9	1.539	0.1093E-01	0.
11	0.	0.	521.8	1.538	-0.1205E-12	0.
12	0.	0.	521.9	1.539	-0.1093E-01	0.
13	0.	0.	612.5	0.9658	0.1096E-01	0.
14	0.	0.	612.4	0.9657	-0.1207E-12	0.
15	0.	0.	612.5	0.9658	-0.1096E-01	0.
16	0.	0.	659.6	0.3350	0.1094E-01	0.
17	0.	0.	659.4	0.3350	-0.1207E-12	0.
18	0.	0.	659.6	0.3350	-0.1094E-01	0.
19	0.	0.	653.1	-0.4768	0.1093E-01	0.
20	0.	0.	653.0	-0.4767	-0.1208E-12	0.
21	0.	0.	653.1	-0.4768	-0.1093E-01	0.
22	0.	0.	575.1	-1.245	0.1090E-01	0.
23	0.	0.	574.9	-1.244	-0.1207E-12	0.
24	0.	0.	575.1	-1.245	-0.1090E-01	0.
25	0.	0.	428.2	-1.908	0.1089E-01	0.
26	0.	0.	428.1	-1.908	-0.1207E-12	0.
27	0.	0.	428.2	-1.908	-0.1089E-01	0.
28	0.	0.	228.9	-2.366	0.1088E-01	0.
29	0.	0.	228.9	-2.365	-0.1206E-12	0.
30	0.	0.	228.9	-2.366	-0.1088E-01	0.
31	0.	0.	0.4830E-48	-2.536	0.1088E-01	0.
32	0.	0.	0.4830E-48	-2.536	-0.1206E-12	0.
33	0.	0.	0.4830E-48	-2.536	-0.1088E-01	0.

DEAD LOAD RATIO= 1.000 KA= 0 KB= 0 KBA= 0 KBB= 0

ELEMENT	RMAD	RMBD	SITADA	SITADB	RFAD	RFBD
1	-0.4815E-06	696.4	0.	0.	9.660	-7.828
2	696.4	1247.	0.	0.	7.828	-5.997
3	1247.	1652.	0.	0.	5.997	-4.165
4	1652.	1892.	0.	0.	4.165	-2.509
5	1892.	2013.	0.	0.	2.509	-0.8528
6	2013.	1996.	0.	0.	0.8528	1.217
7	1996.	1794.	0.	0.	-1.217	3.287

8	1794.	1392.	0.	0.	-3.287	5.411
9	1392.	794.1	0.	0.	-5.411	7.536
10	794.1	-0.3773E-06	0.	0.	-7.536	9.660

11	0.9630E-06	696.4	0.	0.	9.660	-7.828
12	696.4	1247.	0.	0.	7.828	-5.997
13	1247.	1652.	0.	0.	5.997	-4.165
14	1652.	1892.	0.	0.	4.165	-2.509
15	1892.	2013.	0.	0.	2.509	-0.8528
16	2013.	1996.	0.	0.	0.8528	1.217
17	1996.	1794.	0.	0.	-1.217	3.287
18	1794.	1392.	0.	0.	-3.287	5.411
19	1392.	794.1	0.	0.	-5.411	7.536
20	794.1	0.7546E-06	0.	0.	-7.536	9.660
21	-0.4815E-06	696.4	0.	0.	9.660	-7.828
22	696.4	1247.	0.	0.	7.828	-5.997
23	1247.	1652.	0.	0.	5.997	-4.165
24	1652.	1892.	0.	0.	4.165	-2.509
25	1892.	2013.	0.	0.	2.509	-0.8528
26	2013.	1996.	0.	0.	0.8528	1.217
27	1996.	1794.	0.	0.	-1.217	3.287
28	1794.	1392.	0.	0.	-3.287	5.411
29	1392.	794.1	0.	0.	-5.411	7.536
30	794.1	-0.3773E-06	0.	0.	-7.536	9.660
31	-0.1123E-05	0.5615E-06	0.	0.	0.1404E-07	-0.1404E-07
32	0.5615E-06	-0.1123E-05	0.	0.	-0.1404E-07	0.1404E-07
33	-0.4030E-06	-0.2128E-05	0.	0.	-0.1438E-07	0.1438E-07
34	-0.2128E-05	-0.4030E-06	0.	0.	0.1438E-07	-0.1438E-07
35	0.1642E-06	-0.4610E-05	0.	0.	-0.3978E-07	0.3978E-07
36	-0.4610E-05	0.1642E-06	0.	0.	0.3978E-07	-0.3978E-07
37	0.5372E-06	-0.6691E-05	0.	0.	-0.6023E-07	0.6023E-07
38	-0.6691E-05	0.5372E-06	0.	0.	0.6023E-07	-0.6023E-07
39	-0.2336E-04	0.4065E-05	0.	0.	0.2286E-06	-0.2286E-06
40	0.4065E-05	-0.2336E-04	0.	0.	-0.2286E-06	0.2286E-06
41	-0.1316E-05	-0.7310E-05	0.	0.	-0.4995E-07	0.4995E-07

995E-07						
42	-0.7310E-05	-0.1316E-05	0.	0.	0.4995E-07	-0.4
995E-07						
43	-0.1303E-04	-0.1023E-05	0.	0.	0.1001E-06	-0.1
001E-06						
44	-0.1023E-05	-0.1303E-04	0.	0.	-0.1001E-06	0.1
001E-06						
45	0.4414E-05	-0.8365E-05	0.	0.	-0.1065E-06	0.1
065E-06						
46	-0.8365E-05	0.4414E-05	0.	0.	0.1065E-06	-0.1
065E-06						
47	0.9280E-06	-0.4684E-05	0.	0.	-0.4677E-07	0.4
677E-07						
48	-0.4684E-05	0.9280E-06	0.	0.	0.4677E-07	-0.4
677E-07						
49	-0.1607E-06	-0.2051E-05	0.	0.	-0.1575E-07	0.1
575E-07						
50	-0.2051E-05	-0.1607E-06	0.	0.	0.1575E-07	-0.1
575E-07						
51	-0.9010E-06	0.4505E-06	0.	0.	0.1126E-07	-0.1
126E-07						
52	0.4505E-06	-0.9010E-06	0.	0.	-0.1126E-07	0.1
126E-07						
53	-0.4508E-05	0.4093E-05	0.	0.	0.7148E-06	-0.7
148E-06						
54	0.5824E-04	0.1196E-04	0.	0.	-0.6418E-06	0.6
418E-06						
55	-0.9048E-06	0.1748E-05	0.	0.	0.2457E-07	-0.2
457E-07						
56	0.1753E-04	0.4903E-05	0.	0.	-0.9762E-07	0.9
762E-07						
57	0.6122E-04	0.1437E-04	0.	0.	-0.6421E-06	0.6
421E-06						
58	-0.6730E-05	0.2015E-05	0.	0.	0.7288E-06	-0.7
288E-06						
59	0.1894E-04	0.5377E-05	0.	0.	-0.1045E-06	0.1
045E-06						
60	-0.6864E-06	0.1232E-05	0.	0.	0.1776E-07	-0.1
776E-07						
61	0.6193E-04	0.1458E-04	0.	0.	-0.5217E-06	0.5
217E-06						
62	-0.6047E-05	0.1612E-05	0.	0.	0.6383E-06	-0.6
383E-06						
63	0.2549E-04	0.6752E-05	0.	0.	-0.1333E-06	0.1
333E-06						
64	-0.6446E-06	0.1160E-05	0.	0.	0.1671E-07	-0.1
671E-07						
65	-0.4891E-05	0.6811E-05	0.	0.	0.1393E-06	-0.1
393E-06						
66	0.2469E-04	0.4115E-05	0.	0.	-0.1869E-06	0.1
869E-06						

67	-0.1311E-04	0.1006E-04	0.	0.	0.6433E-06	-0.6433E-06
68	0.4982E-04	0.2333E-05	0.	0.	-0.5957E-06	0.5957E-06
69	0.2654E-04	0.4645E-05	0.	0.	-0.1979E-06	0.1979E-06
70	-0.5156E-05	0.6949E-05	0.	0.	0.1441E-06	-0.1441E-06
71	0.5293E-04	0.3209E-05	0.	0.	-0.6178E-06	0.6178E-06
72	-0.1416E-04	0.1002E-04	0.	0.	0.6716E-06	-0.6716E-06
73	0.3426E-04	0.5313E-05	0.	0.	-0.2352E-06	0.2352E-06
74	-0.5321E-05	0.7295E-05	0.	0.	0.1502E-06	-0.1502E-06
75	0.5738E-04	0.4347E-05	0.	0.	-0.5472E-06	0.5472E-06
76	-0.1366E-04	0.9097E-05	0.	0.	0.6322E-06	-0.6322E-06
77	-0.1311E-04	0.1006E-04	0.	0.	0.6433E-06	-0.6433E-06
78	0.4982E-04	0.2333E-05	0.	0.	-0.5957E-06	0.5957E-06
79	-0.4891E-05	0.6811E-05	0.	0.	0.1393E-06	-0.1393E-06
80	0.2469E-04	0.4115E-05	0.	0.	-0.1869E-06	0.1869E-06
81	0.5293E-04	0.3209E-05	0.	0.	-0.6178E-06	0.6178E-06
82	-0.1416E-04	0.1002E-04	0.	0.	0.6716E-06	-0.6716E-06
83	0.2654E-04	0.4645E-05	0.	0.	-0.1979E-06	0.1979E-06
84	-0.5156E-05	0.6949E-05	0.	0.	0.1441E-06	-0.1441E-06
85	0.5738E-04	0.4347E-05	0.	0.	-0.5472E-06	0.5472E-06
86	-0.1366E-04	0.9097E-05	0.	0.	0.6322E-06	-0.6322E-06
87	0.3426E-04	0.5313E-05	0.	0.	-0.2352E-06	0.2352E-06
88	-0.5321E-05	0.7295E-05	0.	0.	0.1502E-06	-0.1502E-06
89	-0.9048E-06	0.1748E-05	0.	0.	0.2457E-07	-0.2457E-07
90	0.1753E-04	0.4903E-05	0.	0.	-0.9762E-07	0.9762E-07
91	-0.4508E-05	0.4093E-05	0.	0.	0.7148E-06	-0.7148E-06
92	0.5824E-04	0.1196E-04	0.	0.	-0.6418E-06	0.6418E-06
93	0.1894E-04	0.5377E-05	0.	0.	-0.1045E-06	0.1045E-06
94	-0.6864E-06	0.1232E-05	0.	0.	0.1776E-07	-0.1776E-07
95	0.6122E-04	0.1437E-04	0.	0.	-0.6421E-06	0.6421E-06
96	-0.6730E-05	0.2015E-05	0.	0.	0.7288E-06	-0.7288E-06
97	0.2549E-04	0.6752E-05	0.	0.	-0.1333E-06	0.1333E-06

333E-06

98	-0.6446E-06	0.1160E-05	0.	0.	0.1671E-07	-0.1671E-07
99	0.6193E-04	0.1458E-04	0.	0.	-0.5217E-06	0.5217E-06
100	-0.6047E-05	0.1612E-05	0.	0.	0.6383E-06	-0.6383E-06

NODE : 41 CUMAX= 660.1 DEAD LOAD RATIO= 1.000

NODE OF MAX. DISPLACEMENT AMONG BEAMS : 18 CUMAXBEAM= 659.6

- -

DEAD LOAD: ELEMENT	MOMENT A	MOMENT B	FORCE A	FORCE B
1	-0.7458E-04	3482.	48.30	-39.14
2	3482.	6235.	39.14	-29.98
3	6235.	8258.	29.98	-20.83
4	8258.	9459.	20.82	-12.54
5	9459.	0.1006E+05	12.55	-4.272
6	0.1006E+05	9982.	4.264	6.086
7	9982.	8969.	-6.080	16.43
8	8969.	6960.	-16.44	27.06
9	6960.	3971.	-27.06	37.68
10	3971.	-0.7291E-04	-37.68	48.30
11	0.1492E-03	3482.	48.30	-39.14

12	3482.	6234.	39.14	-29.98
13	6234.	8257.	29.98	-20.82
14	8257.	9457.	20.81	-12.53
15	9457.	0.1006E+05	12.56	-4.275
16	0.1006E+05	9981.	4.265	6.085
17	9980.	8967.	-6.073	16.42
18	8968.	6959.	-16.43	27.05
19	6959.	3970.	-27.05	37.68
20	3970.	0.1458E-03	-37.68	48.30
21	-0.7458E-04	3482.	48.30	-39.14
22	3482.	6235.	39.14	-29.98
23	6235.	8258.	29.98	-20.83
24	8258.	9459.	20.82	-12.54
25	9459.	0.1006E+05	12.55	-4.272
26	0.1006E+05	9982.	4.264	6.086
27	9982.	8969.	-6.080	16.43
28	8969.	6960.	-16.44	27.06
29	6960.	3971.	-27.06	37.68
30	3971.	-0.7291E-04	-37.68	48.30
31	-0.1627E-01	0.8133E-02	0.2033E-03	-0.2033E-03
32	0.8133E-02	-0.1627E-01	-0.2033E-03	0.2033E-03
33	-0.1557E-01	0.7434E-02	0.1917E-03	-0.1917E-03
34	0.7434E-02	-0.1557E-01	-0.1917E-03	0.1917E-03
35	-0.1494E-01	0.6797E-02	0.1811E-03	-0.1811E-03
36	0.6797E-02	-0.1494E-01	-0.1811E-03	0.1811E-03
37	-0.1443E-01	0.6275E-02	0.1725E-03	-0.1725E-03
38	0.6275E-02	-0.1443E-01	-0.1725E-03	0.1725E-03
39	-0.1416E-01	0.5973E-02	0.1677E-03	-0.1677E-03
40	0.5973E-02	-0.1416E-01	-0.1677E-03	0.1677E-03
41	-0.1394E-01	0.5784E-02	0.1644E-03	-0.1644E-03
42	0.5784E-02	-0.1394E-01	-0.1644E-03	0.1644E-03
43	-0.1398E-01	0.5818E-02	0.1650E-03	-0.1650E-03
44	0.5818E-02	-0.1398E-01	-0.1650E-03	0.1650E-03
45	-0.1420E-01	0.6079E-02	0.1690E-03	-0.1690E-03
46	0.6079E-02	-0.1420E-01	-0.1690E-03	0.1690E-03
47	-0.1473E-01	0.6616E-02	0.1779E-03	-0.1779E-03
48	0.6616E-02	-0.1473E-01	-0.1779E-03	0.1779E-03
49	-0.1543E-01	0.7317E-02	0.1895E-03	-0.1895E-03
50	0.7317E-02	-0.1543E-01	-0.1895E-03	0.1895E-03
51	-0.1621E-01	0.8106E-02	0.2027E-03	-0.2027E-03
52	0.8106E-02	-0.1621E-01	-0.2027E-03	0.2027E-03
53	-0.5528E-01	0.1801E-01	0.6091E-02	-0.6091E-02
54	0.4793	0.9981E-01	-0.5261E-02	0.5261E-02
55	-0.2086E-02	0.3734E-02	0.5389E-04	-0.5389E-04
56	0.1480	0.3371E-01	-0.8837E-03	0.8837E-03
57	0.5037	0.1201	-0.5256E-02	0.5256E-02
58	-0.7291E-01	0.1332E-02	0.6187E-02	-0.6187E-02
59	0.1593	0.3777E-01	-0.9365E-03	0.9365E-03
60	-0.7490E-03	-0.1771E-03	0.5295E-05	-0.5295E-05
61	0.5099	0.1217	-0.4276E-02	0.4276E-02
62	-0.6690E-01	-0.1536E-02	0.5447E-02	-0.5447E-02
63	0.2130	0.5018E-01	-0.1158E-02	0.1158E-02
64	0.6178E-04	-0.1296E-02	-0.1257E-04	0.1257E-04
65	-0.5486E-01	0.5652E-01	0.1326E-02	-0.1326E-02
66	0.1954	0.3368E-01	-0.1470E-02	0.1470E-02
67	-0.1012	0.8196E-01	0.5085E-02	-0.5085E-02

68	0.4126	0.1869E-01	-0.4941E-02	0.4941E-02
69	0.2110	0.3820E-01	-0.1562E-02	0.1562E-02
70	-0.5652E-01	0.5737E-01	0.1356E-02	-0.1356E-02
71	0.4382	0.2578E-01	-0.5124E-02	0.5124E-02
72	-0.1104	0.8153E-01	0.5330E-02	-0.5330E-02
73	0.2762	0.4360E-01	-0.1889E-02	0.1889E-02
74	-0.5831E-01	0.6059E-01	0.1416E-02	-0.1416E-02
75	0.4744	0.3539E-01	-0.4530E-02	0.4530E-02
76	-0.1061	0.7405E-01	0.5004E-02	-0.5004E-02
77	-0.1012	0.8196E-01	0.5085E-02	-0.5085E-02
78	0.4126	0.1869E-01	-0.4941E-02	0.4941E-02
79	-0.5486E-01	0.5652E-01	0.1326E-02	-0.1326E-02
80	0.1954	0.3368E-01	-0.1470E-02	0.1470E-02
81	0.4382	0.2578E-01	-0.5124E-02	0.5124E-02
82	-0.1104	0.8153E-01	0.5330E-02	-0.5330E-02
83	0.2110	0.3820E-01	-0.1562E-02	0.1562E-02
84	-0.5652E-01	0.5737E-01	0.1356E-02	-0.1356E-02
85	0.4744	0.3539E-01	-0.4530E-02	0.4530E-02
86	-0.1061	0.7405E-01	0.5004E-02	-0.5004E-02
87	0.2762	0.4360E-01	-0.1889E-02	0.1889E-02
88	-0.5831E-01	0.6059E-01	0.1416E-02	-0.1416E-02
89	-0.2086E-02	0.3734E-02	0.5389E-04	-0.5389E-04
90	0.1480	0.3371E-01	-0.8837E-03	0.8837E-03
91	-0.5528E-01	0.1801E-01	0.6091E-02	-0.6091E-02
92	0.4793	0.9981E-01	-0.5261E-02	0.5261E-02
93	0.1593	0.3777E-01	-0.9365E-03	0.9365E-03
94	-0.7490E-03	-0.1771E-03	0.5295E-05	-0.5295E-05
95	0.5037	0.1201	-0.5256E-02	0.5256E-02
96	-0.7291E-01	0.1332E-02	0.6187E-02	-0.6187E-02
97	0.2130	0.5018E-01	-0.1158E-02	0.1158E-02
98	0.6178E-04	-0.1296E-02	-0.1257E-04	0.1257E-04
99	0.5099	0.1217	-0.4276E-02	0.4276E-02
100	-0.6690E-01	-0.1536E-02	0.5447E-02	-0.5447E-02

***** END OF DEAD LOAD ANALYSIS *****

- -

***** INCREMENTAL ANALYSIS *****

- -

STAGE : 1

NODE	U(X)	V(Y)	W(Z)	Rot. X	Rot. Y	Rot. Z
1	0.	0.	0.6622E-49	0.3053E-03	-0.3247E-04	0.
2	0.	0.	0.7986E-49	0.3711E-03	0.2851E-18	0.
3	0.	0.	0.6622E-49	0.3053E-03	0.3247E-04	0.
4	0.	0.	0.2401E-01	0.2937E-03	-0.7320E-04	0.
5	0.	0.	0.2921E-01	0.3579E-03	0.2221E-17	0.
6	0.	0.	0.2401E-01	0.2937E-03	0.7320E-04	0.
7	0.	0.	0.4616E-01	0.2589E-03	-0.1344E-03	0.
8	0.	0.	0.5631E-01	0.3182E-03	0.3963E-17	0.

9	0.	0.	0.4616E-01	0.2589E-03	0.1344E-03	0.
10	0.	0.	0.6463E-01	0.2014E-03	-0.2145E-03	0.
11	0.	0.	0.7917E-01	0.2511E-03	0.4715E-17	0.
12	0.	0.	0.6463E-01	0.2014E-03	0.2145E-03	0.
13	0.	0.	0.7673E-01	0.1324E-03	-0.2657E-03	0.
14	0.	0.	0.9439E-01	0.1684E-03	0.4373E-17	0.
15	0.	0.	0.7673E-01	0.1324E-03	0.2657E-03	0.
16	0.	0.	0.8337E-01	0.5001E-04	-0.3550E-03	0.
17	0.	0.	0.1030	0.6674E-04	0.3348E-17	0.
18	0.	0.	0.8337E-01	0.5001E-04	0.3550E-03	0.
19	0.	0.	0.8296E-01	-0.5827E-04	-0.2974E-03	0.
20	0.	0.	0.1028	-0.6875E-04	0.1845E-17	0.
21	0.	0.	0.8296E-01	-0.5827E-04	0.2974E-03	0.
22	0.	0.	0.7305E-01	-0.1610E-03	-0.3331E-03	0.
23	0.	0.	0.9075E-01	-0.1985E-03	0.8200E-18	0.
24	0.	0.	0.7305E-01	-0.1610E-03	0.3331E-03	0.
25	0.	0.	0.5398E-01	-0.2463E-03	-0.1846E-03	0.
26	0.	0.	0.6709E-01	-0.3064E-03	0.2050E-18	0.
27	0.	0.	0.5398E-01	-0.2463E-03	0.1846E-03	0.
28	0.	0.	0.2859E-01	-0.2980E-03	-0.9685E-04	0.
29	0.	0.	0.3550E-01	-0.3702E-03	0.	0.
30	0.	0.	0.2859E-01	-0.2980E-03	0.9685E-04	0.
31	0.	0.	0.7319E-49	-0.3153E-03	-0.3946E-04	0.
32	0.	0.	0.9511E-49	-0.3913E-03	-0.4271E-20	0.
33	0.	0.	0.7319E-49	-0.3153E-03	0.3946E-04	0.

FCT= 0.6303 KA= 1 KB= 1 KBA= 0 KBB= 0

IIA= 16
IIB= 15

ELEMENT	CMA	CMB	SITAA	SITAB	CFA	CFB
1	2.979	537.6	0.	0.	6.713	-6.713
2	543.4	1072.	0.	0.	6.638	-6.638
3	1077.	1591.	0.	0.	6.444	-6.444
4	1595.	1946.	0.	0.	4.864	-4.864
5	1957.	2272.	0.	0.	4.387	-4.387
6	2277.	2170.	0.	0.	-1.186	1.186
7	2179.	2038.	0.	0.	-1.558	1.558
8	2037.	1378.	0.	0.	-7.139	7.139
9	1373.	696.0	0.	0.	-7.326	7.326
10	689.5	3.444	0.	0.	-7.428	7.428
11	-5.958	615.7	0.	0.	7.806	-7.806
12	604.1	1238.	0.	0.	7.956	-7.956
13	1227.	1891.	0.	0.	8.342	-8.342
14	1881.	2362.	0.	0.	6.673	-6.

673
15 2369. 2849. 0. 0. 6.673 -6.
673
16 2854. 2710. 0. 0. -1.607 1.
607
17 2725. 2602. 0. 0. -1.366 1.
366
18 2616. 1704. 0. 0. -9.870 9.
870
19 1715. 838.2 0. 0. -9.496 9.
496
20 851.3 -6.888 0. 0. -9.292 9.
292
21 2.979 537.6 0. 0. 6.713 -6.
713
22 543.4 1072. 0. 0. 6.638 -6.
638
23 1077. 1591. 0. 0. 6.444 -6.
444

24	1595.	1946.	0.	0.	4.864	-4.864
25	1957.	2272.	0.	0.	4.387	-4.387
26	2277.	2170.	0.	0.	-1.186	1.186
27	2179.	2038.	0.	0.	-1.558	1.558
28	2037.	1378.	0.	0.	-7.139	7.139
29	1373.	696.0	0.	0.	-7.326	7.326
30	689.5	3.444	0.	0.	-7.428	7.428
31	7.209	-3.604	0.	0.	-0.9011E-01	0.9011E-01
32	-3.604	7.209	0.	0.	0.9011E-01	-0.9011E-01
33	3.632	12.62	0.	0.	0.7489E-01	-0.7489E-01
34	12.62	3.632	0.	0.	-0.7489E-01	0.7489E-01
35	3.336	26.51	0.	0.	0.1931	-0.1931
36	26.51	3.336	0.	0.	-0.1931	0.1931
37	14.56	33.07	0.	0.	0.1543	-0.1543
38	33.07	14.56	0.	0.	-0.1543	0.1543
39	20.00	38.99	0.	0.	0.1583	-0.1583
40	38.99	20.00	0.	0.	-0.1583	0.1583
41	48.89	29.92	0.	0.	-0.1580	0.1580
42	29.92	48.89	0.	0.	0.1580	-0.1580
43	21.82	44.20	0.	0.	0.1866	-0.1866
44	44.20	21.82	0.	0.	-0.1866	0.1866
45	49.64	24.32	0.	0.	-0.2110	0.2110
46	24.32	49.64	0.	0.	0.2110	-0.2110
47	9.266	31.72	0.	0.	0.1872	-0.1872
48	31.72	9.266	0.	0.	-0.1872	0.1872
49	4.638	16.86	0.	0.	0.1019	-0.1019
50	16.86	4.638	0.	0.	-0.1019	0.1019
51	8.760	-4.380	0.	0.	-0.1095	0.1095
52	-4.380	8.760	0.	0.	0.1095	-0.1095
53	-11.19	3.436	0.	0.	1.215	-1.215
54	-0.1940	-0.1388	0.	0.	0.7653E-03	-0.7653E-03

653E-03

55	-1.107	1.980	0.	0.	0.2858E-01	-0.2
858E-01						
56	-0.7358	1.308	0.	0.	0.1580E-01	-0.1
580E-01						
57	-0.3652	-1.338	0.	0.	-0.1333E-01	0.1
333E-01						
58	-45.03	13.55	0.	0.	4.881	-4.
881						
59	-2.807	4.961	0.	0.	0.5985E-01	-0.5
985E-01						
60	-4.443	7.942	0.	0.	0.1147	-0.1
147						
61	-0.7880E-01	-1.216	0.	0.	-0.1253E-01	0.1
253E-01						
62	-45.76	12.89	0.	0.	4.887	-4.
887						
63	-2.429	4.285	0.	0.	0.4776E-01	-0.4
776E-01						
64	-4.624	8.278	0.	0.	0.1195	-0.1
195						
65	-7.527	10.20	0.	0.	0.2110	-0.2
110						
66	-3.444	4.061	0.	0.	0.6819E-01	-0.6
819E-01						
67	-20.33	14.25	0.	0.	0.9603	-0.9
603						
68	-2.356	-0.6771	0.	0.	0.2107E-01	-0.2
107E-01						
69	-13.47	15.60	0.	0.	0.2628	-0.2
628						
70	-30.36	41.07	0.	0.	0.8503	-0.8
503						
71	-8.795	-3.829	0.	0.	0.6170E-01	-0.6
170E-01						
72	-82.09	57.13	0.	0.	3.867	-3.
867						
73	-11.31	13.09	0.	0.	0.1982	-0.1
982						
74	-32.14	43.81	0.	0.	0.9042	-0.9
042						
75	-5.717	-3.941	0.	0.	0.1832E-01	-0.1
832E-01						
76	-84.20	56.97	0.	0.	3.921	-3.
921						
77	-20.33	14.25	0.	0.	0.9603	-0.9
603						
78	-2.356	-0.6771	0.	0.	0.2107E-01	-0.2
107E-01						
79	-7.527	10.20	0.	0.	0.2110	-0.2
110						

80	-3.444	4.061	0.	0.	0.6819E-01	-0.6819E-01
81	-8.795	-3.829	0.	0.	0.6170E-01	-0.6170E-01
82	-82.09	57.13	0.	0.	3.867	-3.867
83	-13.47	15.60	0.	0.	0.2628	-0.2628
84	-30.36	41.07	0.	0.	0.8503	-0.8503
85	-5.717	-3.941	0.	0.	0.1832E-01	-0.1832E-01
86	-84.20	56.97	0.	0.	3.921	-3.921
87	-11.31	13.09	0.	0.	0.1982	-0.1982
88	-32.14	43.81	0.	0.	0.9042	-0.9042
89	-1.107	1.980	0.	0.	0.2858E-01	-0.2858E-01
90	-0.7358	1.308	0.	0.	0.1580E-01	-0.1580E-01
91	-11.19	3.436	0.	0.	1.215	-1.215
92	-0.1940	-0.1388	0.	0.	0.7653E-03	-0.7653E-03
93	-2.807	4.961	0.	0.	0.5985E-01	-0.5985E-01
94	-4.443	7.942	0.	0.	0.1147	-0.1147
95	-0.3652	-1.338	0.	0.	-0.1333E-01	0.1333E-01
96	-45.03	13.55	0.	0.	4.881	-4.881
97	-2.429	4.285	0.	0.	0.4776E-01	-0.4776E-01
98	-4.624	8.278	0.	0.	0.1195	-0.1195
99	-0.7880E-01	-1.216	0.	0.	-0.1253E-01	0.1253E-01
100	-45.76	12.89	0.	0.	4.887	-4.887

NODE : 42 CUMAX= 538.5 FACTOR= 0.6303

NODE OF MAX. DISPLACEMENT AMONG BEAMS : 17 CUMAXBEAM= 0.1030

- -

STAGE : 2

NODE	U(X)	V(Y)	W(Z)	Rot. X	Rot. Y	Rot. Z
1	0.	0.	0.7214E-49	0.3326E-03	-0.3545E-04	0.
2	0.	0.	0.8670E-49	0.4043E-03	0.3909E-18	0.
3	0.	0.	0.7214E-49	0.3326E-03	0.3545E-04	0.
4	0.	0.	0.2615E-01	0.3199E-03	-0.7992E-04	0.
5	0.	0.	0.3183E-01	0.3901E-03	0.3083E-17	0.
6	0.	0.	0.2615E-01	0.3199E-03	0.7992E-04	0.
7	0.	0.	0.5028E-01	0.2820E-03	-0.1469E-03	0.

8	0.	0.	0.6137E-01	0.3470E-03	0.5625E-17	0.
9	0.	0.	0.5028E-01	0.2820E-03	0.1469E-03	0.
10	0.	0.	0.7041E-01	0.2194E-03	-0.2345E-03	0.
11	0.	0.	0.8631E-01	0.2741E-03	0.6999E-17	0.
12	0.	0.	0.7041E-01	0.2194E-03	0.2345E-03	0.
13	0.	0.	0.8358E-01	0.1442E-03	-0.2908E-03	0.
14	0.	0.	0.1029	0.1843E-03	0.7006E-17	0.
15	0.	0.	0.8358E-01	0.1442E-03	0.2908E-03	0.
16	0.	0.	0.9082E-01	0.5446E-04	-0.3885E-03	0.
17	0.	0.	0.1124	0.7265E-04	0.6113E-17	0.
18	0.	0.	0.9082E-01	0.5446E-04	0.3885E-03	0.
19	0.	0.	0.9037E-01	-0.6350E-04	-0.3251E-03	0.
20	0.	0.	0.1121	-0.7580E-04	0.4502E-17	0.
21	0.	0.	0.9037E-01	-0.6350E-04	0.3251E-03	0.
22	0.	0.	0.7956E-01	-0.1753E-03	-0.3632E-03	0.
23	0.	0.	0.9888E-01	-0.2167E-03	0.3092E-17	0.

24	0.	0.	0.7956E-01	-0.1753E-03	0.3632E-03	0.
25	0.	0.	0.5880E-01	-0.2683E-03	-0.2012E-03	0.
26	0.	0.	0.7308E-01	-0.3340E-03	0.1843E-17	0.
27	0.	0.	0.5880E-01	-0.2683E-03	0.2012E-03	0.
28	0.	0.	0.3114E-01	-0.3246E-03	-0.1055E-03	0.
29	0.	0.	0.3866E-01	-0.4033E-03	0.8384E-18	0.
30	0.	0.	0.3114E-01	-0.3246E-03	0.1055E-03	0.
31	0.	0.	0.7970E-49	-0.3434E-03	-0.4298E-04	0.
32	0.	0.	0.1033E-48	-0.4262E-03	0.7874E-19	0.
33	0.	0.	0.7970E-49	-0.3434E-03	0.4298E-04	0.

FCT= 0.5543E-01 KA= 1 KB= 1 KBA= 0 KBB= 0

IIA= 17
IIB= 16

ELEMENT CFB	CMA	CMB	SITAA	SITAB	CFA	
1	3.250	585.6	0.	0.	7.312	-7.312
2	592.0	1168.	0.	0.	7.231	-7.231
3	1174.	1733.	0.	0.	7.020	-7.020
4	1738.	2120.	0.	0.	5.299	-5.299
5	2132.	2476.	0.	0.	4.777	-4.777
6	2480.	2364.	0.	0.	-1.295	1.295
7	2373.	2220.	0.	0.	-1.702	1.702
8	2219.	1501.	0.	0.	-7.775	7.775
9	1495.	758.0	0.	0.	-7.978	7.978
10	750.8	3.749	0.	0.	-8.089	8.089
11	-6.500	668.3	0.	0.	8.474	-8.474
12	655.6	1343.	0.	0.	8.637	-8.637
13	1332.	2053.	0.	0.	9.058	-9.058
14	2042.	2564.	0.	0.	7.245	-7.245
15	2571.	3093.	0.	0.1332E-05	7.252	-7.252
16	3099.	2942.	0.1334E-05	0.	-1.741	1.741
17	2959.	2826.	0.	0.	-1.473	1.473
18	2842.	1851.	0.	0.	-10.72	10.72
19	1863.	910.6	0.	0.	-10.32	10.32
20	924.8	-7.499	0.	0.	-10.09	10.09
21	3.250	585.6	0.	0.	7.312	-7.312

22	592.0	1168.	0.	0.	7.231	-7.231
23	1174.	1733.	0.	0.	7.020	-7.020
24	1738.	2120.	0.	0.	5.299	-5.299
25	2132.	2476.	0.	0.	4.777	-4.777
26	2480.	2364.	0.	0.	-1.295	1.295
27	2373.	2220.	0.	0.	-1.702	1.702
28	2219.	1501.	0.	0.	-7.775	7.775
29	1495.	758.0	0.	0.	-7.978	7.978
30	750.8	3.749	0.	0.	-8.089	8.089
31	7.871	-3.935	0.	0.	-0.9838E-01	0.9838E-01
32	-3.935	7.871	0.	0.	0.9838E-01	-0.9838E-01
33	3.981	13.76	0.	0.	0.8151E-01	-0.8151E-01
34	13.76	3.981	0.	0.	-0.8151E-01	0.8151E-01
35	3.662	28.95	0.	0.	0.2107	-0.2107
36	28.95	3.662	0.	0.	-0.2107	0.2107
37	15.87	36.20	0.	0.	0.1694	-0.1694
38	36.20	15.87	0.	0.	-0.1694	0.1694

39	21.75	42.82	0.	0.	0.1756	-0.1
756						
40	42.82	21.75	0.	0.	-0.1756	0.1
756						
41	52.96	33.29	0.	0.	-0.1640	0.1
640						
42	33.29	52.96	0.	0.	0.1640	-0.1
640						
43	23.74	48.43	0.	0.	0.2057	-0.2
057						
44	48.43	23.74	0.	0.	-0.2057	0.2
057						
45	54.04	26.60	0.	0.	-0.2287	0.2
287						
46	26.60	54.04	0.	0.	0.2287	-0.2
287						
47	10.12	34.56	0.	0.	0.2037	-0.2
037						
48	34.56	10.12	0.	0.	-0.2037	0.2
037						
49	5.069	18.35	0.	0.	0.1107	-0.1
107						
50	18.35	5.069	0.	0.	-0.1107	0.1
107						
51	9.542	-4.771	0.	0.	-0.1193	0.1
193						
52	-4.771	9.542	0.	0.	0.1193	-0.1
193						
53	-12.17	3.738	0.	0.	1.322	-1.
322						
54	-0.2111	-0.1511	0.	0.	0.8326E-03	-0.8
326E-03						
55	-1.205	2.154	0.	0.	0.3109E-01	-0.3
109E-01						
56	-0.8006	1.423	0.	0.	0.1719E-01	-0.1
719E-01						
57	-0.3974	-1.456	0.	0.	-0.1451E-01	0.1
451E-01						
58	-48.99	14.74	0.	0.	5.310	-5.
310						
59	-3.054	5.397	0.	0.	0.6511E-01	-0.6
511E-01						
60	-4.834	8.641	0.	0.	0.1248	-0.1
248						
61	-0.8573E-01	-1.323	0.	0.	-0.1363E-01	0.1
363E-01						
62	-49.78	14.02	0.	0.	5.317	-5.
317						
63	-2.642	4.662	0.	0.	0.5196E-01	-0.5
196E-01						
64	-5.031	9.006	0.	0.	0.1300	-0.1
300						
65	-8.189	11.10	0.	0.	0.2296	-0.2
296						
66	-3.747	4.419	0.	0.	0.7419E-01	-0.7
419E-01						
67	-22.12	15.50	0.	0.	1.045	-1.
045						
68	-2.564	-0.7366	0.	0.	0.2292E-01	-0.2
292E-01						
69	-14.65	16.97	0.	0.	0.2859	-0.2

859						
70	-33.03	44.68	0.	0.	0.9251	-0.9
251						
71	-9.568	-4.166	0.	0.	0.6713E-01	-0.6
713E-01						
72	-89.31	62.16	0.	0.	4.207	-4.
207						
73	-12.30	14.24	0.	0.	0.2156	-0.2
156						
74	-34.97	47.67	0.	0.	0.9837	-0.9
837						
75	-6.219	-4.288	0.	0.	0.1993E-01	-0.1
993E-01						
76	-91.60	61.99	0.	0.	4.266	-4.
266						
77	-22.12	15.50	0.	0.	1.045	-1.
045						
78	-2.564	-0.7366	0.	0.	0.2292E-01	-0.2
292E-01						
79	-8.189	11.10	0.	0.	0.2296	-0.2
296						
80	-3.747	4.419	0.	0.	0.7419E-01	-0.7
419E-01						
81	-9.568	-4.166	0.	0.	0.6713E-01	-0.6
713E-01						
82	-89.31	62.16	0.	0.	4.207	-4.
207						
83	-14.65	16.97	0.	0.	0.2859	-0.2
859						
84	-33.03	44.68	0.	0.	0.9251	-0.9
251						
85	-6.219	-4.288	0.	0.	0.1993E-01	-0.1
993E-01						
86	-91.60	61.99	0.	0.	4.266	-4.
266						
87	-12.30	14.24	0.	0.	0.2156	-0.2
156						
88	-34.97	47.67	0.	0.	0.9837	-0.9
837						
89	-1.205	2.154	0.	0.	0.3109E-01	-0.3
109E-01						
90	-0.8006	1.423	0.	0.	0.1719E-01	-0.1
719E-01						
91	-12.17	3.738	0.	0.	1.322	-1.
322						
92	-0.2111	-0.1511	0.	0.	0.8326E-03	-0.8
326E-03						
93	-3.054	5.397	0.	0.	0.6511E-01	-0.6
511E-01						
94	-4.834	8.641	0.	0.	0.1248	-0.1
248						

95	-0.3974	-1.456	0.	0.	-0.1451E-01	0.1451E-01
96	-48.99	14.74	0.	0.	5.310	-5.310
97	-2.642	4.662	0.	0.	0.5196E-01	-0.5196E-01
98	-5.031	9.006	0.	0.	0.1300	-0.1300
99	-0.8573E-01	-1.323	0.	0.	-0.1363E-01	0.1363E-01
100	-49.78	14.02	0.	0.	5.317	-5.317

NODE : 42 CUMAX= 585.9 FACTOR= 0.6857

NODE OF MAX. DISPLACEMENT AMONG BEAMS : 17 CUMAXBEAM= 0.1124

IR= 15 JJK1= 0 JJK2= 1 RKT1= 0. RKT2= 0.1833E+09
IR= 16 JJK1= 1 JJK2= 0 RKT1= 0.1833E+09 RKT2= 0.

SECTION F.6

PROGRAM LISTING

The listing of program NONBAN is given below. The listing provided includes comment cards which explain the program logic and define the variables used.

```
c       ****************************************************************
c
c                              PROGRAM NONBAN
c
c       This program performs the nonlinear analysis of
c       multi-girder bridge systems using a grillage analysis.
c       The program accounts for the nonlinear behavior of beams
c       by considering their Moment versus Plastic Hinge Rotation
c       Curves. (M-Q curves)
c       Each M-Q curve should have a total of four linear segments.
c       Each linear segment of M-Q will have a different slope.
c       The term "subhinge" is used to refer to the point at which
c       the slope of M-Q changes.
c       The program uses an incremental analysis procedure.
c       It performs an elastic analysis and checks each beam to
c       find the load increment at which a new subhinge is formed.
c       When a new subhinge forms at one end of a beam element,
c       the stiffness matrix of this beam element is modified to add
c       a rotational spring on that end.
c       The stiffness of the rotational spring is obtained from the M-Q curve.
c       A linear elastic analysis is then performed for this step alone
c       and its results are added to the results of the previous steps.
c       The analysis is continued until either a maximum total rotation
c       criteria is met or when a very large displacement is obtained.
c       The program can perform either a linear elastic or a nonlinear
c       incremental analysis.
c       Check the manual of operations for information on input
c       data format and step-by-step procedure.
c       This program is divided into 50 blocks (labelled 0 to 49) and
c       several subroutines.
c       A description of each block and subroutine is given in this listing.
c       The variables used in the Main program are also defined in this listing
c
c       This program includes sections for use in connection with plate
c       elements, please ignore these sections as the use of plate
c       elements has been discontinued at an early stage of this project.
c
c       ****************************************************************
c
        PROGRAM NONBAN97
c
c       ****************************************************************
c       Block 0
c       Define variable types, set up dimensions and data common blocks
c
c       ****************************************************************
c
        IMPLICIT REAL*8 (A-H,O-Z)
        CHARACTER*64 TITLE,X$
        CHARACTER*16 FNAMEI,FNAMEO
        COMMON/CONT/ICONT,NBEXYC(100),IBJC(600)
        COMMON/FUN0/KGIRD
        COMMON/FUN00/PFORCE,PECCEN,FS4
        COMMON/FUN1/SIZ(50),RMPM5(50)
        COMMON/FUN2/FJGD,RIZGD,RIYGD,RJGD,SIZGD,EBEAMG,GBEAMG,
     &  ASYGD,ASZGD,RMPPGD(5),RKTPGD(5),RLPPGD,SITMAXG
```

```
      COMMON/F1/RKK(300000),P(4000),X(600),Y(600),Z(600),
     *  PX(600),PY(600),PZ(600),RMX(600),RMY(600),RMZ(600)
      COMMON/F2/N,N1,IRG,IRGJ,ISG,ISGJ,NBE,IBE,MP,I1,IR,IS,
     *  LQG,IOV,IG
      COMMON/F3/ER,GR,ES,GS,RMU
      COMMON/F4/IAD(4000),IBB(600),IBBX(6)
      COMMON/F5/RUX,RUY,RU1,RUXY
      COMMON/R1/IA(600),IB(600),IRR(12)
      COMMON/S1/IAS(600),IBS(600),ICS(600),IDS(600),IRR2(24)
      COMMON/FIJ/FJ(50),RIZ(50),RIY(50),RJ(50),RKTP(5,50),
     *  RKTN(5,50),IRKT(600)
      COMMON/NFIJ/NRKT
      COMMON/RMP/RMPP(5,50),RMPN(5,50),RLPP(50),SITMAXP(50),
     *  RLPN(50),SITMAXN(50)
      COMMON/J1/RKK1J(12,12),RLM(12,12),RLM1(12,12),RLM2(12,12),
     *  ASY(600),ASZ(600),RKK1J0(12,12)
      COMMON/J2/IAJ(600),IBJ(600),IIK(600)
      COMMON/J3/JJK1(600),JJK2(600)
      COMMON/J4/RKT(600),RKT1(600),RKT2(600)
      COMMON/J5/RMA(600),RMB(600)
      COMMON/J6/CA(600),SA(600)
      COMMON/J7/CUMAX,CFCT,UMAX,FCT,KA,KB,IRGJ1,LDY
      COMMON/J8/RMPA(600),RMPB(600),CMA(600),CMB(600),RKTA(600),
     *  RKTB(600),RMAD(600),RMBD(600)
      COMMON/J9/IHA(600),IHB(600),IIA(600),IIB(600)
      COMMON/J10/RMA0(600),RMB0(600)

      COMMON/SJ1/IASJ(200),IBSJ(200),ICSJ(200),IDSJ(200)
      COMMON/SJ2/TJ(200),RKKSJ(24,24)
      COMMON/SJ3/U(24),U1(24),U2(24),SP(3,12),UL(12,600)
      COMMON/SJ4/RKKX(12,12),RKKY(12,12),RKK3(12,12),RKKXY(12,12)
     *  ,RRL(12,12)
      COMMON/N1/EBAR(600),GSHEAR(600),EBEAM(50),GBEAM(50),
     *  EBEND(600)
      COMMON/N2/EIG(600),UU(4000),PP(4000)
      COMMON/N3/SIG(600),UUP(12),UUP1(12)
      COMMON/Q2/UUU(4000),SITA1(600),SITA2(600),UUUD(4000),SITAD1(600),
     *SITAD2(600)
      COMMON/Q3/CUMAX0,CFCT0
      COMMON/Q4/IDK(600)
      COMMON/RP/RLMD(6,6),RLMD1(6,6),P0X(6),P1X(6)
      COMMON/PR/IPRINT(600)
      COMMON/DSXY/NDSY,NDSX,DSY(100),IRKTX(100),DSX(20),
     *  IRKTY(20),IDKY(20),IDKX(100)
      COMMON/IDLOD/NDLDC,NDLDU,NLOAD,NDLDU0(2),IPDU1(10),IPDU2(10),
     * IPDC1(100)
      COMMON/VLOD/PDU0(10),PDC0(600,6),PLC0(600,6)
      COMMON/NPPBE/NPPXY(100),NBEXY(100)
      COMMON /NN1/ FMA(600),FMB(600)


      COMMON/RV/RV(5,50),RBET(5,50),IRBT(600)
      COMMON/JB3/JJB1(600),JJB2(600)
      COMMON/JB4/RBT(600),RBT1(600),RBT2(600)
      COMMON/JB5/RFA(600),RFB(600)
      COMMON/JB7/KBA,KBB
```

```
      COMMON/JB8/RFPA(600),RFPB(600),CFA(600),CFB(600),RBTA(600),
     *  RBTB(600),RFAD(600),RFBD(600)
      COMMON/JB9/IHBA(600),IHBB(600),IIBA(600),IIBB(600)
      COMMON/JB10/RFA0(600),RFB0(600)
      COMMON/JB11/ FFA(600),FFB(600)

      DIMENSION FJC(4),RIZC(4),RIYC(4),RJC(4),SIZC(4),EBEAMC(4),
     *  GBEAMC(4),ASYC(4),ASZC(4),RMPPC(5,4),RKTPC(5,4),RLPPC(4),
     *  SITMAXPC(4)

      REAL PDUC(10),IRKTC(600)

c
c     ****************************************************************
c     Block 1
c     Define names for input and output files
c
c     ****************************************************************
c
C     WRITE(*,198)
198   FORMAT(//,' Name of Input Data File : NONBAN.DAT')
c     READ(*,196) FNAMEI
C     WRITE(*,197)
197   FORMAT(/,' Name of Output Data File : NONBAN.OUT')
c     READ(*,196) FNAMEO
196   FORMAT(A16)
c     WRITE(*,195)
195   FORMAT(/,' The Name of File Which Contains Plots (do not use
     *  prfam2.plo as name)')
c     READ(*,196) FNAMEF
c
c     ****************************************************************
c     Block 2
c     Open input and output data files
c
c     ****************************************************************
c
      OPEN(1,FILE='NONBAN9.DAT',STATUS='OLD')
      OPEN(7,FILE='NONBAN9.OUT',STATUS='UNKNOWN')
      OPEN(8,FILE='prfam12.plo',STATUS='UNKNOWN')
      OPEN(10,FILE='figpvd12.dat',STATUS='UNKNOWN')
      OPEN(12,FILE='figpvd12bm.dat',STATUS='UNKNOWN')

c     OPEN(1,STATUS='OLD')
c     OPEN(7,STATUS='UNKNOWN')
c     OPEN(8, STATUS='UNKNOWN')
c     OPEN(10, STATUS='UNKNOWN')
c     OPEN(12, STATUS='UNKNOWN')

c
C*********************************************************************
C     File: FNAMEI --- input data file;                              *
C     File: FNAMEO --- output file;                                  *
C     File: prfam12.plo--- excutable file for plotting curve;        *
C                  this file is to be used only in conjunction with  *
C                  GNUPLOT graphic package in DECterm Work Station   *
```

```
C       File: figpvd12.dat--- data file containing Max. displacement    *
C                             vs. applied load for whole bridge system; *
C       File: figpvd12bm.dat --- data file containing Max. displacement *
C                             of main girder elements vs. applied load; *
C*************************************************************************
c
c
c       ***************************************************************
c
c               This next section sets up the input data
c
c       ***************************************************************
c
c       ***************************************************************
c       Block 3
c       Read Job title
c
c       ***************************************************************
        READ(1,199)TITLE
199     FORMAT(A64)
        WRITE(7,4)TITLE
4       FORMAT(//,5X,A64,/)
c
c       ***************************************************************
c       Block 4
c       set up the automatic mesh generation option
c
c       if NAUTXY is equal to 0, then enter all data(system geometry
c                and applied load) through input file
c       if NAUTXY is greater than 0, then use mesh generation option
c       if NAUTXY is greater than 1, then use load generation option also
C       Subroutine AUTOXY is a subroutine used for automatic mesh generation
c       ***************************************************************
c
        READ(1,*) NAUTXY

        IF(NAUTXY.GE.1) THEN
        CALL AUTOXY(NAUTXY)
        IF(NAUTXY.EQ.-1)GOTO 995
        IF(NAUTXY.EQ.1) GOTO 193
        IF(NAUTXY.GT.1) GOTO 6500
        END IF

C*************************************************************************
C       NAUTXY  : =-1   Error in input data was detected go to 995 for output;
C               : =0    Do not use auto-generation of mesh at all;
C               : =1    Generate geometry of system only;
C               : >1    Generate all including loads;
C*************************************************************************
c
c       ***************************************************************
c       Block 5
c       read general system model information
c
c       ***************************************************************
c
```

```
      READ(1,199) X$
      READ(1,199) X$
      READ(1,*,ERR=995)LDY, RMU, IG
      READ(1,*,ERR=995)N, IRGJ,IRGJ1
      IF(LDY.LE.3)LDYY=LDY
      IF(LDY.GT.3)LDYY=3

      IF(LDY.EQ.7)THEN
        WRITE(*,*)
        WRITE(*,*)
        WRITE(*,*)"WE ARE NOW CALCULATING LF1"
        WRITE(*,*)"NOTE: WE ASSUME ALL THE GIRDERS HAVE THE SAME DEAD LOAD"
        WRITE(*,*)"PLEASE INPUT THE ANALYZING OPTION OF YOUR NONBAN9.DAT"
        READ(*,*)LDY
        LF1LF1=1
      END IF

      IF(LDY.EQ.4.OR.LDY.EQ.5)THEN
              READ(1,*,ERR=995)KGIRD
      END IF

      IF(LDY.EQ.6)THEN
              READ(1,*, ERR=995) KGIRD,PFORCE,PECCEN,FS4
              FS4=7.5*SQRT(FS4*1000)/1000
      END IF


C     ***************************************************************
C     X$       :       Title of this block of input data
C     N        :       Total number of nodes
C     IRGJ     :       Total number of beam elements
C     IRGJ1    :       Number of main girder elements
C                      i.e. the ones to be checked for maximum displacement
C                           and for maximum rotations
C     RMU      :       Poisson's ratio
C     IG       :       = 0  do not include shear deformations
C              :       = 1  include shear deformations
C     LDY      :       = 1  regular output of deformations and moments;
C              :       = 2  Perform elastic solution only.
C              :       = 3  prints everything for tracing program ( showing
C                           the status after each iteration like hinge
C                           location, type, cumulative deflection and
C                           load factor etc.)
C     KGIRD    :       Number of longintudinal beam element.
C     PFORCE   :       the amount of prestressed force acting on the girder's
C                      section.
C     PECCEN :         Eccentricity of prestressed force.
C     FS4      :       The allowing twnsion stress of the material below the
C                      prestressed point.
C     ***************************************************************
C
c     ***************************************************************
c     Block 6
c     Enter beam properties & beam type information
c
c     ***************************************************************
```

```
          IF(LDY.LE.3)GOTO 1663
          READ(1,199)X$
          READ(1,199)X$
          READ(1,*,ERR=995)FJGD,RIZGD,RIYGD,RJGD,SIZGD,EBEAMG,GBEAMG,ASYGD,
         &  ASZGD
          READ(1,*,ERR=995)(RMPPGD(I),I=1,4)
          READ(1,*,ERR=995)(RKTPGD(I),I=1,4)
          READ(1,*,ERR=995)RLPPGD,SITMAXG

1663      READ(1,199) X$
          READ(1,199) X$
          READ(1,*,ERR=995) NRKT
          DO 3020 I=1,NRKT
          READ(1,*,ERR=995) FJ(I),RIZ(I),RIY(I),RJ(I),SIZ(I),EBEAM(I),
         *  GBEAM(I),ASY(I),ASZ(I)

c         ****************************************************************
C                 If only elastic analysis is requested do not enter
C                 properties of M-Q curves
c         ****************************************************************

          IF(LDY.EQ.2) GOTO 3020
          READ(1,*,ERR=995) (RMPP(J,I),J=1,4)
          READ(1,*,ERR=995) (RKTP(J,I),J=1,4)
          READ(1,*,ERR=995) RLPP(I),SITMAXP(I)
          READ(1,*,ERR=995) (RMPN(J,I),J=1,4)
          READ(1,*,ERR=995) (RKTN(J,I),J=1,4)
          READ(1,*,ERR=995) RLPN(I),SITMAXN(I)
                  READ(1,*,ERR=995) (RV(J,I),J=1,4)
                  READ(1,*,ERR=995) (RBET(J,I),J=1,4)
3020      CONTINUE

          IF(LDY.LE.3)THEN
              FJGD=FJ(1)
              RIZGD=RIZ(1)
              RIYGD=RIY(1)
              RJGD=RJ(1)
              SIZGD=SIZ(1)
              EBEAMG=EBEAM(1)
              GBEAMG=GBEAM(1)
              ASYGD=ASY(1)
              ASZGD=ASZ(1)
              DO 3021 I=1,4
              RMPPGD(I)=RMPP(I,1)
              RKTPGD(I)=RKTP(I,1)
3021          CONTINUE
              RLPPGD=RLPP(1)
              SITMAXG=SITMAXP(1)
          END IF

C         ****************************************************************
C         X$          : Title of this block of input data;
C         NRKT        : Total number of different cross sections;
C         FJ(I)       : Area of cross section for beam type I;
C         RIZ(I)      : moment of inertia about Z-axis i.e. major axis;
```

```
C       RIY(I)     : moment of inertia about Y-axis i.e. minor axis;
C       RJ(I)      : torsional inertia;
C       EBEAM(I)   : Young's modulus for beam elements;
C       RMPP(J,I)  : Mp at each sub-hinge point for POSITIVE moment
C                  : of beam type I;
C       RMPN(J,I)  : Mp at each sub-hinge point for NEGATIVE moment
C                  : of beam type I;
C       RKTP(J,I)  : Slopes of M vs. Plastic Rotation for each segment
C                  : for POSITIVE moment in beam type I;
C       RKTN(J,I)  : Slopes of M vs. Plastic Rotation for each segment
C                  : for NEGATIVE moment in beam type I;
C       RLPP(I)    : Length of plastic hinge for POSITIVE moment
C                  : in beam type I;
C       RLPN(I)    : Length of plastic hinge for NEGATIVE moment
C                  : in beam type I;
C       SITMAXP(I): Limit of Plastic hinge rotation for POSITIVE moment
C                  : in beam type I;
C       SITMAXN(I): Limit of Plastic hinge rotation for NEGATIVE moment
C                  : in beam type I;
C                       These are the maximum possible rotations that
C                       the beams can sustain.
c       ***************************************************************

C       ***************************************************************
c       If LDY=2 then only linear elastic analysis is requested
c       and there is no need to perform the adjustments on M-Q that follow
c       ***************************************************************

        IF(LDY.NE.2) THEN
        DO 3022 I=1,NRKT
        DO 3024 J=1,4
        RKTP(J,I)=RKTP(J,I)/RLPP(I)
        RKTN(J,I)=RKTN(J,I)/RLPN(I)

C*****************************************************************************
C       If for concrete bridges we enter moment versus curvature curves
C       we correct these curves to transform them to moment versus rotation
C       by dividing the ordinates by the length of the plastic hinge
C
C       Each moment versus rotation curve has 4 segments
C       The counter J defines the segment under consideration
C       The counter I defines the beam under consideration
C
C       The program cannot allow zero slopes so we substitute
C       a zero slope by a small slope equal to 0.0001
C
C       if only elastic analysis will be performed, there is no need
C       to make the data adjustment
C*****************************************************************************

        IF(RKTP(J,I).EQ.0.0) RKTP(J,I)=1.0E-9
        IF(RKTN(J,I).EQ.0.0) RKTN(J,I)=1.0E-9

        IF(RBET(J,I).EQ.0.0) RBET(J,I)=1.0E-9

C
```

```
3024     CONTINUE
3022     CONTINUE

         DO 9550 I=1,4
         RKTPGD(I)=RKTPGD(I)/RLPPGD
         IF(RKTPGD(I).EQ.0.0)RKTPGD(I)=1.0E-9
9550     CONTINUE
         X1=(RMPPGD(2)-RMPPGD(1))/RKTPGD(1)+(RMPPGD(3)-RMPPGD(2))/RKTPGD(2)
     &   +(RMPPGD(4)-RMPPGD(3))/RKTPGD(3)
         RMPPGD(5)=RMPPGD(4)+RKTPGD(4)*(SITMAXG-X1)
         DO 9545 I=1,NRKT
         X1=(RMPP(2,I)-RMPP(1,I))/RKTP(1,I)+(RMPP(3,I)-RMPP(2,I))/RKTP(2,I)
     &   +(RMPP(4,I)-RMPP(3,I))/RKTP(3,I)
         RMPM5(I)=RMPP(4,I)+RKTP(4,I)*(SITMAXP(I)-X1)
9545     CONTINUE

         END IF

         N1=6*N

c        WRITE(7,*) ' NUMBER OF NODES',N
c        WRITE(7,*) ' NUMBER OF D.O.F',N1
C
c        ****************************************************************
c        There are 6 D.O.F. per node
c        N is the total number of nodes
c        N1 is the number of degrees of freedom
c        ****************************************************************
c
c        ****************************************************************
c        Block 7
c        Read Node coordinates
c
c        ****************************************************************
c
         READ(1,199) X$
         READ(1,199) X$
         READ(1,*,ERR=995)(X(I),I=1,N)

         READ(1,*,ERR=995)(Y(I),I=1,N)

         READ(1,*,ERR=995)(Z(I),I=1,N)

C        ****************************************************************
C        X$              : Title for this block of input data;
C        X(I),Y(I),Z(I)  : X,Y,Z coordinates of all nodes.
C        ****************************************************************
c
c        ****************************************************************
c        Block 8
c        Read beam connectivity data
c
c        ****************************************************************
c        Read this data only if automatic mesh generation is not selected
c        ****************************************************************
```

```
c
      IF(NAUTXY.LT.1) THEN
      IF(IRGJ.EQ.0) GOTO 11
      READ(1,199) X$
      READ(1,199) X$
      READ(1,*,ERR=995)(IAJ(IR),IR=1,IRGJ)
      READ(1,*,ERR=995)(IBJ(IR),IR=1,IRGJ)
      END IF

C     ****************************************************************
C     X$      : Title of this block of input data;
C     IAJ(I)  : Node ID number at end A of element I;
C     IBJ(I)  : Node ID number at end B of element I;
C     ****************************************************************
C
C     ****************************************************************
C     Block 9
C     Read beam type identification data
C
C     ****************************************************************

193   READ(1,*,ERR=995)(IRKT(IR),IR=1,IRGJ)
      DO 11993 IR=1,IRGJ
      IRBT(IR)=IRKT(IR)
11993 CONTINUE
C     READ(1,*,ERR=995)(IDK(IR),IR=1,IRGJ)

C     ****************************************************************
C     IRKT(I) : Section ID number of element I;
C     IDK(I)  : 0-- compact section for steel section only;
C             : 1-- noncompact section for steel section only;
C             : 0-- for concrete sections
C      The variable IDK is no longer needed so you should always enter 0
C     ****************************************************************
C
C     ****************************************************************
C     Block 10
C     Find length and direction cosines for each beam element
C     And give warning when an element has zero length.
C     ****************************************************************
C

      DO 200 IR=1,IRGJ
      DX=X(IBJ(IR))-X(IAJ(IR))
      DY=Y(IBJ(IR))-Y(IAJ(IR))
      DZ=Z(IBJ(IR))-Z(IAJ(IR))
      RL1=DSQRT(DX*DX+DY*DY+DZ*DZ)
      IF(RL1.LT.1.0E-20) THEN
      WRITE(*,202) IR
202   FORMAT(' THE LENGTH OF BEAM ELEMENT ',I5,' IS ZERO')
      GOTO 995
      END IF
      CA(IR)=DX/RL1
      SA(IR)=DY/RL1
200   CONTINUE
```

```
C       ****************************************************************
C       DX,DY,DZ: Coordinates of elements in x, y and z directions
C       RL1(I)   : Length if element I
C       CA(I)    : cosine of angle between the element and X axis.
C       SA(I)    :   sine of angle between the element and X axis.
C       ****************************************************************
c
c       ****************************************************************
c       Block 11
c       Read and set up shear deformation data
c       read this data only if IG =1 (include shear deformations option)
c
c       ****************************************************************

C       DO 85 I=1,NRKT
C85      GBEAM(I)=EBEAM(I)/2.0/(1.0+RMU)

C       ****************************************************************
C       ASY(I),ASZ(I)    : shear areas in Y & Z directions
C       GBEAM : shear modulus for every beam element type
C       ****************************************************************

c       ****************************************************************
c       Block 12
c       Read plate information data.
c       This part is not being used in this version of program.
c       Therefore, enter 0 for the variable ISGJ which gives the
c       number of plate elements.
c
c       ****************************************************************
c

11      IF(NAUTXY.LT.1) THEN
        READ(1,199) X$
        READ(1,199) X$
        READ(1,*,ERR=995) ISGJ
        IF(ISGJ.EQ.0) GOTO 111
c
        READ(1,*,ERR=995) ES
        GS=ES/2.0/(1.0+RMU)
        READ(1,*,ERR=995) RUX,RUY,RU1,RUXY
        READ(1,*,ERR=995)(TJ(I),I=1,ISGJ)
        READ(1,*,ERR=995)(IASJ(I),I=1,ISGJ)
        READ(1,*,ERR=995)(IBSJ(I),I=1,ISGJ)
        READ(1,*,ERR=995)(ICSJ(I),I=1,ISGJ)
        READ(1,*,ERR=995)(IDSJ(I),I=1,ISGJ)

C       ****************************************************************
C       This data is for all plate elements
C       ISGJ     :       Total plate elements
C       ES       :       Young's modulus for plate elements
C       TJ(I)    :       plate thickness
C       IASJ(I),IBSJ(I),ICSJ(I),IDSJ(I) : node numbers  A_____ C
c                                                        ]      ]
c               use this sequence for nodes ---->        ]      ]
c                                                       B]_____]D
```

```
C       ****************************************************************

        DO 86 I=1,ISGJ
86      EBEND(I)=ES
        END IF

C
C       ****************************************************************
C       Block 13
C       Read boundary condition data and set up corresponding
C       degree of freedom numbers.
C
C       ****************************************************************
C

111     READ(1,199) X$
        READ(1,199) X$
        READ(1,*,ERR=995) NBE
        IBE=0
        DO 117 I=1,NBE
        READ(1,*,ERR=995) ITEMP,(IBBX(J),J=1,6)
        NBEXY(I)=ITEMP
        DO 116 J=1,6
        IF(IBBX(J).EQ.1) THEN
        IBE=IBE+1
        IBB(IBE)=6*ITEMP-6+J
        END IF
116     CONTINUE
117     CONTINUE

C       ****************************************************************
C       X$      : Title of this block of input data;
C       NBE     : Total number of constrained nodes;
C       NBEXY(I): ID number of constrained node;
C       IBBX(1) : Constraint of displacement in X axis;   =0 free
C       IBBX(2) : Constraint of displacement in Y axis;   =0 free
C       IBBX(3) : Constraint of displacement in Z axis;   =0 free
C       IBBX(4) : Constraint of rotation about X axis;    =0 free
C       IBBX(5) : Constraint of rotation about Y axis;    =0 free
C       IBBX(6) : Constraint of rotation about Z axis;    =0 free
C       IBB(I)  : constrained d.o.f. ID numbers
C       ****************************************************************

C
C       ****************************************************************
C       Block 14
C       Find correspondence between node numbers, element numbers
C       and degrees of freedom numbers.
C
C       ****************************************************************

C       ****************************************************************
C       This part is for the beam elements
C       ****************************************************************

        DO 44 K=1,N
```

```
        IW=0
        DO 2 IR=1,IRGJ
        IF(IAJ(IR).EQ.K.OR.IBJ(IR).EQ.K) GOTO 3
        GOTO 2
3       IF(K-IAJ(IR).GE.IW) IW=K-IAJ(IR)
        IF(K-IBJ(IR).GE.IW) IW=K-IBJ(IR)
2       CONTINUE

c       ****************************************************************
c       This part is for plate elements; it is not used at this stage
c       ****************************************************************

        DO 145 IS=1,ISGJ
        IF(IASJ(IS).EQ.K.OR.IBSJ(IS).EQ.K.OR.
     *  ICSJ(IS).EQ.K.OR.IDSJ(IS).EQ.K) GOTO 146
        GOTO 145
146     IF(K-IASJ(IS).GE.IW) IW=K-IASJ(IS)
        IF(K-IBSJ(IS).GE.IW) IW=K-IBSJ(IS)
        IF(K-ICSJ(IS).GE.IW) IW=K-ICSJ(IS)
        IF(K-IDSJ(IS).GE.IW) IW=K-IDSJ(IS)
145     CONTINUE

c       ****************************************************************
C               This part is for all elements
c       ****************************************************************

        IW=6*(IW+1)
        IAD(6*K)=IW
        IAD(6*K-1)=IW-1
        IAD(6*K-2)=IW-2
        IAD(6*K-3)=IW-3
        IAD(6*K-4)=IW-4
        IAD(6*K-5)=IW-5
44      CONTINUE

        IAD(1)=1
        DO 52 I=2,N1
        IAD(I)=IAD(I)+IAD(I-1)
52      I1=IAD(I)

        if(i1.gt.300000)then
        write (7,*) 'MAXIMUM SIZE EXCEEDED'
        write(7,*)'the size is ',i1
        end if

C*****************************************************************************
C       IW      : Max. difference between node K and the nodes of any beam
C                 This variable helps define the size and shape of the
C                 original global stiffness matrix.  However, since the
C                 global stiffness matrix is replaced by a one dimensional
C                 array, this variable then gives the relationship between
C                 the global stiffness matrix and the corresponding one
C                 dimensional array
C       IAD(I)  : Address of d.o.f. in the one dimensional array;
C       I1      : Total length (size) of one dimensional array
```

```
C*********************************************************************

c       ***************************************************************
c       Block 15
c       Read and set up concentrated dead load data (when NAUTXY < 2)
c       and the concentrated dead loads will not be incremented
c       ***************************************************************
c

        DO 12 I=1,N
        PX(I)=0.0
        PY(I)=0.0
        PZ(I)=0.0
        RMX(I)=0.0
        RMY(I)=0.0
12      RMZ(I)=0.0

        READ(1,199)X$
        READ(1,199) X$
        READ(1,*,ERR=995) NDLDC
        IF(NDLDC.GT.0) THEN
        READ(1,*,ERR=995) (IPDC1(I),(PDC0(I,J),J=1,6),I=1,NDLDC)
      END IF

C*********************************************************************
C       X$    : Title of this block of input data;
C       NDLDC: Total Number of concentrated dead load;
C       IPDC1(I): Node ID number at which there is a concentrated dead
C               : load applied;
C       PDC0(1~3) : Concentrated forces in x,y and z directions respectively;
C       PDC0(4~6) : Concentrated moments about x,y and z axis respectively;
C       PX,PY,PZ  : Loads in x,y,z directions for dead laod temporarily;
C       MX,MY,MZ  : Moments about x,y,z axes for dead load temporarily;
C*********************************************************************

c       ***************************************************************
c       Block 16
c       Read uniform dead load input data (when NAUTXY < 2)
c       (dead load data is entered as uniform load in z direction)
c       ***************************************************************

17      READ(1,199)X$
        READ(1,199) X$
        READ(1,*,ERR=995) NDLDU
        IF(NDLDU.GT.0) THEN
        READ(1,*,ERR=995) (IPDU1(I),IPDU2(I),PDU0(I),PDUC(I),I=1,NDLDU)

        IF(LF1LF1.EQ.1)THEN
          LF1DL1=PDU0(1)
          LF1DL2=PDUC(1)
          PDU0(1)=0.0
          PDUC(1)=0.0
        END IF

        IF(LDY.LE.3)THEN
          DO 9716 I=1,NDLDU
```

```
          PDUC(I)=PDUC(I)+PDU0(I)
          PDU0(I)=0.0
9716      continue
        END IF

        END IF

C*********************************************************************
C       X$        : Title of this block of input data;
C       NDLDU     : Total number of uniform dead load groups;
C       JPDU1(I)  : Starting ID number of elements in group I;
C       JPDU2(I)  : Ending ID number of elements in group I;
C       PDU0(I)   : Intensity of uniform dead load
C       In one group of dead load , the ID numbers have to be continuous
C       with the same value of this load;
C*********************************************************************

C*********************************************************************
C       Block 17
C       Read input concentrated live load data
C       These are the loads to be incremented
C
C*********************************************************************

6500  READ(1,199)X$
        READ(1,199)X$
        READ(1,*,ERR=995) NLOAD
C       WRITE(7,208)NLOAD
208     FORMAT('NO. LIVE LOAD=',I5)

        DO 216 I=1,NLOAD

C*********************************************************************
C       If NAUTXY=2 use mesh generation to create input load
C       from limited input format. Otherwise use regular input option;
C*********************************************************************

        IF(NAUTXY.EQ.2) THEN
        READ(1,*) JX,JY,PX0,PY0,PZ0,RMX0,RMY0,RMZ0
        J=(JX-1)*NDSY+JY
        GOTO 219
        END IF

C*********************************************************************
C               Regular input option
C*********************************************************************

        READ(1,*,ERR=995)J,PX0,PY0,PZ0,RMX0,RMY0,RMZ0

219     PLC0(I,1)=PX0
        PLC0(I,2)=PY0
        PLC0(I,3)=PZ0
        PLC0(I,4)=RMX0
        PLC0(I,5)=RMY0
        PLC0(I,6)=RMZ0
```

```
216     NPPXY(I)=J

C       ****************************************************************
C       X$      : Title for this block of input data;
C       NLOAD   : Total number of nodes where live load is applied;
C       J       : Node ID number at which live load is applied
C               : for NAUTXY < 2 only;
C       PLC0(J,1~3)   : load in X,Y,Z directions respectively;
C       PLC0(J,4~5)   : moments about X,Y,Z axes respectively;
C       NPPXY(I): Vector listing the nodes where loads are applied.
C       ****************************************************************

C
C*****************************************************************
C       Block 18
C       Identify the nodes for which printout of internal forces
C       is desired
C
C*****************************************************************

        READ(1,*) NPRINT
        READ(1,*)(IPRINT(I),I=1,NPRINT)

c       ****************************************************************
c       NPRINT    : Total number of nodes for printout
c       IPRINT(I): ID number of nodes for printout of internal forces
c       ****************************************************************

C
C*****************************************************************
C        Block 19
C        Printout the data collected this far by calling WRITDATA
C
C*****************************************************************

        CALL WRITDATA
c       WRITE(7,*) ' NUMBER OF NODES ',N
c       WRITE(7,*) ' NUMBER OF D.O.F.',N1

C*****************************************************************
C
C               End of input data
C
C*****************************************************************

c       ****************************************************************
c       Block 20
c       Set up the load vector for dead loads and loads that
C       will not be incremented
c
c       ****************************************************************

c       WRITE(7,*) ' SET UP DEAD LOADS'

        ICONT=1
```

```
      NTYPE=0
      DO 9552 I=1,KGIRD
      IF(IRKT(I).GT.NTYPE)NTYPE=IRKT(I)
9552  CONTINUE
      DO 9554 I=1,NTYPE
      FJC(I)=FJ(I)
      RIZC(I)=RIZ(I)
      RIYC(I)=RIY(I)
      RJC(I)=RJ(I)
      SIZC(I)=SIZ(I)
      EBEAMC(I)=EBEAM(I)
      GBEAMC(I)=GBEAM(I)
      ASYC(I)=ASY(I)
      ASZC(I)=ASZ(I)

      FJ(I)=FJGD
      RIZ(I)=RIZGD
      RIY(I)=RIYGD
      RJ(I)=RJGD
      SIZ(I)=SIZGD
      EBEAM(I)=EBEAMG
      GBEAM(I)=GBEAMG
      ASY(I)=ASYGD
      ASZ(I)=ASZGD
      DO 9556 J=1,4
      RMPPC(J,I)=RMPP(J,I)
      RKTPC(J,I)=RKTP(J,I)
      RMPP(J,I)=RMPPGD(J)
      RKTP(J,I)=RKTPGD(J)

c     write(*,*)"rmpp(j,i)",rmpp(j,i)

9556  CONTINUE
      RLPPC(I)=RLPP(I)
      SITMAXPC(I)=SITMAXP(I)
      RLPP(I)=RLPPGD
      SITMAXP(I)=SITMAXG
9554  CONTINUE

      DO 761 I=1,NBE
      KNC=NBEXY(I)
      DO 761 J=1,KGIRD
      IF(IAJ(J).EQ.KNC)NBEXYC(I)=NBEXYC(I)+1
      IF(IBJ(J).EQ.KNC)NBEXYC(I)=NBEXYC(I)+1
761   CONTINUE
      DO 763 I=1,NBE
      KNC=NBEXYC(I)
      IF(KNC.GE.2)THEN
         DO 765 J=1,KGIRD

C        FOR PRESTRESSED CONCRETE BRIDGE, CONSIDER THE GIRDERS HAVE
C        SIMPLE SUPPORTS AT BOTH END.

         IF(IBJ(J).EQ.NBEXY(I))IBJC(J)=1

C        FOR CONTINUOUS BRIDGE, CONSIDER THE GIRDERS HAVE CONTINUE
```

```
C           DEFORMATIONS AT MIDDLE SUPPORTS.

            IF (LDY.EQ.4)THEN
              IF(IBJ(J).EQ.NBEXY(I))IBJC(J)=0
            END IF


765         CONTINUE
          END IF
763       CONTINUE
          DO 865 I=1,IRGJ
          IRKTC(I)=IRKT(I)
865       CONTINUE
          DO 867 I=KGIRD+1,IRGJ
          IRKT(I)=NRKT
867       CONTINUE

768       IF(ICONT.EQ.2)THEN
          DO 767 I=1,NDLDU
          PDU0(I)=PDUC(I)
767       CONTINUE
          DO 769 I=1,IRGJ
          IRKT(I)=IRKTC(I)
769       CONTINUE

          DO 9558 I=1,NTYPE
          FJ(I)=FJC(I)
          RIZ(I)=RIZC(I)
          RIY(I)=RIYC(I)
          RJ(I)=RJC(I)
          SIZ(I)=SIZC(I)
          EBEAM(I)=EBEAMC(I)
          GBEAM(I)=GBEAMC(I)
          ASY(I)=ASYC(I)
          ASZ(I)=ASZC(I)
          DO 9560 J=1,4
          RMPP(J,I)=RMPPC(J,I)
          RKTP(J,I)=RKTPC(J,I)
9560      CONTINUE
          RLPP(I)=RLPPC(I)
          SITMAXP(I)=SITMAXPC(I)
9558      CONTINUE

          END IF

          DO 16 I=1,NDLDC
          J=IPDC1(I)
c         WRITE(7,*) ' DEAD LOAD',I
          PX(J)=PDC0(I,1)
          PY(J)=PDC0(I,2)
          PZ(J)=PDC0(I,3)
          RMX(J)=PDC0(I,4)
          RMY(J)=PDC0(I,5)
16        RMZ(J)=PDC0(I,6)

c         WRITE(7,*) ' NUMBER OF NODES ' ,N
```

```
c       WRITE(7,*) ' NUMBER OF D.O.F.',N1

C*********************************************************************
C       Block 21
C       Convert the uniform dead load into equivalent
C       concentrated point loads and moments at ends of beam elements
C
C*********************************************************************

        DO 6495 I=1,NDLDU
        J1=IPDU1(I)
        J2=IPDU2(I)
c       WRITE(7,*) ' SET UP UNIFORM DEAD LOAD MATRIX'
        DO 19 IR=J1,J2

        DO 20 IX=1,6
20      P0X(IX)=0.0

C*********************************************************************
C       Call LENGTH to find the length of element
C       P0X gives the equivalent fixed end forces & moments
C       J1, J2 give starting and ending ID number of elements
C             in each group ( continuous and same load )
C       PDU0 is the load intensity
C       RL1 is the length of the element
C*********************************************************************

        CALL LENGTH(IBJ(IR),IAJ(IR),N,X,Y,Z,RL1)

        P0X(2)=-PDU0(I)*RL1/2.0
        P0X(6)=-PDU0(I)*RL1*RL1/12.0

        if(icont.eq.1.and.ibjc(ir).eq.1)then
        p0x(2)=-pdu0(i)*rl1*5.0/8.0
        p0x(6)=-pdu0(i)*rl1*rl1/8.0
        end if


C*********************************************************************
c       Call FRLMD to form the rotation matrix RLMD
c       Call MATTRA to transpose the rotation matrix into RLMD1
c       Call MMT to perform the rotation of load vector from
c              local to global coordinates
c       RLMD is the rotation matrix
c       RLMD1 is the transposed rotation matrix
c       P0X is the load vector in local coordinates
c       P1X is the load vector in global coordinates
C       FMA & FMB are the fixed end moments from uniform loads
C*********************************************************************

        CALL FRLMD(IR)
        CALL MATTRA(6,6,RLMD,RLMD1)
        CALL MMT(6,6,RLMD1,P0X,P1X)
        J=IAJ(IR)
        PX(J)=P1X(1)+PX(J)
```

```
        PY(J)=P1X(2)+PY(J)
        PZ(J)=P1X(3)+PZ(J)
        RMX(J)=P1X(4)+RMX(J)
        RMY(J)=P1X(5)+RMY(J)
        RMZ(J)=P1X(6)+RMZ(J)
        FMA(IR)=P0X(6)
        FFA(IR)=-P0X(2)
        P0X(6)=-P0X(6)

        if(icont.eq.1.and.ibjc(ir).eq.1)then
        p0x(2)=-pdu0(i)*r11*3.0/8.0
        p0x(6)=0.0
        end if


        CALL MMT(6,6,RLMD1,P0X,P1X)
        J=IBJ(IR)
        PX(J)=P1X(1)+PX(J)
        PY(J)=P1X(2)+PY(J)
        PZ(J)=P1X(3)+PZ(J)
        RMX(J)=P1X(4)+RMX(J)
        RMY(J)=P1X(5)+RMY(J)
        RMZ(J)=P1X(6)+RMZ(J)
        FMB(IR)=P0X(6)
        FFB(IR)=-P0X(2)
19      CONTINUE
6495    CONTINUE

c       WRITE(7,*) ' NUMBER OF NODES ', N
c       WRITE(7,*) ' NUMBER OF D.O.F.',N1

C       ****************************************************************
C       Block 22
C       identify analysis option
C
C       ****************************************************************

      IDDL=0

C       ****************************************************************
C       IDDL :=-1  Internal forces due to dead loads are larger than first
C                  sub-hinge.
C            : =0  Perform calculation of internal forces due to dead load
C                  After first stage, if IDDL is still equal to zero, this
C                  means that dead load moments are less than first subhinge;
C            : =1  perfrom incremental analysis of live load
C       ****************************************************************

C*****************************************************************
C        Block 23
C        Initialize variables for analysis
C
C*****************************************************************

        CFCT=0.0
```

```
        IF(ICONT.EQ.2)THEN
        ICONT=0
        GO TO 699
        END IF

        CUMAX=0.0
        WRITE(10,363)CUMAX,CFCT
        WRITE(12,363)CUMAX,CFCT

        DO 1100 IR=1,IRGJ
        IHA(IR)=0
        IHB(IR)=0
        IHBA(IR)=0
        IHBB(IR)=0
        RKT1(IR)=0.0
        RKT2(IR)=0.0
        RBT1(IR)=0.0
        RBT2(IR)=0.0
        JJK1(IR)=0
        JJK2(IR)=0
        JJB1(IR)=0
        JJB2(IR)=0
        SITA1(IR)=0.0
        SITA2(IR)=0.0
        RMAD(IR)=0.0
        RMBD(IR)=0.0
        RFAD(IR)=0.0
        RFBD(IR)=0.0
1100  CONTINUE

c       WRITE(7,*) ' NUMBER OF NODES ' ,N
c       WRITE(7,*) ' NUMBER OF D.O.F.',N1

        DO 67 I=1,N1
        PP(I)=0.0
67      UUU(I)=0.0
699     NSTOP=0

C       ****************************************************************
C       PX(I),PY(I),PZ(I)   : Concentrated dead load in X,Y,Z directions
C       RMX(I),RMY(I),RMZ(I)   : moments about X,Y,Z axes respectively.
C       At the beginning, these variables are considered as dead loads
C       when dead load analysis is finished, they will be set to live load;
C
C       RMAD(I),RMBD(I) : moments at ends A & B due to dead load;
C       CUMAX cumulative maximum displacement;
C       CFCT cumulative load factor;
C       PP is a variable that is no longer used in this version of program
C       UUU cumulative displacement vector;
C       NSTOP stopping criteria (=0 continue analysis, =1 stop);
C               The other variables will be defined further down
c       ****************************************************************

C*********************************************************************
C       Block 24
C       Perform analysis of dead loads only
```

```
C               (or loads that will not be incremented)
C*********************************************************************

C*********************************************************************
c       If NDLDU and or NDLDC are greater than 0
c       then dead loads analysis are performed;
c       go to statement label # 160 to find the internal forces and moments
c       due to dead load only
C
C*********************************************************************

        IF(NDLDU.GT.0.OR.NDLDC.GT.0) THEN
        WRITE(7,138)
138   FORMAT(/,1X,'*** OUTPUT OF DEAD LOAD ANALYSIS ***',/)

c       WRITE(7,*) ' NUMBER OF NODES ', N
c       WRITE(7,*) ' NUMBER OF D.O.F.',N1

        GOTO 160
        END IF

C
C*********************************************************************
C       Block 25
C       Starting point for incremental analysis of live load
C       (analysis of dead loads has been completed)
C*********************************************************************

21      CONTINUE

C*********************************************************************
C       Block 26
C       Initialize variables for incremental live load analysis
C
C*********************************************************************

C*********************************************************************
C       Set up internal moments and permanent deformation
C       (displacement and rotation) vectors from dead loads only
C       RMAD :  dead load moment at end A
C       RMBD :  dead load moment at end B
C       CMA  :  cumulative moment at end A
C       CMB  :  cumulative moment at end B
C       SITAD1 : permanent rotation at end A due to dead load
C       SITAD2 : permanent rotation at end B due to dead load
C       SITA1 : permanent rotation at end A
C       SITA2 : permanent rotation at end B
C       UUUD  : cumulative deformations due to dead loads
C       UUU   : cumulative deformations
C       CFCT  : cumulative load factor
C*********************************************************************

      DO 25 IR=1,IRGJ
      RMAD(IR)=CMA(IR)+RMAD(IR)
      CMA(IR)=0.0
      RMBD(IR)=CMB(IR)+RMBD(IR)
```

```
      CMB(IR)=0.0

        RFAD(IR)=CFA(IR)+RFAD(IR)
        CFA(IR)=0.0
        RFBD(IR)=CFB(IR)+RFBD(IR)
        CFB(IR)=0.0

      IF(ABS(RMAD(IR)).LT.1.0E-06) RMAD(IR)=0.0
      IF(ABS(RMBD(IR)).LT.1.0E-06) RMBD(IR)=0.0

      IF(ABS(RFAD(IR)).LT.1.0E-06) RFAD(IR)=0.0
      IF(ABS(RFBD(IR)).LT.1.0E-06) RFBD(IR)=0.0


      SITAD1(IR)=SITA1(IR)
      SITAD2(IR)=SITA2(IR)

25    CONTINUE

      DO 128 I=1,N1
      UUUD(I)=UUU(I)
      IF(ICONT.EQ.2)GO TO 128
      UUU(I)=0.0
128   CONTINUE

c      CFCTD=CFCT
      CFCT=0.0

      WRITE(7,81)
81      FORMAT(/,' DEAD LOAD: ELEMENT    MOMENT A       MOMENT B
     *       FORCE A        FORCE B ',/)
        DO 118 IR=1,IRGJ
        IF(RMAD(IR).NE.0.0.OR.RMBD(IR).NE.0.0) THEN
        WRITE(7,79) IR,RMAD(IR),RMBD(IR),RFAD(IR),RFBD(IR)
79     FORMAT(14X,I3,7X,G12.4,2X,G12.4,2X,G12.4,2X,G12.4)
        END IF
118   CONTINUE

      WRITE(*,228)
      WRITE(7,228)
228   FORMAT(/,1X,' ***** END OF DEAD LOAD ANALYSIS *****',/)

c       WRITE(7,*) ' NUMBER OF NODES ', N
c       WRITE(7,*) ' NUMBER OF D.O.F.',N1


        IF(ICONT.EQ.2)THEN

        DO 9547 IR=1,IRGJ
        RMA0(IR)=RMAD(IR)
        RMB0(IR)=RMBD(IR)
        RFA0(IR)=RFAD(IR)
        RFB0(IR)=RFBD(IR)
9547    CONTINUE

        DO 697 I=1,N
```

```
        PX(I)=0.0
        PY(I)=0.0
        PZ(I)=0.0
        RMX(I)=0.0
        RMY(I)=0.0
        RMZ(I)=0.0
697     CONTINUE
        GO TO 768
        END IF


      WRITE(*,1007)
      WRITE(7,1007)

C*********************************************************************
C       Block 27
C       Begin incremental analysis of live load
C
C*********************************************************************

      WRITE(*,148)
      WRITE(7,148)
148   FORMAT(/,1X,' ***** INCREMENTAL ANALYSIS  *****')

        IDDL=1

C*********************************************************************
C       set up load vectors
C       PX, PY, PZ are the live load vectors now;
C       MX, MY, MZ are moment vectors of live load now;
C       NPPXY gives the nodes where the live loads are applied;
C       IDDL=1 -> starting live load analysis;
C*********************************************************************

        DO 207 I=1,N
        PX(I)=0.0
        PY(I)=0.0
        PZ(I)=0.0
        RMX(I)=0.0
        RMY(I)=0.0
207     RMZ(I)=0.0

c       WRITE(7,*) ' SET UP LIVE LOAD'

        DO 307 I=1,NLOAD
        J=NPPXY(I)
        PX(J)=PLC0(I,1)
        PY(J)=PLC0(I,2)
        PZ(J)=PLC0(I,3)
        RMX(J)=PLC0(I,4)
        RMY(J)=PLC0(I,5)
        RMZ(J)=PLC0(I,6)
c       WRITE(7,*) ' LOADS', I,PX(J),PY(J),PZ(J),RMX(J),RMY(J),RMZ(J)
307     CONTINUE

        WRITE(7,1007)
```

```
C*********************************************************************
C       Block 28
C       Perform structural analysis
C
C*********************************************************************

160   CONTINUE

1010    II=0
        IF(IDDL.LT.1) THEN
        WRITE(*,1243)
1243    FORMAT(/,' PERFORMING ANALYSIS OF DEAD LOADS',/)
        END IF

        WRITE(*,1240) NSTG
        WRITE(7,1240) NSTG
1240    FORMAT(' STAGE :',I5)


C*********************************************************************
C       Call QUS to setup element stiffness matrices
C               & to assemble global stiffness matrix
C               & to solve for displacements
C*********************************************************************


2000    continue


c       WRITE(7,*) ' NUMBER OF NODES ', N
c       WRITE(7,*) ' NUMBER OF D.O.F.',N1

C       DO 10688 J=1,N
C       WRITE(7,*) ' LOADS', J,PX(J),PY(J),PZ(J),RMX(J),RMY(J),RMZ(J)
10688   CONTINUE

        CALL QUS

c       WRITE(7,*) ' NUMBER OF NODES ', N
c       WRITE(7,*) ' NUMBER OF D.O.F.',N1

C*********************************************************************
C       P     ; Vector for temporary storage
C       UU    : Displacement vector in global coordinates for every DOF
C       UMAX  : Maximum displacement
C       NUMAX : Node at which maximum displacement occurs
C*********************************************************************

        DO 68 I=1,N1
68      UU(I)=P(I)

c       write(*,*)'the total displacement is'
c       write(*,69)(p(i),i=1,n1)
69      format(6e10.4)
```

```
        UMAX=0.0
        DO 10000 I=1,N
        J=6*(I-1)+3
        IF(ABS(UU(J)).GT.ABS(UMAX)) THEN
        UMAX=UU(J)
        NUMAX=I
        END IF
10000   CONTINUE

        IF (DABS(UMAX).GT.1.0D10) THEN
        WRITE(7,899)NUMAX,UMAX
899     FORMAT(3X,'NODE : ',I3,1X,'UMAX=',G12.4,
     *  /,' DISPLACEMENT GOES TO INFINITY ')
        GOTO 999
        END IF

C*********************************************************************
C       Block 29
C       Find internal forces ;
C       Set up local stiffness matrix for each element by calling RODJ;
C       Find local deformations and end moments for each element;
C*********************************************************************

        DO 74 IR=1,IRGJ

        DX=X(IBJ(IR))-X(IAJ(IR))
        DY=Y(IBJ(IR))-Y(IAJ(IR))
        DZ=Z(IBJ(IR))-Z(IAJ(IR))
        RL1=DSQRT(DX**2+DY**2+DZ**2)

        CALL RODJ

        K1=6*IAJ(IR)-5
        K2=6*IBJ(IR)-5

C*********************************************************************
C       RL1 : length of beam element
C       K1  : D.O.F. number of end A of element
C       K2  : D.O.F. number of end B of element
C       Put displacements in global coordinates in vector U
C       Put displacements in local coordinates in U1
C       Put local forces in U2
C       UL is a rearrangment of U1 for each element
C       RMA is the moment at end A for this load increment
C       RMB is the moment at end B for this load increment
C       RMA0 is the moment at end A from the elastic analysis
C       RMB0 is the moment at end B from the elastic analysis
C       The elastic analysis corresponds to iteration no. 0
C       NSTG gives the stage number of live load analysis
C       RLM is the rotation matrix
C       RKK1J0 is the element stiffness matrix in local coordinates
C*********************************************************************
C

        DO 75 I=1,6
```

```
        U(I)=UU(K1+I-1)
75      U(I+6)=UU(K2+I-1)

        CALL MMT(12,12,RLM,U,U1)
        CALL MMT(12,12,RKK1J0,U1,U2)

        DO 76 I=1,6
        UL(I,IR)=U1(I)
        UL(I+6,IR)=U1(I+6)
76      CONTINUE

        RMA(IR)=-U2(6)
        RMB(IR)=U2(12)
        RFA(IR)=U2(2)
        RFB(IR)=U2(8)

C       WRITE (7,*) 'CHECKING', NSTG, IDDL,RMA(IR),RMB(IR), FMA(IR),FMB(IR)
C       WRITE (7,*) 'FIXED END FORCES', RFA(IR),FFA(IR),RFB(IR),FFB(IR)

C*********************************************************************
C       Correct the moments by adjusting for fixed end moments
C*********************************************************************

        IF (IDDL.LT.1) THEN
        RMA(IR)=RMA(IR)+FMA(IR)
        RMB(IR)=RMB(IR)-FMB(IR)
        RFA(IR)=RFA(IR)+FFA(IR)
        RFB(IR)=RFB(IR)+FFB(IR)
        END IF

74      CONTINUE

C*********************************************************************
C         Block 30
C         Print output for first step of calculations
C
C*********************************************************************


        IF(NSTG.EQ.0.AND.LDYY.EQ.3) THEN
        WRITE(7,4212)
4212    FORMAT(/,' ELEMENT     RMA',13X,'RMB',13X,'RFA',13X,'RFB',12X,/)
        DO 4213 IR=1,IRGJ
        DO 4221 J=1,NPRINT
        I=IPRINT(J)
        IF(I.EQ.IAJ(IR).OR.I.EQ.IBJ(IR)) GOTO 4223
4221    CONTINUE
        GOTO 4213
4223    WRITE(7,4230) IR,RMA(IR),RMB(IR),RFA(IR),RFB(IR)
4230    FORMAT(2X,I5,4(4X,G12.4))
4213    CONTINUE
        END IF

C*********************************************************************
C       Block 31
C       Find forces & moments if only elastic analysis option
```

```
C
C       LDY=2 means perform elastic analysis only
C*********************************************************************

        IF(LDYY.EQ.2) THEN
        WRITE(7,78)
78      FORMAT(/,' NODE   U(X)         V(Y)         W(Z)       Rot. X
     *       Rot. Y       Rot. Z ',/)
        DO 80 J=1,NPRINT
        I=IPRINT(J)
        WRITE(7,83)I,P(6*I-5),P(6*I-4),P(6*I-3),P(6*I-2),P(6*I-1),P(6*I)
83      FORMAT(1X,I4,6(G12.4))
80      CONTINUE

        WRITE(7,4212)
        DO 4218 IR=1,IRGJ
c       DO 4232 J=1,NPRINT
c       I=IPRINT(J)
c       IF(I.EQ.IAJ(IR).OR.I.EQ.IBJ(IR)) GOTO 4234
c4232    CONTINUE
c       GOTO 4218
4234    WRITE(7,4230) IR,RMA(IR),RMB(IR),RFA(IR),RFB(IR)
4218    CONTINUE

C*********************************************************************
C       UUU is the matrix containing the cumulative displacements
C       from all the load steps
C       UU is the displacement vector for only one iteration step
C*********************************************************************

        DO 4803 I=1,N1
4803    UUU(I)=UU(I)

C*********************************************************************
C       This section deals with plate elements and is
C       ignored at this stage
C*********************************************************************

        IF(ISGJ.EQ.0) GOTO 4155
        WRITE(7,4078)
        RMAXPL=0.0
        DO 4150 IS=1,ISGJ
        CALL STRSPL(SIGPL,0)
        IF(DABS(SIGPL).GT.RMAXPL) THEN
        RMAXPL=SIGPL
        NSGJ=IS
        END IF
4150    CONTINUE
        WRITE(7,4200) NSGJ,TJ(NSGJ)
4200    FORMAT('NO. OF PLATE:',I5,' THICKNESS=',G12.4)
        SIGMAX=6.0*RMAXPL/TJ(NSGJ)**2
        WRITE(7,4080) NSGJ,RMAXPL,SIGMAX
        IS=NSGJ
        CALL STRSPL(SIGPL,1)

C*********************************************************************
```

```
C       If only elastic analysis is desired stop program
C       by going to statement label # 999
C*********************************************************************

4155    WRITE(*,799)
        WRITE(7,799)
799     FORMAT(/,' Program stopped at end of elastic analysis ')
        GOTO 999
        END IF

C*********************************************************************
C          Block 32
C          Check each element for loading reversal
C
C*********************************************************************

C*********************************************************************
C               CMA is the cumulative moment at end A
C               CMB is the cumulative moment at end B
C*********************************************************************

      IF(IDDL.LT.1) THEN
        WRITE(*,2031)
2031    FORMAT(' CALCULATING DEAD LOAD FACTOR',/)
      END IF

      IF(IDDL.EQ.1) THEN
        WRITE(*,2032)
2032    FORMAT(' CALCULATING LIVE LOAD FACTOR',/)
      END IF

        DO 2002 IR=1,IRGJ

        IF((CMA(IR)+RMAD(IR))*RMA(IR).GT.0.0) RKTA(IR)=1.0
        IF((CMA(IR)+RMAD(IR))*RMA(IR).LT.0.0) RKTA(IR)=-1.0
        IF((CMA(IR)+RMAD(IR))*RMA(IR).EQ.0.0) THEN
        IF(RMA(IR).GT.0.0.OR.(CMA(IR)+RMAD(IR)).GT.0.0) RKTA(IR)=1.0
        IF(RMA(IR).LT.0.0.OR.(CMA(IR)+RMAD(IR)).LT.0.0) RKTA(IR)=-1.0
        END IF

        IF((CMB(IR)+RMBD(IR))*RMB(IR).GT.0.0) RKTB(IR)=1.0
        IF((CMB(IR)+RMBD(IR))*RMB(IR).LT.0.0) RKTB(IR)=-1.0
        IF((CMB(IR)+RMBD(IR))*RMB(IR).EQ.0.0) THEN
        IF(RMB(IR).GT.0.0.OR.(CMB(IR)+RMBD(IR)).GT.0.0) RKTB(IR)=1.0
        IF(RMB(IR).LT.0.0.OR.(CMB(IR)+RMBD(IR)).LT.0.0) RKTB(IR)=-1.0
        END IF

        IF((CFA(IR)+RFAD(IR))*RFA(IR).GT.0.0) RBTA(IR)=1.0
        IF((CFA(IR)+RFAD(IR))*RFA(IR).LT.0.0) RBTA(IR)=-1.0
        IF((CFA(IR)+RFAD(IR))*RFA(IR).EQ.0.0) THEN
        IF(RFA(IR).GT.0.0.OR.(CFA(IR)+RFAD(IR)).GT.0.0) RBTA(IR)=1.0
        IF(RFA(IR).LT.0.0.OR.(CFA(IR)+RFAD(IR)).LT.0.0) RBTA(IR)=-1.0
        END IF

        IF((CFB(IR)+RFBD(IR))*RFB(IR).GT.0.0) RBTB(IR)=1.0
        IF((CFB(IR)+RFBD(IR))*RFB(IR).LT.0.0) RBTB(IR)=-1.0
```

```
      IF((CFB(IR)+RFBD(IR))*RFB(IR).EQ.0.0) THEN
      IF(RFB(IR).GT.0.0.OR.(CFB(IR)+RFBD(IR)).GT.0.0) RBTB(IR)=1.0
      IF(RFB(IR).LT.0.0.OR.(CFB(IR)+RFBD(IR)).LT.0.0) RBTB(IR)=-1.0
      END IF

2002  CONTINUE

C*****************************************************************
C     RKTA(IR)=1.0 : the sign of accumulated moment at the end A
C                    of element IR is the same as that of moment
C                    increment;
C           =-1.0 : the sign of accumulated moment at the end A
C                    of element IR is different from that of moment
C                    increment;
C     RKTB(IR)=1.0 : the sign of accumulated moment at the end B
C                    of element IR is the same as that of moment
C                    increment;
C           =-1.0:  the sign of accumulated moment at the end B
C                    of element IR is different from that of moment
C                    increment;
C*****************************************************************


C*****************************************************************
C     Block 33
C     Identify moment at the next subhinge
C     Adjust moment rotation curves by subtracting Dead load moments
C
C     ****************************************************************

C     ****************************************************************
C     IX & IRKT GIVE THE BEAM ELEMENT TYPE
C     J & JJK1  GIVE THE SUBHINGE NUMBER FOR END OF ELEMENT
C     ITMP TEMPORARY INDICATOR FOR LOADING OR UNLOADING
C     RKTA LOADING OR UNLOADING INDICATOR
C     CMA CUMULATIVE LIVE LOAD MOMENT AT END A
C     RMAD DEAD LOAD MOMENT AT END A
C     RMPA MOMENT LEVEL AT WHICH NEXT SUBHINGE FORMS
C     RMPP ORDINATE OF M-Q CURVE FOR POSITIVE MOMENT
C     RMPN ORDINATE OF M-Q CURVE FOR NEGATIVE MOMENT
C
C     VARIABLES WITH B OR 2 ARE SAME AS ABOVE FOR END A
C
C*****************************************************************

      DO 1002 IR=1,IRGJ

      IX=IRKT(IR)
      J=JJK1(IR)
      ITMP=1
      IF(RKTA(IR).LT.0.0) ITMP=0
      IF((CMA(IR)+RMAD(IR)).GE.0.0) THEN

       IF(J.GT.0) THEN
       RMPA(IR)=RMPPX(J+1*ITMP,IX,IR,1)-RMAD(IR)
       ELSE
```

```
            IF(RMA(IR).GE.0.0) THEN
            RMPA(IR)=RMPPX(1,IX,IR,1)-RMAD(IR)
            ELSE
            RMPA(IR)=-RMPN(1,IX)-RMAD(IR)
            END IF
           END IF
          END IF

          IF((CMA(IR)+RMAD(IR)).LT.0.0) THEN
           IF(J.GT.0) THEN
           RMPA(IR)=-RMPN(J+1*ITMP,IX)-RMAD(IR)
           ELSE
            IF(RMA(IR).LT.0.0) THEN
            RMPA(IR)=-RMPN(1,IX)-RMAD(IR)
            ELSE
            RMPA(IR)=RMPPX(1,IX,IR,1)-RMAD(IR)
            END IF
           END IF
          END IF

c         nh=j+1*itmp
c         write(*,*)"ir,nh,itmp,rmppx(nh,ix,ir,1),rmad(ir),rmpa(ir)"
c         write(*,*)ir,nh,itmp,rmppx(nh,ix,ir,1),rmad(ir),rmpa(ir)

        J=JJK2(IR)
          ITMP=1
          IF(RKTB(IR).LT.0.0) ITMP=0
          IF((CMB(IR)+RMBD(IR)).GE.0.0) THEN
           IF(J.GT.0) THEN
           RMPB(IR)=RMPPX(J+1*ITMP,IX,IR,2)-RMBD(IR)
           ELSE
            IF(RMB(IR).GE.0.0) THEN
            RMPB(IR)=RMPPX(1,IX,IR,2)-RMBD(IR)
            ELSE
            RMPB(IR)=-RMPN(1,IX)-RMBD(IR)
            END IF
           END IF
          END IF

          IF((CMB(IR)+RMBD(IR)).LT.0.0) THEN
           IF(J.GT.0) THEN
           RMPB(IR)=-RMPN(J+1*ITMP,IX)-RMBD(IR)
           ELSE
            IF(RMB(IR).LT.0.0) THEN
            RMPB(IR)=-RMPN(1,IX)-RMBD(IR)
            ELSE
            RMPB(IR)=RMPPX(1,IX,IR,2)-RMBD(IR)
            END IF
           END IF
          END IF


c         nh=j+1*itmp
c         write(*,*)"ir,nh,itmp,rmppx(nh,ix,ir,2),rmbd(ir),rmpb(ir)"
c         write(*,*)ir,nh,itmp,rmppx(nh,ix,ir,2),rmbd(ir),rmpb(ir)
```

```
          IXB=IRBT(IR)
          JB=JJB1(IR)
          ITMP=1
          IF(RBTA(IR).LT.0.0) ITMP=0
          IF((CFA(IR)+RFAD(IR)).GE.0.0) THEN
           IF(JB.GT.0) THEN
           RFPA(IR)=RV(JB+1*ITMP,IXB)-RFAD(IR)
           ELSE
            IF(RFA(IR).GE.0.0) THEN
            RFPA(IR)=RV(1,IXB)-RFAD(IR)
            ELSE
            RFPA(IR)=-RV(1,IXB)-RFAD(IR)
            END IF
           END IF
          END IF

C         WRITE(7,*) ' IR,JB,IXB',IR,JB,ITMP,IXB,RV(JB+1*ITMP,IXB)
C         WRITE(7,*) ' IXB', IXB,RV(1,IXB)
          IF((CFA(IR)+RFAD(IR)).LT.0.0) THEN
           IF(JB.GT.0) THEN
           RFPA(IR)=-RV(JB+1*ITMP,IXB)-RFAD(IR)
           ELSE
            IF(RFA(IR).LT.0.0) THEN
            RFPA(IR)=-RV(1,IXB)-RFAD(IR)
            ELSE
            RFPA(IR)=RV(1,IXB)-RFAD(IR)
            END IF
           END IF
          END IF

C         WRITE(7,*) 'IR,RFPA,RFAD,CFA',IR,RFPA(IR),RFAD(IR),CFA(IR)


        JB=JJB2(IR)
          ITMP=1
          IF(RBTB(IR).LT.0.0) ITMP=0
          IF((CFB(IR)+RFBD(IR)).GE.0.0) THEN
           IF(JB.GT.0) THEN
           RFPB(IR)=RV(JB+1*ITMP,IXB)-RFBD(IR)
           ELSE
            IF(RFB(IR).GE.0.0) THEN
            RFPB(IR)=RV(1,IXB)-RFBD(IR)
            ELSE
            RFPB(IR)=-RV(1,IX)-RFBD(IR)
            END IF
           END IF
          END IF

          IF((CFB(IR)+RFBD(IR)).LT.0.0) THEN
           IF(JB.GT.0) THEN
           RFPB(IR)=-RV(JB+1*ITMP,IXB)-RFBD(IR)
           ELSE
            IF(RFB(IR).LT.0.0) THEN
            RFPB(IR)=-RV(1,IXB)-RFBD(IR)
            ELSE
            RFPB(IR)=RV(1,IX)-RFBD(IR)
```

```
          END IF
        END IF
      END IF


1002    CONTINUE
C*********************************************************************
C         Block 34
C         Initialize cumulative variables
C
C*********************************************************************
C
C*********************************************************************
C       intialize:   CFCT =cumulative load factor
C                    CMA = cumulative moment of live load at end A
C                    CMB = cumulative moment of live load at end B
C                    CUMAX = cumulative maximum displacement
C       NSTG = Stage number of analysis;
C*********************************************************************

        IF(NSTG.EQ.0) THEN
        CUMAX=0.
        CFCT=0.
        DO 2001 IR=1,IRGJ
        CMA(IR)=0.
        CMB(IR)=0.
        CFA(IR)=0.
        CFB(IR)=0.
2001    CONTINUE

        END IF

C*********************************************************************
C       Block 35
C       Check for formation of subhinges after one step
C       in incremental analysis
C
C*********************************************************************

C*********************************************************************
C       Call HINGE
C               Find min. load factor to make one end of any element
C                       reach its next possible sub-hinge
C               Identify the loading stage for each beam element
C               Obtain FCT= load factor increment for this stage
C*********************************************************************

        CALL HINGE(NSTG,IDDL)

c       write(*,*)"the fct=", fct
c       write(*,*)"the icont=",icont


C*********************************************************************
```

```
C       Block 36
C       Verify that the Maximum plastic hinge rotation is not exceeded
C
C*********************************************************************

C*********************************************************************
C          RMA     : is the moment for this stage of calculation
C          RKT1    : is the slope of M-Q curve at this level of loading
C          SITA11  : is the possible incremental rotation at end A
C          SITMAX  : is temporary variable of maximum rotation for
C                    this element.
C          FCT1    : is temporary variable of maximum increment you can
C                    have without exceeding of plastic rotation limit
C          FCT     : is the previously calculated load factor increment
C                    based on moments
C          IRKT    : is the beam type number
C          JJK1 > 0 indicates that a subhinge was formed at this end
C          SITMAXP: plastic hinge rotation limit in positive bending
C          SITMAXN: plastic hinge rotation limit in negative bending
C          SITA1   : accumulated hinge rotation just before this increment
C          NSTOP   : if 1 signals the program to stop
C
C          variables with B and/or 2 are same as above for end B
C                        of beam element
C          We only check the elements previously identified as main girders
C          for stop criteria;
C*********************************************************************

        DO 3000 IR=1,IRGJ1
        IF (ABS (RMA(IR)).LT.1.0E-10) GOTO 3010
        J=IRKT(IR)
        IF(JJK1(IR).NE.0) THEN
        SITA11=RMA(IR)/RKT1(IR)
         IF(SITA1(IR).GT.0.0) SITMAX=SITMAXP(J)
         IF(SITA1(IR).LT.0.0) SITMAX=SITMAXN(J)
         IF(SITA1(IR).EQ.0.0) THEN
          IF(SITA11.GT.0.0) SITMAX=SITMAXP(J)
          IF(SITA11.LT.0.0) SITMAX=SITMAXN(J)
          END IF

         FCT1=(SITMAX-ABS(SITA1(IR)))/(ABS(SITA11))
        IF(FCT1.LT.FCT) THEN
        FCT=FCT1
        NSTOP=1
        END IF

        END IF


3010  continue

        IF(ABS(RMB(IR)).LT.1.0E-10) GOTO 3000

        IF(JJK2(IR).NE.0) THEN
        SITA22=RMB(IR)/RKT2(IR)
```

```
          IF(SITA2(IR).GT.0.0) SITMAX=SITMAXP(J)
          IF(SITA2(IR).LT.0.0) SITMAX=SITMAXN(J)
          IF(SITA2(IR).EQ.0.0) THEN
           IF(SITA22.GT.0.0) SITMAX=SITMAXP(J)
           IF(SITA22.LT.0.0) SITMAX=SITMAXN(J)
         END IF


         FCT1=(SITMAX-DABS(SITA2(IR)))/(DABS(SITA22))
          IF (FCT1.LT.FCT) THEN
          FCT=FCT1
          NSTOP=1
          END IF

         END IF

3000     CONTINUE

         IF (FCT.LT.0. .AND. ABS(FCT).GT.0.5*CFCT) NSTOP=2

C*************************************************************************
C        Block 37
C        Update total load factor
C
C*************************************************************************

C        IF(IDDL.GE.1) CFCT=CFCT+FCT
         CFCT=CFCT+FCT

C*************************************************************************
C           Block 38
C           Update accumulated displacement
C           and find max. displavement in whole system
C
C*************************************************************************


         DO 803 I=1,N1
803      UUU(I)=UUU(I)+UU(I)*FCT

         CUMAX=0.0
         DO 804 I=1,N
         J=6*(I-1)+3
         IF(ABS(UUU(J)).GT.ABS(CUMAX)) THEN
         CUMAX=UUU(J)
         NUMAX=I
         END IF
804      CONTINUE

         WRITE(7,70)
70       FORMAT(/,' NODE    U(X)         V(Y)         W(Z)       Rot. X
     *       Rot. Y        Rot. Z ',/)

         DO 805 J=1,NPRINT
         I=IPRINT(J)
         WRITE(7,71)I,UUU(6*I-5),UUU(6*I-4),UUU(6*I-3),UUU(6*I-2)
```

```
     *   ,UUU(6*I-1),UUU(6*I)
71        FORMAT(1X,I3,6(G12.4))
805       CONTINUE

C*********************************************************************
c         UUU ; cumulative displacement
c         UU  : displacement from this increment
c         FCT : load factor for this increment
c         CUMAX : maximum cumulative displacement
c         NUMAX : Node where max. cumulative displacement occurs
C*********************************************************************

C*********************************************************************
C         Block 39
C         Update accumulated moment in whole system
C
C*********************************************************************

          DO 26 I=1,IRGJ
C         WRITE(7,*) ' FCT, RMA,RMB',FCT,RMA(I),RMB(I),RFA(I),RFB(I)
C         WRITE(7,*) '              ',FCT,CMA(I),CMB(I),CFA(I),CFB(I)
          CMA(I)=CMA(I)+FCT*RMA(I)
          CMB(I)=CMB(I)+FCT*RMB(I)
          CFA(I)=CFA(I)+FCT*RFA(I)
          CFB(I)=CFB(I)+FCT*RFB(I)
26        CONTINUE

C*********************************************************************
c         CMA cumulative moment at end A due to live load only
C         RMA moment due to this load increment
C*********************************************************************

C*********************************************************************
C         Block 40
C         Update max. displacement and plastic rotations for main
C         girder elements
C
c              SITAP0  : MAXIMUM POSSIBLE PLASTIC HINGE ROTATION
C              SITAN0  : MAXIMUM POSSIBLE NEGATIVE HINGE ROTATION
C              CUMAXBM : MAXIMUM DISPLACEMENT IN BEAM ELEMENT
C              NUMAXBM : NODE NUMBER AT WHICH MAXIMUM DISPLACEMENT OCCURS
C              RKT1    : SLOPE OF M-Q CURVE AT THIS STAGE FOR END A
C              RKT2    : SLOPE OF M-Q CURVE AT THIS STAGE FOR END B
C*********************************************************************

          SITAP0=0.0
          SITAN0=0.0
          CUMAXBM=0.0

          DO 3009 IR=1,IRGJ1

          I=IAJ(IR)
          IF(ABS(UUU(6*I-3)).GT.ABS(CUMAXBM)) THEN
          CUMAXBM=UUU(6*I-3)
          NUMAXBM=I
          END IF
```

```
          I=IBJ(IR)
          IF(ABS(UUU(6*I-3)).GT.ABS(CUMAXBM)) THEN
          CUMAXBM=UUU(6*I-3)
          NUMAXBM=I
          END IF

          IF(JJK1(IR).NE.0) THEN
          SITA11=RMA(IR)/RKT1(IR)
          SITA1(IR)=SITA1(IR)+SITA11*FCT
           IF(SITA1(IR).GT.0.0) THEN
            IF(SITA1(IR).GT.SITAP0) SITAP0=SITA1(IR)
           END IF
           IF(SITA1(IR).LT.0.0) THEN
            IF(SITA1(IR).LT.SITAN0) SITAN0=SITA1(IR)
           END IF
          END IF

          IF(JJK2(IR).NE.0) THEN
          SITA22=RMB(IR)/RKT2(IR)
          SITA2(IR)=SITA2(IR)+SITA22*FCT
           IF(SITA2(IR).GT.0.0) THEN
            IF(SITA2(IR).GT.SITAP0) SITAP0=SITA2(IR)
           END IF
           IF(SITA2(IR).LT.0.0) THEN
            IF(SITA2(IR).LT.SITAN0) SITAN0=SITA2(IR)
           END IF
          END IF

3009      CONTINUE
c         write(*,*)'sita1(i)'
c         write(*,*)'***************************'
c         write(*,2007)(sita1(i),i=1,ir)
c2007     format(10e9.4)
c         write(*,*)'sita2(i)'
c         write(*,*)'*******************************'
c         write(*,2007)(sita2(i),i=1,ir)

C*********************************************************************
C         Block 41
C         Update max. plastic rotation for other than main elements
C
C         SITAP00 SAME AS SITAP0 FOR NON MAIN GIRDER ELEMENTS
C         SITAN00 SAME AS SITAN0 FOR NON MAIN GIRDER ELEMENTS
C*********************************************************************

          SITAP00=SITAP0
          SITAN00=SITAN0

          DO 353 IR=IRGJ1+1,IRGJ

          IF(JJK1(IR).NE.0) THEN
          SITA11=RMA(IR)/RKT1(IR)
          SITA1(IR)=SITA1(IR)+SITA11*FCT
           IF(SITA1(IR).GT.0.0) THEN
            IF(SITA1(IR).GT.SITAP00) SITAP00=SITA1(IR)
           END IF
```

```
          IF(SITA1(IR).LT.0.0) THEN
           IF(SITA1(IR).LT.SITAN00) SITAN00=SITA1(IR)
          END IF
         END IF

         IF(JJK2(IR).NE.0) THEN
         SITA22=RMB(IR)/RKT2(IR)
         SITA2(IR)=SITA2(IR)+SITA22*FCT
          IF(SITA2(IR).GT.0.0) THEN
           IF(SITA2(IR).GT.SITAP00) SITAP00=SITA2(IR)
          END IF
          IF(SITA2(IR).LT.0.0) THEN
           IF(SITA2(IR).LT.SITAN00) SITAN00=SITA2(IR)
          END IF
         END IF

353      CONTINUE

C*********************************************************************
C        Block 42
C        Identify elements that reached new subhinges
C
C        Printout ID numbers for the elements which formed new
C                 sub-hinges at this load increment
C        KA = number of elements whose end A reached a sub-hinge
C        KB = number of elements whose end B reached a sub-hinge
C        IIA = contains the ID numbers of elements with A hinged
C        IIB = contains the ID numbers of elements with B hinged
C*********************************************************************

       IF(IDDL.GT.0) THEN
         WRITE(7,350)FCT,KA,KB,KBA,KBB
350      FORMAT(/,3X,'FCT=',G12.4,1X,'KA=',I4,1X,'KB=',I4,
     *           1X,'KBA=',I4,1X,'KBB=',I4/)
       ELSE
       WRITE(7,352)FCT,KA,KB,KBA,KBB
352    FORMAT(/,3X,'DEAD LOAD RATIO=',G12.4,1X,'KA=',I4,1X,'KB=',I4,
     *            1X,'KBA=',I4,1X,'KBB=',I4,/)
       END IF

         IF(KA.NE.0) THEN
         WRITE(7,355)(IIA(K),K=1,KA)
355      FORMAT(3X,'IIA=',10I5)
         END IF
         IF(KB.NE.0) THEN
         WRITE(7,360)(IIB(K),K=1,KB)
360      FORMAT(3X,'IIB=',10I5)
         END IF

         IF(KBA.NE.0) THEN
         WRITE(7,356)(IIBA(K),K=1,KBA)
356      FORMAT(3X,'IIBA=',10I5)
         END IF
         IF(KBB.NE.0) THEN
         WRITE(7,361)(IIBB(K),K=1,KBB)
361      FORMAT(3X,'IIBB=',10I5)
```

```
        END IF

C*********************************************************************
C       Block 43
C       Printout accumulated moments and total plastic rotation
C       for beam element selected for detailed print option
C
C*********************************************************************

      IF(IDDL.GT.0) THEN
        WRITE(7,212)
212     FORMAT(/,' ELEMENT     CMA',13X,'CMB',12X,'SITAA',10X,'SITAB',
     *  13X,'CFA',13X,'CFB',/)
      ELSE
      WRITE(7,152)
152     FORMAT(/,' ELEMENT    RMAD',12X,'RMBD',11X,'SITADA',10X,
     *'SITADB',12X,'RFAD',12X,'RFBD',/)
      END IF

        DO 213 IR=1,IRGJ
        DO 221 J=1,NPRINT
        I=IPRINT(J)
        IF(I.EQ.IAJ(IR).OR.I.EQ.IBJ(IR)) GOTO 223
221     CONTINUE
        GOTO 213
223     WRITE(7,3001) IR,CMA(IR),CMB(IR),SITA1(IR),SITA2(IR),
     *     CFA(IR),CFB(IR)


3001    FORMAT(2X,I5,6(3X,G12.4))
213     CONTINUE

        rmp2=0.0
        rmn2=1e9
        if(LF1LF1.eq.1.and.iddl.eq.1)then
        do 2138 i=1,kgird
        if(cma(i).gt.rmp2)rmp2=cma(i)
        if(cmb(i).gt.rmp2)rmp2=cmb(i)
        if(cma(i).lt.rmn2)rmn2=cma(i)
        if(cmb(i).lt.rmn2)rmn2=cmb(i)
2138    continue
        write(*,*)'the following are fct,Mpos,Mneg created by living load'
        write(*,*)fct,rmp2,rmn2

        WRITE(*,*)"PLEASE INPUT Mpos(max) and Mneg(max) created by dead load"
        read(*,*)rmp1,rmn1
        write(*,*)"Please input the normal moment Mu(pos), Mu(neg)"
        read(*,*)rmp3, rmn3
        write(*,*)"Please input the ultimate LFu "
        read(*,*)rlfu
        write(*,*)
        write(*,*)

        clf11=(rmp3-rmp1)*fct/rmp2
        clf12=(abs(rmn3)-abs(rmn1))*fct/abs(rmn2)
        write(*,*)'to positive section'
```

```
        write(*,2139)rmp1,'+',rmp2,'/',fct,'* LF1=',rmp3
        write(*,*)'LF1=',clf11
        write(*,*)
        write(*,*)'to negative section'
        write(*,2139)rmn1,'+',abs(rmn2),'/',fct,'* LF1=',rmn3
        write(*,*)'LF1=',clf12
        clf=clf11
        if(clf11.gt.clf12)clf=clf12
        write(*,*)'LFu/LF1=',rlfu/clf

2139    format(f10.2,a,f10.2,a,f7.3,a,f10.2)
        stop
        end if


C*********************************************************************
C               print incremented load factors, displacements
C               and moments
C*********************************************************************

      IF(IDDL.GT.0) THEN
        WRITE(7,365)NUMAX,CUMAX,CFCT
        ELSE
        WRITE(7,142)NUMAX,CUMAX,CFCT
142   FORMAT(/,3X,'NODE : ',I3,3X,'CUMAX=',G12.4,3X,'DEAD LOAD RATIO=',
     * G12.4,/)
      END IF

        WRITE(7,367)NUMAXBM,CUMAXBM
        IF(IDDL.GT.0) THEN
        WRITE(10,363) CUMAX,CFCT
        WRITE(12,363) CUMAXBM,CFCT
        END IF
363     FORMAT(G12.4,1X,G12.4)
365     FORMAT(/,3X,'NODE : ',I3,3X,'CUMAX=',G12.4,3X,'FACTOR=',G12.4,
     *  /)
367     FORMAT(3X,'NODE OF MAX. DISPLACEMENT AMONG BEAMS :',I3,3X,
     *  'CUMAXBEAM=',G12.4,/)

C*********************************************************************
C       If LDY=3 , print the status of subhinge formation in selected node
C*********************************************************************

        IF(LDYY.EQ.3) THEN
        DO 1022 IR=1,IRGJ1
        DO 1018 I=1,NPRINT
        J=IPRINT(I)
        IF(J.EQ.IAJ(IR).OR.J.EQ.IBJ(IR)) GOTO 1019
1018    CONTINUE
        GOTO 1022
1019    IF(JJK1(IR).NE.0 .OR. JJK2(IR).NE.0) THEN
        WRITE(7,1021)IR,JJK1(IR),JJK2(IR),RKT1(IR),RKT2(IR)
        END IF

        IF(JJB1(IR).NE.0 .OR. JJB2(IR).NE.0) THEN
```

```
      WRITE(7,1023)IR,JJB1(IR),JJB2(IR),RBT1(IR),RBT2(IR)
      END IF

1023  FORMAT(3X,'IR=',I4,2X,'JJB1=',I3,2X,'JJB2=',I3,2X,'RBT1=',
     * G12.4,2X,'RBT2=',G12.4)

1021  FORMAT(3X,'IR=',I4,2X,'JJK1=',I3,2X,'JJK2=',I3,2X,'RKT1=',
     * G12.4,2X,'RKT2=',G12.4)
1022  CONTINUE
      END IF

C*********************************************************************
C           Block 44
C           This section is for plate elements and is not being used
C           at this stage
C
C*********************************************************************

      IF(ISGJ.EQ.0) GOTO 3015
      WRITE(7,4078)
4078  FORMAT(/,' ---- DEFLECTION AND FORCE AT PLATE
     * ---- ',/)
      RMAXPL=0.0
      DO 4050 IS=1,ISGJ
      CALL STRSPL(SIGPL,0)
      IF(SIGPL.GT.RMAXPL) THEN
      RMAXPL=SIGPL
      NSGJ=IS
      END IF
4050  CONTINUE
      SIGMAX=6.0*RMAXPL/TJ(NSGJ)**2
      WRITE(7,4080) NSGJ,RMAXPL,SIGMAX
4080  FORMAT(/,'  MAXIMUM STRESS AT PLATE ELEMENT :',/,
     * ' ELEMENT :',I3,' MOMENT (PER LENGTH) :',G12.4,
     * ' STRESS :',G12.4,/)
      IS=NSGJ
      CALL STRSPL(SIGPL,1)

3015  CONTINUE

C*********************************************************************
C     If NSTOP=0 then plastic hinge rotation limit was not exceeded
C             so continue calculations by going to statement with label
C             # 3005  otherwise print output and stop
C*********************************************************************

      IF(NSTOP.EQ.0) GOTO 3005

C*********************************************************************
C          Block 45
C          Print out Maximum Plastic Hinge Rotations
C
c          CFCT0 is the cumulative load factor from previous iteration
C*********************************************************************

      CFCT=CFCT0+FCT
```

```
        WRITE(7,3006) SITAP0,SITAN0
3006    FORMAT(/,1X,'MAX. PLASTIC ROTATION IN MAIN BEAM:
     *  SITM(+)=',G12.4,1X,'SITM(-)=',G12.4,/)

        WRITE(7,3008) SITAP00,SITAN00
3008    FORMAT(/,1X,'MAX. PLASTIC ROTATION IN WHOLE SYSTEM:
     *  SITM(+)=',G12.4,1X,'SITM(-)=',G12.4,//,' *** PROGRAM
     *  TERMINATED ***')

        IF (NSTOP.EQ.2) WRITE(7,3019)
3019    FORMAT( //,' *** PROGRAM TERMINATED DUE TO GLOBAL UNLOADING' )


        IF (NSTOP.EQ.1) WRITE(7,3018)
3018    FORMAT( //,' *** PROGRAM TERMINATED AFTER EXCEEDING MAXIMUM
     *      PLASTIC HINGE ROTATION' )

C*********************************************************************
C               Stop by going to statement label # 999
C*********************************************************************

        GOTO 999

C*********************************************************************
C       Block 46
C       Modify value of sub-hinge indicator to identify
C       the point on M-Q curve that each element has reached
C
c       KA number of elements where a new subhinge formed at end A
c       KB number of elements where a new subhinge formed at end B
c       IIA element ID number with new subhinge at A
c       IIB element ID number with new subhinge at B
c       JJK1 subhinge number for element at end A
c       JJK2 subhinge number for element at end B
c       RKTA indicates whether cumulative moment at A increases or decreases
c       RKTB indicates whether cumulative moment at B increases or decreases
C
C*********************************************************************

3005    DO 1003 I=1,KA
        IR=IIA(I)
        IF(RKTA(IR).GT.0.) JJK1(IR)=JJK1(IR)+1
        IF(RKTA(IR).LT.0.) JJK1(IR)=JJK1(IR)-1
        IF(JJK1(IR).LT.0) JJK1(IR)=1

1003    CONTINUE

        DO 1004 I=1,KB
        IR=IIB(I)
        IF(RKTB(IR).GT.0.) JJK2(IR)=JJK2(IR)+1
        IF(RKTB(IR).LT.0.) JJK2(IR)=JJK2(IR)-1
        IF(JJK2(IR).LT.0) JJK2(IR)=1

1004    CONTINUE

C       WRITE(7,*) ' KBA',KBA
```

```
        DO 10030 I=1,KBA
        IR=IIBA(I)
        IF(RBTA(IR).GT.0.) JJB1(IR)=JJB1(IR)+1
        IF(RBTA(IR).LT.0.) JJB1(IR)=JJB1(IR)-1
        IF(JJB1(IR).LT.0) JJB1(IR)=1

C       WRITE(7,*) 'I,IR,JJB1(IR),RBTA(IR)',I,IR,JJB1(IR),RBTA(IR)
10030    CONTINUE

        DO 10040 I=1,KBB
        IR=IIBB(I)
        IF(RBTB(IR).GT.0.) JJB2(IR)=JJB2(IR)+1
        IF(RBTB(IR).LT.0.) JJB2(IR)=JJB2(IR)-1
        IF(JJB2(IR).LT.0) JJB2(IR)=1

10040    CONTINUE

C*********************************************************************
C       Block 47
C       Update slopes of M-Q curve depending on stage of loading
C       of every element
c       *****************************************************************

c       *****************************************************************
C          IHA = 2 indicates that end A has reached last subhinge
C          IHB = 2 indicates that end B has reached last subhinge
C          RKT1 is the slope of M-Q curve at this stage for end A
C          RKT2 is the slope of M-W curve at this stage for end B
C*********************************************************************

        DO 1006 IR=1,IRGJ

        I=IRKT(IR)
        J=JJK1(IR)

        IF((CMA(IR)+RMAD(IR)).EQ.0) JJK1(IR)=0

         IF((CMA(IR)+RMAD(IR)).GE.0.0) THEN
         RKT1(IR)=RKTPX(J,I,IR,1)
          IF(J.GE.4) IHA(IR)=2
         END IF

         IF((CMA(IR)+RMAD(IR)).LT.0.0) THEN
         RKT1(IR)=RKTN(J,I)
          IF(J.GE.4) IHA(IR)=2
         END IF

        IF(J.EQ.-1) THEN
        RKT1(IR)=RKTN(4,I)
        IHA(IR)=2
        END IF

c       write(*,*)'j,i,ir,rkt1(ir)',j,i,ir,rkt1(ir)

1006    CONTINUE
```

```
      DO 1016 IR=1,IRGJ
      I=IRKT(IR)
      J=JJK2(IR)

      IF((CMB(IR)+RMBD(IR)).EQ.0) JJK2(IR)=0

       IF((CMB(IR)+RMBD(IR)).GE.0.0) THEN
       RKT2(IR)=RKTPX(J,I,IR,2)
        IF(J.GE.4) IHB(IR)=2
       END IF

       IF((CMB(IR)+RMBD(IR)).LT.0.0) THEN
       RKT2(IR)=RKTN(J,I)
        IF(J.GE.4) IHB(IR)=2
       END IF

      IF(J.EQ.-1) THEN
      RKT2(IR)=RKTN(4,I)
      IHB(IR)=2
      END IF

c     write(*,*)'j,i,ir,rkt2(ir)',j,i,ir,rkt2(ir)
1016  CONTINUE


      DO 10060 IR=1,IRGJ

      I=IRBT(IR)
      J=JJB1(IR)

      IF((CFA(IR)+RFAD(IR)).EQ.0) JJB1(IR)=0

       IF((CFA(IR)+RFAD(IR)).GE.0.0) THEN
       RBT1(IR)=RBET(J,I)
        IF(J.GE.4) IHBA(IR)=2
       END IF

       IF((CFA(IR)+RFAD(IR)).LT.0.0) THEN
       RBT1(IR)=RBET(J,I)
        IF(J.GE.4) IHBA(IR)=2
       END IF

      IF(J.EQ.-1) THEN
      RBT1(IR)=RBET(4,I)
      IHBA(IR)=2
      END IF

10060  CONTINUE

      DO 10160 IR=1,IRGJ

      I=IRBT(IR)
      J=JJB2(IR)

      IF((CFB(IR)+RFBD(IR)).EQ.0) JJB2(IR)=0
```

```
          IF((CFB(IR)+RFBD(IR)).GE.0.0) THEN
          RBT2(IR)=RBET(J,I)
           IF(J.GE.4) IHBB(IR)=2
          END IF

          IF((CFB(IR)+RFBD(IR)).LT.0.0) THEN
          RBT2(IR)=RBET(J,I)
           IF(J.GE.4) IHBB(IR)=2
          END IF

         IF(J.EQ.-1) THEN
         RBT2(IR)=RBET(4,I)
         IHBB(IR)=2
         END IF

C        WRITE(7,*) ' IR, RBT1,RBT2', IR, RBT1(IR),RBT2(IR)

10160     CONTINUE


         WRITE(*,1007)
         WRITE(7,1007)
1007     FORMAT(/,1X,'- - - - - - - - - - - - - - - - - - - - - - - - - -
     *- - - - - - - - - ',/)

C*********************************************************************
C        If IDDL=0 (calculation of moments  due to dead loads is terminated)
C        then go back to statement with label # 21 for live load analysis
C*********************************************************************

       IF(IDDL.EQ.0) GOTO 21

C*********************************************************************
C        Block 48
C        Update iteration number
C                Check if limiting number of iteration (400) is reached
C                to continue go to statement with label # 1010
C                to STOP go to statement with label # 1011
C
C*********************************************************************

         NSTG=NSTG+1
C        IF (NSTG.EQ.2) GO TO 1011
         IF (NSTG.GT.600) GOTO 1011
         IF(ICONT.EQ.2)THEN
         GO TO 21
         END IF
         GOTO 1010

C*********************************************************************
C        Block 49
C        Print final output then stop
C
C*********************************************************************
```

```
1011    CONTINUE
999     WRITE(*,998) FNAMEO
998     FORMAT(//,5X,'OUT-PUT DATA  FILE :',A16,//,5X,'PLOT CURVE, LOAD
     *  FILE: prfam12.plo  IN WINDOW gnuplot IF YOU WANT ',//,5X,
     *  'AND THEN THE CURVE WILL BE IN FILE :  prfam12.fig',//)

C*********************************************************************
C               Create graphic file for plotting
C*********************************************************************

        CALL FIGPLO(TITLE,NSTG)
        GOTO 996

C*********************************************************************
C               Call WRITDATA to print all input data
C*********************************************************************

995     CALL WRITDATA

996     STOP
        END



C*************************************************************
C       Subroutine HINGE
C       Find min. load factor to make one end of any element
C       reach its next possible sub-hinge
C*************************************************************

        SUBROUTINE HINGE(NSTG,IDDL)
        IMPLICIT REAL*8 (A-H,O-Z)
        COMMON/CONT/ICONT,NBEXYC(100),IBJC(600)
        COMMON/F2/N,N1,IRG,IRGJ,ISG,ISGJ,NBE,IBE,MP,I1,IR,IS,
     *  LQG,IOV,IG
        COMMON/J5/RMA(600),RMB(600)
        COMMON/J7/CUMAX,CFCT,UMAX,FCT,KA,KB,IRGJ1,LDY
        COMMON/J8/RMPA(600),RMPB(600),CMA(600),CMB(600),RKTA(600),
     *  RKTB(600),RMAD(600),RMBD(600)
        COMMON/J9/IHA(600),IHB(600),IIA(600),IIB(600)
        COMMON/H1/CA(600),CB(600),TA(600),TB(600)
        COMMON/Q3/CUMAX0,CFCT0
        COMMON/J3/JJK1(600),JJK2(600)

        COMMON/RV/RV(5,50),RBET(5,50),IRBT(600)
        COMMON/JB3/JJB1(600),JJB2(600)
        COMMON/JB4/RBT(600),RBT1(600),RBT2(600)
        COMMON/JB5/RFA(600),RFB(600)
        COMMON/JB7/KBA,KBB
        COMMON/JB8/RFPA(600),RFPB(600),CFA(600),CFB(600),RBTA(600),
     *  RBTB(600),RFAD(600),RFBD(600)
        COMMON/JB9/IHBA(600),IHBB(600),IIBA(600),IIBB(600)
        COMMON/JB10/RFA0(600),RFB0(600)
        COMMON/JB11/ FFA(600),FFB(600)
```

```
C*********************************************************************
C               intialize variables for first iteration
C
C               CFCT is the cumulative load factor
C               CMA, CMB are cumulative moments at ends A and B
C               CUMAX is the maximum displacement
C*********************************************************************

        IF (NSTG.EQ.0) THEN
        CUMAX=0.
        CFCT=0.
        DO 1 I=1,IRGJ
        CMA(I)=0.0
        CMB(I)=0.0
        CFA(I)=0.0
1       CFB(I)=0.0
        END IF

C*********************************************************************
C               set high load factors as a first check
C               FCT final load factor forthis iteration
C               CA load factor for end A to reach next subhinge
C               CB load factor for end B to reach next subhinge
C*********************************************************************

        FCT=1.0D10
        DO 4 I=1,IRGJ

C       WRITE(7,*) ' MEMBER', I,RMA(I),RMB(I),RFA(I),RFB(I)
        IF (ABS(RMA(I)).LE.1.0D-6) CA(I)=1.0D15
        IF (ABS(RMB(I)).LE.1.0D-6) CB(I)=1.0D15
        IF (ABS(RFA(I)).LE.1.0D-6) TA(I)=1.0D15
        IF (ABS(RFB(I)).LE.1.0D-6) TB(I)=1.0D15
C*********************************************************************
C       To avoid errors due to very small negative moments at
C       simple supports, set CA and CB to be always positive
C*********************************************************************

        IF (ABS(RMA(I)).GT.1.0D-6) THEN
        CA(I)=(RMPA(I)-CMA(I))/RMA(I)
C        IF (RKTA(I).GE.0.0) CA(I)=(RMPA(I)-CMA(I))/RMA(I)
C        IF (RKTA(I).LT.0.0) CA(I)=-(RMPA(I)-CMA(I))/RMA(I)
         IF(JJK1(I).EQ.0) CA(I)=ABS(CA(I))
        END IF
        IF (ABS(RMB(I)).GT.1.0D-6) THEN
        CB(I)=(RMPB(I)-CMB(I))/RMB(I)
C        IF (RKTB(I).GE.0.0) CB(I)=(RMPB(I)-CMB(I))/RMB(I)
C        IF (RKTB(I).LT.0.0) CB(I)=-(RMPB(I)-CMB(I))/RMB(I)
         IF(JJK2(I).EQ.0) CB(I)=ABS(CB(I))
        END IF


        IF (ABS(RFA(I)).GT.1.0D-6) THEN
        TA(I)=(RFPA(I)-CFA(I))/RFA(I)
         IF(JJB1(I).EQ.0) TA(I)=ABS(TA(I))
```

```
        END IF
        IF (ABS(RFB(I)).GT.1.0D-6) THEN
        TB(I)=(RFPB(I)-CFB(I))/RFB(I)
         IF(JJB2(I).EQ.0) TB(I)=ABS(TB(I))
        END IF

        IF (IHA(I).EQ.2) CA(I)=1.0D15
        IF (IHB(I).EQ.2) CB(I)=1.0D15

        IF (IHBA(I).EQ.2) TA(I)=1.0D15
        IF (IHBB(I).EQ.2) TB(I)=1.0D15
C
C       WRITE (7,*) ' CHECK', CA(I),CB(I),TA(I),TB(I)
        IF(ABS(CA(I)).LE.FCT) FCT=abs(CA(I))
        IF(ABS(CB(I)).LE.FCT) FCT=abs(CB(I))
        IF(ABS(TA(I)).LE.FCT) FCT=abs(TA(I))
        IF(ABS(TB(I)).LE.FCT) FCT=abs(TB(I))

c       write(*,*)"ir,ca(i),cb(i)",i,ca(i),cb(i)
c       write(*,*)"ir,ta(i),tb(i)",i,ta(i),tb(i)

4       CONTINUE

      IF(IDDL.LT.1) THEN
       IF((CFCT+FCT).GE.1.0)THEN
       XTEMP=CFCT+FCT-1.0
       FCT=FCT-XTEMP
       IDDL=0

        IF(ICONT.EQ.1)THEN
        IDDL=-2
        ICONT=2

        CFCT=0

        END IF

       ELSE
       IDDL=-1
       END IF
c       CFCT=CFCT+FCT

       IF(NSTG.EQ.0.AND.IDDL.EQ.-1) THEN
       WRITE(*,173)
       WRITE(7,173)
173    FORMAT(/,1X,'SOME ELEMENTS HAVE REACHED YIELDING MOMENT UNDER
     *DEAD LOAD ONLY',/,'CHECK YOUR INPUT DATA TO MAKE SURE THERE IS
     *NO ERROR',/)
        END IF
      END IF

C*********************************************************************
C               identify elements where new subhinges formed
C*********************************************************************
```

```
        if(abs(fct).le.1e-2)then
                fct=1e-2
                write(7,*)"the calculation iterates here"
                write(*,*)"the calculation iterates here"
        end if


        KA=0
        KB=0
        KBA=0
        KBB=0
        DO 14 I=1,IRGJ
        IF(ABS(CA(I)-FCT).LE.1.0D-2) THEN
        KA=KA+1
        IIA(KA)=I
        END IF
        IF(ABS(CB(I)-FCT).LE.1.0D-2) THEN
        KB=KB+1
        IIB(KB)=I
        END IF

        IF(ABS(TA(I)-FCT).LE.1.0D-2) THEN
        KBA=KBA+1
        IIBA(KBA)=I
        END IF
        IF(ABS(TB(I)-FCT).LE.1.0D-2) THEN
        KBB=KBB+1
        IIBB(KBB)=I
        END IF

14      CONTINUE

        CFCT0=CFCT

        RETURN
        END

C*************************************************************
C  Subroutine for calling other procedures to setup equations
C  and solve it
C*************************************************************

        SUBROUTINE QUS
        IMPLICIT REAL*8 (A-H,O-Z)
        COMMON/F1/RKK(300000),P(4000),X(600),Y(600),Z(600),
     *  PX(600),PY(600),PZ(600),RMX(600),RMY(600),RMZ(600)
        COMMON/F2/N,N1,IRG,IRGJ,ISG,ISGJ,NBE,IBE,MP,I1,IR,IS,
     *  LQG,IOV,IG
        COMMON/F3/ER,GR,ES,GS,RMU
        COMMON/F4/IAD(4000),IBB(600),IBBX(6)
        COMMON/R1/IA(600),IB(600),IRR(12)
        COMMON/S1/IAS(600),IBS(600),ICS(600),IDS(600),IRR2(24)
        COMMON/J1/RKK1J(12,12),RLM(12,12),RLM1(12,12),RLM2(12,12),
     *  ASY(600),ASZ(600),RKK1J0(12,12)
        COMMON/J2/IAJ(600),IBJ(600),IIK(600)
        COMMON/J7/CUMAX,CFCT,UMAX,FCT,KA,KB,IRGJ1,LDY
```

```
      COMMON/SJ1/IASJ(200),IBSJ(200),ICSJ(200),IDSJ(200)
      COMMON/SJ2/TJ(200),RKKSJ(24,24)
      COMMON/SJ3/U(24),U1(24),U2(24),SP(3,12),UL(12,600)
      COMMON/N1/EBAR(600),GSHEAR(600),EBEAM(50),GBEAM(50),
     * EBEND(600)
      COMMON/N2/EIG(600),UU(4000),PP(4000)

      COMMON/RV/RV(5,50),RBET(5,50),IRBT(600)
      COMMON/JB3/JJB1(600),JJB2(600)
      COMMON/JB4/RBT(600),RBT1(600),RBT2(600)
      COMMON/JB5/RFA(600),RFB(600)
      COMMON/JB7/KBA,KBB
      COMMON/JB8/RFPA(600),RFPB(600),CFA(600),CFB(600),RBTA(600),
     * RBTB(600),RFAD(600),RFBD(600)
      COMMON/JB9/IHBA(600),IHBB(600),IIBA(600),IIBB(600)
      COMMON/JB10/RFA0(600),RFB0(600)
      COMMON/JB11/ FFA(600),FFB(600)


      DO 55 I=1,I1
55    RKK(I)=0.0

      WRITE(*,200)
200   FORMAT(' SETTING UP STIFFNESS MATRIX OF BEAM ELEMENT ')


c     WRITE(7,*) ' NUMBER OF NODES ', N
c     WRITE(7,*) ' NUMBER OF D.O.F.',N1

      DO 4 IR=1,IRGJ
      CALL RODJ

c     if(ir.eq.2.or.ir.eq.3.or.ir.eq.4.or.ir.eq.15.or.ir.eq.16)then
c     write(*,*)'*********************************'
c     write(*,*)'the number of element is ',ir
c     do 206 i=1,12
c206  write(*,207)(rkk1j0(i,j),j=1,12)
c207  format(6e9.3)
c     end if

      CALL K1PKJ
4     CONTINUE


c     WRITE(7,*) ' NUMBER OF NODES ', N
c     WRITE(7,*) ' NUMBER OF D.O.F.',N1

      IF(ISGJ.EQ.0) GOTO 65
      WRITE(*,205)
205   FORMAT(' SETTING UP STIFFNESS MATRIX OF PLATE ELEMENT ')
      DO 58 IS=1,ISGJ
      CALL PSHELL
      CALL K2PKJ
58    CONTINUE

65    DO 60 J=1,IBE
```

```
        K1=IBB(J)
        K2=IAD(K1)
60      RKK(K2)=1.0D50
C        WRITE(*,1200)(RKK(IAD(I)),I=1,N1)
c        WRITE(7,1200)(RKK(IAD(I)),I=1,N1)
1200    FORMAT(3X,'RKK='/6G12.4)

c       WRITE(7,*) ' NUMBER OF NODES', N

        DO 108 I=1,N
        J=I
C       WRITE(7,*) ' LOADS', I,PX(J),PY(J),PZ(J),RMX(J),RMY(J),RMZ(J)
        P(6*I-5)=PX(I)
        P(6*I-4)=PY(I)
        P(6*I-3)=PZ(I)
        P(6*I-2)=RMX(I)
        P(6*I-1)=RMY(I)
108     P(6*I)=RMZ(I)

        IWARN=1
c       WRITE(7,*) ' NUMBER OF D.O.F.',N1
        DO 2000 I=1,N1
        P(I)=P(I)-PP(I)
        IF ( P(I).NE.0 ) IWARN=0
c       WRITE(7,*) '  D.O.F. ',I,' LOAD',P(I)
2000    CONTINUE

c       write(*,*)'the address of unknown is '
c       write(*,*)'**********************************'
c       write(*,955)(iad(i),i=1,n1)
c955    format(10i8)
c       write(*,*)'the stiffness matrix is'
c       write(*,*)'************************'
c       write(*,956)(rkk(i),i=1,iad(n1))

c956    format(6e10.4)
c       write(*,*)'the force is'
c       write(*,*)'******************************'
c       write(*,956)(p(i),i=1,n1)


        IF(IWARN.EQ.1) WRITE(7,*) ' ALL FORCES ARE EQUAL TO ZERO'

        WRITE(*,210)
210     FORMAT(' SOLVING EQUATIONS ')
        CALL SSSJC

c       DO 2020 I=1,N1
c       WRITE(7,*) '  D.O.F. ',I,' DISPLACEMENT',P(I)
2020    CONTINUE


        RETURN
        END
```

```
C*****************************************************************
C  Subroutine for multiplication of matrix A and B
C*****************************************************************

        SUBROUTINE MMT(M,N,A,B,C)
        IMPLICIT REAL*8 (A-H,O-Z)
        DIMENSION A(M,N),B(N),C(M)
        DO 201 I=1,M
        C(I)=0.0
        DO 202 J=1,N
202     C(I)=C(I)+A(I,J)*B(J)
201     CONTINUE
        RETURN
        END


C*****************************************************************
C  Transpose of matrix A to B
C*****************************************************************

        SUBROUTINE MATTRA(M,N,A,B)
        IMPLICIT REAL*8 (A-H,O-Z)
        DIMENSION A(M,N),B(N,M)
        DO 231 I=1,M
        DO 232 J=1,N
232     B(J,I)=A(I,J)
231     CONTINUE
        RETURN
        END


C*****************************************************************
C  Subroutine for multiplication of matrix A and B
C*****************************************************************

        SUBROUTINE MATMUL(M,N,L,A,B,C)
        IMPLICIT REAL*8 (A-H,O-Z)
        DIMENSION A(M,N),B(N,L),C(M,L)
        DO 241 K=1,L
        DO 242 I=1,M
        C(I,K)=0.0
        DO 243 J=1,N
243     C(I,K)=C(I,K)+A(I,J)*B(J,K)
242     CONTINUE
241     CONTINUE
        RETURN
        END


C*****************************************************************
C   Subroutine to find projections of a vector on X,Y & Z axes
C*****************************************************************
```

```
      SUBROUTINE PROJEC(I,J,N,T,X,Y,Z)
      IMPLICIT REAL*8 (A-H,O-Z)
      DIMENSION T(3),X(N),Y(N),Z(N)
      T(1)=X(I)-X(J)
      T(2)=Y(I)-Y(J)
      T(3)=Z(I)-Z(J)
      RETURN
      END



C*************************************************************
C  Subroutine for the length of two points
C*************************************************************

      SUBROUTINE LENGTH(I,J,N,X,Y,Z,D)
      IMPLICIT REAL*8 (A-H,O-Z)
      DIMENSION X(N),Y(N),Z(N)
      DX=X(I)-X(J)
      DY=Y(I)-Y(J)
      DZ=Z(I)-Z(J)
      D=DSQRT(DX*DX+DY*DY+DZ*DZ)
      RETURN
      END



C*************************************************************
C   Subroutine for solving equations
C*************************************************************

      SUBROUTINE SSSJC
      IMPLICIT REAL*8 (A-H,O-Z)
      COMMON/F1/RKK(300000),P(4000),X(600),Y(600),Z(600),
     *  PX(600),PY(600),PZ(600),RMX(600),RMY(600),RMZ(600)
      COMMON/F2/N,N1,IRG,IRGJ,ISG,ISGJ,NBE,IBE,MP,I1,IR,IS,
     *  LQG,IOV,IG
      COMMON/F4/IAD(4000),IBB(600),IBBX(6)

      DO 211 I=1,N1
      IF(I.EQ.1) GOTO 212
      MI=I-(IAD(I)-IAD(I-1))+1
      GOTO 213
212   MI=I
213   DO 225 J=MI,I
      IF(I.EQ.1) GOTO 214
      IGP=IAD(I-1)+J-MI+1
      GOTO 215
214   IGP=J-MI+1
215   IF(LQG.GT.0.AND.J.EQ.I) GOTO 216
      IF(LQG.GT.0) GOTO 217
      IF(J.EQ.1) GOTO 218
      MJ=J-(IAD(J)-IAD(J-1))+1
```

```
        GOTO 219
218     MJ=J-IAD(J)+1
219     IF(MJ.GE.MI) GOTO 220
        JI=MI
        GOTO 221
220     JI=MJ
221     K1=J-1
        IF(JI.LE.K1) GOTO 222
        GOTO 223
222     DO 224 K=JI,K1
        K2=IAD(I)-I+K
        K3=IAD(K)
        K4=IAD(J)-J+K
224     RKK(IGP)=RKK(IGP)-RKK(K2)*RKK(K3)*RKK(K4)
223     IF(J.EQ.I) GOTO 216
        K5=IAD(J)

        IF(ABS(RKK(K5)).LT.1.0E-15)THEN
        WRITE(*,300)
300    FORMAT(/1X,'Divided by very small value when solving equation',
     *,/,'check your input data file to eliminate this error',/)
       END IF

        RKK(IGP)=RKK(IGP)/RKK(K5)
217     K5=IAD(J)
        P(I)=P(I)-RKK(IGP)*RKK(K5)*P(J)
225     CONTINUE
216     K6=IAD(I)
        IF(RKK(K6).EQ.0.0) GOTO 1000
        P(I)=P(I)/RKK(K6)
211     CONTINUE
        I=N1
226     IF(I.EQ.1)GOTO 233
        MI=I-(IAD(I)-IAD(I-1))+1
        GOTO 234
233     MI=I-IAD(I)+1
234     K7=I-1
        IF(MI.LE.K7) GOTO 227
        GOTO 228
227     DO 229 K=MI,K7
        K9=IAD(I)-I+K
229     P(K)=P(K)-RKK(K9)*P(I)
228     I=I-1
        IF(I.GT.0) GOTO 226
        GOTO 1001
1000    IOV=1
c        WRITE(*,1002)
C        WRITE(7,1002)
1002    FORMAT(3X,'-----------------------------------')
1001    CONTINUE
        RETURN
        END
```

```
C*************************************************************
C   Subroutine for setting up rotation matrix
C*************************************************************

        SUBROUTINE FRLMD(IR)
        IMPLICIT REAL*8 (A-H,O-Z)
        COMMON/J6/CA(600),SA(600)
        COMMON/RP/RLMD(6,6),RLMD1(6,6),P0X(6),P1X(6)

        DO 100 I=1,6
        DO 100 J=1,6
100     RLMD(I,J)=0.0

        RLMD(1,1)=CA(IR)
        RLMD(4,4)=CA(IR)
        RLMD(1,2)=SA(IR)
        RLMD(4,5)=SA(IR)
        RLMD(2,3)=-1.0
        RLMD(5,6)=-1.0
        RLMD(3,1)=-SA(IR)
        RLMD(6,4)=-SA(IR)
        RLMD(3,2)=CA(IR)
        RLMD(6,5)=CA(IR)
        RETURN
        END



C*************************************************************
C   Subroutine for adding beam element stiffness matrix to
C   global matrix
C*************************************************************

        SUBROUTINE K1PKJ
        IMPLICIT REAL*8 (A-H,O-Z)
        COMMON/F1/RKK(300000),P(4000),X(600),Y(600),Z(600),
     *  PX(600),PY(600),PZ(600),RMX(600),RMY(600),RMZ(600)
        COMMON/F2/N,N1,IRG,IRGJ,ISG,ISGJ,NBE,IBE,MP,I1,IR,IS,
     *  LQG,IOV,IG
        COMMON/F4/IAD(4000),IBB(600),IBBX(6)
        COMMON/R1/IA(600),IB(600),IRR(12)
        COMMON/J1/RKK1J(12,12),RLM(12,12),RLM1(12,12),RLM2(12,12),
     *  ASY(600),ASZ(600),RKK1J0(12,12)
        COMMON/J2/IAJ(600),IBJ(600),IIK(600)

        DO 281 J=1,6
        K1=J+6
        IRR(J)=6*(IAJ(IR)-1)+J
281     IRR(K1)=6*(IBJ(IR)-1)+J
        DO 282 J=1,12
        DO 283 K=1,12
        IF(IRR(J).LT.IRR(K))GOTO 283
        K2=IRR(J)
        IC1=IAD(K2)-(IRR(J)-IRR(K))
        RKK(IC1)=RKK(IC1)+RKK1J(J,K)
```

```
283     CONTINUE
282     CONTINUE
        RETURN
        END



C*****************************************************************
C   Subroutine for adding plate element stiffness matrix to
C   global matrix
C*****************************************************************

        SUBROUTINE K2PKJ
        IMPLICIT REAL*8 (A-H,O-Z)
        COMMON/F1/RKK(300000),P(4000),X(600),Y(600),Z(600),
     *  PX(600),PY(600),PZ(600),RMX(600),RMY(600),RMZ(600)
        COMMON/F2/N,N1,IRG,IRGJ,ISG,ISGJ,NBE,IBE,MP,I1,IR,IS,
     *  LQG,IOV,IG
        COMMON/F4/IAD(4000),IBB(600),IBBX(6)
        COMMON/S1/IAS(600),IBS(600),ICS(600),IDS(600),IRR2(24)
        COMMON/SJ1/IASJ(200),IBSJ(200),ICSJ(200),IDSJ(200)
        COMMON/SJ2/TJ(200),RKKSJ(24,24)

        DO 281 J=1,6
        K1=J+6
        K2=J+12
        K3=J+18
        IRR2(J)=6*(IASJ(IS)-1)+J
        IRR2(K1)=6*(IBSJ(IS)-1)+J
        IRR2(K2)=6*(ICSJ(IS)-1)+J
281     IRR2(K3)=6*(IDSJ(IS)-1)+J
        DO 282 J=1,24
        DO 283 K=1,24
        IF(IRR2(J).LT.IRR2(K))GOTO 283
        K4=IRR2(J)
        IC1=IAD(K4)-(IRR2(J)-IRR2(K))
        RKK(IC1)=RKK(IC1)+RKKSJ(J,K)
283     CONTINUE
282     CONTINUE
        RETURN
        END



C*************************************************************
C   Subroutine for setting up plate element stiffness matrix
C*************************************************************

        SUBROUTINE PSHELL
C       NEW SUBROUTINE PSHELL
        IMPLICIT REAL*8 (A-H,O-Z)
        COMMON/F1/RKK(300000),P(4000),X(600),Y(600),Z(600),
     *  PX(600),PY(600),PZ(600),RMX(600),RMY(600),RMZ(600)
        COMMON/F2/N,N1,IRG,IRGJ,ISG,ISGJ,NBE,IBE,MP,I1,IR,IS,
```

```
     *   LQG,IOV,IG
         COMMON/F3/ER,GR,ES,GS,RMU
         COMMON/F5/RUX,RUY,RU1,RUXY
         COMMON/SJ1/IASJ(200),IBSJ(200),ICSJ(200),IDSJ(200)
         COMMON/SJ2/TJ(200),RKKSJ(24,24)
         COMMON/SJ4/RKKX(12,12),RKKY(12,12),RKK3(12,12),RKKXY(12,12)
     *   ,RRL(12,12)
         COMMON/N1/EBAR(600),GSHEAR(600),EBEAM(50),GBEAM(50),
     *   EBEND(600)

         RLB=DSQRT((X(IASJ(IS))-X(IBSJ(IS)))**2
     *   +(Y(IASJ(IS))-Y(IBSJ(IS)))**2
     *   +(Z(IASJ(IS))-Z(IBSJ(IS)))**2)
         RLA=DSQRT((X(IASJ(IS))-X(ICSJ(IS)))**2
     *   +(Y(IASJ(IS))-Y(ICSJ(IS)))**2
     *   +(Z(IASJ(IS))-Z(ICSJ(IS)))**2)
         RLA=RLA*0.5
         RLB=RLB*0.5
         P1=(RLA/RLB)**2
         P2=1./P1

         BET=RLA/RLB
         RETB=1./60./RLA/RLB
         EX=RUX*ES

         EY=RUY*ES

         DX=EX*TJ(IS)**3/12./(1-RMU**2)
         DY=EY*TJ(IS)**3/12./(1-RMU**2)

         D3=RU1*DX

         DXY=RUXY*GS*TJ(IS)**3/12.

         DO 1 I=1,12
         DO 1 J=1,12
     1   RKKX(I,J)=0.0

         RKKX(1,1)=60.
         RKKX(2,1)=0.
         RKKX(2,2)=0.
         RKKX(3,1)=30.
         RKKX(3,2)=0.
         RKKX(3,3)=20.
         RKKX(4,1)=30.
         RKKX(4,2)=0.
         RKKX(4,3)=15.
         RKKX(4,4)=60.
         RKKX(5,1)=0.
         RKKX(5,2)=0.
         RKKX(5,3)=0.
         RKKX(5,4)=0.
         RKKX(5,5)=0.
         RKKX(6,1)=15.
         RKKX(6,2)=0.0
         RKKX(6,3)=10.
```

```
      RKKX(6,4)=30.
      RKKX(6,5)=0.
      RKKX(6,6)=20.
      RKKX(7,1)=-60.
      RKKX(7,2)=0.
      RKKX(7,3)=-30.
      RKKX(7,4)=-30.
      RKKX(7,5)=0.
      RKKX(7,6)=-15.
      RKKX(7,7)=60.
      RKKX(8,1)=0.
      RKKX(8,2)=0.
      RKKX(8,3)=0.
      RKKX(8,4)=0.
      RKKX(8,5)=0.
      RKKX(8,6)=0.
      RKKX(8,7)=0.
      RKKX(8,8)=0.
      RKKX(9,1)=30.
      RKKX(9,2)=0.0
      RKKX(9,3)=10.
      RKKX(9,4)=15.
      RKKX(9,5)=0.0
      RKKX(9,6)=5.
      RKKX(9,7)=-30.
      RKKX(9,8)=0.
      RKKX(9,9)=20.
      RKKX(10,1)=-30.
      RKKX(10,2)=0.
      RKKX(10,3)=-15.
      RKKX(10,4)=-60.
      RKKX(10,5)=0.
      RKKX(10,6)=-30.
      RKKX(10,7)=30.
      RKKX(10,8)=0.
      RKKX(10,9)=-15.
      RKKX(10,10)=60.
      RKKX(11,1)=0.
      RKKX(11,2)=0.
      RKKX(11,3)=0.0
      RKKX(11,4)=0.
      RKKX(11,5)=0.
      RKKX(11,6)=0.
      RKKX(11,7)=0.
      RKKX(11,8)=0.
      RKKX(11,9)=0.0
      RKKX(11,10)=0.
      RKKX(11,11)=0.
      RKKX(12,1)=15.
      RKKX(12,2)=0.
      RKKX(12,3)=5.
      RKKX(12,4)=30.
      RKKX(12,5)=0.
      RKKX(12,6)=10.
      RKKX(12,7)=-15.
      RKKX(12,8)=0.0
```

```
      RKKX(12,9)=10.
      RKKX(12,10)=-30.
      RKKX(12,11)=0.
      RKKX(12,12)=20.
      DO 3 I=1,12
      DO 4 J=1,I
4     RKKX(I,J)=RKKX(I,J)*DX*P2
3     CONTINUE


      RKKY(1,1)=60.
      RKKY(2,1)=-30
      RKKY(2,2)=20.
      RKKY(3,1)=0.
      RKKY(3,2)=0.
      RKKY(3,3)=0.
      RKKY(4,1)=-60.
      RKKY(4,2)=30.
      RKKY(4,3)=0.
      RKKY(4,4)=60.
      RKKY(5,1)=-30.
      RKKY(5,2)=10.
      RKKY(5,3)=0.
      RKKY(5,4)=30.
      RKKY(5,5)=20.
      RKKY(6,1)=0.
      RKKY(6,2)=0.
      RKKY(6,3)=0.
      RKKY(6,4)=0.
      RKKY(6,5)=0.
      RKKY(6,6)=0.
      RKKY(7,1)=30.
      RKKY(7,2)=-15.
      RKKY(7,3)=0.
      RKKY(7,4)=-30.
      RKKY(7,5)=-15.
      RKKY(7,6)=0.
      RKKY(7,7)=60.
      RKKY(8,1)=-15.
      RKKY(8,2)=10.
      RKKY(8,3)=0.
      RKKY(8,4)=15.
      RKKY(8,5)=5.
      RKKY(8,6)=0.
      RKKY(8,7)=-30.
      RKKY(8,8)=20.
      RKKY(9,1)=0.
      RKKY(9,2)=0.
      RKKY(9,3)=0.
      RKKY(9,4)=0.
      RKKY(9,5)=0.
      RKKY(9,6)=0.
      RKKY(9,7)=0.
      RKKY(9,8)=0.
      RKKY(9,9)=0.
      RKKY(10,1)=-30.
```

```
        RKKY(10,2)=15.
        RKKY(10,3)=0.
        RKKY(10,4)=30.
        RKKY(10,5)=15.
        RKKY(10,6)=0.
        RKKY(10,7)=-60.
        RKKY(10,8)=30.
        RKKY(10,9)=0.
        RKKY(10,10)=60.
        RKKY(11,1)=-15.
        RKKY(11,2)=5.
        RKKY(11,3)=0.
        RKKY(11,4)=15.
        RKKY(11,5)=10.
        RKKY(11,6)=0.
        RKKY(11,7)=-30.
        RKKY(11,8)=10.
        RKKY(11,9)=0.
        RKKY(11,10)=30.
        RKKY(11,11)=20.
        RKKY(12,1)=0.
        RKKY(12,2)=0.
        RKKY(12,3)=0.
        RKKY(12,4)=0.
        RKKY(12,5)=0.
        RKKY(12,6)=0.
        RKKY(12,7)=0.
        RKKY(12,8)=0.
        RKKY(12,9)=0.
        RKKY(12,10)=0.
        RKKY(12,11)=0.
        RKKY(12,12)=0.
        DO 13 I=1,12
        DO 14 J=1,I
14      RKKY(I,J)=RKKY(I,J)*DY*P1
13      CONTINUE

C-----------------------------
        RKK3(1,1)=30.
        RKK3(2,1)=-15
        RKK3(2,2)=0.
        RKK3(3,1)=15.
        RKK3(3,2)=-15.
        RKK3(3,3)=0.
        RKK3(4,1)=-30.
        RKK3(4,2)=0.
        RKK3(4,3)=-15.
        RKK3(4,4)=30.
        RKK3(5,1)=0.
        RKK3(5,2)=0.
        RKK3(5,3)=0.
        RKK3(5,4)=15.
        RKK3(5,5)=0.
        RKK3(6,1)=-15.
        RKK3(6,2)=0.
        RKK3(6,3)=0.
```

```
      RKK3(6,4)=15.
      RKK3(6,5)=15.
      RKK3(6,6)=0.
      RKK3(7,1)=-30.
      RKK3(7,2)=15.
      RKK3(7,3)=0.
      RKK3(7,4)=30.
      RKK3(7,5)=0.
      RKK3(7,6)=0.
      RKK3(7,7)=30.
      RKK3(8,1)=15.
      RKK3(8,2)=0.
      RKK3(8,3)=0.
      RKK3(8,4)=0.
      RKK3(8,5)=0.
      RKK3(8,6)=0.
      RKK3(8,7)=-15.
      RKK3(8,8)=0.
      RKK3(9,1)=0.
      RKK3(9,2)=0.
      RKK3(9,3)=0.
      RKK3(9,4)=0.
      RKK3(9,5)=0.
      RKK3(9,6)=0.
      RKK3(9,7)=-15.
      RKK3(9,8)=15.
      RKK3(9,9)=0.
      RKK3(10,1)=30.
      RKK3(10,2)=0.
      RKK3(10,3)=0.
      RKK3(10,4)=-30.
      RKK3(10,5)=-15.
      RKK3(10,6)= 0.
      RKK3(10,7)=-30.
      RKK3(10,8)=0.
      RKK3(10,9)=15.
      RKK3(10,10)=30.
      RKK3(11,1)=0.
      RKK3(11,2)=0.
      RKK3(11,3)=0.
      RKK3(11,4)=-15.
      RKK3(11,5)=0.
      RKK3(11,6)=0.
      RKK3(11,7)=0.
      RKK3(11,8)=0.
      RKK3(11,9)=0.
      RKK3(11,10)=15.
      RKK3(11,11)=0.

      RKK3(12,1)=0.
      RKK3(12,2)=0.
      RKK3(12,3)=0.
      RKK3(12,4)=0.
      RKK3(12,5)=0.
      RKK3(12,6)=0.
      RKK3(12,7)=15.
```

```
        RKK3(12,8)=0.
        RKK3(12,9)=0.
        RKK3(12,10)=-15.
        RKK3(12,11)=-15.
        RKK3(12,12)=0.

        DO 23 I=1,12
        DO 24 J=1,I
24      RKK3(I,J)=RKK3(I,J)*D3
23      CONTINUE

C-------------------------
        RKKXY(1,1)=84.
        RKKXY(2,1)=-6.
        RKKXY(2,2)=8.
        RKKXY(3,1)=6.
        RKKXY(3,2)=0.
        RKKXY(3,3)=8.
        RKKXY(4,1)=-84.
        RKKXY(4,2)=6.
        RKKXY(4,3)=-6.
        RKKXY(4,4)=84.
        RKKXY(5,1)=-6.
        RKKXY(5,2)=-2.
        RKKXY(5,3)=0.
        RKKXY(5,4)=6.
        RKKXY(5,5)=8.
        RKKXY(6,1)=-6.
        RKKXY(6,2)=0.
        RKKXY(6,3)=-8.
        RKKXY(6,4)=6.
        RKKXY(6,5)=0.
        RKKXY(6,6)=8.
        RKKXY(7,1)=-84.
        RKKXY(7,2)=6.
        RKKXY(7,3)=-6.
        RKKXY(7,4)=84.
        RKKXY(7,5)=6.
        RKKXY(7,6)=6.
        RKKXY(7,7)=84.
        RKKXY(8,1)=6.
        RKKXY(8,2)=-8.
        RKKXY(8,3)=0.
        RKKXY(8,4)=-6.
        RKKXY(8,5)=2.
        RKKXY(8,6)=0.
        RKKXY(8,7)=-6.
        RKKXY(8,8)=8.
        RKKXY(9,1)=6.
        RKKXY(9,2)=0.
        RKKXY(9,3)=-2.
        RKKXY(9,4)=-6.
        RKKXY(9,5)=0.
        RKKXY(9,6)=2.
        RKKXY(9,7)=-6.
        RKKXY(9,8)=0.
```

```
      RKKXY(9,9)=8.
      RKKXY(10,1)=84.
      RKKXY(10,2)=-6.
      RKKXY(10,3)=6.
      RKKXY(10,4)=-84.
      RKKXY(10,5)=-6.
      RKKXY(10,6)=-6.
      RKKXY(10,7)=-84.
      RKKXY(10,8)=6.
      RKKXY(10,9)=6.
      RKKXY(10,10)=84.
      RKKXY(11,1)=6.
      RKKXY(11,2)=2.
      RKKXY(11,3)=0.
      RKKXY(11,4)=-6.
      RKKXY(11,5)=-8.
      RKKXY(11,6)=0.
      RKKXY(11,7)=-6.
      RKKXY(11,8)=-2.
      RKKXY(11,9)=0.
      RKKXY(11,10)=6.
      RKKXY(11,11)=8.
      RKKXY(12,1)=-6.
      RKKXY(12,2)=0.
      RKKXY(12,3)=2.
      RKKXY(12,4)=6.
      RKKXY(12,5)=0.
      RKKXY(12,6)=-2.
      RKKXY(12,7)=6.
      RKKXY(12,8)=0.
      RKKXY(12,9)=-8.
      RKKXY(12,10)=-6.
      RKKXY(12,11)=0.
      RKKXY(12,12)=8.
      DO 33 I=1,12
      DO 34 J=1,I
34    RKKXY(I,J)=RKKXY(I,J)*DXY
33    CONTINUE
C-------------------------
      DO 43 I=1,12
      DO 44 J=1,I
44    RKKX(I,J)=RKKX(I,J)+RKKY(I,J)+RKK3(I,J)+RKKXY(I,J)
43    CONTINUE
      DO 5 I=1,24
      DO 5 J=1,24
5     IF (J.GT.I) RKKX(I,J)=RKKX(J,I)
C -------------------------
      DO 53 I=1,12
      DO 53 J=1,12
53    RRL(I,J)=0.
      RRL(1,1)=1.
      RRL(4,4)=1.
      RRL(7,7)=1.
      RRL(10,10)=1.
      RRL(2,2)=2*RLB
      RRL(5,5)=2*RLB
```

```
      RRL(8,8)=2*RLB
      RRL(11,11)=2*RLB
      RRL(3,3)=2*RLA
      RRL(6,6)=2*RLA
      RRL(9,9)=2*RLA
      RRL(12,12)=2*RLA
C-----------------------------
      CALL MATMUL(12,12,12,RKKX,RRL,RKKY)
      CALL MATMUL(12,12,12,RRL,RKKY,RKKX)
      DO 54 I=1,12
      DO 54 J=1,12
54    RKKX(I,J)=RKKX(I,J)*RETB
      DO 56 I=1,24
      DO 56 J=1,I
56    RKKSJ(I,J)=0.0
      RKKSJ(3,3)=RKKX(1,1)
      RKKSJ(4,3)=RKKX(2,1)
      RKKSJ(4,4)=RKKX(2,2)
      RKKSJ(5,3)=RKKX(3,1)
      RKKSJ(5,4)=RKKX(3,2)
      RKKSJ(5,5)=RKKX(3,3)
      RKKSJ(9,3)=RKKX(4,1)
      RKKSJ(9,4)=RKKX(4,2)
      RKKSJ(9,5)=RKKX(4,3)
      RKKSJ(9,9)=RKKX(4,4)
      RKKSJ(10,3)=RKKX(5,1)
      RKKSJ(10,4)=RKKX(5,2)
      RKKSJ(10,5)=RKKX(5,3)
      RKKSJ(10,9)=RKKX(5,4)
      RKKSJ(10,10)=RKKX(5,5)

      RKKSJ(11,3)=RKKX(6,1)
      RKKSJ(11,4)=RKKX(6,2)
      RKKSJ(11,5)=RKKX(6,3)
      RKKSJ(11,9)=RKKX(6,4)
      RKKSJ(11,10)=RKKX(6,5)
      RKKSJ(11,11)=RKKX(6,6)

      RKKSJ(15,3)=RKKX(7,1)
      RKKSJ(15,4)=RKKX(7,2)
      RKKSJ(15,5)=RKKX(7,3)
      RKKSJ(15,9)=RKKX(7,4)
      RKKSJ(15,10)=RKKX(7,5)
      RKKSJ(15,11)=RKKX(7,6)
      RKKSJ(15,15)=RKKX(7,7)

      RKKSJ(16,3)=RKKX(8,1)
      RKKSJ(16,4)=RKKX(8,2)
      RKKSJ(16,5)=RKKX(8,3)
      RKKSJ(16,9)=RKKX(8,4)
      RKKSJ(16,10)=RKKX(8,5)
      RKKSJ(16,11)=RKKX(8,6)
      RKKSJ(16,15)=RKKX(8,7)
      RKKSJ(16,16)=RKKX(8,8)

      RKKSJ(17,3)=RKKX(9,1)
```

```
      RKKSJ(17,4)=RKKX(9,2)
      RKKSJ(17,5)=RKKX(9,3)
      RKKSJ(17,9)=RKKX(9,4)
      RKKSJ(17,10)=RKKX(9,5)
      RKKSJ(17,11)=RKKX(9,6)
      RKKSJ(17,15)=RKKX(9,7)
      RKKSJ(17,16)=RKKX(9,8)
      RKKSJ(17,17)=RKKX(9,9)

      RKKSJ(21,3)=RKKX(10,1)
      RKKSJ(21,4)=RKKX(10,2)
      RKKSJ(21,5)=RKKX(10,3)
      RKKSJ(21,9)=RKKX(10,4)
      RKKSJ(21,10)=RKKX(10,5)
      RKKSJ(21,11)=RKKX(10,6)
      RKKSJ(21,15)=RKKX(10,7)
      RKKSJ(21,16)=RKKX(10,8)
      RKKSJ(21,17)=RKKX(10,9)
      RKKSJ(21,21)=RKKX(10,10)

      RKKSJ(22,3)=RKKX(11,1)
      RKKSJ(22,4)=RKKX(11,2)
      RKKSJ(22,5)=RKKX(11,3)
      RKKSJ(22,9)=RKKX(11,4)
      RKKSJ(22,10)=RKKX(11,5)
      RKKSJ(22,11)=RKKX(11,6)
      RKKSJ(22,15)=RKKX(11,7)
      RKKSJ(22,16)=RKKX(11,8)
      RKKSJ(22,17)=RKKX(11,9)
      RKKSJ(22,21)=RKKX(11,10)
      RKKSJ(22,22)=RKKX(11,11)

      RKKSJ(23,3)=RKKX(12,1)
      RKKSJ(23,4)=RKKX(12,2)
      RKKSJ(23,5)=RKKX(12,3)
      RKKSJ(23,9)=RKKX(12,4)
      RKKSJ(23,10)=RKKX(12,5)
      RKKSJ(23,11)=RKKX(12,6)
      RKKSJ(23,15)=RKKX(12,7)
      RKKSJ(23,16)=RKKX(12,8)
      RKKSJ(23,17)=RKKX(12,9)
      RKKSJ(23,21)=RKKX(12,10)
      RKKSJ(23,22)=RKKX(12,11)
      RKKSJ(23,23)=RKKX(12,12)
      DO 55 I=1,24
      DO 55 J=1,24
      IF(J.GT.I) RKKSJ(I,J)=RKKSJ(J,I)
55    CONTINUE
      RETURN
      END


C*************************************************************
C   Subroutine for finding stress in plate element
```

```
C*************************************************************

      SUBROUTINE STRSPL(SIGPL,IDPR)
      IMPLICIT REAL*8 (A-H,O-Z)
      COMMON/F1/RKK(300000),P(4000),X(600),Y(600),Z(600),
     *  PX(600),PY(600),PZ(600),RMX(600),RMY(600),RMZ(600)
      COMMON/F2/N,N1,IRG,IRGJ,ISG,ISGJ,NBE,IBE,MP,I1,IR,IS,
     *  LQG,IOV,IG
      COMMON/F3/ER,GR,ES,GS,RMU
      COMMON/SJ1/IASJ(200),IBSJ(200),ICSJ(200),IDSJ(200)
      COMMON/SJ2/TJ(200),RKKSJ(24,24)
      COMMON/SJ3/U(24),U1(24),U2(24),SP(3,12),UL(12,600)
      COMMON/SJ4/RKKX(12,12),RKKY(12,12),RKK3(12,12),RKKXY(12,12)
     *  ,RRL(12,12)
      COMMON/N1/EBAR(600),GSHEAR(600),EBEAM(50),GBEAM(50),
     *  EBEND(600)
      COMMON/J7/CUMAX,CFCT,UMAX,FCT,KA,KB,IRGJ1,LDY
      COMMON/N2/EIG(600),UU(4000),PP(4000)
      COMMON/N3/SIG(600),UUP(12),UUP1(12)
      COMMON/Q2/UUU(4000),SITA1(600),SITA2(600),UUUD(4000),SITAD1(600),
     *SITAD2(600)
      DIMENSION ISJ(4)

      SIGPL=0.0
      IX=1
      ISJ(1)=IASJ(IS)
      ISJ(2)=IBSJ(IS)
      ISJ(3)=ICSJ(IS)
      ISJ(4)=IDSJ(IS)
      DO 5045 J=1,4
      UUP(IX)=UUU(6*ISJ(J)-3)
      UUP(IX+1)=UUU(6*ISJ(J)-2)
      UUP(IX+2)=UUU(6*ISJ(J)-1)
      IX=IX+3
5045  CONTINUE
      CALL PSHELL
      CALL MATMUL(12,12,1,RKKX,UUP,UUP1)
      IF(IDPR.EQ.1) THEN
      DO 5050 J=1,4
      IF(J.EQ.1) THEN
      WRITE(*,5080) IS,ISJ(J),(UUP(3*J-3+IX),IX=1,3)
      WRITE(7,5080) IS,ISJ(J),(UUP(3*J-3+IX),IX=1,3)
      ELSE
      WRITE(*,5084) ISJ(J),(UUP(3*J-3+IX),IX=1,3)
      WRITE(7,5084) ISJ(J),(UUP(3*J-3+IX),IX=1,3)
      END IF
      WRITE(*,5082) (UUP1(3*J-3+IX),IX=1,3)
      WRITE(7,5082) (UUP1(3*J-3+IX),IX=1,3)
5050  CONTINUE
      END IF
      DO 5055 J=1,12
      IF(J.EQ.1.OR.J.EQ.4.OR.J.EQ.7.OR.J.EQ.10) GOTO 5055
      IF(DABS(UUP1(J)).GT.SIGPL) SIGPL=UUP1(J)
5055  CONTINUE
5080  FORMAT(' ELEMENT :',I3,'   NODE :',I3,' W=',G12.4,
     *  ' SITX=',G12.4,' SITY=',G12.4)
```

```
5082    FORMAT(25X,'Qz=',G12.4,3X,'Mx=',G12.4,3X,'My=',G12.4)
5084    FORMAT(13X,'   NODE :',I3,' W=',G12.4,
     *  ' SITX=',G12.4,' SITY=',G12.4)
        RETURN
        END



C*************************************************************
C   Subroutine for auto-generation of nodes location and ID
C*************************************************************

        SUBROUTINE LOCAXY(ALFAX,ALFAY)
        IMPLICIT REAL*8 (A-H,O-Z)
        COMMON/F1/RKK(300000),P(4000),X(600),Y(600),Z(600),
     *  PX(600),PY(600),PZ(600),RMX(600),RMY(600),RMZ(600)
        COMMON/F2/N,N1,IRG,IRGJ,ISG,ISGJ,NBE,IBE,MP,I1,IR,IS,
     *  LQG,IOV,IG
        COMMON/J7/CUMAX,CFCT,UMAX,FCT,KA,KB,IRGJ1,LDY
        COMMON/J2/IAJ(600),IBJ(600),IIK(600)
        COMMON/SJ1/IASJ(200),IBSJ(200),ICSJ(200),IDSJ(200)
        COMMON/Q4/IDK(600)
        COMMON/FIJ/FJ(50),RIZ(50),RIY(50),RJ(50),RKTP(5,50),
     *  RKTN(5,50),IRKT(600)
        COMMON/NFIJ/NRKT
        COMMON/DSXY/NDSY,NDSX,DSY(100),IRKTX(100),DSX(20),
     *  IRKTY(20),IDKY(20),IDKX(100)

        IRGJ1=0
        NI=0

        DO 50 I=1,N
50      Z(I)=0.0

c       IF(NDSY.GT.NDSX) GOTO 200
c       IRGJ=(NDSY-1)*NDSX
        DO 100 I=1,NDSX
        DO 90 J=1,NDSY
        NI=NI+1
        X(NI)=DSY(J)*SIN(ALFAY)+(DSX(I)-DSX(1))*COS(ALFAX)
        Y(NI)=DSY(J)*COS(ALFAY)+(DSX(I)-DSX(1))*SIN(ALFAX)
        IF(IRKTY(I).EQ.0) GOTO 90
         IF(J.EQ.1) THEN
         IRGJ1=IRGJ1+1
         IAJ(IRGJ1)=NI
         END IF
         IF(J.EQ.NDSY) THEN
         IBJ(IRGJ1)=NI
         END IF
         IF(J.GT.1.AND.J.LT.NDSY) THEN
         IRGJ1=IRGJ1+1
         IAJ(IRGJ1)=NI
         IBJ(IRGJ1-1)=NI
         END IF
        IRKT(IRGJ1)=IRKTY(I)
        IDK(IRGJ1)=IDKY(I)
```

```
90      CONTINUE
100     CONTINUE
        IRGJ=IRGJ1
        IF(NDSX.EQ.1) GOTO 200
        DO 180 I=1,NDSY
        IF(IRKTX(I).EQ.0) GOTO 180
        DO 190 J=1,NDSX
        NI=I+(J-1)*NDSY
         IF(J.EQ.1) THEN
         IRGJ=IRGJ+1
         IAJ(IRGJ)=NI
         END IF
         IF(J.EQ.NDSX) THEN
         IBJ(IRGJ)=NI
         END IF
         IF(J.GT.1.AND.J.LT.NDSX) THEN
         IRGJ=IRGJ+1
         IAJ(IRGJ)=NI
         IBJ(IRGJ-1)=NI
         END IF
        IRKT(IRGJ)=IRKTX(I)
        IDK(IRGJ)=IDKX(I)
190     CONTINUE
180     CONTINUE
200     RETURN
        END


C*************************************************************
C   Subroutine for writing out all input data
C*************************************************************

        SUBROUTINE WRITDATA
        IMPLICIT REAL*8 (A-H,O-Z)
        COMMON/F1/RKK(300000),P(4000),X(600),Y(600),Z(600),
     *  PX(600),PY(600),PZ(600),RMX(600),RMY(600),RMZ(600)
        COMMON/F2/N,N1,IRG,IRGJ,ISG,ISGJ,NBE,IBE,MP,I1,IR,IS,
     *  LQG,IOV,IG
        COMMON/F3/ER,GR,ES,GS,RMU
        COMMON/F4/IAD(4000),IBB(600),IBBX(6)
        COMMON/F5/RUX,RUY,RU1,RUXY
        COMMON/R1/IA(600),IB(600),IRR(12)
        COMMON/S1/IAS(600),IBS(600),ICS(600),IDS(600),IRR2(24)
        COMMON/FIJ/FJ(50),RIZ(50),RIY(50),RJ(50),RKTP(5,50),
     *  RKTN(5,50),IRKT(600)
        COMMON/NFIJ/NRKT
        COMMON/RMP/RMPP(5,50),RMPN(5,50),RLPP(50),SITMAXP(50),
     *  RLPN(50),SITMAXN(50)
        COMMON/J1/RKK1J(12,12),RLM(12,12),RLM1(12,12),RLM2(12,12),
     *  ASY(600),ASZ(600),RKK1J0(12,12)
        COMMON/J2/IAJ(600),IBJ(600),IIK(600)
        COMMON/J3/JJK1(600),JJK2(600)
        COMMON/J4/RKT(600),RKT1(600),RKT2(600)
        COMMON/J5/RMA(600),RMB(600)
        COMMON/J6/CA(600),SA(600)
```

```
      COMMON/J7/CUMAX,CFCT,UMAX,FCT,KA,KB,IRGJ1,LDY
      COMMON/J8/RMPA(600),RMPB(600),CMA(600),CMB(600),RKTA(600),
     *  RKTB(600),RMAD(600),RMBD(600)
      COMMON/J9/IHA(600),IHB(600),IIA(600),IIB(600)
      COMMON/J10/RMA0(600),RMB0(600)

      COMMON/SJ1/IASJ(200),IBSJ(200),ICSJ(200),IDSJ(200)
      COMMON/SJ2/TJ(200),RKKSJ(24,24)
      COMMON/SJ3/U(24),U1(24),U2(24),SP(3,12),UL(12,600)
      COMMON/SJ4/RKKX(12,12),RKKY(12,12),RKK3(12,12),RKKXY(12,12)
     *  ,RRL(12,12)
      COMMON/N1/EBAR(600),GSHEAR(600),EBEAM(50),GBEAM(50),
     *  EBEND(600)
      COMMON/N2/EIG(600),UU(4000),PP(4000)
      COMMON/N3/SIG(600),UUP(12),UUP1(12)
      COMMON/Q2/UUU(4000),SITA1(600),SITA2(600),UUUD(4000),SITAD1(600),
     *SITAD2(600)
      COMMON/Q3/CUMAX0,CFCT0
      COMMON/Q4/IDK(600)
      COMMON/RP/RLMD(6,6),RLMD1(6,6),P0X(6),P1X(6)
      COMMON/PR/IPRINT(600)
      COMMON/DSXY/NDSY,NDSX,DSY(100),IRKTX(100),DSX(20),
     *  IRKTY(20),IDKY(20),IDKX(100)
      COMMON/IDLOD/NDLDC,NDLDU,NLOAD,NDLDU0(2),IPDU1(10),IPDU2(10),
     * IPDC1(100)
      COMMON/VLOD/PDU0(10),PDC0(600,6),PLC0(600,6)
      COMMON/NPPBE/NPPXY(100),NBEXY(100)

      COMMON/RV/RV(5,50),RBET(5,50),IRBT(600)


      WRITE(7,5)N,IRGJ,IRGJ1,ISGJ,NBE,RMU,IG
5     FORMAT(5X,'N=',I3,5X,'IRGJ=',I3,5X,'IRGJ1=',I3,5X,'ISGJ=',I3/5X,
     *  'NBE=',I3,5X,'RMU=',G12.4,5X,'IG=',I2)

      DO 3030 I=1,NRKT
      WRITE(7,3002)I,FJ(I),RIZ(I),RIY(I),RJ(I),EBEAM(I)
      WRITE(7,3003)RMPP(1,I),RMPP(2,I),RMPP(3,I),RMPP(4,I),RKTP(1,I),
     *  RKTP(2,I),RKTP(3,I),RKTP(4,I),RLPP(I),SITMAXP(I)
      WRITE(7,3004)RMPN(1,I),RMPN(2,I),RMPN(3,I),RMPN(4,I),RKTN(1,I),
     *  RKTN(2,I),RKTN(3,I),RKTN(3,I),RLPN(I),SITMAXN(I)
      WRITE(7,3005) (RV(J,I),J=1,4), (RBET(J,I),J=1,4)

3030  CONTINUE
3003  FORMAT(/,14X,'MPP1=',G12.4,' MPP2=',G12.4,' MPP3=',G12.4,
     *  ' MPP4=',G12.4,/14X,'KTP1=',G12.4,' KTP2=',G12.4,' KTP3=',
     *  G12.4,' KTP4=',G12.4,/,14X,'RLP= ',G12.4,' SITMAXP=',G12.4)
3004  FORMAT(/,14X,'MPN1=',G12.4,' MPN2=',G12.4,' MPN3=',G12.4,
     *  ' MPN4=',G12.4,/14X,'KTN1=',G12.4,' KTN2=',G12.4,' KTN3=',
     *  G12.4,' KTN4=',G12.4,/,14X,'RLN= ',G12.4,' SITMAXN=',G12.4)
3005  FORMAT(/,14X,'RV1  =',G12.4,' RV 2=',G12.4,' RV 3=',G12.4,
     *  ' RV 4=',G12.4,/14X,'KB 1=',G12.4,' KB 2=',G12.4,' KB 3=',
     *  G12.4,' KB 4=',G12.4,/,14X)

3002  FORMAT(/,' MATERIAL :',I3,//1X,'FJ=',G12.4,' IZ=',G12.4,' IY=',
     *  G12.4,' IX=',G12.4,' EBEAM=',G12.4)
```

```
      WRITE(7,3031)
3031  FORMAT(/,5X,'NODE',5X,'X(i)',11X,'Y(i)',11X,'Z(i)',/)
      DO 6 I=1,N
      WRITE(7,7)I,X(I),Y(I),Z(I)
7     FORMAT(4X,I5,3X,G12.4,3X,G12.4,3X,G12.4)
6     CONTINUE

      WRITE(7,3033)
      DO 301 IR=1,IRGJ
      WRITE(7,3034)IR,IAJ(IR),IBJ(IR),IRKT(IR),IDK(IR)
301   CONTINUE
3033  FORMAT(/,'    IR',2X,' IAJ',1X,' IBJ',1X,' IRKT IDK ',/)
3034  FORMAT(1X,5I5)

      IF(ISGJ.NE.0) THEN
      WRITE(7,115) RUX,RUY,RU1,RUXY
115   FORMAT(1X,'RUX,RUY,RU1,RUXY=',4F8.4)
      DO 112 I=1,ISGJ
      WRITE(7,113)I,TJ(I),IASJ(I),IBSJ(I),ICSJ(I),IDSJ(I)
113   FORMAT(3X,'ELEMENT: ',I3,1X,'TJ=',G12.4,1X,'IASJ=',I3,
     1  1X,'IBSJ=',I3,1X,'ICSJ=',1X,I3,1X,'IDSJ=',I3)
112   CONTINUE
      END IF

      WRITE(7,14)(IBB(I),I=1,IBE)
14    FORMAT(3X,'IBB=',3X,10I5)

     IF(NDLDC.GT.0) THEN
      WRITE(7,81)
81    FORMAT(/,' CONCENTRATED DEAD LOAD:',/,
    */,3X,'Node   Pdx   Pdy   Pdz   Mdx   Mdy   Mdz ',/)
      DO 69 I=1,NDLDC
      WRITE(7,79) IPDC1(I),(PDC0(I,J),J=1,6)
79    FORMAT(4X,I5,5X,6G12.4)
69    CONTINUE
     END IF

     IF(NDLDU.GT.0) THEN
      WRITE(7,91)
91    FORMAT(/,' UNIFORM DEAD LOAD:',/,
    */,3X,'From elem.    to elem.          VALUE ',/)
      DO 92 I=1,NDLDU
      WRITE(7,95) IPDU1(I),IPDU2(I),PDU0(I)
95    FORMAT(4X,I5,8X,I5,10X,G12.4)
92    CONTINUE
     END IF

     IF(NLOAD.GT.0) THEN
      WRITE(7,208)NLOAD
208   FORMAT(/,1X,' NO. LIVE LOAD=',I5)
      WRITE(7,264)
264   FORMAT(/,'  NODE      PX         PY          PZ          RMX
    *       RMY       RMZ  ',/)
      DO 265 I=1,NLOAD
      J=NPPXY(I)
```

```
      WRITE(7,266) J,(PLC0(I,J1),J1=1,6)
266     FORMAT(2X,I3,6(G12.4))
265     CONTINUE
      END IF

        WRITE(7,1007)
1007    FORMAT(/,1X,'*****************************************************
     ********************* ',/)
      WRITE(7,1017)
1017  FORMAT(5X,'OUTPUT OF ANALYSIS')
      WRITE(7,1007)

        CALL PLOTXY

        RETURN
        END



C*************************************************************
C   Subroutine for generation of plotting file for plan view
C*************************************************************

        SUBROUTINE PLOTXY
        IMPLICIT REAL*8 (A-H,O-Z)
        COMMON/F1/RKK(300000),P(4000),X(600),Y(600),Z(600),
     *  PX(600),PY(600),PZ(600),RMX(600),RMY(600),RMZ(600)
        COMMON/F2/N,N1,IRG,IRGJ,ISG,ISGJ,NBE,IBE,MP,I1,IR,IS,
     *  LQG,IOV,IG
        COMMON/J2/IAJ(600),IBJ(600),IIK(600)
        COMMON/IDLOD/NDLDC,NDLDU,NLOAD,NDLDU0(2),IPDU1(10),IPDU2(10),
     * IPDC1(100)
       COMMON/VLOD/PDU0(10),PDC0(600,6),PLC0(600,6)
       COMMON/NPPBE/NPPXY(100),NBEXY(100)


        OPEN(20,FILE='prfam12xy.plo',STATUS='UNKNOWN')
        OPEN(22,FILE='prfam12xy.dat',STATUS='UNKNOWN')
        OPEN(24,FILE='prfam12xy.dat1',STATUS='UNKNOWN')
        OPEN(26,FILE='prfam12xy.dat2',STATUS='UNKNOWN')

c       OPEN(20,STATUS='UNKNOWN')
c       OPEN(22,STATUS='UNKNOWN')
c       OPEN(24,STATUS='UNKNOWN')
c       OPEN(26,STATUS='UNKNOWN')

        YMAX=Y(IAJ(1))
        XMAX=X(IAJ(1))
        YMIN=Y(IAJ(1))
        XMIN=X(IAJ(1))
        DO 200 IR=1,IRGJ
        IF(YMAX.LT.Y(IAJ(IR))) YMAX=Y(IAJ(IR))
        IF(XMAX.LT.X(IAJ(IR))) XMAX=X(IAJ(IR))
        IF(YMIN.GT.Y(IAJ(IR))) YMIN=Y(IAJ(IR))
        IF(XMIN.GT.X(IAJ(IR))) XMIN=X(IAJ(IR))
        IF(YMAX.LT.Y(IBJ(IR))) YMAX=Y(IBJ(IR))
```

```
      IF(XMAX.LT.X(IBJ(IR))) XMAX=X(IBJ(IR))
      IF(YMIN.GT.Y(IBJ(IR))) YMIN=Y(IBJ(IR))
      IF(XMIN.GT.X(IBJ(IR))) XMIN=X(IBJ(IR))
200   CONTINUE

      IF(YMAX-YMIN.GT.1.0E-10) THEN
      RATIOX=8.3125/(YMAX-YMIN)
      ELSE
      RATIOX=1.0E20
      END IF

      IF(XMAX-XMIN.GT.1.0E-10) THEN
      RATIOY=6.25/(XMAX-XMIN)
      ELSE
      RATIOY=1.0E20
      END IF

      IF(RATIOX.LE.RATIOY) THEN
      YMAXP=YMAX
      YMINP=YMIN
      XMAXP=RATIOY*XMAX/RATIOX
      XMINP=RATIOY*XMIN/RATIOX
      ELSE
      XMAXP=XMAX
      XMINP=XMIN
      YMAXP=RATIOX*YMAX/RATIOY
      YMINP=RATIOX*YMIN/RATIOY
      END IF

      NPXY=0
      DO 220 IR=1,IRGJ
      WRITE(22,*) Y(IAJ(IR)),X(IAJ(IR))
      WRITE(22,*) Y(IBJ(IR)),X(IBJ(IR))
      NPXY=NPXY+2
      IF(IBJ(IR).NE.IAJ(IR+1).AND.IR.LT.IRGJ) THEN
      WRITE(22,*)
      NPXY=NPXY+1
      END IF
220   CONTINUE

      DO 320 I=1,NBE
      WRITE(24,*) Y(NBEXY(I)),X(NBEXY(I))
      WRITE(24,*) Y(NBEXY(I)),X(NBEXY(I))
      WRITE(24,*)
320   CONTINUE

      DO 420 I=1,NLOAD
      WRITE(26,*) Y(NPPXY(I)),X(NPPXY(I))
      WRITE(26,*) Y(NPPXY(I)),X(NPPXY(I))
      WRITE(26,*)
420   CONTINUE

      WRITE(20,90)
90    FORMAT('set term postscript',/,'set output "prfam12xy.fig"')
      WRITE(20,95)
95    FORMAT('show output')
```

```
      WRITE(20,97)
97    FORMAT('set title" PLOT OF X-Y COORDINATES "')
      WRITE(20,100) NPXY+3*NBE+3*NLOAD+5
100   FORMAT('set nogrid',/,'set samples ',I5,/,'set nokey',
     * /,'set xlabel "Y-dimension"',/,'set ylabel "X-dimension"')
      WRITE(20,110) YMINP,YMAXP
110   FORMAT('set xrange [',G12.4,':',G12.4,']')
      WRITE(20,120) XMINP,XMAXP
120   FORMAT('set yrange [',G12.4,':',G12.4,']')
      WRITE(20,130)
130   FORMAT('plot "prfam12xy.dat" with lines,"prfam12xy.dat1"
     * with linesp 1 3,"prfam12xy.dat2" with linesp 1 4')

      RETURN
      END


C*************************************************************
C     Subroutine for auto-generation of system including load
C     Due to the complexity of explanation of input data in
C     this procedure, it is recommended to find the definition
C     of concerned data in operation manual
C*************************************************************

      SUBROUTINE AUTOXY(NAUTXY)
      IMPLICIT REAL*8 (A-H,O-Z)
      COMMON/F1/RKK(300000),P(4000),X(600),Y(600),Z(600),
     *  PX(600),PY(600),PZ(600),RMX(600),RMY(600),RMZ(600)
      COMMON/F2/N,N1,IRG,IRGJ,ISG,ISGJ,NBE,IBE,MP,I1,IR,IS,
     *  LQG,IOV,IG
      COMMON/F3/ER,GR,ES,GS,RMU
      COMMON/F4/IAD(4000),IBB(600),IBBX(6)
      COMMON/F5/RUX,RUY,RU1,RUXY
      COMMON/R1/IA(600),IB(600),IRR(12)
      COMMON/S1/IAS(600),IBS(600),ICS(600),IDS(600),IRR2(24)
      COMMON/FIJ/FJ(50),RIZ(50),RIY(50),RJ(50),RKTP(5,50),
     *  RKTN(5,50),IRKT(600)
      COMMON/NFIJ/NRKT
      COMMON/RMP/RMPP(5,50),RMPN(5,50),RLPP(50),SITMAXP(50),
     *  RLPN(50),SITMAXN(50)
      COMMON/J1/RKK1J(12,12),RLM(12,12),RLM1(12,12),RLM2(12,12),
     *  ASY(600),ASZ(600),RKK1J0(12,12)
      COMMON/J2/IAJ(600),IBJ(600),IIK(600)
      COMMON/J3/JJK1(600),JJK2(600)
      COMMON/J4/RKT(600),RKT1(600),RKT2(600)
      COMMON/J5/RMA(600),RMB(600)
      COMMON/J6/CA(600),SA(600)
      COMMON/J7/CUMAX,CFCT,UMAX,FCT,KA,KB,IRGJ1,LDY
      COMMON/J8/RMPA(600),RMPB(600),CMA(600),CMB(600),RKTA(600),
     *  RKTB(600),RMAD(600),RMBD(600)
      COMMON/J9/IHA(600),IHB(600),IIA(600),IIB(600)
      COMMON/J10/RMA0(600),RMB0(600)
      COMMON/SJ1/IASJ(200),IBSJ(200),ICSJ(200),IDSJ(200)
      COMMON/SJ2/TJ(200),RKKSJ(24,24)
      COMMON/SJ3/U(24),U1(24),U2(24),SP(3,12),UL(12,600)
```

```
      COMMON/SJ4/RKKX(12,12),RKKY(12,12),RKK3(12,12),RKKXY(12,12)
     *  ,RRL(12,12)
      COMMON/N1/EBAR(600),GSHEAR(600),EBEAM(50),GBEAM(50),
     *  EBEND(600)
      COMMON/N2/EIG(600),UU(4000),PP(4000)
      COMMON/N3/SIG(600),UUP(12),UUP1(12)
      COMMON/Q2/UUU(4000),SITA1(600),SITA2(600),UUUD(4000),SITAD1(600),
     *SITAD2(600)
      COMMON/Q3/CUMAX0,CFCT0
      COMMON/Q4/IDK(600)
      COMMON/RP/RLMD(6,6),RLMD1(6,6),P0X(6),P1X(6)
      COMMON/PR/IPRINT(600)
      COMMON/DSXY/NDSY,NDSX,DSY(100),IRKTX(100),DSX(20),
     *  IRKTY(20),IDKY(20),IDKX(100)
      COMMON/IDLOD/NDLDC,NDLDU,NLOAD,NDLDU0(2),IPDU1(10),IPDU2(10),
     * IPDC1(100)
      COMMON/VLOD/PDU0(10),PDC0(600,6),PLC0(600,6)
      COMMON/NPPBE/NPPXY(100),NBEXY(100)

      READ(1,199) X$
      READ(1,199) X$
      READ(1,*,ERR=995) RMU,IG,LDY

      READ(1,199) X$
      READ(1,199) X$
      READ(1,*,ERR=995) NRKT
      DO 3020 I=1,NRKT
      READ(1,*,ERR=995) FJ(I),RIZ(I),RIY(I),RJ(I),EBEAM(I)
      IF(LDYY.EQ.2) GOTO 3020
      READ(1,*,ERR=995) (RMPP(J,I),J=1,4)
      READ(1,*,ERR=995) (RKTP(J,I),J=1,4)
      READ(1,*,ERR=995) RLPP(I),SITMAXP(I)
      READ(1,*,ERR=995) (RMPN(J,I),J=1,4)
      READ(1,*,ERR=995) (RKTN(J,I),J=1,4)
      READ(1,*,ERR=995) RLPN(I),SITMAXN(I)
3020  CONTINUE

      IF(LDYY.NE.2) THEN
      DO 3022 I=1,NRKT
      DO 3024 J=1,4
      RKTP(J,I)=RKTP(J,I)/RLPP(I)
3024  RKTN(J,I)=RKTN(J,I)/RLPN(I)
      IF(RKTP(J,I).EQ.0.0) RKTP(J,I)=0.5
      IF(RKTN(J,I).EQ.0.0) RKTN(J,I)=0.5
3022  CONTINUE
      END IF

      READ(1,199) X$
      READ(1,199) X$
199   FORMAT(A64)
      READ(1,*,ERR=995) NDSX,NDSY,ALFAX,ALFAY
      N=NDSX*NDSY
      N1=6*N
      READ(1,*,ERR=995)(DSX(I),I=1,NDSX)
      READ(1,*,ERR=995)(IRKTY(I),I=1,NDSX)
      READ(1,*,ERR=995)(DSY(I),I=1,NDSY)
```

```
      READ(1,*,ERR=995)(IRKTX(I),I=1,NDSY)
      DO 370 I=1,10
370   IDKY(I)=0
      DO 375 I=1,100
375   IDKX(I)=0
      CALL LOCAXY(ALFAX,ALFAY)

      IF(NAUTXY.EQ.1) GOTO 6500
      DO 200 IR=1,IRGJ
      DX=X(IBJ(IR))-X(IAJ(IR))
      DY=Y(IBJ(IR))-Y(IAJ(IR))
      DZ=Z(IBJ(IR))-Z(IAJ(IR))
      RL1=DSQRT(DX*DX+DY*DY+DZ*DZ)
      IF(RL1.LT.1.0E-20) THEN
      WRITE(*,202) IR
202   FORMAT(' THE LENGTH OF BEAM ELEMENT ',I5,' IS ZERO')
      GOTO 995
      END IF
      CA(IR)=DX/RL1
      SA(IR)=DY/RL1
200   CONTINUE

      DO 85 I=1,NRKT
85    GBEAM(I)=EBEAM(I)/2.0/(1.0+RMU)

      IF(IG.EQ.1 ) THEN
      READ(1,*,ERR=995)(ASY(I),I=1,IRGJ)
      READ(1,*,ERR=995)(ASZ(I),I=1,IRGJ)
      END IF

11    READ(1,199) X$
      READ(1,199) X$
      READ(1,*,ERR=995) ISGJ
      IF(ISGJ.EQ.0) GOTO 111
      READ(1,*,ERR=995) ES
      GS=ES/2.0/(1.0+RMU)
      READ(1,*,ERR=995) RUX,RUY,RU1,RUXY
      READ(1,*,ERR=995)(TJ(I),I=1,ISGJ)
      READ(1,*,ERR=995)(IASJ(I),I=1,ISGJ)
      READ(1,*,ERR=995)(IBSJ(I),I=1,ISGJ)
      READ(1,*,ERR=995)(ICSJ(I),I=1,ISGJ)
      READ(1,*,ERR=995)(IDSJ(I),I=1,ISGJ)
      DO 86 I=1,ISGJ
86    EBEND(I)=ES

111   READ(1,199) X$
      READ(1,199) X$
      READ(1,*,ERR=995) NBE
      IBE=0
      DO 117 I=1,NBE
      READ(1,*,ERR=995) JX,JY,(IBBX(J),J=1,6)
      IX=(JX-1)*NDSY+JY
      NBEXY(I)=IX
      DO 116 J=1,6
      IF(IBBX(J).EQ.1) THEN
      IBE=IBE+1
```

```
        IBB(IBE)=6*IX-6+J
        END IF
116     CONTINUE
117     CONTINUE

        DO 44 K=1,N
        IW=0
        DO 2 IR=1,IRGJ
        IF(IAJ(IR).EQ.K.OR.IBJ(IR).EQ.K) GOTO 3
        GOTO 2
3       IF(K-IAJ(IR).GE.IW) IW=K-IAJ(IR)
        IF(K-IBJ(IR).GE.IW) IW=K-IBJ(IR)
2       CONTINUE

        DO 145 IS=1,ISGJ
        IF(IASJ(IS).EQ.K.OR.IBSJ(IS).EQ.K.OR.
     *  ICSJ(IS).EQ.K.OR.IDSJ(IS).EQ.K) GOTO 146
        GOTO 145
146     IF(K-IASJ(IS).GE.IW) IW=K-IASJ(IS)
        IF(K-IBSJ(IS).GE.IW) IW=K-IBSJ(IS)
        IF(K-ICSJ(IS).GE.IW) IW=K-ICSJ(IS)
        IF(K-IDSJ(IS).GE.IW) IW=K-IDSJ(IS)
145     CONTINUE

        IW=6*(IW+1)
        IAD(6*K)=IW
        IAD(6*K-1)=IW-1
        IAD(6*K-2)=IW-2
        IAD(6*K-3)=IW-3
        IAD(6*K-4)=IW-4
        IAD(6*K-5)=IW-5
44      CONTINUE
        IAD(1)=1
        DO 52 I=2,N1
        IAD(I)=IAD(I)+IAD(I-1)
52      I1=IAD(I)

        DO 12 I=1,N
        PX(I)=0.0
        PY(I)=0.0
        PZ(I)=0.0
        RMX(I)=0.0
        RMY(I)=0.0
12      RMZ(I)=0.0
        READ(1,199)X$
        READ(1,199) X$
        READ(1,*,ERR=995) NDLDC
        IF(NDLDC.EQ.0) GOTO 17
        DO 16 I=1,NDLDC
        READ(1,*,ERR=995)JX,JY,PX0,PY0,PZ0,RMX0,RMY0,RMZ0
        J=(JX-1)*NDSY+JY
        PX(J)=PX0
        PY(J)=PY0
        PZ(J)=PZ0
        RMX(J)=RMX0
        RMY(J)=RMY0
```

```
16      RMZ(J)=RMZ0

17      READ(1,199)X$
        READ(1,199) X$
        NDLDU=0
        READ(1,*,ERR=995) NDLDU0(1),NDLDU0(2)
c       WRITE(7,6480) NDLDU
c6480   FORMAT(' NO. OF UNI. LOAD=',I5)
        IF(NDLDU0(1).EQ.0.AND.NDLDU0(2).EQ.0) GOTO 6500
        NI=0
        DO 6493 I0=1,2
        NDLDU=NDLDU0(I0)
        DO 6495 I=1,NDLDU
        READ(1,*,ERR=995)J1,J2,PDU0(I)
        IF(I0.EQ.2) THEN
        NI=IRGJ1
        NX=NDSY
        ELSE
        NI=0
        NX=NDSX
        END IF
        DO 35 J0=1,NX
        IF(J0.EQ.J1) GOTO 38
        IF(I0.EQ.1) NI=NI+NDSY-1
        IF(I0.EQ.2) NI=NI+NDSX-1
35      CONTINUE
        GOTO 6495
38      IF(I0.EQ.1) J2=NI+(J2-J1+1)*(NDSY-1)
        IF(I0.EQ.2) J2=NI+(J2-J1+1)*(NDSX-1)
        J1=NI+1
        DO 19 IR=J1,J2
        DO 20 IX=1,6
20      P0X(IX)=0.0
        CALL LENGTH(IBJ(IR),IAJ(IR),N,X,Y,Z,RL1)
        RMAD(IR)=-PDU0(I)*RL1*RL1/12.0
        RMBD(IR)=-PDU0(I)*RL1*RL1/12.0
        P0X(2)=-PDU0(I)*RL1/2.0
        P0X(6)=RMAD(IR)
        CALL FRLMD(IR)
        CALL MATTRA(6,6,RLMD,RLMD1)
        CALL MMT(6,6,RLMD1,P0X,P1X)
        J=IAJ(IR)
        PX(J)=P1X(1)+PX(J)
        PY(J)=P1X(2)+PY(J)
        PZ(J)=P1X(3)+PZ(J)
        RMX(J)=P1X(4)+RMX(J)
        RMY(J)=P1X(5)+RMY(J)
        RMZ(J)=P1X(6)+RMZ(J)
        P0X(6)=-P0X(6)
        CALL MMT(6,6,RLMD1,P0X,P1X)
        J=IBJ(IR)
        PX(J)=P1X(1)+PX(J)
        PY(J)=P1X(2)+PY(J)
        PZ(J)=P1X(3)+PZ(J)
        RMX(J)=P1X(4)+RMX(J)
        RMY(J)=P1X(5)+RMY(J)
```

```
        RMZ(J)=P1X(6)+RMZ(J)
19      CONTINUE
6495    CONTINUE
6493    CONTINUE
        NDLDU=NDLDU0(1)+NDLDU0(2)
        GOTO 6500
995     NAUTXY=-1

6500    RETURN
        END


C*************************************************************
C   Subroutine for generation of plotting file for applied load
C   vs. displacement curves
C*************************************************************

        SUBROUTINE FIGPLO(TITLE,NSTG)
        IMPLICIT REAL*8 (A-H,O-Z)
        CHARACTER*64 TITLE
        COMMON/J7/CUMAX,CFCT,UMAX,FCT,KA,KB,IRGJ1,LDY
        NSTG1=NSTG+5
        XF=CUMAX*1.05
        YF=CFCT*1.05
        WRITE(8,90)
90      FORMAT('set term postscript',/,'set output "prfam12.fig"')
        WRITE(8,95)
95      FORMAT('show output')
        WRITE(8,97)TITLE
97      FORMAT('set title"',A64,'"')
        WRITE(8,100)NSTG1
100     FORMAT('set grid',/,'set samples',I4,/,'set nokey',
     *  /,'set xlabel "Deflection"',/,'set ylabel "Load Factor "')
        WRITE(8,110) XF
110     FORMAT('set xrange [0.0:',G12.4,']')
        WRITE(8,120) YF
120     FORMAT('set yrange [0.0:',G12.4,']')
        WRITE(8,130)
130     FORMAT('plot "figpvd12.dat" with linespoints')

        WRITE(8,92)
92      FORMAT('set term postscript',/'set output "prfam12bm.fig"')
        WRITE(8,95)
        WRITE(8,97)TITLE
        WRITE(8,100)NSTG1
        WRITE(8,110) XF
        WRITE(8,120) YF
        WRITE(8,140)
140     FORMAT('plot "figpvd12bm.dat" with linespoints')

        RETURN
        END

C*************************************************************
C   Subroutine for setting up beam element stiffness matrix
```

```
C***********************************************************

      SUBROUTINE RODJ
C     IG=0  NEGLECT  SHEAR DEFORMATION
C     IG=1  INCLUDE  SHEAR DEFORMATION
      IMPLICIT REAL*8 (A-H,O-Z)
      COMMON/FUN0/KGIRD
      COMMON/FUN00/PFORCE,PECCEN,FS4
      COMMON/CONT/ICONT,NBEXYC(100),IBJC(600)
      COMMON/F1/RKK(300000),P(4000),X(600),Y(600),Z(600),
     *  PX(600),PY(600),PZ(600),RMX(600),RMY(600),RMZ(600)
      COMMON/F2/N,N1,IRG,IRGJ,ISG,ISGJ,NBE,IBE,MP,I1,IR,IS,
     *  LQG,IOV,IG
      COMMON/F3/ER,GR,ES,GS,RMU
      COMMON/J7/CUMAX,CFCT,UMAX,FCT,KA,KB,IRGJ1,LDY
      COMMON/R1/IA(600),IB(600),IRR(12)
      COMMON/J1/RKK1J(12,12),RLM(12,12),RLM1(12,12),RLM2(12,12),
     *  ASY(600),ASZ(600),RKK1J0(12,12)
      COMMON/J2/IAJ(600),IBJ(600),IIK(600)
      COMMON/J3/JJK1(600),JJK2(600)
      COMMON/J4/RKT(600),RKT1(600),RKT2(600)
      COMMON/J6/CA(600),SA(600)
      COMMON/N1/EBAR(600),GSHEAR(600),EBEAM(50),GBEAM(50),
     *  EBEND(600)
      COMMON/FIJ/FJ(50),RIZ(50),RIY(50),RJ(50),RKTP(5,50),
     *  RKTN(5,50),IRKT(600)
      COMMON/NFIJ/NRKT

      COMMON/JB3/JJB1(600),JJB2(600)
      COMMON/JB4/RBT(600),RBT1(600),RBT2(600)



      REAL*8 FE1(3,3),FE2(3,3),FB(3,3),EQ(3,3),TEMP(3,3),TEMP2(3,3)
      REAL*8 STIF22(3,3),STIF11(3,3),STIF12(3,3),STIF21(3,3)
      REAL*8 RL,E,RIZ1,A


      IX=IRKT(IR)
      EBEAMX=EBEAM(IX)
      GBEAMX=GBEAM(IX)
      GBEAMT=GBEAM(IX)
      FJX=FJ(IX)
      RIZX=RIZ(IX)
      RIYX=RIY(IX)
      RJX=RJ(IX)
      ASYG=ASY(IX)
      ASZG=AS2(IX)

      CALL LENGTH(IBJ(IR),IAJ(IR),N,X,Y,Z,RL1)
      IF(RL1.EQ.0.0) THEN
      WRITE(*,201) IR
201   FORMAT(' LENGTH OF BEAM ELEMENT ',I5,' IS ZERO')
      END IF
```

```
      FY=0.0
      FZ=0.0
      IF(IG.EQ.1) THEN
      IF (ASYG.GT.0.) FY=12*EBEAMX*RIZX/GBEAMX/ASYG/RL1**2
      IF (ASZG.GT.0.) FZ=12*EBEAMX*RIYX/GBEAMX/ASZG/RL1**2
      END IF

      H1=EBEAMX*FJX/RL1
      H2=GBEAMT*RJX/RL1
      H3=12*EBEAMX*RIZX/(1+FY)/RL1**3
      H4=12*EBEAMX*RIYX/(1+FZ)/RL1**3
      H5=6*EBEAMX*RIZX/(1+FY)/RL1**2
      H6=6*EBEAMX*RIYX/(1+FZ)/RL1**2
      H7=(4+FZ)*EBEAMX*RIYX/(1+FZ)/RL1
      H8=(4+FY)*EBEAMX*RIZX/(1+FY)/RL1
      H9=(2-FZ)*EBEAMX*RIYX/(1+FZ)/RL1
      H10=(2-FY)*EBEAMX*RIZX/(1+FY)/RL1


C
C     PROGRAM TO CALCULATE THE STIFFNESS MATRIX
C     FOR A BEAM WITH ROTATIONAL AND DISPLACEMENT
C     SPRINGS AT BOTH OR EITHER ENDS.
C
C
C
C
c     RL=100.
c     E=29000000.
c     RIZ1=11000.
c     A=100.

      RL=RL1
      E=EBEAMX
      RIZ1=RIZX
      A=FJX


      BETA1=1.0E16
      BETA2=1.0E16
      RK1=1.0E16
      RK2=1.0E16

      IF(ICONT.EQ.1.AND.IBJC(IR).EQ.1)RK2=1.0E-16

      RLAMDA=1.0E16
      IF (ASZG.NE.0) RLAMDA=GBEAMX*ASZG/RL
      IF(JJK1(IR).NE.0) RK1=RKT1(IR)
      IF(JJK2(IR).NE.0) RK2=RKT2(IR)

      IF (IG.EQ.1) THEN

      BETA=0.

      IF(JJB1(IR).NE.0 .AND.JJB2(IR).EQ.0) BETA=(RBT1(IR)+GBEAMX)/2.
      IF(JJB1(IR).EQ.0 .AND.JJB2(IR).NE.0) BETA=(RBT2(IR)+GBEAMX)/2.
```

```
      IF(JJB1(IR).NE.0 .AND.JJB2(IR).NE.0) BETA=(RBT1(IR)+RBT2(IR))/2.
      IF (BETA.NE.0 .AND. ASZG.NE.0) RLAMDA=BETA*ASZG/RL

      END IF

c     WRITE(7,*) ' IR =',IR,' -------->>   RLAMDA ',RLAMDA

C
C     WRITE(8,*)
C     WRITE(8,*)
C     WRITE(8,*) NK1,NK2,NB1,NB2
C     WRITE(8,*)
C     WRITE(7,*) ' BETA1,BETA2,RK1,RK2,RLAMDA', BETA1,BETA2,RK1,RK2,RLAMDA
C     WRITE(8,*)
C
      DO 10 I=1,3
      DO 10 J=1,3
      FE1(I,J)=0.
      FE2(I,J)=0.
      FB(I,J)=0.
      EQ(I,J)=0.
      TEMP(I,J)=0.
      TEMP2(I,J)=0.
      STIF22(I,J)=0.
      STIF11(I,J)=0.
      STIF12(I,J)=0.
      STIF21(I,J)=0.
10    CONTINUE
C
      FE1(2,2)=1./BETA1
      FE1(3,3)=1./RK1
C
      FE2(2,2)=1./BETA2
      FE2(3,3)=1./RK2
C     WRITE(8,*) ' MATRIX FE1'
      DO 11 I=1,3
C     WRITE(8,200) (FE1(I,J),J=1,3)
11    CONTINUE

C     WRITE(8,*) ' MATRIX FE2'
      DO 12 I=1,3
C     WRITE(8,200) (FE2(I,J),J=1,3)
12    CONTINUE

C
      FB(1,1)=RL/(E*A)
      FB(2,2)=RL**3/(3*E*RIZ1)+1./RLAMDA
      FB(2,3)=RL*RL/(2*E*RIZ1)
      FB(3,3)=RL/(E*RIZ1)
      FB(3,2)=FB(2,3)

      EQ(1,1)=1.
      EQ(2,2)=1.
      EQ(3,2)=RL
      EQ(3,3)=1.
C     WRITE(8,*) ' MATRIX EQ'
```

```
      DO 14 I=1,3
C     WRITE(8,200) (EQ(I,J),J=1,3)
14    CONTINUE

C
      DO 20 I=1,3
      DO 20 J=1,3
      DO 20 K=1,3
      TEMP(I,J)=FE1(I,K)*EQ(K,J)+TEMP(I,J)
20    CONTINUE
C
C     WRITE(8,*) ' MATRIX TEMP'
      DO 21 I=1,3
C     WRITE(8,200) (TEMP(I,J),J=1,3)
21    CONTINUE

      DO 30 I=1,3
      DO 30 J=1,3
      DO 30 K=1,3
      TEMP2(I,J)=EQ(K,I)*TEMP(K,J)+TEMP2(I,J)
30    CONTINUE

C     WRITE(8,*) ' MATRIX TEMP2'
      DO 31 I=1,3
C     WRITE(8,200) (TEMP2(I,J),J=1,3)
31    CONTINUE
C
      DO 40 I=1,3
      DO 40 J=1,3
      FB(I,J)=FB(I,J)+TEMP2(I,J)+FE2(I,J)
40    CONTINUE
C     WRITE(8,*) ' MATRIX FB'
      DO 41 I=1,3
C     WRITE(8,200) (FB(I,J),J=1,3)
41    CONTINUE


      DEN=FB(2,2)*FB(3,3)-FB(2,3)*FB(3,2)
      IF(DEN.LE.1.E-80) WRITE(7,*)' ********* WARNING DEN IS TOO SMALL'
c     WRITE (7,200) DEN
c     IF(DEN.LE.1.E-80) GO TO 500
      IF (DEN.LE.1.E-80) DEN=1.E-80
      STIF22(2,2)=FB(3,3)
      STIF22(3,3)=FB(2,2)
      STIF22(2,3)=-FB(2,3)
      STIF22(3,2)=-FB(3,2)

      STIF22(1,1)=1./FB(1,1)
      DO 50 I=2,3
      DO 50 J=2,3
      STIF22(I,J)=STIF22(I,J)/DEN
50    CONTINUE

      DO 60 I=1,3
      DO 60 J=1,3
      TEMP(I,J)=0.
```

```
        TEMP2(I,J)=0.
60      CONTINUE
        DO 70 I=1,3
        DO 70 J=1,3
        DO 70 K=1,3
        STIF12(I,J)=-EQ(I,K)*STIF22(K,J)+STIF12(I,J)
70      CONTINUE
        DO 80 I=1,3
        DO 80 J=1,3
        DO 80 K=1,3
        STIF11(I,J)=-STIF12(I,K)*EQ(J,K)+STIF11(I,J)
80      CONTINUE
        DO 90 I=1,3
        DO 90 J=1,3
        STIF21(I,J)=STIF12(J,I)
90      CONTINUE
C
C
C       WRITE(8,*) ' MATRIX K11'
        DO 105 I=1,3
C       WRITE(8,200) (STIF11(I,J),J=1,3)
105     CONTINUE

C       WRITE(8,*) ' MATRIX K22'
        DO 110 I=1,3
C       WRITE(8,200) (STIF22(I,J),J=1,3)
110     CONTINUE

C       WRITE(8,*) ' MATRIX K12'
        DO 120 I=1,3
C       WRITE(8,200) (STIF12(I,J),J=1,3)
120     CONTINUE
C
C
500     CONTINUE
C
C
200     FORMAT(3X,3E15.5)


C*****************************************************************
C       Setup element stiffness matrix without plastic hinges
C*****************************************************************

        DO 1 I=1,12
        DO 1 J=1,12
1       RKK1J0(I,J)=0.0

        RKK1J0(1,1)=H1
        RKK1J0(2,2)=STIF11(2,2)
        RKK1J0(3,3)=H4
        RKK1J0(4,4)=H2

        RKK1J0(5,3)=-H6
        RKK1J0(5,5)=H7
```

```
        RKK1J0(6,2)=STIF11(3,2)
        RKK1J0(6,6)=STIF11(3,3)
        RKK1J0(7,1)=-H1
        RKK1J0(7,7)=H1

        RKK1J0(8,2)=STIF21(2,2)
        RKK1J0(8,6)=STIF21(2,3)
        RKK1J0(8,8)=STIF22(2,2)
        RKK1J0(9,3)=-H4
        RKK1J0(9,5)=H6
        RKK1J0(9,9)=H4
        RKK1J0(10,4)=-H2
        RKK1J0(10,10)=H2
        RKK1J0(11,3)=-H6
        RKK1J0(11,5)=H9
        RKK1J0(11,9)=H6
        RKK1J0(11,11)=H7
        RKK1J0(12,2)=STIF21(3,2)
        RKK1J0(12,6)=STIF21(3,3)
        RKK1J0(12,8)=STIF22(3,2)
        RKK1J0(12,12)=STIF22(3,3)

        DO 2 I=1,12
        DO 2 J=1,12
        IF(J.GT.I) RKK1J0(I,J)=RKK1J0(J,I)
2       CONTINUE


        IF(ABS(EBEAMX*RIZX).LT.1.0D-15) THEN
        WRITE(7,205) IR
205     FORMAT(' EBEAM OR RIZ OF ELEMENT',I5,' IS ZERO')
        END IF


C

220   CONTINUE
C*****************************************************************
C       Form rotation matrix
C*****************************************************************
        DO 100 I=1,12
        DO 100 J=1,12
100     RLM(I,J)=0.0

        RLM(1,1)=CA(IR)
        RLM(4,4)=CA(IR)
        RLM(7,7)=CA(IR)
        RLM(10,10)=CA(IR)
        RLM(1,2)=SA(IR)
        RLM(4,5)=SA(IR)
        RLM(7,8)=SA(IR)
        RLM(10,11)=SA(IR)
        RLM(2,3)=-1.0
        RLM(5,6)=-1.0
        RLM(8,9)=-1.0
        RLM(11,12)=-1.0
```

```
      RLM(3,1)=-SA(IR)
      RLM(6,4)=-SA(IR)
      RLM(9,7)=-SA(IR)
      RLM(12,10)=-SA(IR)
      RLM(3,2)=CA(IR)
      RLM(6,5)=CA(IR)
      RLM(9,8)=CA(IR)
      RLM(12,11)=CA(IR)
C-----------------------------------------------------------------
      CALL MATMUL(12,12,12,RKK1J0,RLM,RLM1)
      CALL MATTRA(12,12,RLM,RLM2)
      CALL MATMUL(12,12,12,RLM2,RLM1,RKK1J)

      RETURN
      END


      FUNCTION RMPPX(NH,IX,IR,LR)
      IMPLICIT REAL*8 (A-H,O-Z)
      COMMON/CONT/ICONT,NBEXYC(100),IBJC(600)
      COMMON/FUN0/KGIRD
      COMMON/FUN00/PFORCE,PECCEN,FS4
      COMMON/FUN1/SIZ(50),RMPM5(50)
      COMMON/FUN2/FJGD,RIZGD,RIYGD,RJGD,SIZGD,EBEAMG,GBEAMG,
     & ASYGD,ASZGD,RMPPGD(5),RKTPGD(5),RLPPGD,SITMAXG
      COMMON/FIJ/FJ(50),RIZ(50),RIY(50),RJ(50),RKTP(5,50),
     * RKTN(5,50),IRKT(600)
      COMMON/NFIJ/NRKT
      COMMON/RMP/RMPP(5,50),RMPN(5,50),RLPP(50),SITMAXP(50),
     * RLPN(50),SITMAXN(50)
      COMMON/J10/RMA0(600),RMB0(600)
      COMMON/J7/CUMAX,CFCT,UMAX,FCT,KA,KB,IRGJ1,LDY

      IF(NH.EQ.5)THEN
      RMPPX=RMPM5(IX)
      RETURN
      END IF

      IF(IR.GT.KGIRD.OR.LDY.LE.3)THEN
      RMPPX=RMPP(NH,IX)
      RETURN
      END IF

      IF(ICONT.EQ.1)THEN
      RMPPX=RMPP(NH,IX)
      RETURN
      END IF

      IF(ICONT.NE.1)THEN
        IF(LR.EQ.1)RMAB=RMA0(IR)
        IF(LR.EQ.2)RMAB=RMB0(IR)
        IF(RMAB.LE.0.0)THEN
          X1=ABS(RMAB)/RMPPGD(1)
          RMAB=0.0
```

```
        END IF
      IF(RMAB.GE.RMPPGD(1))THEN
        RM1=RMPPGD(1)
      ELSE

        IF (LDY.EQ.6)THEN
          RM1=SIZ(IX)*(PFORCE/FJGD+(PFORCE*PECCEN-RMAB)/SIZGD+FS4)+RMAB
        END IF


        IF(LDY.EQ.4.OR.LDY.EQ.5)THEN
          RM1=RMAB+SIZ(IX)*(RMPP(1,IX)/SIZ(IX)-RMAB/SIZGD)
        END IF

        IF(RM1.LE.RMAB)RM1=RMAB+.0000001
        IF(RM1.GT.RMPP(1,IX))RM1=RMPP(1,IX)
      END IF

      RMPPX=RMPP(NH,IX)-(RMPP(1,IX)-RM1)/(RMPP(1,IX)-RMPM5(IX))*
     &  (RMPP(NH,IX)-RMPM5(IX))
      END IF
      RETURN
      END



      FUNCTION RKTPX(NH,IX,IR,LR)
      IMPLICIT REAL*8 (A-H,O-Z)
      COMMON/CONT/ICONT,NBEXYC(100),IBJC(600)
      COMMON/FUN0/KGIRD
      COMMON/FUN00/PFORCE,PECCEN,FS4
      COMMON/FUN1/SIZ(50),RMPM5(50)
      COMMON/FUN2/FJGD,RIZGD,RIYGD,RJGD,SIZGD,EBEAMG,GBEAMG,
     &  ASYGD,ASZGD,RMPPGD(5),RKTPGD(5),RLPPGD,SITMAXG
      COMMON/FIJ/FJ(50),RIZ(50),RIY(50),RJ(50),RKTP(5,50),
     *  RKTN(5,50),IRKT(600)
      COMMON/NFIJ/NRKT
      COMMON/RMP/RMPP(5,50),RMPN(5,50),RLPP(50),SITMAXP(50),
     *  RLPN(50),SITMAXN(50)
      COMMON/J10/RMA0(600),RMB0(600)
      COMMON/J7/CUMAX,CFCT,UMAX,FCT,KA,KB,IRGJ1,LDY

      IF(IR.GT.KGIRD.OR.LDY.LE.3)THEN
        RKTPX=RKTP(NH,IX)
        RETURN
      END IF

      IF(ICONT.EQ.1)THEN
        RKTPX=RKTP(NH,IX)
        RETURN
      END IF

      IF(ICONT.NE.1)THEN

        IF(NH.EQ.0)THEN
        RKTPX=RKTP(NH,IX)
```

```
          RETURN
          END IF

        SNH=RMPPX(NH+1,IX,IR,LR)-RMPPX(NH,IX,IR,LR)
        SNH=SNH*RKTP(NH,IX)/(RMPP(NH+1,IX)-RMPP(NH,IX))

          IF(LR.EQ.1)RMAB=RMA0(IR)
          IF(LR.EQ.2)RMAB=RMB0(IR)

          IF(RMAB.LE.0.0)THEN
            X1=ABS(RMAB)/RMPPGD(1)
            RMAB=0.0
          END IF
          IF(RMAB.LE.RMPPGD(NH))THEN
            RKTPX=SNH
            RETURN
          ELSE
            IF(RMAB.LE.RMPPGD(NH+1))THEN
              X1=1-(RMAB-RMPPGD(NH))/(RMPPGD(NH+1)-RMPPGD(NH))
              IF(X1.LT.1.0E-10)THEN
                RKTPX=1.0E16
            ELSE
                RKTPX=(RMPPX(NH+1,IX,IR,LR)-RMAB)/X1/(RMPP(NH+1,IX)-
     &                RMPP(NH,IX))*RKTP(NH,IX)
            END IF
          END IF
        END IF
        END IF
        RETURN
        END
```